

# **Genetic Modulation of the Neonatal Neural Processing of Speech at High and Low Familial Risk for Developmental Dyslexia**

**Stanimira Georgieva**  
Newnham College  
University of Cambridge

*This thesis is submitted for the degree of Doctor of  
Philosophy (PhD)*

*Supervisors: Prof Zoe Kourtzi & Dr Victoria Leong*

*24<sup>th</sup> June 2021*

# PREFACE

---

## Declarations

This thesis is the result of my own work and includes nothing which is the outcome of work done in collaboration except as declared in the preface and specified in the text.

It is not substantially the same as any work that has already been submitted before for any degree or other qualification except as declared in the preface and specified in the text. The relevant research output published or delivered throughout the duration of the dissertation is detailed in Appendix VII.

It does not exceed the prescribed word limit of 60,000 for the School of Biology Degree Committee. The actual word-count excluding captions, footnotes, bibliography and appendices is 54,173.

# SUMMARY PAGE

## **Genetic Modulation of the Neonatal Neural Processing of Speech at High and Low Familial Risk for Developmental Dyslexia**

*Phd Candidate: Stanimira Georgieva*

This is a longitudinal study that aims to identify potential neural oscillatory deficits in neonates associated with genetic and familial risk of dyslexia. Poor awareness of speech sounds (phonology) is the hallmark of dyslexia, across all languages studied so far. Despite the identification of several dyslexia susceptibility genes, little is known about the mechanisms by which genetic abnormalities give rise to neural deficits and how these in turn generate phonological deficits. Here, we hypothesised that common genetic polymorphisms in major dyslexia susceptibility genes (which are involved in developmental processes in-utero), are associated with abnormalities in the cortical microcircuitry, as hence in the functional connectivity and brain-to-speech (B2S) synchrony *at birth*. Identifying potential neonatal neural markers in association with dyslexia would be important for the understanding and supporting phonological development as it occurs during early infancy. One hundred infants (49 at high familial dyslexia risk) were assessed at birth, and half of them were followed up longitudinally at 7.5, 15 and 24 months of age. The current dissertation is focused on the neonatal dataset only. Previously reported single nucleotide polymorphisms (SNPs) – single base alterations in individual nucleotides within a gene - across major dyslexia susceptibility loci were analysed (DCDC2, KIAA0319, ROBO1 and DYX1C1) based on the neonatal blood-spot samples. Electroencephalography (EEG) was used to assess the new-born infants' channel-to-channel network coherence and their neuronal oscillatory processing of prosodically enhanced speech. We predicted lower network coherence, as well as a reduced and delayed B2S synchrony (measured as phase-locking values - PLV) in infants at high familial risk of dyslexia, and in those carrying the less common variants of the tested SNPs. We found evidence for a reduced left hemispheric directed coherence in infants with the rarer ROBO1 and DCDC2 genotypes, independent of their familial risk. In contrast, we found that high familial risk was the strongest indicator of a significant delay in the PLV peak to the onset of speech, despite a similar PLV peak strength between the risk groups. The effect was driven by the infants with dyslexic mothers. Finally, the less common variants of two ROBO1 SNPs were associated with a delayed PLV peak beyond the infant's familial risk. Although not directly tested, we can hypothesise that delays in peaks synchrony can be theoretically related to less synchronised or noisier internal neural environment in relation to dyslexia, which could result in less efficient synchronisation to external stimuli. Together, the neonatal results point toward a measurable dyslexia-risk related neural endophenotypes present at birth. They indicate a possible distinction between the effects of the at-risk genotype on the network coherence measures, and of the familial risk on the efficiency of the brain-to-speech synchrony. The developmental trajectories

of these neonatal effects, and their significance over early phonological development and later dyslexia outcomes remain to be investigated. These results, however, present a potential mechanism for the emergence of an early neurobiological dyslexia-risk profile, which is yet to undergo the developmental, environmental, and experiential influences that would later shape language acquisition and reading skill.

# ACKNOWLEDGEMENTS

This work would have not been possible without the generous donations by the Rosetrees Charitable Trust who funded the project, and by Newnham College and the G C Grindley Funds, who further funded my work.

I will be forever grateful and in owe of my supervisors, who are always there, even from afar, and who inspire me every day: Prof Zoe Kourtzi, for giving me a chance and always finding the time and the right words of encouragement in the moments most needed; and Dr Victoria Leong, for her keen insight, sharp mind, sound advice and unwavering faith in me, which provided me with both an anchoring pole and a guiding light. I could not be more honoured to be their student and mentee.

I further want to thank my advisor Prof Topun Austin, who believed in me enough to support my NHS contract and who made it possible for me to collect the neonatal patient data despite my very limited clinical research experience. Massive thanks also to the neonatal and paediatric research nurses Emma Porter, Kelly Spike and Andrea Edwards, who helped me navigate through the exciting sea of CUH administration and competence training.

It would have been completely impossible to run any of the genetics side of the study without the invaluable guidance of Dr Gusztav Belteki who despite my complete lack of competence and knowhow in molecular biology managed to somehow teach and supervise me. Dr Salvatore Valenti deserves a special mention here, who trained me step-by-step in running the genetics analysis and provided daily support in the wet lab.

I want to extend very special words of gratitude to Dr Kaili Clackson and Dr Valdas Noreika, who were there every day in the lab (next door) with helpful suggestions, sharp observations, kind words, and warm beverages. I would have not loved being in the lab as much without them there. I will be always in debt of Dr Elian Finch who lent me and taught me how to use LENA; and to Professors Stoel-Gammon and Williams for their sharing and guidance on PEEPS.

Finally, I am no one if not for my family, both the one which created me, and the one that I have created here. I want to thank my parents for always trusting me and for never telling me what to do, or what not to. My sister, for being my pillar, my inspiration, and my aspiration. All of the dear friends, near and far, for carrying me through the entire process and for being my partners in late-life writing and crime. Last but not least, all of those families with newborn babies, who decided to partake and are still following up with the study, who trusted me with their most precious and without whom none of this would have ever been possible. THANK YOU!

# LIST OF COMMON ABBREVIATIONS & BASIC DEFINITIONS

---

## Related to Neuroscience and Neuroimaging

AC – auditory cortex (PAC is primary auditory cortex); not to be confused with phase-amplitude coupling, which is not abbreviated here – or is it?

AF – arcuate fasciculus

DTI – Diffusion Tensor Imaging

    FA – fractional anisotropy

EEG – electroencephalography

ERP – evoked-response or event-related potential

(f)MRI – (functional) Magnetic Resonance Imaging

fNIRS – functional Near InfraRed Spectroscopy

GM – gray matter

IFG – inferior frontal gyrus

LFP – local field potentials

MMN/MMR – mismatch negativity/response – in oddball-type paradigms

MTG – middle temporal gyrus

SMG - supramarginal gyrus

STG – superior temporal gyrus

TPJ - temporo-parietal junction

WM – white matter

---

## Related to Linguistics

ADS – adult directed speech

AM – amplitude modulated/tion

    AMHM – Amplitude Modulated Hierarchical Model

CDS – child directed speech.

IDS – infant directed speech.

NR – nursery rhyme

Rise time - the time between the onset and the highest amplitude of the vowel in a syllable.

Prosodic rhythm – stress-pattern of the language.

Phonology/cal – related to the sounds of/in speech.

---

## Related to Genetics

Genotype#1 – two copies of the more common allele in this cohort

/ #2 – two different alleles

/#3 – two copies of the less common allele in this cohort

LD – linkage disequilibrium.

HW – Hardy-Weinberg equilibrium/principal.

SNP – single nucleotide polymorphism.

---

## Related to Computations and Statistics

CI – confidence intervals

FDR – False Discovery Rate

BH – Benjamini-Hochberg

(i)FFT – (inverse) Fast Fourier Transform

GPDC – generalised or extended partial directed coherence (based on PDC)

PLV – phase-locking index

LME – liner-mixed effects

FE – fixed effects

RE – random effects

LSD – least significant difference (Fisher's)

SD – standard deviation

w.l. – Wilk's Lambda

Delta band – <2 Hz in infants; 1-3Hz in adults; – often referred to as slow-wave or low frequency, prosodic rate.

Theta – 2-4Hz in infants; 4-6Hz in adults; - referred to as slow-wave or low frequency, syllabic rate.

Alpha band- 4-6/7Hz in infants; 8-12Hz in adults

Beta – 8-20Hz in infants; 12-20Hz in adults – referred to as fast or high frequency, phonemic rate.

Gamma – >20Hz in both infants and adults, sometimes restricted to >35Hz in adult literature, also phonemic rate.

# TABLE OF CONTENTS

PREFACE.....	1
Declarations.....	2
ACKNOWLEDGEMENTS .....	5
SUMMARY PAGE .....	3
LIST OF COMMON ABBREVIATIONS & BASIC DEFINITIONS.....	8
Related to Neuroscience and Neuroimaging .....	6
Related to Linguistics .....	6
Related to Genetics .....	7
Related to Computations and Statistics .....	7
TABLE OF CONTENTS .....	8
PART ONE	
CHAPTER ONE: GENERAL INTRODUCTION & LITERATURE REVIEW.....	2
1.1    Dissertation Overview.....	2
1.2    Dissertation Aims .....	3
1.3    Review of the Literature to date.....	4
1.3.1    Developmental Dyslexia: Prevalence and Cognitive Characteristics .....	4
1.3.2    The Neurobiology of Dyslexia: from structural and functional abnormalities to impaired oscillatory entrainment to speech.....	14
1.3.3    Heritable Nature and Genetic Susceptibility of Dyslexia .....	35
1.3.4    Research Rationale, Hypotheses & Predictions .....	36
CHAPTER TWO: GENETIC SUSCEPTIBILITY IN DYSLEXIA .....	42
2.1    Candidate SNPs Overview .....	42
2.2    Genetics Chapter Summary .....	45
2.3    Dyslexia Susceptibility Genes: Review of the Literature to date.....	46
2.3.1    Dyslexia Susceptibility Genes Impacting Neuronal Migration .....	46
2.3.2    Dyslexia Susceptibility and Axonal Guidance.....	51
2.4    Genetics: Methods .....	54
2.4.1    Participants.....	54
2.4.2    Sample Collection – Neonatal.....	55
2.4.3    Genotyping Protocol .....	55
2.4.4    Statistical Analysis.....	61

2.5	Genetics: Results .....	62
2.5.1	Allelic and Genotype Frequencies .....	62
2.5.2	Associations between the Familial and Genetic Risk of Dyslexia .....	67
2.6	Genetics: Discussion .....	69
2.6.1	Summary of Genotyping Results .....	69
2.6.2	Implications of the Infants' Genotypes on Studies One and Two .....	69
<b>PART TWO</b>		
<b>CHAPTER THREE: COMMON METHODS.....</b>		<b>73</b>
3.1	Full Project Overview .....	73
3.2	Participants.....	74
3.3	Materials.....	75
3.3.1	Nursery Rhymes .....	75
3.3.2	Calculating the Hilbert-Envelope (baseband) of the Speech Signal .....	77
3.4	Experimental Protocol.....	82
3.4.1	Genetic Data Collection .....	82
3.4.2	EEG Data Collection.....	82
3.5	EEG Data Pre-Processing .....	86
3.5.1	Artifact Rejection: Common Rejection Strategies for Studies One and Two .	86
3.6	Speech-Brain Phase-Locking & Neural Coherence Calculations .....	88
3.6.1	Calculating the Phase-Locking Values between the phase angle series of the speech envelope and EEG .....	90
3.6.2	Calculating the Generalised Partial Directed Coherence between channels during speech presentation .....	90
3.7	Surrogate Baseline Control Analysis.....	92
3.7.1	Phase-Randomised Surrogates .....	93
<b>CHAPTER FOUR: STUDY ONE - Familial and Genetic Risk Effects on the Neonatal Neuronal Entrainment to Speech.....</b>		<b>97</b>
4.1	Study One Aims .....	97
4.2	Study One Keywords .....	97
4.3	Study One: Introduction.....	98
4.3.1	Deficient Neuro-Oscillatory Underpinnings in Dyslexia. ....	98
4.3.2	What Aspect of the Neural Oscillatory Response to Speech is Different in Neonatal Infants at Risk of Dyslexia? .....	98
4.3.3	Measuring phase entrainment at the onset of the speech stream using PLV ....	100
4.4	Study One: Methods .....	101

4.4.1	Participants .....	101
4.4.2	Experimental Materials and Protocol .....	101
4.4.3	Genotyping protocol and Infants' Genotype .....	101
4.4.4	Dyslexia Risk Variables.....	101
4.4.5	Other modelled variables.....	102
4.4.6	EEG pre-processing for the PLV onset analysis.....	103
4.4.7	Statistical Analyses Approaches.....	108
4.5	Study One: Results .....	115
4.5.1	Exploratory Regression Analysis for the PLV onset peaks .....	115
4.5.2	Linear Mixed Effects (LME) Models Analyses for PLV peak latency.....	117
4.5.3	Describing the Effects of The Factors Identified by The LME Models.....	124
4.6	Study One: Discussion .....	127
4.6.1	Summary and Interpretation of the Findings in Study One.....	127
4.6.2	Transition to Study Two.....	129
<b>CHAPTER FIVE: STUDY TWO – Familial and Genetic Risk Effects on the Neonatal Neural Network</b>		
<b>Coherence during Speech Presentation .....</b>		
<b>132</b>		
5.1	Study Two: Aims.....	132
5.2	Study Two Key Words .....	133
5.3	Study Two: Introduction .....	133
5.3.1	Dyslexia and Measures of Neural Connectivity and Network Coherence ....	134
5.3.2	Measuring Oscillatory Coherence Neonatally using GPDC.....	134
5.4	Study Two: Methods .....	136
5.4.1	Participants .....	136
5.4.2	Experimental Materials and Protocol .....	137
5.4.3	Genotyping protocol and Infants' Genotype .....	137
5.4.4	Dyslexia Risk Variables.....	137
5.4.5	EEG pre-processing.....	138
5.4.6	GPDC Outcome Measures.....	145
5.4.7	Statistical Analyses Approach.....	146
5.5	Study Two: Results .....	147
5.5.1	Summary Results: Effects of Genotype and Familial Risk on Infants' four-channel network connectivity at birth .....	147
5.5.2	Detailed GLM Results by Gene .....	149
5.5.3	Controlling for the Effects of the Varied Number of Nursery Rhymes Contributed .....	156

5.5.4	Effects of the Parent of Origin on the Network Coherence Estimates.....	156
5.5.5	Link between delayed PLV latency and Network Coherence .....	157
5.6	Study Two: Discussion.....	158
5.6.1	Summary of the Findings in Study Two .....	158
5.6.2	Link between the Studies One & Two.....	159
<b>PART THREE</b>		
<b>CHAPTER SIX: THE LONGITUDINAL DATASET .....</b>		
162		
6.1	The Aims of the Longitudinal Research Project .....	162
6.2	Brief Rationale & Potential Impact.....	163
6.3	My Role in The Longitudinal Project.....	164
6.4	Data Collection .....	165
6.4.1	Participant Recruitment.....	165
6.4.2	Neuro-Behavioural Data Acquisition .....	166
6.4.3	Background and Home Environment Measures .....	179
6.4.4	Genetics and Cortisol Measures .....	180
6.5	Significance of The Longitudinal Project .....	181
<b>CHAPTER SEVEN: DISCUSSION &amp; CONCLUDING REMARKS.....</b>		
185		
7.1	DISCUSSION .....	185
7.1.1	Summary.....	185
7.1.2	PLV results.....	185
7.1.3	GPDC results .....	191
7.1.4	The Wider Literature Context.....	195
7.1.5	Future Directions Based on the Longitudinal Dataset.....	200
7.1.6	Dissertation Limitations .....	201
7.2	CONCLUSIONS .....	204
<b>BIBLIOGRAPHY.....</b>		
207		
<b>Appendix I.....</b>		
226		
Parental Information Sheet .....		226
Parental Consent Form.....		230
Infant Consent Form.....		231
Full Study Protocol .....		232
<b>Appendix II.....</b>		
243		
II.I Parental Genetics .....		243
Participants .....		243

<b>Genetics Sample Collection</b> .....	243
<b>Genotyping Procedure for the Parental Saliva Samples</b> .....	243
<b>Parental Genotyping Results</b> .....	245
<b>My First PCR Gel</b> .....	252
<b>Appendix III</b> .....	253
<b>III.I Noisy or Artifactual Data Inspection and Quality Control</b> .....	253
<b>III.II Data Cleaning and Rejection by Individual Recording</b> .....	260
<b>III.III Nursery Rhymes Used in Analyses</b> .....	262
<b>Appendix IV</b> .....	263
<b>IV. I Negative PLV onset peak latencies</b> .....	263
<b>IV.II Exploratory Regression Analysis based on the 98% Surrogate Threshold</b> .....	266
<b>IV.III The Family of LME models describing the top 1% variance explained against the lowest information criteria (continued from the main text)</b> .....	267
<b>IV.IV Effects of Other Variables in the LME models</b> .....	273
<b>Appendix V</b> .....	277
<b>V.I Noisy Channels Correction Attempts</b> .....	277
<b>V.II Normalised GPDC Scores by Connection and Familial Risk Group</b> .....	278
<b>V.III FDR Corrections on the Three GLMs by Gene</b> .....	281
<b>V.IV Controlling for number of nursery rhymes by infant</b> .....	285
<b>Appendix VI</b> .....	290
<b>VI.I PEEPS Protocol &amp; Stimuli Adaptation for Online Administration</b> .....	290
<b>Appendix VII</b> .....	311
<b>VII.I Relevant Research Output During PhD Program</b> .....	311
<b>VII.II Methods Paper One</b> .....	312
<b>VII.III Methods Paper Two</b> .....	335



# **PART ONE**

## **CHAPTER ONE**

# **GENERAL INTRODUCTION & LITERATURE REVIEW**

# CHAPTER ONE: GENERAL INTRODUCTION & LITERATURE REVIEW

---

## 1.1 Dissertation Overview

This dissertation focuses on the initial time point of a longitudinal design aimed at understanding the early mechanisms of phonological development as influenced by perinatal risk factors for reading disorder. Additional developmental and environmental measures were acquired in the course of the larger study, which are not reported but merely described in the current paper. The dissertation is organised in three sections. Section 1 (Chapters 1 & 2) introduces the relevant literature and the pre-natal genetic risk factors upon which the project's rationale was built. Section 2 (Chapters 3 to 5) reports two studies focused on understanding the neonatal dependencies between the familial and genetic risk factors of developmental dyslexia and the early neuro-oscillatory markers of differential continuous acoustic speech processing. Section 3 (Chapters 6 & 7) puts the results of the two neonatal studies in the context of the wider project and discusses them in light of the broader literature and possible future investigative directions.

## 1.2 Dissertation Aims

The PhD dissertation aims to advance the current state of knowledge by attempting to:

- (1) Give a comprehensive account of the dyslexia literature through an early neuro-developmental lens and in the context of pre-natal genetic susceptibility.
  
- (2) investigate whether there are congenital oscillatory deficits in neonatal infants at high familial risk of dyslexia as measured by:
  - a. speech-onset phase entrainment
  - b. channel-to-channel network coherence.
  
- (3) uncover systematic relationships between the tentative oscillatory deficits and the genotype in order to define risk profiles of the gene-brain interactions, constrained by familial risk.
  
- (4) Put the identified risk profiles in the context of the wider longitudinal project.

It is important to note that within the time-constraints of the PhD project, testing for dyslexia in our cohort falls outside of the scope of the current work. Therefore, the investigated risk profiles were tested in the longitudinal project against validated measures of language and phonological development instead.

---

## 1.3 Review of the Literature to date

### 1.3.1 Developmental Dyslexia: Prevalence and Cognitive Characteristics

Fisher et al. (2002) defined dyslexia as a specific and significant impairment in reading ability, which cannot be explained by deficits in intelligence, learning opportunity, motivation, or sensory acuity. The authors pointed out that dyslexia was one of the most frequently diagnosed disorders in childhood, representing a further educational and social burden. Dyslexia is a multicomponential reading disorder with complex neurobiological aetiology (Black et al., 2017; Kere, 2014). While various theories on the origins of the reading impairment exist, phonological (speech-sound) processing deficit has been commonly found as the cognitive hallmark of dyslexia (Peterson & Pennington, 2015; Snowling, 2001) and could be one of the potential explanations for the observed difficulties in phoneme-to-grapheme (sound-to-letter) mapping, a prerequisite for reading acquisition (Wagner & Torgesen, 1987).

Dyslexia has an established heritable nature with several contributing candidate genes (Newbury, Monaco, & Paracchini, 2014). As the identified dyslexia susceptibility genes have consistently been implicated in very early neurodevelopment processes of cell migration and axonal guidance, it has been suggested that the affected cortical neuronal circuitries are already altered at birth. The differences in neuronal wiring can be translated into functional changes in the underlying activity and handling of incoming information. One such basic functional change can affect the processing of phonological information, a capacity already available to the new-born infants. At the behavioural level, these differences might not be observable until long after birth, when a child is learning to read. To inform early interventions, there is a keen investment in understanding the mechanisms of the observed phonological processing deficits in developmental dyslexia much earlier. Because of the strong genetic component and the resulting micro-structural modifications in-utero, both the neuroendophenotypical and the cognitive-behavioural characteristics of developmental dyslexia are almost always discussed in the context of a developmental trajectory. Morphological and functional changes and cognitive outcomes are often reviewed as part of a maturation process, with differences in the symptomatology identified in infancy, childhood and adulthood.

### 1.1.1. Prevalence

Dyslexia affects the acquisition of skilled reading in between 5 to 17.5% of children worldwide (S. Shaywitz, 1998). In the UK, the British Dyslexia Association estimates that there are 375,000 pupils with dyslexia each year, and a total of 2 million people are severely affected. It is more frequent in boys than girls, with a ratio between 1:1.35 in non-clinical and 1:2.76 in clinical populations (Jiménez-Bravo, Marrero, & Benítez-Burraco, 2017), however, due to comorbidity with other more externalizing disorders such as attention-deficit/hyperactivity disorder, boys may be coming more often to clinical attention (Peterson & Pennington, 2015).

Dyslexia has been identified in many languages globally and in different language groups, but is less prevalent in languages with shallow orthographies – i.e. with more direct mapping of phonemes onto graphemes, such as Spanish, Italian and Finnish (Jiménez-Bravo, Marrero, & Benítez-Burraco, 2017). Still, problems with fluent reading and the associated early cognitive predictors were similar in five tested European languages (Finnish, Hungarian, Dutch, Portuguese, and French), and phonological awareness specifically was the main predictor of reading ability in each one of those<sup>1</sup> (Peterson & Pennington, 2015). The exception was Finnish where phonological awareness and vocabulary had comparable contributions (Ziegler et al., 2009). Furthermore, the cross-cultural consistency extended to non-orthographic languages as well, such as Chinese (Feng et al., 2020), which is a logographic language - the written symbols represent morphemes (the smallest unit of meaning) rather than phonemes (the smallest unit of sound). Phonological awareness was as important of a predictor of reading skill in Chinese as in the other reported languages.

### 1.1.2. Cognitive and Behavioural Characteristics of developmental dyslexia

Peterson & Pennington (2015) gave a brief overview of the history of dyslexia, starting from the first coining of the term at the turn of the 20th century to label a variety of reading disabilities in children. The popular view throughout the 20th century was that dyslexia was a visual processing disorder, and it is still sometimes seen as a visual processing

---

<sup>1</sup> It should be said, however, that the NeuroDys study (N>2100 children (8-12 years old) across eight European countries: Austria, France, Germany, The Netherlands, Switzerland, Finland, Hungary, and the United Kingdom; with common inclusion criteria for the study) failed to find any common genetic predictors (single markers or haplotypes) of case-status or reading/spelling skills in the metanalysis (J. Becker et al., 2014).

impairment in the public eye despite lack of empirical support (Peterson & Pennington, 2015). The contemporary scientific consensus is that although there may be a suboptimal visual attention component to it, dyslexia is a neurodevelopment disorder of a linguistic nature with a primary cognitive deficit in phonological awareness. The neurodevelopmental disorder classification (DSM5, American Psychiatric Association, 2013) postulates that dyslexia is a heritable, life-long conditions with an early, potentially pre-natal onset, and does not represent a transient developmental lag (Snowling et al., 2020). Indeed, evidence for phonological processing difficulties in dyslexic individuals has been identified from early childhood (de Bree & Wijnen, 2016 in Thomson & Jarmulowicz (Eds.); Dębska et al., 2016 - although they did not find differences in pre-school children; Lohvansuu et al., 2018; Łuniewska et al., 2019). In fact, the lion share of the literature implicates phonological difficulties in reading acquisition even prior to learning to read (Shaywitz & Shaywitz, 2005). In the early 2000s, Goswami steered the discussion on phonological issues in dyslexia towards a deficit in the ability to follow the speech prosodic rhythm – the specific patterns of intonation and stress in a given language (Goswami et al., 2002). The phonological deficits were attributed to a failure to perceive the onsets (Goswami, 2011; Hämäläinen et al., 2005; Leong et al., 2011; Thomson & Goswami, 2010) of the distinct phonological units with the highest power in the speech envelope (ie. stressed vowels), leading to a difficulty in finding the boundaries of the prosodic utterance. In English, these boundaries occur at the syllabic (~4Hz) and stress (~2Hz) rates.

### ***The role of prosodic boundaries in phonological inferences in early development***

Speech-sound perception obeys several organizational principles. Phonemic information is encoded by short high-frequency (>20Hz, or gamma) amplitude modulated cues, such as formant transitions between the consonant and vowel, and voicing (i.e. /da/ versus /ta/). The speech envelope correlates with slow-wave speech features such as the syllabic rate and the prosodic (stress) rhythm. The syllables in English occur roughly four times per second (~4Hz, or theta rate) in the adult speech and twice per second in child- or infant-directed speech (ADS, CDS and IDS respectively) (Leong et al., 2014). The prosodic rhythm is given by the alterations of stressed (**Strong**) and non-stressed (**weak**) syllables (i.e., in English, it is usually S-w-S-w) and can be measured by the interstress interval between onset rise times. The syllable's rise time is the time between the onset and the highest amplitude of the vowel. The prosodic rhythm is phase-locked to the onset rise time of the strong syllables in the speech stream, as they are the auditory events around the audible edges of speech with steepest increase in energy. The prosodic rhythm in English is usually

measured at around ~2Hz (or delta rate), and there seems to be a considerable cross-language consistency in the rate of the interstress interval (Dauer, 1983).

The prosodic speech segmentation is important for language acquisition, especially in early childhood. It provides the early language learners with cues to the statistical regularities between phonemes that exist in their native language and define boundaries of larger semantic units such as morphemes and words (Gervain et al., 2008; Mehler et al., 1988; Peña et al., 2002; Thiessen et al., 2005). Meltzoff, Kuhl, Movellan & Sejnowski (2009) suggested that expressive and receptive speech learning processes follow Piagetian stages. Initial ability to perceive all sounds within the human production spectrum is lost by 6 months, when tuning in to speech sound (phonology) of the mother tongue happens. Between 6-12 months, infants use statistical learning to infer the regularities and important prosodic speech patterns in their primary language (or two languages, if bilingual – and it takes them slightly longer). In this period, they develop a good discrimination of their native phonemes present and learn to ignore the irrelevant phonemes characteristic of other language systems (classic example here is the lack of discrimination between the /l/ and /r/ sounds for Japanese infants). This process of ‘tuning-in’ is a natural automatic by-exposure trial-and-error learning experience and is heavily dependent on the social interactions with the primary caregiver in which they build accurate prosodic speech segmentation inferences. The child uses those cues to infer when the meaningful speech units start and end, and to scaffold their future, more intricate understanding of the spoken word on them (Friedrich & Friederici, 2015; Graf Estes & Hurley, 2013; Leong et al., 2014; Singh et al., 2009; Zhang et al., 2011). Humans start using the prosodic stress boundaries to segment the speech stream into meaningful sound units in the very early language development stages, potentially even prior to birth. Rise time discrimination abilities have been reported impaired in dyslexic children of different languages (Goswami 2011, 2015). McPhillips et al (2000) argued that dyslexic children do not ‘unlearn’ their primitive reflexes and are delayed in disengaging from the phoneme decoding and moving to the full-word sound decoding, even after intensive phonological training programs. According to these authors, the dyslexic children take on a focus-on-every-sound processed strategy which might be helpful for them in the initial stages of learning to speak but is interfering with the subsequent fluency stages.

Importantly, there are key differences between human adult- and infant-directed speech; the critical low frequency carrier band that organises the amplitude modulated structure

(or envelope) of the speech signal over time seems to follow a maturation trajectory, whereby it goes from the delta range in early infancy to theta in adulthood (Leong et al., 2017). Leong & Goswami (2015) used an Amplitude Modulated Hierarchical Model (AMHM) to demonstrate that CDS has a three-tier nested hierarchical structure of amplitude modulation (AM) based on the Hilbert transform of the speech signal across all spectral bands, centred around 2Hz, 5Hz and 20Hz. In the constructed AMHMs, the 2Hz AM peak (i.e. the prosodic modulation peak) was the master orchestrator at the highest level of nesting and with the highest measured energy. This was different to ADS where the peak organising frequency was centred between 4-6Hz. Thus, it was the delta AM frequency that the infant's brain was able to follow best, and which may be providing them with linguistic cues to start fitting structure to the speech they hear (Thiessen et al., 2005).

### ***The Special Case of Prosody in Infant-Directed Speech***

IDS is a prosodically-enhanced speaking register naturally used by adults to engage infants' attention and convey affective warmth, and infants seem to show preference to IDS already in the first weeks of life (Cooper & Aslin, 1990; Fernald, 1989). For example, 2-9-day-olds had a tendency towards higher oxygenated blood-flow in fNIRS when listening to pre-recorded IDS-told stories than to the same stories in the ADS register (Saito et al., 2007). An added benefit for researchers comes from the fact that infants find IDS more engaging, which facilitate experimental procedures and higher data retention in infant-oriented paradigms.

IDS also supported language learning directly because the exaggerated amplitude and frequency modulation entrained the infants' brain response more strongly than normal speech (Thiessen et al., 2005), thereby supporting infants' phonological parsing of the speech signal (Leong et al., 2014; Zhang et al., 2011). The parsing of auditory information based on the slow frequencies in the IDS had a key role in word acquisition (Graf Estes & Hurley, 2013) as early as 3 months of age (Friedrich & Friederici, 2015), and retention for at least 24 hours at the age of 7-8 months (Singh et al., 2009) but not yet at 3 month. Already at birth, infants could distinguish between language structures with different rhythmic signatures (i.e. stress- vs syllable-timed) (Nazzi et al., 1998). Four-day old-French and 2-month-old American infants were able to distinguish between two foreign for them languages even after the speech signal had been low-pass filtered (i.e. with preserved prosodic but impoverished phonemic structure), as long as they were familiar with at least

one the presented languages (Mehler et al., 1988). Thus, the young infants were likely basing their language discrimination abilities on the prosodic cues remaining intact and were moreover able to extend these abilities to other languages with a similar prosodic structure but not to rhythmically different languages (Nazzi, Bertochini & Mehler, 1988). Infants, however, learn with an incredible speed and their phonemic indifference seemed to only last for a few months. By 2-3 months of age, infants responded differentially to phonemes that only varied in their place of articulation (i.e. /ba/ vs /ga/). In a seminal paper, these precocious discrimination abilities were found in the latency of the time-locked EEG waveform consisting of two positive peaks between 200-400ms post stimulus onset (Ghislaine Dehaene-Lambertz & Dehaene, 1994). By 6 months of age, infants had developed the ability to discriminate their maternal language from rhythmically similar languages (Molnar et al., 2014). Pena, Pitaluga & Mehler, (2010) showed that even infants who were born prematurely had reached that capacity by the time they would have been at their 6 months post-term age. As their experience with language grows, twenty-month and 28-month-old infants were able to use the prosodic information of the sentences in French to infer the syntactic categories (semantically significant in French) of ambiguous words based on the prosodic structure of the sentence, and to correctly identify the intended word meaning, indicated by preferential gaze time (de Carvalho et al., 2017).

Thus, in many languages, stress pattern (or mora, in Japanese) perception was an important prerequisite for the development of phonological skills as early as a few days after birth (Mehler et al., 1988). The early accurate encoding of the key low frequency features of the IDS envelope had developmental value for infants beginning to form the scaffolding structure of their mental lexicon (Leong & Goswami, 2015). If they were poor at following the slow modulation peaks in IDS, they would potentially benefit less from the prosodically enhanced speech input and would require more effort in forming accurate speech-sound representations early on. At high risk of dyslexia, already at 6 months, infants displayed reduced behavioural sensitivity (as measured by conditional head turning) to the available phonological information, and to passive phonological discrimination (Leppänen et al., 2002; Richardson et al., 2003).

### ***Phonological processing deficits in dyslexia***

In the theoretical accounts that bind dyslexia to problems in phonological processing (Ramus et al., 2003; Snowling, 2001; Vellutino et al., 2004), the reading difficulties are attributed to the difficulties in parsing words and phrases into their constituent sounds

(Stanovich, 1988). The impairment is in the crucial ability to attend to and manipulate linguistic sounds for the establishment and automisation of the letter-to-sound correspondences, which normally facilitate fluency in written word recognition in both alphabetic (script represents phonemes) and logographic (script represents morphemes and syllables) orthographies (Peterson & Pennington, 2015). Narrowing down on the specific aspects of phonological impairment in dyslexia, Ramus & Szenkovits (2008) predicted that it was the efficiency of access to the representations of the speech-sound units that was impaired, and not the phonological representations themselves. In line with this, previously, Wagner & Torgesen (1987) highlighted the importance of the ability to maintain a phonological representation in working memory for lexical access. They related the underperformance of dyslexic children on rapid naming tasks to a deficit in using the available phonological information to efficiently access the lexical (and sublexical in Ramus & Szenkovits, 2008) units. The reduced speed of access thwarts the automisation of the sound-letter mapping and potentially puts a further strain on the executive functions (Nicolson & Fawcett 2019).

Ramus & Szenkovits (2008) further identified the three main dimensions of deficit in dyslexia, which have often been used in research to test for reading and cognitive differences between dyslexic and typical (pre-)readers. These were: a) poor phonological awareness measured by the phoneme deletion task (i.e. saying 'dice' without /d/); b) poor performance on rapid automatized naming (or RAN, i.e. naming rapidly over-learned items such as colours); c) inefficient phonological or verbal short-term memory (VSTM, tested by tasks such as digit span and nonword repetition). Phonological awareness relies on a conscious access or attention to the needed phonemes, RAN retrieves phonological representations from memory storage, and VSTM is responsible for passively maintaining or actively manipulating phonological items in the short-term memory buffers (Ramus & Szenkovits, 2008). In dyslexia, all three dimensions of phonological access have been reported compromised in English, however, the loading of each of the three components varied between languages. In German, for example, a language with a more transparent orthography than English, the phonological awareness deficit seemed to be less severe in children with dyslexia, and to be almost completely outgrown by adulthood (Soltész et al., 2013).

Although all the three dimensions rely to some degree on phonological representations, they also employ a myriad of other capacities such as an increased working memory load. In half-a-decade-long series of experiments, Ramus & Szenkovits (2008) found that

phonological representations remained intact in their dyslexic participants. When presented with a series of words and nonwords to recall, their dyslexic participants' performance deteriorated with increasing the phonological similarity between words and nonword at the same rate as it did in the control group. Thus, the phonological deficit did not reflect a deterioration of the phonological representations as compared to controls but rather was a function of an increased task-demand in the domains of VSTM and conscious effortful processing. The authors termed those constraints collectively as a deficient *access* to phonological representations in dyslexia. Furthermore, dyslexic university students seemed to have acquired their native language phonological assimilation rules (speaking rate or context dependent deletions, insertions or substitutions of phonemes) comparable to controls (Szenkovits et al., 2016). The implication from this study was that the dyslexic students' phonological representations must have been intact for their phonological 'grammar' to fair against the control group's, despite still showing the phonological access deficits typical of dyslexic readers.

While there has been a general agreement that deficits in phonological access or processing have a pivotal role in dyslexia, the phonology-centred theories incurred some criticism on being too reductionist and focused on the phonological symptoms rather than the causes leading to poor reading ability (Nicolson & Fawcett, 2019). Perhaps the most prominent criticism has been on their inability to directly account for motor and sensory impairments often detected in dyslexic individuals.

The suboptimal visual spatial attention theories hypothesised that the reading deficits in dyslexia were caused by an inability to efficiently switch the visual attention to a new specific place while still keeping concentrated on the current location (Facoetti et al., 2003). This notion was supported by data showing an increased visual crowding effect, a diminished fixation accuracy, and differences in eye-movements in dyslexic individuals, who additionally benefited more from larger fonts (Eden et al., 1994). At the neural level, the problem was attributed to disruptions in the lateral geniculate nuclei's (LGN) magnocellular layers which resulted in dyslexic adults and children processing visual, auditory, and movement-related stimuli differently (Stein, 2018). However, Sperling et al (2005) concluded that dyslexic children perform as well as non-dyslexic children when presented with magnocellular response-evoking clear images in a visual signal-in-noise discrimination task. In contrast, when visual noise was introduced to the images, the dyslexic children underperformed significantly, and their high-noise contrast thresholds

correlated with their performance on RAN, and moderately with measures of vocabulary, non-word reading and reading comprehension, which was symptomatic of an executive functioning rather than visual-spatial discrimination deficit.

A different idea situated the problem in visual-auditory integration instead of purely a visual attention or rapid auditory processing deficit (Nicolson and Fawcett, 2019). However, Gori et al (2020) tested dyslexic children using audio-visual cues in a multisensory temporal integration task where they had to judge the distance between stimuli. While their multi-sensory thresholds fared well against matched typical readers, their unimodal visual and auditory thresholds were significantly higher as they required a larger gap between stimuli to make a correct temporal judgement. Furthermore, the temporal skills in the auditory modality and reading ability in a subgroup of the dyslexic children were positively correlated. Gori et al (2020) concluded that multisensory processing was not in itself impaired in dyslexia, rather, the limitations on multisensory integration were attributed to suboptimal temporal processing of the unisensory inputs.

Generalizing over the variety of deficits described in dyslexia, Nicolson and Fawcett (2019) argued for a universal automatization deficit across multiple domains in dyslexia, of which visual-auditory integration and phonological processing were examples. The failure was in making routine everyday tasks and skills automatic across the board, including but not limited to reading and motor-related skills, in such wise placing a strain on their working memory capacity. Notably, however, Ramus et al (2003) failed to find a general automaticity deficit in their pool of dyslexic participants (although, note the study had N=13-16) on the several motor and sensory-motor tasks.

The traditional argument in favour of the phonological deficit-centred hypotheses has been that the sensory or motor impairments were not present in all dyslexic individuals and were therefore more likely indicative of comorbidities rather than central to dyslexia (Ramus et al., 2003); though it should be noted that phonological deficits as measured on one or more of the available tests discussed above have been absent in some dyslexic individuals in most studies too. Ramus et al (2003) tested dyslexic and matched university students on a variety of psychometric, visual, auditory, motor, and phonological tests and found that only phonological skills successfully segregated the two groups in their sample. Sensory and motor impairments at 1.65 standard deviations (SDs) under the mean of the control performance were observed in only a proportion of the dyslexic participants. Typically, auditory and visual impairments were characteristic of only about a third of the

dyslexic readers (Ramus, 2001). White et al (2006) also showed that the motor deficits in their school-aged children sample did not explain reading skills over and beyond the phonological processing impairments measured. The dyslexic group were significantly impaired on phonological but not on sensory-motor tasks, and phonological and visual stress tasks impairments were present in almost every individual child (six out of the 23 children diagnosed with dyslexia had a phonological score within 1.65 SDs below the mean value of the control group, with the rest remaining below that mark). Ramus (2004) argued that the available neurobiological evidence is consistent with a specific phonological deficit in dyslexia. The symptomatic heterogeneity Ramus attributed to the presence of cortical abnormalities (i.e. ectopias found in post-mortem studied of dyslexic brains) in widespread brain networks participating in a variety of cognitive domains, some of which may not be directly related to dyslexia. In fact, the 'phonological brain network' itself is broad and shows deficits in many functional areas, some of which have general domains (Black et al., 2017). It could potentially be better described as several networks associated with the three phonological dimensions – reduced phonological awareness, slow retrieval and limited VSTM, each one of which could have different type and distribution of ectopias, which could give rise to marker individual differences in dyslexia, as well as different comorbidities associated with one or more of the affected functional areas. The related neural noise hypothesis of Hoefft and collaborators offered an even more fundamental account of the multifaceted dyslexia deficits (Hancock, Pugh, et al., 2017). Neural noise, or higher random variability in the firing activity of neurons, was linked to increased neuronal excitability. When a neuron is close to its spiking threshold (i.e. in a highly excitable state) at baseline, spontaneous firing occurs more frequently, which can reduce synchronisation within the neural network or between it and external stimuli. According to the authors, the roots of such suboptimal activation patterns can be traced back to genetic modulation of the glutamatergic pathways in brain regions where dyslexia susceptibility genes were highly expressed (ie temporo-parietal and occipital-temporal cortices) (Meng et al., 2005). Less reliable (noisier) functional neural base would exacerbate noisy stimuli conditions and would lead to timing difficulties in many domains, including phonological, multisensory integration and sensory-motor skills. Deficits in speech-sound timing perception have been observed in the early infancy of at-risk pre-linguistic children (Molfese, 2002; Guttorm et al., 2005). Vanvooren et al., (2017) compared children at high and low familial risk of dyslexia longitudinally before and during reading acquisition and found that speech-in-noise perception before learning to read was the strongest predictor of contemporary phonological skills and later reading ability.

In summary, the phonological (and potentially other sensory-motor and executive functions) deficits in dyslexia have been at least partially ascribed to a reduced ability to access and manipulate speech-sound related information due to a broadly distributed reduction in neural timing accuracy. Importantly, if minor common genetic variations give rise to micro-scale wiring changes in the available neural architecture, it could be inferred that the most reliably observable differences at the behavioural level would be found in those capacities most sensitive to issues in timing. In the case of the behavioural and cognitive deficits described in dyslexia, the phonological skills would be the most vulnerable to neuronal noise and disturbances is timing.

### **1.3.2 The Neurobiology of Dyslexia: from structural and functional abnormalities to impaired oscillatory entrainment to speech.**

By birth, the large white matter tracts are in place and the structural and functional sensory-motor white-matter networks have started developing. The first year of life is characterised by a rapid gray matter growth, and maturation and myelination of the microstructure of the already existent large-scale white matter tracts (Gilmore et al., 2018). The fundamental structure – *the tabula rasa* - and functional architecture are ready to be shaped in the coming years. At birth, infants already discriminate the rhythmic structures in language (i.e. Nazzi et al., 1998) and can recognise their mother's voice (DeCasper & Fifer, 1980), both examples of rudimentary phonological 'skills'. In dyslexia, some evidence (albeit based on a limited number of studies and participants in them) suggests the neural infrastructure is less well-organised cortically and subcortically (Galaburda et al., 1990, 2005), with a slightly coarser cortical columnar arrangement (Casanova et al., 2002). These observations were likely due to the micro abnormalities in the neuronal wiring (i.e. disprusias, ectopias, misguided axonal connections) associated with the dyslexia-susceptibility common genetic variations outlined briefly in Section 1.3.3 below, and in more detail in *Chapter 2*. It is essential to highlight that due to the nature of the post-mortem experiments, the structural cortical abnormalities described have been observed in a limited number of brains only (i.e. Casanova et al., 2002 was a case study). Even though focal cortical aberration are a logical prediction based on the associated genetic susceptibility, the evidence of them in humans is still rudimentary so it would be premature to generalise on their presence in all dyslexic brains. They can be at best implicated as a potential mechanism for the genetic susceptibility to dyslexia in the early days of life, but they cannot predict future dyslexia. Dyslexia is a compound multifaceted deviation in the complex cognitive capacity of reading and cannot be easily reduced to

neurostructural changes. The cortical aberrations can only contribute to explaining dyslexia neurobiological aetiology. Structural modifications in utero likely lead to functional abnormalities already measurable at birth, and the characteristic behavioural and cognitive symptoms in infancy and later life. Whether it is functional wiring between neurons or noisy communications via potentially modified neurotransmitter release parameters (Sperling et al., 2005), the greater variability in the intrinsic neural firing and greater cortical excitability is likely to result in less accurate neural processing, and hence - in a reduced signal-to-noise ratio, as discussed previously (Hancock et al., 2017; Nicolson & Fawcett, 2019). The increased neuronal structural and functional 'noise' would interfere with the performance precision of broad neural networks such as the reading network, and with timing-sensitive processes such as those needed for reading and phonological acuity. A rich literature of neuroimaging evidence in both grey and white matter (GM and WM) changes, as well as abnormalities in functional neural electrophysiological or haemodynamic responses, attests to the spatial and temporal deviations in dyslexic populations of all ages, starting notably, at birth (Table 1-1 below).

*Table 1-1. A summary of the white and gray matter structures reported in language development studies and the earliest detection in typical development and at dyslexia risk.*

Typical Development		Dyslexia	
WM structure and volume changes	When		When
Leftward AF assymetry	early infancy; childhood; adulthood	Abnormal lateralisation in AF and SLF	12 months; school-aged children; adults
<b>Functional network: left dorsal (posterior temporal and inferior parietal regions)</b>			
Left prisylian region (planum temporale and Heschl's gyrus)	at birth and to adulthood	Atypical rightward assymetry in planum temporale (perisylian/temporal-parietal)	school-aged boys but not girls; reading adults
Left SMG, STG, AG, IFG	perinatally; childhood; adulthood	Left STG and bilateral MTG	delayed in pre-schoolers
		Left FG, STS, middle-frontal and pre-central gyri	reduced activation in 10-year-olds
		Left IPL	reduced surface area in 5-year-olds
		Left occipital-temporal region (small)	reduced activation at school age
		Total brain size	reduced in all ages

### 1.3.2.1 White Matter Microstructure and Lateralisation Abnormalities in Dyslexia

Xia, Hancock & Hoeft (2017) described developmental dyslexia as a decoding-based reading-disorder with a neurobiological aetiology of anomalies in the left temporo-parietal and possibly occipital-temporal cortex. Cross-sectional and longitudinal neuroimaging studies have suggested that dyslexia-risk related differences are already present in early infancy and are similar to the observed impairments in the left reading network demonstrated in mature dyslexic readers (Black et al., 2017). Dyslexia related changes in WM micro-structure and volume have been detected throughout development, including perinatally. The left arcuate fasciculus (AF, *Figure 1-1* below), a large WM tracts running between the temporo-parietal junction (TPJ) and the frontal cortex, is the most reported site of alteration in dyslexia studies (Vandermosten et al., 2012) from early infancy (Langer et al., 2015) and childhood to well into reading age (Boets et al., 2013; Huber et al., 2018; Lou et al., 2018; Saygin et al., 2013; Su et al., 2018; Torre et al., 2019; Vandermosten et al., 2012; Wang et al., 2017).

There is a multitude of indications that already in the very first months of life, adult-like structural<sup>2</sup> organisation can be observed, and similar functional linguistic networks are to some extent present in the left perisylvian regions when neonates listen to sentences in their mother-tongue (Dehaene-Lambertz et al., 2010; Dehaene-Lambertz, et al., 2006; Dubois et al., 2009). A cross-sectional DTI tractography and clustering analyses of the dorsal (phonological) and ventral (semantic) language-related WM pathways in the first weeks after birth (2-22 weeks) and in early adulthood (21-27 years old) found dorsal-ventral segregation and WM structural similarities in the two groups (Dubois et al., 2015). Furthermore, the leftward asymmetry in the AF was already present in these initial weeks postnatally (Dubois et al., 2015). The fractional anisotropy (a measure of WM integrity determined by the amount of myelination and the positioning of the axonal fibres) of the left temporo-parietal WM tract correlated with individual differences in standardized

---

<sup>2</sup> Interestingly, the fact that these structures are there at birth does not necessarily indicate that they are not further shaped by experience. (Huber et al., 2018) highlighted a difference between experience-based changes (rapid WM plasticity during an intense reading intervention for children with RD) and structural differences (less permeable to change). The left AF and the left ILF were involved in experience dependent reading performance (effective learning throughout the intense intervention), as a part of a wider WM network. In contrast, WM connections of the posterior corpus callosum with the left inferior frontal-occipital fasciculus showed no change with the intervention but predicted the children's initial reading skills and the ease of learning, in association.

reading scores in typically developing 8-year-olds (Niogi & McCandliss, 2006), and was significantly lower in children with reading-disability-range scores. Abnormal lateralization has also been described with respect to the superior longitudinal fasciculus (SLF), which showed increased right hemisphere volume and rightward asymmetry associated with reading ability in dyslexic compared to control school-aged children (Zhao et al., 2016). Preliterary, however, Saygin et al (2013) confirmed the unique contribution of the left AF volume to the phonological awareness of 40 English-speaking kindergarteners, against other closely related WM tracts (including the parietal portion of the SLF). Left AF microstructural integrity has also been positively correlated with phonological awareness in European and Chinese samples (Vandermosten et al., 2012; Su et al., 2018). Finally, Langer et al (2015) reported reduced microstructural integrity in the central part of the left AF tract for infants at high familial risk of dyslexia at 10-12 months of age, which correlated with the infants' expressive language abilities (Langer et al., 2015).

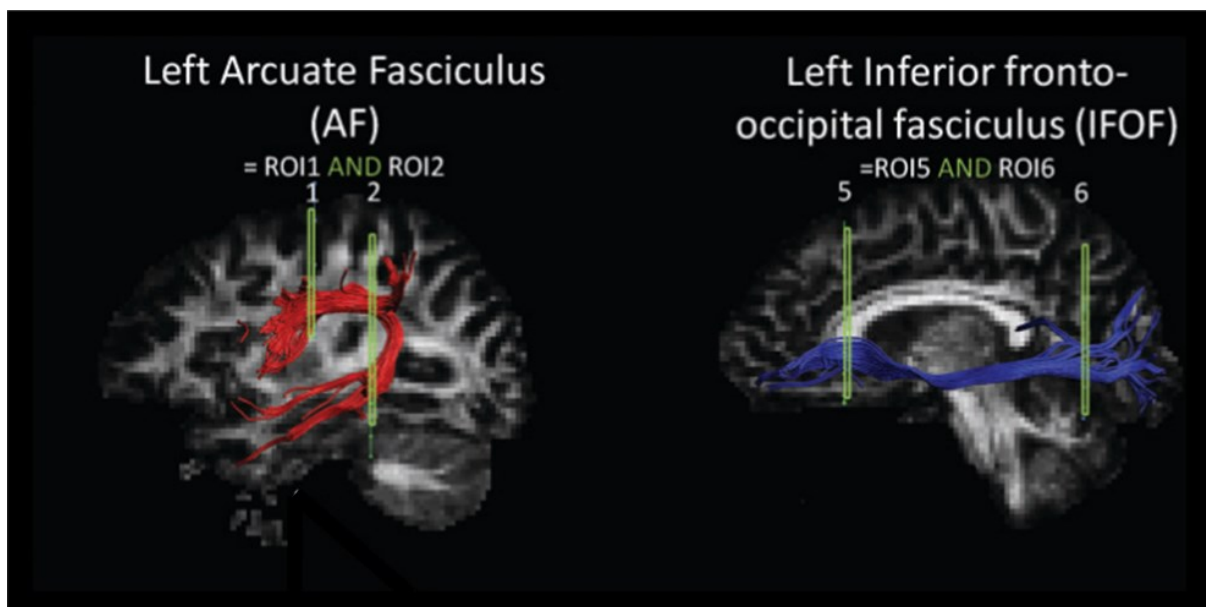
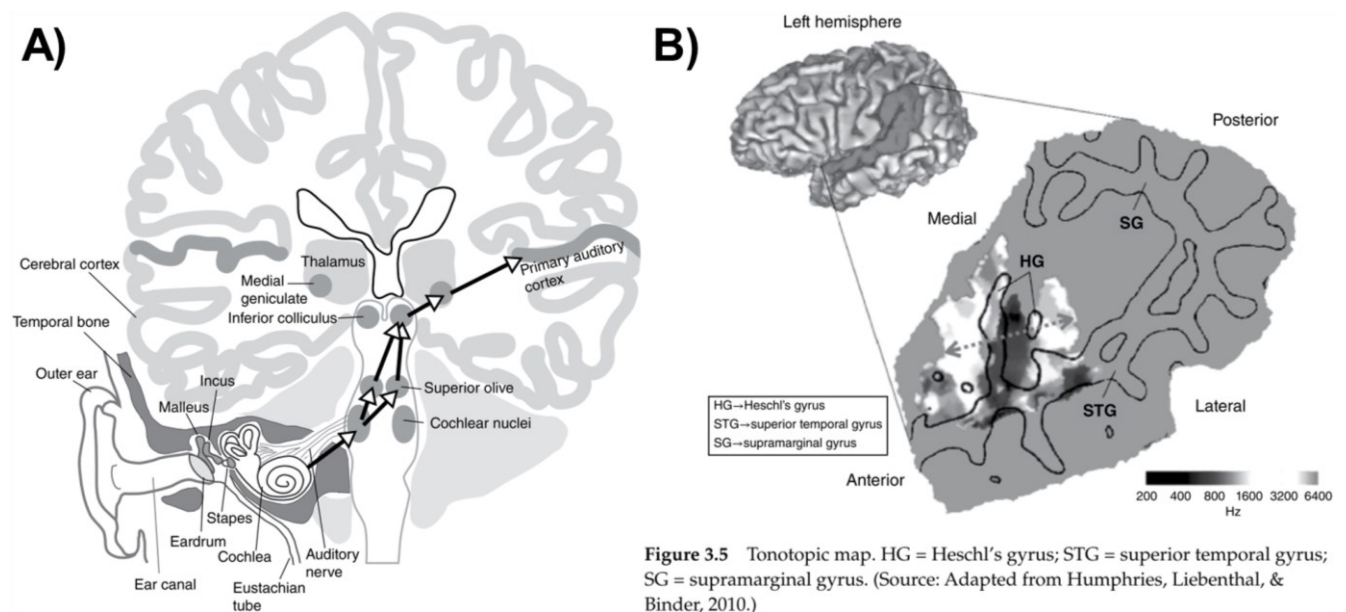


Figure 1-1. Copied and adapted from (Vandermosten et al., 2012, Figure 1) – an example subject's white-matter fibre tracking images of the left hemisphere arcuate fasciculus (AF), frequently implicated in typical and dyslexic neural processing in language.

### 1.3.2.2. Functional 'Reading Network' Connectivity Abnormalities in Dyslexia

Alongside the structural organisation of the reading system in the brain, the typically described functional reading networks recruit the left dorsal system: including the supramarginal gyrus (SMG), the superior temporal gyrus (STG, *Figure 1-2* below), and the inferior frontal gyrus (IFG) for phonological processing (Black et al., 2017). Additionally,

evidence suggests that these left-lateralised dorsal systems are to some extent already present perinatally (Dehaene-Lambertz et al., 2010), and respond selectively to phonological over other acoustic information (Dehaene-Lambertz, 2000; Dehaene-Lambertz & Baillet, 1998). In line with this suggestion, when processing the phonological properties of a stimulus (i.e. when detecting a phonemic difference between syllables but generalising over several speakers), 2-6 days old infants experienced an ERP shift towards dorsal posterior temporal and inferior parietal regions, consistent with phonological processing markers in adults (Dehaene-Lambertz & Pena, 2001). Apart from the already well-developed left AF asymmetry providing a fast-tract phonological “highway” to connect the left and right temporal with left frontal processing areas, fMRI studies have testified to a leftward activation preference in the language related regions in response to specifically linguistically-structured auditory stimuli in new-born and 3-month old infants (Dehaene-Lambertz et al., 2008; Dehaene-Lambertz, Hertz-Pannier, & Dubois, 2006). In week one (2-5 days old), optical imaging showed a greater concentration of total haemoglobin to normal but not reversed (i.e. played backwards) recordings of IDS in the temporal channels overlaying the lower portion of the Sylvian fissure (Peña et al., 2003). An elongation of the left planum temporale and a thickening of the left Heschl’s gyrus were confirmed at the ages of 2-16 weeks in a structural MRI study (Glaser et al., 2011). At 2-3 months of age, the left STG and the angular gyrus activated in response to auditory signals phonetically consistent with the infants’ native language (i.e. forward and backward IDS), and the right prefrontal areas responded specifically to IDS register in awake infants only (Dehaene-Lambertz et al., 2002). Furthermore, the left planum temporale areas responded preferentially to speech but not to similarly temporally phrased music pieces (Dehaene-Lambertz et al., 2010).



**Figure 3.5** Tonotopic map. HG = Heschl's gyrus; STG = superior temporal gyrus; SG = supramarginal gyrus. (Source: Adapted from Humphries, Liebenthal, & Binder, 2010.)

*Figure 1-2. Copied and adapted from (Jones & Schnupp, 2021, combining Figures 3.1 and 3.5). A: a schematic representation of the hierarchy of language information processing from the ear, subcortically and up to the primary auditory cortex. B: A schematic representation of the left hemispheric planum temporale along the Sylvian fissure. The zoomed and unfolded image shows the tonotopic map representation within the structures in this region relevant to language processing and implicated in dyslexia (risk).*

A number of studies have identified pre-literate differences in dorsal phonology-associated functional networks for children at high familial risk of dyslexia. Pre-schoolers with (a risk of) dyslexia had consistently atypical phonology-network activation on a rhyme judgement tasks in a longitudinal fMRI study when they were tested two years apart (Łuniewska et al., 2019). Bilateral STG and left middle temporal gyrus (MTG) were amongst the structures with delayed development in children who were eventually diagnosed with dyslexia. Notably, the high-risk group of children who did not develop dyslexia also presented hypoactivation in those regions but were able to compensate to a typical phonological performance by additionally employing higher-order regions. In contrast, pre-literate 5-year-olds at familial risk of dyslexia did not manifest compensatory activation and demonstrated impaired performance on an initial sound matching task when compared to their low-risk counterparts (Raschle et al., 2012). There were sizeable differences in the task-related functional response in favour of the low-risk group in the left STG and bilateral MTG, as well as bilaterally in the cerebellum. The hypoactivity in these phonological processing regions in young children at risk of dyslexia were conducive of the phonological deficit predating the reading acquisition failure.

In literate children, Altarelli et al (2013) estimated the cortical thickness in individually defined word-activated areas of dyslexic and control groups across two datasets and reported a reduction in a small left occipital-temporal region. Using an anatomical outlining criteria based on postmortem dyslexia examinations by Galaburda, Sandies & Gerschwind (1978), the same authors revealed that dyslexic boys but not girls had atypical rightward asymmetry in the surface area of the planum temporale compared to a leftward bias in typical readers (Altarelli et al., 2014). A series of meta-analyses concluded that a left occipital-temporal region was most consistently under-activated in dyslexic children (Richlan et al., 2011), while in dyslexic adults, the functional abnormalities encompassed atypical left hemisphere temporal-parietal and perisylvian networks in association with impoverished performance of both linguistic and phonological tasks (Richlan et al. 2013). Ramus et al (2018), however, cautioned that methodological inconsistencies and sample-size limitations often rendered reading disorder related structural and functional MRI studies inconsistent and underpowered. After reviewing four decades of literature, the only finding of certain consistency was the reduced total brain size in dyslexia, irrespective of age of the study group, or how the volume was measured (that conclusion was supported by (Peyre et al., 2020)). Still, a recent sizeable cross-cultural study measured language-evoked fMRI responses in 96 10-year-old Chinese and French students and observed cross-language similarities in the reading network. Left FG, STG, superior temporal sulcus (STS) and precentral and middle frontal gyri correlated with reading skills across all children (Feng et al., 2020). As half of the volunteers were experiencing reading difficulties, the collaborators were able to ascertain that the dyslexia related functional differences were also broadly consistent across languages. Left FG, STS, middle frontal, and precentral gyri had greater word-related activation in fluent than poor readers of both French and Chinese.

Collectively and with some consistency, white and gray matter left temporal-parietal regions (left AF, left planum temporale including STG) have been identified as hypo-activated or atypically lateralized in both their structural and functional connectivity in dyslexia. Atypical left parietal-temporal and temporal-occipital sulcal basin patterns (described by a higher number of basins at the expense of size) characterized both school-aged dyslexic children (in whom it also correlated with reading performance), and pre-literate children at familial dyslexia risk (Im et al., 2016). The primary sulcal pattern is related to structural and functional cortical organisation, and is largely prenatally determined with strong genetic influences (Im et al., 2016). Additionally, the severity of maternal dyslexia predicted the child's cortical surface area in the left inferior parietal

lobule, but not the cortical thickness in the same region at the age of 5 (Black et al., 2012). These findings signified at least partially prenatal (related to surface area) rather than experiential (related to thickness) origins of the effect. Taken together, these evidence (while still acknowledging the underpower of some of the supporting studies), along with the post-mortem accounts of morphological changes in the neural infrastructure in the language networks, allowed for the prediction of a *very early* (prenatal) onset of dyslexia-(risk)-related abnormalities in the electrophysiological activity of the neural ensemble. These abnormalities have been detected as changes in the electrical or magnetic potentials at the scalp level, predominantly using electro- and magnetoencephalography (EEG and MEG), and functional near infrared spectroscopy (fNIRS).

### **1.3.2.3 Neurobiology of Developmental Dyslexia: a deficit in the neuronal entrainment to speech?**

So far, we described the cognitive-behavioural phenotypes of dyslexia in light of the proposed theoretical frameworks, and the underlying neuroendophenotype of structural and functional connectivity abnormalities. We next described what is known about early language processing in terms of rhythm perception and cortical oscillatory response. Then we looked into why the conceptualisation of prosody as ‘rhythmic waves’ is useful (although by no means exhaustive) in describing the phonological deficits in dyslexia. Finally, we concluded that it should be possible to detect the shortfalls in the brain’s ability to track rhythmic prosodic patterns at birth in the context of familial dyslexia risk.

#### ***Cortical tracking of the amplitude fluctuations in speech over time can be already observed in the newly born human brain.***

Humans are already born with specific preferences for the temporal structure and characteristics of their linguistic input. *Table 1-2* below summarises the developmental trajectory of cortical rhythmic tracking in the first half-year of life. Neonates at less than 6 days old responded more readily to syllable sequences if they contained an immediate repetition pattern, rather than if no, or if non-adjacent repetition was presented (Gervain et al., 2008). The preference was detected using optical imaging and peaked over bilateral temporal and left frontal channels already in the first few trials, suggesting that a perceptual repetition detection mechanism was already in place and ready to track the acoustic structure of the incoming signal. Furthermore, as reviewed above, infants could recognise the rhythmic structure of their native language from other rhythmically different

languages at birth, and from rhythmically similar languages by 6 months. Peña et al (2010) showed that the power of the cortical oscillatory responses in the gamma band to ADS was able to distinguish between the infants' native (Spanish) over a rhythmically close foreign (Italian) language for infants older than 4-6 months, even if they had been born pre-term (Peña et al., 2010). Whether these extremely early oscillatory responses have any functional significance for linguistic processing could not be clarified. However, the results indicated that slow rate activity had already started forming by 6 months after conception and was at least capable of entraining to the acoustic language input, consistent with the idea that while still in the womb, infants process auditory information lowpass-filtered by the amniotic fluid (Armitage et al, 1980).

By postnatal day 6, infants were able to decipher the temporal modulations in the auditory signal by selectively showing sustained (200ms to 2s around stimulus presentation) haemodynamic response at the encoded frequency (Telkemeyer et al., 2009). The infants were presented with amplitude modulated (AM) noise stimuli in the prominent syllabic (3-6Hz) and phonemic (40-80Hz) frequencies for Dutch speech and showed a preferential oxygenated haemoglobin concentration increase in response to the 40Hz and to a lesser degree, to the 6Hz (alpha in neonates) signal modulations. Notably, Telkemeyer and collaborators later investigated the oscillatory electrophysiological response to the same fast and slow amplitude modulated noise stimuli in a different group of infants in their first half-a-year of life (Telkemeyer et al., 2011). They were able to detect a sustained (in 9-second time windows) cortical theta desynchronisation in response to both the fast and slow frequency modulation in the auditory signal at 6 month and to a lesser degree at 3 months. No high-frequency cortical (de)synchronisation response was detected for these amplitude-modulated noise stimuli.

Ortiz Barajas and colleagues set off to describe the evolution of cortical entrainment to natural speech in the first months of life (Ortiz Barajas et al., 2021). In a cross-sectional longitudinal study, they recorded EEG from two groups of native French infants, under 5 days and at 6 months while they were listening to a female speaker narrating the story of *Goldilocks and the Three Bears* in a mild IDS register in their native and two foreign languages: a rhythmically similar (Spanish) and different (English). The researchers evaluated two measures of entrainment: amplitude tracking calculated as the cross-correlation between the speech-envelope and EEG evoked-response in the time domain; and phase tracking, calculated as the phase-coherence between the Hilbert filtered

envelope of the speech and the EEG response in the syllabic rate of the sentences<sup>3</sup>. In the neonatal infants, both amplitude and phase tracking followed all three languages alike. Conversely, the amplitude tracking at 6 months differentiated between the native and the rhythmically distinct foreign languages (but not the rhythmically similar one), while the phase tracking still showed no language effects. However, in a previous study, the inter-trial phase locking synchronisation in delta/theta (2-4Hz) during 1-second around stimulus presentation was able to segregate between the ERPs to native and non-native phonemic deviants in a group of 6-month-old infants (Ortiz-Mantilla et al., 2013), in their left and to a lesser degree right auditory cortex in source space (based on individual anatomical MRIs). This came to show that different phase and amplitude tracking metrics could produce convergent patterns for different aspects of the cortical oscillatory speech-response. Interestingly, in Ortiz-Mantilla et al (2013), only the native phonemic contrasts induced a temporal spectral evolution in gamma (around 30-35Hz) in the same time window, selectively only in the frontal source (the anterior cingulate). Assuming that the gamma response was related to the phonemic structure of the presented syllables, the authors construed that gamma cortical oscillations supported syllable discrimination and the initiation of rudimentary phonemic memory representations. Slow-wave modulations then nested the power in gamma to provide salient cues for parsing and attention to the phonemic features.

IDS-based entrainment has further been reported in the cortex of 7-month olds in English (Kalashnikova, Peter, et al., 2018) and German (Jessen et al., 2019), and at 4-month olds in English, within the earliest demonstration of delta and theta tracking, as well as phase-amplitude coupling of delta with gamma and beta (Attaheri et al., 2020). In the first study to measure cortical entrainment to continuous natural speech signal in infants, Kalashnikova et al (2018) used the temporal response function (a regression fit between the speech envelope and the EEG) to predict the EEG signal from both IDS and ADS stimuli. The correlation values between the measured and predicted EEG signals were taken to index the non-frequency-resolved cortical tracking of the speech envelope in both registers. Within this metric, infants were able to track IDS but not ADS in a small central frontal cluster at 7 months of age. Moreover, Attaheri et al (2020) demonstrated that delta (2Hz)

---

<sup>3</sup> The syllabic rate of the sentences was calculated as the number of peaks per second in their speech envelopes rounded to the closest integer. This was not dissimilar to how the frequency rate of entrainment to IDS is calculated in the current thesis, with the difference that we used the number of syllables rather than the number of envelope peaks related to the syllables; we envision that the two produce a very similar syllabic rate.

was significantly stronger than theta when tracking speech in 4- to 7-month-olds and participated in significant phase-amplitude coupling with beta and gamma. The result was converging with the findings that unlike in adults, where theta (4-6Hz) orchestrates the oscillatory temporal organisation in response to speech, in infants, delta is the carrier frequency (Leong, et al., 2017; Leong & Goswami, 2015). As suggested by Ortiz Barajas et al., (2021), slow-frequency high-power carriers in IDS (2-4Hz) governed the parsing of the speech stream into smaller units of acoustic and later linguistic information (Thiessen et al., 2005), and nested the finer-grained acoustic information at higher frequencies (5Hz and 20Hz) (Leong & Goswami, 2015). This hierarchical structure carries implicit information that helps the naïve listeners compute phonological-sound mapping based on statistical learning principals and without presuming any linguistic knowledge (Leong & Goswami, 2015; Peña et al., 2002).

In later childhood, entrainment correlated with specific language outcome measures (Cutini et al., 2016; De Vos et al., 2016, 2020; Gou et al., 2011; Lehongre et al., 2013; Molinaro et al., 2016; Power et al., 2013, 2016; Vanvooren et al., 2017). Power et al (2012) measured high-density EEG in 23 school-aged children (~13 years old) to show entrainment to pre-recorded speech stimuli. The experiment played the syllable /ba/ repeatedly at 2Hz either only in the auditory stream, or while watching a video of a talking head mouthing the syllable. Three conditions were presented: auditory-visual (AV), auditory only (A), and visual only (V), and children had to press a button as soon as they detect the occasional rhythm violations in each condition. Power et al (2012) found delta entrainment at 2Hz in all the three streams. Entrainment peak was also found in the theta (at 4Hz) band in the conditions containing an auditory stimulus only (i.e. AV and A). The strength of theta correlated with standardised language measures of phoneme deletion, phonological short-term memory, and rapid automatized naming. Finally, the preferred phase of theta changed between the A and the AV conditions, indicating a potential cross-modal phase resetting mechanism in speech perception.

*Table 1-2. A summary of the empirical evidence found in the literature to the developmental trajectories of the measured cortical rhythms in the context of speech processing in the first half-year of life.*

<b>Evolution of Speech-Processing Cortical Rhythms in Early Infancy</b>		
<b>Cortical Response</b>	<b>Age</b>	<b>Significance</b>
Slow-wave phase coherence	6-7 months post conception (neonatally, pre-term birth)	Early response to repetitive stimuli with typical rightward lateralisation of the SW response
Amplitude and phase tracking of syllabic rhythm	< 5 days old (term)	Track speech input but does not discriminate yet for language's rhythmic class
Detection of repetition patterns	< 6 days old (term)	Preference for repetitive syllabic patterns
Power in gamma to ADS	4-6 months postnatally even if born pre-term	Distinguish between native and rhythmically similar languages
Power tracking in delta and theta	4-7 months	Selective response to slow but not faster AMs in speech vocoded noise
Amplitude tracking of syllabic rhythm	at 6 months	Discriminate for language rhythmic class
Theta synchrony to fast and slow-wave AM noise	at 6 months	Cross-frequency coupling orchestrated by the amplitude of the slow-wave rhythm
Gamma response (ERP/EROs) to native phonemic deviants	at 6 months	Discriminate between native and non-native phonemes, localised in left auditory cortex
Phase-amplitude coupling between delta-beta & delta-theta	at 7 months	Phase-amplitude coupling response to IDS regulated by the phase of the slow-wave rhythm

### ***Theories of Speech Processing Based on Cortical Oscillations***

Giraud & Poeppel (2012) put forward a comprehensive yet parsimonious perspective that in language processing, temporal reorganisation of the endogenous neuronal oscillatory activity has been employed in the course of evolutionary specialization as a mechanism for segregating information and organising spike timing. Language, due to the presence of rhythmic components in speech, offers a unique naturally occurring model of a direct functional neural-to-speech mapping, in which the influences of intrinsic and stimulus-driven oscillatory activity can be measured and compared in different conditions.

Importantly, neither language, nor neural language processing is necessarily fully rhythmic. In a recent review of the state-of-the-art knowledge of language representation in the brain, Jones & Schnupp (2021) describe a hierarchical neural speech-processing stream starting from the outer and inner ear and going all the way to associative cortical areas and back (*Figure 1-2* above). The physical attributes of the acoustic waveform are encoded in the early pathways from the inner ear via the auditory nerve fibres to auditory-relevant structures within the brainstem and the thalamus, and from there to the primary auditory cortex. These aspects of the speech signal could be described as low-level acoustic features which have largely tonotopic representation in these largely early (sub)cortical neural pathways whereby voiced speech sounds exhibit a harmonic structure while unvoiced

sounds have noise-like spectra. The nerve fibres produce a temporal pattern of bands at time interval of the voice pitch rate of vowels and thus the auditory nerve fibres convey information about 'periodicity pitch by phase-locking their discharges to salient features of the temporal fine structure of the speech sounds with sub-millisecond accuracy' (Jones & Schnupp, 2021). To detect such features as voicing and determine voice pitch, the brain also tracks the sharp peaks at regular intervals in the spectrum to identify harmonics and periodicities in the temporal waveform. Such pitch information provided by the detected harmonicity, or periodicity is a vital cue for identifying speakers and prosodic information. This largely acoustic representation in the auditory nerve, brainstem, thalamus and primary auditory cortex (i.e *Figure 1-2A*) progresses to a more linguistic representation in the STG (i.e *Figure 1-2B*), and more semantic representation in higher cortical areas of motor and associative cortex and beyond structures classically attributed to auditory processing. Crucially, moving higher in the hierarchy of the process, the tonotopic representation is no longer found and instead information processing is increasingly aperiodic. It is critical to instruct the reader that these distinctions are not strict and there is plenty of overlap between processing capacities prior to and within the cortex. The hierarchical description outlined here is useful to conceptualise the representational process, it is nonetheless a simplified picture which omits the feedback and parallel processing features which were not within the scope of the current dissertation but are however an integral part of language processing. It is also important to reiterate here that the simpler rhythmic processing of the speech signal that is the focus of this dissertation does not necessarily represent linguistic but likely speech-specific acoustic information processing in humans. As such, it has been detected at birth and does potentially contribute towards the understanding of the neural correlates of the lower-level deficits in dyslexia. That is not to say that it can account for any of the more complex cognitive aspects described in dyslexia, which are likely the result of intricate interactive processes starting in the womb and carrying on through life. The rhythmic-centred hypotheses tested here (as well as the background theories that informed them such as the temporal sampling theory of Goswami (2011) and the theta-gamma oscillatory coupling of Giraud & Ramus, 2013) do not contribute toward accounting for the cognitive aspects of the disorder based on the current data and state of knowledge. The lower-level processing features demonstrated here could however pre-date the more complex aspects of phonological processing and cognitive phenotypes in dyslexia and could participate in modulating their developmental pathways by acting as risk or resilience factors.

Animal studies of the primary auditory cortex have shown that delta (2-4Hz) and theta (4-6Hz) rhythms were important for auditory perception and communication abilities across different mammalian species (Lakatos et al., 2005; 2016). Chandrasekaran et al (2010) tested the cortical encoding of the structure of natural acoustic scenes in the macaque primary auditory cortex by measures of local field potentials (LFPs, a direct measure of the summation of activity of large neuronal populations intracranially) as well as multiunit spiking activity (spikes of the neuron(s) closest to the probe are reliably detected but a single neuron cannot be isolated). The LFPs phase-locked to the temporal structure of natural sounds and showed amplitude modulation peaks in the 2-9Hz and 16-30Hz bands, while the 9-16Hz activity remained at baseline levels. The increased power of the LFPs and the spiking activity was in phase with the temporal structures of the auditory stimuli up to 25Hz, and the cortical sites showed local spectral selectivity predicting the phase-locking and power increase in that site. The multiunit spiking activity was also phase-locked to the LFPs under 30Hz, showing a direct relationship between the network connectivity (i.e. LFP) and the neuronal spiking response at these low frequencies. Albeit a much more direct measure of network activity, the LFP response here can be paralleled by the network response at the scalp level as measured by EEG in human primates. The spike-time gating by the phase of the LFP oscillations in response to the temporal structure of the natural sounds supports the idea that neuronal representations of a complex acoustic signal in the primary auditory cortex are driven by the temporal dynamics in the stimulus.

Translationally, a similar temporal organisation process could be employed via salience-based phase-resetting of the endogenous neural activity to gate the power-modulations in the neural evoked response to the complex natural human speech signal. Cortical oscillations have been detected in response to auditory speech encoding in the human language-processing areas identified in the previous section (left Heschl's gyrus, planum temporale, STG, STS, IPL and IFG) (Poeppel, 2014).

Giraud & Poeppel (2012) proposed that the phase-resetting of the slow cortical oscillations (theta and delta) in response to prominent speech units scaffolds the power in the high-frequency oscillations (beta, gamma) in response to the phonemic information. Phase-resetting would allow for the underlying oscillatory neural activity to align to the phase of the envelope of the incoming speech signal. Potentially through this mechanism, the brain could encode simultaneously the temporal structure of the amplitude modulations at different frequencies present in natural speech (Doelling et al., 2014). For Goswami

(2011), the prominent speech units which reset the phase of the endogenous oscillations are the most pronounced amplitude rise times within the syllables. In English, they coincide with the prosodic pattern in the delta-theta range. Supporting this idea, the sharp changes in the amplitude of the delta-theta bands were the temporal cues in the speech envelope to drive the neural oscillations in the auditory cortex and increase intelligibility in an MEG experiment with young adults (Doelling et al., 2014). Cortical entrainment response to the higher frequencies in speech (i.e. in beta and gamma, corresponding to the energy in the phonemic structures) have also been reported (Attaheri et al., 2020; Benasich et al., 2008; De Vos et al., 2016; Gou et al., 2011; Lizarazu et al., 2019; Ortiz-Mantilla et al., 2013; Poeppel, 2014; S. Telkemeyer et al., 2009).

Giraud & Poeppel (2012) hypothesised that since neuronal populations are working in the time-domain within the available framework of oscillatory phenomena, the brain uses this readily existing structure in parsing and decoding of continuous speech. Similar to the process described in other primates above, the intrinsic neuronal oscillations generated in the human auditory cortex interact with the spiking activity in response to the speech signal such that salient points in the speech input cause phase resetting of the intrinsic oscillations. Giraud & Poeppel (2012), refined by Giraud & Ramus (2013), focused their model on the gamma [25-35Hz] (phonemic) and theta-delta [2-8Hz] (syllabic, prosodic) range oscillations. The amplitude of theta entrains to and tracks the speech signal envelope (Ahissar et al., 2001). The phase of theta shapes the phase and amplitude of gamma via an interaction between a pyramidal-interneuron theta (PINT) and gamma (PING) networks, whereby theta ramps up gamma excitability for three to four gamma cycles (presumably coinciding with the rise time), and then releases it between syllables, to enable phase-locking of gamma to the next syllable. This intrinsically generated continuous gamma activity becomes stronger and more in phase with theta as individual neurons become more likely to fire in response to auditory stimulation at each gamma cycle. Gamma reflects phoneme-driven spike trains and in turns gets organised by nesting in the envelope-tracking theta oscillation, and thus the brain signal aligns to the incoming speech signal (*Figure 1-3*). Oscillatory activity is largely believed to be regulated by the inhibitory activity of the interneurons which participate in the PING and PINT networks (Borgers et al., 2005).

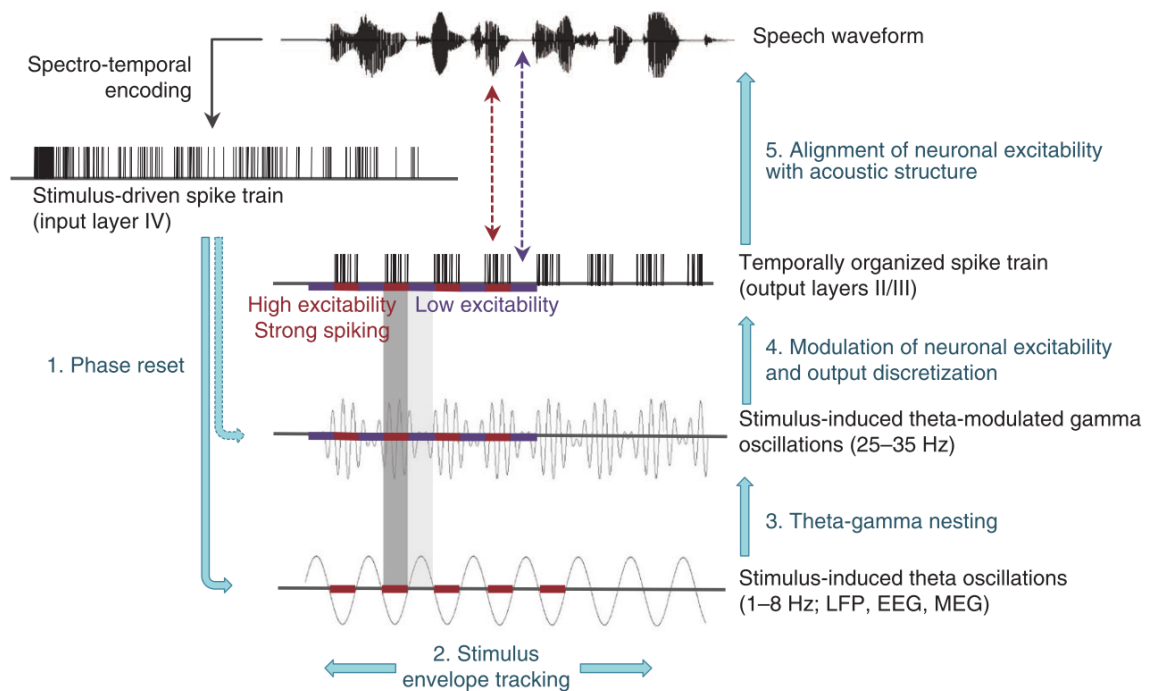


**Figure 1** A theory of early oscillation-based operations in speech perception. Five operations allow connected speech to be parsed by cortical theta and gamma oscillations. We assume a high-resolution spectro-temporal representation of speech in primary auditory cortex. We represent a typical spike train in layer IV cortical neurons. Most of these neurons phase-lock to speech amplitude modulations. Response onset elicits a reset of theta oscillations in superficial layers (step 1) where auditory cortex output is generated. After reset, theta oscillations track the speech envelope (step 2). Theta reset induces a transient pause in gamma activity and a subsequent reset of gamma oscillations. Theta and gamma generators that are weakly coupled at rest become more strongly coupled and nested (step 3). Gamma power controls the excitability of neurons generating the feedforward signal from A1 to higher order areas (step 4). Neuronal excitability phase aligns to speech modulations (step 5): gamma tends to be strong when the energy in the signal is weak.

*Figure 1-3. Copied from (Giraud & Poeppel, 2012): Schematic representation of gamma-theta nesting hypothesis of language processing. DOI: 10.1038/nn.3063*

Anatomically, stimulus driven spikes are encoded by thalamocortical pyramidal neurons in the intermediate layer IV, which then transmit the signal to more superficial layers II/III of the primary auditory cortex, where oscillatory LFPs are typically measured (Giraud & Poeppel, 2012). Note that this is still the low-level features speech processing hierarchy depicted in *Figure 1-2A*. This periodic modulation of the firing likelihood of the layers II/III/IV neurons gives rise to the discretization of the continuous speech signal into slow-wave time-matched representations to be outputted to the higher-level (i.e. non-primary-sensory) cortex. Indeed, the same authors reported that next level (i.e. Brodmann area 22, overlaying regions such as the posterior STG and planum temporale, *Figure 1-2B*) tracked speech in theta and delta but not in gamma, despite the fact that non-phase-coupled gamma oscillations were present there. Thus, both the phase of gamma (encoded in the phase of

theta) and the spiking rate, contain relevant cues to be transmitted to the next processing level (*Figure 1-3*), and the slow-wave amplitude modulations bridge the low-level auditory response and the higher-level (phonological) processing.

Two points of caution should be made here. Although theta-gamma phase-coupling is likely to play a role in processing some of the basic acoustic features of speech such as voicing and pitching and come into play when encoding phonological and speaker-identity information, it is unlikely to describe the more complex stages of language processing that lead to comprehension and semantic processing. Additionally, while endogenous oscillatory activity in the theta band has been detected in response to speech and can regulate the phase of the gamma bursts in response to frequency formants in vowels, still it is possible that these represent transient rather than sustained activation patterns. The phase resetting of theta in response to the high-amplitude speech modulations can be viewed as an evoked response or an evoked oscillation (ie ERP or ERO). Possibly the highest power in the onset response comes from the invariant initial spike time of a large population of neurons in the primary auditory cortex (i.e Heil, 1997). Heil (1997) concluded that sound onsets are salient and behaviourally relevant and most auditory neurons (in the feline cortex) discharge spike locked to such transients.

An important feature of the anatomical organization of speech rhythm processing is hemispheric asymmetry. fMRI, EEG(-fMRI) and MEG experiments have attested that gamma entrainment happens bilaterally (though some sources claimed in the left auditory cortex, see research cited in Giraud & Poeppel, 2012), while the right hemisphere shows a preference for slower temporal modulations (Abrams et al., 2008; Giraud et al., 2007; Lehongre et al., 2013; Lizarazu et al., 2021; Morillon, 2010; Poelmans et al., 2012). This observation has to an extent been corroborated by Hämäläinen et al (2012), who found that the syllabic band modulations at 2-4Hz were more pronounced in the right hemisphere, while the tracking of the phonemic band at 20Hz was bilateral.

Similar lateralisation patterns in response to speech(-like) temporal modulations in the auditory stream have already started to form by birth. Rightward specialisation for slow-wave temporal modulations has been described in term (Telkemeyer et al., 2009), and even pre-term (Daneshvarfard et al., 2019) new-born infants. Premature infants at 29-32 weeks gestational age tested around postnatal day 3 with optical imaging had an mismatch

negativity (MMN) response (a special type of EEG evoked response described in more detail in the following section) to phonemic (/ba/ vs /ga/) and voice (female vs male) deviants in the right inferior frontal region, and only to phonemic deviants in the left inferior frontal region (Mahmoudzadeh et al., 2013). The left IFG also had MMNs time-locked more precisely to the onset of the phonemic than the voice deviant (Mahmoudzadeh et al., 2017). These very young infants also showed the replicable pattern of preferential right hemisphere processing of the slow-wave syllabic modulation, here identifiable by the spectral properties of the cortical response to the syllable repetitions, which was modulated by age (Daneshvarfard et al., 2019). In another EEG-fNIRS study of auditory evoked responses, healthy term neonatal infants showed preferential processing of phonemic-register signal bilaterally, and a weaker right hemisphere lateralisation for the slow modulation frequencies (Telkemeyer et al., 2009). These functional asymmetries were also found in the ERP and haemoglobin response functions of 3- and 6-month old infants, as published by the same group (Telkemeyer et al., 2011). They seemed to be preserved throughout the early childhood years. The lateralisation pattern was replicated in an EEG experiment with Dutch 5-year-olds who had the patience to listen to speech-weighted white noise at 4Hz and 20Hz (Vanvooren et al., 2014). The right hemisphere entrained ASSRs<sup>4</sup> to the 4Hz modulation band, while the 20Hz processing was distributed bilaterally.

Dyslexia may be an example of impaired abilities to follow temporal features of speech-sound important for phonological processing (Goswami, 2011; Leong et al., 2011, 2014; Leong & Goswami, 2014a, 2014b; Power et al., 2013; Soltész et al., 2013). Entrainment deficits have been assumed to arise from affected temporal coding within the primary auditory cortex due to a deficit in auditory rhythm perception (Molinaro et al., 2016; Poelmans et al., 2012; Power et al., 2013; Power et al., 2012). Deficient processing of the rapidly changing auditory information could underlie at least to some extent the deficient development of the phonological processing, which in turn would contribute to reading and spelling risk during language acquisition.

### ***Neural Entrainment Gone Wrong in Dyslexia: theory and evidence.***

---

<sup>4</sup>Auditory steady state response potentials (ASSRs) are oscillations synchronous to the frequency of the incoming auditory stimulus. Believed to be generated from the auditory brainstem (ABS) and to propagate to subcortical and cortical neuronal populations. Can be measure at the scalp EEG level (Dicton et al., 2003).

Paralleling cortical speech entrainment, the process of phonological development begins while in the womb. The uterine wall and amniotic fluid act as a low-pass filter that transmits the prosodic rhythm to the developing foetus (Armitage et al, 1980). Consequently, typically developing neonates can remember voices and stories that they hear during the third trimester of pregnancy (DeCasper & Fifer, 1980; DeCasper & Spence, 1986), presumably by using prosodic cues. Conversely, neonates at-risk for dyslexia already show neural differences in speech sound processing at birth (Guttorm et al., 2001; Leppänen et al., 2010; Mahmoudzadeh et al., 2013; Molfese, 2000)). The neural processing of speech is constraint by the available neural infrastructure; and as reviewed in this and the following chapters, dyslexic neural infrastructure features abnormal developmental axonal trajectories and abnormal cortical architecture characterised by ectopias, heterotopias and changes in total brain volume, and white matter volume and structure. These abnormalities, in turn, would disrupt the generation of synchronous activity in local and long-range neuronal ensembles. A number of influential proposals link dyslexia to mismanagement of cortical oscillatory activity in both adults and children<sup>5</sup> (Giraud &

---

<sup>5</sup> Importantly, a recent extensive conceptual replication attempt on the brain-to-speech entrainment findings in dyslexia failed by and large to find any differences between dyslexic (N=19) and typically reading (N=20) French adults on any measures of amplitude or phase synchronisation to the speech signal; and found only limited differences in the amplitude cross-correlation metrics between the MEG brain response and AM-ed white noise stimuli (Lizarazu et al., 2021). Albeit in a mid-range sample size, the authors meticulously compared a variety of B2S synchrony metrics previously reported in the literature, including in the current review (SNP, PLV, inter-hemispheric phase synchronization, coherence, and phase and amplitude cross-correlation) against three modulation frequencies (2Hz, 5Hz and 30Hz) and contrasting the hemispheric lateralization effects. They found no group differences in any of the entrainment metrics in response to the speech signal. The typical readers had a stronger amplitude cross-correlation at 30Hz in left auditory cortex in response to AM-ed noise, and marginally higher amplitude response at 2Hz in the right auditory cortex. Furthermore, they observed that the amplitude cross-correlation values were left lateralized for control participants at 30Hz, whereas they were bilateral in the dyslexic group, the difference being marginally significant. At 5Hz, both groups showed bilateral responses, and at 2Hz the cross-correlation values in the dyslexic group preferred the left hemisphere, while the values were bilateral in the control group. Thus, the replication results could be viewed as weakly consistent with the literature reviewed above claiming entrainment disruptions differentially in the right-hemispheric delta/theta and the left-hemispheric beta/gamma bands to amplitude modulations in the auditory signal, although they raise a serious concern about the reliability of differences found in response to natural speech stimuli. An emphatic take-home message from the authors besides the wide methodological inconsistencies in the field, was additionally the implication that dyslexia-related group differences are likely to be of small effect sizes and embedded in other neural activity adding noise to the entrainment measurements. The authors' recommendations were for future studies to employ larger groups of participants to ensure reliable and replicable results.

Poeppel, 2012; Goswami, 2011; Hancock, Pugh, et al., 2017; Jiménez-Bravo et al., 2017; Neef et al., 2017; Soltész et al., 2013; Hämäläinen et al., 2012; Lehongre et al., 2011, 2013; Soltész et al., 2013). For example, it has been previously shown that in children with formal dyslexia diagnosis, the auditory temporal reference frame for speech processing was atypical, as measured by the preferred phase of the low frequency (delta) oscillations (Power et al., 2013). The group differences in phase preference could imply suboptimal phase alignment of the dyslexic participants to the phase of delta in the speech stream, i.e. they may have been entraining to the 'wrong' part of the speech signal. Additionally, dyslexic adolescents had an atypically high for their age left hemisphere beta response (Power et al., 2016). Off-phase alignment could interfere with the accurate perception of the linguistic structure, while the anomalously high beta response could affect the quality of phonemic encoding. Collectively, the fast and slow oscillatory deficits could underlie dyslexia's hallmark impairments in phonological processing.

Finally, in addition to the reviewed reports of abnormal lateralisation of white matter structures in young infants at dyslexia risk, there are indications of disturbances also in the established language-related functional asymmetry of right-hemispheric specialization for slow and bilateral for fast frequencies (Daneshvarfard et al., 2019; Dehaene-Lambertz, 2000; Telkemeyer et al., 2009). Weaker entrainment during processing of the speech sound in the right hemisphere and a reduced or absent right hemisphere lateralization have been reported in dyslexia (Molinaro et al., 2016; Power et al., 2013, 2016). Cutini et al (2016) found functionally atypical right-hemisphere processing of slow temporal speech modulations in dyslexic children. Molinaro et al (2016) found that the impaired neural entrainment to speech in the delta range was related to an impaired feed-forward connectivity from the right auditory cortex to the left higher processing areas (left IFG) cross-sectionally. The unidirectional connectivity impairment was consistent with the idea that the slow-wave entrainment deficits (as suggested by Goswami (2011) and others) provided a less accurate oscillatory output from the primary auditory to higher processing areas, which in turn affected the ensuing higher-order speech sampling computations in both children and adults with dyslexia.

The tentative modulation of cortical processing of the rhythmic features of speech in early infancy by dyslexia risk is at this stage only speculative. Most of the research up to date reported associations between event-related response potentials (EPR) to linguistic-based auditory stimulation and later reading pathologies (i.e., Leppänen et al., 2012). Of the

existing studies, the majority employ an oddball-type of paradigm where a rare deviant stimulus is embedded in a long stream of subtly different standard stimuli. The outcome measure of the oddball paradigm is a negative deflection in the EEG trace, time-locked to the deviant as compared to the standard and is therefore referred to as the mismatch negativity (MMN) or mismatch response (MMR). Atypical MMN to phonologically relevant deviants in infants (including neonates) at high familial risk of dyslexia have been found predictive of phonological and letter-naming skill at pre-school age, and of reading and writing skills at school age (Leppänen et al., 2012; Leppänen et al., 2010; Leppänen et al., 2002). Van Zuijen et al (2012) were able to detect a frontal-central MMN to a temporal-structure deviant at 2 and 17 months (Van Zuijen et al., 2013) of age in Dutch infants at low but not at high risk of reading disorder. The amplitude of the MMN was correlated to language comprehension at the age of 4 and reading fluency at school in the same children (Van Zuijen et al., 2012). The high-risk group of poor readers at school did not show an MMN when they were 2 months old, whereas the fluent readers from the high and low risk backgrounds had discernible topological differences in their MMN (Van Zuijen et al., 2013). Thus, the temporal processing deficits observed in neonates at dyslexia risk have been connected to later inferior phonological and reading outcomes. What is yet unclear is whether the temporal deficits are related to disruptions of the continuous oscillatory cortical tracking of the temporal modulations within the speech signal.

### ***Dyslexia susceptibility related changes in neuronal activity from the start?***

Extensive literature lends insight into how by the time of birth, the neural architecture of the infant's brain has already started specializing in the processing of complex acoustic, potentially even linguistic information. The basic neural structure is ready for the ensuing speedy learning of temporal cues and statistical regularities to help parse and encode the idiosyncrasies of their native tongue. Already having mastered how to follow closely the slow-wave amplitude modulations delivered by the envelope of the speech signal, and enhanced by IDS, the newly born brain can start immediately fine-tuning to the high-frequencies that carry the phonemic information and inferring the morphological structure of their language. Dyslexia risk, from the very start, has been linked to reduced specialisation and more frequent mismatches in the neural encoding of the speech(-like) temporal dynamics, both of which have been associated with poorer prognosis for phonological and reading acquisition. Early structural and functional connectivity alterations have been described in association with dyslexia risk and outcomes and likely contribute to noisier neural environment, and therefore, lowered timing precision. Leading

up to the described microstructural gray and white matter abnormalities are complex molecular processes of neuronal migration and axonal guidance toward forming connections and building the cortical circuitry during early neural development. It is in these processes that the dyslexia susceptibility genes most frequently implicated in the literature participate. Although it cannot be directly tested, the resulting disruptions in the cortical circuitry could in turn lead to disruptions in the cortical oscillatory response to the prosodic rhythm in speech. Converging evidence described above demonstrated that these cortical disruptions could be measured reduced timing precision of the ERP or the oscillatory response. We speculate, therefore, that the heritability and genetic risk factors in dyslexia would be connected to measurable imprecisions of the cortical oscillatory response to the prosodic rhythm of the speech signal, and that these effects would be already present at birth.

In the following sections, we briefly outline the heritability and genetic susceptibility factors in dyslexia, which are reviewed in a greater detail in Chapter 2, and then we formulate the specific rationale, hypotheses and predictions pertaining to the two neonatal studies included in this dissertation.

### **1.3.3 Heritable Nature and Genetic Susceptibility of Dyslexia**

Dyslexia is a highly heritable disorder (heritability estimates ~50%; Grigorenko, 2004). When comparing monozygotic (MZ) to same-sex dizygotic twins (DZ), a heritability of .53 was obtained for spelling skills, increasing to .75 when intelligence was controlled for (Stevenson et al., 1987). Additionally, Defries, Fulker, & Labuda (1987) provide evidence for the hereditary nature of reading disability in reporting that MZ twins had higher resemblance than DZ twins (.77 and .50, respectively), on all measures including reading recognition, spelling and digit span (Defries et al., 1987). Rutter and Yule (1975) additionally reported that 34% of children with dyslexia had at least one parent or sibling with reading impairment, which presents four-fold risk compared to 9% for children with typical reading skills (Rutter & Yule, 1975). Gilger et al (1991) calculated that a male child with a dyslexic first-degree relative (parent or sibling) has 50% chance of being diagnosed with dyslexia themselves (against 7-10% in the general population) (Gilger et al., 1991).

Genetics studies have consistently implicated the genes abbreviated in HGNC Database as *DYX1C1*, *DCDC2*, *KIAA0319*, and *ROBO1*, as genes associated with language development

deficits such as developmental dyslexia (Bates et al., 2011; Becker et al., 2014; Eicher et al., 2014; Jiménez-Bravo, Marrero, & Benítez-Burraco, 2017; Scerri et al., 2012). These genes have all been implicated in axonal guidance and neuronal migration mechanisms (Carrion-Castillo, Franke, & Fisher, 2013; Kere, 2014; Meng et al., 2005; Paracchini, Scerri, & Monaco, 2007; Peschansky et al., 2010). Animal studies have demonstrated that disruptions of these genes resulted in abnormal grey and white matter structure (Adler et al., 2013; Burbridge et al., 2008; Currier, Etchegaray, Haight, Galaburda, & Rosen, 2011). Comparative studies investigating the effects of these genes have revealed neocortical and hippocampal changes closely corresponding to those found post-mortem in human dyslexic cases (Rosen et al., 2007). In humans, genome-wide association (GWAS) and empirical candidate genes studies have linked common, often single-nucleotide, genetic variations on these genes with dyslexia-related behavioural and neuroendophenotypes (Mascheretti et al., 2017; Mascheretti et al., 2014; Neef et al., 2017).

Given that most of the structural alterations associated with these four dyslexia risk genes occur in early prenatal stages of neural development, it was reasonable to hypothesise that the deficits reviewed above would already be there and can be measured in neonatal infants in association with these genes. Thus, we tested for three common single nucleotide polymorphisms in the *DYX1C1* gene, seven on *DCDC2*, two on *KIAA0319*, and four on *ROBO1*, described in *Table 2-1* in Chapter 2. These candidate genes were selected as they were the most consistently reported risk carriers in the reviewed cognitive neuropsychology literature. Furthermore, as they were all shown to participate in the processes of neuronal migration or axonal guidance during early neurodevelopment, and their risk phenotypes resulted in ectopias and misguided axonal connections, they conferred a theoretically plausible mechanism for the tentative abnormalities in the cortical oscillatory connectivity.

### **1.3.4 Research Rationale, Hypotheses & Predictions**

#### **1.3.4.1 Research Rationale**

The genetic risk-associated early neuronal oscillatory modulations are a prediction based on the genetic profiles we review below, the language networks that are already structurally and functionally present at birth, as well as the oscillatory connectivity changes found in dyslexic children and adults in later life. Oscillatory responses to speech acoustics

have been demonstrated in pre-term infants, so very early signs of the hindered cortical wiring and temporal tracking of speech linked to genetic risk of dyslexia are not unlikely in the neonatal brain. How familial risk, genetic risk and neuronal oscillatory endophenotypes come together to influence language ability is not completely clear but there is accumulating evidence that these factors already interact during the prenatal development. In two studies, we set out to understand the relationships between the genetically incurred dyslexia risk and cortical entrainment to speech, as well as the underlying network connectivity in EEG sensor space of the neonatal brain, all in the context of familial risk of dyslexia. We argue that it is essential to study the influences of familial and genetic risk on infants' (1) oscillatory response to speech and (2) intrinsic network connectivity *at birth*, as we hypothesise that at-risk infants are set on a suboptimal developmental trajectory in early in-utero development. Finally, as this dissertation is a part of a longitudinal study (described in *Chapter 6*), a further aim of the full study was to follow the trajectories of high and low risk infants over the first two years of life, and to assess the developmental interactions between genetics and the oscillatory processing of speech, as well as early phonological processing outcomes. We believe that understanding the early properties of the cortical oscillatory activity in the context of genetic risk would provide a mechanistic stance on how the state of the functional neuronal architecture at birth could hamper the initial stages of entrainment to speech. These initial entrainment stages have been highlighted as essential for building up the adequate word-segmentation and accurate phonemic perception needed for future phonological skills and reading acquisition.

***The advantages of addressing these questions in the neonatal brain.***

The gene-associated neural changes and reading deficits likely feed into each other (see (Xia et al., 2017) for reviews and commentaries on this) making the neurobiological aetiology of dyslexia complex, multifactorial, and developmentally modulated. It would also make empirically addressing the neurobiological side of the aetiology very challenging. Despite the major pitfall of being unable to test for dyslexia as an outcome measure in the current design, investigating these early neurobiological effects in the neonatal brain provided two clear advantages. On the one hand, there were literature motivated indications that the infants' genetic background should be related neuro-oscillatory pathology (as a measure of direct stimulus-to-brain mapping) at birth. Secondly, the neonatal design reduced the number of variables contributing to the neurobiological link being tested. Although there were undoubtedly some linguistic environmental impacts already acting from 'outside the womb', they would have been markedly limited in

modulating the neuronal entrainment and network coherence compared to even a few weeks later. External factors while in the womb alter genetic expression (epigenetically) and therefore the effect we describe here related to dyslexia risk could never be fully contributed by allelic variance only. We were able to account for some circumstantial variables around the birth, such as weight and infections markers, which we thought would be the most significant contributors outside of the theoretically defined predictors. As the language exposure would have been limited to predominantly in the womb, we could confine the complex question of dyslexia's neurobiological aetiology to a genetically modulated early neurobiological mechanism of predisposition with the dyslexia proxy measure defined as familial dyslexia history.

#### **1.3.4.2 Study One: Familial and Genetic Risk Effects on the Neonatal Neuronal Entrainment to Speech – Hypotheses and Predictions**

In dyslexia, there are indications of temporal abnormalities (most commonly reported as changes in the amplitude or latency of the evoked response potentials) in the processing of speech-sound shortly after birth, associated with increased familial risk (i.e. (Guttorm<sup>1</sup> et al., 2010; Leppänen et al., 2012; Leppänen et al., 2010; Molfese, 2000; Van Zuijen et al., 2013). These neonatal and early infancy deviations, which have been related to later phonological processing and reading skills, have been attributed to less synchronised or noisier endogenous neural environment and faulty cortical wiring resulting from the observed aberrant neuronal migration and axonal connections leading to disruptions in the micro-circuitry of the cortex associated with the dyslexia susceptibility genes. The functioning of the cortical micro-circuitry can be measured not only as a stimulus-evoked timed EEG response, as previously reported, but also as imprecisions of the cortical oscillatory response to the prosodic rhythm of the speech signal, time-locked to the speech signal onset. The disruptions in the cortical micro-circuitry are likely to lead to disruptions in the timing of oscillatory response of speech, as has been previously suggested. Despite the general agreement in the literature on the hereditary nature of dyslexia and the high replicability of specific genetic variations, the links between the changes in the genotype and the neuro-endophenotypes of irregular continuous temporal processing of speech in the cortex are not straightforward. Here, we addressed the question of how the genetic and familial risk of dyslexia come together to confer a tentative dyslexia-related early speech-locked oscillatory response to the prosodic features of speech-sound signal. As it is not possible not directly test the relationship between the genes and the predicted neural response changes, but converging evidence points towards such a link, we aimed to

understand better how the two are related in the context of the infants' familial risk of dyslexia. Due to the pre-natal influences of the susceptibility genes, we predicted that the risk-related mechanisms leading to inferior continuous speech tracking should be already present at birth.

#### **1.3.4.3 Study Two: Familial and Genetic Risk Effects on the Neonatal Neural Network Coherence during Speech Presentation – Hypotheses and Predictions**

A related framing of the temporal processing issues implicated the dyslexia genotype-related cortical microstructure aberrations, and specifically, abnormalities in neuronal migration (Hancock et al 2017), in creating a noisier endogenous neural environment (Centanni et al., 2018; Nicolson & Fawcett, 2019; Perrachione et al., 2016; Vanvooren et al., 2017; Yoncheva et al., 2014). A consequence of the noisier neuronal activity patterns would be short- and longer-range discordant structural and functional coherence. Long- and short-range neural connections can be approximated using signal connectivity metrics. Partial directed coherence (PDC) shows the lagged dependencies between two oscillatory time series (in frequency and phase) and the directionality of the signal transfer in the network. The results from PDC in the source-space have been interpreted in a similar ways as functional connectivity in fMRI (Molinaro et al, 2016).

In the second study, we attempted detecting the putative changes in the sensory-space within- and across-hemispheric directed coherence in association with the neonatal genetic and familial risk, using the measures of generalised PDC (GPDC). From previous literature, we know that structural abnormalities with implication on connectivity and lateralization are already present close to birth. It has also been demonstrated that functional neural coherence is suboptimal in children and adults with dyslexia, and that the issue is directional whereby impaired speech-sound processing in the primary auditory cortices passes suboptimal entrainment information to highest processing areas (Lizarazu et al., 2020; Molinaro et al., 2016). We expected here to be able to detect directed coherence abnormalities in at-familial-risk infants precociously at birth, and in association with the risk-related genotypes as alleged drivers of the atypical connectivity.



## **CHAPTER TWO**

# **GENETIC SUSCEPTIBILITY IN DYSLEXIA**

# CHAPTER TWO: GENETIC SUSCEPTIBILITY IN DYSLEXIA

## 2.1 Candidate SNPs Overview

This is a candidate gene approach in a case-control type design, aiming to identify the potential effect of previously reported dyslexia susceptibility common genetic variants on the surface-measurable cortical oscillatory dynamics related to the continuous processing of speech in the neonatal brain. As briefly outlined in the introductory chapter, we selected a total of 16 single nucleotide polymorphisms (SNPs) across 4 dyslexia candidate genes (*Table 2-1*), all involved in neuronal migratory and axonal guidance processes in animal studies (*Figure 2-1*). Specific SNPs have been implicated in an gene-phenotype association studies with either reading and spelling skills or the related cognitive and neural components (Bates et al., 2010; Chen et al., 2017; Darki et al., 2014; Hannula-Jouppi et al., 2005; Liebig et al., 2020; Mascheretti et al., 2014; Müller et al., 2017; Neef et al., 2017; Scerri et al., 2012). Furthermore, several of the individual polymorphisms of interest (on KIAA0319 and DCDC2) have been connected to syllabic oddball MMN markers in dyslexic (Czamara et al., 2011) and ABS response reliability in at-risk (Centanni et al., 2018) children.

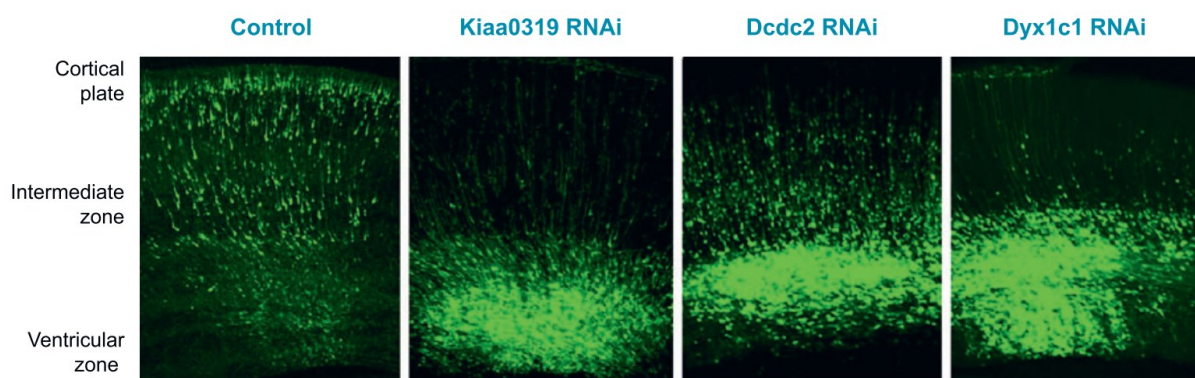


**Figure 3**

RNA interference (RNAi) of *Kiaa0319*, *Dcdc2*, and *Dyx1c1* disrupts migration in the developing rat neocortex. Images of sections of embryonic rat neocortex are shown four days after the electroporation of short hairpin RNA (shRNA) vectors and an EGFP vector, as described by Bai et al. (3). In the control experiment, where cells were transfected with a neutral shRNA, most of the neurons migrated well away from the ventricular zone and many reach the cortical plate. Neurons transfected with shRNA vectors against *Kiaa0319*, *Dcdc2*, and *Dyx1c1* migrate abnormally and are arrested in the ventricular and intermediate zones. Credit: Joe LoTurco, University of Connecticut.

*Figure 2-1. Copied from (Paracchini et al., 2007). DOI: 10.1146/annurev.genom.8.080706.092312*

In our neonatal and parental samples, we tested for three common SNP variants on the *DYX1C1* gene, seven on *DCDC2*, two on *KIAA0319*, and four on *ROBO1*, delineated in *Table 4-1* below. All populational genetics are reported here as percentages of known samples, based on the data from three British studies: the TWINSUK (3574 individuals, re3data.org, 2020) and Avon Longitudinal Study of Parents And Children (ALSPAC, 3708 individuals, (Northstone et al., 2019)), and 1000 Genomes Project Consortium phase 3 GBR segment (91 individuals, ("A Global Reference for Human Genetic Variation," 2015)). The descriptive information for each of the SNPs is derived from the gnomAD (Karczewski et al., 2021), *Ensembl - European Bioinformatic Institute*, (Howe et al., 2021) and dbSNP - *National Centre for Biotechnology Information*, (Sherry et al., 2001) databases.

As shown in *Table 2-1*, all the seven SNPs on the *DCDC2* gene are non-protein-coding intron variants, and so are the four SNPs overlapping the *ROBO1* gene (although note that the rs9853895 SNP partakes also in a reported nonsense-mediated mRNA decay (NMD) transcript splice<sup>6</sup> variant). One of the SNPs coinciding the *DYX1C1* gene is also an intronal variant, while the rs17819126 SNP is a missense variant – a nonsynonymous point substitution in the mRNA coding sequence of the gene which results in an often functionally inconsequential amino acid substitution in the corresponding region in the encoded protein. The third *DYX1C1* SNP is a variant of the 5' untranslated region (5'-UTR is the RNA sequence immediately upstream of the start codon) of the exonal part of the gene. Albeit non-protein-coding, the 5'-UTR participates in the regulation of the corresponding mRNA translation. Finally, both SNPs tested for on the *KIAA0319* gene are exonal variants, one is a missense point mutation, while the other one is a part of a non-coding transcript variant of the gene<sup>7</sup>. The non-coding gene variants most frequently arise by skipping the start or end part of an exonal sequence, potentially in this way removing the start or stop codons of the

---

<sup>6</sup> The splice site is the locus between an exon and an intron. Common genetic variations may occur when the splicing of the encoding site results in excluding some exonal parts and/or including different intronal parts into the transcript mRNA.

<sup>7</sup> Note that rs2143340 actually overlays the *KIAA0319/TTRAP/THEM2* intergenic locus, which has been shown to affect gene expression of the *KIAA0319* gene and has strong associations in the literature with reading disability (Pinel et al., 2012); TTRAP (TRAF and TNF receptor-associated protein) or TDP2 (tyrosyl-DNA phosphodiesterase 2); TRAF is TNF receptor associated factor; TNF is tumour necrosis factor. THEM2 (thioesterase superfamily member 2) has been updated to ACOT13 (acyl-CoA thioesterase 13), according to the HUGO gene nomenclature committee (HGNC).

relevant genes. Most non-coding transcripts are intermediary splicing variants which still contain some intronal non-coding mRNA (Dhamija & Menon, 2018). Thus, most of the SNPs which we test do not participate in protein encoding processes but rather in regulatory processes around transcription and splicing. It can be speculated these SNP contribute to variations in regulatory functions with much milder and more complex effects on their related phenotypes than any potential changes in the protein encoding regions. This could lead to the lower effect sizes of the SNPs on associated neuroendophenotypes. It may be indicative of the intrinsic complexity in the relationship between the dyslexia susceptibility genes reviewed in the literature on the one hand, and the multifaceted neurobiological and behavioural characteristics of dyslexia, on the other.

Table 2-1. Summary descriptive of the 16 SNPs of interest in known British samples (comprising English and Scottish population) based on ensemb.org and dbSNP databases. Please note the table only shows citations available in the two databases which do not contain an exhaustive list of literature reports of the associated phenotypes.

GENE	SNP	Chromosome	Location (bp)	Variant Type	Reference Allele (Ancestral)	Alternatives	VIC/FAM	Phenotype
DYX1C1	rs3743204	15	55498112	intron	T	G	G/T	
	rs3743205	15	55498332	5 prime UTR	C	A, G, T	C/T	
	rs17819126	15	55497712	missense	C	A, T	C/T	Dyslexia risk factor (T)
KIAA0319	rs4504469	6	24588656	missense	C	G, T	C/T	
	rs2143340	6	24658843	non-coding transcript exon	A	G, T	A/G	Genetic risk for poor reading performance
DCDC2	rs793842	6	24224260	intron	T	C	C/T	Neuroimaging genetics of specific reading disability, developmental language disorder, developmental dyslexia, information processing speed
	rs793862	6	24206972	intron	A	C, G, T	A/G	Haplotype with rs807701, A is the risk allele
	rs807701	6	24273563	intron	G	A	A/G	Haplotype with rs793862; dyslexia risk increasing in combination with rs793862.
	rs2328819	6	24333258	intron	G	C	C/G	left temporal gray and white matter structures during development
	rs2792682	6	24272156	intron	A	C	C/A	gray and white matter during development, normal variation in reading and spelling
	rs7751169	6	24351696	intron	G	A	A/G	left temporal gray and white matter structures during development
	rs9460974	6	24188719	intron	T	C	C/T	speech sound disorder; white and gray matter development, specific language impairment
ROBO1	rs6803202	3	79450003	intron	C	T	C/T	cognitive predictor of dyslexia, specific learning disabilities, expressive vocabulary in infancy.
	rs7644521	3	79735384	intron	T	C	C/T	white matter structure in corpus callosum
	rs333491	3	78759700	intron	A	G	A/G	
	rs9853895	3	79536008	intron;NMD transcript	C	T	C/T	white matter structure in corpus callosum

## 2.2 Genetics Chapter Summary

The current chapter intends to expand on the genetic susceptibility of dyslexia review briefly mentioned in *Chapter 1*. It further details the known associations of the selected SNPs with neurobiological and cognitive (reading-related) phenotypes. Additionally, the chapter presents the genotyping procedures employed in the current study to identify the sample genetics in our cohort of infants (parental genetics are detailed in *Appendix II.I*).

Next, it performs a detailed descriptive analysis of the genotypical distribution in our sample and compare those to other published British samples. Finally, it discusses the genotyping results in the context of the two studies in the dissertation, reporting genetic risk factors on neuro-oscillatory functioning in relation to speech.

---

## 2.3 Dyslexia Susceptibility Genes: Review of the Literature to date

Both the dbSNP and Ensembl databases had phenotypical entries for four of the seven DCDC2 SNPs tested here in relation to dyslexia and reading disorders (Chen et al., 2017; Darki et al., 2012, 2014; Eicher et al., 2015; Neef et al., 2017). The remaining three SNPs had been related to white and gray matter structures maturation during development, and normal reading ability variations (Darki et al., 2012, 2014). Across all seven DCDC2 SNPs, the reported associations came from both neuroimaging studies and behavioural and reading assessments. Two of the ROBO1 SNPs had shown strong associations with reading difficulties and other cognitive predictors in developmental dyslexia (Bates et al., 2011; Mascheretti et al., 2014), while the other two were reportedly predictive of white-matter structures in the corpus callosum (Darki et al., 2017). Darki et al (2014) found the KIAA0319 rs2143340 SNP to be a risk factor for poor reading performance, while Mascheretti et al (2014) implicated rs4504469 as a part of a three-way risk haplotype for developmental dyslexia. Finally, the three DYX1C1 SNPs in the study had been identified as dyslexia risk factors (Bates et al., 2010; Darki et al., 2012; Lim et al., 2011).

### 2.3.1 Dyslexia Susceptibility Genes Impacting Neuronal Migration

#### 2.3.1.1 DYX1C1: Mechanism of Effect and Association with Dyslexia

The ENSG00000256061 dyslexia susceptibility 1 candidate 1 gene (here abbreviated as **DYX1C1**, on chromosome 15q21.3) was first identified in a large Finnish family with two putative variants. The variants were then found to be associated with dyslexia in a larger Finnish population sample (Becker et al., 2014), in the UK and US in dyslexic selected samples, and with reading and spelling in an unselected Australian twin study sample (Bates et al., 2011). Selected samples are those collected from individuals at high familial risk, and they were specifically selected for dyslexia. Note, however, that the link with

dyslexia has not always been replicated, for example, in smaller samples from UK, Italy, US and India (Darki et al., 2012).

Downregulating *DYX1C1* using RNA interference (RNAi) disrupted neuronal migration of premigratory neurons in the ventricular zone rats' brains (Rosen et al., 2007). Examination of the neural tissue four days post in-utero manipulation revealed that transfected neurons were "arrested in migration" (Figure 2-1, rightmost panel). Furthermore, the authors observed that the transfected adult rat brains had similar pathologies to the ones reported in human dyslexia brains studied post-mortem, such as pockets of unmigrated neurons in periventricular white matter, ectopias with abnormal radial orientation in neocortex and white matter (WM), and hippocampal pyramidal cell migration abnormalities. Tapia-Paez, Tammimies, Massinen, Roy & Kere (2008) proposed a functional role of three proteins in the promoter region of *DYX1C1* as binding factors to regulate dyslexia-related SNPs. In humans, the rs3743204 SNP, located on the *DYX1C1* gene, showed an age-modulated effect on WM volume in a left hemisphere temporal-parietal cluster in relation to verbal intelligence (Darki et al., 2012). In a cross-sectional longitudinal design, Darki et al (2012) reported that the genetic influence ramped up with age in the same individuals, and between the ages of 6 and 25 years old (participants were tested twice with a two-year gap), potentially implicating the *DYX1C1* SNP not only in neuronal migration during in-utero development, but also in experience-based structural WM changes in adulthood. In the identified left temporal-parietal cluster, WM volume was significantly correlated with reading abilities when gender, age and handedness were accounted for. WM tractography, on the other hand, did not identify any significant tracts correlating with the SNPs on *DYX1C1*, but with SNPs located on the *KIAA0319* and *DCDC2* genes instead.

### ***Linkage Disequilibrium between the *DYX1C1* SNPs of interest***

The Linkage disequilibrium (LD) structure of (a specific part of) a gene indicates the likelihood of the constituting SNPs (usually in a close proximity of each other as measured in the number of base-pairs or bps) to be inherited together. Here, the LD structure was inferred from the other British samples on the published database in Ensemble.org and is not based on our sample. Therefore, we used it only to infer potential dependencies between the SNPs of interest, but no SNPs were excluded from analyses on the basis of higher likelihood of coinheritance in the general population.

There are three measures relevant to describing LD between two SNPs: the distances between them in bps, the  $D'$  and  $r^2$ . The  $D'$  measure is given by the difference between the observed and expected frequency of co-inheritance of a specific combination of two SNP variants. It is assumed that if in a perfect state of heritable equilibrium, the two SNPs are inherited independently of each other and so the distance between their expected and actualised co-inheritance is  $D'=0$ .  $r^2$  is the correlation coefficient between the two loci, varying from 0 to mean not co-inherited at all, to 1 meaning complete linkage disequilibrium. That is, the higher values of  $r^2$  indicate that the two SNPs are often co-inherited and are likely to form a haplotype. It may mean that their effects are not independent from each other. Please note that the *Ensembl* database only stores LD information between two SNPs if they have a value of  $r^2 > .05$ .

For the three SNPs we tested on the *DYX1C1* gene, the rs3743204 had a high frequency of coinheritance with the other two *DYX1C1* SNPs but the correlation coefficients were low for both linkages, indicating that they were not very likely to consistently form a haplotype (Figure 2-2).

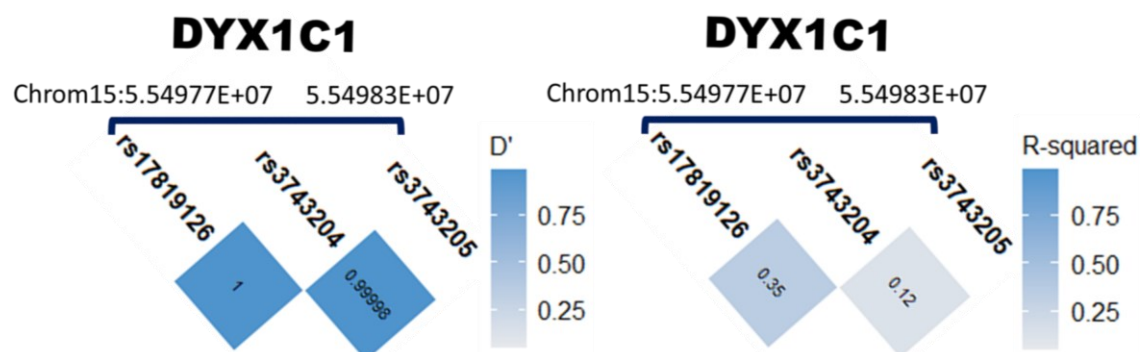


Figure 2-2. Pairwise Linkage Disequilibrium plots for the 3 SNPs tested overlaying the *DYX1C1* gene; Numbers in the squares are  $D'$  on the left and  $R^2$  on the right. Only linkages with a correlation coefficient  $R^2 > .05$  are plotted. The order of the SNPs on chromosome 15 between the outer base-pair locations are schematically represented on the line above the plot.

### 2.3.1.2 KIAA0319 and DCDC2: Mechanism of Effect and Association with Dyslexia

The ENSG00000146038 doublecortin domain containing protein 2 (*DCDC2*) and the ENSG00000137261 *KIAA0319* genes (both on chromosome 6p22.2), are collectively the most replicated loci on chromosome 6 in relation to dyslexia/reading disability (Neef et al.,

2017), language impairment, and verbal language and cognition (Eicher et al., 2014). They have been referred to as dyslexia susceptibility 2 genes, or the *DYX2* locus. SNPs overlaying the *KIAA0319* site have been associated with general reading abilities in 7-9 year old children in the ALSPAC (UK) cohort, and the strength of the association increased when controlling for IQ (Paracchini et al., 2008). Associated SNPs on *KIAA0319* were also predictive of noisier auditory brainstem (ABS) entrainment to the stop consonant in the syllable (/da/) in school-aged native German speakers (Neef et al., 2017).

The influence of the gene-expression patterns of *KIAA0319* during the development of the cerebral neocortex has been recognized in both human and mouse fetuses (Paracchini et al., 2006). In rats, the down-regulation of a homologue of a dyslexia-risk associated *KIAA0319* haplotype - a set of two or more allele variants which often located in close proximity and have a high probability of being inherited together in a given population - lead to the suboptimal neuronal migration during cerebral cortex development - see the two middle panels of *Figure 2-1* (Paracchini et al., 2006). *KIAA0319* encodes a plasma membrane protein in the early endosomes (Velayos-Baeza et al., 2010). The early endosomes (cell organelles with intra- and extra-cellular and transmembrane domains, responsible for endosomal trafficking) in neurons have importance for cell fate decisions, polarity, migration and axon outgrowth and guidance (Choo Yap & Winckler 2012). Peschansky et al. (2010) demonstrated that while in-utero knocking down *KIAA0319* in rats via RNAi lead to periventricular heterotopias (dislocated groups of neurons, similar to those described in association with the *DYX1C1* polymorphisms), overexpressing the *KIAA0319* not only did not affect development but could also acted as a resilience factor to rescue the phenotype. Additionally, the knock-down neurons in the same study displayed dendritic heterotrophy, implicating the *KIAA0319* further in post-migration neuronal wiring. This finding is in line with the documented role of the *KIAA0319* in the negative regulation of dendritic development through processes that stop, prevent or reduce the frequency or extend of dendrite development (Neef et al., 2017). In humans, adults with a dyslexia-susceptibility haplotype within *KIAA0319* showed left prefrontal and temporal deficits in auditory steady-state responses (ASSRs) to noise modulations at 30Hz (Pinel et al., 2012). Non-dyslexic adults carrying the same haplotype had a reduced leftward functional asymmetry more similar to dyslexic than to fluent readers (Pinel et al., 2012) in areas roughly corresponding to locations prone to cortical ectopias in post-mortem examinations of human dyslexic brains (Ramus, 2004). Three dyslexia-risk associated SNPs

on the KIAA0319 were also predictive of noisier auditory brainstem (ABS) entrainment to stop-consonants in school-aged native German speakers (Neef et al., 2017).

Evidence for relation of DCDC2 SNPs with developmental dyslexia, both as single-markers and in a haplotype, has been replicated in many different studies and samples, including cohorts from Germany, the US, the UK (Schumacher et al., 2007), Sweden (Darki et al., 2012, 2014), and Hong Kong and China (Chen et al., 2017; Waye et al., 2017).

DCDC2 is widely expressed in the inferior and medial temporal cortices, where diminished activation has been reported in association with dyslexia (Schumacher et al., 2007). SNPs located on this gene have also been associated with visual learning and sound perception (Neef et al., 2017). The DCDC2 encodes a doublecortin domain-containing protein that binds with tubulin to enhance microtubule polymerization (Neef et al., 2017), involved in establishing the cell's polarity, and thus influencing neuronal migration (Darki et al., 2012). Structurally, rats knocked down for DCDC2 in-utero using the RNAi technique exhibited significantly diminished neuronal migration (Meng et al., 2005) and the resulting periventricular heterotopias (Burbridge et al., 2008) during neuronal plate development. Functionally, mice locally knockdown for DCDC2 showed a deficit in rapid auditory processing (Truong et al., 2014), and degraded spike timing when encoding rapid sensory input measured directly in the somatosensory cortex (Che et al., 2014). In humans, one SNP on DCDC2 - rs793842 - showed a strong association with both total white matter volume, and WMV in a left temporal-parietal cluster in relation to reading abilities in children and adult fluent readers, independently of age, gender and handedness (Darki et al., 2012). The lack of interaction with age indicated that the effect of the SNP may be related to the earlier neuronal development and not as much axonal maturation and myelination during childhood. In both the children and the adults in the study, the WMV effects correlated significantly with reading comprehension and reading accuracy.

Due to the proximity of DCDC2 and KIAA0319 on chromosome 6 (*Figure 2-3*), dyslexia-risk haplotypes formed between SNPs within DCDC2 and KIAA0319 are commonly found (Becker et al., 2014). Using diffusion tensor imaging, Darki et al. (2012) predicted the connectivity strength of the WM tracts in a region overlapping the left superior longitudinal fasciculus (close to the arcuate fasciculus, sometimes used interchangeably) and the corpus callosum from the non-dyslexic volunteers' genotypical pattern of co-variation between the

DCDC2 and KIAA0319 SNPs. This region contained temporal-parietal tracts, which connected the middle temporal gyrus (MTG) to the left angular (LA) and supramarginal gyri (SMG), with the inter-hemispheric pathways terminating in the left and right superior parietal lobule and the superior division of the lateral occipital cortex (Darki et al., 2012).

### ***Linkage Disequilibrium between the KIAA0319 and DCDC2 SNPs of interest.***

The SNPs of interest overlaying the DCDC2 and KIAA0319 genes in our sample were also located within a proximity of each other on chromosome 6. The available LD structure is plotted in *Figure 2-3* below. Again, despite the high frequency of co-inheritance and frequent reporting as haplotypes, no two SNPs have a correlation higher than  $R^2=.80$  and were all considered separately in our sample as well.

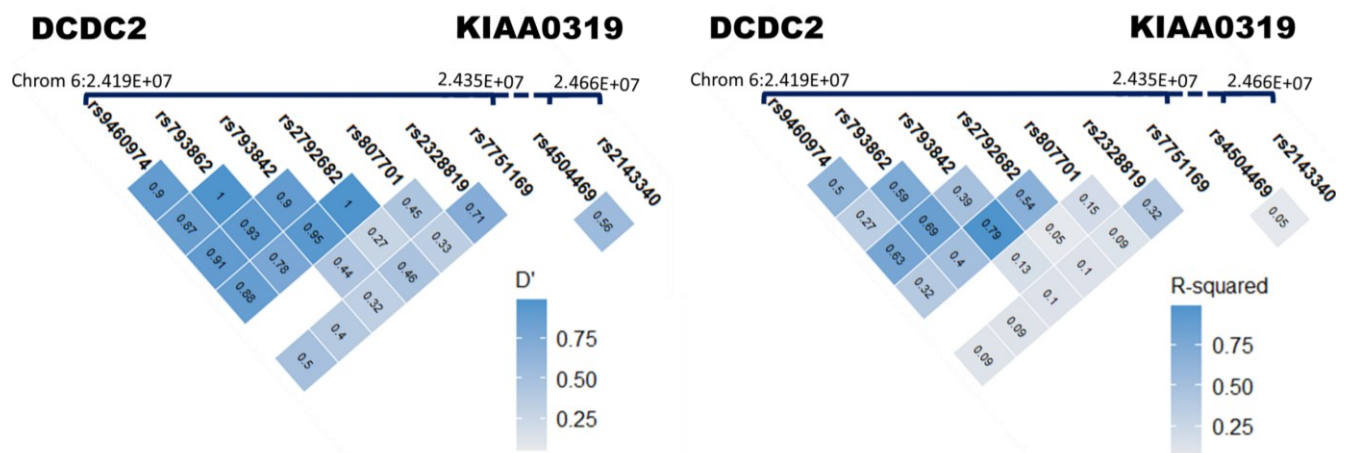


*Figure 2-3. Pairwise Linkage Disequilibrium plots for the 7 DCDC2 and 2 KIAA0319 SNPs tested; Numbers in the squares are D' on the left and R<sup>2</sup> on the right. Only linkages with a correlation coefficient R<sup>2</sup> >.05 are plotted. The order of the SNPs on chromosome 6 between the outer base-pair locations on each gene are schematically represented on the line above the plot.*

## **2.3.2 Dyslexia Susceptibility and Axonal Guidance**

### **2.3.2.1 ROBO1: Mechanism of Effect and Association with Dyslexia**

The ENSG00000169855 human homolog 1 of the roundabout gene originally identified in *Drosophila* (ROBO1, on chromosome 3p12.3), is the main candidate gene in the DYX5 dyslexia risk region (Schumacher et al., 2007). ROBO1 has been associated with dyslexia-related neurolinguistic traits in samples from Italy (Mascheretti et al., 2014) and Finland (Nopola-Hemmi et al., 2001). It has also been associated with phonological deficits in large

US samples (Hannula-Jouppi et al., 2005; Stein et al., 2004), and in school-aged Australian twins (Bates et al., 2011).

The *ROBO1* gene expresses a *ROBO1* protein that forms a receptor for the slit molecule (Neuhaus-Follini & Bashaw, 2015). The slit ligands help regulate axon branching, pathfinding and neuronal migration (Andrews et al., 2006). During the axonal growth in the neuronal plate development, the slit proteins are expressed at the floorplate and their binding acts as a repellent for the post-midline-crossing neurons. Underexpression of *ROBO1* results in the axons crossing the midline back and forth too many times, leading to abnormalities in axonal targeting in *ROBO1* knockout mice (Andrews et al., 2006). The midline is a neurodevelopmental precursor structure in the brain that later serves as a basis for forming the corpus callosum. A potential mechanism of the *ROBO1*'s influence on the axons crossing over the midline comes from its binding the slit proteins at the midline. The slit proteins silence netrin (an axonal-attractor present at the midline) and prevents it from binding the growing axons again after they cross the midline. For example, homozygous *ROBO1* knockout mice (who were unable to express *ROBO1* proteins) did not survive long after birth but prenatally displayed major pathfinding deficits in the corpus callosum and hippocampal commissure. They had abnormalities in corticothalamic and thalamocortical axonal targeting, with a significantly increased number of interneurons migrating into the neocortex, particularly in the rostral and parietal but not in the caudal regions (Andrews et al., 2006). In contrast, during the normal critical periods for avian vocal learning, *ROBO1* was developmentally upregulated in the forebrain part of a neural circuit connecting to the brainstem's vocal motor-neurons in independent lineages of vocal-learning birds (songbirds, parrots and hummingbirds) but not in non-learning birds (Wang et al., 2015). In humans, a splice variant of the *ROBO1* gene has been found to be more common in the temporal lobe of the developing neocortex, while the shorter isoform of the same splice variant was also marginally enhanced in the prefrontal cortex (Johnson et al., 2009). Thus, in both humans and other animals, *ROBO1* has been developmentally upregulated in the forebrain, thalamocortical pathways and temporal cortex - areas important in humans for language and speech-sound processing, while its downregulation has been associated with abnormalities in neuronal wiring processes such as axonal guidance, pathway finding, and neuronal migration, in those areas. It is worth noting that Hannula-Jouppi et al. (2005) localized a translocation splice variant in the *DYX5* region of chromosome 3 with a specific rare haplotype (consisting of two silent exonal SNPs and four SNPs in the 3' UTR) that segregated individuals with dyslexia in a large Finnish pedigree

family. The authors used the haplotype as an assay to study the expression of ROBO1 in an independent sample of genomic and chromosomal DNA from four dyslexic individuals, which showed that the mRNA was only weakly or not at all transcribed from the alleles that segregated with dyslexia. Furthermore, same authors reported multiple coding differences in ROBO1 between humans, apes and mice, by identifying exons and splice variants specific to humans, which might help explain the difference in gravity on phenotypes of heterozygous loss of ROBO1 in mouse and human (Hannula-Jouppi et al., 2005). It should be noted that the relationship of this specific ROBO1 translocation with dyslexia has not been replicated outside a few families in the Finnish population (Schumacher et al., 2007). Even though these results lent a strong indication of the role of ROBO1 in severe reading impairment, they do not represent an exhaustive causal mechanism of genetic influence on dyslexia, which likely has an extremely complex multifactorial neurobiological aetiology, modulated by a strong epigenetic component (Ramus, 2004; Xia et al., 2017). Still, (Mascheretti et al., 2014) found that the “A” allele of ROBO1’s SNP rs333491A/G was associated with phenotype of reduced mental calculation accuracy, as well as reading-related deficits in a GWAS of quantitative dyslexia-related phenotypes. Furthermore, Bates et al. (2011) tested a total of 144 ROBO1 SNPs against phonological buffer deficits (a common cognitive dyslexia marker) and reading and spelling traits in a twin-study with a cohort of 1177 randomly-selected individuals (11 triplets) in Australia. The study identified significant associations with phonological buffer capacity for 21 SNPs (the strongest associations were for rs6803202 and rs4535189 with the nonword repetition test); with forward digit span (related to phonological span) for 22 SNPs; with reading and spelling ability for only one SNP (rs1995402 - did not survive multiple comparisons); and with working memory for 5 SNPs (the strongest association was with rs333491, but it did not survive multiple comparisons).

### ***Linkage Disequilibrium between the ROBO1 SNPs of interest***

The chromosomal context map and the LD structure of the four included ROBO1 SNPs are given in *Figure 2-4*. Evidently, the SNPs of interest have low rates of co-occurrence and all but the rs6803202-rs9853895 pair have a correlation of  $R^2 < .05$ . For the rs6803202-rs9853895 pair, LD was still below 80%, so the two SNP could not be considered in disequilibrium.

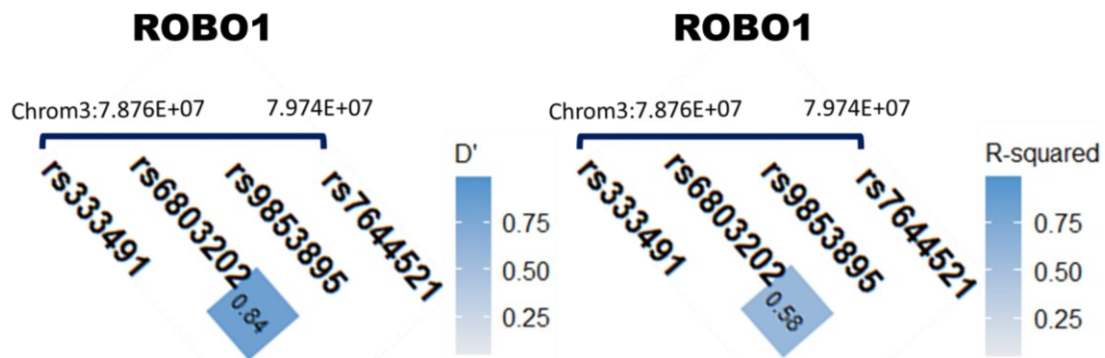


Figure 2-4. Pairwise Linkage Disequilibrium plots for the 4 SNPs tested overlaying *ROBO1*; Numbers in the squares are  $D'$  on the left and  $R^2$  on the right. Only linkages with a correlation coefficient  $R^2 > .05$  are plotted. The order of the SNPs on chromosome 3 between the outer base-pair locations are schematically represented on the line above the plot.

Taken together, there is a vast literature suggesting a strong genetic component to the aetiology of reading disorders. Despite the considerable individual heterogeneity, there are consistent indications in both human and other animal studies that dyslexia susceptibility genetic variations exert an influence on the way that the brain is "wired-up" during early development, well before literacy age. A significant proportion of the gene-related neural structural and functional modifications are potentially in place already prior to birth.

## 2.4 Genetics: Methods

### 2.4.1 Participants

The full set of 96 infants (after excluding those who withdrew consent or did not meet the study's inclusion criteria) is included in the genetics analysis here. The sample's descriptive characteristics are identical to the ones given in Chapter 3. Infants 1-12 were genotyped by P.C. prior to the start of my doctoral project (Cyr, 2016). The protocol followed for the genotyping of the remaining infants' samples was identical and was established by the manufacturer of the genotyping materials.

### 2.4.2 Sample Collection – Neonatal

*Genetic Sampling:* To identify each infant's genetic profile on the SNPs of interest, blood spot samples were collected from each infant on a Guthrie card, using a standard heel lance technique (Saavedra-Matiz et al., 2013).

The heel prick was done at the end of each experimental session, after the EEG protocol described in *Chapter 3* had been completed. The size of the heel lance was chosen based on the weight of the infant. The area of the heel to be punctured was sterilised, and a button-operated spring ejector blade was applied on it, which produces a 2-3mm slice. Four drops of blood were collected at the designated areas on the Guthrie card. Any remaining blood was absorbed using sterile cotton tampons, and if necessary, a plaster. In most cases, the infants appeared to remain asleep or in the state of a quiet restfulness when the heel lance was applied. Most infants had a startle reaction at the prick but settled in a few seconds. Few infants showed a minor distress at the procedure and needed to be comforted by a parent.

The majority of the blood spot samples were collected at the neuroimaging suite by the experimenter (me for the latter 50 infants) who underwent a formal training and certification to be able to perform the procedure. The blood cards were then stored in a designated fridge at 4-8 C for up to one year prior to analysis. Several samples have been collected by neonatal or paediatric ward staff, most frequently that happened for infants who were recruited on postnatal day 5, as they already had a heel-prick procedure scheduled on that day for the national neonatal blood spot screening program.

### 2.4.3 Genotyping Protocol

All the 16 SNPs of interest within the four candidate genes (*Table 2-1*) were genotyped to tests for the presence of either two copies of the reference allele (homozygous 1), the alteration (homozygous 2), or both alleles (heterozygous).

A set of previously tested samples with known genotypes (or templates) were used as a positive template control, or PTC, in a selected number of reaction plates. One PTC of known genotype was added in some plates to replicate the genotyping with all reagents, and to confirm that the reagent assays were working consistently over time.

The genotyping was conducted as a quantitative polymerase chain-reaction (qPCR) using the commercially available predesigned *Taqman SNP Genotyping Assays and GTXpress Master Mix* in 384-well plates on a *QuantStudio 6 Flex 6900HT Sequence Detection System (LifeTechnologies)*.

#### *The procedure for DNA extraction and stabilising*

First, genomic DNA was extracted from a 3-mm puncture from the Guthrie blood cards and immediately stabilized. The protocol for stabilizing the genomic DNA consisted of the following steps:

- a. 50µL of TaqMan Extract All Reagents Lysis solution was added to each testing sample (the 3mm puncture).
- b. The mix tubes were briefly vortexed.
- c. The mix tubes were then incubated at 95°C for 3 minutes.
- d. 50µL of TaqMan Extract All Reagents DNA Stabilizing solution was next added to each tube immediately after incubation.
- e. The tubes were again briefly vortexed and then centrifuged at 45,000 revolutions per minute (RPM) for 1 minute to allow for the separation of the supernatant with the stabilized genomic DNA from the remaining precipitate.
- f. The thus stabilized DNA sample templates were either immediately used in a qPCR reaction plate or stored in a fridge at 4-8°C.

#### *The procedure for genotyping using qPCR*

Next, the samples' genomic DNA was amplified in the presence of a primer and two probes, one for the reference and one for the alternative allele of the SNP being tested. In this procedure, each of the two probes was attached to two markers – a reporter dye (which fluoresced), and quencher (which prevented fluorescence). Two different reporter dyes

were used for the two alleles of the SNP, where the order of the alleles corresponded to their association with the probe reporter dyes: the allele 1 was always marked with the VIC™ dye and appeared as a red marker, while the allele 2 was stained by the FAM™ dye which was given in blue. The quencher was detached when a complementary strand of the genomic DNA was present in the sample, thus allowing for the fluorescent marker to activate and indicate the allelic presence. Homozygous samples showed fluorescence for only one of the two alleles, while heterozygous - for both. All samples in this study were run in duplicates for better reliability of the results – both copies of each sample should have indicated identical alleles. For each SNP genotyping assay, two no-template controls (NTC) were also included in every plate, whereby two wells per assay were prepared with water instead of sample DNA in order to confirm that the fluorescence detected in the samples was due to the presence of the sample and not solely to the presence of the probes in the solution. Selected reaction plates also included positive template control samples (PTCs as defined above) to test for the reliability of the used reagents over time.

The protocol to prepare the reaction well-plates for DNA amplification and fluorescence-detection consisted of the following steps:

- a. In each well of the 10 $\mu$ L 384-well reaction plate, 5  $\mu$ L of *TaqMan GTXpress Master Mix* and 2.5 $\mu$ L of nucleotide-free water were pipetted.
- b. 0.5 $\mu$ L of each of the 16 SNP Genotyping Assays (reagents) were added to one of the 24 rows of wells on the plate. The total reaction volume at this step was therefore 8 $\mu$ L per well.
- c. *MicroAmp* clear optical adhesive film (*ThermoFisher*) was used to seal the reaction plate before it was centrifuged for a few minutes to shift all contents to the bottom of the wells and remove any air bubbles generated while pipetting.
- d. The adhesive film was removed and 2 $\mu$ L of each infant's stabilised genomic sample DNA template was added in to two wells for each line of reagents so that the samples were tested in duplicates. That meant that there was a total of 11 infants' samples tested in duplicates for each reaction plate. The two rightmost columns of each plate were left free of genomic template and used as NTC, as described above. In selected plates, one of the 11 samples was dedicated to a PTC. At this step, the total reaction volume per well was 10 $\mu$ L at this step.

- e. The ready reaction well-plate was again covered with a transparent optical adhesive film and centrifuged briefly. The adhesive film was replaced one final time after centrifuging, and tightly sealed while the air was removed by running a non-reflective comb in-between the edges of all individual wells.
- f. Finally, the *QuandStudio 6* thermal cycler was set up for each run from a pre-saved program template. The sequence for each run was carefully checked beforehand. Each run went through a holding stage for 20s in which the DNA polymerase was activated at 95°C. This was followed by a cycling stage (between 48-56 cycles) whereby every cycle consisted of two steps: a) genomic DNA denaturation for 3s at 95°C; and b) annealing and extension for 30s at 60°C. The DNA denaturation is a process of “melting” the double stranded DNA into single DNA strands and loosening the secondary connections by applying the highest temperature that the polymerase withstands according to the manufacturer’s prescription. During the combined process of annealing and extension, the complimentary sequences (if present) in the DNA were allowed to hybridise at an optimal for the polymerase temperature and to extend the primer. Each such cycle took about 3.5 minutes, and the entire qPCR experiment ran for a total of between 50-60 minutes depending on the number of cycles.
- g. After the final cycle, the endpoint fluorescence reading was performed at 25°C. During each qPCR run, the change in fluorescence (measured by the  $\Delta R_n$  value) per cycle for each well was plotted online to track the fluorescent accumulation as the genomic DNA is denaturated and amplified (an example run’s amplification plot is shown in *Figure 2-5* below). Amplification plots thus represented the accumulation of fluorescent product over the duration of the qPCR experiment. The *QuandStudio 6 Flex System* software used the  $\Delta R_n$  fluorescence measurement in each well to discriminate which alleles were present in it. The allelic discrimination results for each individual sample were then plotted on a scatterplot of Allele 1 versus Allele 2 (there were two dots for each sample as the samples were run in duplicates, see *Figure 2-6* below). The threshold for quality of each sample reading was left at default (97.5%).

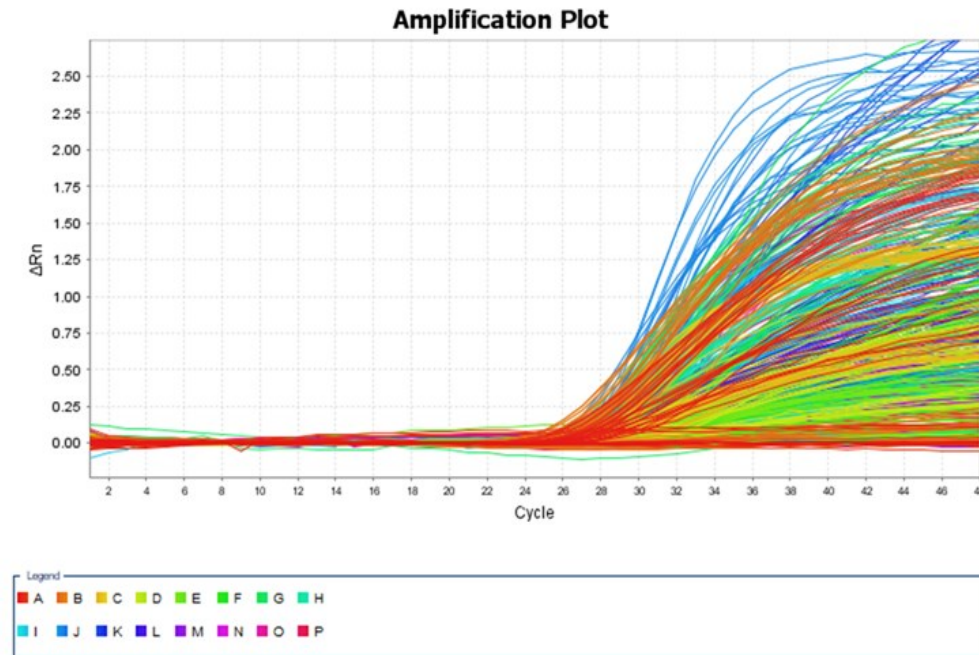


*Figure 2-5. Example amplification plot (the fluorescent signal from each sample is plotted against cycle number) for each of the SNPs. The different colours stand for different SNPs and each line represents one of the 384 wells.*

The scatterplot discriminated between groups based on the total fluorescence ( $Rn$ ) values clustering. The clusters were formed when the two SNP alleles were labelled using fluorescent probes emitting colour. The signal from the VIC (red) dye was displayed on the X axis and the signal from the FAM (blue) dye was displayed on the Y axis. If both dyes were emitting in equal proportions, the sample was classified as having both alleles present. The distinct fluorescence colour contribution of each dye or their co-localization (in the case of heterozygotes) led to the distinct clusters in the plot.

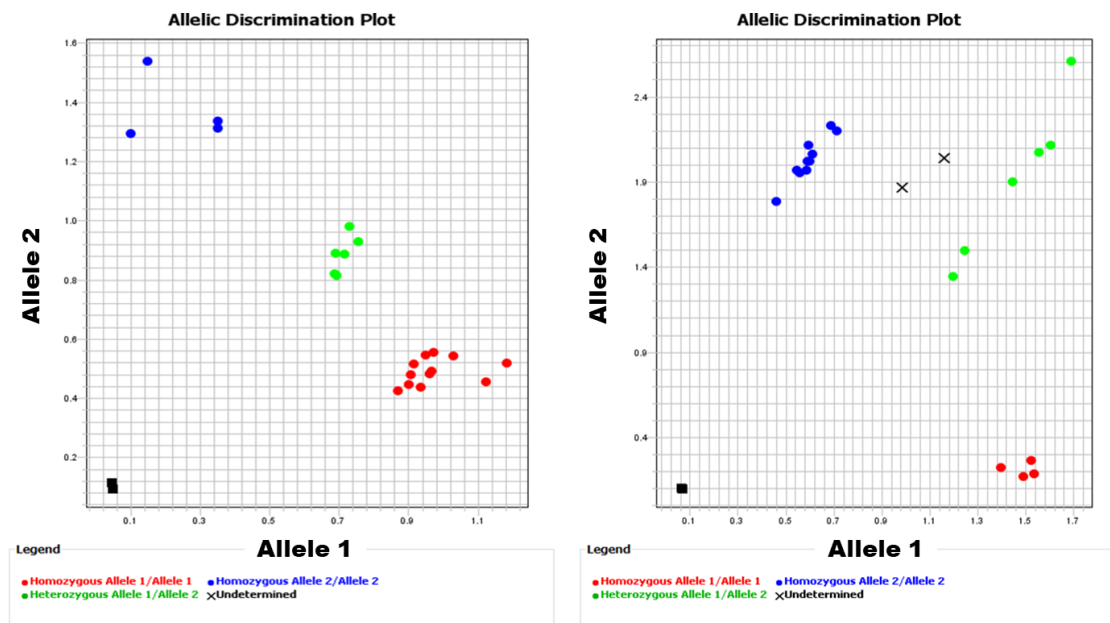


Figure 2-6. An AD scatterplot for two example assays over two separate runs (384 wells plates). Each dot/cross/square represents an individual well. A) Genotyping worked for all samples; B) Failed in two wells (indicated by the black crosses in the scatterplot) when they could not be definitively classified. There are two dots/squares for each sample as the samples were run in duplicates. Allele 1 homozygotes are clustered in red in the bottom right corner. Allele 2 homozygotes are clustered in blue in the top left corner. Heterozygotes are clustered in green in the middle of the plot. NTCs are clustered in black squares and are oriented to the origin.

Of the 16 tested SNPs, one SNP on the DCDC2 gene (rs9460974) did not produce consistent results against the positive control for the infants' blood-spot samples on repeated attempts and across several reaction plates. It was suspected that the reagent for this SNP was not functioning properly although this suspicion has not been systematically tested due to limited availability of time and resources. Instead, the rs9460974 SNP was not included in any reporting hereafter. Thus, we analysed the genetic profiles for 15 SNPs in the neonatal infants.

A total of 10 infants were re-tested on several occasions (4 infant samples were repeated more than 3 times) by re-performing the entire procedure from extracting and stabilising the DNA to running the qPCR experiment. This was done for quality control to ensure that the reagents and the procedure worked consistently over time and to control for my error

rate in genotyping as part of my learning curve. Only the results from plates that matched the original genotyping were admitted to analysis. If there were errors in pipetting or a mismatch on any SNPs (apart from the one that was deemed unreliable), the entire plates were rerun if sufficient DNA template was available for the infants tested.

## 2.4.4 Statistical Analysis

### 2.4.4.1 Frequency distribution of the infants' genotypes

The Ensembl, dbSNP and gnomAD databases are used here to review the prevalence of genomic variation within our sample in the context of other published samples from Great Britain.

We assumed that all SNPs tested follow the Hardy-Weinberg (HW) equilibrium for common genetic variations (Andrews, 2010), and we reported the expected allelic frequencies according to the HW principle of quadratic equation. The HW principle applies to the general population when it is assumed that a gene is not evolving, that is, the allelic frequency remains constant across the generations. The HW assumes no processes of mutation, selective mating or natural selection are acting on the gene (i.e. there is no new alleles generated by mutation or deletion, and no advantage for a particular copy of the gene in terms of survival or mating). Finally, the HW principle applies to a population of a very large size (or the entire population) where there is no genetic drifts or migration in and out of the gene-pool. Although for any given gene, some or all of the HW assumption can be violated in a varying degree at any given time, common genetic variations such as the SNPs that we are testing here are assumed to be in HW equilibrium over long periods of time.

For all plots, Allele1 indicates the more common allele in our sample. Also, for consistency and ease of expression, genotype#1 hereafter refers to the homozygous genotype for the more common allele in our sample population (irrespective of whether this was the reference or the alternative allele in *Table 2-1*). Genotype#2 is therefore the heterozygous genotype, and genotype#3 is the homozygous for the less common allele in the current sample.

#### 2.4.4.2 Testing for the association between familial and genetic risk

To estimate whether there was a statistical association between the infants' genotype on the SNPs of interest and their familial dyslexia risk independent chi-square tests were performed on each SNP against familial risk. The genotype on each SNP was defined as described above, whereby genotype#1 denoted the heterozygous variant for the most common allele in our sample. Familial risk here was defined as high (the infant had one or more first-degree dyslexic relative) or low (the infant had no first-degree relatives with dyslexia).

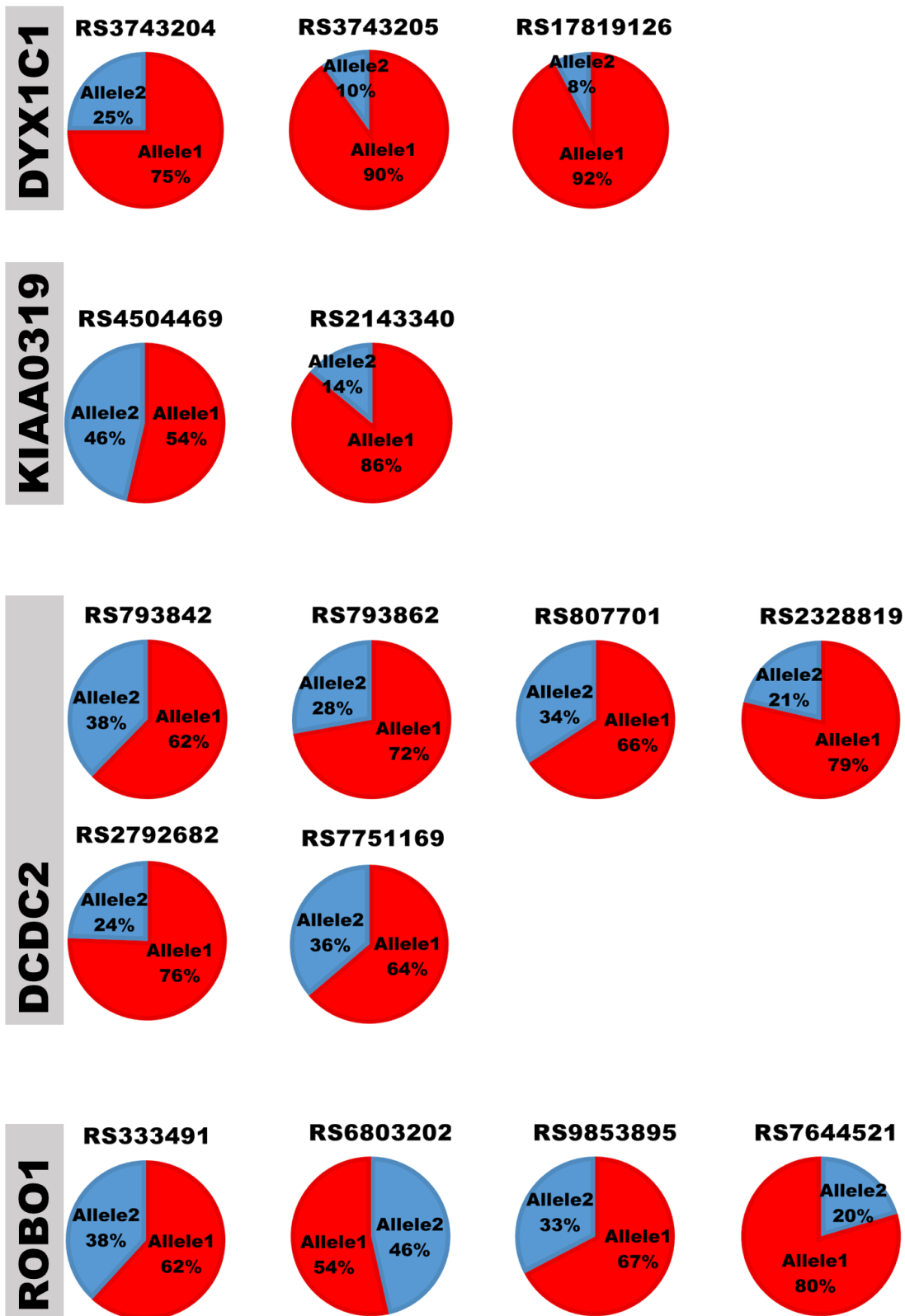
---

## 2.5 Genetics: Results

### 2.5.1 Allelic and Genotype Frequencies

*Figure 2-7A* and *Table 2-2* below show the allelic frequency of our sample for each of the SNPs to facilitate comparison with published databases of other British samples. *Figure 2-7B* shows the genotype for each SNP (expressed as a percentage of the total sample count, N).

A)



B)

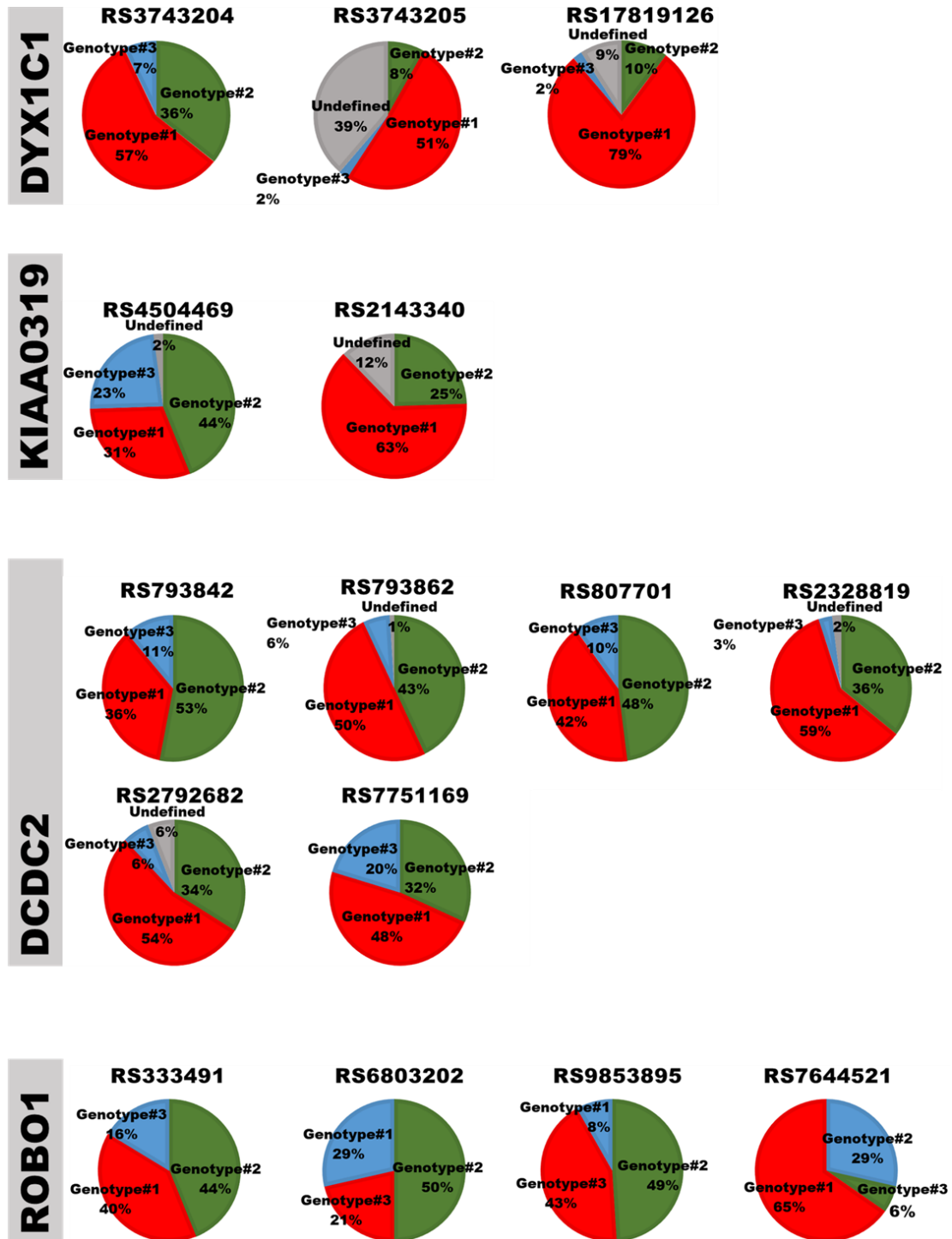


Figure 2-7. Allelic frequency (A) and genotype frequency (B) by SNP and gene in our sample. Genotype#1 was always heterozygous for allele 1 in these pie charts.

*Allelic Frequencies in Our Samples follow the Hardy-Weinberg Equilibrium*

In *Table 2-2* below, the allelic frequencies in our sample calculated via both the HW equation and as an actual percentage of alleles present per sample are compared against the allelic frequency of the known British populations as published in Ensembl and dbSNP. It can be first observed that the allelic frequencies for all SNPs in our sample match tightly the expected allelic frequencies according to the HW equilibrium. They also follow closely the previously reported allelic frequencies in other British samples of various sizes. It reassured us that our observations fall within the realm of expected frequencies, especially considering my little experience in performing genotyping.

*Table 2-2. Allelic distribution in our and other British studies by SNP. The final column gives the minor-allele heterozygous genotype frequency by SNP to help identify genotypes with insufficient number of infants for further analyses.*

GENE	SNP	1000 Genomes (GBR sub- population)	UKTWINs	ALSPAC	Allelic frequency (HW)	Allelic frq (actual)	Genotype#3
<b>DYX1C1</b>	<b>rs3743204</b>	84.6% (154)	78.9% (2821)	79.9% (3080)	75.59%	75.00%	7.14%
	<b>rs3743205</b>	97.8% (178)	94.0% (3361)	94.9% (3656)	91.29%	90.00%	3.33%
	<b>rs17819126</b>	94.0% (171)	93.4% (3388)	93.0% (3584)	93.01%	92.13%	2.25%
<b>KIAA0319</b>	<b>rs4504469</b>	50.5% (46)	59.0% (2109)	59.7% (2300)	55.90%	53.65%	23.96%
	<b>rs2143340</b>	85.2% (155)	84.3% (3013)	84.3% (3248)	84.91%	86.05%	0.00%
<b>DCDC2</b>	<b>rs793842</b>	63.7% (116)	61.5% (2370)	61.4% (2195)	59.76%	62.24%	11.22%
	<b>rs793862</b>	74.7% (136)	74.4% (2658)	74% (2852)	71.07%	72.16%	6.19%
	<b>rs807701</b>	66.5% (121)	66.2% (2365)	66.4% (2559)	64.68%	65.82%	10.20%
	<b>rs2328819</b>	72.5% (132)	75.4% (2695)	75.5% (2911)	77.73%	78.65%	3.13%
	<b>rs2792682</b>	78.6% (174)	78.4% (3020)	78.7% (2812)	75.90%	75.54%	6.52%
	<b>rs7751169</b>	62.6% (114)	65.3% (2515)	66.6% (2380)	69.25%	63.78%	20.41%
<b>ROBO1</b>	<b>rs6803202</b>	56.6% (103)	51.6% (1845)	50.2% (1934)	53.45%	46.43%	28.57%
	<b>rs7644521</b>	80.2% (146)	81.5% (2914)	82.5% (3180)	80.81%	79.59%	6.12%
	<b>rs333491</b>	61.5% (112)	55.8% (1994)	55.1% (2125)	63.08%	61.73%	16.33%
	<b>rs9853895</b>	61.0% (131)	60.9% (2176)	60.1% (2325)	65.47%	67.35%	8.16%

Table 2-2 also presents the frequencies of genotype#3 in the current sample to highlight any SPNs for which the incidence of the minor allele was lower than 5% and therefore not feasible for group analyses. The frequencies of genotypes #1 and #2 are depicted in the pie charts in Figure 2-7B above, as is the percentage of undefined samples per assay, for which the genotyping procedure did not work, and which partially contributed to the low incidence of genotype#3 for some of the assays.

Four SNPs of interest had a genotype#3 frequency lower than 5%: rs3743205 (3.33%) and rs1781926 (2.25%) on DYX1C1, rs2143340 (0% - note that (Neef et al., 2017) also excluded this SNP for insufficient number of samples) on KIAA0319, and rs2328819 (3.13%) on DCDC2. All four SNPs had missing values, which presumably contributed to the low incidence of genotype#3 (Table 2-3 below).

Table 2-3. Number of Samples for which the Genotyping Procedure did not work by SNP and Gene.

Gene	SNP	Missing Data
<b>KIAA0319</b>		
	rs4504469	2 nans
	rs2143340	12 nans; 2 genotypes only
<b>DYX1C1</b>		
	<b>rs3743204</b>	<b>none</b>
	rs3743205	37 nans
	rs17819126	8 nans
<b>DCDC2</b>		
	<b>rs793842</b>	<b>none</b>
	rs793862	1 nan
	<b>rs807701</b>	<b>none</b>
	rs2328819	2 nans
	rs2792682	7 nans
	<b>rs7751169</b>	<b>none</b>
<b>ROBO1</b>		
	<b>rs6803202</b>	<b>none</b>
	<b>rs7644521</b>	<b>none</b>
	<b>rs333491</b>	<b>none</b>
	<b>rs9853895</b>	<b>none</b>

*Table 2-3* demonstrates that in total, six SNPs had missing values for a variable number of infants: rs3743205 had 37 missing values; rs17819126 - eight; rs2792682 - seven; rs2328819 and rs4504469 has two each; and rs793862 had one. Missing values were primarily attributable to failure in genotyping due to noise while reading the fluorescence output in one or both samples genotyped in duplicates (the sample quality had to be above 97.5% for successful reading). The noisy samples could have been caused by several factors, most likely relating to either pipetting errors, or insufficient amount of blood (and therefore, DNA), or a combination of the two. Since we did not pre-amplify the samples as a part of the established protocol, we were not able to salvage low quantity samples which may have not had enough template DNA for all assays. Furthermore, due to limitations in time and resources, we were not always able to re-perform the genotyping procedure. None of the remaining eight SNPs, which were successfully assigned in all infants, had a genotype#3 frequency <5%, with the closest SNP to the cut-off - rs7644521 (6.12% on ROBO1).

For the two main studies describing the neuro-oscillatory effects in *Chapters 4* and *5*, we only tested the 8 remaining SNPs comprising the full dataset. This was done to allow for sufficient degrees of freedom and number of observations per condition in the respective statistical models tested.

### 2.5.2 Associations between the Familial and Genetic Risk of Dyslexia

None of the 8 SNPs assessed had a significant association with the infants' familial risk group (Kruskal-Wallis  $KW\chi^2$  statistics and p values are reported in *Table 2-4* below, all *n.s.* at  $\alpha=.05$ ). That is to say, in our sample, there was not enough evidence for a statistical dependence between the infants' familial risk of dyslexia and their genotype on any of the eight SNPs of interest across the three dyslexia susceptibility genes.

Table 2-4. Individual Chi-square statistics and significance level by SNP on the difference between the observed and expected distributions of infants' genotypes given their dyslexia risk status the null hypothesis.

Individual Chi-square Tests by Group: FamRisk(2) x Genotype(3)				
Gene	SNP	KW $\chi^2$	df	p
<b>ROBO1</b>	rs7644521	1.440	2	0.487
	rs9853895	1.238	2	0.529
	rs6803202	1.064	2	0.587
	rs333491	1.069	2	0.586
<b>DYX1C1</b>	rs3743204	4.886	2	0.087
<b>DCDC2</b>	rs7751169	1.517	2	0.468
	rs807701	5.218	2	0.074
	rs793842	5.127	2	0.077

Histograms demonstrating the distribution of the infants' genotypes across the eight remaining SNPs tabulated against their familial risk is shown in Figure 2-8 below.



Figure 2-8. Genotype Distribution by Familial Risk Groups of the Neonatal Infants.

---

## 2.6 Genetics: Discussion

### 2.6.1 Summary of Genotyping Results

There were no associations found in our sample between the SNPs of interest across the dyslexia susceptibility genes, and the cohort's familial risk of dyslexia. That is not to say that there is no association, as we were unable to test for that in the neonatal infants. It is possible that the link between the SNPs on the susceptibility genes tested and the likelihood of the infants to have a first-degree relative with dyslexia is not strong enough to be detected with our sample size (N=96). However, the genotypical and allelic distributions in our sample resembled those described in previous genotyping studies which gave us the reassurance that the genotype representation in our study fits that of larger British population reported previously.

Next, we used the genotyping results on the SNPs of interest as genetic risk factors in a candidate gene approach in two studies investigating the genetic and familial risk influences on the neonatal neuro-oscillatory processing of infant-directed speech.

### 2.6.2 Implications of the Infants' Genotypes on Studies One and Two

As reviewed before, previous research has connected several of the SNPs of interest in this study to neuronal speech processing deficits in dyslexic children and adults. For example, Czamara et al (2011) found a relationship between KIAA0319 and DCDC2 rare variants and a late MMN component to syllabic oddball stimuli in 8-19-year-old German dyslexic readers. The auditory MMN to minimal differences in syllables, which is the time-locked EEG marker of auditory oddball stimuli, was reduced in dyslexia susceptibility KIAA0319 and DCDC2 variant carriers (Giraud & Ramus, 2013). SNPs on the same genes have been found to predict a measure of the consistency of the auditory brain stem response to a syllable stimulus in pre- or literate children (Centanni et al., 2018; Liebig et al., 2020; Neef et al., 2017). Building upon these findings, we asked if there was an association between continuous neural-oscillatory response to the speech signal, and the genetic variation on the susceptibility genes in our sample of neonatal infants. Furthermore, we addressed the

link between the genotype and the sensor-space network connectivity metrics during infant-directed speech presentation.

We estimated the required sample size in addressing these questions based on previously published work reporting the variance explained in a continuous ABS response to syllable stimuli by the top three genetic risk components tested (Neef et al., 2017). We used the reported  $R^2$ , which ranged from 26.4-26.8%, as the closest approximation of the expected effect size of genotype in our studies. Thus, we expected a medium-sized effect of around 0.26-0.27 for the genetic risk factors introduced in this chapter. To identify a predictor for each of our oscillatory outcome measures (either the brain-to-speech phase synchrony, or the network connectivity) with a power goal of 0.9, based on the estimated medium effect size, a total sample size of between  $N=88-95$  was required. It is worth noting that although the studies are conceptually similar to the ones used for an effect-size reference, the use of different neural metrics, age groups and the distinction between familial risk and dyslexia diagnosis, these power calculations were only referential, rather than prescriptive.



# **PART TWO**

## **CHAPTER THREE**

### **COMMON METHODS**

## CHAPTER THREE: COMMON METHODS

---

### 3.1 Full Project Overview

The doctoral project spanned a longitudinal study that aimed to identify potential neural oscillatory response deficits in neonates associated with genetic and familial risk of dyslexia. The full longitudinal project identified neonatal neuro-oscillatory dyslexia risk related markers, and their associations with both familial and genetic dyslexia susceptibility. One-hundred infants (49 at high and 51 at low familial risk) were assessed at birth and half of those were followed up longitudinally at three additional timepoints: at 7.5, 15 and 23 months of age. We followed up the developmental trajectories of these infants on a multitude of neural, environmental, socio-emotional and phonological developmental measures. We tested their neural oscillatory response to the prosodic rhythm at the onset of the speech signal at birth and re-tested them again when the infants were 7.5 months and 15 months old. We additionally took control neural measures in the form of a resting state EEG recording, and an oddball ERP task (of which risk-related differences have been reported in the literature). Moreover, we evaluated the mediating effects of the early language environment that the infants were experiencing (in the form of a full-day home audio recording), the standard developmental indices of the infants and parental mood and traits, as well as the parent-infant language based social interactions on a variety of tasks increasing in complexity with age. Finally, we measured the infants' expressive phonological skills at the age of 21-23 months, as an early predictor of later dyslexia outcomes.

A schematic representation of the longitudinal setup is given in *Figure 3-1* below. In the focus of this doctoral dissertation is solely the report on a subset of data from the longitudinal study that aimed to identify potential neural biomarkers of dyslexia risk in neonates and to elucidate specific genotypes that are associated with these neural deficits (leftmost green panel in *Figure 3-1*). Only the neonatal data analyses, methods and results are reported in the following three chapters. A detailed description of the full longitudinal project with all collected measures and intended questions to address is provided in *Chapter 6*, and the relationship between the current report and the longitudinal study is discussed in *Chapter 7*.

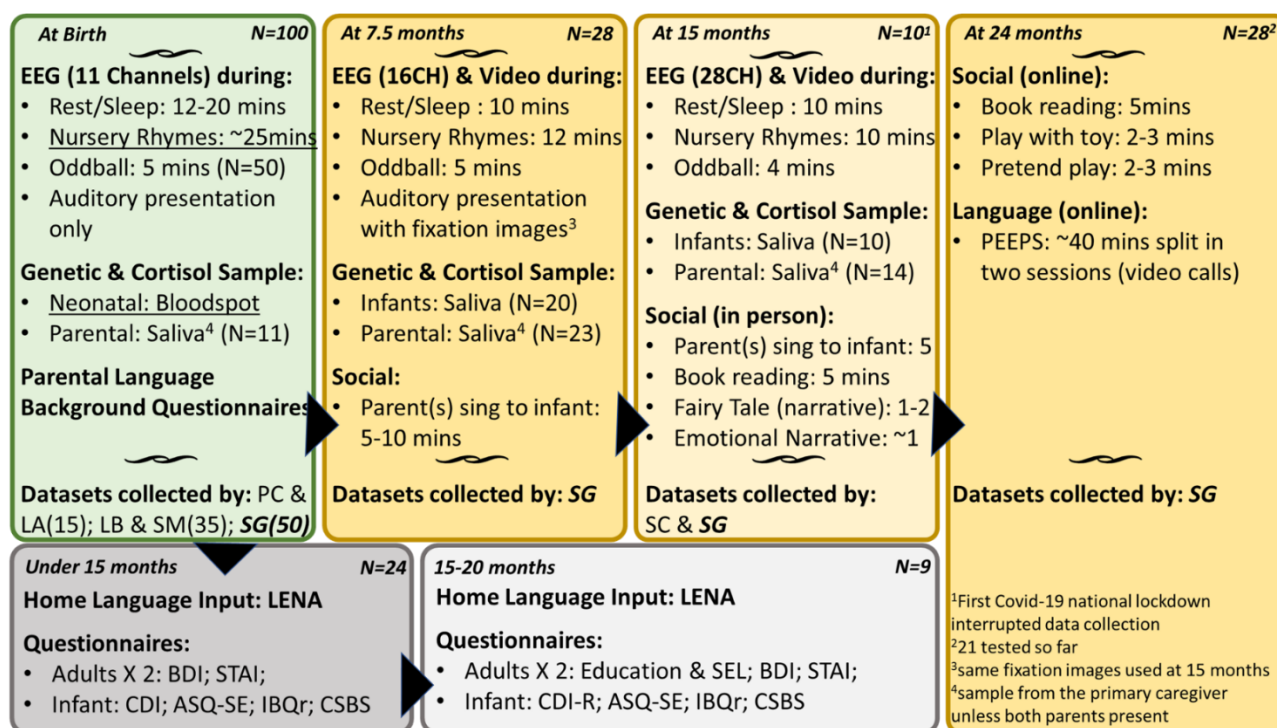


Figure 3-1. Overview of the data acquisition sessions and their progression in time. The top row presents the lab sessions, highlighting the features that change between sessions, the number of participants or samples per session, as well as the junior team-members who contributed towards the experimental design and data collection. The leftmost green panel singles out the session of focus for this dissertation, and the underlined tasks are those reported in the researched studies presented in Chapters 2 to 5.

## 3.2 Participants

A total of N=102 families with a new-born infant were recruited to take part in the study, and data from N=96 families were included in the final analysis. The final two infants were never tested as they were born in the period at the onset of the Covid-19 pandemic when all in-person research activities were suspended. One family withdrew consent before the full set of measures was completed. Three other families were subsequently deemed ineligible according to the selection criteria following complications with the infant. The data produced by those families were archived and were not further processed or included in any reports.

A total of 46 (24F) neonatal infants were at high and 50 (18F) at low familial risk of dyslexia. Infants at high familial risk of dyslexia were identified from families with at least one dyslexic parent (34 with confirmed diagnosis where one infant has two dyslexic parents, 12 self-reported). Control neonates were recruited from families with no history of dyslexia. For both high-risk and control low-risk groups, the families were screened for other developmental or learning disorders (e.g. autism, ADHD, dyspraxia, dyscalculia) in the infant's first-degree relatives and excluded if any were present. There were four pairs of fraternal twins in our sample, two pairs were at low risk and two pairs were at high risk.

The recruitment of the families for this PhD projects was done as a part of a longitudinal study, which is detailed in *Chapter 6* and its timeline is schematically presented in *Figure 3-1*. Only the dataset acquired during the *At Birth* panel (top leftmost green panel in *Figure 3-1*) are reported in this dissertation. Following the brief outline here, a more comprehensive description of the participating families and the recruitment process is given in *Chapter 6.1*.

---

### 3.3 Materials

This dissertation reports the initial section of a longitudinal project that ran throughout the course of my entire PhD program and is described in more detail in Chapter 6. The materials and methods reported in the following four chapters were retested with small variations three times within the first 1.5 years of life in our cohort of infants (schematic representation of the used materials by data-collection session is shown in *Figure 3-1*). The materials reported in this dissertation are outlined in the green (top leftmost) panel of *Figure 3-1* and are underlined for clarity.

#### 3.3.1 Nursery Rhymes

Fifty-eight NR stimuli were taken from a published corpus (Leong & Goswami, 2015) of strongly rhythmic infant directed speech (IDS) spoken verses in order to elicit strong neuronal entrainment to the temporal modulation patterns in IDS (Leong & Goswami, 2015). Nursery rhymes were 16.78s in duration on average (SD = 7.77s) and included familiar rhymes such as *Mary had a little lamb*, *Incy wincy spider*, and *The wheels on the bus*

*go round and round*. The full list of stimuli and their durations is provided in *Appendix III.III*. All NRs were narrated by one of six native British female speakers (21 NRs were produced by two speakers). The presentation of the NRs was counterbalanced across participants in three pseudorandomized orders. The volume of all the NRs was equalized to an average of 60dB using the sound processing software Praat (Boersma, & Weenink, 2016).

For the analysis of both the PLV and GPDC scores, we only used nursery rhymes in a duple meter – that is, nursery rhymes for which every phrase (prosodic stress foot) consisted of two syllables, one stressed and one unstressed. Thirty-nine of the 58 recorded nursery rhymes (those were 24 NRs over 6 speakers, see *Appendix III.III*) in our experimental battery had a duple meter, so that was the highest number of onset trials that each infant in the datasets for both studies could contribute to the subsequent analyses.

For each NR, we determined its syllabic rate in order to test the infants' neuro-oscillatory entrainment to the prominent carrier frequency in the speech envelope (Goswami, 2011; Greenberg et al., 2003; Leong, Kalashnikova, et al., 2017; Leong & Goswami, 2015; Ortiz Barajas et al., 2021; Thwaites et al., 2015). There were twofold reasons for using the syllabic frequency. The theoretical background reviewed in the introductory chapter suggested that because they help them parse the more complex acoustic information, infants would preferentially track the slow amplitude modulations in the human speech, normally falling in the delta-theta range (2-4Hz) and corresponding to the syllabic or prosodic pattern. The nursery rhymes used here fell in the IDS register, their modulation frequencies were slower than normal adult speech, and their syllabic rates were taken as their most prominent modulating frequencies. The second reason for focusing the analyses on the syllabic rate of the nursery rhymes was more practical: as we estimated that the measured between risk-groups effects would have a small-to-medium effect sizes, we chose to concentrate on the most prominent feature of the speech signal, that both befitted the theoretical rationale, and optimised our chances of detecting the group effects of interest.

The syllabic frequency of a NR was determined by the syllable presentation rate within one second of speech. The IDS had lower syllabic rate than normal adult speech. Here, the syllabic rate of the NRs was derived by dividing the total number of syllables (stressed or non-stressed vowels or consonant-vowel combinations) in the NR recording by the

duration of the speech in seconds. The NRs differed slightly in their peak syllabic rate, with a range between 2.2-3.9Hz, and an average (and median) of 3.1Hz (SD=0.47Hz).

### 3.3.2 Calculating the Hilbert-Envelope (baseband) of the Speech Signal

The speech amplitude envelope for each nursery rhyme was extracted to estimate the high-power slow-frequency carrier waves in the IDS signal. The speech Hilbert envelope was used in both studies to calculate the power in the frequencies that matched the closest the syllabic rates of the presented nursery rhymes. The neural entrainment and coherence indices were then calculated in the same frequencies and tested on how well they tracked the carrier amplitude modulations.

First, the digital auditory signal for each nursery rhyme was Hilbert-transformed to extract the complex envelope of the analytic signal of the speech. The advantage of the Hilbert transforms was that the resulting complex analytic signal had the same power values and frequency characteristics as the original real timeseries, and it allowed for the calculation of the instantaneous amplitude and frequency for the real timeseries. Thus, we got the frequency information in the time domain, and the absolute magnitude of the analytic signal was the complex envelope of the real timeseries.

The Hilbert transformation process converted the real timeseries of the speech signal into a complex signal representation by rotating it in the frequency domain by 90° from the real into the imaginary plain. The rotation was counterclockwise for positive frequencies under the Nyquist frequency and was equivalent to multiplying the positive complex frequency spectrum by  $*-i$ . The rotation was clockwise for the negative frequencies, or equivalent to  $*i$ . In this way, we could rotate orthogonally between the real (cos) – imaginary (sin) axes for each frequency in time (i.e.  $\cos wt \rightarrow \sin wt \rightarrow -\cos wt \rightarrow -\sin wt \rightarrow \cos wt$ ). In the time domain, this procedure was essentially a filter that shift the phase of the composing oscillations by  $\frac{1}{\pi t}$  without modifying their amplitude.

In Matlab, the Hilbert transform was computed as an orthogonal shift in the frequency domain. In the first step, the real timeseries data were transform from the time to the frequency domain by applying the discrete Fast Fourier Transform (FFT) to the real timeseries input, or a point-by-point convolution in time of the real signal with a series of complex sinewaves with amplitude  $A$  and frequency  $f$ , represented by the exponential formula:

3- 1

$$S = Ae^{-i2\pi ft}$$

The product of the convolution between a complex sine function above and the real signal was a complex FFT representation of the real signal in the frequency domain, or:

3- 2

$$FFT(f) = \sum_{t=1}^n \cos(\theta) + i \sin(\theta) = \sum_{t=1}^n x_t e^{-i2\pi f(t-1)n^{-1}}$$

$n$ =total number of data/time points,  $0 < f \leq$  Nyquist frequency;  $x$  was the real timeseries.

The resulting FFT coefficients consisted of two complex sinewaves (complex exponents) of equal amplitude travelling through the polar space in opposite directions. The positive frequencies travelled in the counterclockwise direction, and the negative travel clockwise. The real part of the FFT coefficients related to the power at each frequency, whereby the magnitude of the oscillation was given by the absolute magnitude of the complex signal.

3- 3

$$M = |\cos(\theta) + i\sin(\theta)| = \sqrt{\cos(\theta)^2 + \sin(\theta)^2}$$

Although the FFT readily provided the power spectra in the frequency space, it offered no time varying frequency information as the convolved sine waves had constant power throughout the entire oscillation  $(-\infty$  to  $+\infty)$ . As the FFT was a linear transform, it allowed for reverting between the time and frequency domains without any information loss, but it did not allow for frequency information in the time domain. To this aim, the Hilbert transform was used.

In the Hilbert transform, the complex FFT spectra were shifted by 90° at each frequency along the real-imaginary quadrature to get the Hilbert transform at that frequency.

Practically, in Matlab this was achieved by doubling the complex polar representation of the positive frequencies and nullifying the negative ones. As previously described, this was equivalent to multiplying  $i$  in the imaginary part of the complex number by  $-i^*i(=1)$  or  $i^*i(=-1)$  and adding those to the original positive and negative FFT coefficients, respectively. The direct current (i.e the zero) and Nyquist frequencies were left untouched. The sum of the original signal and its Hilbert transform were referred to as the analytic signal.

The analytic signal was then the complex signal produced by taking the original signal and adding its Hilbert transform. As the Hilbert transform was derived by shifting the original signal by 90°, the two components are orthogonal to each other.

3- 4

$$g(t) = \cos(\omega t) + i \sin(\omega t) = e^{i\omega t}$$

$$\omega = 2\pi f_c$$

$f_c$  are the carrier frequencies of the real timeseries input.

Therefore, the analytic signal can be reduced to a complex exponential whose frequency spectrum had an entirely positive domain. The inverse FFT (iFFT) was next applied to the complex exponent to transfer the analytic signal from the frequency back to the time domain. The analytic signal in the time domain was still a complex number.

Both components of the analytic signal had the same amount of energy because the Hilbert transform bore no effect on the amplitude of the original signal. However, they were in orthogonal phase to each other, and the phase changed periodically. The amplitude of the analytic signal was the instantaneous amplitude of the real signal in the time domain.

Although the Hilbert transform was more easily computed in the frequency domain, the Hilbert-envelope was derived in the time domain. Therefore, the complex envelope of the speech timeseries was the modulus or the complex magnitude of the analytic signal, that is the magnitude of the vector from the origin to the value of the analytic signal in the complex plain (for completion: the phase was given by the angle between the complex vector and the positive real axis in radians; and the rate of change in the phase angle was

the instantaneous frequency of the timeseries). The complex envelope, or the Hilbert-envelope, was therefore:

3- 5

$$|G_r + iG_i| = \sqrt{G_r^2 + G_i^2}$$

$G_r$  and  $G_i$  are respectively the real and imaginary part of the analytic speech signal in the time domain.

Finally, the complex envelope of the speech signal as derived here was down-sampled to 250Hz to match the EEG sampling rate.

### ***Calculating Instantaneous Phase Series of the Speech Envelope and the EEG traces***

In the next step, the phase-locking values between the speech and the neural signals were calculated. The phase angles for both the Hilbert-envelope timeseries of the speech signal and the NR-evoked EEG onset epochs, were derived using a complex Morlet wavelet decomposition. The complex Morley wavelet function was a complex sine wave passed through a Gaussian kernel, according to:

3- 6

$$S = Ae^{-i2\pi ft} e^{\frac{-(t-m)^2}{2s^2}}$$

but as the mean  $m=0$  for the Gaussian kernel, then

3- 7

$$S = Ae^{-i2\pi ft} e^{\frac{-t^2}{2s^2}}$$

As the power of the oscillation decayed towards the edges of the wavelet, the complex wavelet transform of the real timeseries allowed for the extraction of information about time-varying frequency features of the real signal (as did the Hilbert transform).

The complex wavelet transform (cwt function in *MATLAB*) made use of a prototype wavelet function referred to as mother- or analysis-wavelet. The mother-wavelet used here ('cmor1-0.1') was a complex wavelet with a bandwidth  $Fb$  of 1Hz and a central frequency

$F_c$  of .1Hz. The bandwidth was a speed-of-decay parameter in the time domain and the inverse of the variance in frequency in the frequency domain. Increasing  $F_b$  narrowed the frequency spread of the wavelet around the central frequency while in the time domain it slowed down the decay of the wavelet. The multi-frequency resolution of the wavelet function was achieved by scaling and shifting the mother-wavelet via changing the time-varying index  $t$  in the wavelet function above by a scaling factor  $a$  and a shifting factor  $d$  according to

3- 8

$$t = \frac{t - d}{a}$$

The scaling factor  $a$  was inversely proportional to the frequency  $f$  with a constant of proportionality equal to the  $F_c$  of the mother wavelet. Thus, the scaling factor was related to how stretched or compressed the analysing wavelet was, with high scaling factors stretching the wavelet more. High scaling factors were therefore more suited for detecting the lower frequencies in the real signal. The shifting factor  $d$  was not related to the central frequency  $F_c$ . Here, we input the scaling vector  $a$  for different  $F_c$ , while for the shifting  $d$ , the built-in default in the *cwt* in *MATLAB* was used.

In the next step, the derived series of complex 'daughter' wavelets were point-by-point convolved with both the speech envelope (derived above), and the EEG timeseries. Here, each EEG channel represented an independent timeseries. As in the Hilbert transform described earlier, the result of the convolution between the complex wavelet and the real timeseries signal was a complex polar vector (or a complex exponent) in the frequency domain.

Similar to the Fourier and the Hilbert transforms, the real part of the wavelet convolution coefficients amounted to the frequency power spectrum, and power spectrum was symmetrical, i.e. the amplitudes in the positive and the negative frequencies were identical. As before, the power per frequency was equivalent to the absolute magnitude of the complex number (i.e. that is also the length of the vector in the polar space). The phase series of the frequency spectrum were derived by taking the angle in radians between the positive real axis and the complex vector, for both the speech envelope and the EEG traces.

---

## 3.4 Experimental Protocol

The experimental design, preprocessing steps and main hypotheses are outlined in *Figure 3-4* below.

### 3.4.1 Genetic Data Collection

*Genetic Sampling:* To perform genotyping, blood spot samples were collected from each infant a Guthrie card, using a standard heel lance technique (Saavedra-Matiz et al., 2013

Please see Chapter 2 for description of genetic data analysis.

### 3.4.2 EEG Data Collection

#### *EEG Acquisition Environment*

The EEG experimental testing was conducted onsite at the neuroimaging facilities within the Rosie Maternity Hospital (CUHs). The infant had his/her head circumference measured either by a midwife on the ward, or by the experimenter, and then an appropriate EEG cap was fit on the infant's head for the duration of the experiment. The infant was then swaddled and laid on the pre-warmed up bassinet of a Panda Resuscitation trolley with the lights dimmed to encourage a restful state (*Figure 3-2*).

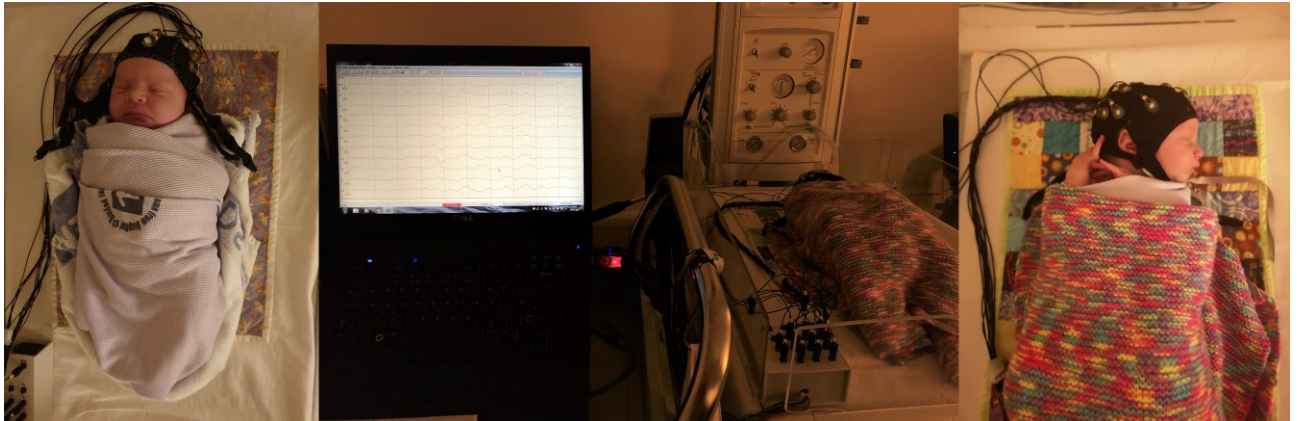


Figure 3-2. EEG data acquisition set up. All images were provided by the parents and parental consent was given for their use.

### ***EEG Acquisition Parameters***

EEG was recorded at a sampling rate of 250Hz in 11 active electrodes using a V-amp amplifier and BrainVisionRecorder software (BrainProducts GmbH, 2013) running on a Dell Latitude 5500 laptop with an operating system (OS) of Windows7 Enterprise (Figure 3-1). TEN20 (12.5% NaCl content, 2.15 molar NaCl; D.O. Weaver & Co, Colorado, USA) conductive and adhesive paste was applied to each ring electrode prior to fitting the cap on the infant's head. Impedance was brought down to below 20kOhms in all EEG recordings; however, impedance rarely exceeded 4kOhms in any given channel. The channels were located on the standard 10-20 montage, with a location between F7 and C3 used for common grounding, and Cz was used as an online reference (Figure 3-3). The Cz reference was retained in all the subsequent analyses.

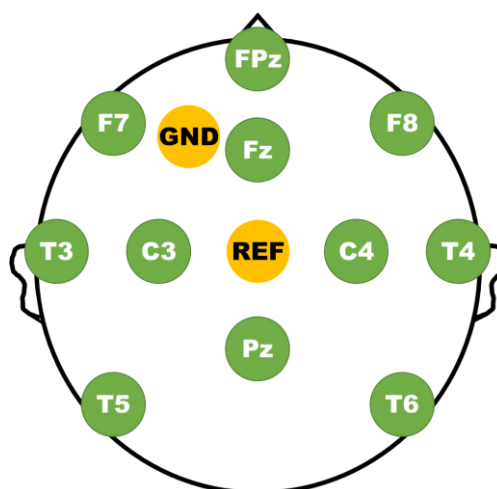


Figure 3-3. EEG montage: EEG channels are shown in green, and their reference (Cz) and common ground are shown in yellow.

### *Nursery Rhyme Task*

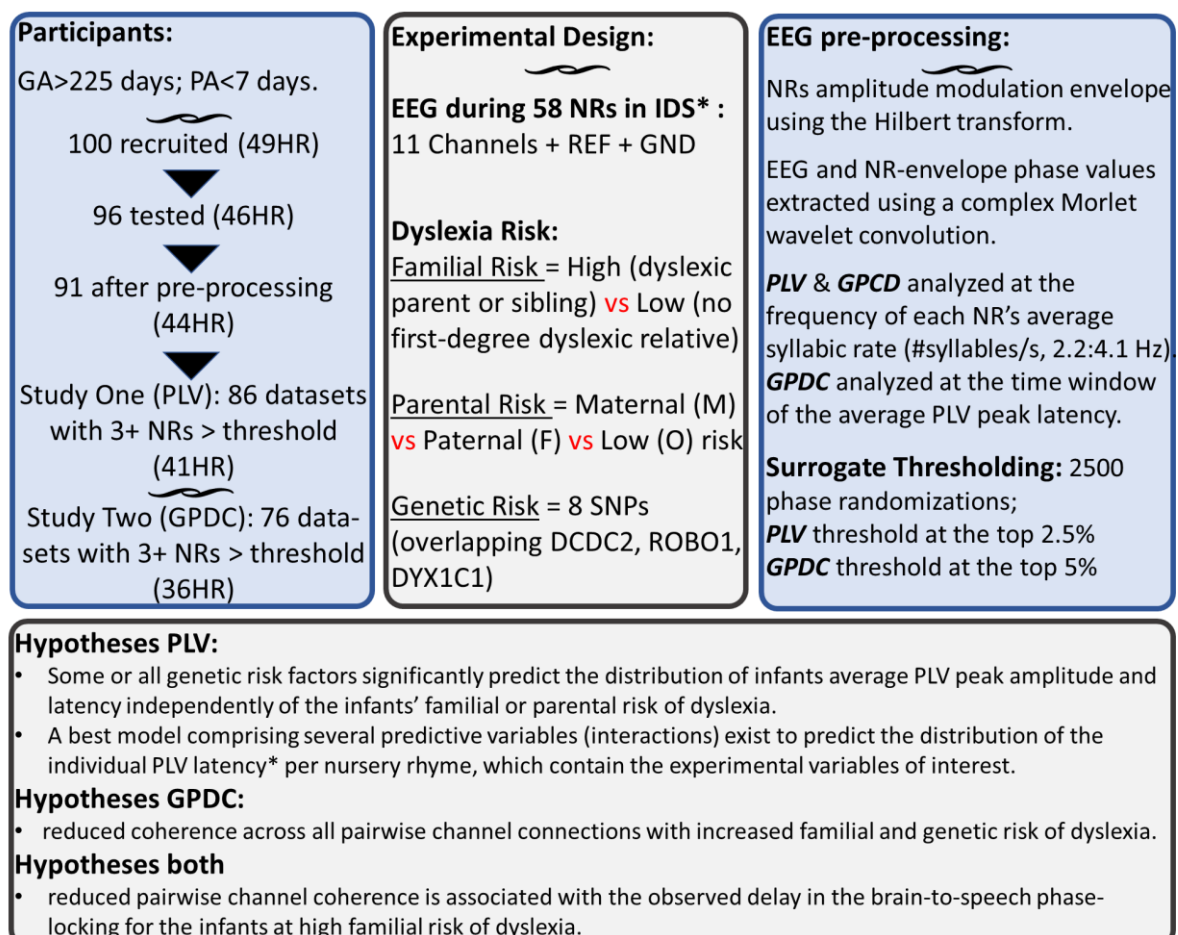
After ensuring that the infant was calm and settled, the nursery rhymes were played one at a time through Logitech Z150 speakers connected via an extension jack to the stimulus presentation laptop (Lenovo AMD A10 Radeon R6 with Windows 8.1 OS, 8GB 64-bit outputting at 1.9GHz). The speakers were mounted on tripods and positioned at either side of the trolley levelled with the infant's head, about 35cm away from the infant's head. The output volume of the nursery rhymes measured at the position in the cot where the infant's head lied was at a sound level of 59.8 dB at the presentation laptop's volume set to 5%. The total duration of the task was 45 minutes on average per infant, depending on the length of the movement breaks taken in between the NRs. Not all infants completed the full session, with seven infants completing fewer than 50 NRs, three of who completed fewer than half. Thus, the total EEG recording time lasted between 45-60 minutes per infant. The experiment was delivered via Presentation (Neurobehavioral Systems; first 50 participants), or *MATLAB* 2015b (Mathworks; last 50 participants) software. A digital triggering system was used to communicate between the stimulus-presentation and the EEG-acquisition laptops, thus keeping any potential hardware induced timing delays in the EEG stimulus onset markers constant.

In around 30% of the neonatal EEG recordings, a delay was present between the auditory stimulus onset and the marker of the EEG recording's timestamp. The average delay was estimated to be of around 49ms (ranges between 37-56ms) and was suspected to be present in at least 30 infants. After the presence of a delay was established, a series of systematic tests were performed on the stimulus presentation script in *MATLAB*, as well as on the hardware running the experiment. This was achieved by using an auxiliary device which measures with a millisecond precision the time-delay between the stimulus being loaded in the auditory buffer memory channel and the actual onset of the auditory output, relative to the command line sending the trigger stamp to the EEG acquisition apparatus. The auxiliary device was generously lent to us by a neighbouring lab. After the delay was confirmed, the stimulus presentation coding sequence in *MATLAB* was updated to optimally minimize the delay. The subsequent systematic tests confirmed that the delay with the updated sequence had an average of 2ms (0-4ms range).

As the delay for each individual recording could not be estimated retrospectively, we addressed this issue by removing the 60ms time-window around the recorded stimulus

onset from the analyses. We acknowledge that the lower timing precision in 30% of the recordings means a lower precision in connectivity calculations, especially when testing for the phase of the oscillations and we discuss the implications further in *Chapter 7*.

Finally, in 16 neonatal recordings, one or more nursery rhyme stimuli did not run until the end. They were either accidentally cut short due to an experimental error, or due to an urgent situation with the infant which required an immediate interruption of the experimental procedure. In the cases where nursery rhymes did not play until the end of the auditory vector, the last recorded second of the corresponding EEG episode was removed, thus making the EEG epoch time-locked to the nursery rhyme one second shorter. If the resulting EEG epoch was shorter than a continuous total of two seconds, that epoch was fully removed from all further analyses.



\*only PLV latency tested as PLV amplitude was not predicted by any of the tested variables.

Figure 3-4. A schematic representation of the experimental design and operational definitions, preprocessing steps and hypotheses.

## 3.5 EEG Data Pre-Processing

The recorded EEG signals were imported and pre-processed in *MATLAB* 2017-2020b (MathWorks). Continuous raw data (the example shown in *Figure 3-5* had a visual notch-filter applied for the 50Hz line-noise) were band-pass filtered between 0.2-40Hz and segmented from one second before the start of each NR to its end. Segmented data were next visually inspected for noise and artifacts, and noisy sections were manually rejected, as described in the following section.

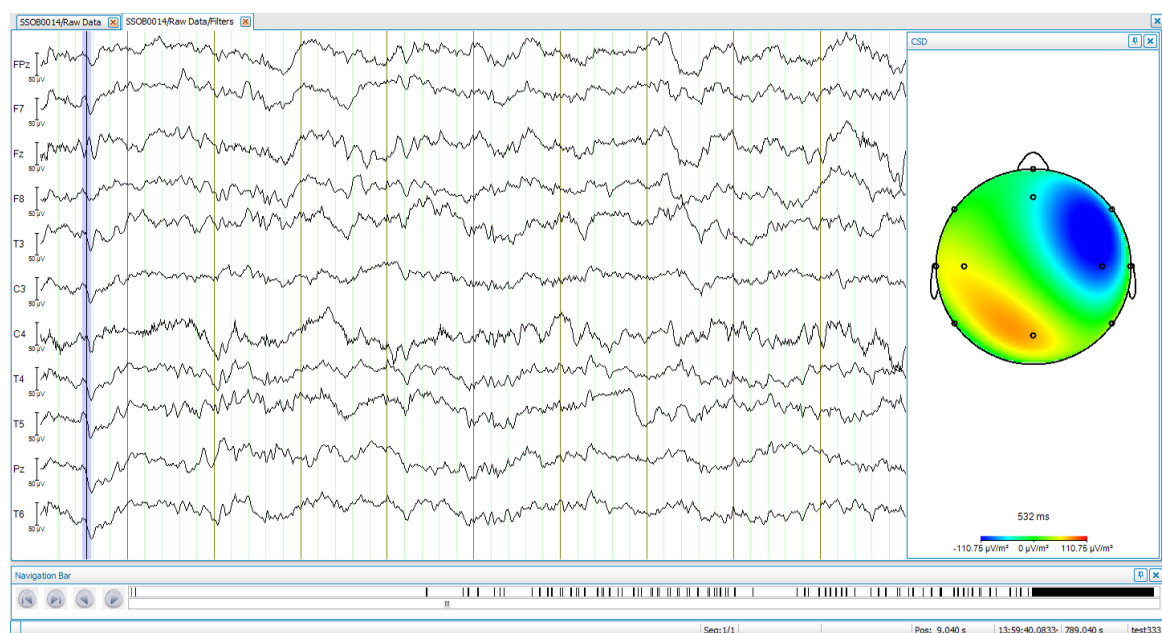


*Figure 3-5. Raw neonatal EEG for an example infant.*

### 3.5.1 Artifact Rejection: Common Rejection Strategies for Studies One and Two

For the two studies describing the brain-to-speech phase-locking and the network coherence analyses in *Chapters 4* and *5*, respectively, only the initial 2.5 s of each nursery rhyme were used. The nursery rhyme segments were epoched from 200ms prior to the NR onset to 2.5s in the stimulus presentation. For each infant, the thus created 58 epochs of 2.7s in length were saved as an individual dataset in the EEGLAB compatible format (*.set* and *.fdt*).

Next, the onset segment of every NR in the infant's dataset was visually inspected for general noise and movement-related artifacts.

### ***Epoch-Level Rejection***

To retain the maximal amount of data, data rejection was performed at the individual channel level for each epoch. That is if noise was present in one or more channels in an epoch, only those channels were rejected for that epoch. In rare case, this happens when a very small eye-blink was localised in the frontal channels only, or when a channel temporarily lost contact with the skin and resulted in a temporary localised increase in noise impedance, for example. More often, however, there was noise in specific channels only when the infant's head tilted momentarily to one side as the channels on that side were affected by the pressure of the head on them, while the rest of the channels remained unaffected. Another example was if the infant happened to wiggle their arm out of the swaddle and briefly touch an electrode before they were swaddled back in the break between the nursery rhymes. In 41 of the infants, one or more channels ( $M=2.22$ ,  $range=1:5$ ) were noisy in four or more NR epochs. An example for channel rejection in a single nursery rhyme onset epoch is given in *Appendix Figure III-1*.

The full NR epoch was rejected if it had fewer than three noise-free channels remaining. The most common reasons for epoch rejection included blink-like activity that affects most channels despite being most prominent in the four frontal channels; movement/muscle-related activity; head movements, gentle spontaneous and sporadic suckling behaviours; and occasionally the poorer fit of the EEG cap around the ear-lobe areas, or the mechanical/equipment related noise artefacts described in *Appendix III*. An example of an entire nursery rhyme onset epoch marked for removal is given in *Appendix III.I, Figure III-1* (fifth trial in the top panel, marked by a red down-facing arrow). On average, the infants contributed  $M=41.26$  ( $SD=10.99$ ,  $range=5:57$ ) clean NR onset epochs after artefact rejection. A full list of NR epochs and channels rejected by individual infant is included in *Appendix III.II*

### ***Participant-Level Rejection***

The entire infant's dataset was rejected if they had all channels noisy or had fewer than five epochs with more than three channels retained. The recordings derived from five infants

did not fit those criteria therefore did not contribute enough useable data to be included in further analyses (*Appendix III.II*).

---

### 3.6 Speech-Brain Phase-Locking & Neural Coherence Calculations

We used two measures of connectivity to meet the study aims defined at the end of *Chapter 1*: the phase-locking value (PLV - a non-directed measure) was used to compute brain-to-speech connectivity; and the general partial directed coherence (GPDC) was used to compute within-brain network connectivity. Thus, the PLV metric helped us estimate the group differences in neural oscillatory tracking of the prominent features of the speech signal, whereas GPDC was used to measure the neuro-oscillatory network capacity in the dominant speech frequency.

The time-lagged PLV and GPDC connectivity estimates were calculated in 2s sliding windows with a 40ms offset, starting at 200ms prior to stimulus presentation, and ending at 2.5s post stimulus onset, producing 18 overlapping subsamples (voxels) of the [-0.2 2.5ms] time-window around the onset of the nursery rhymes (*Figure 3-6* below). Both connectivity analyses were done in the frequency of the syllabic rate of the nursery rhymes which ranged between 2.2-3.9Hz, as described in *Section 3.2.1*. Hereafter, the phase angle series included in the analysis were the phase angle series for the frequency closest to the syllabic rate of the analysed nursery rhyme only.

The PLV onset peaks were operationally defined as at least three consecutive 40ms-spaced moving windows of 2s for which the PLV was higher than the pre-defined surrogate threshold. The rule of three time-voxels was applied to ensure that the detected effects over the threshold were not due to a sporadic spike in the PLV measure for that time window but rather a reliable trend of increased phase-locking of the neural to the speech signal. As the nursery rhymes presented to the infants had a stable frequency and amplitude signatures throughout the initial 2 seconds of recording, it was expected that the peak phase-locking should have a briefly sustained rather than a spiking profile. The PLV onset peak's strength and latency were defined as the value and timing of the highest of the first cluster of three-or-more post-onset PLV time-voxels above threshold (*Figure 3-6*).

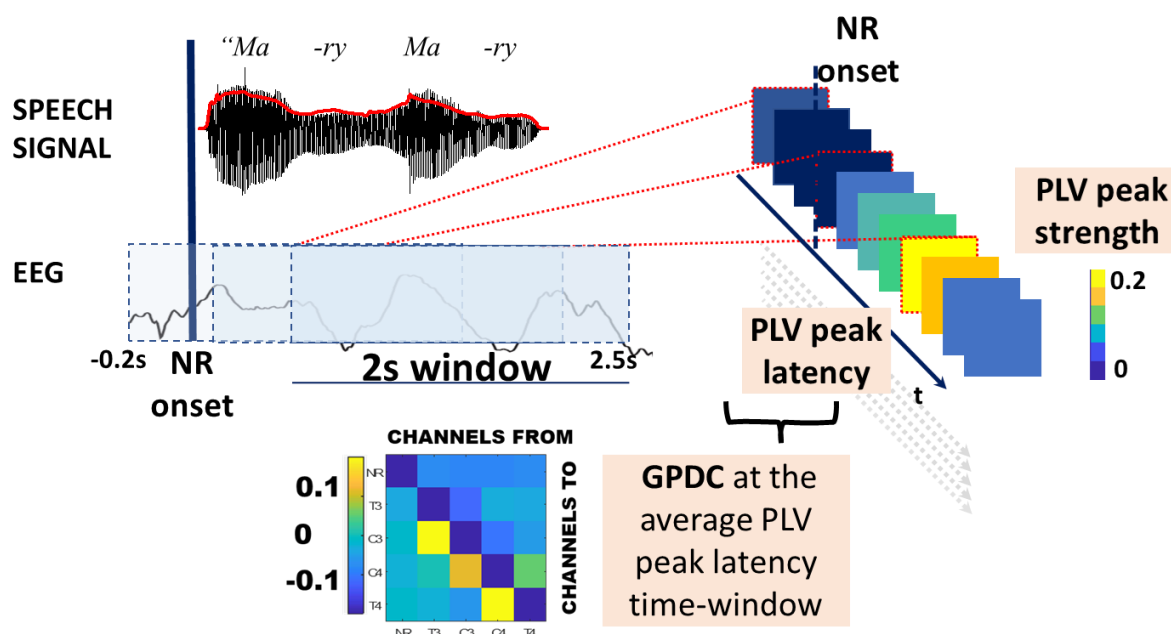


Figure 3-6. Calculating the PLV onset peak and its latency: the EEG signal was aligned to the speech signal and PLV was calculated for a moving window of 2s (with a 40ms offset). The PLV peak strength was given by the highest PLV value among the first occurrence of three (or more) consecutive values above threshold. The PLV peak latency was given by the timing of the highest value. The average PLV latency over all infants was used as the onset of the 2-second time-window in which GPDC was calculated between the four participating channels and between the channels and the NRs. The speech signal waveform representation here was modified from (Leong & Goswami, 2014b) DOI: 10.3389/fnhum.2014.00096.

Based on the PLV time-lagged connectivity time-series, an optimal time-window was identified in which to perform the further GPDC analysis. This corresponded to the median latency at which peak PLV connectivity was reached across infants (In Figure 3-6, this would correspond to the PLV peak latency time marker, for which the median was taken across all nursery rhymes and infants), indicating a maximal response in infants' neural phase locking to the speech envelope or 'speech onset response' (Leong & Goswami, 2014a; Lizarazu et al., 2020; Mahmoudzadeh et al., 2013; Power et al., 2013) for an optimal coherence alignment. Although the latency of the PLV peak was expected to differ between individual infants and between nursery rhymes, not all infants contributed to both analyses, and if they did, they did not necessarily contribute the same nursery rhymes to both analyses. Therefore, it was not always possible or practical to calculate the GPDC matrices in the latency time-window of the individual PLV onset peaks, and so the median latency was used instead.

### 3.6.1 Calculating the Phase-Locking Values between the phase angle series of the speech envelope and EEG

The phase-locking value (PLV) between the speech envelope and the EEG timeseries was given by the difference between their phase-angle series in the frequency domain. Thus, for each channel at the syllabic frequency of interest, PLVs were calculated according to the formula:

3- 9

$$PLV_{i,j}(t) = \frac{1}{N} \cdot \left| \sum_{n=1}^N e^{i(\varphi_i(t,n) - \varphi_j(t,n))} \right|$$

where  $N$  was the total number of epochs,  $n$  was the current epoch at time  $t$ , and  $\varphi_i$  and  $\varphi_j$  were the phase angles of the EEG and the speech envelope, respectively, measured in radians.

The phase-locking value varied between [0:1] with higher values indicating stronger synchronisation between the phase series derived from the complex envelope of the speech signal and EEG timeseries.

### 3.6.2 Calculating the Generalised Partial Directed Coherence between channels during speech presentation

GPDC was calculated between the brain and the speech signals in the syllabic frequency of each NR. GPDC is a Granger-causality based measure of the degree of predictability between the spectral estimators of one continuous signal (here, EEG channel or speech envelope) by another in a multivariate autoregressive model (MVAR), allowing for instantaneous effects. Only channels T3, C3, C4, and T4, were included in the GPDC calculations here. EEG epochs which had channels T3, T4, C3 or C4 removed were not included in the GPDC calculations, as using fewer channels would change the structure of the causal autoregressive model, leading to unmatched data across participants. A more detailed account of selection criteria for the four-channel network is described in *Chapter 5*.

Here, GPDC was calculated between on the complex morlet wavelet transform of the voltage values of four EEG channels (T3, T4, C3 & C4) and the Hilbert-transformed amplitude envelope of the speech signals. For each NR, the five signals (4 x EEG channels and 1 x speech envelope) were described as multivariate time-series processes with instantaneous effects as:

3- 10

$$Y(t) = \sum_{k=0}^p A(k)Y(t-k) + W(t)$$

Where  $k$  was the lag between the processes, starting from 0 to the model order  $p$ ,  $A$  was the positive square (5x5) covariance matrix of model parameters, and  $W(t)$  was the estimated zero-mean uncorrelated white noise diagonal covariance matrix so that  $\Lambda = \text{diag}(\lambda^2) = \text{cov}(W(t))$ .

The spectral version of the extended multivariate model given by the FFT of the time-series signals above was then:

3- 11

$$Y(f) = A(f)Y(f) + W(f)$$

Where the frequency-domain model parameter matrix was defined as:

3- 12

$$A(f) = A(0) + \sum_{k=1}^p A(k)e^{-2\pi i f k \Delta t}$$

Using the spectral model coefficients, the partial directed coherence between two signals  $i$  and  $j$  was given by the equation in (Faes & Nollo, 2011):

3- 13

$$X(f)_{i \rightarrow j} = \frac{\frac{1}{\lambda_i} A_{ij}(f)}{\sqrt{P_{jj}(f)}}$$

where  $P_{jj}(f)$  was the  $jj$  element in the inverse spectral matrix  $P(f) = \underline{A}^H(f)\Lambda^{-1}\underline{A}(f)$ ; therefore:

3- 14

$$X(f)_{i \rightarrow j} = \frac{\frac{1}{\lambda_i} A_{ij}(f)}{\sqrt{\sum_{m=1}^M \frac{1}{\lambda_m^2} |A_{mj}(f)|^2}}$$

$[m_0 .. M]$  are the elements in the diagonal matrix, and  $m_0=i$ .

In study two, we only reported GPDC values in the direction of speech signal toward the four EEG channels, as it was not possible for infants' EEG to have influenced the pre-recorded speech signal. However, the full GPDC matrix was calculated in both directions for quality control purposes, and described in *Appendix V.II*.

---

### 3.7 Surrogate Baseline Control Analysis

As spurious connectivity within and between oscillatory systems can occur or be measured at the scalp-level, especially for sparse networks (Deuker et al., 2009; Santamaria et al., 2020) and as higher power (amplitude) in the oscillations can in some cases drive higher phase connectivity metrics between them, the calculated connectivity metrics were baselined-corrected using surrogate data generated via random phase permutation.

The surrogate EEG datasets were used to calculate a surrogate distribution of randomised phase connectivity values (surrogate PLV and GPDC) and threshold the original PLVs and GPDC scores against those randomly distributed phase-surrogates. The same phase permuted surrogate EEG data series were used for calculating both connectivity metrics. However, the thresholding applied against the surrogate PLVs distribution was stricter than that applied to the GPDC values as the original phase-locking values were noisier compared to the calculated directed coherence metrics. The different thresholding approaches were elaborated in the respective chapters for studies one (PLV) and two

(GPDC). Here, the common methods for calculating the common phase-randomised EEG data series are detailed in *Section 3.6.1*.

### 3.7.1 Phase-Randomised Surrogates

The surrogate EEG data series were created using a phase randomization procedure. The phase randomisation procedure was implemented by generating a series of random phase versions of each infant's EEG dataset (hereafter referred to as surrogates). In the surrogates, the phase values at the frequency of interest (the syllabic rate of the NR) were randomised within each onset epoch, while the power of the oscillation was kept constant.

The phase randomisation here was implemented using the *phaseran.m* (Leontitsis, 2002) function from *MATLAB's Chaotic Systems Toolbox* (Leontitsis, 2021).

First, the FFT was applied to the input EEG timeseries. Again, the absolute magnitude of the resulting complex FFT coefficients provided the power of the frequency spectrum, while the  $90^\circ$  arctangent of the real to imaginary part (the counterclockwise shift) of the complex output of the FFT in radians contained the phase information for each frequency.

Next, the phase surrogates were created by multiplying the phase angle in radians by a random number between 0 and 1 for each frequency bin. The original imaginary part was then substituted by these newly created phase values. Finally, the original real part (amplitude) and the newly derived imaginary part (phase) of the signal were put back together to form the phase-randomised analytical signal.

The real part of the inverse FFT (iFFT) was used to convert back to the time series data. Note that since the FFT was a symmetric transformation, normally the analytical signal that we input to the FFT would be fully restored back to its time-domain equivalent by applying the iFFT. However, since we modified the phase angle series of the spectrum, the real part of the time-series signal that the iFFT outputted was no longer equivalent to the original real part of the original EEG signal. Instead, we derived a phase-shuffled surrogate timeseries. The process was repeated 2500 times to produce a distribution of randomly phase-permuted surrogate timeseries.

Finally, for both connectivity metrics, the same step-by-step strategy as described above was employed whereby the surrogate timeseries were transformed to the frequency domain using the complex Morlet wavelet function. The PLVs were then calculated between the phase of the surrogates and the Hilbert envelope of the NRs in the same way as with the original EEG timeseries. Similarly, the GPDC matrices for the four selected channels of the surrogate EEG data series and the speech envelope time-series were derived to produce the surrogate GPDC distribution.



## **CHAPTER FOUR**

### **STUDY ONE: Familial and Genetic Risk Effects on the Neonatal Neuronal Entrainment to Speech**

# CHAPTER FOUR: STUDY ONE - Familial and Genetic Risk Effects on the Neonatal Neuronal Entrainment to Speech

---

## 4.1 Study One Aims

The study advances the current state of knowledge by assessing whether there are:

- (1) congenital oscillatory deficits in the neonates at high familial risk of dyslexia;
- (2) associations between familial risk and selected single nucleotide polymorphisms (SNPs) in the three described genes and neural-to-speech synchrony.

### *Rationale and Hypotheses*

In neonatal infants (assuming minimal environmental influences outside the uterus), genetic dyslexia risk factors, as well individual differences relating to the birth experience, could contribute to faulty oscillatory speech processing, which fails to phase-reset to (and therefore, entrain to) the relevant speech cues. Importantly, we need to study these neonatal factors in the context of the infants' familial risk of dyslexia as, as described in the introductory chapter, prenatal environmental influences would have been already on the way and parental dyslexia would likely be one of the contributing risk factors, potentially independent of the small-to-medium expected effects of the genetically incurred risk.

We hypothesised here that when presented with IDS up-to 7 days postnatally, infants would already exhibit less accurate speech-onset phase entrainment to the slow-amplitude modulation in the speech signal if they were susceptible to dyslexia due to their familial history or genetic makeup.

---

## 4.2 Study One Keywords

PLV, brain-to-speech phase entrainment, parental dyslexia, genetic dyslexia risk, oscillations.

---

## 4.3 Study One: Introduction

### 4.3.1 Deficient Neuro-Oscillatory Underpinnings in Dyslexia.

There is a widespread consensus on the phonological impairments presented in dyslexic adults and children, as well as on the hereditary nature of dyslexia. Despite the high replicability of specific genetic variations, however, the links between the changes in the genotype and the neurophysiological and cognitive phenotype of impaired phonological processing are less straightforward. There is a general agreement that the influences that lead to later phonological impairment have a very early, potentially prenatal onset. The faulty neural wiring due to the observed aberrant neuronal migration and axonal connections associated with dyslexia susceptibility genes lead to disruptions in the micro-circuitry of the cortex. Cortical micro-circuitry structure has been linked to neuronal oscillations, which have been shown to track the amplitude modulations of (or entrain to) the complex speech signal in all ages (and many species). The faulty wiring, incurred during the early neuronal development in utero, could bring about faulty entrainment at birth, which to an extent could be predictive of later phonological development. Here, we address what are the exact aspects of neuronal oscillatory mechanisms of speech-tracking that are abnormal at birth; and what are the main contributing factors to these mechanisms. Importantly, the question is addressed prior to major additional language-input related plasticity (an environmental factor) which at the time of birth is likely to have a comparatively smaller impact.

### 4.3.2 What Aspect of the Neural Oscillatory Response to Speech is Different in Neonatal Infants at Risk of Dyslexia?

The high-power amplitude modulations in the human speech signal (or envelope) arise from prominent syllabic and prosodic inflections (such as rise time), which follow a  $\sim 2$  -  $\sim 4$  Hz rhythms and in western languages often signify the beginning of morphological units. Goswami (2011) emphasized that slow temporal modulations of syllabic/prosodic encoding are impaired in dyslexia. The temporal profile of dyslexic entrainment-to-rhythm deficits have been characterised as less efficient neural phase alignment to amplitude-

modulating frequencies in speech at under 20Hz (Leong & Goswami, 2014b). Dyslexic adults were significantly out of phase by entraining to an earlier angle of the theta rhythm (4Hz, Leong & Goswami, 2014a). Dyslexic teenaged children had lower reconstruction accuracy than reading- and chronological-age matched controls in the 0-2Hz amplitude modulation frequencies of the speech envelope (Power et al., 2016).

### ***Slow Oscillations and Sharp Edges***

Delta or theta govern the parsing of the speech stream and nest the finer-grained high-frequency acoustic information (Leong et al., 2017; Leong & Goswami, 2015), so misalignment in these bands could provide suboptimal scaffolding upon which phonological awareness is built. In the first few months of life, infants rely on automated statistical learning processes, which are known to be regulated by the slow-frequency modulating structure of the speech input. In the case of the infant-directed speech (here represented by nursery rhymes), the high-power slow-frequency features are additionally exaggerated in the syllabic and prosodic registers and give the infants clear and pronounced clues, especially towards the sharp onset edges of the individual phrases. In the literature, sharp onset edges are the primary cues that both guide language learning (Gervain et al., 2008; Mehler et al., 1988; Peña et al., 2002; Thiessen et al., 2005) and have been suggested to be suboptimally utilised by the developing brain in dyslexia (Goswami 2011).

Thus, neonatal neural entrainment to sharp onset edges of (ID) speech could be a potential robust marker of suboptimal at-risk envelope tracking at birth. There are already some indications of such deficiency (Guttorm<sup>1</sup> et al., 2010; Leppänen et al., 2012; Leppänen et al., 2010; Molfese, 2000; Van Zuijen et al., 2013), in relation to impaired reading performance in later years. Continuous oscillatory entrainment deficits, related to familial and genetic risk effects have not been demonstrated at birth yet, although they are a viable prediction based on the existing literature addressed. Additionally, it is unclear what aspects of oscillatory processing are impaired, and to what dyslexia risk factors or individual differences surrounding birth these impairments may relate. In this study, we set out to reduce the gap on these questions.

### 4.3.3 Measuring phase entrainment at the onset of the speech stream using PLV

There were both theoretical and practical reasons to study the infants' neural phase-locking at the onset of the speech phrase. According to the theta-gamma embedded theory of Giraud & Poeppel (2012), the phase-resting of theta happens as a response to slow-wave modulations of the incoming speech signal. The phase-locking is additionally most prominent at the sharp edges around the onset of speech signal (Heil, 1997) which are the primary cues used by naïve language learners to parse the speech signal and infer the boundaries of speech units (Gervain et al., 2008; Mehler et al., 1988; Peña et al., 2002; Thiessen et al., 2005). The onset of the speech signal would be where the phase of theta would change from tracking the endogenous oscillatory activity to tracking the exogenous input and therefore would be most likely where differences between groups in slow-wave phase-resetting would be most prominent. On the more practical side, time and computational constraints did now allow us to calculate and study PLV for the entirety of each NRS (which also varied in their duration), so we decided to limit the analysis window to the part of the NRs which were theoretically most relevant and most likely to contain the difference between groups. Therefore, we selected those 18 adjacent time-windows at the onset of each NR, which were likely to reflect the phase-resetting to the syllabic-rate slow-wave modulations in the incoming speech signal.

We opted for the phase-locking value (PLV) as a measure of the phase coherence at the onset of speech as it measures the clustering of the differences in the phase-angle series between the speech and the neural signal. As such, PLV did not take into account the actual instantaneous phase values but rather, how consistently the phase series were between the two signals. For that reason, PLV was deemed more appropriate than more recently developed measures such as the weighted/phase-lag index (w/PLI) which is not sensitive to the consistency of the phase distribution between the two signals; or the phase-slope index (PSI), which measures whether the phase lag between the two signals is consistently positive or consistently negative but could be insensitive in the case of strong bidirectional phase slope consistency which could be a plausible scenario in the context of rhythmic NRs. Thus, PLV is recommended in cases where there is a specific hypothesis about phase consistency between the two signals (for an in-depth review on this, refer to Cohen, 2014) as it was found to be the most sensitive to detecting phase-clustering or connectivity regardless of the phase-angle differences themselves.

---

## 4.4 Study One: Methods

### 4.4.1 Participants

A total of N=91 neonatal infants (52 boys, 44 at high familial risk of dyslexia) contributed to the PLV analysis after the pre-processing steps described in Chapter 3.

After thresholding the onset PLVs at 97.5% above the surrogate baseline (procedure described below), 86 infants remained to contribute three or more nursery rhyme onset epochs and thus qualify for the analyses. Of those 86 infants, 50 were boys, and 41 were at high familial dyslexia risk.

### 4.4.2 Experimental Materials and Protocol

The experimental materials and the protocol followed are as described in *Chapter 3*.

### 4.4.3 Genotyping protocol and Infants' Genotype

The genotyping protocol is detailed in Chapter 4, and the genotyping results and the analysis genetic profiles of the infants included in the PLV onset dataset are described in the same chapter.

### 4.4.4 Dyslexia Risk Variables

In Study One, the effect of familial and genetic risk of dyslexia on the phase coherence between the neonatal EEG (brain) and the envelope carrier at the onset of the nursery rhymes (speech) they listened to, were evaluated.

*Familial risk* of dyslexia, also here referred to as parental risk, was defined by the infants' dyslexic parent. Thus, the familial risk between-subject variable had three levels: M for maternal risk (N=16 neonates); F for paternal (N=24), and O for low risk (N=45). Notably one of the infants had two dyslexic parents and could not be grouped by the parent of origin and has therefore been excluded from analyses featuring the parent of origin variable.

To test the thresholding sensitivity of the surrogate phase-randomisation procedure (described in the next section) only, we defined familial risk as high (a group of all infants with at least one dyslexic parent, N=41) or low risk of dyslexia (same as above, N=45). The high-risk level here did not fully nest the parental risk variable, and thus contributed towards a slightly different proportion of the variance, so we were able to use it to test the sensitivity of the threshold applied on the outcome PLV variable.

*Genetic risk* was defined as carrying the less common genotype (here always abbreviated as genotype#3) on any of the eight successfully genotyped SNPs across the three susceptibility genes, as detailed out in Chapter 2.

#### 4.4.5 Other modelled variables

In the Linear Mixed effects analyses detailed below, additional factors expected to contribute to explanatory power were included in the models.

The fixed-effect (FE) variables fell in two categories; one was variables relating to the individual infants: birth weight, gestational age<sup>8</sup>, sex, C-reactive protein (CRP) infection markers, and the number of nursery rhymes they contributed to the analysis; as well as the experimental variable of interest - genetic and parental risk group. The other FE category comprised factors relating to the measurement parameters (channel of effect and hemisphere of effect). The random effects (RE) related to the experimental parameters (the

---

<sup>8</sup> A systematic literature review identified birth weight and gestation age as the most reliable perinatal predictors of the likelihood of developing later reading disorder (Sara Mascheretti et al., 2018)

infant's and the nursery rhyme's identity, the syllable rate of the current and previously heard nursery rhymes, and the duration of the inter-trial-interval (ITI) <sup>9</sup>.

#### 4.4.6 EEG pre-processing for the PLV onset analysis

For the purposes of the regression analyses reported in *Section 4.5 Results* below, the EEG recordings for the PLV onset analyses were pre-processed following the steps detailed in *Chapter 3*.

Seven out of the 11 recorded EEG channels were analysed for the level of phase-locking between the neural and the speech signals. The selected channels were: T3 and T4; T5 and T6; C3 and C4; and Pz. The remaining four frontal channels were not included in any of the reported analyses. The selection of a region of interest in temporal and central channels only was motivated by the literature describing the strongest brain-to-speech connectivity values in those areas in children and adult populations (Altarelli et al., 2013; Feng et al., 2020; Xia et al., 2017), and in other neonatal studies (Dehaene-Lambertz et al., 2010; Dubois et al., 2015; Glasel et al., 2011). It was further practical to focus the scope of the measured PLV effects in fewer channels to reduce to error (noise) in the distribution of the modelled variables describing the PLV peaks and optimise the chance of detecting the effects in the predictor factors.

##### ***Thresholding the PLVs of the original EEG signal by the surrogate phase-randomized EEG***

All PLVs calculated between the EEG and the speech envelope signals were normalized by subtracting the 97.5<sup>th</sup> centile of the surrogate PLVs across the 2500 phase-randomisation runs. PLVs were normalized separately for every channel and NR epoch and individually in each infant. Thus, only the top 2.5% of the genuine PLV values in each channel, onset epoch, and infant, were retained.

---

<sup>9</sup> A key with all variables and their abbreviations for the model formulae is provided in the List of Abbreviations & Basic Definitions

Unlike the standard baselining procedure<sup>10</sup> in published studies evaluating coherence in infant samples, where the surrogate metrics are stacked in a pooled “super-subject” and thresholded at 95% surrogate cut-off (i.e. Leong, et al., 2017), here we use the individual infant’s own surrogate phase-randomised EEG set as the more conservative baseline. We considered the pooled baselining approach to be less suitable for the current PLV analyses because it was not strict enough to deal well with the noisier PLV metric. The greater variability incurred by pooling over individual epochs and surrogate datasets resulted in a lower absolute threshold, which in turn brought more individual PLVs above the threshold. Increasing the lenience, however, seemed to also increase the noise in the metric (i.e. more values above threshold and closer or prior to the onset of the nursery rhyme) upon inspecting the individual PLVs in each channel, trial, and infant.

Furthermore, the individually baselined PLVs still appeared noisy still above the 95%tile of the surrogate distribution upon visual inspection (examples of individual results panels are shown in *Figure 4-1*). A yet stricter 97.5<sup>th</sup> %tile threshold was therefore used. That meant that only PLVs above the top 2.5% of the phase-randomised surrogates’ distribution were included in the ensuing analyses.

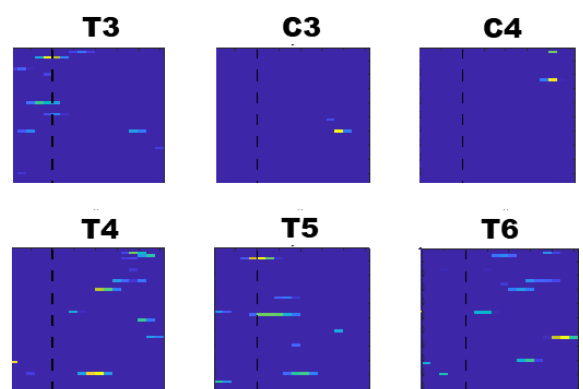
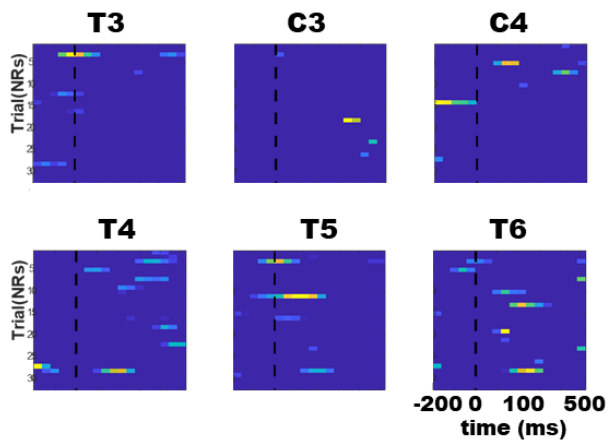
---

<sup>10</sup> The standard “super-subject” baselining approach was used for the network coherence GPDC values in Study 2 and is therefore described in greater detail in Chapter 5.

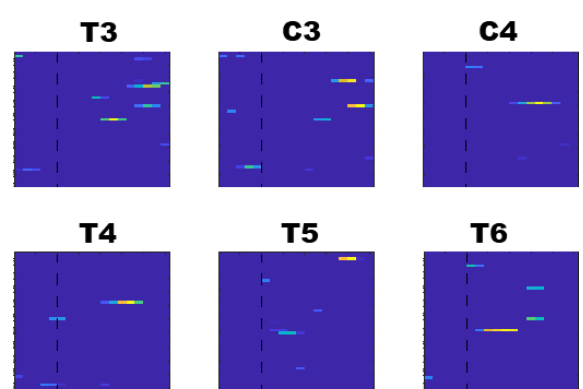
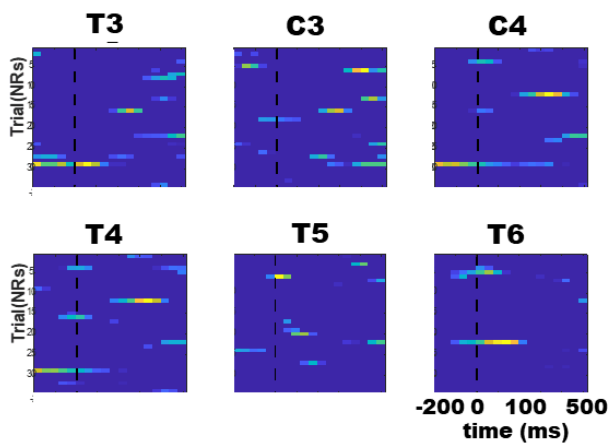
## 95% Individual Surrogate Threshold

## 97.5% Individual Surrogate Threshold

### Infant: SPELL084



### Infant: SPELL032



### Infant: SPELL002

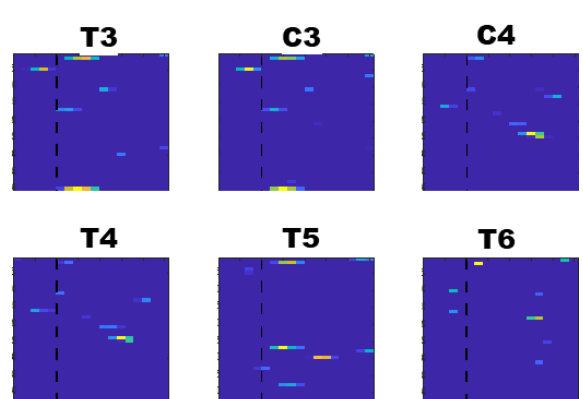
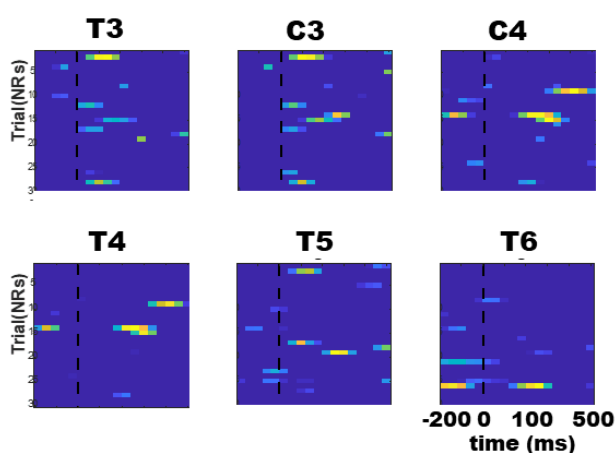


Figure 4-1. Individual results from the thresholding procedure in three example infants at two example cut-off levels: PLVs above 95% and 97.5% of the random-phase surrogate distribution threshold. The surrogate thresholds were calculated individually for each infant within channel and nursery rhymes. Plots are separated by named channel. Nursery rhyme onset epoch are plotted on the y-axis, onset time (only

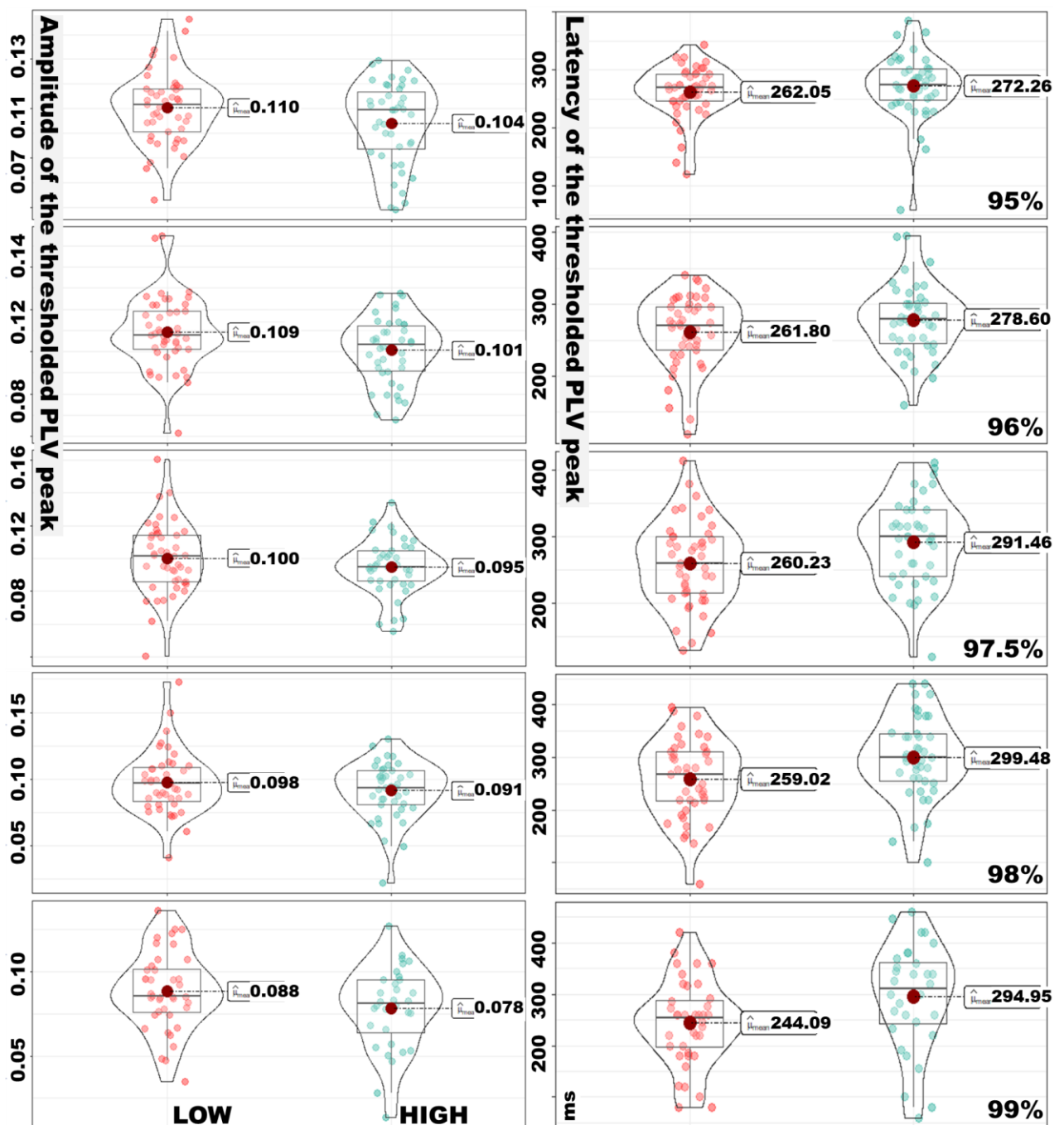
the initial 500ms post stimulus onset) – on the x-axis. Brighter colours on the scale indicate larger relative difference between the PLV values and the random surrogate distribution.

Finally, the 97.5% threshold was tested retrospectively to check for the sensitivity of the PLV peak amplitude and latency values to segregate between the infants at low and high familial risk of dyslexia. The effect size (Cohen's *d* values) is plotted against each level of the threshold above between 95% and 99% value of each infant's surrogate phase randomisations (*Figure 4-2* and *Table 4-1* below).

*Table 4-1. Sample size, effect size (Cohen's *d*), observed power and t-test statistics at the different levels of surrogate thresholding.*

Threshold (%surrogate distribution)	N	Effect Size ( <i>d</i> <sup>^</sup> )	Observed Power	<i>t</i> <sub>Welch</sub> & <i>p</i> Statistics
95.0%	88	0.203	0.157	<i>t</i> =-0.95, <i>p</i> =.35
96.0%	87	0.337	0.340	<i>t</i> =-1.57, <i>p</i> =.12
<b>97.5%</b>	<b>86</b>	<b>0.486</b>	<b>0.596</b>	<b><i>t</i>=-2.25, <i>p</i>&lt;.03</b>
98.0%	84	0.527	0.647	<i>t</i> =-2.41, <i>p</i> <.02
99.0%	72	0.556	0.618	<i>t</i> =-2.28, <i>p</i> <.03

As can be seen in *Figure 4.2*, the distribution of latency values is similar at all levels of the thresholding, however the sensitivity of the comparison increases with the stricter baselining procedure. In hindsight, choosing an even stricter threshold would have probably increased our chances of detecting a difference in the subsequent analyses as the size of the effect increases with the stricter 98% and 99% cut-offs. However, we consider the 97.5% cut-off sensitive enough for detecting the differences between the infants grouped by their familiar risk circumstances, or by their genotype. The 97.5% threshold is used hereafter in all the analyses; however, the backward stepwise and the best subset regression models were also tested retrospectively with the 98% threshold (as it offers the most optimal effect size – observed power balance of the ones tested) to verify that the results of the 97.5% threshold hold. The results from the exploratory regression analyses with the PLVs thresholded at 98% of the surrogate distribution are presented in *Appendix IV.II*.



**Difference between LOW & HIGH familial dyslexia risk in the PLV peak amplitude & latency at each surrogate threshold level.**

Figure 4-2. Amplitude and latency differences between infants at high and low familial risk of dyslexia at different levels of the surrogate threshold.

**PLV Outcome Measures**

The two outcome measures for the PLV analyses were the strength (amplitude) and the latency of the PLV onset peak, as defined in *Section 3.5* in the Common Methods chapter.

Only PLV peaks with a positive latency are included in the formal regression models described in *Sections 4.5.2 and 4.5.3*. The PLV peaks with a negative latency are further described in *Appendix IV.1* and further discussed in *Chapter 7*.

#### 4.4.7 Statistical Analyses Approaches

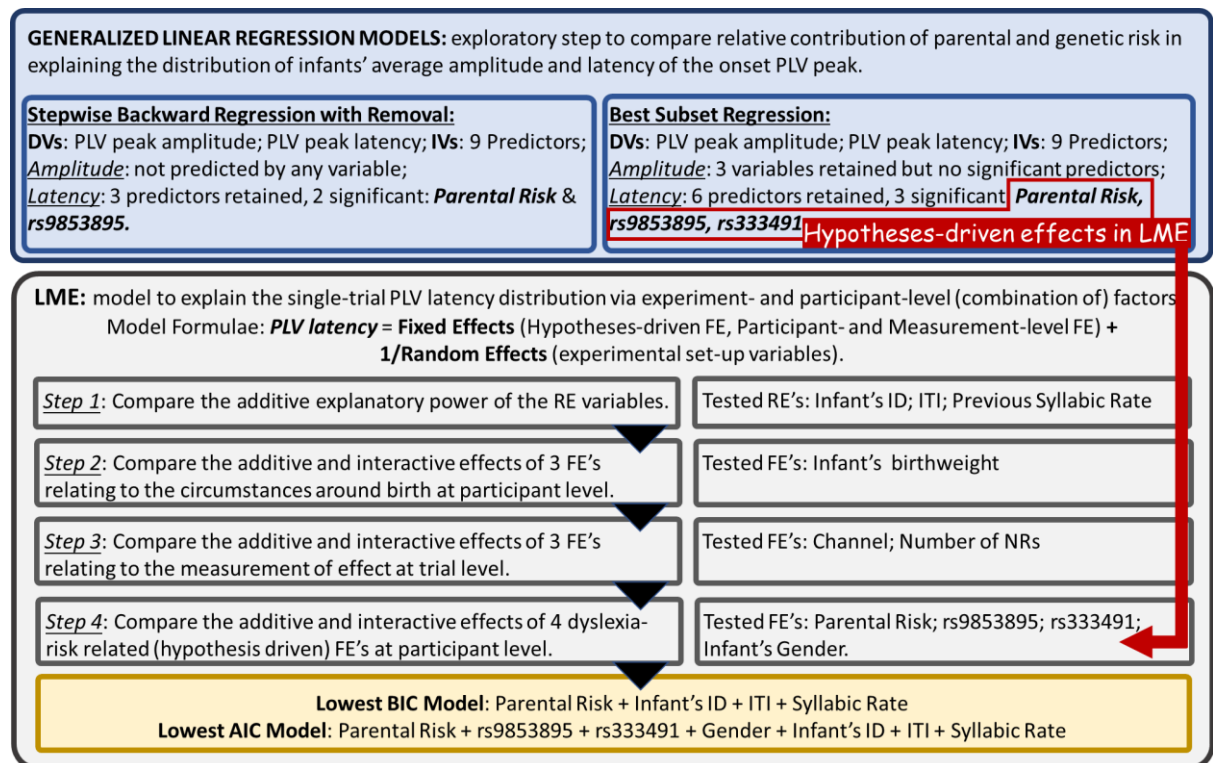


Figure 4-3. A summary of the design of the regression models presenting the variables entered at each step. The top blue panels demonstrate the two exploratory GLRMs and the bottom gray panels show the steps of the LMEs and the order of variables entered in them. The bottom yellow panel show the two LME models with the lowest information criteria overall.

##### 4.4.7.1 Exploratory Regression Models on the Strength and the Latency of the PLV Peak Distributions.

To understand better the explanatory contributions of the genetic and familial risk predictors, two exploratory generalized linear regression models each were fit on the PLV strength and latency dependent variables. Those were the backward stepwise and the best subset regressions. All four analyses were run in *Statistica* (TIBCO Statistica® v14.0.0, r2020). For the backward stepwise regression with removal, the entry and exclusion p-

criteria were set to  $\alpha=.05$ . For the best subset regression analysis, the model was set to optimising the adjusted effect-size coefficient  $R^2$  (i.e. optimising the percentage variance explained) with the lowest complexity, as measured by the number of factors included in the model.

Eighty-five infants (40 at high risk) contributed to the four analyses. Each infant's PLV peak and latency values were averaged over all nursery rhyme onset epochs. Note that the infant who had two dyslexic parents was excluded from the regression models described here.

There were 9 categorical predictor variables in each of the regression models: the infants' parental risk type with three levels (M/F/O), and the infant's genotype on the 8 remaining SNPs with three levels each. Thus, for every regression model run, there were 85 observations with 9 factors, or 9.4(4) observations per categorical predictor variable.

As no risk factors were identified to predict significantly the strength of PLV response (see *Results section 4.5.1* below), only the effects on the PLV peak latency were further tested at the following step in the linear mixed effects model.

#### **4.4.7.2 Linear Mixed-Effects Models to Test for the Main Mechanisms Contributing to the Latency Distribution of the PLV Peaks**

##### ***LME: Introduction and Purpose***

In the next step of the analysis, the linear mixed effect models (LME) were used to assess the mechanisms by which the genetic and familial risk factors identified by the regression models in the previous step, influenced the onset timing distribution of the neonates' oscillatory tracking of the input speech signal. The genetic and familial risk factors were tested in conjunction with other variables pertaining to the characteristics of the infants and measurements (fixed effects) or experimental setup (random effects). Models were compared based on their best fit at the lowest complexity. The LME approach helped us assess many different combinations of (interacting) factors explained best the observed distribution of PLV latencies.

All LME models were run in *MATLAB* using the *fitlme* function. To limit the level of complexity permitted, no more than two variables were allowed to interact.

The best model selection was based on three model parameters: the adjusted correlation coefficient  $R^2$  to optimise the percentage of explained variance; and the Akaike's Information Criteria (AIC) and the Bayesian Information Criteria (BIC) to assess the fitness of the model to the data, and to minimise the model's complexity as measured by the number of included parameters and interactions between them. Generally, the complexity of the model increased with the variance explained, therefore the more parsimonious models with high explanatory power with fewer predictors, and fewer interactions between those predictors, were considered to have a better fit.

### ***Information Criteria in LME Model Selection***

Both AIC and BIC are often used in selecting a subset of predictor variables in regression models and both penalize the loglikelihood of the models to be compared in a slightly different way.

The general format for AIC and BIC is:

$$4-1 \quad [-2\text{LogLikelihood} + kp]$$

where  $p$  is the degrees of freedom and directly depends on the number of parameters included in the model. They differ in that  $k=2$  for AIC, while  $k=\log(n)$  for BIC, where  $n$  is the number of observations (the rows dimension). Thus, both penalise the higher number of factors in the model, but BIC also depends directly on the sample size and tends to penalise the more complex models more strictly.

The AIC is the slightly less conservative criterion used when there are effects of different sizes to be considered. There is no assumption that a true model exists, it is looking for the model with the best fit of the dimensionality present in the data. It is an estimate of the constant and the distance between the fitted log likelihood of the model and the true likelihood function of the data so the AIC can be termed as a type of a goodness-of-fit measure. The lower AIC (i.e. smaller distance between the predicted and the real likelihood function) is therefore closer to the truth, as the AIC understands it. Thus, the implicit aim of the AIC is to achieve a low prediction error and to optimize the fit of the model. However,

this gives rise to the most frequently pointed out problem with the AIC – it can be prone to overfitting and to choosing a larger model than the BIC. This is especially notable in larger samples (as in our case) where the AIC can expand to encompass smaller effects at a larger  $N$ , that is, the AIC can improve with the addition of small effects. This could lead to the AIC picking a more complex model than the BIC, so it is advised that the AIC is relied on more heavily in situations where a false negative result is considered more misleading than a false positive result.

On the other hand, the BIC answers a slightly different question as it assumes that there is a best model, and it attempts to identify it given the available parameters. The use of the BIC is therefore more consistent with model selection given a different number of parameters than is with minimising prediction error. It aims to identify the main drivers of the effect as a function of the posterior probability of the model being true such that the lower the BIC, the higher the log likelihood of the model being the true underlying configuration of the data as observed. As it is looking for the main drivers and not for the significance of the smaller effects, the BIC is less tolerant than the AIC to larger number of factors included in the model and penalises more complex models more strictly. It also tends to converge towards a specific selection of model parameters as the number of observations increases and is therefore more likely than the AIC to prefer a smaller model, especially at a larger  $N$ . The main problem cited for the BIC is thus the danger of selecting a model which underfits the data. Therefore, it is advised to rely more heavily on the BIC when a false positive result is considered more costly than a false negative.

In practice, the consensus seems to be that neither measure is ideal and based on the specific assumptions of the model design and parameters, they may make slightly different predictions, so it is best to take both into account. Therefore, we report the results of several models based on both those criteria and show that albeit slight differences in model selection, the selected models converge on the factors which they highlight as the most important in explaining the distribution of PLV peak latencies in our cohort of infants. Still, the Bayesian information criterion seemed conceptually slightly closer to our modelling aims here – i.e. identifying an underlying mechanism of variables working together to produce a peak, so results which optimise the BIC were taken with higher gravity. However, both ICs were always plotted and taken into consideration as a reference.

### ***LME Model Selection Steps***

We ran the LME model in four steps, starting from the random-effect variables and introducing a new variable at the beginning of each following step. This was necessary due to our computational constraints whereby for the PC to maintain a matrix with all possible permutations of 5 interacting variables, it took 48.4GB of the random-access memory (RAM), or 75% of the available physical memory of the machine used to run the models. Seven interacting variables took in the order of 63.8GB (>99%) of RAM. Targeted selective introduction of variables was therefore more practical in terms of memory usage and computational time.

Based on the adjusted R<sup>2</sup>, AI and BI criteria, the factors which comprised the best fit models were passed onto the following step. A new set of variables was then tested on whether it improved the fit within the thus far selected best model. Importantly, the models' formulae were at first coded blindly. That is to say, the comprising variables were not revealed until after the model selection was performed based on the current set of model parameters. Thus, for each step, we first identified the model with the best fit at the lowest complexity, and only then we uncovered the identity of the included variable(s).

Four of the fixed effects relating to the individual infants were of theoretical interest and were core experimental variable so they were by default included in the final set of models to be tested against each other. Those four factors were the infants' *Parental Risk* group (M=mother; F=Father; or O=low risk), their genotype on the SNPs identified as most important by the exploratory regression models (selection reported in the Results *Section 4.5.1*), and their biological *Sex* (M=male; F=female). From here on, we refer to these four factors as the experimental fixed effects factors.

In the *first step*, the five random effects variables were tested, according to the formula:

4-2

$$\text{'LAT} \sim 1 + (1|\text{Variable V})\text{'}$$

$$\text{'LAT} \sim 1 + (1|\text{Variable V}) + (1|\text{Variable W})\text{'}$$

$$\text{'LAT} \sim 1 + (1|\text{Variable V}) + (1|\text{Variable W}) + (1|\text{Variable X})\text{'}$$

$$\text{'LAT} \sim 1 + (1|\text{Variable V}) + (1|\text{Variable W}) + (1|\text{Variable X}) + (1|\text{Variable Y})\text{'}$$

'LAT ~1 + (1|Variable V) + (1|Variable W) + (1| Variable X) + (1| Variable Y) + (1| Variable Z)'

The equations above were written out as they were entered into the *MATLAB* function. The 'LAT~' indicated that the dependent variable was the latency of the peak; the (1|Variable V) terms signifies a random effect variable. Variables V-Z here stand for the five blindly tested random effects, with one extra variable introduced at each level: *infant's ID, nursery rhyme ID, syllabic rate of the current and of the previously presented nursery rhyme, and the ITI*. 1 stood for the intercept term.

The ITI explains 22.7% of the variance while none of the other random effects (RE) explain any variance on their own. In combination, ITI and the infant's ID variables explain 29.5% together; and ITI, the infant's ID and the syllabic rate of the previous nursery rhyme variables together explain 29.9% of the variance in the latencies of the PLV peaks. Both the AIC and BIC parameters decreased from the one to two RE factors model. AIC was still lower with the three REs model, while BIC marginally increased. Thus, the three RE factors selected to include in the LME model at Step 1 were *ITI, infant's ID and syllabic rate of the previously presented nursery rhyme*. The total number of models ran in step 1 is 13.

In the *second step*, the three fixed effects (FE) of the neonatal parameters were tested against each other: the infants' birthweight, gestational age (+ age at testing), and their highest CRP infection markers count whilst hospitalised. The basic formula of the models tested at step 2 was:

4-3

'LAT ~1 + Variable A + (1|ITI) + (1|INFANTID) + (1|SR\_prev)'

'LAT ~1 + Variable A + B + (1|ITI) + (1|INFANTID) + (1|SR\_prev)'

'LAT ~1 + Variable A + B + C+ (1|ITI) + (1|INFANTID) + (1|SR\_prev)'

'LAT ~1 + Variable A\*B + C + (1|ITI) + (1|INFANTID) + (1|SR\_prev)'

*Equations (4-3)* follow the same nomenclature as in *equations (4-2)*. Again, variables A-C stand for the three blindly tested fixed effects, with one extra variable introduced at each level.

In this model, all the three FEs were allowed to interact with each other only to the first order. Adding the infants birth weight in the model as a covariate marginally increased the variance explained, whereas adding any other variable or a combination of variables either lowered the adjusted R<sup>2</sup> or did not affect it. All additions to the model increased both the AIC and BIC parameters, however, the birth weight variable contributed the least to that increase. Thus, only the birth weight variable was selected for the next step of modelling. The adjusted R<sup>2</sup> after the addition of birth weight increased to 30.0% variance explained. The total number of models ran in step 2 was 13.

In *step 3*, the three fixed-effects experimental measurement variables were tested against each other: *channel of the effect, hemisphere of the effect, and number of nursery rhymes contributing to the effect measured*. Note that since the channel variable was nested in the hemisphere variable, they could not be added together in the same model as one of the two variables would not be of full rank. Their effects were therefore tested separately of each other.

4-4

'LAT ~1 + Variable A + Birth Weight + (1|ITI) + (1|INFANTID) + (1|SR\_prev)'

'LAT ~1 + Variable A + B + Birth Weight + (1|ITI) + (1|INFANTID) + (1|SR\_prev)'

In *equation (4-4)*, we did not model for an interaction between either (*Channel x N<sup>o</sup> Nursery Rhymes*) or (*Hemisphere x N<sup>o</sup> Nursery Rhymes*) as there was no interest in these interactions at this step. Furthermore, if either combination of variables was retained at this step, their interaction was tested in the following modelling step.

In general, adding the *Channel* variable increased the variance explained above adding the *Hemisphere* variable, which was expected as *Channel* had more levels which allowed it to track the variance better. For the same reason, however, it added more to the complexity of the model. Adding both the channel and the number of nursery rhymes FE predictors marginally increases both the fit and the complexity, more than adding the hemisphere and nursery rhymes together. *Channel* and *N<sup>o</sup> Nursery Rhymes* were the final two FEs variables added at this step of modelling. The total number of models ran in step 3 was 5.

In the *fourth step*, the all fixed- and random-effects variables were added alongside the fixed-effects of the experimental design of interest: infants' parental risk, and their genotype on the two ROBO SNPs identified in the regression models. All FE variables in this step of modelling were allowed to interact with one other variable, apart from the two ROBO1 SNPs together. We did not model for relatedness between any of the SNPs tested in this sample. The asterisk in *Equation 4-5* below denotes when a variable is permitted to interact with some or all of the other variables.

4-5

$$\text{'LAT} \sim 1 + \text{Parental Risk}^* + \text{rs9853895}^* + \text{rs333491}^* + \text{Gender}^* + \text{No Nursery Rhymes}^* + \text{Channel}^* + \text{Birth Weight}^* + (1|\text{ITI}) + (1|\text{INFANTID}) + (1|\text{SR\_prev})\text{'}$$

As the *Parental Risk* factor was a categorical predictor, it was entered in the form of three dummy effect variables. The LME was only able to test the effects of the different levels of the dummy variable each against a reference dummy level (here, the reference level was the low-risk group). Thus, the differences were reported here as the maternal risk compared to the low-risk group, and the paternal risk compared to the low-risk group. The two SNPs variables were entered as ordinal, as they were coded according to the predicted effect, from the lowest (genotype#1) to the highest (genotype#3) risk incurred.

All possible combinations of the fixed effects variables were tested, starting when only one FE variable was included in the model, and gradually increasing the modelled complexity until all variables were in the model. The total number of models ran in step four was 1,214,649.

The best models were finally identified as the most parsimonious models in two categories: the models with the lowest BI and AI criteria overall; and the models with the lowest BI and AI criteria in the top 1% range of variance explained as measured by the adjusted R<sup>2</sup>.

---

## 4.5 Study One: Results

### 4.5.1 Exploratory Regression Analysis for the PLV onset peaks

Two regression models are run on the thresholded PLVs above 97.5% of the surrogate phase-locking distribution: a backward stepwise removal procedure where independent

factors were entered in the model with  $p < .05$  and retained in the model at  $p < .10$ ; and the best subset procedure whereby the most parsimonious combination of factors that derives the most variance explained as measured by the model's adjusted  $R^2$  was selected.

For the strength of the PLV peaks, neither model significantly explained the distribution of values. No factors were retained at the specified significance level in the stepwise regression. Three factors were selected as the best subset but neither of them significantly predicted the distribution of the strength of PLVs in the current sample, with the total variance explained at 3.75% (Table 4-2 below).

For the latency of the PLV onset peaks, the backward stepwise regression identified three factors to be retained in the model, with two of them significantly predicting the latency values: Parental Risk at  $F_{(2,78)} = 6.71$ ,  $p < .002$ ,  $\eta^2 = .15$ ; and rs9853895 (ROBO1) at  $F_{(2,78)} = 3.24$ ,  $p < .045$ ,  $\eta^2 = .08$ . The model with three variables was significant at  $F_{(6,78)} = 4.19$ ,  $p < .002$ ,  $R^2_{adj} = .19$ . The best subset model comprised six factors in total, with three of them significantly predicting the latency values: Parental Risk at  $F_{(2,72)} = 7.80$ ,  $p < .001$ ,  $\eta^2 = .18$ ; rs9853895 (ROBO1) at  $F_{(2,72)} = 4.29$ ,  $p < .018$ ,  $\eta^2 = .11$ ; and rs333491 (ROBO1) at  $F_{(2,72)} = 4.10$ ,  $p < .021$ ,  $\eta^2 = .10$ . This model with six variables was significant at  $F_{(12,72)} = 2.80$ ,  $p < .004$ ,  $R^2_{adj} = .20$ .

Table 4-2. Results from the regression models for the two dependent variables: the latency and strength of the PLV onset peak.

PLV Peak Latency	Stepwise backward removal [.05-.10]	Best Subset based on Adj R <sup>2</sup>
N vars in the model	3	6
Variables at p<.05	Parental Risk: $F_{(2,78)} = 6.71$ , $p < .002$ ; rs9853895: $F_{(2,78)} = 3.24$ , $p < .045$ .	Parental Risk: $F_{(2,72)} = 7.80$ , $p < .001$ ; rs9853895: $F_{(2,72)} = 4.29$ , $p < .018$ ; rs333491: $F_{(2,72)} = 4.10$ , $p < .021$ .
Variance explained (Adj R <sup>2</sup> )	18.54%	20.46%
PLV Peak Strength	Stepwise backward removal [.05-.10]	Best Subset based on Adj R <sup>2</sup>
N vars in the model	-	3
Variables at p<.05	-	-
Variance explained (Adj R <sup>2</sup> )	-	3.75%

The stepwise backward removal model was stricter in identifying three variables, with two of them under the 5% cut-off for significance and a small effect size (under 20%).

Consistent with the less strict best subset model (which also assigned a small effect size on the three significant variables it identified), Parental Risk and one of the ROBO1 SNPs best

predicted the spread of the PLV onset latencies, consistent with the hypothesised effect of familial and genetic dyslexia risk on the synchronous EEG onset response timed to the speech stimuli.

### 4.5.2 Linear Mixed Effects (LME) Models Analyses for PLV peak latency

*Figure 4-4* below plots the variance explained of all the 1,214,649 LME models, as measured by the adjusted  $R^2$ , against the two information criteria AIC and BIC. The values were ordered by the information criteria, and the model with the highest explanatory power of 39.24%, was marked in red (the full formula is given in *Appendix IV.III*). An important observation in *Figure 4-4* was that the most complex models did not deliver the highest variance explained, which made it less likely that the models with the highest  $R^2$  would overfit the distribution of the PLV peak latency values. Additionally, in the models with mid-range information criteria, the variance explained grew together with the AIC and BIC parameters, unlike the edges of the distribution.

Hereafter, the report is focused on the simplest models with the lowest information criteria, either overall (Equations (*BIC1*) and (*AIC1*)), or when only the top 1% of models with highest variance explained as measured by the adjusted  $R^2$  (Equations (*BIC2*) and (*AIC2*)), were considered.

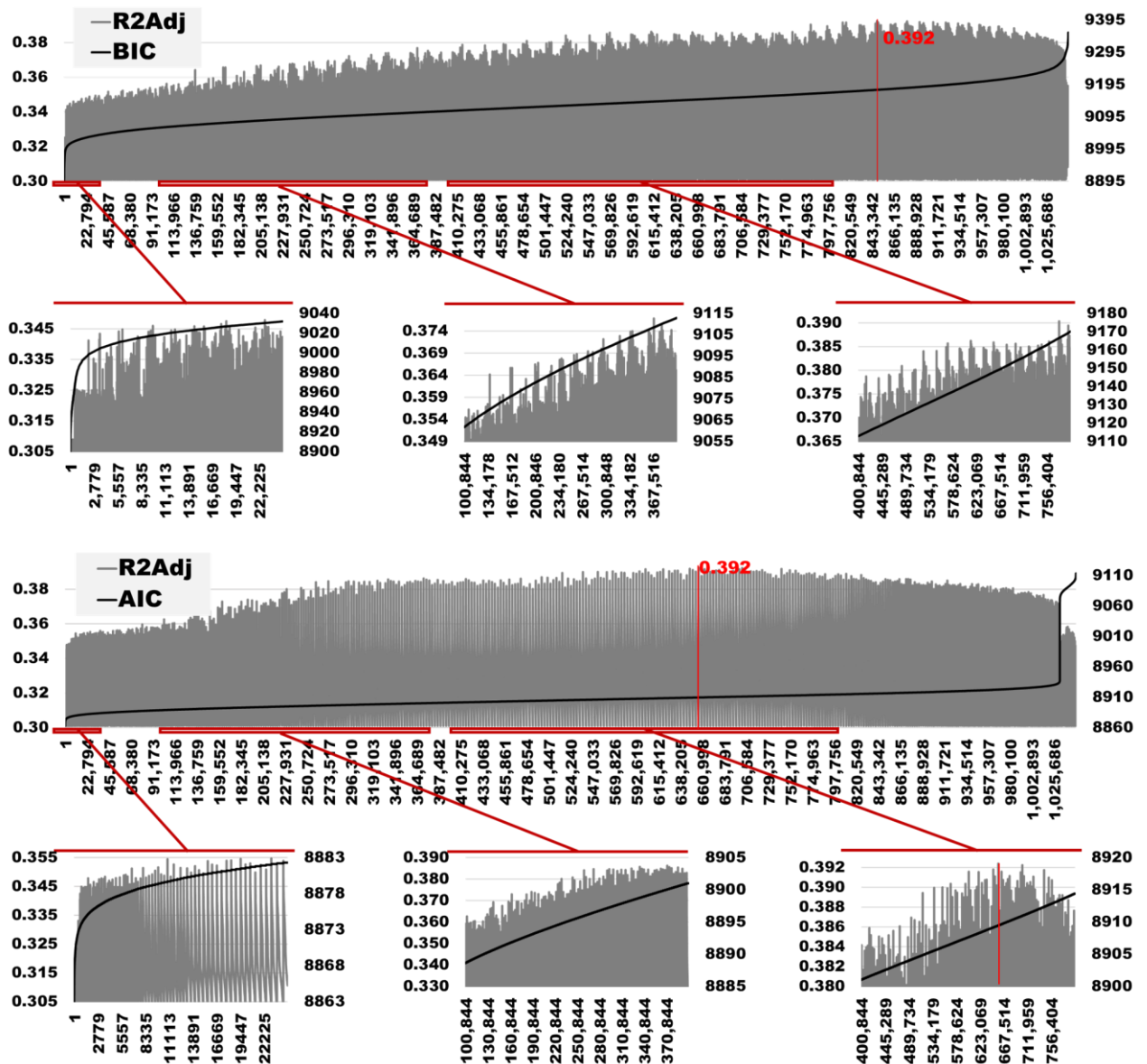


Figure 4-4. The distribution of  $R^2$  (gray bars) & BIC and  $R^2$  & AIC parameters for all models, ordered by the respective information criterion (black lines in the respective plots). The left y-axis plots the values for  $R^2$ , and the right - for B/AIC. The red bar indicates the model with the highest  $R^2$ . The three zoomed-in panels underneath show a closed-up look at the underlined areas of the plot to demonstrate the change in the slope of the BIC and AIC distributions throughout, as well as the distribution of  $R^2$  values in that region. As can be seen, the slope of the line changes for different sections of the distribution. Specifically at low and high  $R^2$  values, they have no linear dependency with B/AIC.

Despite not giving us an immediate indication of the best model selection, Figure 4-4 was informative of the non-linear relationship between the B/AIC and the adjusted  $R^2$  in the tested models. It reassured that the models with highest variance explained were not the

most complex models and that in the more parsimonious categories of models (in the leftmost bottom panels for both ICs, there were still models with comparatively high explanatory power. Finally, it demonstrated that when ordered by the AIC, the variance explained of the tested models tended to oscillate between higher and lower values for models that had very similar AIC values, which raised further suspicions for the reliability of the AIC as a model parameter in the current paradigm.

*Results by the Most Parsimonious of All LME Models Ran*

When considering only the simplest models (Equations (BIC1) and (AIC1) below), the fixed-effects factors predicting the variance in the latencies of the PLV peak at alpha lower than 5% were the infants' *Parental Risk* and their genotype on the *rs9853985* ROBO1 SNP. The full set of effects in the simplest models are given in *Tables IV-2* and *IV-3* for models ordered according to the BIC and AIC respectively, in *Appendix IV.III*.

The model with the lowest BIC parameter with an adjusted  $R^2=.3053$  (ordinary  $R^2=.3073$ ), AIC= 8867.3, BIC= 8899.2, LogLikelihood= -4426.6, was

(BIC 1)

$$'LAT \sim 1 + ParentalRisk + (1|ITI) + (1|INFANTID) + (1|SR_prev)'$$

As before, the (BIC1) equation represented the *MATLAB* input where 'LAT~' indicated that the dependent variable was the onset peak's latency, the random effects were denoted as '(1|Variable X)', and the fixed effects as 'Variable A'. 1 stood in for the effect of the intercept.

The model with the lowest AIC parameter had an adjusted  $R^2=.2908$  (ordinary  $R^2=.2958$ ), AIC= 8861.7, BIC= 8907.4, LogLikelihood= -4420.9, and was given by the formula:

(AIC 1)

$$'LAT \sim 1 + rs333491 + rs9853895 + Gender + ParentalRisk + (1|ITI) + (1|INFANTID) + (1|SR_prev)'$$

Low risk infants did not differ significantly from infants with paternal dyslexia risk, the former having a phase-locking peak 22.58ms (SE=14.99ms) earlier on average than the latter,  $t_{(701)}=1.51$ ,  $p=.132$ . In contrast, the infants at maternal risk of dyslexia had a phase-locking peak on average 51.56ms (SE=17.24) later than the low-risk infants,  $t_{(701)}=2.96$ ,  $p<.0032$  (Table IV-3 in Appendix IV.III).

As an ordinal FE variable, the rs9853985 ROBO1 SNP predicted the distribution of the PLV peak latencies at  $B=26.90$ ,  $t_{(701)}=2.74$ ,  $p<.0064$  whereby the rs9853985 genotype#1 group tended to have shorter peak latencies than the genotype#3 group (Table IV-3 in Appendix IV.III).

***Results by the Most Parsimonious of LME Models Ran with the top 1% Explanatory Power.***

In Figure 4-5 below are the distributions of the models with the highest 1% values of adjusted  $R^2$ , ordered by their AIC and BIC parameters from lowest to highest (12,478 models in total). Both the AIC and the BIC distribution plots have two observable peaks. The first peaks spread over the lowest 1000 criteria scores (the red squares to the left, zoomed in on underneath), with the highest  $R^2$  values of .386 in this region. At the low end of the AIC and the BIC scores, the distribution curves for both the information criteria take a logarithmic shape, while their corresponding adjusted  $R^2$  values show a small initial increase followed by a downward slope. The second peak of adjusted  $R^2$  scores for both distribution plots spans between 2000-8000<sup>th</sup> criteria values (highlighted in the red rectangle on the right). Again, the adjusted  $R^2$  values follow an inverse U-shaped curve characterised by an initial increase and then a slower decrease, with the highest values for this peak at adjusted  $R^2=.392$ . Both the information criteria in these regions of the graphs grow linearly at a steady pace. Finally, towards their high tail end, both the AIC and BIC distributions take an exponential shape, while the corresponding adjusted  $R^2$  values of the models decrease seemingly linearly.

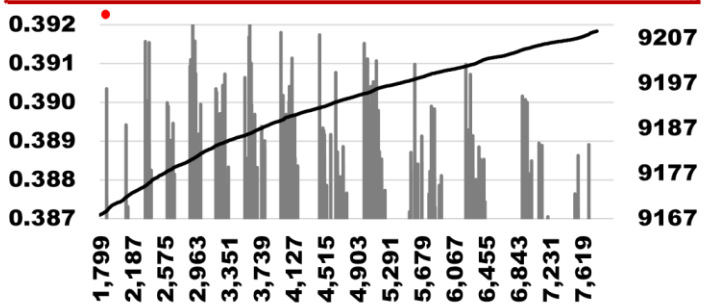
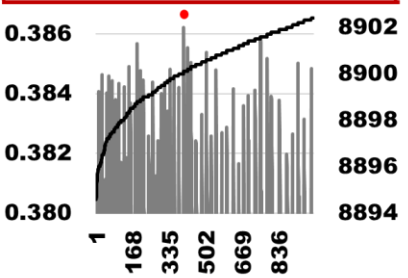
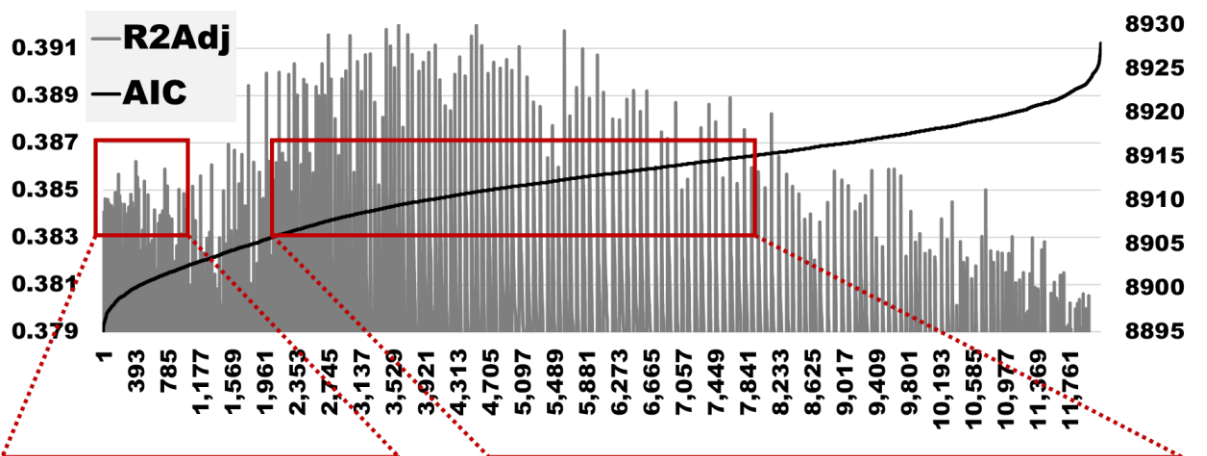
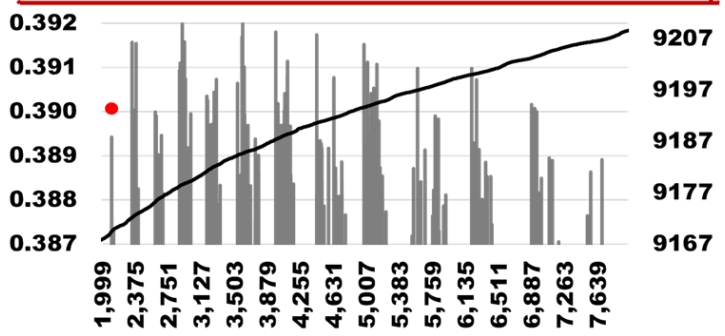
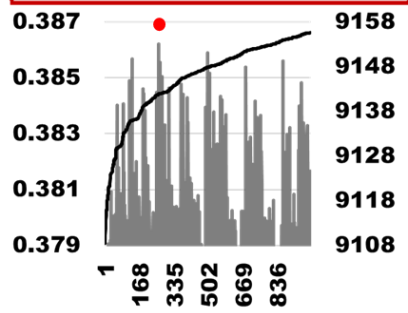
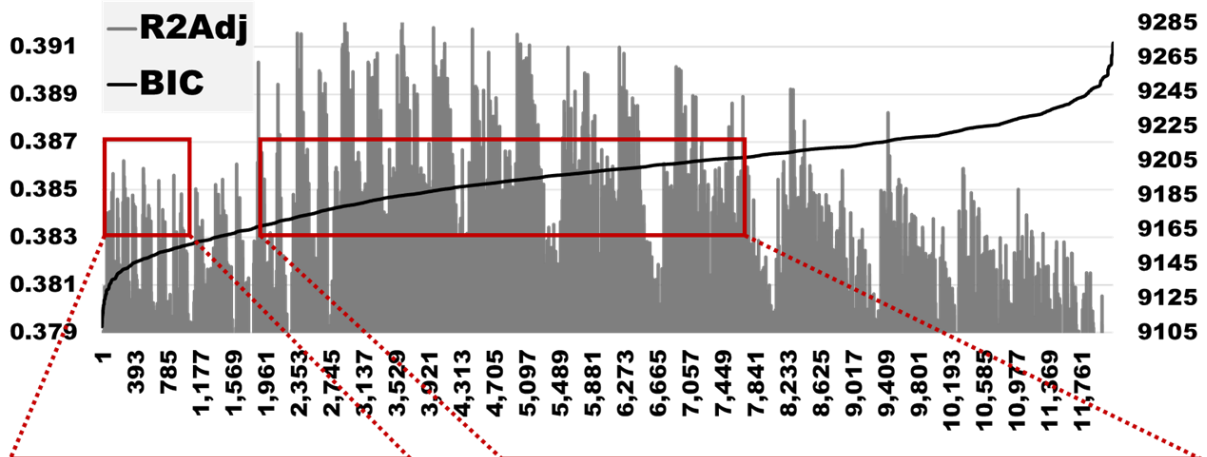


Figure 4-5. The distribution of  $R^2$  (gray bars) and BIC & AIC parameters for the top 1% of model with highest  $R^2$ , ordered by the respective information criterion (black lines in the respective plots). The left y-axis again plots the values for  $R^2$ , and the right - for B/AIC. The  $R^2$  distribution has a bimodal shape whereby there is a small initial peak (marked by the smaller red square) and a second larger peak (marked by the long red rectangle). It is also notable that the B/AIC line in the initial  $R^2$  peak region has a logarithmic shape with a rapid growth of either criterion, while it is mostly linear in the second peak region. The  $R^2$  values vary substantially within both zoomed regions, indicating no relationship with the ICs behaviour. The little red dot in the small initial peak indicates the model with the highest  $R^2$ ; while in the longer secondary peak, it indicates the lowest regional complexity at the optimal  $R^2$  value.

Considering only the top 1% of models with highest variance explained, the model (BIC2) had the lowest BIC parameter with adjusted  $R^2=.3769$  (original  $R^2=.413$ ),  $AIC=8898.6$ ,  $BIC=9108.5$ ,  $\text{LogLikelihood}=-4403$ :

(BIC 2)

' $LAT \sim 1 + N^{\circ}NurseryRhymes * Channel + BirthWeight * Channel + rs9853895 * Channel + Channel * ParentalRisk + (1|ITI) + (1|INFANTID) + (1|SR_{prev})$ '

In the same category of the highest 1% variance explained, the model (AIC2) was with the lowest AIC parameter with adjusted  $R^2=.3776$  (original  $R^2=.4217$ ),  $AIC=8894.6$ ,  $BIC=9145.5$ ,  $\text{LogLikelihood}=-4392.3$ :

(AIC 2)

' $LAT \sim 1 + N^{\circ}NurseryRhymes * rs333491 + N^{\circ}NurseryRhymes * Channel + N^{\circ}NurseryRhymes * ParentalRisk + BirthWeight * Channel + BirthWeight * ParentalRisk + rs9853895 * Channel + rs333491 * ParentalRisk + Channel * ParentalRisk + Gender + (1|ITI) + (1|INFANTID) + (1|SR_{prev})$ '

A further detailed description of the family of models in the top 1% of adjusted variance explained is given in the *Appendix IV.III*. It is worth noting that all models gravitated towards the same variables, which in different interactive combinations contributed an additional 8-9% of explanatory power over the simplest models (AIC1) and (BIC1) shown above, however, at the expense of an increase in the information criteria. In summary, the most frequently implicated variables in this family of models were the *Parental Risk* and

one of the ROBO1 SNPs (*rs9853895*), often modulated by the *Channel* of effect and the *Birth Weight* of the infant. The *Channel* of effect variable tended to interact with (all) other variables and was thus potentially prone to overfitting the model. The fixed effects of the *Channel* variable were driven by the PLV peaks in channels T4 and C4 which occurred earlier than in C3. The latency of the PLV peak in channel C3 was entered as the reference value for the dummy effects *Channel* variables. The direction of effect was reversed for channels T4 and T5, as well as for Pz, against C3, in the interaction term with the ROBO1 SNP (*rs9853895 X Channel*). Tables of the effects in the (*BIC2*) and (*AIC2*) models (*Tables IV-4* and *IV-5*, respectively), as well as of the model with the highest variance explained across all (*Table IV-6*), can be found in Appendix IV.III.

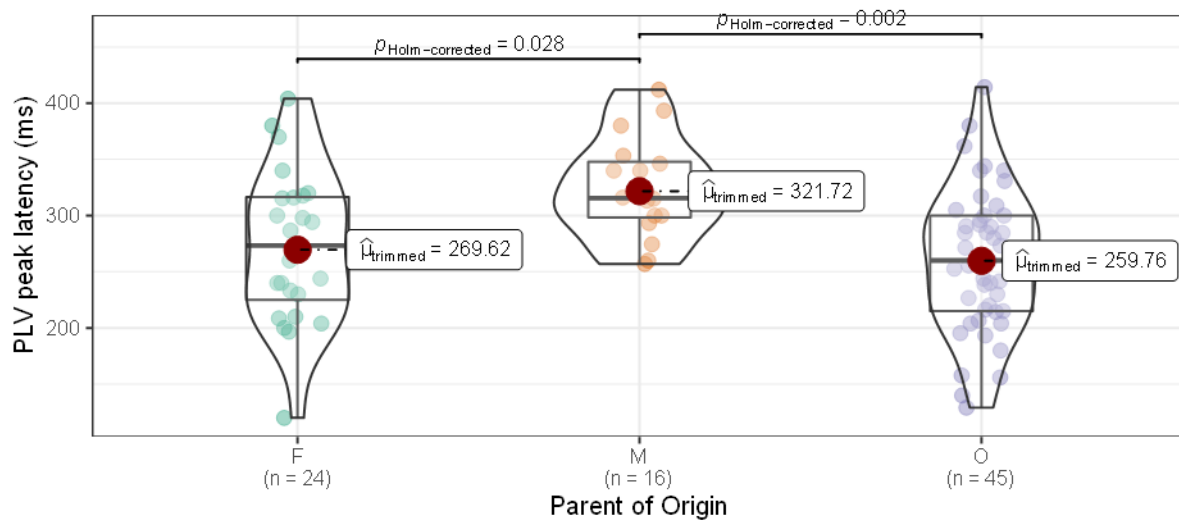
Importantly, when we increased the number of models under consideration to the top 2% of those with the highest explained variance – i.e. doubling the number of models to 24,293, there were only 13 AIC and 10 BIC values lower than the lowest ones for the top 1% of the models. Taking it even further, when the top 5% of the highest adjusted R<sup>2</sup> values were considered (60,732 models), only 171 BIC and 152 AIC values were lower than the lowest ones for the top 1% of the models. Thus, reducing the adjusted R<sup>2</sup> values under consideration did not entail a proportional decrease in either of the two information criteria. On the contrary, both the information criteria had a similar shape of the distribution when all models were considered as when only a subsection of the models was plotted. These observations gave us confidence that when we looked at only the top 1% of models, at least at the lower end of the plots, the BIC and AIC values were not atypically high compared to the rest of the models with lower adjusted R<sup>2</sup> values. That is, we were not in the high-end exponential increase region of the BIC and AIC values plotted on the rightmost side of *Figure 4-4* above, which would have been indicative of overfitting the PLV peak latency values. In summary, regardless of what proportion of models we considered or what information criteria we used in model selection, the single most reliable and consistently present factor in predicting the distribution of PLV onset latencies was the infant's Parental Risk of dyslexia. The second factor identified in all reviewed models (apart from model B1) was the infant's genotype on the ROBO1 SNP *rs9853895*. For both those factors, post-hoc analysis for their main effect was performed next.

### 4.5.3 Describing the Effects of The Factors Identified by The LME Models

Evidently, the **parental risk factor** was present in all models explaining the variance in the PLV peak latencies in our neonatal dataset, from the least to the most complex model. When the PLV latency values were broken down by a parent of origin, we saw that the infants with a dyslexic mother had the slowest phase locking to the nursery rhymes, compared to both groups with a dyslexic father and with no first-degree familial risk (statistics from the LME models were reported in the previous section and in *Table IV-2(B1) in Appendix IV.III*). Here, a robust one-way ANOVA with three levels on the parental dyslexia variable was run to test the group differences at the infant level (rather than the trial level, as the results from the LME). The ANOVA confirmed the LME result that there were significant differences between two out of the three groups at  $F(2,27.27) = 9.88$ ,  $p < .001$ ,  $\xi = .50$ . The corrected post-hoc tests revealed a significant difference between infants with a dyslexic mother and both low risk infants ( $p < .002$ ), and infants with a dyslexic father ( $p < .028$ ). A violin plot of the tested effects is shown in *Figure 4-6* below.

## The Effect of the Parent of Origin on the Latency of the PLV peak

$$F_{\text{trimmed-mean}}(2,27.27) = 9.88, p = 0.001, \hat{\xi} = 0.50, CI_{95\%} [0.29, 0.73], n_{\text{obs}} = 85$$



Pairwise test: **Yuen's trimmed means test** ; Comparisons shown: **only significant**

Figure 4-6. A violin plot demonstrating the effects of parental dyslexia group on the latency of the PLV onset peaks at the infant level (i.e. every dot represents a mean latency for the infant PLV onset peaks). M=maternal; F=paternal; O=low risk group. Statistics reported are for the robust Yuen's trimmed mean test using 80% of the total distribution of values to deal with potential outliers (referred to in the text as robust ANOVA).

The **ROB1 SNP rs9853895** factor demonstrated an increase in the latency for the PLV peaks from genotype#1 toward genotype#3 when the distribution of the individual peak latencies were plotted per trial (Figure 4-7B), as well as when the average latency for each infant was plotted against their genotype (Figure 4-7A). Note that the plot in Figure 4-6B matches the effect as modeled by the LME model. A robust one-way ANOVA with 3 levels on the rs9853895 variable (genotypes#1-3) was run and did not show a significant effect but a strong tendency towards an increase in the latency of the PLV peaks with the higher risk genotypes, at  $p=.05$ , n.s. (Figure 4-6A).

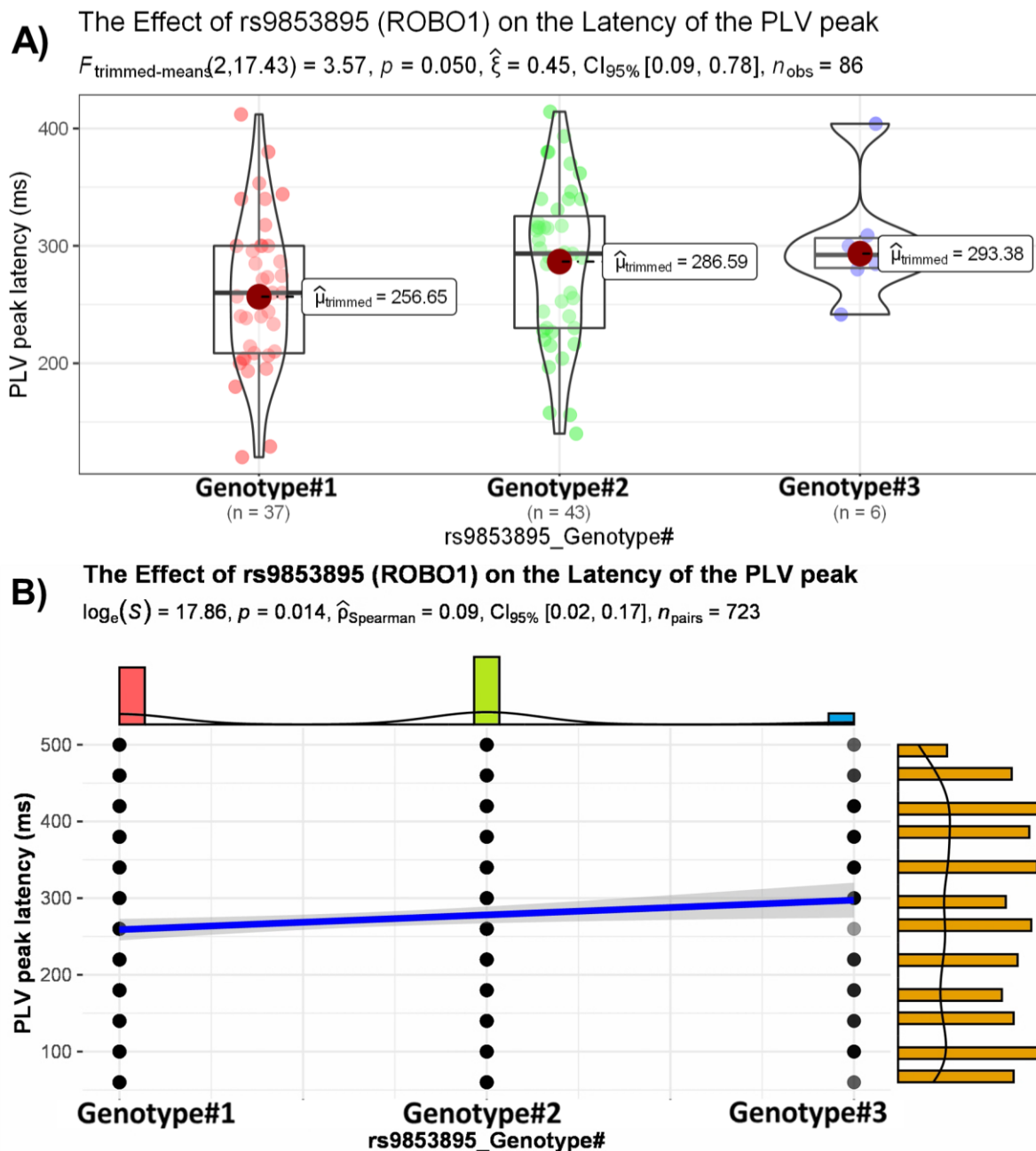


Figure 4-7. A violin plot for infant's mean latency (A) and a regression line for individual trials (B), demonstrating the effects of rs9853895 genotype on the latency of the PLV onset peaks. A: at every dot represents a mean latency for the infant PLV onset peaks (Scatterplot of the effect by infants is in Appendix IV.IV, Figure IV-2); B: every dot represent latency on an individual trial. M=maternal; F=paternal; O=low risk group. Statistics reported are for the robust Yuen's trimmed mean test using 80% of the total distribution of values to deal with potential outliers (referred to in the text as robust ANOVA).

The main effects of both the parental and genetic (ROBO1 SNP) risk variables were in the predicted direction whereby infants at high (maternal) risk showed delayed phase-locking to the speech signal, and so did infants with the less common variant of rs9853895.

---

## 4.6 Study One: Discussion

### 4.6.1 Summary and Interpretation of the Findings in Study One

We set out to understand what aspects of neonatal neuro-oscillatory speech entrainment could be related to dyslexia risk, and what were the major contributing risk factors to this tentative effect. The LME approach confirmed the importance of the Parental Risk and one of the ROBO1 SNPs in predicting the distribution of the PLV onset peak latencies over individual trials, which was also shown over individual infants by the regression models. Beyond confirming the regression models, the LME models contributed little explanatory information on the configuration of factors to describe the onset latency distribution, and the combination of different variables only contributed to a maximum of 39.2% of the variance (ie. medium explanatory power). Increasing the complexity of the model did not help much and hindered the interpretability of the results. So, we employed caution in interpreting any results beyond the main effects of the factors confirming the regression analyses.

Maternal dyslexia was the strongest indicator of a significant delay in the PLV peak at the onset of speech. PLV peak latency but not accuracy changes were likely to signal a timing issue in the entrainment of the endogenous brain activity to the speech input whereby the phase-resetting to prominent speech cues in the at-risk infants took a little longer. The effect could be related to underlying connectivity disturbances in the cortical microstructural wiring, predicted by the genetic influences on the neural development described in *Chapter 2*. Maternal dyslexia as the most prominent risk factor has been reported before (Black et al., 2012). Black et al (2012) found that the severity of maternal dyslexia was related to individual differences in the child's cortical gray matter surface area (especially in the left inferior parietal lobule) at the age of 5. Cortical surface area is by large developmentally defined in-utero and subjected to strong genetic influences (Gilmore et al., 2018; Jha et al., 2018; Winkler et al., 2010). The mechanisms of effect from microstructural changes in the cortex and cortical surface area to cortical entrainment to speech are only speculative at this stage but it is probable that the results reported by Black et al (2012) are relevant to the cortical effects found here, and both converge on attributing these effects to early prenatal development likely symptomatic of currently unknown epigenetic or intrauterine-environmental influences.

Additionally, the less common variants of two ROBO1 SNPs were associated with a delayed PLV peak beyond the infant's familial risk. There were some indications that the genotype on at least one of the SNPs (rs9853895) modulated the speed of reaching peak entrainment differentially by channel whereby the left central channel was only faster than the right temporal ones when they were interacting with the effects of the SNP. Reduced right lateralization effects have been reported previously related to familial risk of dyslexia risk in neonatal infants i.e. (Daneshvarfard et al., 2019; S. Telkemeyer et al., 2009; Vandermosten et al., 2015; Vanvooren et al., 2014) but have not been linked to a specific genotype to the best of our knowledge.

The latency of the PLV representing the neural response to the onset of the speech signal was found to differ between infants based on their dyslexia risk status. The onset speech response was of interest as it was most likely to contain the theorised phase resetting of the ongoing endogenous brain activity to high-amplitude slow-frequency modulatory features of the incoming IDS stimuli, which as reviewed and hypothesised in Chapter 1, was predicted to be suboptimal in infants at risk of dyslexia. As we infer that the delay in the phase connectivity to the stimulus is a failure in processing of the prosodic pattern, we interpret it to signal a risk factor for future problems for phonological development. We could not test this assumption in the neonatal dataset; however, a measure of expressive phonological skills is acquired from the same cohort of children at the age of 2 years, so we hope to be able to address this query in the near future. The distinction must be made here that although we predicted that the delay in the onset response to the NRs in infants at risk of dyslexia based on the theoretical background postulating that theta phase resetting (Giraud & Poeppel, 2013) at the sharp edges of the speech signal (Goswami, 2011), we did not explicitly test, hence confirm, any of the background theories. The effects described here could be explained by a multitude of theoretical propositions, and likely have a broader origin, and can be readily viewed as either disturbances in the periodic and aperiodic neural activity resulting the delay in the phase coupling of the neural to the speech signal, or as delayed evoked response. Thus, the results could also be interpreted in the light of increased neural noise (Hancock, Pugh, & Hoeft, 2017), contributing to less sharp spike timing of the primary auditory neurons, leading to a delay in peak synchronicity time-locked to the onset of the NRs.

The observed delays in entrainment to the most-prominent speech-onset cues of the syllables could be the prerequisite of a minor at this age deficit, which could however have a snowball effect down the developmental trajectory. Language learning in early infancy is dependent upon accurate entrainment timing to the amplitude modulations in speech. The initial delays reported here could bring to reduced entrainment accuracy in later months, leading to misparsing the ongoing acoustic input repeatedly, a process shown to be important for phonemic and word-boundary recognition. If uninterrupted, this snowball effect may trigger phonological processing impairments, which in the long run impede the quick and accurate sound-to-print mapping and normal reading skills acquisition. It is important to highlight here, however, that these early neuroanatomic predictors of language processing in neonates could not be directly related to neural correlates language or dyslexia outcomes based on the data presented in this thesis only. Here, their use is limited to describing the possible risk factors to speech processing in neonates. There are many important factors that come into play in the years of language acquisition between the neonatal infancy and the beginning of school age, some of these factors are later on reviewed in *Chapter 6* in the context of the longitudinal project. The neonatal results discussed here give an important insight into the starting point but their usefulness in terms of predicting future dyslexia outcomes is yet to be tested in the longitudinal aspect of the project. We would advise caution in the reader when drawing conclusions about their predictive power in terms of language (dis)ability outcomes.

#### **4.6.2 Transition to Study Two**

It was hypothesised that the dyslexia-risk related phase-locking delay was attributable to timing inaccuracy of the cortical oscillatory entrainment to the speech signal, due to genetic-risk incurred faulty cortical wiring. Associated morphological and lateralization abnormalities in structural and functional connectivity, as well as in the timing of responses to auditory events at birth have been reviewed in *Chapter 1*. Building on this previous literature, and the phase-locking latency effects reported here, in Study Two we investigated whether there were genetic and familial dyslexia risk related connectivity modifications in the sensor-space network during speech presentation at birth.



## **CHAPTER FIVE**

### **STUDY TWO: Familial and Genetic Risk Effects on the Neonatal Neural Network Coherence during Speech Presentation**

# CHAPTER FIVE: STUDY TWO – Familial and Genetic Risk Effects on the Neonatal Neural Network Coherence during Speech Presentation

---

## 5.1 Study Two: Aims

The study advances the current state of knowledge by assessing whether there are:

- (1) deficits in the synchronisation capacity of the sensor-space network in the neonates at high familial risk of dyslexia;
- (2) associations between familial risk and selected single nucleotide polymorphisms (SNPs) in the three described genes and the pattern of channel-to-channel network coherence.

### *Research question and predictions*

The question we address in this chapter is what the background connectivity in the network is while it is processing the speech information. It has been hypothesised that a dyslexia-bound increased endogenous noise likely leads to the suboptimal processing of the incoming speech signal in primary and secondary sensory areas (Boets et al., 2013; Hancock, Richlan, et al., 2017; Molinaro et al., 2016; Ramus, 2004; Xia et al., 2017), and those timing issues in the entrainment are then passed forward to higher associative areas. The accurate processing timing of the speech signal at various time scales would depend on how efficiently the different sites can establish a synchrony in phase to the incoming signal (i.e. phase-reset to the prominent syllabic stress units) and to each other. In study two, we set out to assess the generic and familial neonatal risk factors on the synchronous efficiency within the cortical network by testing the measures of GPDC in a four-channel grid. The reading ability related modulation of GPDC has been tested before in dyslexic children and adults in MEG at a larger network scale in source-space (Molinaro et al., 2016). Bases on hypotheses of increased neuronal activation noise in the temporal-parietal areas over which our channels were approximately located, we predict reduced coherence across all pairwise channel connections with increased both familial and genetic risk of dyslexia.

## 5.2 Study Two Key Words

GPDC, genetic and familial dyslexia risk, channel pairwise coherence patterns.

---

## 5.3 Study Two: Introduction

In Study One, we established that infants at high familial risk of dyslexia are slower to reach peak connectivity to the phase of the syllabic modulation frequency in the infant-directed speech that they were exposed to. There was a further risk-related effect of the genotype on at least one of the tested susceptibility genes. From a mechanistic standpoint, we could infer that the issue in the neural-to-speech phase-locking was primarily in the onset timing of the neural phase-locking response, rather than the ability to trace it (although there were also some indications for an impairment in the ability to trace it, albeit statistically not as powerful)<sup>11</sup>. The issue of poor timing has been raised in the context of dyslexia on numerous occasions (Hancock, Pugh, et al., 2017; Hancock, Richlan, et al., 2017; Leong & Goswami, 2014b; Molfese et al., 2002; Nicolson & Fawcett, 2019; Ziegler et al., 2009). It has been attributed to noisy endogenous neural environment due to the faulty cortical wiring on which we previously elaborated. The noisy endogenous oscillations in dyslexia have been observed in adults and children cross-sectionally using network coherence metrics such as PDC (Molinaro, 2016). Here, we tested whether we could measure similar network coherence disturbance already at the start of life and in relation to the genetic susceptibility influences, which were the main predicted driver of sub-optimal neural network connectivity. Again, we assessed this prediction in the context of the infants' familial dyslexia risk as an approximate heritability measure, with potentially distinct effects from the genetically incurred risk factors but reflecting intrauterine environmental influences. A positive result would suggest that the hypothesised noisy neural environment is already noisy at birth and could be interpreted as an indication of a risk factor for the speech-processing capacity of the at-risk infants which could potentially underlie the delayed latency response seen in study one.

---

<sup>11</sup> For more detailed commentary, see the discussion chapter and *Appendix IV.II*).

### 5.3.1 Dyslexia and Measures of Neural Connectivity and Network Coherence

Neuroimaging studies (mostly employing MRI) have suggested an impairment of the left reading network in dyslexia in terms of both structural and functional connectivity throughout the course of development (Black, Xia & Hoeft, 2017). In typically developing infants, the leftward asymmetry in the AF has been found at birth (i.e. Dubois et al., 2015) and the microstructural integrity of the left AF has been associated with both the development of reading skills and reading disorder (RD). Given that developmentally, adult-like structural connectivity patterns in the described network have been reported in the first weeks of life, and that the genetic variation related to dyslexia susceptibility exert strong prenatal influences, the possibility exists that the prerequisite for the group differences in phase-locking to speech reported in study one had already been staged, albeit not determined, in those early days of neurodevelopment prior to birth. In later life, Lou et al (2018) reconstructed WM networks connecting in the left AF in 57 11-year-olds using network-based statistical parameters and identified left temporal-occipital and temporal-parietal networks with a decreased streamline in the dyslexic children and positively correlated with literacy. Wang et al found faster and earlier WM development prior to reading acquisition in subsequent good versus poor readers and a positive association between WM maturation and reading development using a longitudinal design (Wang et al., 2017). Žarić et al (2018) corroborated the atypical AF diffusivity in Dutch children with dyslexia between 8-11 years of age.

The established risk-related structural and functional connectivity abnormalities neonatally would inevitably lead to increased variability in the generation of neural responses to auditory stimuli, which have been related to future phonological processing and reading ability (Guttorm et al., 2010; Leppänen et al., 2010; Molfese, 2000; Molfese et al., 2002; Molfese et al., 2001). The higher variability is associated with noisier, or less synchronised endogenous neural environment, which could be expressed as reduced network coherence, could limit the processing capacity of the network.

### 5.3.2 Measuring Oscillatory Coherence Neonatally using GPDC

Long- and short-range neural wiring can be approximated using neural functional connectivity measures. The partial directed coherence (PDC) shows the lagged

dependencies between two oscillatory time series (in frequency and phase) and the directionality of the signal transfer in the network. It has been interpreted in a similar way as functional connectivity in fMRI (Molinaro et al., 2016). Importantly, PCD measured in sensor or even in source space (i.e. between EEG electrodes) does not measure structural or functional connectivity in the same way as MRI does as it is not defined in terms of underlying anatomical structures. Instead, it measures the connectivity between an external information and the brain's processing of that information, including (stimulus-driven) internal information tracking within the brain. Some features of this information tracking, including its directionality and broad topology, have been interpreted as consistent with functional neural connectivity measures of information processing in MRI.

PDC is computed according to the multivariate autoregressive model and is conceptually based on the principle of Granger causality (Granger, 1969), whereby a timeseries  $x$  is said to granger-cause timeseries  $y$  if the prediction error for the current state of  $y$  is reduced by a measure of the past state of  $x$  (Babiloni et al., 2007); a direction of effect can be inferred as the predictability is not necessarily reciprocal.

The PDC model is a multivariate full spectral measure of the influence that each channel has directly on each other channel (Baccalá & Sameshima, 2001). Faes & Nollo (2011) extended the PDC model to the generalised PDC or GPDC, to account for the instantaneous effects among the timeseries due to the significant effect that instantaneous correlations had on estimates of coupling and causality. The authors demonstrated that whenever the time resolution was lower than the time scale of the coupling lag between the two timeseries, neglecting the instantaneous correlations between them lead to misrepresentation and misinterpretation of lagged effects and therefore, heavily modified connectivity patterns (Faes & Nollo, 2011). They extended the GPDC to address the issue. The GPDC measure was particularly well-suited for addressing the connectivity patterns within the four-channel network in this study as it allowed for the simultaneous estimation not only of the amount of connectivity present in the network, but also of the flow of information from one channel to every other within different time scales. As GPDC accounted for the instantaneous connectivity effects between the tested timeseries, we could be confident in the derived coherence estimates in the low syllabic-rate frequency bands of interest (2-4Hz). The directionality of GPDC contributed to our design the additional benefit of an in-built sanity check. We could measure the flow of information between the four-channel EEG network and the envelope timeseries of the speech signal,

expecting to only see information sent from the speech channel towards the EEG but not the other way around as it should not be possible to predict the pre-recorded speech stimuli from the infants' EEG signals<sup>12</sup>. The information flow in the opposite direction would indicate spurious connectivity resulting most likely from a lack of fit between either the chosen set of parameters and the model, or the structure of the data and the model.

PDC can also be understood as a measure of information being passed in the brain, which could be affected by the quality of the information being encoded and passed (Saygin et al., 2013; Seidl, 2014). PDC was interpreted by Molinaro et al (2016) to mean a flow of information from one location to another in the brain at a specific encoding frequency. In the current study, GPCD was measured while the infants listened to IDS. Thus, GPDC here would indicate the strength of the encoding to the concurrent stimulus and how well this encoding is passed between channel locations. In our four-channel network, we would be unable to interpret any local specificity even in the sensor space, but the directionality of the measure is temporally defined so we could trust it.

---

## 5.4 Study Two: Methods

### 5.4.1 Participants

After undertaking the pre-processing steps as described in *Chapter 3*, 91 “clean” participant datasets remain. The GPDC calculations assessed the connectivity within a network and required an input of a connectivity matrix of a full rank. Thus, for each infant only trials with all four channels comprising the GPDC matrix under investigation could be used. From the 91 clean datasets, 15 infants contributed an insufficient number of qualifying nursery rhyme onset epochs of at least 2s in length and with all the four channels intact (qualifying epochs here refer to the epochs containing the nursery rhymes in duple meter as outlined in *Section 3.2.1, Chapter 3*). Consequently, a total of N=76 infants (33F, 36 at high familial risk of dyslexia with two-thirds falling on the paternal side) constituted the dataset used in the GPDC analysis.

---

<sup>12</sup> Details of these control analyses are given in *Appendix V.IV*

## 5.4.2 Experimental Materials and Protocol

The experimental materials and the protocol followed are as described in *Chapter 3*.

## 5.4.3 Genotyping protocol and Infants' Genotype

The genotyping protocol is detailed in *Chapter 2*, and the genotyping results and the analysed genetic profiles of the 76 infants included here in the four-channel network GPDC analysis were as described in *Chapter 2*.

Only the SNPs without any missing values across all infants were added as factors in any of the linear models. This was done to allow for sufficient degrees of freedom and number of observations per condition. As evident from *Table 2-3* and detailed in *Chapter 2*, 7 out of the 15 SNPs across all 4 genes had missing values for varying number of infants. The remaining 8 SNPs tested here spanned 3 of the genes reviewed in *Chapter 2*: *DYX1C1*; *DCDC2* and *ROBO1*.

## 5.4.4 Dyslexia Risk Variables

In Study Two, the effect of familial and genetic risk of dyslexia on the generalised partial directed coherence in the four-channel network were evaluated in sensor space.

*Familial risk* of dyslexia was operationally defined in two ways. High familial risk described infants who had one or more first-degree relatives with dyslexia (N=37); low familial risk was defined in infants with no first-degree relatives with dyslexia (0, N=39). Moreover, high familial risk infants were further grouped by their parent of risk origin – those with dyslexic mothers (M; N=12); and those with dyslexic fathers (F, N=24). Again, as one of the infants had two dyslexic parents and could not be grouped by their parent of origin, they were excluded from analyses featuring the parent of origin variable.

As in Study One, *Genetic risk* was defined by carrying the less common genotype (here always abbreviated as genotype#3) on any of the eight successfully genotyped SNPs across the three susceptibility genes, as detailed out in Chapter 2.

### 5.4.5 EEG pre-processing

The estimation of a positively defined covariance matrix for the calculation of generalised partial directed coherence (GPDC) required an additional EEG pre-processing criterion to be applied to the GPDC dataset beyond those described in *Chapter 3*. The input dataset matrix for the GPDC calculations needed to be of full rank, that is, there could be no missing EEG channels for the modelled matrix to be consistent across all tested neonatal datasets.

To retain data from all infants, we attempted a few noisy channels correction procedures, detailed out in *Appendix V Section V.I*. These generally included either applying an interpolation or calculating a representative summary value of the remaining channels, for the noisy channel to be excluded. Unfortunately, given the sparsity of the network of 11 channels, standard spherical interpolations were deemed unfit, and the calculated summary values either produced a singularity in the cross-correlation matrix (if standardized statistics such as mean and standard deviation were used), or were not validated by previous literature (if random stochastic noise was introduced). Therefore, we opted for the more conservative approach of defining a region of interest based on the channels' positioning on the head and how likely they were to bear noise in any given neonatal dataset.

#### ***Channels of interest selection***

For the purposes of estimating the network coherence, we calculate the GPDC between the Hilbert-envelope of the speech signal and a set of four selected channels of interest. The four-channel matrix comprises the two central (C3 and C4) and two temporal (T3 and T4) channels, all for located on a single central arch spanning from the top of one ear to the other (depicted in *Figure 5-1*). The selection was motivated by previous findings of primary and secondary auditory cortex (temporal-parietal) dyslexia-related connectivity abnormalities. There was also the practical reason for selecting this set of channels that GPDC could only be calculated at the presence of all selected channels, i.e. no channels per

epoch could be noisy or missing. Selecting this combination of four channels amongst the original 11 ensured the retention of the highest proportion of data.

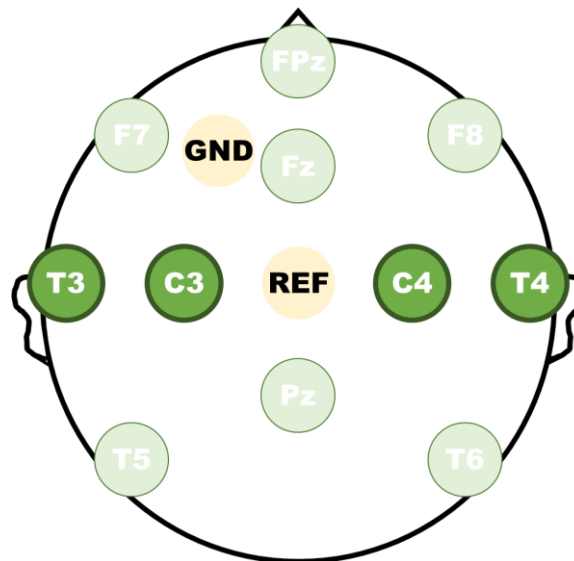


Figure 5-1. The four channels selected for the GPDC analysis are highlighted in full colour on the 11-channel montage.

All nursery rhymes were manually inspected for noisy segments in the four channels included in these analyses and were excluded if an artifactual source was suspected. A total of 15 infants (out of the 91 datasets remaining after the pre-processing procedure described in *Chapter 3*) were further excluded from the GPDC analyses described hereafter on the bases of providing fewer than three nursery-rhyme onset epochs with all the four channels unaffected by noise or artifacts. For the remaining infants ( $N=76$ ), the range of nursery rhyme onset epochs included for analyses was 3-38,  $M = 24.37$ ,  $SD = 9.23$ .

### ***Normalising the GPDC values of the original EEG by the surrogate phase-randomized EEG***

The calculated GPDC measures were normalised against the phase-randomized EEG surrogate datasets, generated as described in the Common Methods *Chapter 3*. Here, the GPDC values within the EEG network, and between the four-channel EEG matrix and the speech envelope, were normalized by subtracting the 95th centile of the surrogate data connectivity values, pooled over infants, randomisation iterations, and nursery rhymes. Only values above the 95<sup>th</sup> percentile were retained. We refer to the pooled surrogate dataset as a super-subject surrogate dataset. Note that this approach differs from the thresholding procedure described for PLV in *Chapter 4*, where each individual infant's

phase-locking estimates for a given channel and nursery rhyme onset epochs were measured against the 97<sup>th</sup> percentile threshold of the matched surrogate dataset for that infant. The more stringent baselining procedure in *Chapter 4* was necessary as the PLVs between the neural oscillatory signal and the speech envelope were a noisier metric than the GPDC values employed as a network connectivity measure in the current chapter.

Therefore, here we pooled over the surrogate GPDC values across infants and nursery rhymes in creating a surrogate super-subject GPDC distribution for each channel, in the following steps:

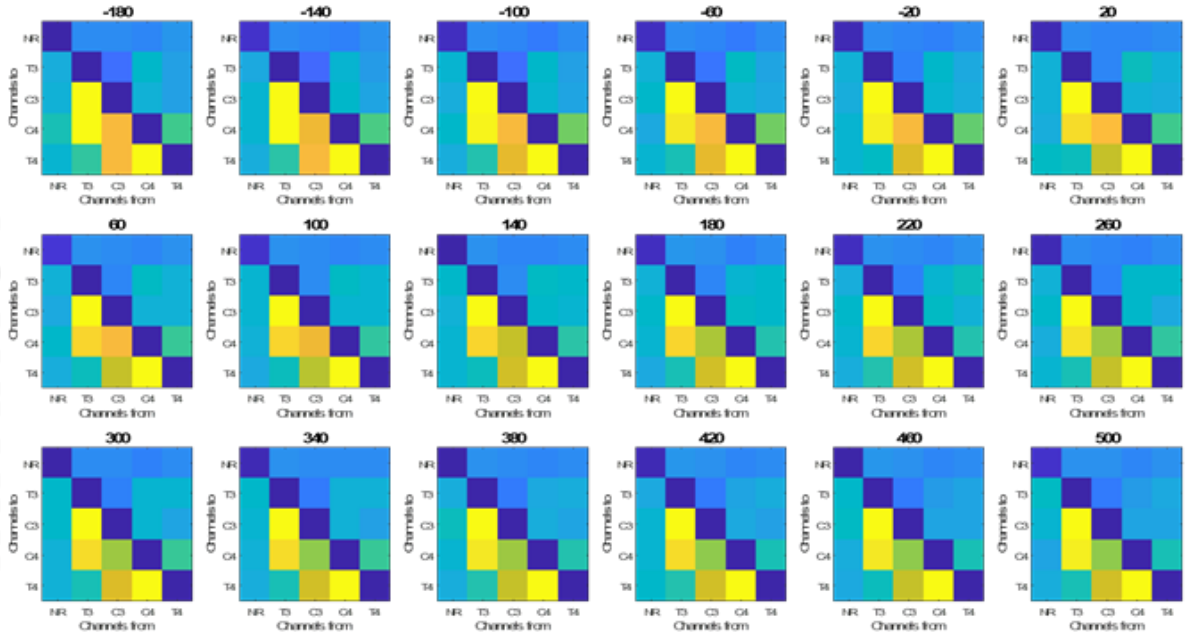
*Step 1:* All NRs (range between 3-38 on the first dimension) and surrogates (2500 iterations along the second dimension) were concatenated for each participant, thus collapsing first two dimensions of the matrix for each individual infant. The result was a three-dimensional matrix with:  $3:38 \times 2,500 = 7,500:95,000$  X 5 (one speech-envelope + four EEG channels, hereafter referred to as sending or outputting row channels) X 5 (one speech-envelope + four EEG channels, hereafter referred to as receiving or inputting column channels).

As outlined in *Section 3.5* in the Common Methods chapter, only the GPDC matrix calculated in the time-window corresponding to the median latency of the PLV onset peak across all nursery rhymes and infants was analysed. That time-window corresponded to ~240ms post stimulus onset<sup>13</sup>. Notably, upon visual inspection there seemed to be only minor differences between the connectivity patterns across the 18 overlapping time-windows for which we estimated coherence (an example plot showing the point-by-point patterns for three randomly selected infants is shown in *Figure 5-2* below). Furthermore, even if the time-window in which the GPDC matrix was calculated was not the optimal one for a given infant, the misalignment would likely reduce rather than increase the measured coherence and thus make it more probable that we miss a true result rather than detect a false one.

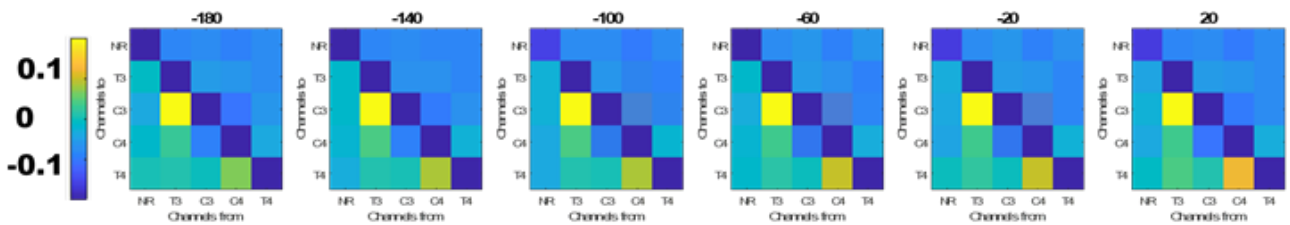
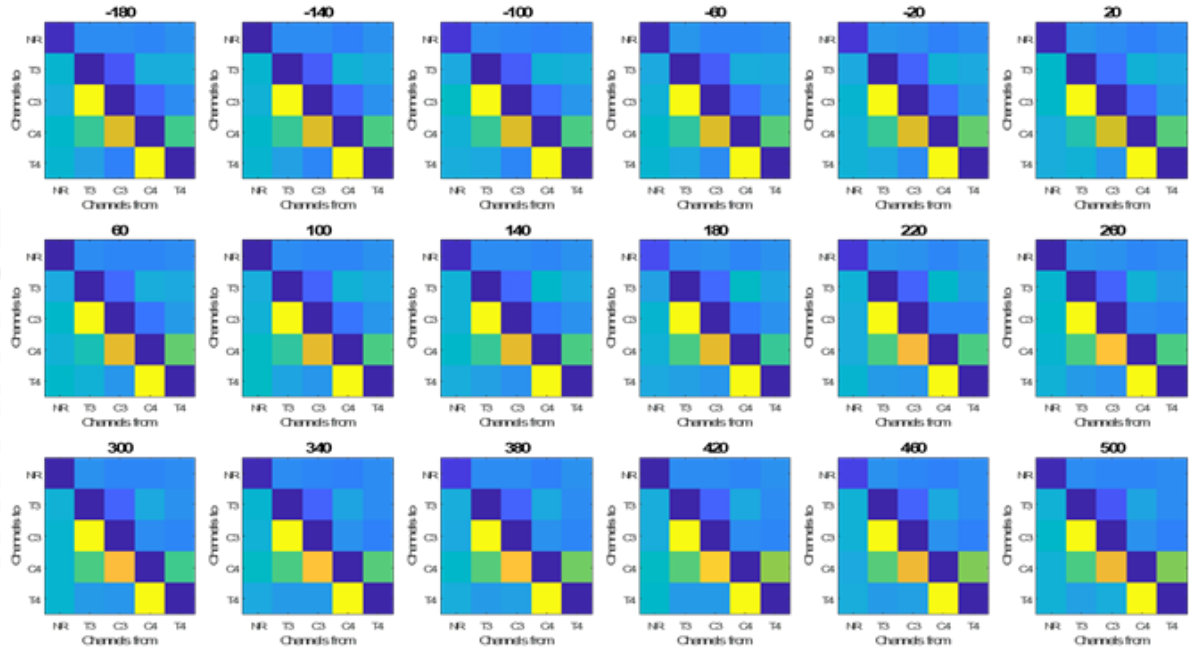
---

<sup>13</sup> The median latency of the PLV onset peak across infants and nursery rhymes is an estimation here and not an exact value due to the different distribution of values and thresholding criteria applied in the PLV and GPDC analyses. In such a way, there are several infants who contributed to the PLV but not the GPDC metrics. Conversely, there were infants who did not produce PLV peaks above threshold but for whom GPDC values were calculated. Thus, the 240ms time-window was taken as the median latency of PLV onset peak of the infants contributing to the PLV but not necessarily to the GPDC analysis. Despite the acknowledged differences, we believe the estimate to be close enough to the true median latency for the set of infants comprising the current analysis' cohort as well.

**INFANT01**



**INFANT02**



**INFANT03**

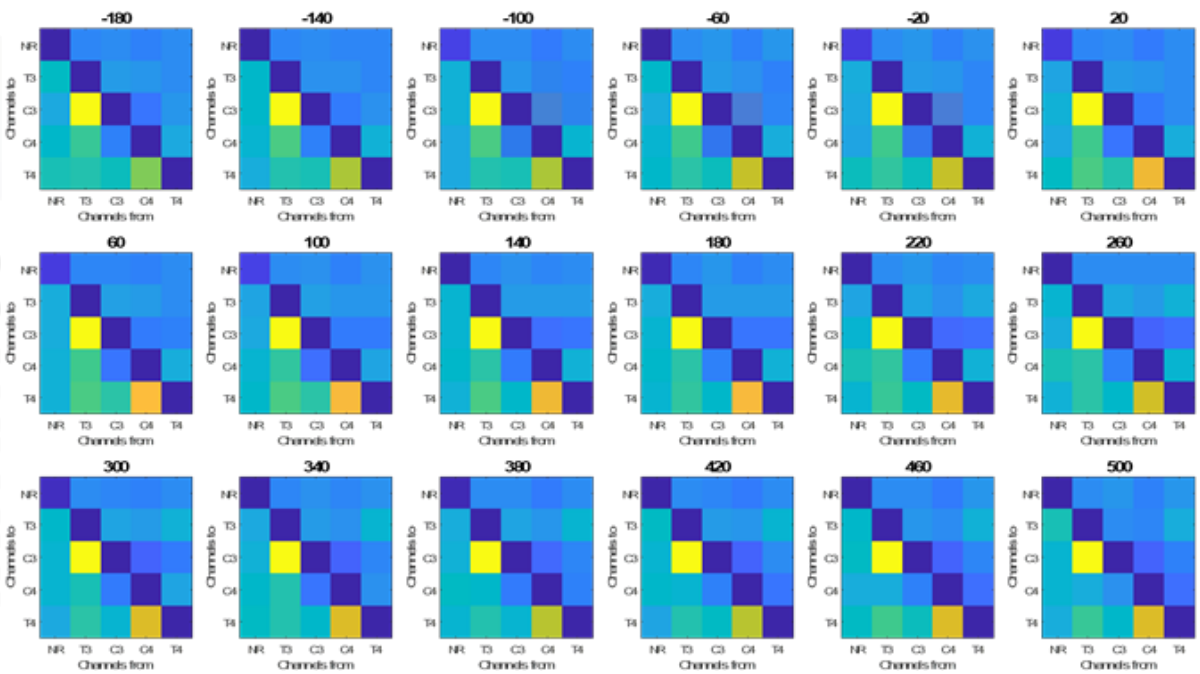


*Figure 5-2. The full time-course of different onsets between -200:500ms of the normalised GPDC values at the onset of the nursery rhyme trials for three example infants. The GPDCs were calculated at the indicated onset to 2s after it. The numbers above the plots indicate the time as locked to the stimulus onset. The sending channels are plotted in the x-axis (including the speech envelope channels NRS), and the receiving channels are plotted on the y-axis for cross-correlation each plot. Brighter colours indicate higher normalised coherence values for that channel pair.*

*Step 2:* All Infants' (N=76) matrices are concatenated into a super-subject along the first dimension. The super-subject matrix has the size of:

9425000 X 5 output channels X 5 input channels X 1 timepoint (240ms)

*Step 3:* We compute the 95%tile over the first dimension of the super-subject matrix.

*Step 4:* For each individual infant (*Figure 5-3* below) and each connection (channel-to-channel; channel-to-nursery-rhyme, and nursery-rhyme-to-channel), we test the individual GPDC estimate against the 95% percentile of the super-subject surrogate threshold. Only connections consistently significantly above the threshold are further included in the analysis.

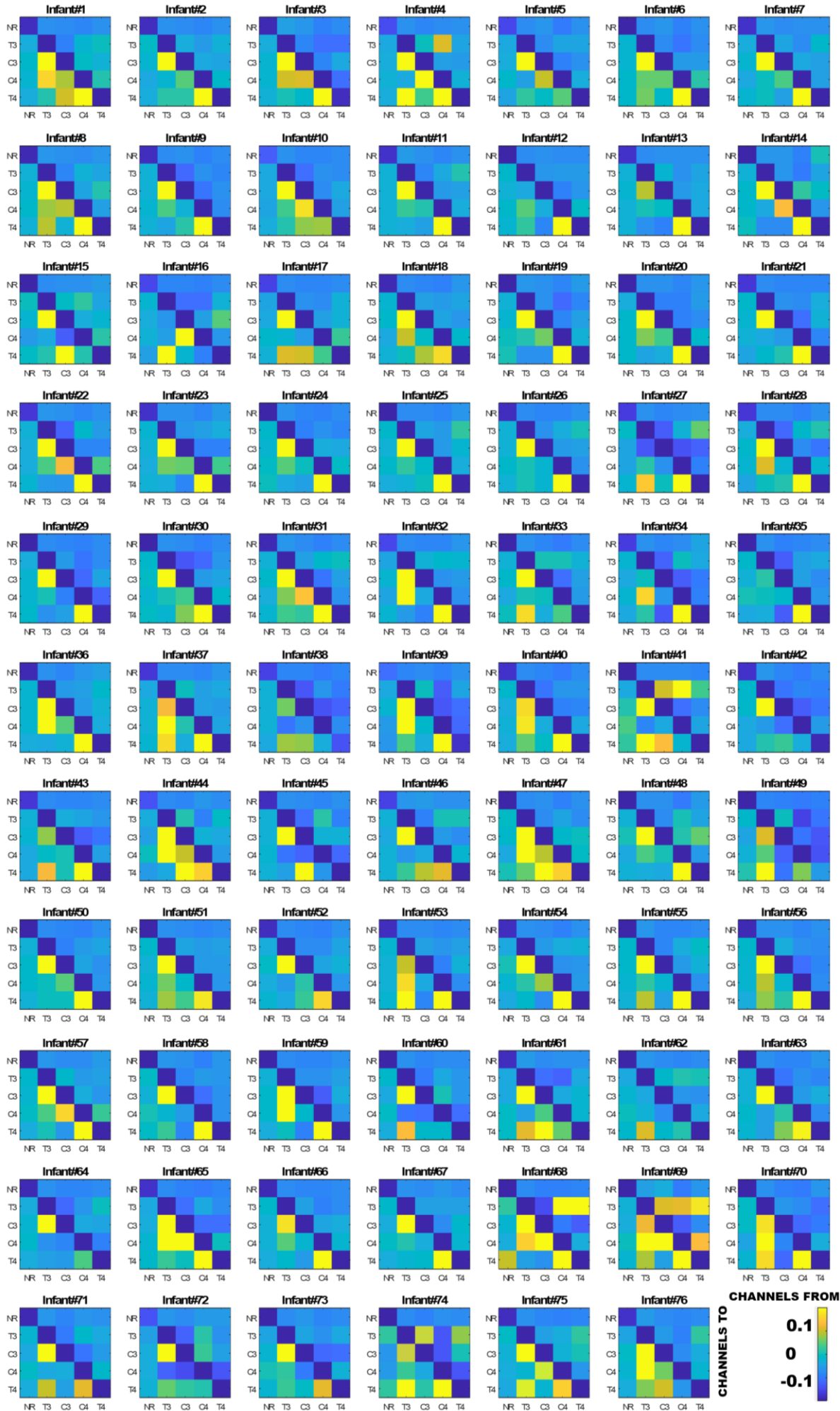


Figure 5-3. All individual infants' normalised GPDC cross-correlation plots in the 260ms onset time-point. Again, GPDC was calculated over a 2-second period, starting at 260ms post stimulus onset. The sending channels are plotted in the x-axis (including the speech envelope channels NRS), and the receiving channels are plotted on the y-axis for cross-correlation each plot. Brighter colours indicate higher normalised coherence values for that channel pair.

### Normalization Procedure Results

As listed in Table 5-1, the twelve possible channel-to-channel coherence values were tested in twelve individual t-tests against the surrogate threshold.

Table 5-1. Average normalised GPDC values for each channel-to-channel connection pairs across all infants. The 12 normalised coherence values were tested against the baseline with a mean  $M=0$  of no difference to baseline (BH-FDR corrected). The four pairwise connections significantly above threshold are highlighted in bold.

<b>All Infants: Test of means against 95%tile Surrogate Threshold</b>								
<b>T<sup>2</sup>(casewise MD)=1308.93 F<sub>(12,64)</sub>=93.08 p=0.0000</b>								
<b>Variable</b>	<b>Mean</b>	<b>Std.Dv.</b>	<b>N</b>	<b>Std.Err.</b>	<b>t-value</b>	<b>df</b>	<b>p</b>	<b>BH-FDR q</b>
'C3'-'C4'	0.017	0.076	76	0.009	1.911	75	0.060	0.065
'C3'-'T3'	-0.032	0.029	76	0.003	-9.574	75	0.000	0.000
'C3'-'T4'	0.000	0.047	76	0.005	-0.040	75	0.968	0.968
'C4'-'C3'	-0.037	0.020	76	0.002	-16.221	75	0.000	0.000
'C4'-'T3'	-0.021	0.045	76	0.005	-4.057	75	0.000	0.000
<b>'C4'-'T4'</b>	<b>0.175</b>	<b>0.153</b>	<b>76</b>	<b>0.018</b>	<b>10.007</b>	<b>75</b>	<b>0.000</b>	<b>0.000</b>
<b>'T3'-'C3'</b>	<b>0.274</b>	<b>0.169</b>	<b>76</b>	<b>0.019</b>	<b>14.126</b>	<b>75</b>	<b>0.000</b>	<b>0.000</b>
<b>'T3'-'C4'</b>	<b>0.029</b>	<b>0.073</b>	<b>76</b>	<b>0.008</b>	<b>3.484</b>	<b>75</b>	<b>0.001</b>	<b>0.001</b>
<b>'T3'-'T4'</b>	<b>0.032</b>	<b>0.088</b>	<b>76</b>	<b>0.010</b>	<b>3.207</b>	<b>75</b>	<b>0.002</b>	<b>0.002</b>
'T4'-'C3'	-0.027	0.019	76	0.002	-12.569	75	0.000	0.000
'T4'-'C4'	-0.023	0.022	76	0.003	-8.899	75	0.000	0.000
'T4'-'T3'	-0.018	0.030	76	0.003	-5.055	75	0.000	0.000

Four of the twelve connections' means were significantly above the surrogate threshold (T3->C3, T3->C4, T3->T4, and C4->T4) (Table 5-1 above). Accordingly, these four connections were used in the further analyses. Note that one more connection pair was above the threshold (C3->C4), however, it was not found to be significantly above, implying that for considerable number of infants it was not consistently above the cut-off point. We did not include that channel-pair in the analyses as we opted for the more conservative approach.

Conversely, one left->right connection (C3->T4), as well as all connections in the right->left direction had an average coherence value significantly *below* the 95th percentile threshold. This was unsurprising given the individual input-output channel maps in *Figure 5-3*. It can be seen already at the individual infant level that the values on the left below the diagonal were consistently above threshold for most infants, while the values in the top right above the diagonal were consistently below the 95%tile surrogate cut-off.

The full set of normalised GPDC values in each channel-to-channel pair, grouped by infant's familial risk of dyslexia, is provided in *Appendix V.II*.

The 95%tile super-subject surrogate threshold provided a cut-off point of a randomly defined normal distribution for the surrogate connectivity values across all infants. A specific connection being consistently and significantly below the 95%tile cut-off was a result of the majority of infants having GPDC scores lower than the top 5% of the random normal distribution of the connectivity values. That is to say, those scores came from within 95% of the random normal distribution of coherence values. Consequentially, it could not be excluded that those values resulted from spurious connectivity rather than from genuine coherence between the channels in response to the experimental manipulation (i.e the nursery rhymes linguistic input).

#### 5.4.6 GPDC Outcome Measures

The normalised generalised partial directed coherence (GPDC) values measured between the four connection pairs with means significantly above the surrogate threshold, were the dependent variables used in the following generalised linear model analyses: T3->C3, T3->C4, T3->T4, and C4->T4.

To increase the available degrees of freedom and help with interpretability, we collapsed the four connections in two levels of the within-subject variable *Connection*: two within the same side of the head (ipsilateral; T3->C3 and C4->T4) and two between hemispheres (contralateral; T3->C4, T3->T4).

## 5.4.7 Statistical Analyses Approach

### 5.4.7.1 Testing the Main Effects and Interaction between Genetic and Familial Risk

The effects of the genetic and familial risk factors on the partial directed coherence scores were formally tested in the four connection pairs above the 95% surrogate threshold: (T3->C3, T3->C4, T3->T4, and C4->T4).

For each of the three remaining genes, we ran a general linear model (GLM) with the following terms: SNPs (3 levels each, between-subjects) x Familial Risk (2 levels, between-subjects) x Connection (2 levels, within-subjects).

*DYX1C1*. Only one SNP remains to be included in the GLM for the *DYX1C1* gene. Thus, a 3(rs3743204) x 2(Familial Risk) x 2(Connection) ANOVA (GLM) is fit on the four GPDC connections.

*DCDC2*. Three SNPs located on the *DCDC2* gene are included in the GLM here. There are two more SNPs for which fewer than 3 infants were undetermined. However, there are not enough DFs to calculate a model with 5 SNPs and missing value so only SNPs for which the full set of infants were successfully genotyped are included. Thus, a 3(rs793842) x 3(rs807701) x 3(rs7751169) x 2(Familial Risk) x 2(Connection) GLM is performed on the four GPDC values.

*ROBO1*. All four SNPs for the *ROBO1* gene were included with no missing values. We ran a 3(rs333491) x 3(rs9853895) x 3(rs6803202) x 3(rs7644521) x 2(Familial Risk) x 2(Connection) GLM on the four pairwise GPDC connections.

### ***Overall FDR Correction***

False Discovery Rate was estimated over all effects in the three genes, applying both the Benjamini-Hochberg (BH) and the Storey methods. The associated error-rate q-values were reported alongside the raw p-values. Storey's FDR estimate was more powerful than BH at smaller number of comparisons, i.e less than 100. The q-value indicated how many false positives should have been expected after choosing a significance limit (i.e. at the given p-

value). A detailed account of how the p-value cut-off was calculated for the current analysis and the FDR corrections were applied is given in *Appendix V.III*.

#### **5.4.7.2 Controlling for the Effects of the Varied Number of Nursery Rhymes Contributed**

Despite the consistency in the connectivity patterns that the four-channel matrices exhibited, there was still a sizeable variability in how much data each neonatal infant contributed to the analyses. We tested whether (1) the number of contributed nursery rhymes differed systematically between familial risk groups; (2) whether the number of nursery rhymes contributed predicted significantly the by-pair coherence values for the connections that were above surrogate threshold.

#### **5.4.7.3 Testing the Main Effects of the Parent of Origin**

As there were significant differences in the brain-to-speech phase coherence indices based on the infants' parental risk status (i.e. whether the familial dyslexia risk originated from the mother (M), the father (F), or neither (O)), we also formally tested the network coherence indices for statistical differences based of the parent of origin. As the size of the parental risk groups differed and the GPDC values were not normally distributed for each connection and risk group, four separate non-parametric Kruskal-Wallis comparisons were computed on the normalised GPDC values in the four connection pairs: T3->C3; T3->C4; T3->T4; and T4->C4. Unfortunately, in the GPDC dataset, the chances of detecting a parental risk effect were reduced by the size of the groups to be compared: only 12 infants included in the GPDC analyses dataset had maternal dyslexia.

---

## **5.5 Study Two: Results**

### **5.5.1 Summary Results: Effects of Genotype and Familial Risk on Infants' four-channel network connectivity at birth**

The table below shows a summary of the significant main effects and interactions by SNP for each of the three genes (see *Chapter 2* for a justification on genes included), each of which was analysed in a separate GLM model taking the GPDC values in the ipsi- and contralateral connection pairs as the dependent variable, and the infants' genotype by SNP and familial risk as the between-subjects grouping factors. In all three models, a main effect of *Connection* was observed where electrode locations within the same hemisphere showed stronger neural connectivity (GPDC) than electrode locations across hemispheres.

Importantly, two SNPs showed significant interaction effects with *Connection*: *rs7751169* (on *DCDC2*) and *rs9853895* (on *ROBO1*), suggesting that the genotype was modulating the network connectivity strength. The interaction between *rs9853895* X *Connection* remained significant after accounting for the FDR corrections. Another *ROBO1* SNP *rs333391* had a differential effect at the levels of the *Familial Risk* and the *Connection* variables in a significant three-way interaction. Full details of these results are reported next.

*Table 5-2. Significant effects across the three generalised linear models ran, one for each SNP. Uncorrected p-values <.05 are indicated with a tick. BH-FDR corrected p-values are reported in the main text alongside.*

	Main Effect	Interaction w/ FamRisk	Interaction w/ Connection	Interaction w/ FamRisk & Connection
<b>DCDC2</b>				
"rs793842"	-	-	-	-
"rs807701"	-	-	-	-
rs7751169	-	-	✓	-
FamRisk	-	-	-	-
Connection	✓	-	-	-
<b>DYX1C1</b>				
rs3743204	-	-	-	-
FamRisk	-	-	-	-
Connection	✓	-	-	-
<b>ROBO1</b>				
"rs333491"	-	-	-	✓
rs9853895	-	-	✓	-
rs6803202	-	-	-	-
rs7644521	-	-	-	-
FamRisk	-	-	-	-
Connection	✓	-	-	-

### 5.5.2 Detailed GLM Results by Gene

As a general note, the main effect of Connection was strongly significant in all models by gene. The specific effect parameters for each gene are detailed in the dedicated paragraphs below. All GLMs highlighted the effects of *Connection* in the same direction. As shown in *Figure 5-4* the effect was driven by the ipsilateral connections being significantly stronger than contralateral ones, reflecting a foreseeable proximity effect. Furthermore, there was also a significant difference between the two ipsilateral connection pairs whereby the normalised coherence in the left hemispheric pair was consistently significantly higher than the normalised coherence between the right-hemispheric pair of channels. Finally, the T3-C3 directed coherence was significantly higher than all other pairs.

The Main Effects of Connection on the GPDC scores

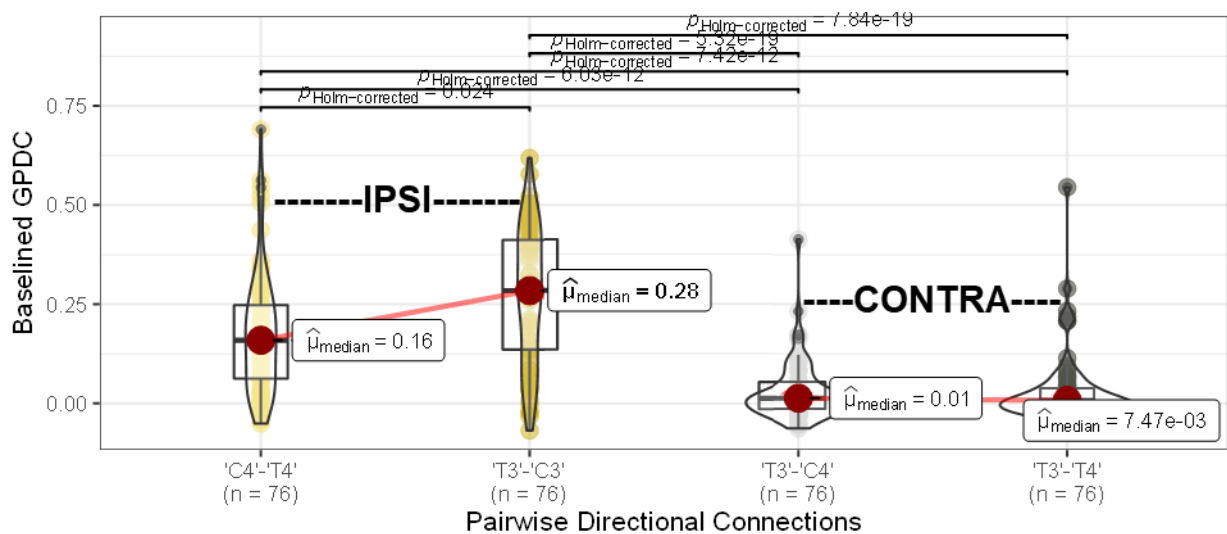


*Figure 5-4.* A representative violin plot of the main effect of the Connection variable on the baselined GPDC scores in the four connection pairs. Significant post-hoc differences between connection pairs are indicated with the bars above the violins, the corrected p-values are reported on the bars.

#### ***DYX1C1: rs3743204***

Only the main effect of Connection was significant in this model at  $F_{(2,69)}=26.14$ ,  $p<.00001$ ,  $\eta^2=.431$ ,  $w.l.=569$ . The effect remained under the 1% error rate when FDR was estimated using both methods of BH- $q<.00001$ , and Storey- $q<.00001$ .

***DCDC2: rs793842; rs807701 & rs7751169***

The main effect of Connection was again significant at  $F_{(2,61)}=27.10$ ,  $p<.00001$ ,  $\eta^2=.47$ ,  $w.l.=.53$ . The interaction between (Connection x rs7751169) was also significant at  $F_{(4,122)}=2.72$ ,  $p<.033$ ,  $\eta^2=.082$ ,  $w.l.=.843$ .

Post-hoc Fisher's LSD test showed that the significant interaction between (Connection x rs7751169) came from the rs7751169-1 having higher connectivity in the left ipsilateral T3->C3 connection than both other genotypes (rs7751169#1>rs7751169#2 at  $p<.02$ , and rs7751169#1>rs7751169#3 at  $p<.0002$ , LSD corrected), demonstrated in the *Figure 5-5* below<sup>14</sup>.

---

<sup>14</sup> When controlling for FRD using both the BH and the Storey methods, only the Connection term remained under the 1% error rate (BH-q<.00001, Storey-q<.00001). The (Connection x rs7751169) had an error rate of Storey-q=.075, BH-q=.166. Details on all corrections are given in *Appendix V.III*.

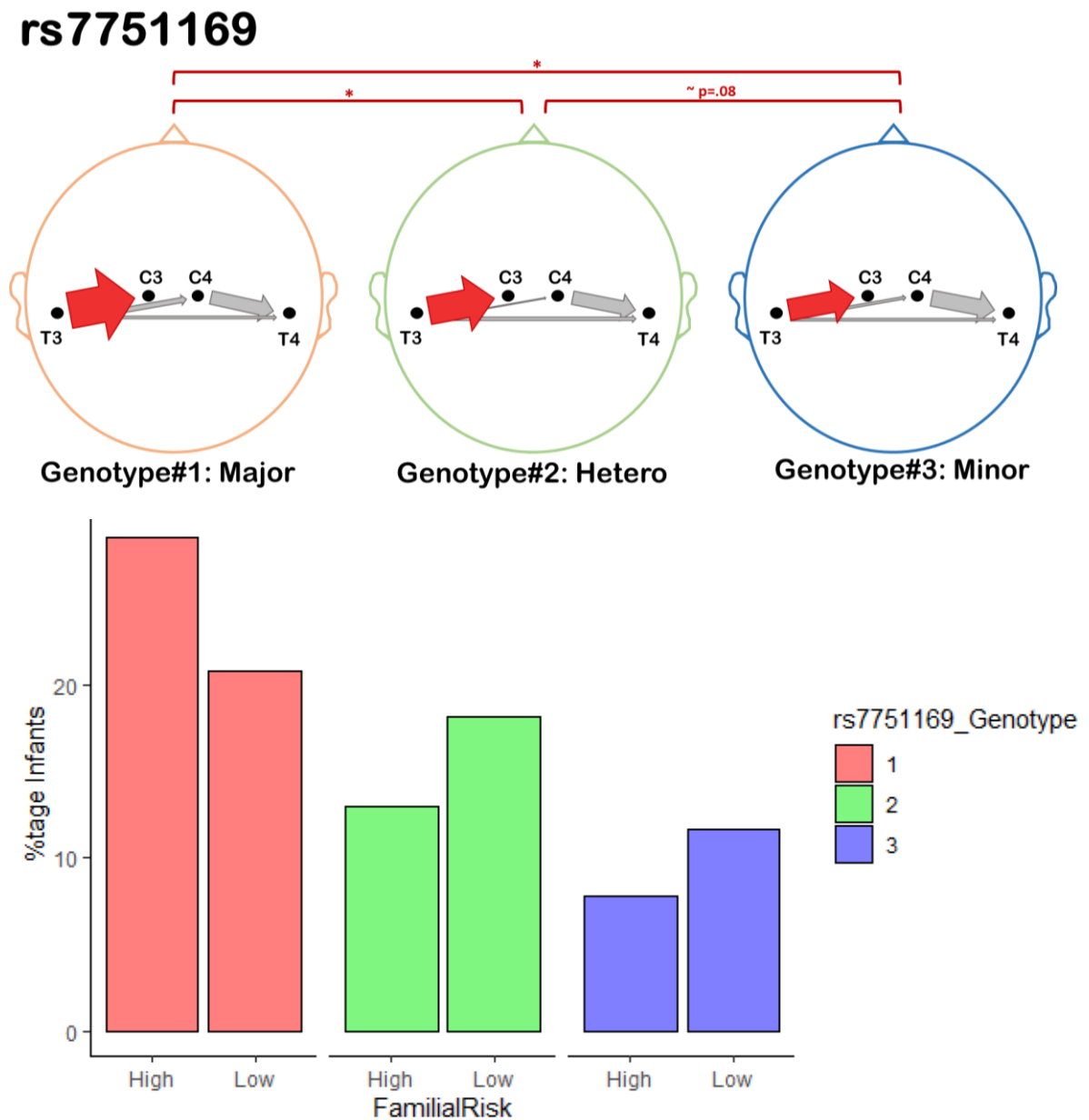


Figure 5-5. The main effects of rs7751169 (DCDC2) genotype on the normalised GPDC values. The direction of the arrows indicates the direction of coherence; the size of the arrows matches to the value of the GPDC metric; the red arrows mark significant differences between genotype groups. The red bars above the heads mark the groups which were significantly different (A). A histogram of the percentage of infants in each genotype group split by their familial dyslexia risk: high and low (B).

We further assessed the frequency of the three rs7751169 genotypes in each Familial risk group, and this did not differ between the high and low risk infants, Pearson's  $\chi^2_{(2)} = 2.58$ ,  $p = .275$ , n.s.

**ROB01: rs333491; rs9853895; rs6803202 & rs7644521**

The main effect of Connection was again significant at  $F_{(2,57)}=11.95, p<.00005, \eta^2=.295, w.l.=.705$  (see *Figures 5-6 and 5-7*). Fisher's LSD correction ran post-hoc confirmed that the main effect of Connection came from the fact that expectedly, the ipsilateral connections had higher coherence than the contralateral ones ( $p<.00001$  for Fisher's LSD for both DVs).

Importantly, the interaction between (Connection x rs9853895 SNP) was significant at  $F_{(2,114)}=3.29, p<.014, \eta^2=.104, w.l.=.804$ . Fisher's LSD post-hoc test on the interaction term between (Connection x rs9853895) revealed that the effect was driven by the large difference between the two levels of the Connection variable, as well as by the difference between rs9853895#1>rs9853895#2 ( $p<.00008$ ) and rs9853895-1>rs9853895-3 ( $p<.025$ ) in the ipsilateral left hemisphere directed coherence (T3->C4, *Figure 5-6* below)<sup>15</sup>.

---

<sup>15</sup> Controlling for FRD using the BH method, the Connection term remained under the 1% error rate (BH-q<.00001, Storey-q<.00001). When estimating the FDR via the Storey method, the (Connection x rs9853895) was also significant under the 5% error rate with Storey-q=.04, while it was only under the 9% error rate in the BH correction, BH-q=.088. Finally, the (Connection x Familial Risk x rs333491) interaction did not remain significant after accounting for false discovery rate with an error rate of Storey-q=.075, BH-q=.166.

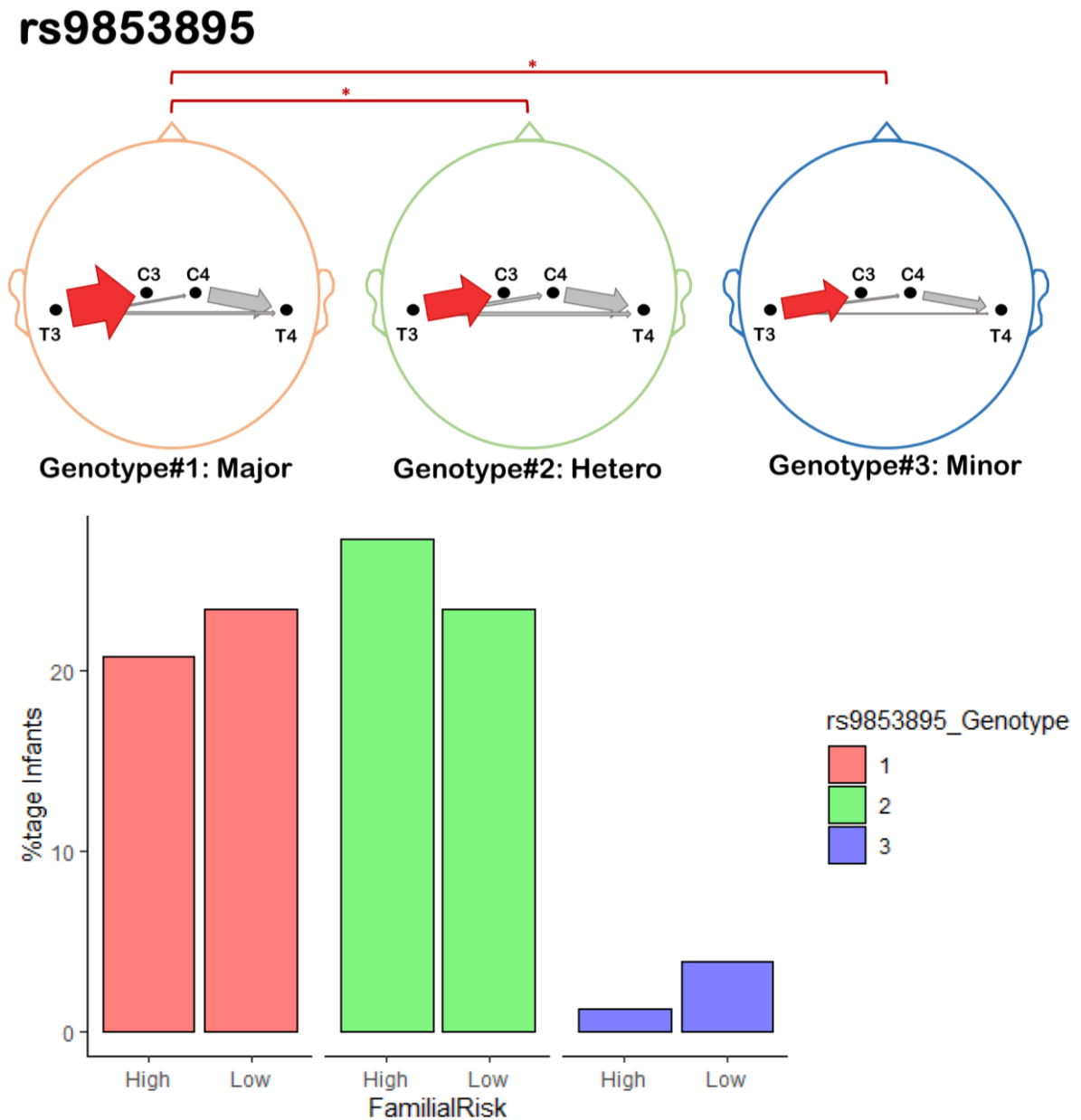


Figure 5-6. The main effects of rs9853895 (ROB01) genotype on the normalised GPDC values. The direction of the arrows indicates the direction of coherence; the size of the arrows matches to the value of the GPDC metric; the red arrows mark significant differences between genotype groups. The red bars above the heads mark the groups which were significantly different (A). A histogram of the percentage of infants in each genotype group split by their familial dyslexia risk: high and low (B).

The proportion of the three rs9853895 genotypes did not differ significantly between the high and low risk infants, Pearson's  $\chi^2_{(2)} = 1.17, p = .557, n.s.$

Additionally, the three-way interaction between (Connection x Familial Risk x rs333491 SNP) was also significant at  $F_{(4,114)}=2.71, p<.034, \eta^2=.087, w.l.=.834$ . Fisher's LSD post-hoc test on the three-way interaction term between (Connection x Familial Risk x rs333491, *Figure 5-7* below) revealed that the effect was again driven by the differences between the two levels of the Connection variable. Additionally, in infants at low familial risk of dyslexia, the rs333491#1 homozygous genotype showed higher GPDC than the heterozygous infants in the left ipsilateral connection (T3->C3, rs333491#1>rs333491#2 at  $p<.018$ , Fisher's LSD corrected), while only rs333491#3 infants had higher coherence than the heterozygous infants in the high-risk group for T3->C3 (rs333491#3>rs333491#2 at  $p<.003$  Fisher's LSD corrected). Infants in the low-risk group carrying the rs333491-3 genotype had higher GPDC than the heterozygous infants at low risk in the contralateral T3->C4 connection (rs333491#3>rs333491#2 at  $p<.043$ , LSD corrected). The rs333491#3 infants also had higher directed connectivity than both other genotype groups for the right ipsilateral connection C4->T4 (rs333491#3>rs333491#1 at  $p<.009$ , and rs333491#3>rs333491#2 at  $p<.001$  Fisher's LSD corrected). Finally, going against the overall pattern, both the left and right ipsilateral connections showed higher connectivity in the infants at high familial risk than those at low familial risk in the rs333491#3 genotype only (high risk > low risk at  $p<.027$  for the left connection, and at  $p<.031$  for the right connection, Fisher's LSD corrected).

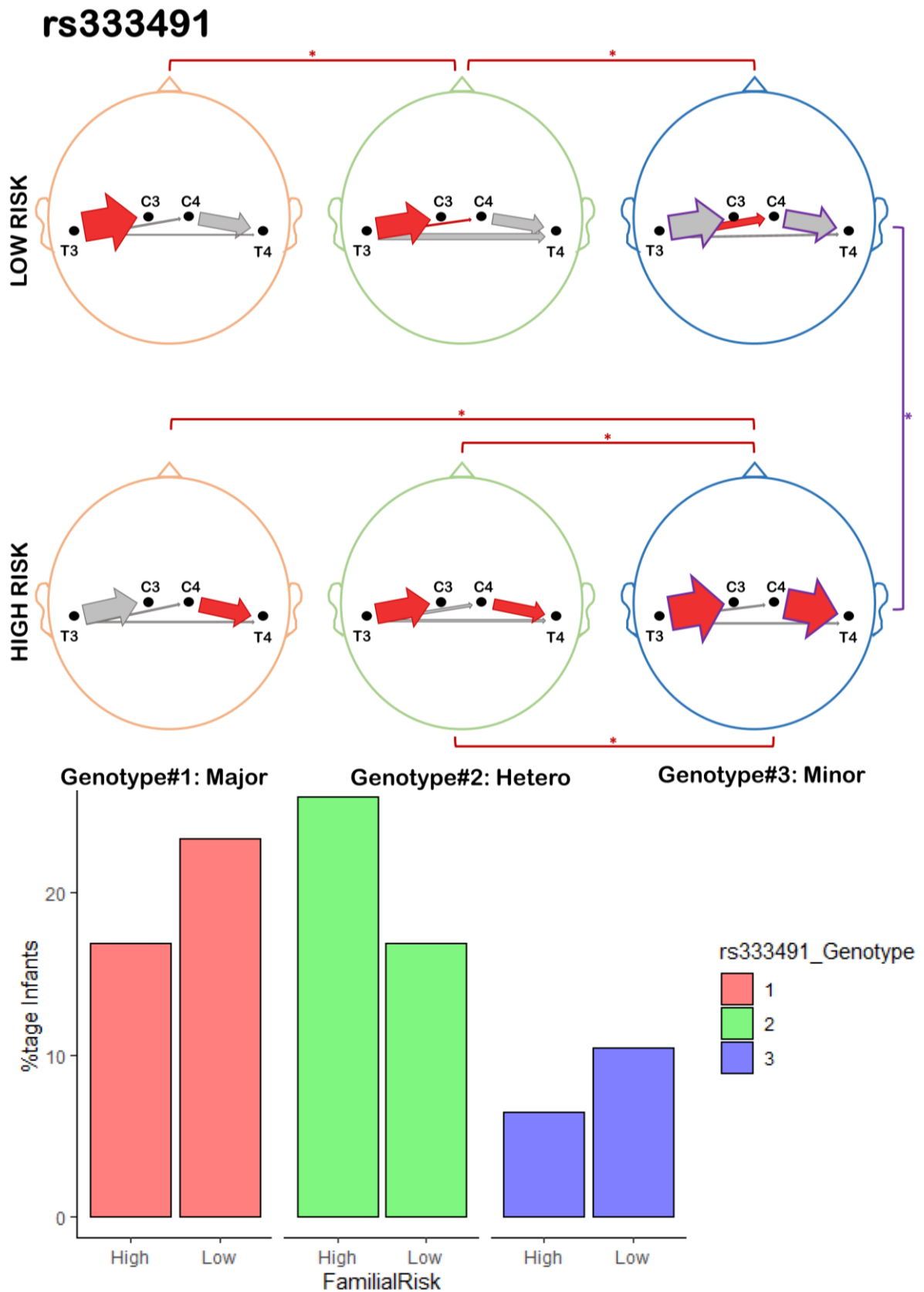


Figure 5-7. The main effects of rs9853895 (ROB01) genotype on the normalised GPDC values. The direction of the arrows indicates the direction of coherence; the size of the arrows matches to the value of the GPDC metric; the red arrows mark significant differences between

*genotype groups. The red bars above the heads mark the groups which were significantly different. The purple bar on the righthand side indices the significant difference between the high and low familial risk groups in the arrows surrounded by a purple borderline (A). A histogram of the percentage of infants in each genotype group split by their familial dyslexia risk: high and low (B).*

The three genotypes of the rs333491 SNP did not differ in their distribution between the two familial risk groups,  $\chi^2_{(2)}=3.33$ ,  $p=.189$ , *n.s.*

### 5.5.3 Controlling for the Effects of the Varied Number of Nursery Rhymes Contributed

The results from the control analyses involving the number of nursery rhymes onset epochs contributed by each infant are detailed in *Appendix V.IV*. Briefly, a multivariate t-test comparison confirmed that the number of contributed nursery rhymes did not differ between familial risk groups. The number of onset speech epochs did not predict the thresholded GPDC values for the ipsilateral connections (T3-> C3 and C4->T4). However, it was a significant predictor of GPDC in the contralateral connection pairs (T3->C3 and T3->T4).

### 5.5.4 Effects of the Parent of Origin on the Network Coherence Estimates

To test the effects of the parent of origin (i.e. mother (M), father (F) and no familial risk (O)), four Kruskal-Wallis non-parametric tests were run on normalized GPDC scores in the four connection pairs. Neither connection pair showed a significant difference in the GPDC values between the three parental risk groups (chi-square statistics detailed below).

There was no significant difference between parental dyslexia groups neither in the two ipsilateral connections: in the T3 to C3 normalized coherence values,  $KW\chi^2_{(2)}= 0.91433$ ,  $df = 2$ ,  $p= .633$ , *n.s.* (*Figure 5-8A* below) and in the C4 to T4 normalized GPDC,  $KW\chi^2_{(2)}= 0.65036$ ,  $p= .722$ , *n.s.* (*Figure 5-8B*); nor in the two contralateral ones: for T3 to C4,  $KW\chi^2_{(2)}= 1.7817$ ,  $p= .41$ , *n.s.* (*Figure 5-8C*), and for T3 to T4,  $KW\chi^2_{(2)}= 1.0536$ ,  $p = .59$ , *n.s.* (*Figure 5-8D*).

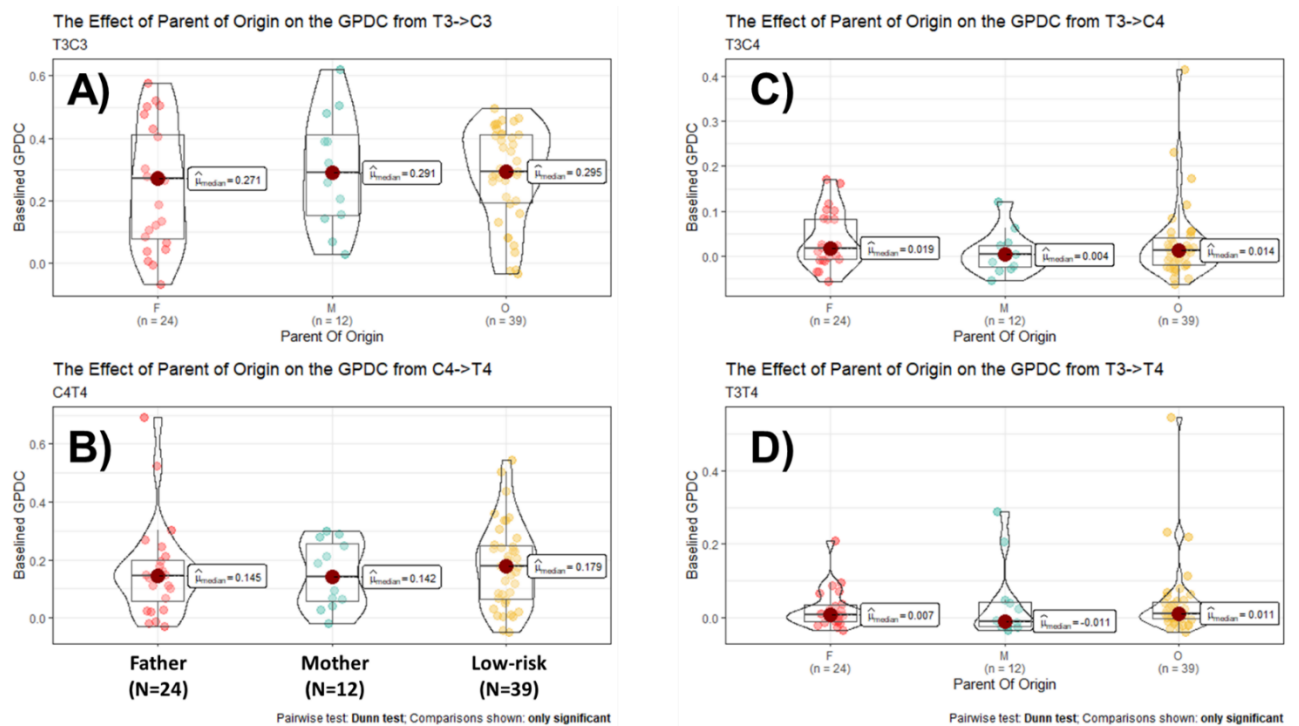


Figure 5-8. Violin plots showing the distribution of normalised GPDC values for each parental risk group in the four pairwise channel connections: T3->C3 (A), T3->C4 (B), T3->T4 (C), and C4->T4 (D).

### 5.5.5 Link between delayed PLV latency and Network Coherence

Finally, we tested the prediction that reduced channel-to-channel network coherence was associated with the observed delay in the brain-to-speech phase-locking for the infants at (maternal and genetic) risk of dyslexia in Study One.

A backward stepwise regression with removal was used to estimate the predictive power of the four GPDC channel-pairs above surrogate threshold on the individual infants' PLV latencies, accounting for the infants' familial risk status. The regression model was not significant at 5% alpha level,  $F_{(1,72)}=3.78$ ,  $p=.056$ , *n.s.* The regression model retained only one predictor variable, T3->C3,  $R^2 = .22$ ,  $AdjR^2 = .04$ . Therefore, there was no significant predictive power of the connectivity between channel pairs over the average PLV latency distribution in the current set of infants (N=74). However, the direction of the relationship between the measured coherence in the T3->C3 channel-pair and the latency of the PLV onset peaks was as predicted, the higher the coherence measured, the lower the latency (Figure 5.9 below)

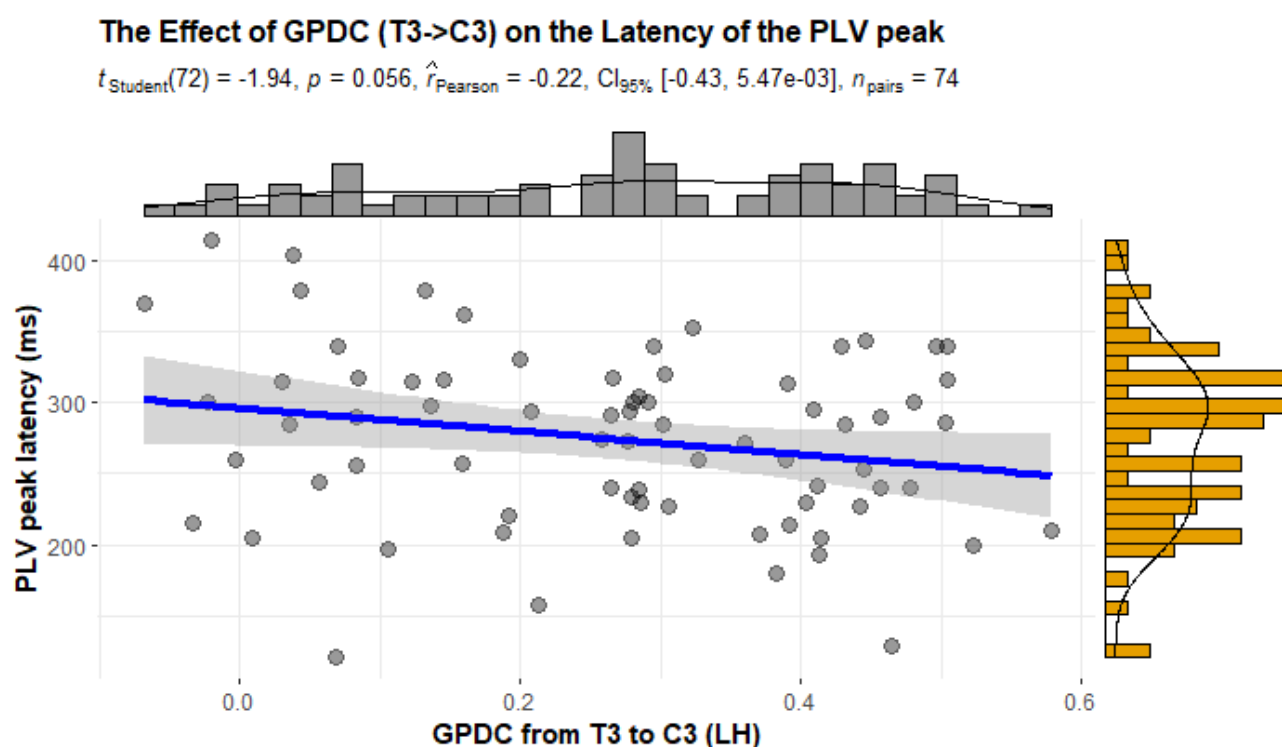


Figure 5-9. A scatterplot of the PLV onset latencies (y-axis) against the GPDC (coherence, x-axis) measured between the T3->C3 channel-pair in the current set of infants. Bar plots and line chart above each axis show the histogram distribution of the respective variable. The blue line is the fitted regression line, and the gray shading around it depicts the 95% confidence interval.

## 5.6 Study Two: Discussion

### 5.6.1 Summary of the Findings in Study Two

We found evidence for a reduced left hemispheric directed coherence (temporal-to-central channel) in infants carrying the genotype#3 variants of the ROBO1 and DCDC2 SNPs, independent of the infants' familial risk. There was an additional trend toward increased right hemispheric directed (top-to-bottom, i.e. central-to-temporal channel) coherence in the genotype#3 variants of the ROBO1 gene in infants at high familial risk only.

We interpreted these results to indicate a processing capacity limitation of the underlying noisier neural network in relation to genetic susceptibility incurred by genes previously implicated with a more excitable endogenous neural activation. The results were also in line with findings of reduced left-hemispheric white and gray matter connectivity in MRI-

based infant research showing reduced leftward lateralisation to acoustic speech processing in children at risk of dyslexia (Black et al., 2012; Langer et al., 2015; Łuniewska et al., 2019; Niogi & McCandliss, 2006; Raschle et al., 2012; Xia et al., 2017; Zhao et al., 2016). These findings were most readily compatible with the theoretical frameworks of neural noise hypotheses as proposed by (Hancock, Pugh, et al., 2017). The neural noise framework predicts higher variability in random neural activity associated with the impact of increased DCDC2 risk variants expression in temporal-parietal and temporal-occipital areas, leading to a reduction in timing accuracy and therefore, in cortical synchronicity within and between those areas. Activation noise from increased neural excitability in reading-associated cortical networks underlie the low-level sensory processing deficits reported in the literature, as well as the future phonological problems.

### 5.6.2 Link between the Studies One & Two

Study One dealt with how the acoustic speech signal was processed differentially between groups as it arrived in the neonatal brain. In Study Two, we tried to understand better the signal processing capacities of the network itself when embedded in the signal presentation. Theoretically, the two should be related as we hypothesised that the cortical miswiring resulting from prenatal genetic influences would lead to noisier (i.e. more variable) processing capacity within the network, leading to diminished signal synchronisation. In this way, the PLV and GPDC metrics within the same infants and speech onset epochs should be theoretically related so that infants with lower network coherence should also have delayed brain-to-speech phase-locking. We tested this hypothesis, accounting also for infants' familial risk but no significant effect was detected in the current sample of infants. Still, the regression line fitted between the GPDC from T3->C3 and the PLV latency values per infant pointed in the predicted direction. It should be noted that the sample size of this test was smaller than that of the PLV and GPDC studies described in *Chapters 4* and *5* as not all infants had sufficient number of trials in both metrics. Further implications are discussed in *Chapter 7*.



# **PART THREE**

## **CHAPTER SIX**

### **THE LONGITUDINAL DATASET**

## CHAPTER SIX: THE LONGITUDINAL DATASET

---

### 6.1 The Aims of the Longitudinal Research Project

- (1) Identify potential neural biomarkers of dyslexia risk in neonates, and
- (2) Elucidate specific genotypes that are associated with these neural deficits
- (3) Identify “risk profiles” based on the interaction between genetics and the oscillatory processing of speech, and
- (4) Follow the developmental trajectories of the infants with both the high and low risk profiles over the first two years of life
- (5) Evaluate the mediating effects of the quality of the early home language environment in the developmental trajectories of infants of both low- and high-risk profiles by improving or deteriorating the neuronal entrainment to the available speech inputs.

A schematic representation of the main aims and proposed influences in the longitudinal project are given in *Figure 6-1* below.

The first two project aims were addressed at birth in the two studies reported in the previous Section 2 by measuring the neonatal neural oscillatory response to speech, as well as their sensory-space network connectivity. These two metrics were contrasted between infants of different genotypes on the dyslexia susceptibility genes, and of different familial risk groups. Thus, we identified which neural markers were related to genetic and familial risk profiles (aim 3 as outlined above).

To address aims (4) and (5), we measured longitudinally the development of a proportion of our neonatal cohort on the same neural processing measures in two additional time-points (described in detail in *Sections 6.4.2.2* and *6.4.2.3*). Our intentions for the future are to evaluate how the metrics collected at the older ages fair against the infants’ neonatal neural “performance”. We additionally collected samples of the home language environment for the families who remained in the study, as well as the infants’ early developmental markers on social and language parameters, the families’ educational and

socio-economic background, and the individual differences in parental mood and personality traits. All these measures would give us an interim snapshot of the home environment for the infants of high and low risk profiles.

The final aim (5) would make use of a phonological outcome measure that we acquired at the age of 23 months using a test of early expressive phonological skills (PEEPS, described in detail in Section 6.4.2.4). We would be able to evaluate whether the high and low risk profiles identified at birth are associated with differential performance on the phonological test, and whether this putative association is mediated by the quality of the early home (language) environment.

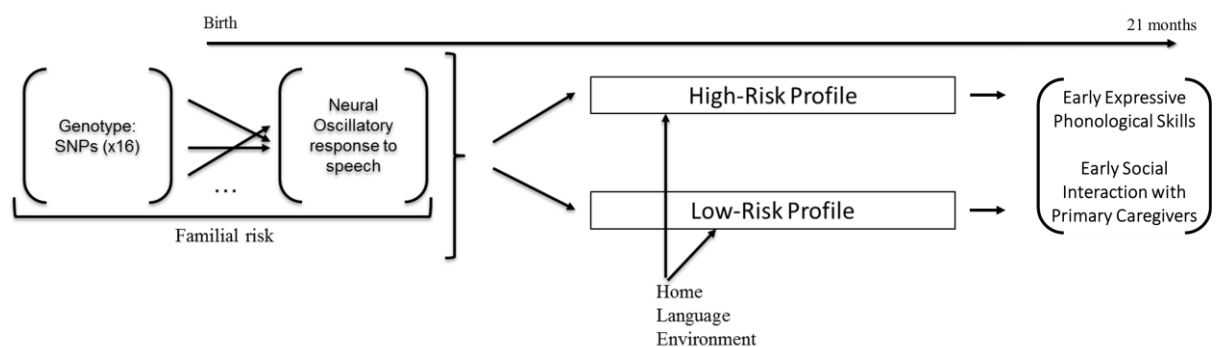


Figure 6-1. A schematic representation of the key factors and their hypothesised dependencies tested in the course of the longitudinal study.

## 6.2 Brief Rationale & Potential Impact

Phonological development (which goes awry in dyslexia) begins in utero and continues throughout the first years of a child's life. Thus, the 'phonological deficit' is incurred well before the dyslexic child reaches schooling age and attempts learning to read.

Consequently, effective intervention for dyslexia should ideally begin *before* children enter school, to support phonological development *as it occurs* during the early years. To target such early intervention appropriately (given limited educational resources), reliable biomarkers are needed to identify those children who are at highest risk for developing dyslexia.

---

### 6.3 My Role in The Longitudinal Project

This doctoral dissertation reports a subset of data from a longitudinal study that aimed to identify potential neural biomarkers of dyslexia risk in neonates and to elucidate specific genotypes that are associated with these neural deficits. Additionally, the wider study assessed the quality of the early home language environment as a potential resilience factor for poor language development. As an outcome measure at around two years of age, we tested the expressive phonological skills using PEEPS, a tool adapted for the age group of 18-30 months. One-hundred infants (49 at high and 51 at low familial risk) were assessed at birth and half of those were followed up longitudinally at three additional timepoints: at 7.5, 15 and 23 months of age.

My role in the wider project was two-fold. In the first place, I completed the second half of neonatal data collection that had started prior to my PhD program, and conducted all the electrophysiological processing, genotyping and statistical analyses for the at-birth time-point (the green panel of *Figure 3-1* in *Chapter 3*). These are the data reported in the current thesis.

My second principal contribution to the wider project was to convert the study from a single time-point into a longitudinal one, which was approved by the East of England – Cambridge Central Research Ethics Committee during my first year of studies. I next went on to set up the home-language measurements and design the experimental protocols for the to the lab-based testing sessions at 7.5 and later at 15 months<sup>16</sup> (the top two middle and bottom two panels in *Figure 3-1*). The home- and following lab-based measurements were running in parallel but remain to be processed and analysed. Finally, I helped convert the test of expressive phonological skills used with the now around 2 years old toddlers for virtual application during the first national lockdown (the right-most panel in *Figure 3-1*). I have since been testing the families who still wished to remain in the study, online.

---

<sup>16</sup> The experimental protocol at the 15-month time-point included three socially interactive paradigms designed in collaboration with an MPhil student, who also pre-processed the EEG data for that time point. The results from those experiments are reported in her MPhil thesis (Carozza, 2020).

---

## 6.4 Data Collection

### 6.4.1 Participant Recruitment

One hundred and two neonatal infants and their families were recruited in the period between March 2016 and Jan 2020. Families were recruited to the study in two ways: (1) prior to their delivery date via leaflets and advertisements placed in the Rosie Maternity Hospital (which sees 6000 live births a year) and in other communal areas; and (2) shortly after they had given birth in Rosie Maternity Hospital, where we approached them in person on the post-natal wards and invited them to take part. Written informed consent was obtained from parents for themselves and on behalf of their infants after fully explaining the experimental procedures and the implications of genetic testing. In follow-up sessions, the parents gave consent for video and photographs to be taken during the experiments and used in presentations and reports. No reimbursement was offered to the families for their participation. The study was approved by East of England – Cambridge Central Research Ethics Committee (REC Ref: 15/EE/0165). The protocol, information sheet and consent form templates are attached in *Appendix I*.

The first 50 families with a new-born infant were recruited prior to the start of my PhD program by an MPhil student (P.C.), two research assistants (L.A. and L.B.) and a consultant neonatologist (S.M.). P.C. and L.A. collected 15 neonatal datasets in the period between March 2016 – August 2016. L.B and S.M. collected 35 additional datasets between December 2016 – July 2017 (*Figure 3-1*, green panel). The remaining 50 families were recruited and tested by me between September 2018 – December 2019 and consented to participate in the research study longitudinally. The latter 50 families were invited to take part in research in person twice more, when the participating infants were ~ 7.5 and 15 months of age. These families are currently participating in the final testing stage of the study, whereby the now toddlers (23-24 months old) are assessed on their expressive phonological skills in an online video call.

At the time of testing at birth, all neonates were healthy full-term infants (born at >255 days, or >36w+3d), with a normal 20-week anomaly scan and no evidence of intrauterine growth restriction or perinatal hypoxia-ischaemia at birth. All infants had passed the Newborn and Infant Physical Examination (NIPE) and had their hearing tests performed on

the ward by the Hearing Screen Team in the Rosie Hospital prior to the experiment. Two infants had an inconclusive hearing screen bilaterally at the time of the experiment, presumably due to very young age (<24 hours postnatally). Normal hearing was confirmed at a subsequent follow up screening, therefore these infants were retained in the study. All infants had English as a native maternal tongue, and four infants had exposure to a second primary language (French, German, Hungarian, and Italian). All parents reported no known visual, hearing, or neurological problems. A brief summary of the dyslexia-risk related characteristics of the participating infants and their parents is given in the Common Methods (*Chapter 3.1*).

At the second testing session, 28 of the longitudinally recruited infants<sup>17</sup> came back to the lab at the age of  $M=224.7$  ( $SD = 25.3$ ) days, 10 girls, 9 at high familial risk of dyslexia, as defined in *Chapter 3.1* (*Figure 3-1*, second upper panel).

Ten infants came back to the lab for the third time at the age of  $M=461.8$  ( $SD=31.6$ ) days, 4 girls, 3 at high familial risk. Four more families had agreed to take part in the study, and some were scheduled in for testing when national lockdown was instated in the UK and all in-person research ceased in April 2020. The data at the 15 months testing age were collected in collaboration with S.C., an MPhil student (*Figure 3-1*, third upper panel).

Finally, 28 families agreed to take part in the online testing session at around 2 years of infant's age. Twenty-one infants have already had their early expressive phonological skills measured. They were at the age for  $M=710.6$ , ( $SD=30.9$ ) days in the first online session, and  $M=715.6$  ( $SD=32.3$ ) at the second one, 8 girls, 7 at high familial dyslexia risk. Seven more infants are awaiting to become of testing age (*Figure 3-1*, rightmost panel).

## 6.4.2 Neuro-Behavioural Data Acquisition

---

<sup>17</sup> In fact, 32 participating families were willing to participate in the follow-up sessions, however, three families did not reply to my emails until after their infant had significantly outgrown the targeted age of participation, so they were invited to come back for the next testing session at 15 months.

In all experimental procedures which involved the concurrent recording of EEG in this cohort, the presentation order of tasks within the protocol was fixed between participants and age groups, and follow the order outlined in *Figure 3-1*. A summary of all tasks used at each age group with a brief statement on the main variations is provided in the same figure.

#### 6.4.2.1 Neonatal Data Collection

##### *Neuroimaging Procedure*

The EEG experimental setup was as described in *Chapter 3*, including the same EEG montage, and presentation and acquisition platforms.

*Sleep/Resting State:* After the EEG cap was put on the infant's head, and they were securely swaddled in the bassinette, the acquisition sequence began with 12-20 minutes of resting state or sleep for the infants. This was a passive protocol in which the neonates did not receive any overt sensory stimulation. They were left to settle in a quiet darkened room, and the EEG was recorded while they appeared in quiet restfulness or sleep (it was sometimes difficult to visually assess by looking at the infant whether they were asleep or not, and I lacked training in neonatal polysomnographic EEG reading).

*Infant-Directed Speech Entrainment:* Next, a set of pre-recorded nursery rhymes was played to the baby via speakers for another 20 minutes. The nursery rhymes protocol is described in greater detail in *Chapter 3* (Common Methods).

*The Oddball Paradigm:* A standard measure of non-speech sound processing was taken using an auditory oddball. MMN has been reported in newborn infants (i.e., Daneshvarfard et al., 2019; Ghislaine Dehaene-Lambertz et al., 2008; Mahmoudzadeh et al., 2017) in association with dyslexia risk and impoverished reading and phonological outcomes (Guttorm et al., 2001; Guttorm<sup>1</sup> et al., 2010; He et al., 2007; Leppänen et al., 2012; Leppänen et al., 2010; Van Zuijen et al., 2013). Thus, we used two syllables which differed in their rise-time: /wa/ was the frequent stimulus, and /ba/ was the deviant. We recorded a female native British speaker producing multiple repetitions of both syllables. Then, using the analysis toolbox in Praat (Boersma & Weenink, 2016), we selected one copy of each syllable to be the closest match in pitch (frequency), amplitude (loudness) and duration (*Table 6-1*

below). Finally, the two selected iterations were amplitude adjusted (Praat) to both have an average amplitude of 60dB so that the two syllables most perceptibly and objectively differed in the duration of their rise-time.

The test consisted of a total of 300 stimuli, with 15% deviants, presented at roughly 1Hz with a randomly jittered inter-stimulus interval of between 700-950ms. There were at least three frequent /wa/ played between two deviants /ba/. The total running time was 5 minutes, with the initial minute featuring only the frequent syllables to establish habituation.

*Table 6-1. Acoustic characteristics of the syllable stimuli used in the oddball paradigm.*

<b>Syllable</b>	<b>Pitch [Hz]</b>	<b>Intensity [dB]</b>	<b>Intensity equalized [dB]</b>	<b>Duration [s]</b>	<b>Rise time [s]</b>
<b>[ba:]</b>	170.10	74.41	60.00	0.290	0.054
<b>[wa:]</b>	169.90	75.26	60.00	0.293	0.108
<b><i>Difference</i></b>	<b><i>0.20</i></b>	<b><i>0.85</i></b>	<b><i>0.00</i></b>	<b><i>0.003</i></b>	<b><i>0.500</i></b>

In the longitudinal aspect of the study, the 50 latest participating families were invited back to the lab for two additional testing sessions, at 7.5 months apart, and for an online testing session at around the infant's age of 2 years.

#### **6.4.2.2 Data Collection Session Two: at the infants' 7.5 months of age.**

##### ***Latest Modifications in the Experimental Materials & Setup***

In the second testing session, the EEG setup and the testing protocol were very similar to those used during the at-birth testing.

The three main differences were the EEG montage, which was modified to include 5 additional channels (16 channels in total, *Figure 6-2B* below), the addition of a socially

interactive test between the infant and their parent (no EEG acquired), and the videorecording of the entire testing session. All videos were recorded with the purpose to be later coded for behavioural characteristics, and segments of on-task attention or movement (especially useful at the artifact-rejection EEG pre-processing step). The parent(s) accompanying the infant to the testing session were seated on a comfortable chair positioned at 45° angle of the infant's frontal vision field (*Figure 6-2D*). The parent's chair was slightly tucked behind the infant's so that they were still visually available if needed for comfort, but sustained eye contact was not comfortable. Additionally, the parents were instructed to avoid eye contact with their infant during the presentation of stimuli, and if the infant persisted to seek their attention, to try and redirect their interest back to the experiment by pointing and looking at the screen themselves. A depiction of the experimental setup is given in *Figure 6-2A, C & D*.

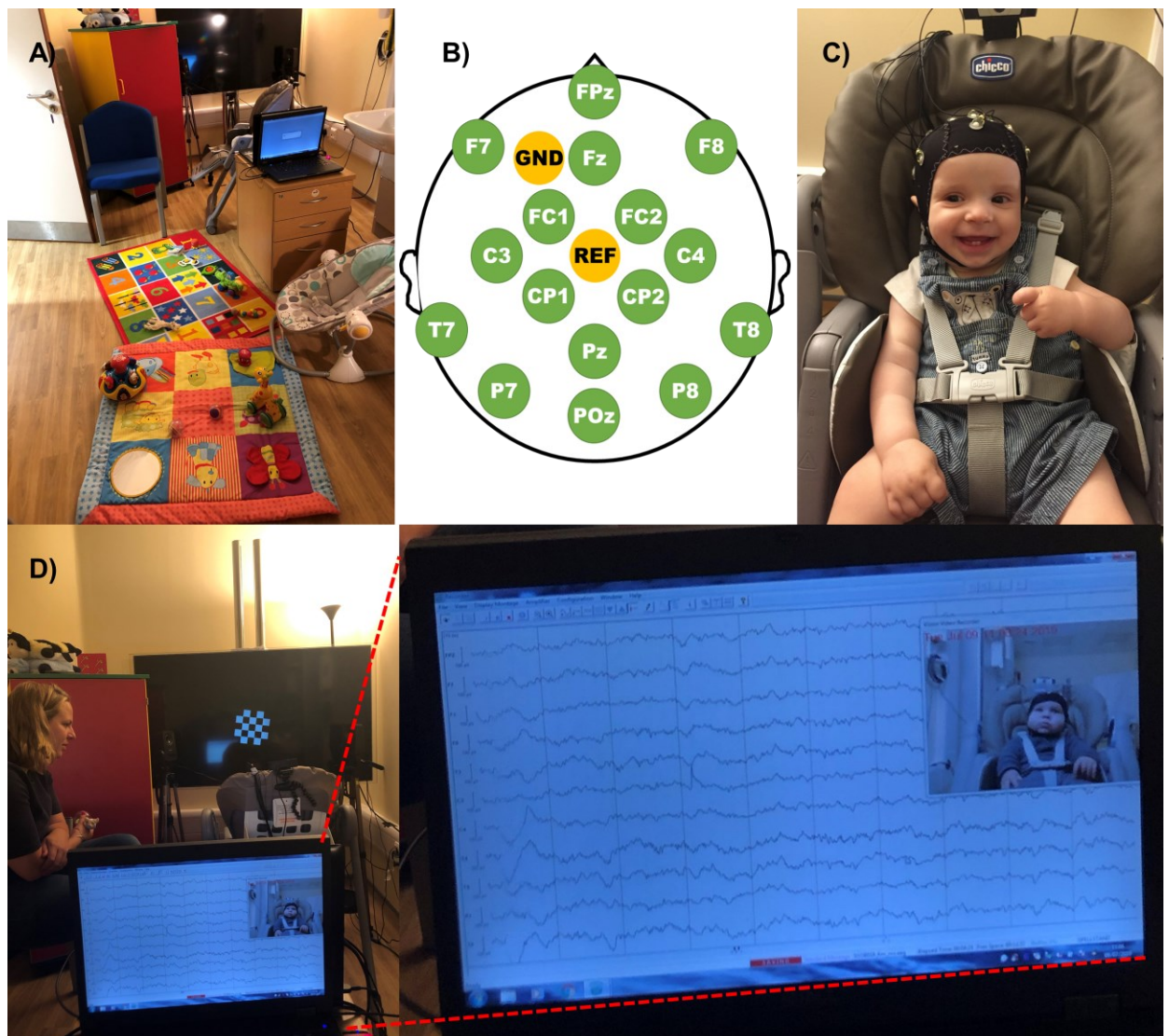


Figure 6-2. The full experimental setup on arrival (A); the EEG montage (B) used at 7.5 months; an infant during the social 'singing' paradigm (C); setup during the presentation of the nursery rhymes with the mother sitting behind the cabinet, zoomed in on the EEG and video feed of the infant (D). Parental consent was obtained for the use of all images.

All video materials presented throughout the resting state and the oddball paradigm were age-appropriate set of short (silent) videos designed to engage infant's attention and keep them happy and entertained throughout (Figure 6-2). They were derived from clips of popular children's programmes. They were presented without or with sound, in an alternating manner, as a compromise between minimizing auditory stimulation during the resting state recording and keeping the infant soothed and engaged throughout.

Two cameras were recording throughout the entire testing session. One was attached to the bottom of the TV screen in the midline, with the entire infant in its focal field, at an angle of about 60°. The recording from that camera was controlled by the Brain Vision EEG acquisition software and was time-locked to the onset and offset of the EEG acquisition sequence. The second camera was placed on the top of the infant's chair and high enough to not be visible to the infant. It was recording the vision field of the infant (i.e. the TV screen for the first three tasks, and the parent in the final task).

### ***Neuroimaging Procedure***

The infants arrived at the same neuroimaging facilities in the Rosie Hospital as in the previous testing session. They were allowed to explore the lab's environment and play on the floor with provided toys for about 5 minutes under parental supervision. The parent(s) also played with the infant and distracted them while the cap was attached, and impedance was brought down to below 10k $\Omega$ s. Throughout the entire session, the short attention span typical of the 7.5-month age group required frequent breaks in between experimental presentations and using entertainment techniques such as blowing soap bubbles and passing toys (Bell et al., 2012; Noreika et al., 2020). At the age of 7-8 months, the infants were less comfortable with sitting still for prolonged amounts of time and less tolerant of the EEG cap. To minimize large-scale body and head movements, the infants were seated and strapped in a Chicco Polly Magic Relax high-chair (Artsana, S.p.a., Como-Italia) in front of 55-inch television screen with a 1920x1080 pixels resolution, connected to the presentation laptop via an HDMI cable and set on mute. To limit the saccadic eye movements throughout the EEG recording and keep the infants entertained for as long as possible, either a short "attention getter" video, or a rotating fixation image, was presented at the centre of the TV screen throughout all tasks for which EEG was simultaneously recorded.

During the resting state procedure, the infants were presented with a series of 13 short videos on the TV screen,  $M=59.35s$  ( $SD=9.79s$ ), which were automatically advanced by the *MATLAB* script and had a total duration of  $\sim 12.87$  minutes.

Next, a modified version of the infant-directed speech entrainment procedure presented at birth was used whereby only the longest 22 out of the 58 nursery rhymes were played to the infants. The poems presentation lasted between 12-20 minutes. The range in total time

was due to the variable length of inter-stimulus intervals, as the experiment was manually advanced by a button press when the infant was ready for the next trial. Furthermore, unlike the neonatal protocol, at this testing age the nursery rhymes were accompanied by a rotating visual stimulus presented in the centre of the TV screen on a black background (*Figure 6-2D*) at 90cm from the infant's head and a visual angle of 20°.

Finally, the oddball stimuli used at birth were played again for 5 minutes, with the silent videos presented in the centre of the TV screen. Often, the infant's attention was diminished by the time of the oddball paradigm, and we had to blow soap bubbles towards the TV screen to keep the infant entertained and occupied.

### ***Social Interaction Test***

At the end of the second experimental visit, the infant listened to their parent(s) sing or recite nursery rhymes of their choice (inclusive of but not restricted to the ones that we presented). The parents were sent the text of suggested nursery rhymes ahead of the testing session and were provided with a printed copy during the session if desired. The infant's and their caregiver's chairs were rotated towards each other to maintain eye-contact which the infants found comforting. A microphone attached to a digital signal reader was placed away from the parent's mouth and equidistant to the infant's position to measure the amplitude of the acoustic output online. The experimenter, standing out of sight for the infant, kept track of the volume and indicated to the parent if adjustments were necessary. For this task, one of the cameras was relocated to just above the parent's left shoulder and had the infant in its recording field, while the other one remained atop the infant's chair and was now facing the parent. This task continued for about 5 minutes, or until the infant seemed compliant and happy to listen to their parent sing. If two parents were accompanying the infant to the testing session, both were asked to sing.

#### **6.4.2.3 Data Collection Session Three: at the infants' 15 months of age.**

### ***Latest Modifications in the Experimental Materials & Setup***

In the third session, the EEG testing *materials* were identical as the previous testing session with the sole difference that the EEG recording time was further reduced (see *Figure 3-1* for specifics). This was imposed by the lower compliance of the older infants with sitting still in

a highchair. For many of them, it signified mealtime and although they were given snacks in the breaks, they became fussy when food was not being constantly provided. Additionally, wearing the EEG cap had by this age become more of a nuisance for now they were indicating an increased awareness and often frustration with it.

The *experimental imaging setup* at 15 months was substantially modified. First, the site of testing was relocated from the imaging facilities in the Rosie Hospital to the Baby-LINC laboratory in the Experimental Psychology department. The 'baby lab' was more spacious and appropriate for the now fully mobile infants. Second, a 28-channel Geodesic Sensor Net (EGI, Oregon) was used with a GES300 amplifier for the EEG acquisition at this age. The accompanying Geodesic acquisition software, installed on a Macintosh laptop provided by the manufacturer, recorded both the EEG traces and the corresponding time-locked videos. The same Ten20 paste as the one used in the previous testing session was squirted in the wells around the EEG channels prior to the infant's arrival to the lab. The cap was applied to the infant's head taking care to place it accurately and to minimize the need for repositioning the channels on the head. Although the channels were sparse and spread out far apart, too much adjustment still presented a risk of smearing the paste between channels and bridging connections. The impedance was next brought to below 50k $\Omega$ s wherever possible, as prescribed by the manufacturer. At this older age of the infants, there was a trade-off between how long we spend adjusting the quality of the EEG trace at each channel, and the duration of the infant's favourable mood. Furthermore, many infants disliked us adjusting the cap and would not let us do it for a very long time. Thus, we prioritised the temporal-parietal and frontal-central channels in reducing the impedance. The infants were sat in the same highchair as used in the previous testing session, in front of a 49-inch TV screen connected to the presentation desktop machine (DELL). The EEG part of the experiment was controlled by a *MATLAB* script running on Ubuntu (Linux) OS<sup>18</sup>, and inside a testing booth with dark walls and a dark curtain instead of a door (*Figure 6-3* below). The parent sat on a comfortable chair just outside the testing boot at around 45° angle behind the infant's chair. Again, the parent was immediately available for comfort if needed, but was instructed to try redirecting the infant's attention back to the experimental presentation whenever possible.

---

<sup>18</sup> We dry-piloted the conversion between the two operating systems (Windows to Linux), and the timing accuracy of the stimulus presentation and EEG markers was double checked to ensure any delays were below < 2ms.



(i.e. having to stay home on a rainy day) – order was randomly assigned. Together, the two emotional narratives lasted for  $M=66.37s$  ( $SD=70.47s$ ). This task was done after the EEG procedure.

The *fairy-tale narrative* was one out of three by-choice: *Jack & The Beanstalk*, *Little Red Riding Hood*, and *Hansel and Gretel*. The parents were sent a bullet-point summary to remind them of the tales beforehand and were offered a reference sheet with the same bullet-points during the testing session but were not restricted to script. The fairy-tale took  $M=47.42s$  ( $SD=59.36s$ ). This task was also done after the EEG procedure, and the order was pseudorandomised with the *emotional narrative* task.

For all three behavioural social interaction tasks, the parent was sat on the floor in one of the corners of the room and the infant was sat either in a low-chair next to their parent, or in their lap, depending on the infant's preference (*Figure 6-4* below). The experimenters hid behind the wall of the testing booth to not present a distraction. Three cameras were recording during the tasks; two were close-ups of the infant's and the parent's upper-body (focusing on their faces), and the third one was a wide-view of the entire experimental setup with the infant-parent dyad. The three video-recordings were used in a subsequent analysis of the infant-parent social interactional synchrony designed and performed by S.C. The results from this analysis were and described in her MPhil dissertation (Carozza, 2020).

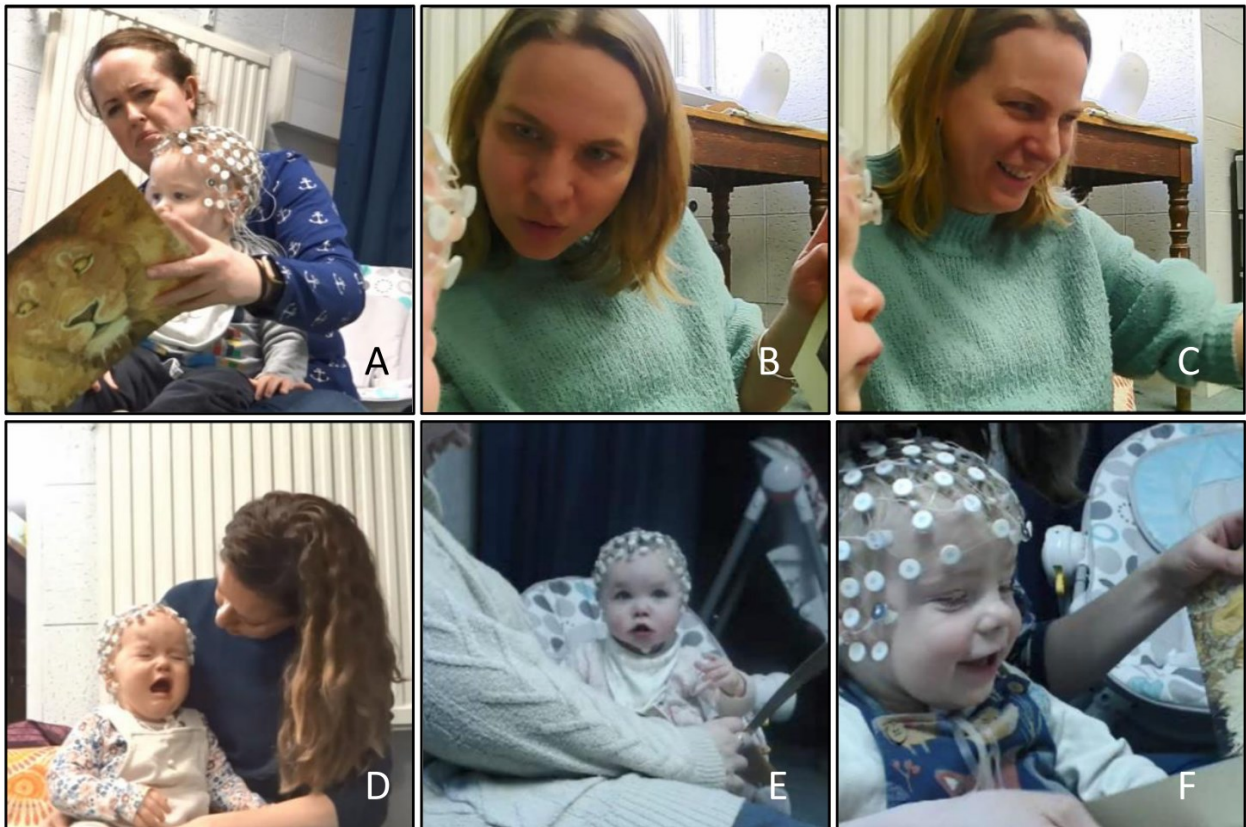


Figure 6-4. Copied from Carozza, S (2020) Examples of the behavioural socio-emotional tasks coding. Socioemotional state could be negative (A & D), neutral (B & E), or positive (C & F).. The tasks depicted were the wordless book reading (A-C, F), and the social or the fairy-tale narrative (D & E). Parental consent was obtained for the use of all images.

#### 6.4.2.4 Data Collection Session Four: between 23-24 months of age

The fourth data-collection session was conducted entirely online via a video-chat during the Covid-19 pandemic. The data-collection was divided between two separate calls of around 45 minutes each, done within a week of each other (*Figure 3-1*, rightmost panel). Each call had a social interaction part between the parent(s) and the infants (5-10 minutes, with the experimenter's microphone and camera off), and a vocabulary task led by the experimenter (15-30 minutes).

All video-calls were done and recorded using the Microsoft Teams account within the Department of Psychology. The parents used a mobile device (a tablet, laptop or phone) so that they could move around if the child found it difficult to keep still during the experiment. Prior to the testing session, we ask the parents to choose a quiet room and

limit the amount of background noise and possible diversions throughout. The most common distractive behaviour so far has been the child's fascination with the buttons on the laptop's keyboard.

### ***Social Interaction Protocols***

The social interactive synchrony task of picture-book reading was repeated with the now nearly two years olds. The parents were asked to download a digital copy of the same wordless book *The Lion and the Mouse* and "read" it together with the child at the beginning of the first the session.

The second session started with *free-play* instead. The parent(s) and infant played together by spending a couple of minutes each on: 1) rolling around a toy car/train; 2) role-play with a favourite soft toy; and 3) passing a ball.

### ***Test of Early Phonological Awareness***

The Profiles of Early Expressive Phonological Skills (PEEPS), to the best of our knowledge, is the only test created to date to comparatively assess the phonological development specifically in toddlers aged 18-36 months (Stoel-Gammon & Williams, 2013). In the current study, we used the basic word list version of PEEPS, which comprised 40 common English words<sup>19</sup>. No child was expected to know or be able to pronounce all the words, and the parents were reassured in advance that normal variation in the performance was expected.

In the protocol we followed, the experimenter used up to three categories of prompts for every word, twice each, and the toddler's responses were coded accordingly, whereby the final score was based on their best attempt, not necessarily their first one. For example, if the child said the word spontaneously out of context after the end of PEEPS, it was scored as a spontaneous utterance, even if they had previously been prompted to the word during the test.

---

<sup>19</sup> We adapted some of the words to British English, for example, for 'cookie' we accepted also 'biscuit'. The full list of words is given in *Appendix VI*

As the test was running online rather than in-person, the toddlers were sometimes shy to interact or reluctant to engage in a conversation with the experimenter. We requested the parents' assistance in those situations, and they attempted to direct the child's attention to the image or demonstrate the word on their own face or body. For two of the 21 infants tested so far, the parents reported that the child uses most of the target words in their daily language, but the child was unwilling to name them during the experiment. For these two children, a spreadsheet with the target words was emailed for the parents to indicate which of the words the child was able to use, and if so, how s/he pronounced them.

***Covid-19 Lockdowns Adaptation:***

PEEPS had been designed for a live administration and is sensitive to the experimenter's ability to engage the infant's interest and attention. It was developed to be used as an interactive face-to-face game between the experimenter and the child. In normal circumstances, for the 21-27-month age-group, the target words are elicited by toys and by demonstrating actions or parts of the face and body on the infant or the experimenter. This setup was, however, not possible in the context of lockdown. Still, it was essential to measure our cohort's performance on PEEPS prior to the end of my PhD program, as it gave us the only direct estimate of the phonological development to date as a possible predictor of later reading difficulties. Therefore, we modified the test for an online administration, and piloted it to make sure it produces usable results, comparable to those produced by the traditional methodology. In doing so, we sought the advice and guidance of the test creators, professors Stoel-Gammon and Williams. We piloted the online delivery of the test, as well as the effectiveness of the selected images (high-resolution stockshare images, refer to *Appendix VI.I*) in eliciting the target words, with 3 native British children close to the age group as our study's cohort (~2 years old). A medical student intern, D.P., helped with the preparation of the target images and recruitment of the pilot participants.



Figure 6-5. Stills from MS Teams video calls during PEEPS at 23 months: (A) presenting an image on the screen; (B) presenting an object/action.

In the online version of PEEPS, we split the target words in blocks of 3-4, and delivered a short entertaining video for up to 2 seconds after each block (the same videos were shown during the resting and oddball paradigms in the previous testing ages). Some of the words were elicited by the selected images shown in a MS PowerPoint presentation, while others were elicited by the experimenter in the video-chat window showing the child objects and actions (Figure 6-5).

### 6.4.3 Background and Home Environment Measures

#### *Home Language Environment Assessment*

Infants' early home language environment was measured via the Language Environment Analysis (LENA, (Ganek & Eriks-Brophy, 2016)) system which consists of a compact digital recorder mounted on a piece of clothing (a vest) worn by the child. The system was sent to participants' homes and provided a continuous acoustic recording for up to 16 hours throughout the day. The LENA system came with a validated linguistic analytic software, which helped with extracting measures such as word-count and conversational turns from the recording. Assessment of the early home language environment would assist us in drawing a better-rounded picture of the factors shaping the early language development in our cohort.

#### *Other Measures of Language and Socio-Emotional Development*

Between the testing sessions, the parents were mailed questionnaires pertaining to their mood and temperament, and their infants' language development. Please note that S.C.

digitised the questionnaires so that they could be completed during the periods of lockdown. Thus, around the 15-month testing period, the participants complete the questionnaires online on the university-approved encrypted platform QualtricsXM (Qualtrics, Provo, UT, 2020), rather than the mailed physical copies.

*Language measures.* Infants' early language development was assessed in-between testing sessions (the bottom two panels in *Figure 3-1*) using the MacArthur-Bates Communicative Development Inventories (CDIs, (Jackson-Maldonado, 2012)), emailed or posted for the parents to fill in. Concurrently, *socio-emotional measures* were reported by the parents in standardized tools such as the Ages and Stages Questionnaire (ASQ2:SE by Squires et al., 2015), the Infant Behaviour Questionnaire (IBQ by Gartstein & Rothbart, 2003), and the Communication and Symbolic Behaviour Scales Developmental Profile (CBSB-DP, Wetherby & Prizant, 2002).

Within the same packet of questionnaires, maternal and paternal socio-emotional wellbeing was also measured by the Beck Depression Inventory (BDI by (BECK, 1961)), and both parents' temperament will be assessed using the Adult Temperament Questionnaire (ATQ) (Derryberry & Rothbart, 1988) and the State-Trait Anxiety Inventory for Adults (STAI-AD) (Spielberger, 1983).

#### 6.4.4 Genetics and Cortisol Measures

##### *At birth*

Genetic samples were obtained from all infants at birth as detailed in Chapter 2. Additionally, 11 parents provided a saliva sample at birth. The parental genetic sample collection, processing and descriptive statistical analyses are fully specified in *Appendix III*. Only a proportion of the parental saliva sample was used for genotyping – the remainder was stored for future cortisol analysis.

##### *In later testing sessions*

In the follow-up sessions, both infants and parents contributed saliva samples, using the age-appropriate collection kit (Stratech, Ely, UK). For the infants, this was achieved by

letting them suck on 20cm-long saliva collection stick 2mm in diameter, held at the other end by the parent for safety. The parental saliva contribution was the same as in the testing session at birth (described in *Appendix II.I*). Several parents contributed saliva in more than one session. The benefit of repeated collection was twofold. On the one hand, we intend to in the future have the samples analysed for the levels of cortisol, which could be used as an indicator of parental stress levels at each time-point and has been related to the child's early cognitive development (Gilmore et al., 2018). The social stress levels measured at each time might therefore be important indicator for the infant's language input and learning. On the other hand, the multiple saliva samples from the same individuals gave us the opportunity to test the reliability of our genotyping experimental protocol as the two independently collected samples should have produced identical results. The conducted reliability tests are elaborated on in *Appendix II.I*

---

## 6.5 Significance of The Longitudinal Project

As it was our goal to deepen the understanding of early phonological development in the very early years of life, which we tentatively contributed to familial and genetic dyslexia risk, it was pivotal to extend the project over the initial neonatal assessment and to a time-point in which we could directly measure beginners' phonological skills.

A literature of numerous investigations and published perspectives has recognised that reading disorder is multifaceted but also, multi-factorial (Bishop, 2015; Black et al., 2017; Ramus et al., 2018; Xia et al., 2017). Additionally, it is simultaneously expressed with cross-cultural consistency and contextual specificity (Feng et al., 2020; Peterson & Pennington, 2015; Silani et al., 2005). Therefore, studying the perinatal risk factors and their influences on the neuroendophenotype was focally informative of the relatively environment-less-dependent early neurobiological mechanisms conferring acoustic speech processing abnormalities at birth, and linked in the literature to subpar phonological skills in later life. However, studying those factors in isolation could ever provide only a limited mechanistical stance on the relationship between neuro-biological risk and phonological processing. Other factors immediately relevant and modulating this relationship early on, amongst many, the infants social, emotional, and lexical development – all shown to play a big part in early language acquisition (Becker et al., 2017; Eaves et al., 2016; Leong, et al.,

2017; Molfese & Molfese, 2002; Newbury et al., 2014; Torre et al., 2019). These factors are further dependent on parental characteristics and input, such as their stress levels and emotional health, as well as the quantity and quality of their linguistic interactions with their infant (Hart & Risley, 1995; Kalashnikova et al., 2018; Newbury et al., 2014; Ozernov-Palchik et al., 2019; Rindermann & Baumeister, 2015; Torre et al., 2019). Across the lifetime, the familial SES and home language environment have been predictive of reading skills (Mascheretti et al., 2018).

The measures described in this chapter were narrowly targeting those factors based on previous literature we found most relevant and informative of the context in which the infants in our cohort were growing up in their first two years of life. It is the aim of the current PhD dissertation to anchor the discussion of those putative interactive environmental factors to the identified neonatal risk profiles and track the impaired but also potentially resilient acoustic and linguistic development as it unfolds and culminates in the measured early expressive phonological skills.



## **CHAPTER SEVEN**

# **GENERAL DISCUSSION & CONCLUDING REMARKS**

# CHAPTER SEVEN: DISCUSSION & CONCLUDING REMARKS

---

## 7.1 DISCUSSION

### 7.1.1 Summary

Together, the neonatal results pointed toward a measurable dyslexia-risk related neural endophenotypes present at birth. They indicated a possible distinction whereby the infants' familial dyslexia risk conferred delays in optimal stimulus phase-locking, which were not influenced to the same extent by the infants' genetic background in the susceptibility genes tested. On the other hand, infants' genetic but not familial risk implied a diminished cortical speech-signal processing capacity, as measured by directed coherence in a small temporal-central four-channel network. The developmental trajectories of these neonatal effects, and their significance over early phonological development and later dyslexia outcomes remained to be investigated further. Some of the arising questions could be addressed in the full longitudinal project.

### 7.1.2 PLV results

We found that the maternal dyslexia was the strongest indicator of a significant delay in the PLV peak to the onset of speech, despite a similar PLV peak strength between all three (maternal, paternal, and low) risk groups. There were all some indications that the less common variant of one and the more common variant of another ROBO1 SNPs were associated with a delayed PLV peak beyond the infant's familial risk, but these results were less reliable.

The take-home messages from the neonatal results of brain-to-speech phase-locking were two. On the one hand, we confirmed that neonatal oscillatory entrainment to the most prominent speech cue at the onset of the acoustic signal is less efficient (and potentially also off-phase) at high risk of dyslexia. This inefficiency characterised both infants with a first-degree dyslexic relative, and infants with a rarer copy of known susceptibility common genetic variants. Secondly, the neonatal results informed that genetic risk factors involved in early neuronal mass construction (the implicated here ROBO1 participates in axonal guidance) can be associated to the functional efficiency of rudimentary information

processing. Importantly, a direct link between gene-related aberrant cortical connectivity and the deficiencies found in neural connectivity metrics cannot be made based on the existing literature or the current results, although they do provide another line of converging evidence to this hypothesis. Additionally, the reduced efficiency may not be symptomatic of future much more complex dyslexia-related problems at this stage, but it could present an initial risk factor in the developmental trajectory of neural speech processing. This risk factor may in turn interact with the developmental language developmental to influence future language outcomes indirectly.

Furthermore, the results pointed to two important features of the neural speech entrainment mechanism at birth in the context of dyslexia risk. Firstly, at this very early age, it was the efficiency of phase-locking that showed group differences, not necessarily the phase alignment accuracy (although there were indications that this was also reduced, and potentially the size of the accuracy effect was smaller so it could not be reliably detected in the current sample). Second, both the familial and the genetic risk factors underlaid the neural mechanism of impaired phase-locking efficiency. The theory behind the genetic pathway of influence was slightly clearer – dyslexia risk genes create minor disruptions in the cortical microstructure wiring, leading to less sharp timing accuracy of the stimulus-induced phase-locking to high-power edges in the speech signal. Still, it should be emphasised again that even the purest and earliest of genetic influence on the neonatal neurodevelopment in the context of language processing are bound to be tainted by the experiences in the womb. As previously reviewed, already prenatally, foetuses are exposed to a low-passed version of the parental speech patterns. It is not within the scope of the current study to account for all the prenatal environmental or epigenetic factors that would have influenced the development of the early neural speech responses. In the LME models, we tried to account for several experimental variables, or variables surrounding the experience around birth, that could have influenced the latency of the peak phase-alignment outside of the genetic and familial risk factors, but the list of variables was neither exhaustive, not directly targeting confounding effects of the intrauterine environment. Thus, the pattern of results in the thesis speak more readily to the genetic influences of the possible deficiencies in the mechanisms of speech processing in the neonatal brain at dyslexia risk, but do not offer a causal account for these deficits, or a direct link to dyslexia development.

The maternal dyslexia risk effect was even less well motivated at the early postnatal age. Studies that have previously suggested a specific maternal dyslexia related risk, have done so at a much later age, when social cues and phase-entrainment speech experience have already had the chance to exert an important effect (Black et al., 2012; Kalashnikova, et al., 2018; Pettigrew et al., 2016). Here, infants to a dyslexic mother were on average 50ms later at their phase-locking onset response than the rest of the infants. One possibility for the origin of the observed pattern are prenatal epigenetic influences of the environment in and outside of the womb. At such an early age, we have to at least partially attribute importance to intrauterine factors, most likely related to epigenetic or genetic-environment interaction effects in the prenatal environment (although such links in relation to reading disability have only had a weak support in the literature – i.e. Pettigrew *et al.*, 2016). Even if we assumed that there was an epigenetic component to this effect, it likely would not hold beyond the neonatal neurofunctional differences described here and have little impact on the future dyslexia outcomes. Perinatal maternal dyslexia specific risk effects have been speculated in the literature only once before, to the best of our knowledge. In Black *et al* (2012), the severity of maternal dyslexia was the sole and strong predictor of the likely prenatally determined cortical surface area in the inferior parietal lobule for pre-literate children at the age of 5 (Black *et al.*, 2012). Focal aberrations in the microstructure of the cortical neural network due to genetic risk factors could be contributing towards both the altered cortical surface area, as reported by Black *et al.* (2012), and the delayed phase-locking response reported here. However, Black et al (2012) did not test for genetic risk factors, and the effects of genotype in the current study were neither strong, nor reliable. Albeit plausible, this explanation is very speculative and would need further investigation, either within the data collected in this longitudinal study, or in other cohorts. It may require also a more comprehensive account of the parental genotyping effects than what we were able to achieve in the current study (detailed in *Appendix II.I*). Although based on very limited data, there was no evidence to suggest that parental genetics influenced in any way their infant's dyslexia risk status in the current sample.

As the direction of affect is similar for the dyslexic fathers as for the dyslexic mother (but the differences are not statistically significant), an alternative possibility is that the maternal effect is stronger due to the sheer physical proximity of the dyslexic parent prenatally. The infants may have picked up on the subtle differences in the slow-frequency amplitude modulations in the maternal more than the paternal speech. The slow-frequency envelope of the maternal speech signal is likely one of the most present and prominent

features of the prenatal acoustic environment due to the low-pass filtering properties on the amniotic fluid surrounding the foetus (Armitage, Baldwin & Vince, 1980). Previous studies have shown that amplitude modulation of the speech produced by dyslexic adults was characterised by shorter syllabic intervals and reduced slow-to-high cross-frequency synchronisation (Leong & Goswami, 2014a). It is to some extent possible that infants could have gotten accustomed to entraining to the distinctive dyslexic speech production prenatally. Although this suggestion possibly describes the main effect of the primary caregiver in the post-natal environment, it is still farfetched for it to be the primary explanation of the perinatal effects described here. In fact, it is highly unlikely that a mere proximity effect prenatally would have any direct impact on dyslexia outcomes in later life. Kalashnikova *et al* (2017) reported that it was the infants' dyslexia (risk) status and not maternal dyslexia that was the significant predictor of the prosodic features of maternal IDS in the first 6 months of life. In that study, the mothers picked up on the social cues from their infant with respect to interest and engagement with prosodic patterns in IDS. The prosodic structure of maternal IDS was based on those cues and not on their own dyslexia risk status. As there are few social cues from the foetus relating to their interest and engagement with IDS prior to birth, we have very little ground to assume that dyslexic mother's IDS prior to or close to birth would have differed (although see Leong & Goswami 2014a for non-IDS). At least partially, we need to allow for poorly understood early epigenetic influences on the neonatal speech-processing delay described here.

Inevitably, the way that we defined and calculated the PLV onset peaks as phase resetting of the brain processing signal to match the phase of the incoming stimuli (ie the NRs) call for a discussion on whether it would be more appropriate to view them as evoked events (i.e. ERRs or EROs) rather than continuous sustain oscillations. The phase-locking to the onset of speech for the duration of 2.5 seconds, which in the IDS used here corresponded to a phrase with a two strong-weak syllables pattern (S-w-S-w, or /MA-ry-Ma-ry [*quite contrary*]), Figure 3-6, or roughly 2-4Hz of stress rate. The PLV onset response here can be interpreted as a measure of how the endogenous neural activity (which could be produced by synchronous cortical oscillators or not) was reset to the prominent features of the incoming stimuli, resulting in a time-resolved (in steps of 40ms) phase mapping between the speech input and the neonatal brain response. Interpreting the PLC onset response as reflecting a change in the endogenous oscillatory neural activity is a helpful but not imperative formulation of neural processing of speech although it could be a useful modality when thinking about phonological processing as it highlights its rhythmicity.

However, it is equally plausible to review the onset phase-locking peaks as multiple individual responses of highly similar and synchronised onset-favouring spikes of the PAC neurons to high-power onset-of-speech events (Heil, 1997), rather than ubiquitous continuous oscillations. Heil (1997) concluded that the shape (latency-acceleration to cosine square rise functions of the stimulus) and latency of the initial spike times of neurons in the primary auditory cortex (of cats) had a striking similarity when obtained from a variety of neurons, while still showing a sensitivity to acceleration and rate of change of peak pressure in the stimulus waveform. The initial discharges of most auditory neurons in PAC were evoked by the stimulus onset and the PAC neurons were particularly well suited to tackle the issue of onset encoding because they preferentially responded to sound onset. Because of the striking similarity in the shape of the functions across the neuronal pool tested, the sound onset produced a predictable spatial-temporal first-time spiking, which the author speculated could be used for instantaneous tracking of fast transient temporal features in the incoming auditory signal. These strong and consistent neuronal responses could actually be locked to individual peaks in the repetitive envelope fluctuations (i.e. instead of oscillating, they are synchronously responding to the incoming power fluctuations) and phase-locking of the spikes to the AM signals or clicks may constitute a rapid series of alike onsets for a given neuron, 'as if each cycle is an effective excitatory stimulus'. Sound onsets are salient and behaviourally relevant stimuli and most [primary] auditory [cortex] neurons discharge spike locked to such transients (Heil, 1997). In either the oscillatory or the evoked response interpretations of the PLV onset peak in the current work, it is important to make the distinction that in Study One, we did not track ongoing oscillations 'dancing' to the ongoing NRs signal, but rather a change in the underlying neural activity in response to the power in formant frequencies at the onset of speech. So, the discussion should be concerned with whether the endogenous oscillatory neural activity surrounding the speech input was an adequate representation of phonological processing on one hand, and of the onset response on the other. Oscillations could be a useful representation here because they are conceptually easy to interpret in the context of processing an ongoing rhythmic activity and could be symptomatic of changes in the neural tracking. On the other hand, it could be difficult to agree on what constitutes an oscillation underlying speech tracking as oscillatory responses tend to be brief and transient in the brain but their computed estimates tend to rely on the assumption that they are sustained and stochastic processes (Donoghue et al., 2021). Additionally, oscillations are problematic for interpretation because of a multitude of issues in the assumptions made when calculating them, primarily concerning the difficulty in disambiguating periodic from aperiodic endogenous neural activity and artifacts in their

power and phase representations (Donoghue et al., 2021). Finally, the measured transitory oscillatory response here (if we assume it was such) would have likely been a by-product of the tonotopic structure of primary auditory cortex (Heil, 1997; Jones & Schnupp, 2021) but as such, related more to the physical features of the auditory aspect of speech and would have little direct contribution towards the complex cognitive aspects of dyslexia.

There is a theoretical background predicting that the nature of the ongoing brain activity, as well as the brain's response is oscillatory of nature (i.e. Giraud & Poeppel, 2012). There is some empirical support to this idea, however there is also strong evidence that aperiodic activity plays a part in both the endogenous workings of the brain, and of the processing of the incoming speech signal (Heil, 1997; Jones & Schnupp, 2021). In either case, we were not really in the position to solve this debate with the current dataset. The current results cannot not (dis-)confirm oscillatory theories as they did not even directly test them. Suboptimal processing could well be coming from noisier endogenous environment rather than oscillatory phase resetting, and this would involve oscillatory as well as aperiodic activity.

An important word of caution here should be the presence of PLV onset peaks prior to the stimulus onset in some nursery rhymes, as mentioned in *Chapter 4.4.6*, and discussed in more detail in *Appendix IV.I*. Between 20-25% of the PLV peaks above the selected surrogate threshold had a negative latency. As discussed in *Appendix IV.I*, although some of them may be attributable to the trigger delay issues outlined in *Chapter 3.3.2*, or to intrinsic noise, the percentage of negative latencies was too high to be ignored. Note that on some of these "negative" trials, there would have been more than one PLV peaks detected, however, the first/highest peak was always the one selected for further analyses. We were unable to explain it on the account of a predictor variable such as the ITI from or the syllabic rate of the previously presented nursery rhyme, tested in simple regressions. There was still the possibility that delays in the EEG triggering system existed which we were not aware but such speculation at this stage would be impossible to confirm or exclude conclusively. Alternative unmeasured effects were likely at play, including potentially unfit PLV calculation parameters, although we used standard *MATLAB* functions for the calculations and to the best of our knowledge, no negative PLV latencies have been previously reported. If we were to interpret the phase-resetting at the onset of the NRs as stimulus-evoked responses for which the phase of the ongoing brain signal is more consistently in phase with the NRs instantaneously or just prior to its onset, and it fades away forward in time as

it is not a sustained oscillatory but rather an evoked response with a transient periodicity. Such interpretation would be consistent with the animal studies reviewed (i.e. Heil, 1997) above showing a great affinity of neurons in the primary auditory cortex to respond instantly and with great consistency to sharp changes at the onset of the auditory signal. This, the peak of the phase synchrony would be detected in time-windows containing the initial 40-80ms post-stimulus presentation, most of which are plotted as 'negative peaks' here. Further investigation is needed to understand better the origins of these effects.

### 7.1.3 GPDC results

In general, when investigating the network connectivity properties during IDS exposure, we found the previously reported and expected left lateralization effect. All infants had higher coherence during speech presentation within the left hemisphere compared to the right hemisphere, irrespective of their familial or genetic risk status (*Figure 7-1*, as well as the individual infants' plots in *Figure 5-3* and the connection comparison plots in *Figure 5-4* in *Chapter 5*). This was reassuring since previous literature stipulates that linguistic stimuli related early left lateralization should be present at birth (Peña et al., 2003). Please note that using GPDC, we measured the phase coherence from one signal to the other as defined in Granger causality terms, and not the strength of the oscillatory response to the syllabic speech signal, which would have generated the opposite prediction, i.e., slow-wave oscillatory responses to low frequencies in speech have been demonstrated in the right hemisphere preferentially. Additionally, only the left-to-right directed coherence was consistently higher than the surrogate threshold, thus all analysed connections had an output channel located to the left of their input channel (note that T3->C3 and C4->T4 also follow that pattern despite being on the same side of the head) (*Figure 7-1*).

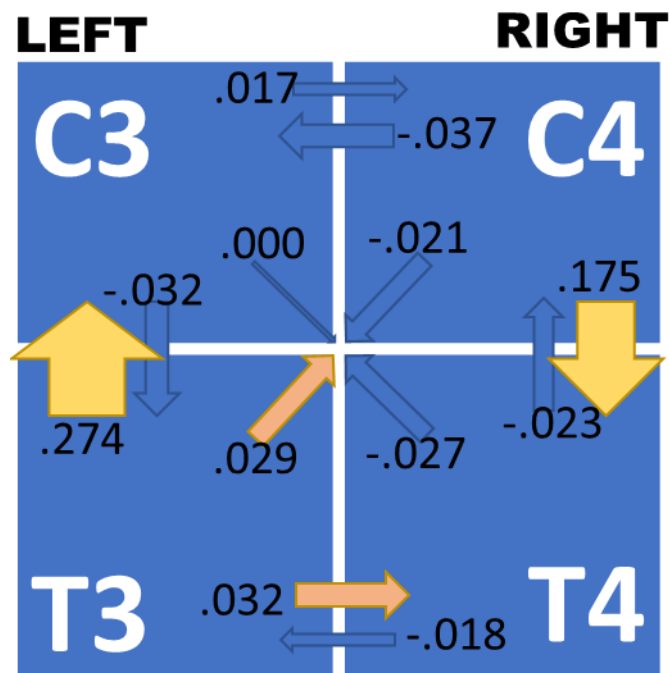


Figure 7-1. Normalized GPDC pairwise coherence, averaged across all infants regardless of their genetic or familial risk status. Yellow/orange arrows indicate directed coherence values significantly above the surrogate threshold. The direction of the arrow indicated the direction of coherence.

### ***Dyslexia Related Differences in Functional Network Coherence***

We found evidence for a reduced left hemispheric directed coherence in infants with the rarer ROBO1 and DCDC2 genotypes, independent of their familial risk. Interestingly, (Hancock, Pugh, et al., 2017) envisioned that a DCDC2 risk genotype affected cortical morphology and could lead to an overexcitatory neural spiking activity (i.e. increased intrinsic noise (Che et al., 2014, 2016; Meng et al., 2005; Smith et al., 2016; Truong et al., 2014)) and therefore – reduced reliability in the neural connectivity patterns. At the cortical macroscale EEG recordings in humans, assuming much subtler minor aberrations, this effect may be paralleled by the undermined oscillatory activity as measured by network coherence.

The reduction of left-hemispheric directed coherence at the syllabic rate was measured from the temporal (T3) towards the central channel (C3). Notably, when modelling the PLV onset peak latencies in all infants, we noticed that for many models, the *Channel* effect was driven by channel C3 (left) having a significantly delayed peak latency compared to T4 (right). However, when the influence of the ROBO1 SNP rs9853895 was accounted for, the

effect reversed so that now C3 (left central) was in fact faster to optimally phase-lock than T4 (right temporal). As this effect was observed in the non-directional measure, we cannot comment on its significance, however, as the effect reversed from typical to atypical with the introduction of susceptibility gene, it can be noted as a cautious observation. Together, these observations broadly resemble the findings of Molinaro et al (2016), indicating an impaired feed-forward connectivity (measured as PDC in source space) between the right primary auditory cortex (PAC) and the left IFG (higher area) in school-aged children and adults with dyslexia. We tested none of the right-to-left GPDC connections for between group effects, as they were all under the chosen random surrogate distribution threshold. Therefore, we cannot know for sure whether our results replicate fully the findings of Molinaro et al (2016), only that they are pointing in a similar direction. An *emphatic* word of caution should be added here that despite drawing parallels between the current results and empirical findings from source space or functional connectivity in fMRI, these are to be interpreted as broad similarities in hemispheric patterns only. With the current study, we were in no position to make any cortical structure inferences or draw conclusions about the underlying sources of the sensor-space connections tested here.

Importantly, converging evidence has been reported in the MRI literature in adults (Boets et al., 2013). In a full-brain fMRI protocol, Boets et al presented dyslexic and normally reading volunteers with four phonetically identical but acoustically different categories of non-words. Multi-voxel pattern analysis was used to assess the quality of the phonemic representations in the primary and secondary auditory cortex, which proved intact in the dyslexic group. However, similar to the reduced T3-to-C3 coherence found in study two, the functional connectivity between the left STG (i.e. left temporal - alongside the right PAC) and the left IFG (i.e. the same higher left area as reported by Molinaro et al, 2016) was reduced in the dyslexic group. Additionally, Boets *et al.* (2013), found that the left STG to left IFG (i.e. left hemisphere temporal-to-higher) functional connectedness correlated with behavioural phonological measures of word and non-word reading, spelling, phonological awareness, VSTM, and lexical access. In a follow-up experiment with the same participants, Boets et al (2013) discovered that the hampered left-hemisphere bridge between the left IFG – left STG in dyslexic individuals was in fact effected by a reduced WM integrity in the left AF, and specifically the segment of the AF tract which connected directly posterior temporal and inferior frontal areas. The left IFG was implicated in sensory-motor integration and correlated with effortful phonological processing but did not contribute to discerning the phonological structure of the auditory input. The authors speculated that

instead, it accesses the phonological representations in the auditory cortices for higher level processing. With these comprehensive findings, Boets et al (2013) additionally corroborated the conclusion from Ramus & Szenkovits (2008) that phonological representations remained intact but were less accessible in dyslexia at the neurostructural and neurofunctional level.

One lack of finding of interest was the missing parental dyslexia effect in GPDC. We originally predicted that infants at high familial risk of dyslexia (did not specify whether maternal or paternal or both) would have reduced connectivity compared to those at low risk. There was no indication of such an effect in any of the tests that we ran separately for each pairwise connection (see *Figure 5-8*). This was surprising and could be due to low power to detect the difference, as we only had 12 infants in the maternal dyslexia group (36 in both parent-groups). Plotting all individual values, however, there did not seem to be a trend towards dyslexia-risk incurred GPDC reduction, even with the small number of observations. To the best of our knowledge, there were no previous studies reporting G/PDC results differentially for at-risk of dyslexia groups, and only one found a difference between groups after dyslexia diagnosis (i.e. in children who can read, and adults). It is therefore hard to speculate whether the lack of effect was due to a general lack of sensitivity of this measure to dyslexia risk, or mostly to lack of sufficient power in the current study. If GPDC here was interpreted as a measure of the capacity of the underlying cortical network to accurately represent the speech waveform, rather than a performance measure, such as the PLV, then we could theorise that the network connectivity capacity would be more prone to a genetic rather than a familial risk influence. In that case, we would more readily detect the hypothetically larger effects of the SNPs tested than the hypothetically smaller (or no) effect of parental dyslexia.

#### ***PLV and GPDC results reviewed together.***

There are strong literature indications that the results for network connectivity and neuronal entrainment (i.e. in the two studies reported here) may be functionally related. That is, the 'out of synch' endogenous network coherence could be underlying the stimulus related phase-locking delay.

The connection between the Studies One and Two reported in this dissertation was tested in a subset of the infants who had enough trials for both metrics. We found that the

parental dyslexia, as well as genetic risk, predicted the infants' efficiency in getting phase-locked to the speech signal, while solely the infant's genetic risk was related to reduced or shifted coherence between the channels. There are many indications in the literature that the dyslexia susceptibility genetic variants tested here lead to minor focal cortical connectivity anomalies. These anomalies leading to reduced coherence, as indicated in Study Two, could impact on the timing accuracy of entraining to the incoming speech signal and on passing it to higher cortical areas for processing (i.e. as described in older children and adults with dyslexia by Molinaro et al, (2016)). Next, the reduced timing accuracy of the information processing could be envisioned driving the less efficient phase resetting to the incoming acoustic speech signal, as reported in Study One. The speculation was formally tested for whether the interaction between the genotype and the GPDC patterns predicts the PLV results above familial risk alone. Although no significant effect of GPDC on the PLV latency was detected in the current sample, the regression line fitted between the GPDC from T3->C3 and the PLV latency values per infant pointed in the predicted direction.

Finally, there stands the question of whether the dyslexia risk modulated coherence patterns could be speech stimulus independent. Although less likely considering the left lateralization effects observed, it is possible that the abnormal network coherence patterns in relation to genetic dyslexia susceptibility are present in the GPDC network even without overt speech input. This alternate hypothesis is not theoretically incompatible with the increased neuronal noise assumption. To test this suggestion, we would need to perform the GPDC calculations in a match section of the already collected resting state data and compare for similar coherence patterns pre-stimulus presentation in the same infants.

#### 7.1.4 The Wider Literature Context

As reviewed in the introductory *Chapter 1*, there is already considerable evidence that dyslexia-risk related neural changes could be readily observable as early as a few days postnatally, both in terms of structural white-matter modifications observable in magnetic imaging, and of electrical processing of information measured via E/MEG. The presence of these early abnormalities is anticipated by the heritable nature of the reading disorder, as well as by the associated susceptibility genetic links, which confer their influence on the cortical wiring in the early prenatal weeks of neuronal development. As the genetics-associated changes in the cortical microstructure develop prenatally, dyslexic children have

less well-tuned speech sound discrimination *at birth* already, presumably attributable to the increased endogenous neuronal variability.

In older children and adults, brain-behaviour association studies show correlations of neural structure and function with dyslexic traits. The four susceptibility genes of interest in the current work have been related to dyslexic behavioural phenotypes, and neuroendophenotypes. In a cross-sectional longitudinal study, Darki et al (2012) found that genetic variation in three dyslexia susceptibility genes were associated with reduced WM volume in the left temporo-parietal tracts, which in turn influenced reading abilities in children and young adults. Importantly, the observed relationship between WM volume and one of the risk genotypes was mediated by age, indicating developmental dynamics in the role of WM structures in dyslexia. These structural modulations in turn influence functional neuronal connectivity.

The predictive power of early risk-modulated neural activity (usually measured via E/MEG) on later language and reading skill outcomes has been backed by previous literature. As reviewed in Chapter 1, early MMN markers in neonatal and young infants have been consistently related to later reading (Leppänen et al., 2012; Leppänen et al., 2010; Leppänen et al., 2002; Van Zuijen et al., 2012, 2013). The auditory processing of cues related to the temporal envelope of the speech was an important predictor of school-aged phonology and literacy skills, consistent with a previous quantitative metanalysis (Cristia et al., 2014). Furthermore, ERPs to pseudoword at 6 months predicted 44% of the reading speed at 14 years, and the predictive power improved when accounting for preschool levels of letter naming, phonology and verbal short-term memory capacity (Lohvansuu et al., 2018). Reduced MMN with a delayed latency characterized high- compared to low-risk infants at 6 months, and the latency delays at birth (Guttorm et al., 2010) and at 6 months (Benasich et al., 2006) were related to expressive and receptive language abilities at late infancy and pre-school age. Guttorm et al (2010) also reported that it was the same high-risk new-born infants who had a slower positive-to-negative polarity shift in the right hemisphere to also demonstrate significantly poorer phonological skills at 5 years of age. Finally, Molfese (2000) was able to predict the reading disability outcomes at school-age from a negative ERP peak latency at birth in the same children, using a discriminant function analysis. Two canonical discriminant functions were identified, loading primarily on the negative neonatal ERP peaks in the left and right frontal channels, which successfully classified 81.25% of the children's reading outcome as control, dyslexic, or

poor readers at the age of 8 years. Despite the limited pool of neonatal studies in the context of dyslexia risk, and the small sample sizes reported in them, a link between the irregular neonatal neural processing of temporal structure in the auditory stream and later inferior phonological and reading outcomes has been replicable. With the current work, we contribute to this line of literature by demonstrating that dyslexia risk is related to disruptions of the cortical tracking of the temporal modulations of the speech signal in the new-born brain. It provides a continuous measure of group differences in brain-to-speech mapping, which could well be the underlying functional deficit behind other measures of temporal deficits in response to speech(-like) stimuli.

The finely tuned relationship between linguistic sound and rhythm and literacy (Thomson & Jarmulowicz, 2016), requires a sharp timing precision in encoding small acoustic differences at a very high pace. Even minor disturbances due to an increased intrinsic neuronal noise could impede the accurate parsing of the acoustic speech signal based on the prominent surges of high-power (i.e. sharp edges, rise time frequency in English, etc). Thus, noisy (or more variable) endogenous neural synchrony could be at least partially responsible for neuro-oscillatory delays that we observed in the current work, and potentially the phonological impairments described in adult and infant dyslexic (pre-)readers in later life.

In early infancy, it is the entrainment to the slow-wave high-power envelope modulation which tracks the significant acoustic events in speech that guides statistical phonological and morphological learning (Banai & Ahissar, 2018; G. Dehaene-Lambertz & Gliga, 2004; Gabay et al., 2015; Thiessen et al., 2005). Dyslexia risk in the current work confers a delayed entrainment to those slow-wave amplitude modulations, defined by the syllabic speech rate. This effect would be predicted by theories emphasising slow-wave entrainment defects as the major driver of phonological deficits in early pre-linguistic infants at dyslexia risk (i.e., the temporal sampling impairment hypothesis (Goswami, 2011)). It is also broadly consistent with accounts of increased neural variability, or neural noise, impeding adequate endogenous neural synchrony (as shown in study two) and entrainment to external speech stimuli (study one) as a prerequisite for later phonological deficits. Furthermore, although both amplitude and latency of entrainment issues can be envisioned by the neural noise hypothesis, its assumption that inconsistent firing times of the cortical neurons compromise the detected oscillatory activity, would imply a more

readily observable latency rather than amplitude effect on neural entrainment to speech, as seen in Study One.

In adults, and to some extent literate children post reading acquisition – that is, post dyslexia diagnosis, the picture is slightly different. Apart from slow-wave tracking impairment, there have been differences also reported at higher frequency rates, relating to phonemic power in the speech spectra, and hence, phonological processing. For example, in a MEG ASSRs study, Lehongre, Ramus, Villiermet, Schwartz, & Giraud (2011) found abnormal processing in high gamma frequencies whereby subjects with dyslexia had reduced left hemisphere bias for the 30Hz band which correlated in magnitude with deficits in phonological processing. Additionally, they found enhanced entrainment in 50-80Hz bands bilaterally compared to controls, suggesting that phonemic oversampling may characterize dyslexia (Giraud & Ramus, 2013). The oversampling correlated with phonological memory deficit. The gamma oversampling and lack of hemispheric gamma asymmetry in dyslexic individuals were replicated a few years later in a simultaneous fMRI-EEG study (Lehongre et al., 2013), while Vanvooren et al (2014) observed immature hemispheric specialization patterns of beta synchronisation in dyslexic children in an EEG experiment. Higher signal-to-noise ratio (SNR) at 20Hz (beta) was related to better phonological awareness in the dyslexic adolescent readers but not in controls (De Vos et al., 2016). Higher, and therefore less mature response to phonemic stimuli in dyslexic adult and child readers (i.e. phonemic oversampling) has been attributed to heightened neuronal excitability and reduced timing accuracy<sup>20</sup>, as was the reduced coupling in the slower frequency modulations describing the pre-linguistic children's entrainment to speech. Thus, these may well be different manifestations of the same underlying problem.

---

<sup>20</sup> Reduced timing accuracy has been reported across modalities, including multisensory integration (Gori et al., 2020), signal-in-noise perception (Sperling et al., 2005), and deficient inhibition (Hancock, Pugh, et al., 2017). For example, inferior cortical alpha response has been reported in dyslexia (De Vos et al., 2016). The cortical activity in the alpha band (centred around 10Hz in adults, and 6Hz in infants) helps organise the temporal representation of the speech signal by facilitating the selective inhibition of the irrelevant information. Straus, Wostman & Oblesser (2014) previously demonstrated that alpha plays a significant role for speech processing in noisy conditions by exercising an excitatory-inhibitory top-down modulation on the cortical speech tracking thus gating the auditory selective attention and inhibiting the processing of task-irrelevant information. Auditory selective attention has been linked to phonological skills (Yoncheva et al., 2014). Reduced stimulus-synchronised alpha activity was shown in dyslexia, and was correlated to reading skill in typical but not in dyslexic adolescent readers (De Vos et al., 2016).

Importantly, the implication would be that the phonemic representation is not central issue but rather, the timing properties of the processing of the phonemic information, which is captured by the amplitude modulations of the slow-wave carrier frequencies in the speech spectra. Whether attributed to endogenously noisy neural spiking environment or not, the phonemic processing deficits are likely an issue of timing; of correctly locking to the high-power surges within the speech stream on the one hand (Power et al 2013, 2016, the results from the current dissertation), but also of oversampling the phonemic register (potentially to compensate for reduced timing accuracy but in doing so, overloading the executive processing system). Indeed, in a half a decade-long series of experiments, Ramus & Szenkovits (2008) found phonological representations to remain intact in their dyslexic participants (Ramus & Szenkovits, 2008; Szenkovits et al., 2016). In fact, there were some signs of the opposite pattern, that phonological representations were somewhat too prominent in dyslexia. For example, Lizarazu et al (2015) found that 30Hz beta power was enhanced in dyslexic over normal readers in school-aged children and in adults. Serniclaes, Van Heghe, Mousty, Carré, & Sprenger-Charolles (2004) report over-specified (allophonic) rather than under-specified phonemic representations in native French school aged dyslexic children (Serniclaes et al., 2004). Cutini et al (2016) discussed that phonetic rate processing is atypically enhanced in dyslexic children because they might have more vigorous response to phonemic information. Like British dyslexic adolescents who retained an atypical for their age left hemisphere beta peak in (Power et al., 2016), Serniclaes et al (2004) found that at school age, the dyslexic children in their sample also maintained a higher sensitivity to phonemic distinctions irrelevant of their mother tongue, not dissimilar to typically developing infants who are predisposed to perceiving all potential phonemic categories of all world languages. While typically developing children seem to lose that predisposition in early childhood, this may not be happening in the same way for dyslexic children. The dyslexic children continued to perceive the allophones, implying that they might have had more sensitive temporal fine-graining capabilities (Cutini et al., 2016).

Notably, atypical phonemic rate processing has been more readily reported in reading children and adults as opposed to pre-literate children, indicating that the phonemic rate disturbances are likely a consequence, rather than the cause of a faulty maturation process (Lizarazu et al., 2015). Underlying this problem is an earlier system with a poor ability to resonate with the amplitude modulation of cross-frequency synchronisation of syllabic-to-phonemic scale. Retaining some non-native phonemic contrast may make the process of phoneme-to-grapheme matching, that is essentially reading, more effortful and attention-

loading, thus reducing working memory capacity. These findings of phonemic oversampling can help explain the previously described verbal short-term memory impairment (Giraud & Ramus, 2013), as it could mean that dyslexic individuals are compelled to perceive, store, and mentally manipulate subphonemic information, not directly relevant to the accuracy of speech perception. This account would also fit with the broad range of findings indicating atypical temporal entrainment and reduced efficiency in the phase alignment in dyslexia, summarised by the idea that increased neural noise and excitability in reading-associated cortical networks lead to low-level sensory and phonological processing deficits in dyslexia.

### **7.1.5 Future Directions Based on the Longitudinal Dataset**

The larger project encompassed the opportunity to longitudinally track and potentially even assess phonological development (one of the early dyslexia hallmarks) in the same cohort. A wide range of measures spanning the neurobiological ones at birth (described in the current dissertation), to increasingly more complex cognitive and social-emotional developmental tests, and culminating in expressive phonological skills assessment, were employed within the course of the study to reflect the multifactorial influences which potentially contribute to future reading disability. Within the larger project, the neonatal results described in the current dissertation presented the initial snapshot and anchor the longitudinal discussion. Still, the link between the genetically conferred risk and the functional alterations due to inferior wiring found here is not deterministic, potentially it is not even indicative as an early dyslexia marker. It just points to a mechanistic difference, the consequences of which in cognitive and behavioural terms are at this stage only speculative. To become indicative, these results need to be checked against the phonological and reading outcomes, and while reading age is out of the scope of the longitudinal project, early phonological assessment was performed on these infants. Therefore, the value of the mechanism reported in the neonatal dataset is that it can be used to generate hypotheses about the developmental progression between this initial snapshot and the tentative early outcomes. For example, we can observe in the interim how resilience is compiled in those infants who were at highest risk initially and started off as having a less optimally connected neural environment. We can track those trajectories as they unfold in time and be able to target additional influences on them, such as those incurred by the early language environment and social interactions between the child and their primary caregivers. The additional social, emotional and language inputs are of great importance for tuning the young brain to their native linguistic environment and are

predicted to have important modulating effects on their language developmental trajectories. Furthermore, if it is to be found that there is a measurable early behavioural/cognitive/neural outcome and it is developmentally determined in time, it could provide inspiration for befitting early intervention tools.

## 7.1.6 Dissertation Limitations

### 7.1.6.1 Empirical and Theoretical Shortcomings

One of the major limitations of the project is that we have not been able to test for dyslexia as a definitive outcome measure of the early neurobiological risk factors identified here. Although the substantial theoretical and empirical pre-linguistic literature has made a link to later reading and spelling abilities (i.e. Xia et al (2017), Goswami (2011), Leppänen et al., 2012; Van Zuijen et al., 2013, Guttorm et al., 2010 amongst others), the link here remains indirect.

Furthermore, in the current dissertation, the link between Studies One and Two was circumstantial. We expect that the delayed response in phase-locking would be underlaid by the infant's reduced network coherence. This prediction partially relied on the assumption that the directed coherence measured at the syllabic rate here were in response to the presented acoustic speech signal. This assumption is corroborated by the left lateralisation effects found. However, we did not test for the dependencies between the PLV and the GPDC results. This was partially due to timing constraints, and partially to the limited degrees of freedom available with 8 genetic and 1 familial risk predictors, given the size of the sample when both measures were present ( $N=74$ ).

It is important to reemphasise here that in some of our neonatal EEG recordings, a delay was present between the auditory stimulus onset and the marker of the EEG recording's timestamp. The average delay was estimated to be of around 49ms and affected at least 30% of the recordings. As the delay for each individual recording could not be estimated retrospectively, the onset time-window of 60ms around the recorded stimulus onset was not analysed. We acknowledge that the lower timing precision in 30% of the recordings means a lower precision in connectivity calculations, especially when testing for the phase of the oscillations. However, due to the slow temporal characteristics of the infant-directed

speech signal to which the EEG signal is locked, and the fact that we were only measuring the phase coherence in the syllabic rate of the nursery rhymes (all under 4Hz), we note that a delay of an average of 49ms is albeit measurement-noise inducing, not detrimental. It is also worth noting that the timing problem would have affected more severely the measurement of brain-to-speech phase-locking (i.e. the coherence of the EEG signal to the speech signal of the nursery rhymes, as measured by the PLV) than the channel-to-channel measures of coherence (i.e. the state of the EEG network connectivity, as measured by GPDC).

An important limitation is that we did not specifically test for rightward preferential oscillatory response to slow-wave frequencies in speech, as previously reported. This would have been measured as a hemisphere effect on the GPDC from the speech channel (NRs) to the four EEG channels in all infants, but especially in the low-risk infants.

A further PLV calculation pitfall came from the unaccounted-for presence of negative latencies in the PLV onset peaks on some nursery rhymes. We were not able to explain why the phase differences between the EEG and the speech envelope signals were more consistent before the onset of the nursery rhyme than after, on some trials. A possible interpretation would be to view the phase-resetting at the onset of the NRs as stimulus-evoked responses for which the phase of the ongoing brain signal is more consistent with the phase of the NRs just before or instantaneously at the onset of stimulus presentation, and it fades away forward in time as it is not a sustained oscillatory but rather an evoked response with a transient periodicity. Such a view would be consistent with animal models showing a great affinity of neurons in the primary auditory cortex (where we were likely recording from predominantly) to sharp changes at the onset of the auditory signal whose response to AM periodic signals can be seen a multitude of highly consistent individual responses to an excitatory stimulus (Heil, 1997). Further investigation is needed to understand better the distribution and possible causes of this result.

An additional potential problem with interpretation specifically in the neonatal dataset comes from our inability to account for the sleep-alert state of the infants. There is extensive adult-based research stating that there are differential sleep-wake cycle effects on neural measures, such as MMN for example (Noreika et al., 2020). It is very likely that the alertness state of the infant influenced directly the neural oscillatory measures that we

investigated. It was beyond the scope of the project to account for neonatal sleep-wake cycles, the EEG scoring for those required specialist training that was unfeasible to acquire in the short time scale of the project. We are aware of at least one published automated neonatal sleep-scoring algorithm (Koolen et al., 2017), however, the understanding and implementation of it in the current dataset as nor feasible within the time constraints of the project. It is of some consolation that, as with the motion related artifacts described below, we expect that the effect of sleep-cycle related neuronal fluctuations would have been equal across risk groups.

A final empirical shortcoming of the dissertation was that despite having a sample size close to the one calculated for detecting the envisioned low-to-medium genetic effects with high power, the effect-sizes reported in Studies One and Two were still low. With all modelled factors in study one, we reported between 30-39% explained variance in the PLV distribution when both familial and genetic risk factors, as well as other circumstantial variables, were accounted for. Although this can be considered a healthy medium size variance explained, given that we modelled many major theoretical contributors, a larger proportion explained could have been expected. Furthermore, the reported effect sizes in Study Two specifically for the genetic factors ranged between .07-.09 for a single SNP. The effect size of *connection of effect* (i.e. which channel-pair GPDC was measured in), ranged between .29-.47, which was unsurprising given the major difference in effect between the channel pairs.

#### 7.1.6.1 Technical Limitations

Technically, one of the major problems with the measures reported here was limited amount of clean EEG data, which was the main reason for calculating the GPDC metric in a small 4-channel network only. Additionally, due to the sparse coverage of the 11 channels on the head, normal interpolation of noisy channels was not appropriate, while the correction techniques attempted that worked with the GPDC matrix calculations were not validated by other studies.

Issues with data retentions are typical in infant EEG research, specifically due to limited cooperation time in experiments, and movement prevalence throughout the recording. In fact, the neonatal infants presented less of a problem compared to the older ages tested, as they were swaddled and if they were in a quite restfulness, or in a sleep state, their

movements were minimal. Still, the time on experiment did vary between infants, if they woke up and were fussy or for some other reason active, they would sometimes not be able to complete the full experiment or would create a lot of movement related artifacts. It should be further noted that in this line of experiments, we did not account for spontaneous muscle activity during the experiment, which was not overtly visible. We did not measure respiration and heart rate (ECG) or ocular activity (EOG), as the infant's comfort and minimizing fiddling were prioritized. For other involuntary motions, for example, if the infant were making tiny suckling motions, not visible to the experimenter, they would not have been accounted for during the artifact rejection stage but may have presented frequency power contortions in the spectrum (Georgieva et al., 2020; Noreika et al., 2020). Such motions could have had a modulating effect in the frequency bands of interested in the study in the syllabic rate (2.2-3.9Hz), if they happened to suckle 2-4 times per second. Still, we assumed here that if any such influences occurred, they did so sporadically in all infants and there were no systematic differences in movement and sleep patterns between groups.

A second technical/skill-based limitation of the dissertation was that we were unable to test for all the genetic predictors (16 polymorphisms in total) that we set off to test originally. As the selection of the SNPs was based on previous positive results in the dyslexia literature, the SNPs excluded from the current analysis had been consistently implicated in reading development processes and could have potentially stronger effect than the ones reported here. It is not unreasonable to also speculate that they might have had different directions of effects, potentially opposing, or negating some of the findings in this report. The single most cardinal reason for the undetermined genotyping samples was my inexperience and inefficient speed in running PCR experiments (a picture of my first gel run as a training experience in the first year of the doctoral program is attached in *Appendix III*). Due to my little experience, most undetermined samples were quite probably due to my errors in pipetting. A secondary constraint came from the availability of time in the wet lab and funding so the margin for learning, error and retesting the samples, was narrow.

---

## 7.2 CONCLUSIONS

Overall, we found evidence for a reduced left hemispheric directed coherence in infants with the rarer ROBO1 and DCDC2 genotypes, independent of their familial risk. In contrast, we found

that the high familial risk was the strongest indicator of a significant delay in the PLV peak to the onset of speech, despite a similar PLV peak strength between the risk groups. The effect was driven by the infants with a dyslexic mother. Finally, the less common variants of two ROBO1 SNPs were associated with a delayed PLV peak beyond the infant's familial risk.

Together, the neonatal results point toward a measurable dyslexia-risk related neural endophenotypes present at birth. They indicate a possible distinction between the effects of the at-risk genotype on the network coherence measures, and of the familial risk on the efficiency of the brain-to-speech synchrony. The developmental trajectories of these neonatal effects, and their significance over early phonological development and later dyslexia outcomes remain to be investigated. These results, however, present a potential mechanism for the emergence of an early neurobiological dyslexia-risk profile, which is yet to undergo the developmental, environmental, and experiential influences that would later shape language acquisition and reading skill.



## BIBLIOGRAPHY

- A global reference for human genetic variation. (2015). *Nature*, 526(7571), 68–74. <https://doi.org/10.1038/nature15393>
- Abrams, D. A., Nicol, T., Zecker, S., & Kraus, N. (2008). *Behavioral/Systems/Cognitive Right-Hemisphere Auditory Cortex Is Dominant for Coding Syllable Patterns in Speech*. <https://doi.org/10.1523/JNEUROSCI.0187-08.2008>
- Ahissar, E., Nagarajan, S., Ahissar, M., Protopapas, A., Mahncke, H., & Merzenich, M. M. (2001). Speech comprehension is correlated with temporal response patterns recorded from auditory cortex. *Proceedings of the National Academy of Sciences*, 98(23), 13367–13372. <https://doi.org/10.1073/pnas.201400998>
- Altarelli, I., Leroy, F., Monzalvo, K., Fluss, J., Billard, C., Dehaene-Lambertz, G., Galaburda, A. M., & Ramus, F. (2014). Planum temporale asymmetry in developmental dyslexia: Revisiting an old question. *Human Brain Mapping*, 35(12), 5717–5735. <https://doi.org/10.1002/hbm.22579>
- Altarelli, I., Monzalvo, K., Iannuzzi, S., Fluss, J., Billard, C., Ramus, F., & Dehaene-Lambertz, G. (2013). A functionally guided approach to the morphometry of occipitotemporal regions in developmental dyslexia: Evidence for differential effects in boys and girls. *Journal of Neuroscience*, 33(27), 11296–11301. <https://doi.org/10.1523/JNEUROSCI.5854-12.2013>
- Andrews, W. (2006). Robo1 regulates the development of major axon tracts and interneuron migration in the forebrain. *Development*, 133(11), 2243–2252. <https://doi.org/10.1242/dev.02379>
- Attaheri, A., Choidealbha, Á. N., Di Liberto, G. M., Rocha, S., Brusini, P., Mead, N., Olawole-Scott, H., Boutris, P., Gibbon, S., Williams, I., Goswami, U., Grey, C., & Flanagan, S. (2020). Delta-And theta-band cortical tracking and phase-amplitude coupling to sung speech by infants. *BioRxiv*, 1–36. <https://doi.org/10.1101/2020.10.12.329326>
- Babiloni, F., Astolfi, L., Cincotti, F., Mattia, D., Tocci, A., Tarantino, A., Marciani, M. G., Salinari, S., Gao, S., Colosimo, A., & De Vico Fallani, F. (2007). Cortical activity and connectivity of human brain during the prisoner's dilemma: An EEG hyperscanning study. *Annual International Conference of the IEEE Engineering in Medicine and Biology - Proceedings*. <https://doi.org/10.1109/IEMBS.2007.4353452>
- Bacalá, L. A., & Sameshima, K. (2001). Partial directed coherence: A new concept in neural structure determination. *Biological Cybernetics*, 84(6), 463–474. <https://doi.org/10.1007/PL00007990>
- Banai, K., & Ahissar, M. (2018). Poor sensitivity to sound statistics impairs the acquisition of speech categories in dyslexia. *Language, Cognition and Neuroscience*, 33(3), 321–332. <https://doi.org/10.1080/23273798.2017.1408851>
- Bates, T. C., Lind, P. A., Luciano, M., Montgomery, G. W., Martin, N. G., & Wright, M. J. (2010). Dyslexia and DYX1C1: Deficits in reading and spelling associated with a missense mutation. *Molecular Psychiatry*, 15(12), 1190–1196. <https://doi.org/10.1038/mp.2009.120>
- Bates, Timothy C., Luciano, M., Medland, S. E., Montgomery, G. W., Wright, M. J., & Martin, N. G. (2011). Genetic variance in a component of the language acquisition device: ROBO1 polymorphisms associated with phonological buffer deficits. *Behavior Genetics*, 41(1), 50–57. <https://doi.org/10.1007/s10519-010-9402-9>

- Beck, A. T. (1961). An Inventory for Measuring Depression. *Archives of General Psychiatry*, 4(6), 561. <https://doi.org/10.1001/archpsyc.1961.01710120031004>
- Becker, J., Czamara, D., Scerri, T. S., Ramus, F., Csépe, V., Talcott, J. B., Stein, J., Morris, A., Ludwig, K. U., Hoffmann, P., Honbolygó, F., Tóth, D., Fauchereau, F., Bogliotti, C., Iannuzzi, S., Chaix, Y., Valdois, S., Billard, C., George, F., ... Schumacher, J. (2014). Genetic analysis of dyslexia candidate genes in the European cross-linguistic NeuroDys cohort. *European Journal of Human Genetics*, 22(5), 675–680. <https://doi.org/10.1038/ejhg.2013.199>
- Becker, N., Vasconcelos, M., Oliveira, V., Santos, F. C. Dos, Bizarro, L., Almeida, R. M. M. D., Salles, J. F. De, & Carvalho, M. R. S. (2017). Genetic and environmental risk factors for developmental dyslexia in children: systematic review of the last decade. *Developmental Neuropsychology*, 42(7–8), 423–445. <https://doi.org/10.1080/87565641.2017.1374960>
- Bell, M. A., Cuevas, K., Bell, M. A., & Cuevas, K. (2012). *Using EEG to Study Cognitive Development : Issues and Practices Using EEG to Study Cognitive Development : Issues and Practices*. 8372(May). <https://doi.org/10.1080/15248372.2012.691143>
- Benasich, A. A., Choudhury, N., Friedman, J. T., Realpe-Bonilla, T., Chojnowska, C., & Gou, Z. (2006). The infant as a prelinguistic model for language learning impairments: Predicting from event-related potentials to behavior. *Neuropsychologia*, 44(3), 396–411. <https://doi.org/10.1016/j.neuropsychologia.2005.06.004>
- Benasich, A. A., Gou, Z., Choudhury, N., & Harris, K. D. (2008). Early cognitive and language skills are linked to resting frontal gamma power across the first 3 years. *Behavioural Brain Research*, 195(2), 215–222. <https://doi.org/10.1016/j.bbr.2008.08.049>
- Bishop, D. V. M. (2015). The interface between genetics and psychology: lessons from developmental dyslexia. *Proceedings of the Royal Society B: Biological Sciences*, 282(1806), 20143139–20143139. <https://doi.org/10.1098/rspb.2014.3139>
- Black, J. M., Tanaka, H., Stanley, L., Nagamine, M., Zakerani, N., Thurston, A., Kesler, S., Hulme, C., Lyytinen, H., Glover, G. H., Serrone, C., Raman, M. M., Reiss, A. L., & Hoeft, F. (2012). Maternal history of reading difficulty is associated with reduced language-related gray matter in beginning readers. *NeuroImage*, 59(3), 3021–3032. <https://doi.org/10.1016/j.neuroimage.2011.10.024>
- Black, J. M., Xia, Z., & Hoeft, F. (2017). Neurobiological bases of reading disorder part II: The importance of developmental considerations in typical and atypical reading. *Language and Linguistics Compass*, 11(10), 1–26. <https://doi.org/10.1111/lnc3.12252>
- Boets, B., Op De Beeck, H. P., Vandermosten, M., Scott, S. K., Gillebert, C. R., Mantini, D., Bulthé, J., Sunaert, S., Wouters, J., & Ghesquière, P. (2013). Intact but less accessible phonetic representations in adults with dyslexia. *Science*, 342(6163), 1251–1254. <https://doi.org/10.1126/science.1244333>
- Borgers, C., Epstein, S., & Kopell, N. J. (2005). Background gamma rhythmicity and attention in cortical local circuits: A computational study. *Proceedings of the National Academy of Sciences*, 102(19), 7002–7007. <https://doi.org/10.1073/pnas.0502366102>
- Bree, E., & Wijnen, F. (2016). *Chapter 7. Word Stress Competence and Literacy in Dutch Children with a Family Risk of Dyslexia and Children with Dyslexia* (pp. 135–162). <https://doi.org/10.1075/tilar.17.07bre>
- Carozza, S. (2020). *The role of parent-child interactions in infant language development: Exploring associations between synchrony and infant neural entrainment to speech*.
- Casanova, M. F., Buxhoeveden, D. P., Cohen, M., Switala, A. E., and Roy, E. L. (2002). Minicolumnar pathology in dyslexia. *Ann. Neurol.* 52, 108–110. doi:

<https://doi.org/10.1002/ana.10226>

- Centanni, T. M., Pantazis, D., Truong, D. T., Gruen, J. R., Gabrieli, J. D. E., & Hogan, T. P. (2018). Increased variability of stimulus-driven cortical responses is associated with genetic variability in children with and without dyslexia. *Developmental Cognitive Neuroscience*, 34(January), 7–17. <https://doi.org/10.1016/j.dcn.2018.05.008>
- Chandrasekaran, C., Tureson, H. K., Brown, C. H., & Ghazanfar, A. A. (2010). *The Influence of Natural Scene Dynamics on Auditory Cortical Activity*. <https://doi.org/10.1523/JNEUROSCI.3174-10.2010>
- Che, A., Girgenti, M. J., & Loturco, J. (2014). The dyslexia-associated gene *dcdc2* is required for spike-timing precision in mouse neocortex. *Biological Psychiatry*, 76(5), 387–396. <https://doi.org/10.1016/j.biopsych.2013.08.018>
- Che, A., Truong, D. T., Fitch, R. H., & Lo Turco, J. J. (2016). Mutation of the dyslexia-associated gene *Dcdc2* enhances glutamatergic synaptic transmission between layer 4 neurons in mouse neocortex. *Cerebral Cortex*, 26(9), 3705–3718. <https://doi.org/10.1093/cercor/bhv168>
- Chen, Y., Zhao, H., Zhang, Y. X., & Zuo, P. X. (2017). DCDC2 gene polymorphisms are associated with developmental dyslexia in Chinese Uyghur children. *Neural Regeneration Research*, 12(2), 259–266. <https://doi.org/10.4103/1673-5374.200809>
- Cooper, R. P., & Aslin, R. N. (1990). Preference for Infant-Directed Speech in the First Month after Birth. *Child Development*, 61(5), 1584. <https://doi.org/10.2307/1130766>
- Cristia, A., Seidl, A., Junge, C., Soderstrom, M., & Hagoort, P. (2014). Predicting individual variation in language from infant speech perception measures. *Child Development*, 85(4), 1330–1345. <https://doi.org/10.1111/cdev.12193>
- Cutini, S., Szűcs, D., Mead, N., Huss, M., & Goswami, U. (2016). Atypical right hemisphere response to slow temporal modulations in children with developmental dyslexia. *NeuroImage*, 143, 40–49. <https://doi.org/10.1016/j.neuroimage.2016.08.012>
- Cyr, Peppar Elizabeth, P.-P. (2016). *Master of Philosophy Dissertation Potential Biomarkers for Dyslexia Risk in Neonates* (Issue July 2016).
- Czamara, D., Bruder, J., Becker, J., Bartling, J., Hoffmann, P., Ludwig, K. U., Müller-Myhsok, B., & Schulte-Körne, G. (2011). Association of a Rare Variant with Mismatch Negativity in a Region Between KIAA0319 and DCDC2 in Dyslexia. *Behavior Genetics*, 41(1), 110–119. <https://doi.org/10.1007/s10519-010-9413-6>
- Daneshvarfard, F., Abrishami Moghaddam, H., Dehaene-Lambertz, G., Kongolo, G., Wallois, F., & Mahmoudzadeh, M. (2019). Neurodevelopment and asymmetry of auditory-related responses to repetitive syllabic stimuli in preterm neonates based on frequency-domain analysis. *Scientific Reports*, 9(1), 10654. <https://doi.org/10.1038/s41598-019-47064-0>
- Darki, F., Massinen, S., Salmela, E., Matsson, H., Peyrard-Janvid, M., Klingberg, T., & Kere, J. (2017). Human ROBO1 regulates white matter structure in corpus callosum. *Brain Structure and Function*, 222(2), 707–716. <https://doi.org/10.1007/s00429-016-1240-y>
- Darki, F., Peyrard-Janvid, M., Matsson, H., Kere, J., & Klingberg, T. (2012). Three Dyslexia Susceptibility Genes, DYX1C1, DCDC2, and KIAA0319, Affect Temporoparietal White Matter Structure. *Biological Psychiatry*, 72(8), 671–676. <https://doi.org/10.1016/j.biopsych.2012.05.008>
- Darki, F., Peyrard-Janvid, M., Matsson, H., Kere, J., & Klingberg, T. (2014). DCDC2 Polymorphism is Associated with Left Temporoparietal Gray and White Matter Structures during

- Development. *Journal of Neuroscience*, 34(43), 14455–14462.  
<https://doi.org/10.1523/JNEUROSCI.1216-14.2014>
- Dauer, R. M. (1983). Stress-timing and syllable-timing reanalyzed. *Journal of Phonetics*, 11(1), 51–62. [https://doi.org/10.1016/s0095-4470\(19\)30776-4](https://doi.org/10.1016/s0095-4470(19)30776-4)
- de Carvalho, A., Dautriche, I., Lin, I., & Christophe, A. (2017). Phrasal prosody constrains syntactic analysis in toddlers. *Cognition*, 163, 67–79.  
<https://doi.org/10.1016/j.cognition.2017.02.018>
- De Vos, A., Vanderauwera, J., Vanvooren, S., Vandermosten, M., Ghesquière, P., & Wouters, J. (2020). The relation between neurofunctional and neurostructural determinants of phonological processing in pre-readers. *Developmental Cognitive Neuroscience*, 46.  
<https://doi.org/10.1016/j.dcn.2020.100874>
- De Vos, A., Vanvooren, S., Vanderauwera, J., Ghesquière, P., Wouters, J., Vos, A. De, Vanvooren, S., Vanderauwera, J., Ghesquière, P., & Wouters, J. (2016). Brain & Language Atypical neural synchronization to speech envelope modulations in dyslexia. *Brain and Language*, 164, 106–117. <https://doi.org/10.1016/j.bandl.2016.10.002>
- Dębska, A., Łuniewska, M., Chyl, K., Banaszkiwicz, A., Żelechowska, A., Wypych, M., Marchewka, A., Pugh, K. R., & Jednoróg, K. (2016). Neural basis of phonological awareness in beginning readers with familial risk of dyslexia—Results from shallow orthography. *NeuroImage*, 132, 406–416. <https://doi.org/10.1016/j.neuroimage.2016.02.063>
- DeCasper, A., & Fifer, W. (1980). Of human bonding: newborns prefer their mothers' voices. *Science*, 208(4448), 1174–1176. <https://doi.org/10.1126/science.7375928>
- DeCasper, A. J., & Spence, M. J. (1986). Prenatal maternal speech influences newborns' perception of speech sounds. *Infant Behavior and Development*, 9(2), 133–150.  
[https://doi.org/10.1016/0163-6383\(86\)90025-1](https://doi.org/10.1016/0163-6383(86)90025-1)
- Defries, J. C., Fulker, D. W., & Labuda, M. C. (1987). Evidence for a genetic aetiology in reading disability of twins. *Nature*, 329(6139), 537–539. <https://doi.org/10.1038/329537a0>
- Dehaene-Lambertz, G. (2000). Cerebral specialization for speech and non-speech stimuli in infants. *Journal of Cognitive Neuroscience*, 12(3), 449–460.  
<https://doi.org/10.1162/089892900562264>
- Dehaene-Lambertz, G., & Baillet, S. (1998). A phonological representation in the infant brain. *NeuroReport*, 9(8), 1885–1888. <https://doi.org/10.1097/00001756-199806010-00040>
- Dehaene-Lambertz, G., & Gliga, T. (2004). Common neural basis for phoneme processing in infants and adults. *Journal of Cognitive Neuroscience*, 16(8), 1375–1387.  
<https://doi.org/10.1162/0898929042304714>
- Dehaene-Lambertz, G., Montavont, A., Jobert, A., Alliol, L., Dubois, J., Hertz-Pannier, L., & Dehaene, S. (2010). Language or music, mother or Mozart? Structural and environmental influences on infants' language networks. *Brain and Language*, 114(2), 53–65.  
<https://doi.org/10.1016/j.bandl.2009.09.003>
- Dehaene-Lambertz, G., & Pena, M. (2001). Electrophysiological evidence for automatic phonetic processing in neonates. *NeuroReport*, 12(14), 3155–3158.  
<https://doi.org/10.1097/00001756-200110080-00034>
- Dehaene-Lambertz, Ghislaine, & Dehaene, S. (1994). Speed and cerebral correlates of syllable discrimination in infants. *Nature*, 370(6487), 292–295.  
<https://doi.org/10.1038/370292a0>

- Dehaene-Lambertz, Ghislaine, Dehaene, S., & Hertz-Pannier, L. (2002). Functional neuroimaging of speech perception in infants. *Science*, *298*(5600), 2013–2015. <https://doi.org/10.1126/science.1077066>
- Dehaene-Lambertz, Ghislaine, Hertz-Pannier, L., & Dubois, J. (2006). Nature and nurture in language acquisition: anatomical and functional brain-imaging studies in infants. *Trends in Neurosciences*, *29*(7), 367–373. <https://doi.org/10.1016/j.tins.2006.05.011>
- Dehaene-Lambertz, Ghislaine, Hertz-Pannier, L., Dubois, J., & Dehaene, S. (2008). How does early brain organization promote language acquisition in humans? *European Review*, *16*(4), 399–411. <https://doi.org/10.1017/S1062798708000513>
- Dehaene-Lambertz, Ghislaine, Hertz-Pannier, L., Dubois, J., Mériaux, S., Roche, A., Sigman, M., & Dehaene, S. (2006). Functional organization of perisylvian activation during presentation of sentences in preverbal infants. *Proceedings of the National Academy of Sciences of the United States of America*, *103*(38), 14240–14245. <https://doi.org/10.1073/pnas.0606302103>
- Derryberry, D., & Rothbart, M. K. (1988). Arousal, affect, and attention as components of temperament. *Journal of Personality and Social Psychology*, *55*(6), 958–966. <https://doi.org/10.1037/0022-3514.55.6.958>
- Deuker, L., Bullmore, E. T., Smith, M., Christensen, S., Nathan, P. J., Rockstroh, B., & Bassett, D. S. (2009). Reproducibility of graph metrics of human brain functional networks. *NeuroImage*, *47*(4), 1460–1468. <https://doi.org/10.1016/j.neuroimage.2009.05.035>
- Doelling, K. B., Arnal, L. H., Ghitza, O., & Poeppel, D. (2014). Acoustic landmarks drive delta-theta oscillations to enable speech comprehension by facilitating perceptual parsing. *NeuroImage*, *85*, 761–768. <https://doi.org/10.1016/j.neuroimage.2013.06.035>
- Donoghue, T., Schaworonkoff, N., & Voytek, B. (2021). Methodological considerations for studying neural oscillations. *European Journal of Neuroscience*, *ejn.15361*. <https://doi.org/10.1111/ejn.15361>
- Dubois, J., Hertz-Pannier, L., Cachia, A., Mangin, J. F., Le Bihan, D., & Dehaene-Lambertz, G. (2009). Structural Asymmetries in the Infant Language and Sensori-Motor Networks. *Cerebral Cortex*, *19*(2), 414–423. <https://doi.org/10.1093/cercor/bhn097>
- Dubois, Jessica, Poupon, C., Thirion, B., Simonnet, H., Kulikova, S., Leroy, F., Hertz-Pannier, L., & Dehaene-Lambertz, G. (2015). *Exploring the Early Organization and Maturation of Linguistic Pathways in the Human Infant Brain*. <https://doi.org/10.1093/cercor/bhv082>
- Eaves, B. S., Feldman, N. H., Griffiths, T. L., Shafto, P., Jr, B. S. E., Feldman, N. H., Griffiths, T. L., & Shafto, P. (2016). *Psychological Review Infant-Directed Speech Is Consistent With Teaching Infant-Directed Speech Is Consistent With Teaching*. *123*(4).
- Eden, G. F., Stein, J. F., Wood, H. M., & Wood, F. B. (1994). Differences in eye movements and reading problems in dyslexic and normal children. *Vision Research*, *34*(10), 1345–1358. [https://doi.org/10.1016/0042-6989\(94\)90209-7](https://doi.org/10.1016/0042-6989(94)90209-7)
- Eicher, J D, Stein, C. M., Deng, F., Ciesla, A. A., Powers, N. R., Boada, R., Smith, S. D., Pennington, B. F., Iyengar, S. K., Lewis, B. A., & Gruen, J. R. (2015). The DYX2 locus and neurochemical signaling genes contribute to speech sound disorder and related neurocognitive domains. *Genes, Brain and Behavior*, *14*, 377–385. <https://doi.org/10.1111/gbb.12214>
- Eicher, John D., Powers, N. R., Miller, L. L., Mueller, K. L., Mascheretti, S., Marino, C., Willcutt, E. G., DeFries, J. C., Olson, R. K., Smith, S. D., Pennington, B. F., Tomblin, J. B., Ring, S. M., & Gruen, J. R. (2014). Characterization of the DYX2 locus on chromosome 6p22 with reading disability, language impairment, and IQ. *Human Genetics*, *133*(7). <https://doi.org/10.1007/s00439->

014-1427-3

- Faes, L., & Nollo, G. (2011). Multivariate Frequency Domain Analysis of Causal Interactions in Physiological Time Series. *Biomedical Engineering, Trends in Electronics, Communications and Software*. <https://doi.org/10.5772/13065>
- Facoetti, A., Luisa, M., Paganoni, P., Umilta, C., & Gastone, G. (2003). 1-s2.0-S0926641002001489-main. 15, 154–164.
- Feng, X., Altarelli, I., Monzalvo, K., Ding, G., Ramus, F., Shu, H., Dehaene, S., Meng, X., & Dehaene-Lambertz, G. (2020). A universal reading network and its modulation by writing system and reading ability in French and Chinese children. *ELife*, 9, 1–30. <https://doi.org/10.7554/eLife.54591>
- Fernald, A. (1989). Intonation and Communicative Intent in Mothers' Speech to Infants: Is the Melody the Message? *Child Development*, 60(6), 1497. <https://doi.org/10.2307/1130938>
- Fisher, S. E., Francks, C., Marlow, A. J., MacPhie, I. L., Newbury, D. F., Cardon, L. R., Ishikawa-Brush, Y., Richardson, A. J., Talcott, J. B., Gayán, J., Olson, R. K., Pennington, B. F., Smith, S. D., DeFries, J. C., Stein, J. F., & Monaco, A. P. (2002). Independent genome-wide scans identify a chromosome 18 quantitative-trait locus influencing dyslexia. *Nature Genetics*, 30(1), 86–91. <https://doi.org/10.1038/ng792>
- Friedrich, M., & Friederici, A. D. (2015). *The origins of word learning: Brain responses of 3-month-olds indicate their rapid association of objects and words*. 1–13. <https://doi.org/10.1111/desc.12357>
- Gabay, Y., Thiessen, E. D., & Holt, L. L. (2015). *Impaired Statistical Learning in Developmental Dyslexia*. [https://doi.org/10.1044/2015\\_JSLHR-L-14-0324](https://doi.org/10.1044/2015_JSLHR-L-14-0324)
- Ganek, H., & Eriks-Brophy, A. (2016). The Language ENvironment Analysis (LENA) System: A Literature Review. *Proceedings of the Joint Workshop on NLP for Computer Assisted Language Learning and NLP for Language Acquisition at SLTC, UmeÅ\textyen, 16th November 2016*, 130, 24–32.
- Gartstein, M. A., & Rothbart, M. K. (2003). Studying infant temperament via the Revised Infant Behavior Questionnaire. *Infant Behavior and Development*. [https://doi.org/10.1016/S0163-6383\(02\)00169-8](https://doi.org/10.1016/S0163-6383(02)00169-8)
- Georgieva, S., Lester, S., Noreika, V., Yilmaz, M. N., Wass, S., & Leong, V. (2020). Toward the Understanding of Topographical and Spectral Signatures of Infant Movement Artifacts in Naturalistic EEG. *Frontiers in Neuroscience*, 14(April), 1–15. <https://doi.org/10.3389/fnins.2020.00352>
- Gervain, J., Macagno, F., Cogoi, S., Peña, M., & Mehler, J. (2008). The neonate brain detects speech structure. *Proceedings of the National Academy of Sciences of the United States of America*, 105(37), 14222–14227. <https://doi.org/10.1073/pnas.0806530105>
- Gilger, J. W., Pennington, B. F., & Defries, J. C. (1991). Risk for reading disability as a function of parental history in three family studies. *Reading and Writing*, 3(3–4), 205–217. <https://doi.org/10.1007/BF00354958>
- Gilmore, J. H., Knickmeyer, R. C., & Gao, W. (2018). *Imaging structural and functional brain development in early childhood*. <https://doi.org/10.1038/nrn.2018.1>
- Giraud, A.-L., Kleinschmidt, A., Poeppel, D., Lund, T. E., Frackowiak, R. S. J., & Laufs, H. (2007). Endogenous Cortical Rhythms Determine Cerebral Specialization for Speech Perception and Production. *Neuron*, 56(6), 1127–1134. <https://doi.org/10.1016/j.neuron.2007.09.038>

- Giraud, A. L., & Poeppel, D. (2012). Cortical oscillations and speech processing: Emerging computational principles and operations. *Nature Neuroscience*, *15*(4), 511–517. <https://doi.org/10.1038/nn.3063>
- Giraud, A. L., & Ramus, F. (2013). Neurogenetics and auditory processing in developmental dyslexia. *Current Opinion in Neurobiology*, *23*(1), 37–42. <https://doi.org/10.1016/j.conb.2012.09.003>
- Glaser, H., Leroy, F., Dubois, J., Hertz-Pannier, L., Mangin, J. F., & Dehaene-Lambertz, G. (2011). A robust cerebral asymmetry in the infant brain: The rightward superior temporal sulcus. *NeuroImage*, *58*(3), 716–723. <https://doi.org/10.1016/j.neuroimage.2011.06.016>
- Gori, M., Ober, K. M., Tinelli, F., & Coubard, O. A. (2020). Temporal representation impairment in developmental dyslexia for unisensory and multisensory stimuli. *Developmental Science*, *23*(5), 1–17. <https://doi.org/10.1111/desc.12977>
- Goswami, U., Thomson, J., Richardson, U., Stainthorp, R., Hughes, D., Rosen, S., & Scott, S. K. (2002). Amplitude envelope onsets and developmental dyslexia: A new hypothesis. *Proceedings of the National Academy of Sciences*. <https://doi.org/10.1073/pnas.122368599>
- Goswami, Usha. (2011). A temporal sampling framework for developmental dyslexia. *Trends in Cognitive Sciences*, *15*(1), 3–10. <https://doi.org/10.1016/j.tics.2010.10.001>
- Gou, Z., Choudhury, N., & Benasich, A. A. (2011). Resting frontal gamma power at 16, 24 and 36 months predicts individual differences in language and cognition at 4 and 5 years. *Behavioural Brain Research*, *220*(2), 263–270. <https://doi.org/10.1016/j.bbr.2011.01.048>
- Graf Estes, K., & Hurley, K. (2013). Infant-Directed Prosody Helps Infants Map Sounds to Meanings. *Infancy*, *18*(5), 797–824. <https://doi.org/10.1111/inf.12006>
- Granger, C. J. W. (1969). Investigating Causal Relations by Econometric Models and Cross-spectral Methods Authors (s): C. W. J. Granger Published by: The Econometric Society Stable URL: <http://www.jstor.org/stable/1912791> Accessed: 25-03-2016 19:26 UTC Your use of the JS. *Econometrica*, *37*(3), 424–438.
- Greenberg, S., Carvey, H., Hitchcock, L., & Chang, S. (2003). Temporal properties of spontaneous speech - A syllable-centric perspective. *Journal of Phonetics*, *31*(3–4), 465–485. <https://doi.org/10.1016/j.wocn.2003.09.005>
- Guttorm, T. K., Leppänen, P. H. T., Richardson, U., & Lyytinen, H. (2001). Event-related potentials and consonant differentiation in newborns with familial risk for dyslexia. *Journal of Learning Disabilities*, *34*(6), 534–544. <https://doi.org/10.1177/002221940103400606>
- Guttorm<sup>1</sup>, T. K., Leppänen<sup>1</sup>, P. H. T., Hämäläinen<sup>1</sup>, J. A., Eklund<sup>1</sup>, K. M., & Lyytinen<sup>1</sup>, H. J. (2010). Newborn Event-Related Potentials Predict Poorer Pre-Reading Skills in Children at Risk for Dyslexia. *Journal of Learning Disabilities*, *43*(5), 391–401. <https://doi.org/10.1177/0022219409345005>
- Gwin, J. T., Gramann, K., Makeig, S., & Ferris, D. P. (2010). Removal of movement artifact from high-density EEG recorded during walking and running. *Journal of Neurophysiology*, *103*(6), 3526–3534. <https://doi.org/10.1152/jn.00105.2010>
- Hämäläinen, J. A., Rupp, A., Soltész, F., Szücs, D., & Goswami, U. (2012). Reduced phase locking to slow amplitude modulation in adults with dyslexia: An MEG study. *NeuroImage*, *59*(3), 2952–2961. <https://doi.org/10.1016/j.neuroimage.2011.09.075>
- Hämäläinen, J., Leppänen, P. H. T., Torppa, M., Müller, K., & Lyytinen, H. (2005). Detection of sound rise time by adults with dyslexia. *Brain and Language*, *94*(1), 32–42. <https://doi.org/10.1016/j.bandl.2004.11.005>

- Hancock, R., Pugh, K. R., & Hoefl, F. (2017). Neural Noise Hypothesis of Developmental Dyslexia. *Trends in Cognitive Sciences*, 21(6), 434–448. <https://doi.org/10.1016/j.tics.2017.03.008>
- Hancock, R., Richlan, F., & Hoefl, F. (2017). Possible roles for fronto-striatal circuits in reading disorder. *Neuroscience and Biobehavioral Reviews*, 72, 243–260. <https://doi.org/10.1016/j.neubiorev.2016.10.025>
- Hannula-Jouppi, K., Kaminen-Ahola, N., Taipale, M., Eklund, R., Nopola-Hemmi, J., Kääriäinen, H., & Kere, J. (2005). The axon guidance receptor gene ROBO1 is a candidate gene for developmental dyslexia. *PLoS Genetics*, 1(4), 0467–0474. <https://doi.org/10.1371/journal.pgen.0010050>
- Hart, B., & Risley, T. R. (1995). Meaningful differences in the everyday experiences of young American children. *Paul H Brookes Publishing*, 3824577. <https://doi.org/10.1007/s00431-005-0010-2>
- He, C., Hotson, L., & Trainor, L. J. (2007). Mismatch responses to pitch changes in early infancy. *Journal of Cognitive Neuroscience*, 19(5), 878–892. <https://doi.org/10.1162/jocn.2007.19.5.878>
- Heil, P. (1997). Auditory cortical onset responses revisited. II. Response strength. *Journal of Neurophysiology*, 77(5), 2642–2660. <https://doi.org/10.1152/jn.1997.77.5.2642>
- Howe, K. L., Achuthan, P., Allen, J., Allen, J., Alvarez-Jarreta, J., Ridwan Amode, M., Armean, I. M., Azov, A. G., Bennett, R., Bhai, J., Billis, K., Boddu, S., Charkhchi, M., Cummins, C., da Rin Fioretto, L., Davidson, C., Dodiya, K., El Houdaigui, B., Fatima, R., ... Flicek, P. (2021). Ensembl 2021. *Nucleic Acids Research*, 49(D1), D884–D891. <https://doi.org/10.1093/nar/gkaa942>
- Huber, E., Donnelly, P. M., Rokem, A., & Yeatman, J. D. (2018). Rapid and widespread white matter plasticity during an intensive reading intervention. *Nature Communications*, 9(1). <https://doi.org/10.1038/s41467-018-04627-5>
- Im, K., Raschle, N. M., Smith, S. A., Ellen Grant, P., & Gaab, N. (2016). Atypical Sulcal Pattern in Children with Developmental Dyslexia and At-Risk Kindergarteners. *Cerebral Cortex*, 26(3), 1138–1148. <https://doi.org/10.1093/cercor/bhu305>
- Jackson-Maldonado, D. (2012). MacArthur-Bates Communicative Development Inventories. In *The Encyclopedia of Applied Linguistics*. <https://doi.org/10.1002/9781405198431.wbeal0745>
- Jessen, S., Fiedler, L., Münte, T. F., & Obleser, J. (2019). Quantifying the individual auditory and visual brain response in 7-month-old infants watching a brief cartoon movie. *NeuroImage*, 202(April), 116060. <https://doi.org/10.1016/j.neuroimage.2019.116060>
- Jha, S. C., Xia, K., Eric Schmitt, J., Ahn, M., Girault, J. B., Murphy, V. A., Li, G., Wang, L., Shen, D., Zou, F., Zhu, H., Styner, M., Knickmeyer, R. C., Gilmore, J. H., & John Gilmore, C. H. (2018). *Genetic influences on neonatal cortical thickness and surface area*. <https://doi.org/10.1002/hbm.24340>
- Jiménez-Bravo, M., Marrero, V., & Benítez-Burraco, A. (2017). An oscillopathic approach to developmental dyslexia: From genes to speech processing. In *Behavioural Brain Research* (Vol. 329, pp. 84–95). <https://doi.org/10.1016/j.bbr.2017.03.048>
- Johnson, M. B., Kawasawa, Y. I., Mason, C. E., Krsnik, Ž., Coppola, G., Bogdanović, D., Geschwind, D. H., Mane, S. M., State, M. W., & Šestan, N. (2009). Functional and Evolutionary Insights into Human Brain Development through Global Transcriptome Analysis. *Neuron*, 62(4), 494–509. <https://doi.org/10.1016/j.neuron.2009.03.027>

- Jones, O. P., & Schnupp, J. W. H. (2021). How Does the Brain Represent Speech? *The Handbook of Speech Perception*, 58–96. <https://doi.org/10.1002/9781119184096.ch3>
- Jung, T. P., Makeig, S., Humphries, C., Lee, T. W., Mckeown, M. J., Iragui, V., & Sejnowski, T. J. (2000). Removing electroencephalographic artifacts by blind source separation. *Psychophysiology*, 37(2), 163–178. <https://doi.org/10.1017/S0048577200980259>
- Kalashnikova, M., Goswami, U., & Burnham, D. (2018). Mothers speak differently to infants at risk for dyslexia. *Developmental Science*, 21(1), 1–15. <https://doi.org/10.1111/desc.12487>
- Kalashnikova, M., Peter, V., Di Liberto, G. M., Lalor, E. C., & Burnham, D. (2018). Infant-directed speech facilitates seven-month-old infants' cortical tracking of speech. *Scientific Reports*, 8(1), 13745. <https://doi.org/10.1038/s41598-018-32150-6>
- Karczewski, K. J., Francioli, L. C., Tiao, G., Cummings, B. B., Alföldi, J., Wang, Q., Collins, R. L., Laricchia, K. M., Ganna, A., Birnbaum, D. P., Gauthier, L. D., Brand, H., Solomonson, M., Watts, N. A., Rhodes, D., Singer-Berk, M., England, E. M., Seaby, E. G., Kosmicki, J. A., ... Consortium, G. A. D. (2021). Author Correction: The mutational constraint spectrum quantified from variation in 141,456 humans. *Nature*, 590(7846), E53–E53. <https://doi.org/10.1038/s41586-020-03174-8>
- Koolen, N., Oberdorfer, L., Rona, Z., Giordano, V., Werther, T., Klebermass-Schrehof, K., Stevenson, N., & Vanhatalo, S. (2017). Automated classification of neonatal sleep states using EEG. *Clinical Neurophysiology*, 128(6), 1100–1108. <https://doi.org/10.1016/j.clinph.2017.02.025>
- Langer, N., Peysakhovich, B., Zuk, J., Drottar, M., Sliva, D. D., Smith, S., Becker, B. L. C. C., Grant, P. E., & Gaab, N. (2015). White Matter Alterations in Infants at Risk for Developmental Dyslexia. *Cerebral Cortex*, 27(2), bhv281. <https://doi.org/10.1093/cercor/bhv281>
- Lehongre, K., Morillon, B., Giraud, A.-L. L., & Ramus, F. (2013). Impaired auditory sampling in dyslexia: further evidence from combined fMRI and EEG. *Frontiers in Human Neuroscience*, 7(August), 1–8. <https://doi.org/10.3389/fnhum.2013.00454>
- Lehongre, K., Ramus, F., Villiermet, N., Schwartz, D., & Giraud, A. L. (2011). Altered low-gamma sampling in auditory cortex accounts for the three main facets of dyslexia. *Neuron*, 72(6), 1080–1090. <https://doi.org/10.1016/j.neuron.2011.11.002>
- Leong, V., Byrne, E., Clackson, K., Georgieva, S., Lam, S., & Wass, S. (2017). Speaker gaze increases information coupling between infant and adult brains. *Proceedings of the National Academy of Sciences*, 114(50), 201702493. <https://doi.org/10.1073/pnas.1702493114>
- Leong, V., & Goswami, U. (2014a). Assessment of rhythmic entrainment at multiple timescales in dyslexia: Evidence for disruption to syllable timing. *Hearing Research*, 308, 141–161. <https://doi.org/10.1016/j.heares.2013.07.015>
- Leong, V., & Goswami, U. (2014b). Impaired extraction of speech rhythm from temporal modulation patterns in speech in developmental dyslexia. *Frontiers in Human Neuroscience*, 8(February), 1–14. <https://doi.org/10.3389/fnhum.2014.00096>
- Leong, V., & Goswami, U. (2015). Acoustic-emergent phonology in the amplitude envelope of child-directed speech. *PLoS ONE*, 10(12), 1–37. <https://doi.org/10.1371/journal.pone.0144411>
- Leong, V., Hämäläinen, J., Soltész, F., & Goswami, U. (2011). Rise time perception and detection of syllable stress in adults with developmental dyslexia. *Journal of Memory and Language*, 64(1), 59–73. <https://doi.org/10.1016/j.jml.2010.09.003>
- Leong, V., Kalashnikova, M., Burnham, D., & Goswami, U. (2017). The Temporal Modulation

- Structure of Infant-Directed Speech. *Open Mind*, 1(2), 78–90.  
[https://doi.org/10.1162/OPMI\\_a\\_00008](https://doi.org/10.1162/OPMI_a_00008)
- Leong, V., Stone, M. A., Turner, R. E., & Goswami, U. (2014). A role for amplitude modulation phase relationships in speech rhythm perception. *The Journal of the Acoustical Society of America*, 136(1), 366–381. <https://doi.org/10.1121/1.4883366>
- Leppänen, P.H.T., Hämäläinen, J. A., Guttorm, T. K., Eklund, K. M., Salminen, H., Tanskanen, A., Torppa, M., Puolakanaho, A., Richardson, U., Pennala, R., & Lyytinen, H. (2012). Infant brain responses associated with reading-related skills before school and at school age. *Neurophysiologie Clinique/Clinical Neurophysiology*, 42(1–2), 35–41.  
<https://doi.org/10.1016/j.neucli.2011.08.005>
- Leppänen, Paavo H.T., Hämäläinen, J. A., Salminen, H. K., Eklund, K. M., Guttorm, T. K., Lohvansuu, K., Puolakanaho, A., & Lyytinen, H. (2010). Newborn brain event-related potentials revealing atypical processing of sound frequency and the subsequent association with later literacy skills in children with familial dyslexia. *Cortex*, 46(10), 1362–1376. <https://doi.org/10.1016/j.cortex.2010.06.003>
- Leppänen, Paavo H T, Richardson, U., Pihko, E., Eklund, K. M., Guttorm, T. K., Aro, M., & Lyytinen, H. (2002). Developmental Neuropsychology Brain Responses to Changes in Speech Sound Durations Differ Between Infants With and Without Familial Risk for Dyslexia) Brain Responses to Changes in Speech Sound Durations Differ Between Infants With and Without Familial Ri. *Developmental Neuropsychology*, 22(1), 407–422.  
[https://doi.org/10.1207/S15326942dn2201\\_4](https://doi.org/10.1207/S15326942dn2201_4)
- Liebig, J., Friederici, A. D., & Neef, N. E. (2020). Auditory brainstem measures and genotyping boost the prediction of literacy: A longitudinal study on early markers of dyslexia. *Developmental Cognitive Neuroscience*, 46(October), 100869.  
<https://doi.org/10.1016/j.dcn.2020.100869>
- Lim, C. K. P., Ho, C. S. H., Chou, C. H. N., & Waye, M. M. Y. (2011). Association of the rs3743205 variant of DYX1C1 with dyslexia in Chinese children. *Behavioral and Brain Functions*, 7.  
<https://doi.org/10.1186/1744-9081-7-16>
- Lizarazu, M., Lallier, M., Bourguignon, M., Carreiras, M., & Molinaro, N. (2020). Impaired neural response to speech edges in dyslexia. *Cortex*, 135, 207–218.  
<https://doi.org/10.1016/j.cortex.2020.09.033>
- Lizarazu, M., Lallier, M., & Molinaro, N. (2019). Phase – amplitude coupling between theta and gamma oscillations adapts to speech rate Phase – amplitude coupling between theta and gamma. *April*. <https://doi.org/10.1111/nyas.14099>
- Lizarazu, M., Lallier, M., Molinaro, N., Bourguignon, M., Paz-Alonso, P. M., Lerma-Usabiaga, G., & Carreiras, M. (2015). Developmental evaluation of atypical auditory sampling in dyslexia: Functional and structural evidence. *Human Brain Mapping*, 36(12).  
<https://doi.org/10.1002/hbm.22986>
- Lizarazu, M., Scotto di Covella, L., van Wassenhove, V., Rivière, D., Mizzi, R., Lehongre, K., Hertz-Pannier, L., & Ramus, F. (2021). Neural entrainment to speech and nonspeech in dyslexia: Conceptual replication and extension of previous investigations. *Cortex*, 137(February), 160–178. <https://doi.org/10.1016/j.cortex.2020.12.024>
- Lohvansuu, K., Hämäläinen, J. A., Ervast, L., Lyytinen, H., & Leppänen, P. H. T. (2018). Longitudinal interactions between brain and cognitive measures on reading development from 6 months to 14 years. *Neuropsychologia*, 108, 6–12.  
<https://doi.org/10.1016/j.neuropsychologia.2017.11.018>

- Lou, C., Duan, X., Altarelli, I., Sweeney, J. A., Ramus, F., Zhao, J., & Jingjing Zhao, C. (2018). *White matter network connectivity deficits in developmental dyslexia*. <https://doi.org/10.1002/hbm.24390>
- Łuniewska, M., Chyl, K., Dębska, A., Banaszekiewicz, A., Żelechowska, A., Marchewka, A., Grabowska, A., & Jednoróg, K. (2019). Children With Dyslexia and Familial Risk for Dyslexia Present Atypical Development of the Neuronal Phonological Network. *Frontiers in Neuroscience*, *13*, 1287. <https://doi.org/10.3389/fnins.2019.01287>
- Mahmoudzadeh, M., Dehaene-Lambertz, G., Fournier, M., Kongolo, G., Goudjil, S., Dubois, J., Grebe, R., & Wallois, F. (2013). Syllabic discrimination in premature human infants prior to complete formation of cortical layers. *Proceedings of the National Academy of Sciences of the United States of America*, *110*(12), 4846–4851. <https://doi.org/10.1073/pnas.1212220110>
- Mahmoudzadeh, M., Wallois, F., Kongolo, G., Goudjil, S., & Dehaene-Lambertz, G. (2017). Functional maps at the onset of auditory inputs in very early preterm human neonates. *Cerebral Cortex*, *27*(4), 2500–2512. <https://doi.org/10.1093/cercor/bhw103>
- Mascheretti, S., De Luca, A., Trezzi, V., Peruzzo, D., Nordio, A., Marino, C., & Arrigoni, F. (2017). Neurogenetics of developmental dyslexia: From genes to behavior through brain neuroimaging and cognitive and sensorial mechanisms. In *Translational Psychiatry*. <https://doi.org/10.1038/tp.2016.240>
- Mascheretti, Sara, Andreola, C., Scaini, S., & Sulpizio, S. (2018). Beyond genes: A systematic review of environmental risk factors in specific reading disorder. *Research in Developmental Disabilities*, *82*(March), 147–152. <https://doi.org/10.1016/j.ridd.2018.03.005>
- Mascheretti, Sara, Riva, V., Giorda, R., Beri, S., Lanzoni, L. F. E., Cellino, M. R., & Marino, C. (2014). KIAA0319 and ROBO1: Evidence on association with reading and pleiotropic effects on language and mathematics abilities in developmental dyslexia. *Journal of Human Genetics*, *59*(4), 189–197. <https://doi.org/10.1038/jhg.2013.141>
- McPhillips, M., Hepper, P. G., & Mulhern, G. (2000). Effects of replicating primary-reflex movements on specific reading difficulties in children: A randomised, double-blind, controlled trial. *Lancet*, *355*(9203), 537–541. [https://doi.org/10.1016/S0140-6736\(99\)02179-0](https://doi.org/10.1016/S0140-6736(99)02179-0)
- Mehler, J., Jusczyk, P., Lambertz, G., Halsted, N., Bertoncini, J., & Amiel-Tison, C. (1988). A precursor of language acquisition in young infants. *Cognition*, *29*(2), 143–178. [https://doi.org/10.1016/0010-0277\(88\)90035-2](https://doi.org/10.1016/0010-0277(88)90035-2)
- Meltzoff, A. N., Kuhl, P. K., Movellan, J., & Sejnowski, T. J. (2009). *of Learning*. *325*(July), 284–289.
- Meng, H., Smith, S. D., Hager, K., Held, M., Liu, J., Olson, R. K., Pennington, B. F., DeFries, J. C., Gelernter, J., O'Reilly-Pol, T., Somlo, S., Skudlarski, P., Shaywitz, S. E., Shaywitz, B. A., Marchione, K., Wang, Y., Paramasivam, M., LoTurco, J. J., Page, G. P., & Gruen, J. R. (2005). DCDC2 is associated with reading disability and modulates neuronal development in the brain. *Proceedings of the National Academy of Sciences of the United States of America*. <https://doi.org/10.1073/pnas.0508591102>
- Molfese, D. L. (2000). Predicting Dyslexia at 8 Years of Age Using Neonatal Brain Responses. *Brain and Language*, *72*(3), 238–245. <https://doi.org/10.1006/brln.2000.2287>
- Molfese, D. L., Molfese, V. J., Key, S., Modydin, A., Kelle~, S., & Terrell, S. (2002). Reading and Cognitive Abilities: Longitudinal Studies of Brain and Behavior Changes in Young Children. *Annals of Dyslexia*, *52*.

- Molfese, V. J., & Molfese, D. L. (2002). Environmental and Social Influences on Reading Skills as Indexed by Brain and Behavioral Responses. *Annals of Dyslexia*, 52.
- Molfese, V. J., Molfese, D. L., & Modgline, A. A. (2001). Newborn and Preschool Predictors of Second-Grade Reading Scores. *Journal of Learning Disabilities*, 34(6), 545–554. <https://doi.org/10.1177/002221940103400607>
- Molinaro, N., Lizarazu, M., & Lallier, M. (2016). *Out-of-Synchrony Speech Entrainment in Developmental Dyslexia*. 2783(April), 2767–2783. <https://doi.org/10.1002/hbm.23206>
- Molnar, M., Gervain, J., & Carreiras, M. (2014). Within-rhythm class native language discrimination abilities of basque-Spanish monolingual and bilingual infants at 3.5 months of age. *Infancy*, 19(3), 326–337. <https://doi.org/10.1111/infa.12041>
- Morillon, B. (2010). Neurophysiological origin of human brain asymmetry for speech and language. *Proceedings of the National Academy of Sciences of the United States of America*, 107(43), 18688–18693. <https://doi.org/10.1073/pnas.1007189107/-/DCSupplemental.www.pnas.org/cgi/doi/10.1073/pnas.1007189107>
- Müller, B., Schaadt, G., Boltze, J., Emmrich, F., Skeide, M. A., Neef, N. E., Kraft, I., Brauer, J., Friederici, A. D., Kirsten, H., & Wilcke, A. (2017). ATP2C2 and DYX1C1 are putative modulators of dyslexia-related MMR. *Brain and Behavior*, 7(11), 1–12. <https://doi.org/10.1002/brb3.851>
- Nazzi, T., Bertoni, J., & Mehler, J. (1998). Language Discrimination by Newborns: Toward an Understanding of the Role of Rhythm. *Journal of Experimental Psychology: Human Perception and Performance*, 24(3), 756–766. <https://doi.org/10.1037/0096-1523.24.3.756>
- Neef, N. E., Müller, B., Liebig, J., Schaadt, G., Grigutsch, M., Gunter, T. C., Wilcke, A., Kirsten, H., Skeide, M. A., Kraft, I., Kraus, N., Emmrich, F., Brauer, J., Boltze, J., & Friederici, A. D. (2017). Dyslexia risk gene relates to representation of sound in the auditory brainstem. *Developmental Cognitive Neuroscience*, 24(February), 63–71. <https://doi.org/10.1016/j.dcn.2017.01.008>
- Neuhaus-Follini, A., & Bashaw, G. J. (2015). Crossing the embryonic midline: molecular mechanisms regulating axon responsiveness at an intermediate target. *Wiley Interdisciplinary Reviews: Developmental Biology*, 4(4), 377–389. <https://doi.org/10.1002/wdev.185>
- Newbury, D. F., Monaco, A. P., & Paracchini, S. (2014). Reading and language disorders: The importance of both quantity and quality. *Genes*, 5(2), 285–309. <https://doi.org/10.3390/genes5020285>
- Nicolson, R. I., & Fawcett, A. J. (2019). Development of dyslexia: The delayed neural commitment framework. *Frontiers in Behavioral Neuroscience*, 13. <https://doi.org/10.3389/fnbeh.2019.00112>
- Niogi, S. N., & McCandliss, B. D. (2006). Left lateralized white matter microstructure accounts for individual differences in reading ability and disability. *Neuropsychologia*, 44(11), 2178–2188. <https://doi.org/10.1016/j.neuropsychologia.2006.01.011>
- Nopola-Hemmi, J., Myllyluoma, B., Haltia, T., Taipale, M., Ollikainen, V., Ahonen, T., Voutilainen, A., Kere, J., & Widén, E. (2001). A dominant gene for developmental dyslexia on chromosome 3. *Journal of Medical Genetics*, 38(10), 658–664. <https://doi.org/10.1136/JMG.38.10.658>
- Noreika, V., Georgieva, S., Wass, S., & Leong, V. (2020). 14 challenges and their solutions for conducting social neuroscience and longitudinal EEG research with infants. *Infant Behavior*

- and Development*, 58(June 2019), 101393. <https://doi.org/10.1016/j.infbeh.2019.101393>
- Northstone, K., Lewcock, M., Groom, A., Boyd, A., Macleod, J., Timpson, N., & Wells, N. (2019). *Open Peer Review The Avon Longitudinal Study of Parents and Children (ALSPAC): an update on the enrolled sample of index children in 2019 [version 1; peer review: 2 approved]*. <https://doi.org/10.12688/wellcomeopenres.15132.1>
- Orekhova, E. V., Stroganova, T. A., Posikera, I. N., & Elam, M. (2006). EEG theta rhythm in infants and preschool children. *Clinical Neurophysiology*, 117(5), 1047–1062. <https://doi.org/10.1016/j.clinph.2005.12.027>
- Ortiz-Mantilla, S., Hamalainen, J. A., Musacchia, G., & Benasich, A. A. (2013). Enhancement of Gamma Oscillations Indicates Preferential Processing of Native over Foreign Phonemic Contrasts in Infants. *Journal of Neuroscience*, 33(48), 18746–18754. <https://doi.org/10.1523/JNEUROSCI.3260-13.2013>
- Ortiz Barajas, M. C., Guevara, R., & Gervain, J. (2021). The origins and development of speech envelope tracking during the first months of life. *Developmental Cognitive Neuroscience*, 48. <https://doi.org/10.1016/j.dcn.2021.100915>
- Ozernov-Palchik, O., Norton, E. S., Wang, Y., Beach, S. D., Zuk, J., Wolf, M., Gabrieli, J. D. E., & Gaab, N. (2019). The relationship between socioeconomic status and white matter microstructure in pre-reading children: A longitudinal investigation. *Human Brain Mapping*, 40(3), 741–754. <https://doi.org/10.1002/hbm.24407>
- Paracchini, S., Scerri, T., & Monaco, A. P. (2007). The Genetic Lexicon of Dyslexia. *Annual Review of Genomics and Human Genetics*, 8(1), 57–79. <https://doi.org/10.1146/annurev.genom.8.080706.092312>
- Paracchini, S., Steer, C. D., Buckingham, L. L., Morris, A. P., Ring, S., Scerri, T., Stein, J., Pembrey, M. E., Ragoussis, J., Golding, J., & Monaco, A. P. (2008). Association of the KIAA0319 dyslexia susceptibility gene with reading skills in the general population. *American Journal of Psychiatry*, 165(12), 1576–1584. <https://doi.org/10.1176/appi.ajp.2008.07121872>
- Paracchini, S., Thomas, A., Castro, S., Lai, C., Paramasivam, M., Wang, Y., Keating, B. J., Taylor, J. M., Hacking, D. F., Scerri, T., Francks, C., Richardson, A. J., Wade-Martins, R., Stein, J. F., Knight, J. C., Copp, A. J., LoTurco, J., & Monaco, A. P. (2006). The chromosome 6p22 haplotype associated with dyslexia reduces the expression of KIAA0319, a novel gene involved in neuronal migration. *Human Molecular Genetics*, 15(10), 1659–1666. <https://doi.org/10.1093/hmg/ddl089>
- Peña, M., Bonatti, L. L., Nespor, M., & Mehler, J. (2002). Signal-driven computations in speech processing. *Science*, 298(5593), 604–607. <https://doi.org/10.1126/science.1072901>
- Peña, M., Maki, A., Kovačić, D., Dehaene-Lambertz, G., Koizumit, H., Bouquet, F., & Mehler, J. (2003). Sounds and silence: An optical topography study of language recognition at birth. *Proceedings of the National Academy of Sciences of the United States of America*, 100(20), 11702–11705. <https://doi.org/10.1073/pnas.1934290100>
- Peña, M., Pittaluga, E., & Mehler, J. (2010). Language acquisition in premature and full-term infants. *Proceedings of the National Academy of Sciences of the United States of America*, 107(8), 3823–3828. <https://doi.org/10.1073/pnas.0914326107>
- Perrachione, T. K., Del Tufo, S. N., Winter, R., Murtagh, J., Cyr, A., Chang, P., Halverson, K., Ghosh, S. S., Christodoulou, J. A., & Gabrieli, J. D. E. (2016). Dysfunction of Rapid Neural Adaptation in Dyslexia. *Neuron*, 92(6), 1383–1397. <https://doi.org/10.1016/j.neuron.2016.11.020>
- Peterson, R. L., & Pennington, B. F. (2015). Developmental dyslexia. *Annual Review of Clinical Psychology*, 11, 283–307. <https://doi.org/10.1146/annurev-clinpsy-032814-112842>

- Pettigrew, K. A., Frinton, E., Nudel, R., Chan, M. T. M., Thompson, P., Hayiou-Thomas, M. E., Talcott, J. B., Stein, J., Monaco, A. P., Hulme, C., Snowling, M. J., Newbury, D. F., & Paracchini, S. (2016). Further evidence for a parent-of-origin effect at the NOP9 locus on language-related phenotypes. *Journal of Neurodevelopmental Disorders*, *8*(1), 1–8. <https://doi.org/10.1186/s11689-016-9157-6>
- Peyre, H., Mohanpuria, N., Jednoróg, K., Heim, S., Grande, M., van Ermingen-Marbach, M., Altarelli, I., Monzalvo, K., Williams, C. M., Germanaud, D., Toro, R., & Ramus, F. (2020). Neuroanatomy of dyslexia: An allometric approach. *European Journal of Neuroscience*, *January*, 1–15. <https://doi.org/10.1111/ejn.14690>
- Pinel, P., Fauchereau, F., Moreno, A., Barbot, A., Lathrop, M., Zelenika, D., Le Bihan, D., Poline, J. B. J.-B., Bourgeron, T., & Dehaene, S. (2012). Genetic Variants of FOXP2 and KIAA0319/TTRAP/THEM2 Locus Are Associated with Altered Brain Activation in Distinct Language-Related Regions. *Journal of Neuroscience*, *32*(3), 817–825. <https://doi.org/10.1523/JNEUROSCI.5996-10.2012>
- Poelmans, H., Luts, H., Vandermosten, M., Ghesquière, P., & Wouters, J. (2012). Hemispheric asymmetry of auditory steady-state responses to monaural and diotic stimulation. *JARO - Journal of the Association for Research in Otolaryngology*, *13*(6), 867–876. <https://doi.org/10.1007/s10162-012-0348-x>
- Poeppel, D. (2014). The neuroanatomic and neurophysiological infrastructure for speech and language. *Current Opinion in Neurobiology*, *28*, 142–149. <https://doi.org/10.1016/j.conb.2014.07.005>
- Power, Alan J., Colling, L. J., Mead, N., Barnes, L., & Goswami, U. (2016). Neural encoding of the speech envelope by children with developmental dyslexia. *Brain and Language*, *160*, 1–10. <https://doi.org/10.1016/j.bandl.2016.06.006>
- Power, Alan J., Mead, N., Barnes, L., & Goswami, U. (2013). Neural entrainment to rhythmic speech in children with developmental dyslexia. *Frontiers in Human Neuroscience*, *7*(November), 1–19. <https://doi.org/10.3389/fnhum.2013.00777>
- Power, Alan James, Mead, N., Barnes, L., Goswami, U., Pena, M., Obleser, J., & Vihman, M. (2012). *Neural entrainment to rhythmically presented auditory, visual, and audio-visual speech in children*. <https://doi.org/10.3389/fpsyg.2012.00216>
- Puolakanaho, A., Ahonen, T., Aro, M., Eklund, K., Leppänen, P. H. T., Poikkeus, A.-M., Tolvanen, A., Torppa, M., & Lyytinen, H. (2008). Developmental Links of Very Early Phonological and Language Skills to Second Grade Reading Outcomes. *Journal of Learning Disabilities*, *41*(4), 353–370. <https://doi.org/10.1177/0022219407311747>
- Ramus, F. (2001). Talk of two theories. *Nature*, *412*(6845), 393–394. <https://doi.org/10.1038/35086683>
- Ramus, F. (2004). Neurobiology of dyslexia: A reinterpretation of the data. *Trends in Neurosciences*, *27*(12), 720–726. <https://doi.org/10.1016/j.tins.2004.10.004>
- Ramus, F., Altarelli, I., Jednoróg, K., Zhao, J., & Scotto di Covella, L. (2018). Neuroanatomy of developmental dyslexia: Pitfalls and promise. *Neuroscience and Biobehavioral Reviews*, *84*(August 2017), 434–452. <https://doi.org/10.1016/j.neubiorev.2017.08.001>
- Ramus, F., Rosen, S., Dakin, S. C., Day, B. L., Castellote, J. M., White, S., & Frith, U. (2003). Theories of developmental dyslexia: insights from a multiple case study of dyslexic adults. *Brain*, *126*(4), 841–865. <https://doi.org/10.1093/brain/awg076>
- Ramus, F., & Szenkovits, G. (2008). What Phonological Deficit? *Quarterly Journal of Experimental Psychology*, *61*(1), 129–141. <https://doi.org/10.1080/17470210701508822>

- Raschle, N. M., Zuk, J., Gaab, N., & Harvard, C. (2012). Functional characteristics of developmental dyslexia in left-hemispheric posterior brain regions predate reading onset. *Proceedings of the National Academy of Sciences of the United States of America*, *109*(6), 2156–2161. <https://doi.org/10.1073/pnas.1107721109>
- Richardson, U., Leppänen, P. H. T., Leiwo, M., & Lyytinen, H. (2003). Speech perception of infants with high familial risk for dyslexia differ at the age of 6 months. *Developmental Neuropsychology*, *23*(3), 385–397. [https://doi.org/10.1207/S15326942DN2303\\_5](https://doi.org/10.1207/S15326942DN2303_5)
- Rindermann, H., & Baumeister, A. E. E. (2015). Parents' SES vs. parental educational behavior and children's development: A reanalysis of the Hart and Risley study. *Learning and Individual Differences*, *37*, 133–138. <https://doi.org/10.1016/j.lindif.2014.12.005>
- Rosen, G. D., Bai, J., Wang, Y., Fiondella, C. G., Threlkeld, S. W., LoTurco, J. J., & Galaburda, A. M. (2007). Disruption of Neuronal Migration by RNAi of *Dyx1c1* Results in Neocortical and Hippocampal Malformations. *Cerebral Cortex*, *17*(11), 2562–2572. <https://doi.org/10.1093/cercor/bhl162>
- Rutter, M., & Yule, W. (1975). the Concept of Specific Reading Retardation. *Journal of Child Psychology and Psychiatry*, *16*(3), 181–197. <https://doi.org/10.1111/j.1469-7610.1975.tb01269.x>
- Saito, Y., Aoyama, S., Kondo, T., Fukumoto, R., Konishi, N., Nakamura, K., Kobayashi, M., & Toshima, T. (2007). Frontal cerebral blood flow change associated with infant-directed speech. *Archives of Disease in Childhood: Fetal and Neonatal Edition*, *92*(2), 113–116. <https://doi.org/10.1136/adc.2006.097949>
- Santamaria, L., Noreika, V., Georgieva, S., Clackson, K., Wass, S., & Leong, V. (2020). Emotional valence modulates the topology of the parent-infant inter-brain network. *NeuroImage*, *207*(November 2019), 116341. <https://doi.org/10.1016/j.neuroimage.2019.116341>
- Saygin, Z. M., Norton, E. S., Osher, D. E., Beach, S. D., Cyr, A. B., Ozernov-Palchik, O., Yendiki, A., Fischl, B., Gaab, N., & Gabrieli, J. D. E. (2013). Tracking the roots of reading ability: White matter volume and integrity correlate with phonological awareness in prereading and early-reading kindergarten children. *Journal of Neuroscience*, *33*(33), 13251–13258. <https://doi.org/10.1523/JNEUROSCI.4383-12.2013>
- Scerri, T. S., Darki, F., Newbury, D. F., Whitehouse, A. J. O., Peyrard-Janvid, M., Matsson, H., Ang, Q. W., Pennell, C. E., Ring, S., Stein, J., Morris, A. P., Monaco, A. P., Kere, J., Talcott, J. B., Klingberg, T., & Paracchini, S. (2012). The Dyslexia Candidate Locus on 2p12 Is Associated with General Cognitive Ability and White Matter Structure. *PLoS ONE*, *7*(11). <https://doi.org/10.1371/journal.pone.0050321>
- Schumacher, J., Hoffmann, P., Schmä, C., Schulte-Körne, G., & Nöthen, M. M. (2007). Genetics of dyslexia: The evolving landscape. *Journal of Medical Genetics*, *44*(5), 289–297. <https://doi.org/10.1136/jmg.2006.046516>
- Seidl, A. H. (2014). Regulation of conduction time along axons. *Neuroscience*, *276*, 126–134. <https://doi.org/10.1016/j.neuroscience.2013.06.047>
- Serniclaes, W., Van Heghe, S., Mousty, P., Carré, R., & Sprenger-Charolles, L. (2004). Allophonic mode of speech perception in dyslexia. *Journal of Experimental Child Psychology*, *87*(4), 336–361. <https://doi.org/10.1016/j.jecp.2004.02.001>
- Shaywitz, S. (1998). *Current Concepts CURRENT CONCEPTS D YSLEXIA* (Vol. 338).
- Shaywitz, S. E., & Shaywitz, B. A. (2005). Dyslexia (specific reading disability). *Biological Psychiatry*, *57*(11), 1301–1309. <https://doi.org/10.1016/j.biopsych.2005.01.043>

- Sherry, S. T., Ward, M.-H., Kholodov, M., Baker, J., Phan, L., Smigielski, E. M., & Sirotkin, K. (2001). dbSNP: the NCBI database of genetic variation. In *Nucleic Acids Research* (Vol. 29, Issue 1). <http://www.ncbi.nlm.nih.gov/SNP>.
- Silani, G., Frith, U., Demonet, J. F., Fazio, F., Perani, D., Price, C., Frith, C. D., & Paulesu, E. (2005). Brain abnormalities underlying altered activation in dyslexia: A voxel based morphometry study. *Brain*, *128*(10), 2453–2461. <https://doi.org/10.1093/brain/awh579>
- Singh, L., Nestor, S., Parikh, C., & Yull, A. (2009). Influences of Infant-Directed Speech on Early Word Recognition. *Infancy*, *14*(6), 654–666. <https://doi.org/10.1080/15250000903263973>
- Smith, S. D., Meng, H., Smith, S. D., Hager, K., Held, M., Liu, J., Olson, R. K., Pennington, B. F., Defries, J. C., Gelernter, J., Reilly-pol, T. O., Somlo, S., Skudlarski, P., & Shaywitz, S. E. (2016). *From The Cover : DCDC2 is associated with reading disability and modulates neuronal development in the brain DCDC2 is associated with reading disability and modulates neuronal development in the brain*. *102*(December 2005). <https://doi.org/10.1073/pnas.0508591102>
- Snowling, M. J. (2001). From Language to Reading and Dyslexia. *Dyslexia*, *7*(1), 37–46. <https://doi.org/10.1002/dys.185>
- Snowling, M. J., Hulme, C., & Nation, K. (2020). Defining and understanding dyslexia: past, present and future. *Oxford Review of Education*, *46*(4), 501–513. <https://doi.org/10.1080/03054985.2020.1765756>
- Soltész, F., Szucs, D., Leong, V., White, S., & Goswami, U. (2013). Differential Entrainment of Neuroelectric Delta Oscillations in Developmental Dyslexia. *PLoS ONE*, *8*(10). <https://doi.org/10.1371/journal.pone.0076608>
- Sperling, A. J., Lu, Z.-L., Manis, F. R., & Seidenberg, M. S. (2005). *Deficits in perceptual noise exclusion in developmental dyslexia B R I E F C O M M U N I C A T I O N S*. *8*. <https://doi.org/10.1038/nm1474>
- Stanovich, K. E. (1988). Explaining the Differences Between the Dyslexic and the Garden-Variety Poor Reader. *Journal of Learning Disabilities*, *21*(10), 590–604. <https://doi.org/10.1177/002221948802101003>
- Stein, C. M., Schick, J. H., Gerry Taylor, H., Shriberg, L. D., Millard, C., Kundtz-Kluge, A., Russo, K., Minich, N., Hansen, A., Freebairn, L. A., Elston, R. C., Lewis, B. A., & Iyengar, S. K. (2004). Pleiotropic Effects of a Chromosome 3 Locus on Speech-Sound Disorder and Reading. *The American Journal of Human Genetics*, *74*(2), 283–297. <https://doi.org/10.1086/381562>
- Stevenson, J., Graham, P., Fredman, G., & McLoughlin, V. (1987). A twin study of genetic influences on reading and spelling ability and disability. *Journal of Child Psychology and Psychiatry*, *28*(2), 229–247. <https://doi.org/10.1111/j.1469-7610.1987.tb00207.x>
- Stoel-Gammon, C., & Williams, A. L. (2013). Early phonological development: Creating an assessment test. *Clinical Linguistics and Phonetics*, *27*(4), 278–286. <https://doi.org/10.3109/02699206.2013.766764>
- Stroganova, T. A., Orekhova, E. V., & Posikera, I. N. (1999). EEG alpha rhythm in infants. *Clinical Neurophysiology*, *110*(6), 997–1012. [https://doi.org/10.1016/S1388-2457\(98\)00009-1](https://doi.org/10.1016/S1388-2457(98)00009-1)
- Su, M., Zhao, J., Thiebaut de Schotten, M., Zhou, W., Gong, G., Ramus, F., & Shu, H. (2018). Alterations in white matter pathways underlying phonological and morphological processing in Chinese developmental dyslexia. *Developmental Cognitive Neuroscience*, *31*(April), 11–19. <https://doi.org/10.1016/j.dcn.2018.04.002>

- Szenkovits, G., Darma, Q., Darcy, I., & Ramus, F. (2016). Exploring dyslexics' phonological deficit II: Phonological grammar. *First Language*. <https://doi.org/10.1177/0142723716648841>
- Tapia-Paez, I., Tammimies, K., Massinen, S., Roy, A. L., & Kere, J. (2008). The complex of TFII-I, PARP1, and SFPQ proteins regulates the DYX1C1 gene implicated in neuronal migration and dyslexia. *The FASEB Journal*, 22(8), 3001–3009. <https://doi.org/10.1096/fj.07-104455>
- Telkemeyer, S., Rossi, S., Koch, S. P., Nierhaus, T., Steinbrink, J., Poeppel, D., Obrig, H., & Wartenburger, I. (2009). Sensitivity of Newborn Auditory Cortex to the Temporal Structure of Sounds. *Journal of Neuroscience*, 29(47), 14726–14733. <https://doi.org/10.1523/JNEUROSCI.1246-09.2009>
- Telkemeyer, Silke, Rossi, S., Nierhaus, T., Steinbrink, J., Obrig, H., & Wartenburger, I. (2011). Acoustic processing of temporally modulated sounds in infants: Evidence from a combined near-infrared spectroscopy and EEG study. *Frontiers in Psychology*, 2(APR), 1–14. <https://doi.org/10.3389/fpsyg.2011.00062>
- Thiessen, E. D., Hill, E. A., & Saffran, J. R. (2005). Infant-Directed Speech Facilitates Word Segmentation. *Infancy*, 7(1), 53–71. [https://doi.org/10.1207/s15327078in0701\\_5](https://doi.org/10.1207/s15327078in0701_5)
- Thomson, J. M., & Goswami, U. (2010). Learning novel phonological representations in developmental dyslexia: associations with basic auditory processing of rise time and phonological awareness. *Reading and Writing*, 23(5), 453–473. <https://doi.org/10.1007/s11145-009-9167-9>
- Thwaites, A., Nimmo-Smith, I., Fonteneau, E., Patterson, R. D., Buttery, P., & Marslen-Wilson, W. D. (2015). Tracking cortical entrainment in neural activity: auditory processes in human temporal cortex. *Frontiers in Computational Neuroscience*, 9(February), 1–14. <https://doi.org/10.3389/fncom.2015.00005>
- Torre, G.-A. A., McKay, C. C., & Matejko, A. A. (2019). The Early Language Environment and the Neuroanatomical Foundations for Reading. *The Journal of Neuroscience*, 39(7), 1136–1138. <https://doi.org/10.1523/JNEUROSCI.2895-18.2018>
- Truong, D. T., Che, A., Rendall, A. R., Szalkowski, C. E., LoTurco, J. J., Galaburda, A. M., & Holly Fitch, R. (2014). Mutation of *Dcdc2* in mice leads to impairments in auditory processing and memory ability. *Genes, Brain and Behavior*, 13(8), 802–811. <https://doi.org/10.1111/gbb.12170>
- Van Zuijen, T. L., Plakas, A., Maassen, B. A. M., Been, P., Maurits, N. M., Krikhaar, E., van Driel, J., & van der Leij, A. (2012). Temporal auditory processing at 17 months of age is associated with preliterate language comprehension and later word reading fluency: An ERP study. *Neuroscience Letters*, 528(1), 31–35. <https://doi.org/10.1016/j.neulet.2012.08.058>
- Van Zuijen, T. L., Plakas, A., Maassen, B. A. M., Maurits, N. M., & Van der Leij, A. (2013). Infant ERPs separate children at risk of dyslexia who become good readers from those who become poor readers. *Developmental Science*, 16(4), 554–563. <https://doi.org/10.1111/desc.12049>
- Vandermosten, M., Boets, B., Poelmans, H., Sunaert, S., Wouters, J., & Ghesquière, P. (2012). A tractography study in dyslexia: Neuroanatomic correlates of orthographic, phonological and speech processing. *Brain*, 135(3), 935–948. <https://doi.org/10.1093/brain/awr363>
- Vandermosten, M., Boets, B., Wouters, J., & Ghesquière, P. (2012). A qualitative and quantitative review of diffusion tensor imaging studies in reading and dyslexia. *Neuroscience and Biobehavioral Reviews*, 36(6), 1532–1552. <https://doi.org/10.1016/j.neubiorev.2012.04.002>
- Vandermosten, M., Vanderauwera, J., Theys, C., De Vos, A., Vanvooren, S., Sunaert, S., Wouters, J.,

- & Ghesquière, P. (2015). A DTI tractography study in pre-readers at risk for dyslexia. *Developmental Cognitive Neuroscience, 14*, 8–15. <https://doi.org/10.1016/j.dcn.2015.05.006>
- Vanvooren, S., Poelmans, H., De Vos, A., Ghesquière, P., & Wouters, J. (2017). Do prereaders' auditory processing and speech perception predict later literacy? *Research in Developmental Disabilities, 70*, 138–151. <https://doi.org/10.1016/j.ridd.2017.09.005>
- Vanvooren, S., Poelmans, H., Hofmann, M., Ghesquière, P., & Wouters, J. (2014). Hemispheric asymmetry in auditory processing of speech envelope modulations in prereading children. *Journal of Neuroscience, 34*(4), 1523–1529. <https://doi.org/10.1523/JNEUROSCI.3209-13.2014>
- Velayos-Baeza, A., Levecque, C., Kobayashi, K., Holloway, Z. G., & Monaco, A. P. (2010). The dyslexia-associated KIAA0319 protein undergoes proteolytic processing with  $\gamma$ -secretase-independent intramembrane cleavage. *Journal of Biological Chemistry, 285*(51), 40148–40162. <https://doi.org/10.1074/jbc.M110.145961>
- Vellutino, F. R., Fletcher, J. M., Snowling, M. J., & Scanlon, D. M. (2004). Specific reading disability (dyslexia): What have we learned in the past four decades? *Journal of Child Psychology and Psychiatry and Allied Disciplines, 45*(1), 2–40. <https://doi.org/10.1046/j.0021-9630.2003.00305.x>
- Wagner, R. K., & Torgesen, J. K. (1987). The nature of phonological processing and its causal role in the acquisition of reading skills. *Psychological Bulletin, 101*(2), 192–212. <https://doi.org/10.1037/0033-2909.101.2.192>
- Wang, R., Chen, C. C., Hara, E., Rivas, M. V., Roulhac, P. L., Howard, J. T., Chakraborty, M., Audet, J. N., & Jarvis, E. D. (2015). Convergent differential regulation of SLIT-ROBO axon guidance genes in the brains of vocal learners. *Journal of Comparative Neurology, 523*(6), 892–906. <https://doi.org/10.1002/cne.23719>
- Wang, Y., Mauer, M. V., Raney, T., Peysakhovich, B., Becker, B. L. C., Sliva, D. D., & Gaab, N. (2017). Development of tract-specific white matter pathways during early reading development in at-risk children and typical controls. *Cerebral Cortex, 27*(4), 2469–2485. <https://doi.org/10.1093/cercor/bhw095>
- Waye, M. M. Y., Poo, L. K., & Ho, C. S.-H. (2017). Study of Genetic Association With DCDC2 and Developmental Dyslexia in Hong Kong Chinese Children. *Clinical Practice & Epidemiology in Mental Health, 13*(1), 104–114. <https://doi.org/10.2174/1745017901713010104>
- White, S., Milne, E., Rosen, S., Hansen, P., Swettenham, J., Frith, U., & Ramus, F. (2006). The role of sensorimotor impairments in dyslexia: a multiple case study of dyslexic children. *Developmental Science, 9*(3), 237–255. <https://doi.org/10.1111/j.1467-7687.2006.00483.x>
- Winkler, A. M., Kochunov, P., Blangero, J., Almasy, L., Zilles, K., Fox, P. T., Duggirala, R., & Glahn, D. C. (2010). Cortical thickness or grey matter volume? The importance of selecting the phenotype for imaging genetics studies. *NeuroImage, 53*(3), 1135–1146. <https://doi.org/10.1016/j.neuroimage.2009.12.028>
- Xia, Z., Hancock, R., & Hoeft, F. (2017). Neurobiological bases of reading disorder Part I: Etiological investigations. *Language and Linguistics Compass, 11*(4), 1–18. <https://doi.org/10.1111/lnc3.12239>
- Yoncheva, Y., Maurer, U., Zevin, J. D., & McCandliss, B. D. (2014). Selective attention to phonology dynamically modulates initial encoding of auditory words within the left hemisphere. *NeuroImage, 97*, 262–270. <https://doi.org/10.1016/j.neuroimage.2014.04.006>
- Žarić, G., Timmers, I., Gerretsen, P., González, G. F., Tijms, J., van der Molen, M. W., Blomert, L., &

- Bonte, M. (2018). Atypical white matter connectivity in dyslexic readers of a fairly transparent orthography. *Frontiers in Psychology, 9*(JUN).  
<https://doi.org/10.3389/fpsyg.2018.01147>
- Zhang, Y., Koerner, T., Miller, S., Grice-Patil, Z., Svec, A., Akbari, D., Tusler, L., & Carney, E. (2011). Neural coding of formant-exaggerated speech in the infant brain. *Developmental Science, 14*(3), 566–581. <https://doi.org/10.1111/j.1467-7687.2010.01004.x>
- Zhao, J., Thiebaut de Schotten, M., Altarelli, I., Dubois, J., & Ramus, F. (2016). Altered hemispheric lateralization of white matter pathways in developmental dyslexia: Evidence from spherical deconvolution tractography. *Cortex, 76*, 51–62.  
<https://doi.org/10.1016/j.cortex.2015.12.004>
- Ziegler, J. C., Pech-Georgel, C., George, F., & Lorenzi, C. (2009). Speech-perception-in-noise deficits in dyslexia. *Developmental Science, 12*(5), 732–745.  
<https://doi.org/10.1111/j.1467-7687.2009.00817.x>

# Appendix I

---

## Parental Information Sheet

**Dr Topun Austin**

*Consultant Neonatologist*

**Dr Victoria Leong**

*Affiliated Lecturer, Department of Psychology, University of Cambridge*

**Dr Gusztav Belteki**

*Consultant Neonatologist*

**Stanimira Georgieva**

*Research Student, University of Cambridge*

### Parental Information Sheet

#### **Study Title: Longitudinal Dyslexia Study in Newborn Infants (Study 1)**

Dear Parent

We would like to invite you to take part in a research study about your baby. Before you decide, we would like to explain why the research is being done and what it involves. Please take the time to read the following information carefully. Please feel free to talk to others about the study if you wish.

***What are we trying to find out?***

We aim to identify neural and genetic characteristics in newborn infants that, in future studies, can be used to predict whether a child will develop a reading difficulty.

Dyslexia is a difficulty in learning to read despite normal intelligence and educational opportunity. Children who are born into a family with a history of dyslexia have a 4-fold increased risk of dyslexia themselves, as compared to their peers with no family history. Although some risk genes for dyslexia have recently been identified, we do not know how these genes affect the developing brain and produce difficulties with reading.

Learning to read requires the brain to make mappings between letters and speech sounds. The brain of a dyslexic child struggles to form these letter-sound mappings because it does not represent speech sounds accurately. This problem with speech sound processing is present even from birth. In this study, we want to use neuroimaging to understand how the brains of genetically high-risk newborns process speech sounds differently from those of low-risk newborns. Furthermore, we want to assess whether the quality of infants' home language environment during their first year-and-half of life can help improve how their brains process speech sounds. We hope in a future study to be able to test enriched home language environment as a potential resilience factor to developing dyslexia.

***Do I have to take part?***

It is entirely up to you. We will describe the study and go through this information sheet. If you would like to participate, we will then ask you to sign a consent form to show you have agreed to take part. You are free to withdraw at any time, without giving a reason. This will not affect the standard of care you receive.

***Who is eligible to participate?***

We are looking for two groups of healthy full-term newborn infants. You will be eligible to participate if:

(1) At least one of your baby's immediate family members (father, mother or sibling) has a diagnosis of dyslexia; OR

(2) None of your baby's immediate family members (father, mother or sibling) have a diagnosis of dyslexia

Additionally, both parents should be fluent English-speakers, and English should be the maternal native language.

### ***How will the study be conducted?***

The project consists of two separate neuroimaging studies. Study 1 will consist of 4 testing sessions every 6 months, starting at your baby's birth. The first session will take place in Rosie Hospital and we will measure your infant's brain activity using electroencephalography (EEG). We will also take a small blood sample from your infant in a similar manner to the hospitals' routine neonatal screening procedure for genetic testing; and correspondingly, a saliva sample from both parents where possible. At further three time points (6, 12 and 18 months) we would like to measure your infant's EEG and take further saliva tests. We would also like to measure conversation in the home with a sound recording device. We will provide training on this device and ask that you return via the post (appropriate packing to return will be provided).

### ***What does participation in Study 1 involve?***

In the first session of Study 1, your baby will take part in a 1-hour EEG recording within the first 7 days of life. We will measure brain activity while your baby is resting quietly, as well as while s/he is listening to a female voice speaking or singing nursery rhymes. We will also like your permission to take a small blood spot sample from your baby for genetic testing. A few drops of blood will be taken using a standard heel lance. This procedure is similar to the routine blood glucose test, bilirubin test and Guthrie test which babies have and does not cause undue distress. Only 4 dyslexia genes will be assessed. Additionally, we would like to take a saliva sample from both parents where possible to test the same genes and additional hormones in the parents.

EEG is a completely safe technique for measuring spontaneous brain activity such as neuronal oscillations. It measures the very weak electrical signals that are naturally generated by the brain during activities like listening or seeing. EEG measures these signals passively and does not generate any electricity. It works like a thermometer – i.e. it does not put anything in or take anything out, it just measures what's already there.

The EEG measurement involves your baby wearing a stretchy cap which contains embedded sensors that passively measure brain activity. A small amount of gel will be used to ensure that the sensors have a good contact with your baby's scalp. This gel is safe for infants and can be easily wiped off after the recording session. No electricity is produced by the cap and the procedure is completely safe. Many infants fall asleep during the EEG recording session.

Apart from the saliva samples, the baby's parents will be asked to complete several short standardised tests for reading, spelling, memory and general ability in order to assess reading and cognitive skills. These short tests will take no more than 45 minutes per person to complete.

We would like to measure your infant's brain activity at 6, 12 and 18 months. Again, we will measure your infant's brain activity using EEG while resting, and while listening to spoken or sang speech, and as they grow older, while performing more complex learning tasks, which would also be video-recorded. In the final session (at 18 months), we would also like to measure their very early language development. In all sessions, we would like to take a new saliva sample from the baby and their parents where possible. We will also ask you to fill in standard questionnaires about your infants cognitive and language development, as well as about your mood and temperament.

We will provide you with a sound recording device for home, designed specifically to measure language development in children of various ages. It is a small recorder attached to a little vest that your infant can wear. We will ask you to keep the device on for a few hours throughout the day and then to post it back to us using a pre-paid envelope. The information stored on the device is encrypted and requires a software key to decode so accessing it is not possible if the device is lost in the post. The device gives us the option of either exporting the full speech recording, or only speech characteristics, such as pitch, loudness, amount of background noise. If you feel like the device might record sensitive information that you do not wish to disclose, you can choose not to take part or for us to only have access to the speech statistics and not the actual contents.

***Are there risks or disadvantages to participating?***

This study has received ethical clearance and the EEG technique has been widely used for infant research for many years. There is no evidence of any disadvantages or risks associated with taking part in an EEG study. However, if your infant experiences distress for any reason, you are free to withdraw from the study at any point without explanation.

***What are the possible benefits of taking part?***

Research is designed to benefit society by gaining new knowledge. As this research is at a very preliminary stage, we will not be able to predict the outcome of individual infants who participate in the study. **Therefore we will not be able to provide an assessment of your child's individual risk for dyslexia.** However, the knowledge that we gain from the results of this study could lead in future to earlier identification of, and support for, infants who are at high risk for dyslexia in later life.

***How will the information about my baby and me be used?***

If you decide to take part in this study, your baby will be assigned a unique identification number. At Cambridge University Hospitals NHS Foundation Trust, we will securely keep the link between your baby's personal details and this identification number so that if we need to, we can identify patient results. Any information that we collect in the study will be kept completely confidential and in a secure place. Only authorised people involved in the study will have access to it. Other than the researchers, the Research and Development (R&D) Department at Cambridge University Hospitals NHS Foundation Trust will have access to the data collected during the study. This will be for audit and monitoring purposes.

The results of the study will be presented at conferences and written up in journals. Results are presented in terms of groups of individuals. The data will be totally anonymous, without any means of identifying the individuals involved.

***Who is organising and funding the research?***

This study is being organised by the University of Cambridge in collaboration with Cambridge University Hospitals NHS Foundation Trust. The study is funded by the Rosetrees Trust for Medical Research.

Families will not be paid a fee for participation, however travel expenses will be compensated (mileage at 40p per mile or public transport fare)

Thank you for considering participating in our study, please don't hesitate to contact us if you have any further questions. Some FAQs, particularly about the genetic testing, are shown on the next page.

***Contact Information:***

**Stanimira Georgieva**

**Research Student, University of Cambridge**

Dr Topun Austin

Consultant neonatologist

Dr Victoria Leong  
Affiliated Lecturer, University of Cambridge

Dr Gusztav Belteki  
Consultant neonatologist

## Frequently Asked Questions

### ***Where will the DNA be analysed?***

The DNA samples will be analysed by Dr Gusztav Belteki and his research staff here in Cambridge.

### ***Can the DNA be used to test if my child has any other health problems (such as Spina Bifida)?***

No. This DNA will not be used by our team to test for any other genetic abnormalities.

### ***Can the DNA be used to test whether any family member will develop a disease later in life (such as breast cancer or Alzheimer's Disease)?***

No. We will not use the DNA to test for any other genetic risk markers.

### ***If I am ever asked by anyone if my child had genetic screening, what should I say?***

You should say that your child has not had genetic screening, as we are not conducting screening tests on the DNA.

### ***Can my doctor contact you to find out the results of the DNA tests?***

No. The DNA will be used for research purposes only. In addition, if your doctor ever wishes to conduct a DNA test, the doctor may take their own DNA sample, so there will be no need for your doctor to contact the study.

### ***Will my GP be informed of my participation?***

We will inform your GP of your participation if you give us consent to do so.

### ***Who has reviewed the study?***

All research in the NHS is looked at by an independent group of people, called a Research Ethics Committee to protect your safety, rights, wellbeing and dignity. This study has been reviewed and given favourable opinion by the NHS Research Ethics Committee.

### ***What if there is a problem?***

If you have any concern about any aspect of this study, you should ask to speak to the researchers, who will do their best to answer your questions. If you remain unhappy and wish to complain formally, you can do this through the NHS complaints procedure. The Patient Advice and Liaison Service (PALS) can be contacted on 01223 216756, 01223 257257, 01223 274432 or 01223 274431. You can withdraw your child from the study at any stage without explanation if you wish to do so. However, we would like to use the data (on an anonymous basis) up to the time of your withdrawal.

---

## Parental Consent Form

### Title : Longitudinal Dyslexia Study in Newborn Infants (Study 1)

Lead Investigators: Dr Topun Austin, Dr Victoria Leong, Dr Gusztav Belteki

#### Informed consent for parent's participation in Study 1 of the study

Please initial box

1. I confirm that I have read and understand the information sheet version 4 (short) dated 1<sup>st</sup> March 2019 for my participation in Study 1 –EEG+genetics - of the Dyslexia Biomarkers study. I have had the opportunity to consider the information, ask questions and have had these answered satisfactorily.
2. I understand that my participation is voluntary and that I am free to withdraw from the study at any time, without giving reason and without my medical care or legal rights being affected.
3. I agree that the relevant sections of my medical records and data collected during the study may be looked at by members of the research team, and made available to the NHS Trust Research & Development Department for audit and monitoring purposes. I understand that such access will be in accordance with the Data Protection Act 1998 and 2018 and medical confidentiality rules. I give permission for the individuals to have access to my records.
4. I agree that any personal data collected as part of the Dyslexia Biomarkers study will be recorded electronically and analysed by members of the research team. These data might be stored for up to 25 years.
5. I agree to provide 4 saliva samples (at infant's birth, 6, 12 and 18 months). I understand that it would be stored and used in accordance with the above-mentioned codes of practice.
6. I understand that my speech at my home will be audio-recorded and the acquired data will be stored and used in accordance with the above-mentioned codes of practice. I agree to give access to *the full speech recording / recording's descriptive features only* [**cross out the irrelevant**].
7. I confirm that I give my full consent to take part in the above study.

\_\_\_\_\_  
Name of Research Subject      Patient identification number

\_\_\_\_\_  
Name of Parent or Guardian      Relationship to Child      Signature, date, time

\_\_\_\_\_  
Name of Research member      Signature, date, time

## Infant Consent Form

### Title : Longitudinal Dyslexia Study in Newborn Infants (Study 1)

Lead Investigators: Dr Topun Austin, Dr Victoria Leong, Dr Gusztav Belteki

#### Informed consent for infant's participation in Study 1 of the study

Please initial box

1. I confirm that I have read and understand the information sheet version version 4 (short) dated 1<sup>st</sup> March 2019 for the participation **of my infant** in Study 1 – EEG+genetics - of the Dyslexia Biomarkers study. I have had the opportunity to consider the information, ask questions and have had these answered satisfactorily.
  
2. I understand that **my infant's participation** is voluntary and that I am free to withdraw **my infant** from the study at any time, without giving reason and without **my infant's** medical care or legal rights being affected.
  
3. I agree that the relevant sections of **my infant's** medical records and data collected during the study may be looked at by members of the research team, and made available to the NHS Trust Research & Development Department for audit and monitoring purposes. I understand that such access will be in accordance with the Data Protection Act 1998 and 2018, and medical confidentiality rules. I give permission for the individuals to have access to **my infant's** records.
  
4. I agree that **my infant's** personal data collected as part of the Dyslexia Biomarkers study will be recorded electronically and analysed by members of the research team. These data might be stored for up to 25 years.
  
5. I agree that **my infant provides a blood spot sample (at birth only) or a saliva sample (at 6, 12 or 18 months)**. I understand that it will be stored and used in accordance with the above-mentioned codes of practice.
  
6. I understand that **my infant's speech** at home will be audio-recorded and the acquired data will be stored and used in accordance with the above-mentioned codes of practice. I agree to give access to *the full speech recording / recording's descriptive features only* **[cross out the irrelevant]**.
  
7. I confirm that I give my full consent to take part in the above study.

\_\_\_\_\_  
 Name of Research Subject      Patient identification number

\_\_\_\_\_  
 Name of Parent or Guardian      Relationship to Child      Signature, date, time

\_\_\_\_\_  
 Name of Research member      Signature, date,

---

## Full Study Protocol

### RESEARCH PROTOCOL

#### Project Title: Dyslexia Study in Newborn Infants

This is a longitudinal study that aims to identify potential neural biomarkers of dyslexia risk in neonates and to elucidate specific genotypes that are associated with these neural deficits. Additionally, the quality of the early home language environment will be assessed as a potential resilience factor for poor language development. Poor awareness of speech sounds (phonology) is the hallmark of dyslexia, across all languages studied so far. Despite the identification of several dyslexia susceptibility genes over the last 2 decades, little is known about the mechanisms by which genetic abnormalities give rise to neural deficits and how these in turn generate a phonological deficit. Here, it is hypothesised that genetic polymorphisms in major dyslexia susceptibility genes (which are involved in developmental processes operating during early brain development), are associated with abnormalities in cortical microcircuitry, as well as structural and functional connectivity in language regions of the brain. Previously reported single nucleotide polymorphisms (SNPs) across major dyslexia susceptibility loci will be analysed (DCDC2, KIAA0319, ROBO1 and DYX1C1). Electroencephalography (EEG) will be used to assess infants' neural oscillatory processing of the speech signal. Magnetic resonance imaging (fMRI and DTI) and functional near infrared spectroscopy (fNIRS) will be employed to assess the structural and functional integrity of infants' neural language circuits. 100 infants (50 high-risk and 50 control) will be assessed longitudinally at 4 timepoints : at birth, 6, 12 and 18 months of age. At each timepoint, infants' brain development, language and socio-emotional development will be assessed, and a measure of infants' home language environment will also be taken.

## 1 BACKGROUND

### 1.1 The phonological deficit in dyslexia

Dyslexia is a neurodevelopmental disorder that affects the acquisition of skilled reading in ~7% of children worldwide (Goswami, 2011). In the UK, the British Dyslexia Association estimates that there are 375,000 pupils with dyslexia, and a total of 2 million people are severely affected. Dyslexia is a highly heritable disorder (heritability estimates ~50%; Grigorenko, 2004). Children who are born into a family with a history of dyslexia have a 4-fold increase in risk in comparison to control children. A cognitive hallmark of dyslexia is poor phonological awareness (Snowling, 2000) - an impairment in the ability to accurately represent and manipulate speech sounds of different grain-sizes, such as prosodic stress patterns, syllables and phonemes. The process of phonological development begins while in the womb. The uterine wall and amniotic fluid act as a low-pass filter that transmits the prosody and rhythm of speech to the developing fetus (Armitage et al, 1980). Consequently, typically-developing neonates can remember voices and stories that they hear during the third trimester of pregnancy (de Casper & Fifer, 1980; de Casper & Spence, 1986), presumably using prosodic cues. Conversely, neonates at-risk for dyslexia already show neural differences in speech sound processing *at birth* (Leppänen et al., 1999; Guttorm et al., 2001). This indicates that one of the primary biological causal mechanisms in dyslexia is altered brain development *in utero*, which implicates the genetic blueprint for building neural

architecture. Indeed, the genetics of dyslexia is starting to shed light on how the dyslexic brain may be "wired-up" differently during early development.

## 1.2 From genes to neural wiring

Dyslexia is thought to be the result of the concomitant effect of *multiple* genetic and environmental factors. Four of the most replicable dyslexia susceptibility genes - DCDC2 (Chr 6), KIAA0319 (Chr 6), ROBO1 (Chr 3) and DYX1C1 (Chr 15) - all have very *early* developmental roles in wiring-up the fetal brain. These 4 genes are all implicated in axonal guidance and *neuronal migration* mechanisms (Paracchini et al, 2007; Meng et al, 2005; Pechansky et al, 2009; Carrion-Castillo et al, 2013; Kere 2014). It has now been demonstrated in several *animal* studies (rat or mouse models) that the knockdown of these genes results in abnormal neuronal migration patterns, ectopias and changes in gray and white matter structure (e.g. Burbridge et al, 2008; Currier et al, 2011; Adler et al, 2013), consistent with the anatomical anomalies observed in post mortem examination of the human dyslexic brain (Galaburda & Kemper, 1979; Humphreys et al, 1990). Genetic neuroimaging studies with *human* dyslexics are now urgently needed to understand the mechanisms by which faulty genes give rise to neural deficits during human development, but these are only just beginning to be carried out. For example, one recent study with *child and adult* dyslexic individuals (aged 6 to 25) reported associations between polymorphisms in the DCDC2, KIAA0319 and DYX1C1 genes, and white matter pathway integrity, particularly tracts connecting the middle temporal gyrus and the inferior parietal lobe (Darki et al, 2012). These results suggest that genetic mutations in dyslexia could fundamentally alter the way that the dyslexic brain is "wired-up" during early development.

## 1.3 From faulty wiring to faulty phonology

One recent proposal suggests that the "faulty wiring" due to aberrant neuronal migration leads to disruptions in the local micro-circuitry of the cortex, due to the over- or under-shoot of neurones to their expected laminar location (Giraud & Ramus, 2013). This in turn disrupts the generation of synchronous ***oscillatory activity*** in local neuronal ensembles. For example, in the auditory cortex, spontaneous bursts of oscillatory activity occur at delta (1-3 Hz), theta (4-7 Hz) and gamma (25-80 Hz) rates, which can be observed using scalp electroencephalography (EEG). Neuronal oscillatory activity in the auditory cortex is thought to have a key role in parsing the speech signal into syllables and phonemes (Giraud & Poeppel, 2012), and in the detection of speech rhythm and prosody (Leong et al, 2014a). These phonological abilities are all impaired in dyslexia (Goswami, 2011; Goswami & Leong, 2014a, Goswami & Leong, 2014b, Leong et al, 2011). Indeed, previous research by ourselves and others has confirmed the presence of oscillatory deficits in both adults and children with dyslexia (Hamalainen et al, 2012; Soltesz et al, 2013; Lehongre et al, 2011). Further, in typically-developing children, resting state oscillatory activity (e.g. gamma power) during infancy is predictive of later language ability (Benasich et al, 2008; Gou et al, 2011). The current proposed study advances the current state of knowledge by attempting to (a) demonstrate congenital oscillatory deficits in *neonates at-risk for dyslexia*, and (2) uncover systematic relationships between oscillatory deficits and genotype.

## 1.4 The home language environment

Infant-directed speech (IDS) is a prosodically-enhanced speaking register that is naturally used by adults to engage the infants' attention and convey affective warmth (Fernald, 1989; Cooper & Aslin, 1989). IDS also supports language learning directly because the exaggerated amplitude and frequency modulation patterns in the speech signal entrain neuronal oscillations in the infant brain more strongly than normal speech, thereby supporting infants' phonological parsing of the speech signal (Zhang et al, 2011; Leong et al, 2014b). Therefore, the amount and quality of IDS used by adult caregivers when speaking to infants in the home environment should be positively related to infants' language development. Further, a high-quality home language environment may confer resilience for infants at high-risk for developmental dyslexia, normalizing their language development trajectories over time.

## 2 STUDY AIMS & RATIONALE

The aims of this research project are to:

- (1) Identify potential neural biomarkers of dyslexia risk in neonates, and
- (2) Elucidate specific genotypes that are associated with these neural deficits
- (3) Identify potential resilience factors in the early language environment

### 2.1 Rationale & Potential Impact

Phonological development (which goes awry in dyslexia) begins in utero and continues throughout the first years of a child's life. Thus, the 'phonological deficit' is incurred well before the dyslexic child reaches schooling age and attempts (and fails) to learn to read. Consequently, effective intervention for dyslexia should ideally begin *before* children enter school, to support phonological development *as it occurs* during the early years. To target such early intervention appropriately (given limited educational resources), reliable biomarkers are needed to identify those children who are at highest-risk for developing dyslexia. The neuro-genetic risk markers identified in the previous pilot study are the first step toward this aim. The validity and reliability of these biomarkers (and the interaction of these factors with the home language environment) will be assessed in the current full-scale study that follows at-risk infants longitudinally until preschool age when their phonological skills and success in the early stages of learning to read can be assessed using early psychological tests for language ability.

## 3 METHOD

### 3.1 Participants and Recruitment

A total of 100 neonates will participate in the study: 50 'at-risk' and 50 control neonates [*Power calculation: To identify 2 genetic/environmental predictors for infants' language outcomes with 0.9 power, where each predictor has a large effect size (0.35, as indicated from our pilot findings), a total size of 40 per group is required (50 with 20% attrition)*]. All neonates will be healthy full-term infants, with a normal 20-week anomaly scan and no evidence of intrauterine growth restriction or perinatal hypoxia-ischaemia at birth. At-risk neonates will be identified from families in which at least one first-degree relative (i.e. parent or sibling) has a confirmed diagnosis of developmental dyslexia. Mothers will be recruited to the study in two ways: (1) prior to their delivery date via leaflets and advertisements placed in the Rosie Maternity Hospital (which sees 6000 live births a year) and in other communal areas; and (2) shortly after they have given birth in Rosie Maternity

Hospital, where they may be approached in person by research staff, or they may elect to volunteer for the study after reading a leaflet placed in the hospital wards. Informed consent will be obtained from the mothers after fully explaining the experimental procedures and the implications of genetic testing. Given the estimated incidence of dyslexia (7%), it is expected that 420 out of the 6000 babies born in a year at the Rosie will eventually receive a diagnosis of dyslexia (although not all of these will have a first-degree relative with dyslexia). We aim to identify 50 of these high-risk neonates. Control neonates will be recruited from families with no history of dyslexia. For both at-risk and control groups, any families with at least one first-degree relative who has a developmental or learning disorder (e.g. autism, ADHD, dyspraxia, dyscalculia) will be excluded.

### 3.2 Neuroimaging Procedure

*Electroencephalography (EEG).* Neuronal oscillatory activity in neonates will be measured using a high-density EEG montage. Measurements will be made at birth (within 7 days), and repeated at 6, 12 and 18 months of age. Neural activity will be assessed at all ages during (a) "resting state" and (b) passive listening to speech. For (a), a passive protocol will be used in which the neonate does not receive any overt sensory stimulation. Spontaneous brain activity will be measured while neonates are lying in a darkened and quiet environment. For (b), the neonate will hear children's poems that are read by female adults. Impairments in neuronal oscillatory function may be observed in children with reading difficulties, both during resting state (Schiavone et al, 2014), and while listening to speech (Power et al, 2013). Additionally, older infants at 6, 12 and 18 months will also participate in a third social learning paradigm with their parents, to assess the quality of parent-child communication and learning. For this paradigm, infants' and mothers' brain activity will be concurrently assessed to measure mutual neuronal oscillatory entrainment. The experiment will also be video recorded to allow for the off-line identification and analysis of the relevant behaviours.

*Magnetic Resonance Imaging (MRI).* T1 and T2-weighted structural and resting state fMRI scans will be collected in a subset of infants whose parents indicate additional consent. The MRI scan will be conducted within 3 months from the date of the initial EEG measurement, and will be used functional and structural connectivity (e.g. diffusion tensor imaging, DTI). [Appendix 1](#) provides more details on the proposed MRI scanning procedures.

*Functional Near-Infrared Spectroscopy (fNIRS).* To be collected simultaneously with the EEG. fNIRS provides images of functionally connected regions by using near-infrared light to measure regional changes in oxy- and deoxy-haemoglobin concentration in the brain. In fNIRS, optical measurements are collected from an array of optical fibres placed over the head. It is portable and silent, allowing infants to be studied continuously by the bedside.

UCL Biomedical Optics Laboratory have developed a multichannel fNIRS system that employs up to 16 pairs of laser diodes, at near-infrared wavelengths of 770nm and 850nm, and 16 photodiode detectors. Each source is modulated at a different frequency in the range 2-4 kHz and are illuminated simultaneously. A Fourier transform of the diffusely reflected intensity measured at each detector can then be used to isolate the contribution from each source. The combined use of fNIRS and EEG is safe and practical and has been used extensively in studies on newborn infants (Cooper et al, 2011; Chalia et al, 2016). Our research group has designed a flexible cap based on the EasyCap EEG cap that can house

the optodes (light sources and detectors) and EEG electrodes in an array configuration that will allow for optimal data acquisition.

### 3.3 Genotyping Procedure

Genetic samples will be obtained from all infants at birth by collecting a blood spot on a filter paper, taken using a standard heel lance. Genetic samples will also be obtained from both parents using a saliva sample. Genomic DNA will be isolated from the blood spots as described (Saavedra-Matiz et al, 2013). The following 16 single nucleotide polymorphisms (SNPs) will be genotyped:

DYX1C1 (Chr 15)	DCDC2 (Chr 6)	KIAA0319 (Chr 6)	ROBO1 (Chr 3)
rs3743204	rs793842	rs4504469	rs333491
rs3743205	rs793862	rs6935076	rs6803202
rs17819126	rs807701	rs4504469	rs9853895
	rs2328819	rs114138463	rs7644521
	rs279268		

These polymorphisms contain dyslexia susceptibility genes replicated by independent studies (Kere, 2014) and some of them have been reported to be associated with phonological deficits (Bates et al, 2011) and deficits in brain white matter volume and structure (Darki et al, 2012). Genotyping will be conducted using Taqman SNP Genotyping Assays (Life Technologies) on a 7900HT Sequence Detection System (Life Technologies).

### 3.4 Early Language Environment Assessment

Infants' early home language environment will be assessed at each time-point (i.e., 0, 6, 12 and 18 months) using the LENA system which consists of a compact digital recorder mounted on a piece of clothing (a vest) that is worn by the child. The system will be sent to participants' homes and will provide continuous audio recordings for up to 24 hours (starting in the morning, continuing throughout the day). Parents will have the option of consenting to either full speech extraction, or to limit the data to only summary statistical features (i.e. pitch, duration, environmental noise) but not the actual speech content. Additionally, questionnaires will be used to assess the family's socio-economic status and overall quality of care (Observational Record of the Caregiving Environment).

### 3.5 Measures of Language and Socio-Emotional Development

*Language measures.* Infants' early language development will be assessed at all time-points using standardized assessment tools such as the MacArthur-Bates Communicative Development Inventories (CDIs). At 18 months of age, a test for early phonological development such as Profiles of Early Expressive Phonological Skills (PEEPS) will be administered. Parents' language skill will also be assessed using standardized measures of reading, spelling and phonology (e.g. Wide-Range Achievement Test [WRAT], Phonological Assessment Battery [PhAB]).

*Socio-emotional measures.* Infants' socioemotional development will be assessed at all time-points by parent report using standardized tools such as the Ages and Stages Questionnaire (ASQ), and Infant Behavior Questionnaire (IBQ). Maternal socio-emotional wellbeing will be

assessed using the Beck Depression Inventory (BDI), and both parents' temperament will be assessed using the Adult Temperament Questionnaire (ATQ). At 18 months, infants' stress reactivity will be assessed using a mild social stress task (e.g. Still Face Paradigm).

In the context of the Covid-19 outbreak, during periods when physical distancing is necessary, the measures of language and socioemotional development will be administered via online video-conferencing instead of through face-to-face assessment. Further, participants will complete online questionnaires (using the university-approved encrypted platform Qualtrics) rather than physical copies of all questionnaires. This modification will enable follow up assessments to continue in a safe and timely manner. The research team will contact parents to explain and obtain verbal consent for video-conferencing sessions, rather than inviting them for a laboratory visit, as planned prior to the Covid-19 outbreak. If the parent does not want to take part, or does not have the technology available, their assessment will either be delayed or omitted until Covid-19 restrictions are lifted.

### 3.6 Data Analysis: Identification of Neurogenetic Risk Markers of Dyslexia

Step 1: For both resting state and passive listening conditions, a comprehensive set of EEG oscillatory indices across the 5 frequency bands (delta (1-3 Hz), theta (4-7 Hz), alpha (8-12 Hz), beta (13-25 Hz) and gamma (26-40 Hz)) will be computed as potential neural biomarkers of risk. These indices will include the (a) power and (b) phase pattern in each frequency band, as well as the (c) power-power (d) phase-phase and (e) phase-power relationships *between* all pairs of frequency bands. Similarly, MRI measures of structural and functional connectivity will be computed.

Step 2: These EEG and MRI indices will be assessed statistically for group differences using a Repeated Measures ANCOVA (entering gestational age, gender and socio-economic status as covariates), where an Index x Group interaction is predicted. To detect the predicted interaction with 0.95 power, given only a small effect size (0.15) and 20 oscillatory indices, a total sample size of 36 (18 per group) is required. However, a larger sample size of 50 will be used to accommodate the planned regression analysis in Step 4 (with 20% attrition).

Step 3: Out of all the measured indices, a sub-set of N neural indices with the strongest combined discriminatory power (i.e. classification of at-risk vs. control status with >75% accuracy) will be identified via logistic regression. These N oscillatory indices will form the set of ***"neural biomarkers of dyslexia risk"***.

Step 4: Multiple linear regression analysis will then be used to identify the strongest *genetic* predictors associated with each of the N neural biomarkers (note: we are performing genetic prediction of a neuroendophenotype, not of the dyslexia phenotype. This is a more proximal relationship and should yield more robust results than a gene-phenotype prediction). That is, each of the 15 SNPs will be entered in forwards or backwards stepwise regressions to explain variance in oscillatory index 1. The process will then be repeated until neural index N. To identify 2 genetic/environmental predictors for each neural index with 0.9 power, where each genetic predictor has a large effect size (0.35), a total sample size of 40 is required (50 with 20% attrition). Note that if the genetic predictors have only a medium effect size (0.25), a similar sample size (45) is sufficient to detect 1 instead of 2 genetic predictors per neural biomarker. Also note that each SNP may be associated with any number of neural indices.

As illustrated in Figure 1, the result of this 4-step analysis will yield: (1) A set of N neural biomarkers that reliably distinguish between at-risk and control infants (target of >75% accuracy); (2) Up to 2 genetic predictors that are associated with each neural biomarker.

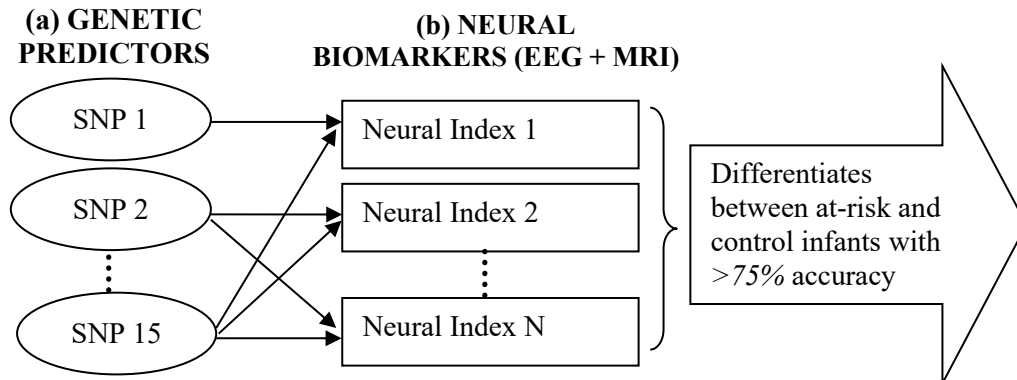


*Figure 1. The aim of the study is to identify a set of neural biomarkers (b, EEG and MRI indices) that reliably distinguish between at-risk and control infants. Further, up to 2 genetic predictors (a, SNPs) that are linked to each neural biomarker will be identified via regression analyses. Each SNP may contribute to any number of neural biomarkers.*

### 3.7 Timeline

The proposed project will run for 5 years from Oct 2017 – Oct 2022. Participant recruitment and neuroimaging will be performed on a rolling basis from Jan 2018 - Dec 2020 (36 months). Genetic data will be collected and stored for batch analysis for the same period. Data analysis and writing-up for publication are planned also on a rolling basis from Jan 2019 - Oct 2022.

## 4 ETHICAL CONSIDERATIONS

Approval from the Research Ethics Committee Approval has been obtained. EEG and MRI are standard clinical tools that are routinely and safely used for newborn infants. However, MRI scanning of young infants can be a challenging undertaking. Other groups in the UK have successfully scanned neonatal infants, and groups elsewhere have begun to develop brain atlases based on large longitudinal studies involving imaging at birth and at several time points within the first few years of life. There is therefore a strong precedence for the scanning of young infants. We will utilise the successful techniques adopted by other groups in the UK and every effort will be made to make the children and their parents comfortable. We will also ensure that scanning time is kept to a minimum.

The following risks/discomforts and safeguards will be highlighted to the parent during the process of obtaining consent for participation in the study:

1. The MRI scan may be mildly stressful for your child if they wake up during the scan because it will involve lying in a noisy machine in an enclosed small space. To minimise the amount of noise your child will be fitted with earplugs or earphones and you can sit near to your child throughout the scan. We will wait with you to ensure your baby is fast asleep before scanning begins. Children are only scanned while sleeping naturally. A member of the research team will monitor your child throughout the scan and if your child wakes up, the scanning will be stopped immediately. The MRI scan does not use radiation. There is no

evidence that the magnetic field used by the scanner has any harmful effects. If your baby does become even mildly distressed, the scanning can be stopped immediately.

2. Sometimes an MRI scan will identify an unexpected abnormality in an apparently normally developing child. If a problem is identified by the MRI, your GP will be contacted and an appropriate follow-up appointment will be arranged. However, it is up to you to decide whether or not you would like the research team to notify your GP of your baby's participation in this study.

3. A further consideration for the home-based speech environment recordings might be that parents are sensitive about the incidental collection of personal information. Parents will be reassured from the beginning that all data will be reported in an anonymized form, and that the data will only be processed by qualified members of the research team that have undergone rigorous checks and training. Additionally, parents will be advised that they can opt out of either the full study, or any component of it, at any point. They would also be offered the choice to only allow researchers access to the anonymized statistics of the home acoustic environment (without any semantic information or identifiers), rather than the full audio recordings.

Informed consent will be obtained from the parents of the infants to be recruited in the study. The explanation will be performed and consent will be taken by the research investigator, with aid of a written Information Sheet and Consent Form.

## REFERENCES

- Adler, W.T., Platt, M.P., Mehlhorn, A.J., Haight, J.L., Currier, T.A., et al. (2013). Position of neocortical neurons transfected at different gestational ages with shRNA targeted against candidate dyslexia susceptibility genes. *PLoS ONE* 8(5): e65179.
- Armitage, S.E., Baldwin, B.A., & Vince, M.A. (1980). The fetal environment of sheep. *Science*, 208, 1173-1174.
- Bates, T.C., Luciano, M., Medland, S.E., et al (2011). Genetic variance in a component of the language acquisition device: ROBO1 polymorphisms associated with phonological buffer deficits. *Behaviour Genetics*, 41, 50-57.
- Benasich, A.A., Gou, Z., Choudhury, N. & Harris, K. D. (2008). Early cognitive and language skills are linked to Resting frontal gamma power across the first three years. *Behavioral Brain Research*, 95, 215-222.
- Burbridge, T., Wang, Y., Volz, A., Peschansky, V., Lisann, L, et al. (2008) Postnatal analysis of the effect of embryonic knockdown and overexpression of candidate dyslexia susceptibility gene DCDC2. *Neuroscience* 152: 723–733.
- Carrion-Castillo, A., Franke, B., & Fisher, S.E. (2013). Molecular genetics of dyslexia : An overview. *Dyslexia*, 19, 214-240.
- Cooper, R.P. & Aslin, R.N. (1989). The language environment of the young infant: Implications for early perceptual development. *Canadian Journal of Psychology*, 43, 247-265.
- Currier, T.A., Etchegaray, M.A., Haight, J.L., et al (2011) The effects of embryonic knockdown of the candidate dyslexia susceptibility gene homologue DYX1C1 on the distribution of GABAergic neurons in the cerebral cortex. *Neuroscience* 172, 535–546.
- Darki, F., Peyrard-Janvid, M., Matsson, H., et al (2012). Three dyslexia susceptibility genes, DYX1C1, DCDC2, and KIAA0319, affect temporo-parietal white matter structure. *Biological Psychiatry*, 72, 671-676.

- DeCasper, A. J., & Fifer, W. P. (1980). Of human bonding: Newborns prefer their mothers' voices. *Science*, 208, 1174–1176.
- DeCasper, A. J., & Spence, M. J. (1986). Prenatal maternal speech influences newborns' perception of speech sounds. *Infant Behavior and Development*, 9, 133–150.
- Fernald, A. (1989). Intonation and communicative intent in mother's speech to infants: Is the melody the message? *Child Development*, 60, 1497-1510.
- Galaburda, A.M., & Kemper, T.L. (1979). Cytoarchitectonic abnormalities in developmental dyslexia: a case study. *Annals of Neurology*, 6, 94-100.
- Giraud, A.L. & Poeppel, D. (2012). Cortical oscillations and speech processing: Emerging computational principles and operations. *Nature Neuroscience*, 15, 511-517.
- Giraud, A. L., & Ramus, F. (2013). Neurogenetics and auditory processing in developmental dyslexia. *Current Opinion in Neurobiology*, 23, 37-42.
- Goswami, U. (2011). A temporal sampling framework for developmental dyslexia. *Trends in Cognitive Sciences*, 15, 1 3-10.
- Gou, Z., Choudhury, N. & Benasich, A.A. (2011). Resting frontal gamma power at 16, 24 and 36 months predicts individual differences in language and cognition at 4 and 5 years. *Behavioral Brain Research*, 220, 2, 263-270.
- Grigorenko, E.L. (2004). Genetic bases of developmental dyslexia: a capsule review of heritability estimates. *Enfance*. 56, 273–288.
- Guttorm, T.K., Leppänen, P.H.T., Richardson, U., & Lyytinen, H. (2001). Event-related potentials and consonant differentiation in newborns with familial risk for dyslexia. *Journal of Learning Disabilities*, 34(6), 534-544.
- Hämäläinen, J.A., Rupp, A., Soltész, F., Szücs D, Goswami U. (2012). Reduced phase locking to slow amplitude modulation in adults with dyslexia: An MEG study. *Neuroimage*, 59, 2952–2961.
- Humphreys, P., Kaufmann, W.E., & Galaburda, A.M. (1990). Developmental dyslexia in women: neuropathological findings in three cases. *Annals of Neurology*, 28, 727-738.
- Kere, J. (2014). The molecular genetics and neurobiology of developmental dyslexia as model of a complex phenotype. *Biochemical and Biophysical Research Communications*, 452, 236–243.
- Lehongre, K., Ramus, F., Villiermet, N., Schwartz, D., & Giraud, A. L. (2011). Altered low-gamma sampling in auditory cortex accounts for the three main facets of dyslexia. *Neuron* 72, 1080–1090
- Leong, V., & Goswami, U. (2014a). Assessment of rhythmic entrainment at multiple timescales in dyslexia : Evidence for disruption to syllable timing. *Hearing Research*, 308, 141-161.
- Leong, V., & Goswami, U. (2014b). Impaired extraction of speech rhythm from temporal modulation patterns in speech in developmental dyslexia. *Frontiers in Human Neuroscience*, 8:96.
- Leong, V., Hamalainen, J., Soltesz, F., & Goswami, U. (2011). Rise time perception and detection of syllable stress in adults with developmental dyslexia. *Journal of Memory and Language*, 64, 59–73.
- Leong, V., Stone, M., Turner, R. & Goswami, U. (2014a). A role for amplitude modulation phase relationships in speech rhythm perception. *Journal of the Acoustical Society of America*, 136, 366-381.
- Leong, V., Kalashnikova, M., Burnham, D., & Goswami, U. (2014b). Infant-directed speech enhances temporal rhythmic structure in the envelope. *Proceedings of the 15th Annual Conference of the International Speech Communication Association (ISCA)*, Singapore, Sept 14-18, 2014.
- Leppänen, P.H.T., Pihko, E., Eklund, K.M. & Lyytinen, H. (1999) Cortical responses of infants with and without a genetic risk for dyslexia: II. Group effects, *Neuroreport* 10 (5), 967–973.
- Meng, H., et al. (2005). DCDC2 is associated with reading disability and modulates neuronal development in the brain. *Proceedings of the National Academy of Sciences of the United States of America*, 102, 17053-17058.

Paracchini, S. et al. (2006). The chromosome 6p22 haplotype associated with dyslexia reduces the expression of KIAA0319, a novel gene involved in neuronal migration. *Human Molecular Genetics*, 15, 1659-1666.

Pechansky, V.J., et al. (2009). The effect of variation in expression of the candidate dyslexia susceptibility gene homolog Kiaa0319 on neuronal migration and dendritic morphology in the rat. *Cerebral Cortex*, 20, 884–897.

Power, A.J., Mead, N., Barnes, L. & Goswami, U. (2013). Neural entrainment to rhythmic speech in children with developmental dyslexia. *Frontiers in Human Neuroscience*, 7:777.

Rosen, G.D., et al. (2007). Disruption of neuronal migration by targeted RNAi knockdown of *Dyx1c1* results in neocortical and hippocampal malformations. *Cerebral Cortex*, 17, 2562-2572.

Schiavone, G., Linkenkaer-Hansen, K., Maurits, N.M., Plakas, A., Maasen, B.A.M., Mansvelter, H., van der Leij, A., & Van Zuijlen, T. (2014). Preliteracy signatures of poor-reading abilities in resting-state EEG. *Frontiers in Human Neuroscience*, 8:735.

Snowling, M.J. (2000). *Dyslexia* (2nd Edition), Oxford, U.K : Blackwell Publishers.

Soltész, F., Szucs, D., Leong, V., White, S., & Goswami, U. (2013). Atypical entrainment of Delta oscillations to rhythmic stimulus streams in developmental dyslexia, *PLOS One*, 8(10): e76608.

Saavedra-Matiz ,C.A., Isabelle, J.T., Biski, C.K., et al (2013). Cost-effective and scalable DNA extraction method from dried blood spots. *Clinical Chemistry*, 59, 1045-1051.

Zhang, Y., Koerner, T., Miller, S., Grice-Patil, Z., Svec, A., Akbari, D., Tusler, L. & Carney, E. (2011), Neural coding of formant-exaggerated speech in the infant brain. *Developmental Science*, 14, 566–581.

## Appendix 1 – MRI Scanning Procedures and Equipment

### **1. Staff: Research Nurse, 1 study staff, 1 radiographer**

#### **1.1 Preparation**

- Schedule the daytime appointment to correspond with the child’s normal feeding or nap time.
- Prior to the appointment:
  - Ask parents how long the child typically takes to fall asleep after feeding, how deeply the child sleeps, and whether the child sleeps on the stomach.
  - Let parents know not to dress child in metal (including clothing clasps).
  - Alert parents to keep child’s routine as close to normal as possible.
- A nurse will always present for the scan sessions. The nurse sits in the scan room during scanning, along with the mother (usually). The nurse monitors the infant's pulse and blood pressure. A Staff member also stays in the room.

#### **1.2 Scan Procedures**

- Greet parents, go over consent form, screening form and explain procedures to follow.
- Make sure there is NO METAL on mother or child
  - Keep a supply of plain white shirts in different sizes in case mother dresses child in an outfit containing metal.
- Dim lights/noise in scan room and waiting area. Increase air temperature in scan room.
- Scan room lights on and the set-up is ready to go
- Bring mother and child into scanner room.
- Child to be swaddled as normal routine at home (possible to bring usual blanket in from home) and placed onto MR bed and connect head coil.
- Connect the child’s foot to the pulse oximeter (SP02 GripSensor Ref 9399B, SN 3155707 for use with InVivo Pulse Ox, SP021, Ref 9311).

- Insert earplugs
  - Cover each earplug with surgical tape (to keep in place)
- Wait at least 5 minutes after child appears to be sleeping, to make sure he/she is thoroughly asleep.
- If the child doesn't fall asleep within 10-15 minutes then a staff member takes over.
- During scan, mother and nurse sit in front of the scanner on plastic chairs – able to see infant and research staff in the control room.
- Scan is stopped if child wakes up. But not if child jerks/moves in sleep.
- Staff member with informs scan technician of movement so technician can start it over right away.
- If child absolutely cannot fall asleep, scan may be rescheduled.

### 1.3 Equipment List

1. Soft changing table for parents to change nappies.
2. Earplugs (for neonates and infants)
3. Surgical tape (neonates)
4. Vacuum seal pillow (neonates)
5. Warmer
6. Little head cushion (neonates)
7. Swaddling blankets (neonates)
8. Pulse Ox and toe grip attachment: SP02 GripSensor Ref 9399B, SN 3155707 for use with InVivo Pulse Ox, SP021, Ref 9311 (neonates)
9. Rocker for scan room (plastic or wooden)
10. Extra t-shirts
11. Wipes and nappies
12. Neonate and regular dummies
13. Memory foam on scanner bed (typical scan bed cushion)
14. Pillow case to go over the whole set up on scanner bed
15. Two velcro straps: One for child and one to keep vacuum seal pillow from interfering with head coil as it firms up. Seems that only the one for the vac seal does anything. Other one just makes it clear that child will not roll off scan bed (neonates)
16. Suction device for stuffy noses (neonates)
17. Headphones (nothing special but child sized) with extra pieces of memory foam for sound protection (Bilsom Viking V2 and 3M 1435 3 months and older)
18. Vitamin E taped on right side of headphones

## 2 MRI tech

- Scans should be seamless (don't let machine make adjustments between scans as this will cause breaks in the noise that will wake up the infant)
  - Copy adjustment settings from first scan to the rest of the scans.
- Scan tech checks scan as they come in and reruns scans as necessary
  - Scan technician relies on staff in the scan room to ring alarm if it should be started over before finishing (based on how amount of child movement).

## 3 Tips

- Tap child's stomach in time with the scanner.
- Pressure of hand on child's stomach (or pressure of weighted blanket or heat pad) can be very important esp. for children who sleep on their stomach or who want to roll over.

# Appendix II

---

## II.I Parental Genetics

### Participants

Eleven parents of 7 infants provided a saliva sample at birth (*Figure 3-1*, green panel on top left).

Thirty-seven parental (across 32 individual parents) and 30 infantile (across 19 individual infants) saliva samples were collected (*Figure 3-1*, middle two top panels) using the age-appropriate collection kit.

Thus, the 48 samples came from 41 parents (28 mothers and 13 fathers) to 29 participating infants. Seven parents (six mothers and one father) contributed two samples at two separate data-collection time-points, and one parental couple had twins in the study. Twenty-two of the parents had a child at high familial risk of dyslexia, and 11 (4 mothers) of them are dyslexic themselves.

### Genetics Sample Collection

Parents agreed to provide a saliva sample for genotyping and cortisol analyses, by spitting a minimum of 1ml of saliva in a 10-ml sterile tube (Stratech, Ely, UK). Parents were advised not to eat or drink for at least half an hour before the sample was secreted. The saliva samples were stored in a fridge at 4-8 C for up to two hours, then frozen at -20 C for up to 12 months prior to analysis.

### Genotyping Procedure for the Parental Saliva Samples

A proportion of the parental saliva samples (100 $\mu$ L, roughly around 10% of the secreted material) was used to extract genomic DNA in accordance with the guidelines provided by the manufacturer of the genotyping products. The same 16 single nucleotide polymorphisms (SNPs) as in the infants', were genotyped for each parental sample (Table 2-1 in Chapter 2). Genotyping was conducted using the same Taqman SNP Genotyping Assays (Life Technologies) on a 6900HT Sequence Detection System (Life Technologies).

Of the 16 tested SNPs, one SNP on the DCDC2 gene (rs9460974) did not produce consistent results against the positive control (known samples) in the infants' blood-spot reaction plates on repeated attempts. It was suspected that the reagent was not functioning properly. rs9460974 was not included in any analyses after genotyping for neither the infants', not the parental data.

### ***Procedure for DNA extraction and PCR***

Genotyping was conducted as a quantitative polymerase chain-reaction (qPCR) using commercially available Taqman SNP Genotyping Assays and GTXpress Master Mix in 384-well plates on a Quant Studio 6 Flex machine (LifeTechnologies).

First, genomic DNA was extracted from 100 $\mu$ L of thwarted saliva and immediately stabilized.

The protocol for stabilizing genomic DNA consisted in the following steps:

- a. 50 $\mu$ L of TaqMan Extract All Reagents Lysis solution was added to each sample (100 $\mu$ L saliva).
- b. The mix tubes were briefly vortexed.
- c. The mix tubes were incubated at 95°C for 3 minutes.
- d. 50 $\mu$ L of TaqMan Extract All Reagents DNA Stabilizing solution was added to each tube immediately after incubation.
- e. The tubes were briefly vortexed and then centrifuged at 45000 repetitions/minute (RPM) for 1 minute to allow for the entire volume to mix down at the bottom of the Eppendorf tube.
- f. Thus, stabilized DNA sample templates were either immediately used in a reaction plate or stored in a fridge at 4-8°C.

The step-by-step PCR procedure for the parental saliva samples was identical to the one described for the infant blood spot samples in *Chapter 2*.

Initially, a blood-spot sample of a known genetic profile was used as a positive template control (PTC) of the same individual's saliva sample. All genotyping profiles were identical

in the two tissues apart from the results for rs17819126 (DYX1C1). The test was repeated three times and the results for that SNP were inconsistent for the saliva sample only. It was suspected that the reagent for that SNP was not working properly with the saliva samples, so it was not further used in the saliva genotyping protocol. The PTC was added to every other parental genotyping well-plate. Finally, all seven individual parents who provided saliva samples twice were genotypes according to both samples. There were no discrepancies between the two genetic profiles delivered by each sample, however, there were some undetermined wells by SNP.

## Parental Genotyping Results

### *Allelic and Genotype Frequencies*

As a general note, the genotyping of the parental saliva samples was less successful than that of the infant blood samples, with all 14 remaining SNPs having at least one missing value. This was at least partially due to the reduced likelihood of genetic material available in epithelial cells in the saliva compared to the blood tissues. Percentagewise, the allelic and the genotype frequencies in the adult sample resemble closely the distribution in the infants and the previously reported distribution in known sample for the UK. This is true for both the HW equilibrium distribution, and the actual allelic frequencies (*Table II-1*). Importantly, the most common allele 1 was always the same allele for parents and infants.

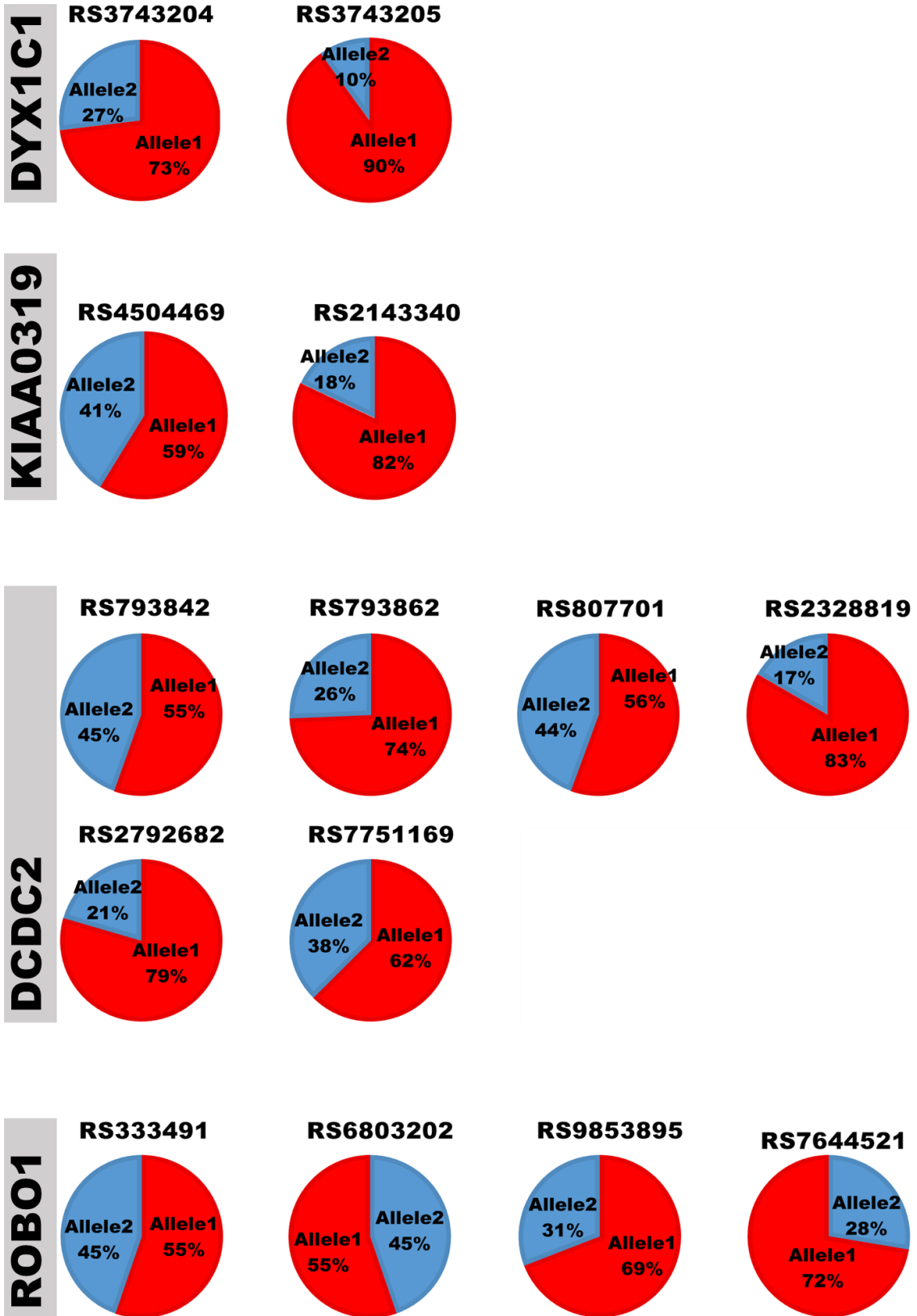
*Figure II-1A* and *Table II-1* below show the allelic frequency of the parental DNA sample for each of the SNPs to facilitate comparison with published databases of other British samples, as well as with their infants'. *Figure II-1B* shows the parental genotype for each SNP (expressed as a percentage of the total sample count, N). Undetermined again refers to samples which we were unable to classify as either genotype, likely due to human pipetting error, or more lack of sufficient genomic DNA template in the saliva sample.

Table II-1. Allelic distribution in the parental, infant samples for this study, and in other British studies by SNP. The Genotype#3 columns give the minor-allele heterozygous frequency by SNP to help identify genotypes with insufficient number of individuals for further analyses.

GENE	SNP	1000 Genomes (GBR sub-population)		UKTWINS	ALSPAC	Allelic frequency (HW)		Allelic frq (actual) *child*	Genotype#3 *child*	Allelic frequency (HW)		Allelic frq (actual) *parent*	Genotype#3 *parent*
		84.6% (154)	84.6% (154)			*child*	*parent*						
DYX1C1	rs3743204	84.6% (154)	78.9% (2821)	79.9% (3080)	75.59%	75.00%	75.00%	7.14%	73.38%	73.08%	7.69%		
	rs3743205	97.8% (178)	94.0% (3361)	94.9% (3656)	91.29%	90.00%	90.00%	3.33%	90.83%	90.00%	2.50%		
KIAA0319	rs4504469	50.5% (46)	59.0% (2109)	59.7% (2300)	55.90%	53.65%	53.65%	23.96%	61.24%	58.75%	20.00%		
	rs2143340	85.2% (155)	84.3% (3013)	84.3% (3248)	84.91%	86.05%	86.05%	0.00%	86.23%	82.05%	10.26%		
DCDC2	rs793842	63.7% (116)	61.5% (2370)	61.4% (2195)	59.76%	62.24%	62.24%	11.22%	56.95%	55.41%	21.62%		
	rs793862	74.7% (136)	74.4% (2658)	74% (2852)	71.07%	72.16%	72.16%	6.19%	73.52%	74.32%	5.41%		
ROBO1	rs807701	66.5% (121)	66.2% (2365)	66.4% (2559)	64.68%	65.82%	65.82%	10.20%	52.70%	55.56%	16.67%		
	rs2328819	72.5% (132)	75.4% (2695)	75.5% (2911)	77.73%	78.65%	78.65%	3.13%	83.33%	83.33%	2.78%		
ROBO1	rs2792682	78.6% (174)	78.4% (3020)	78.7% (2812)	75.90%	75.54%	75.54%	6.52%	78.45%	79.49%	2.56%		
	rs7751169	62.6% (114)	65.3% (2515)	66.6% (2380)	69.25%	63.78%	63.78%	20.41%	63.25%	62.50%	15.00%		
ROBO1	rs6803202	56.6% (103)	51.6% (1845)	50.2% (1934)	53.45%	46.43%	46.43%	21.43%	53.80%	44.74%	18.42%		
	rs7644521	80.2% (146)	81.5% (2914)	82.5% (3180)	80.81%	79.59%	79.59%	6.12%	72.55%	27.63%	7.89%		
ROBO1	rs333491	61.5% (112)	55.8% (1994)	55.1% (2125)	63.08%	61.73%	61.73%	16.33%	53.80%	55.26%	18.42%		
	rs9853895	61.0% (131)	60.9% (2176)	60.1% (2325)	65.47%	67.35%	67.35%	8.16%	70.71%	69.12%	11.76%		

Similar to the infants' genotypical results, there were several SNPs in the parental sample with frequency of genotype#3 lower than 5% (*Table II-1*). Those were two overlapping SNPs in the parents and the infants: rs3743205-genotype#3=2.5% on DYX1C1 and rs2328819-genotype#3=2.78% on DCDC2. There was an additional SNP on DCDC2 rs2792682-genotype#3=2.56%. As with their infants, parents also had the rs7644521 SNP on ROBO1 with a genotype#3 frequency close to 5%, with the addition of rs793862 (DCDC2) in the same incidence category. The striking difference between the sampled infants and their parents was that for the KIAA0319 SNP rs2143340, we failed to identify a single infant carrying the genotype#3, whereas 10% of their parents had genotype#3 (*Table II-1* above and *Figure II-1B* below).

A)



B)

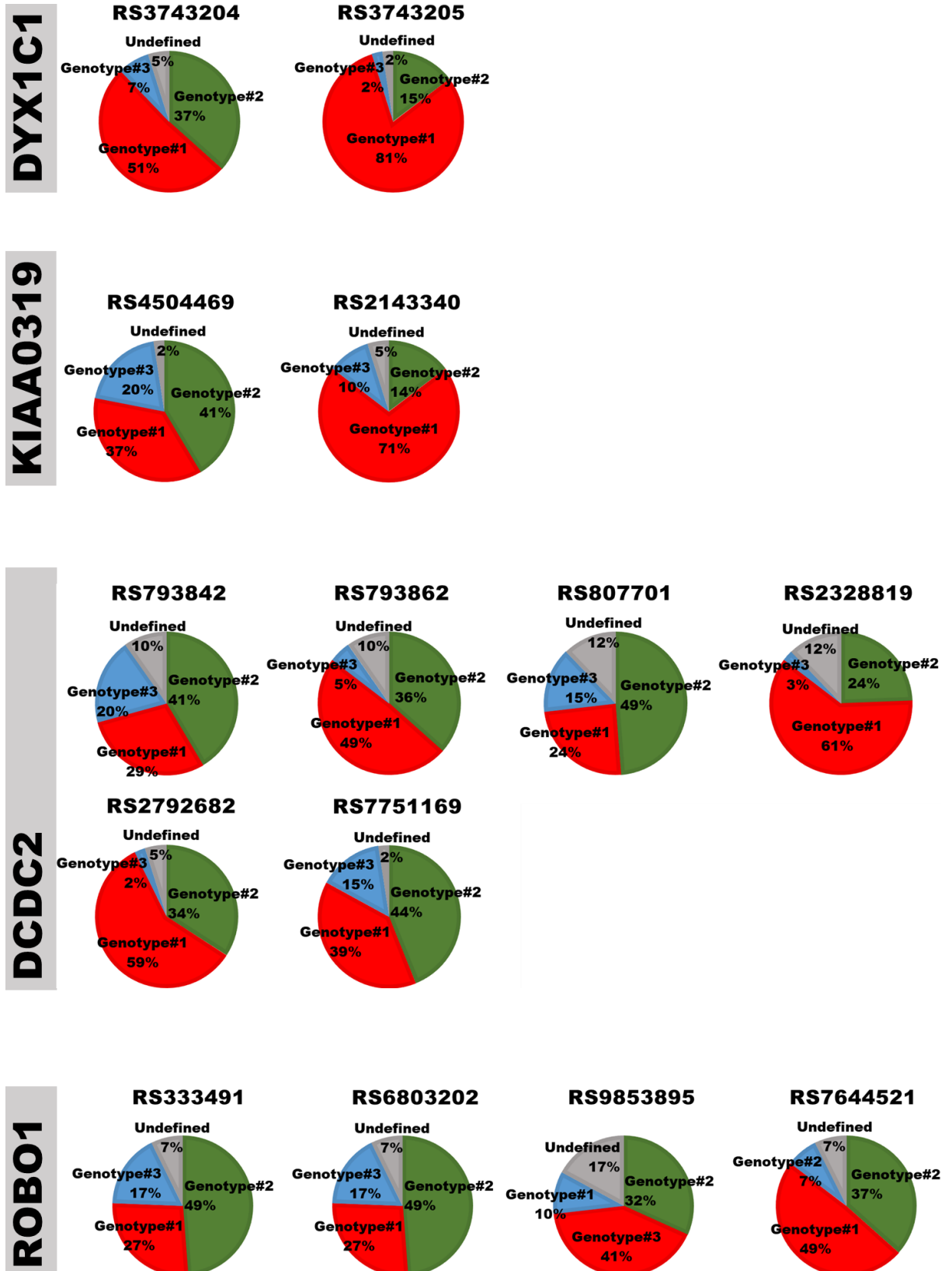


Figure II-1. Allelic frequency (A) and genotype frequency (B) by SNP and gene in the parental saliva sample. Genotype#1 was always heterozygous for allele 1 in these pie charts.

### ***Cross-tabulation between Parental Genetics and Dyslexia***

To estimate whether there was a statistical association between the parental genotype on the 14 SNPs tested and whether they were dyslexic, 14 independent chi-square tests were performed for each SNP. As before, for each SNP, genotype#1 denoted the heterozygous variant for the most common allele in the current parental (and always the same as infant) sample.

None of the 14 SNPs assessed had a significant association with parental (Kruskal-Wallis  $KW\chi^2$  statistics and p values are reported in *Table II-2* below, all *n.s.* at  $\alpha=.05$ ).

Interestingly, no dyslexic parents in our sample carried either the hetero-, or the homozygous version of the less common allele of rs2143340 – i.e., only genotype#1 for this SNP was present.

*Table II-2. Chi-square statistics and significance level by SNP on the difference between the observed and expected distributions of parental genotype given parental dyslexia under the null hypothesis.*

<b>Individual Chi-square Tests by Group: DyslexicOrNot(2) x Genotype(3)</b>				
<b>Gene</b>	<b>SNP</b>	<b>KW<math>\chi^2</math></b>	<b>df</b>	<b>p</b>
<b>ROBO1</b>	rs7644521	0.095	2	0.954
	rs9853895	1.176	2	0.555
	rs6803202	0.668	2	0.716
	rs333491	4.320	2	0.115
<b>KIAA0319</b>	rs2143340	4.637	2	0.098
	rs4504469	0.886	2	0.642
<b>DCDC2</b>	rs7751169	2.407	2	0.300
	rs2792682	0.413	2	0.813
	rs2328819	0.480	2	0.787
	rs807701	0.514	2	0.773
	rs793862	5.141	2	0.076
	rs793842	1.470	2	0.479
<b>DYX1C1</b>	rs3743205	0.646	2	0.724
	rs3743204	0.138	2	0.933

Histograms demonstrating the distribution of the parental genotypes across the 14 SNPs, with dyslexic parents plotted to the left, and typically reading parents plotted to the right in *Figure II-2* below.

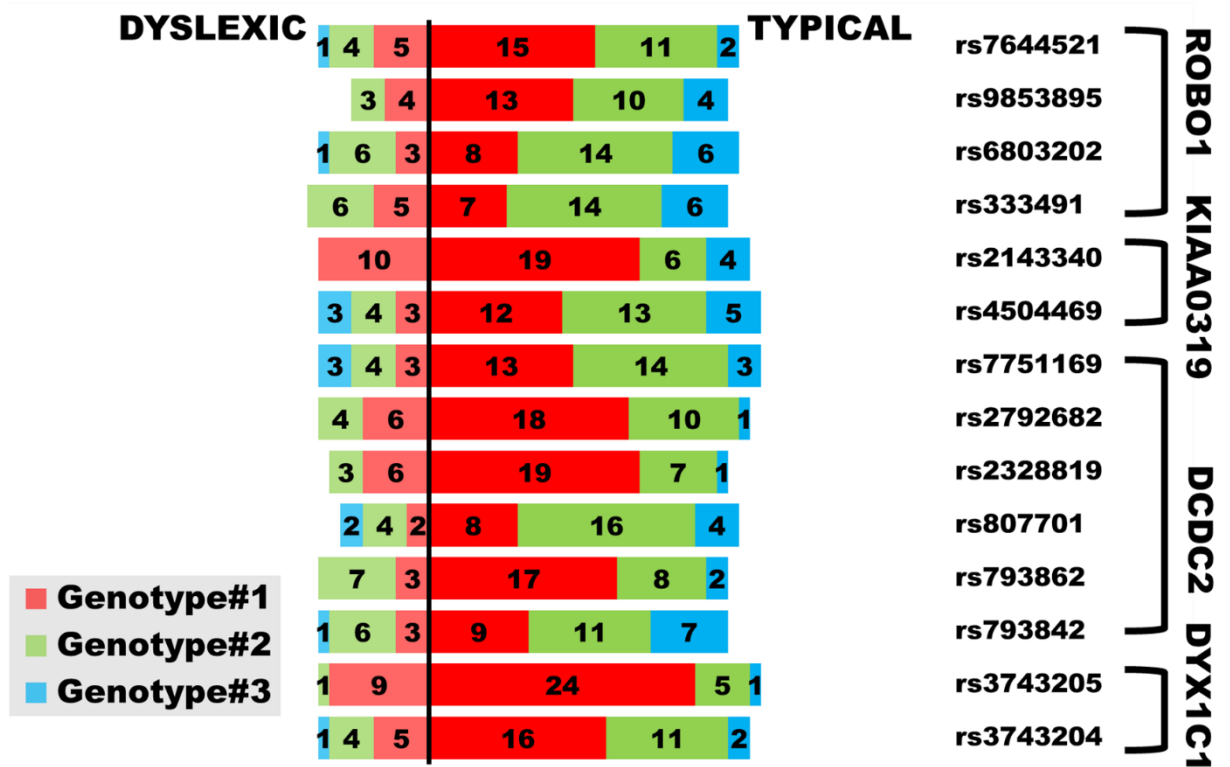
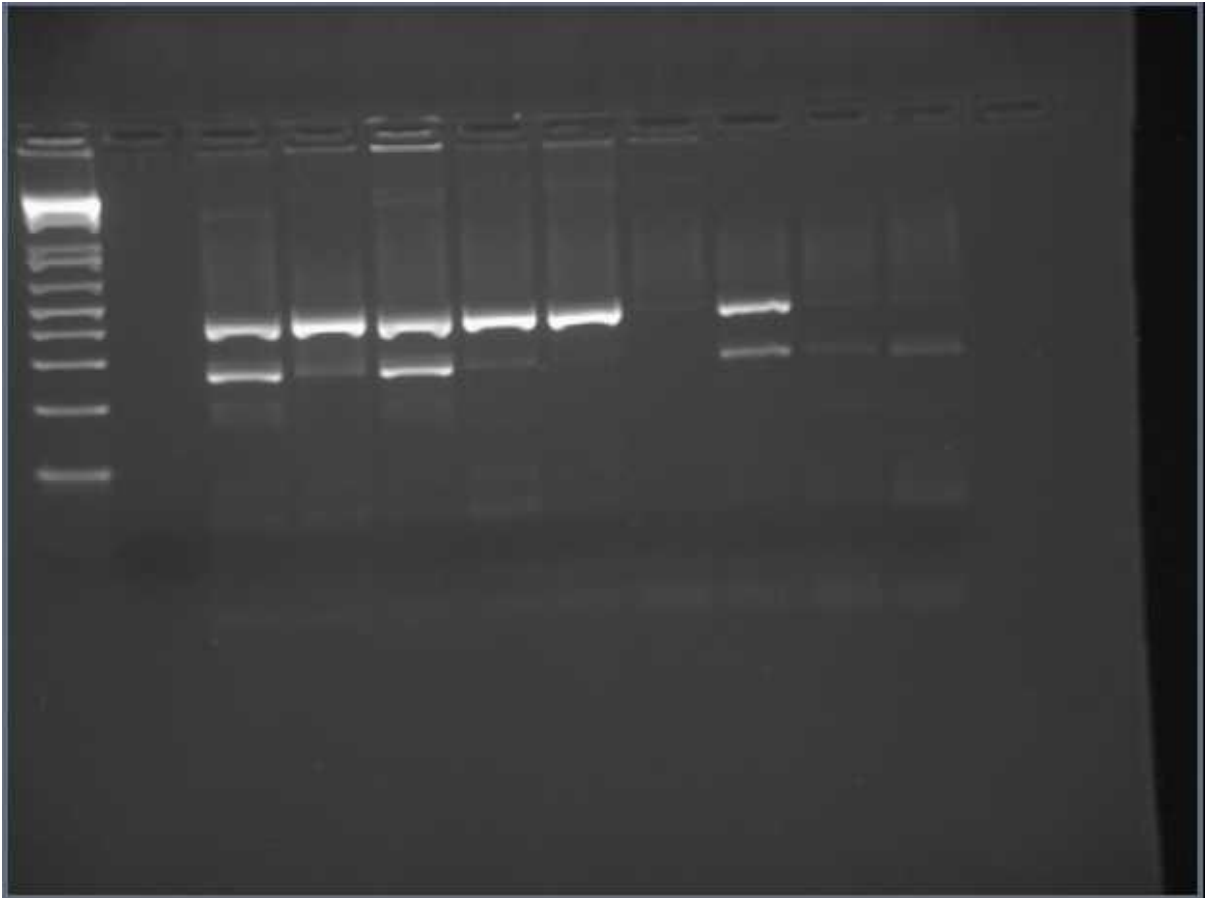


*Figure II-2. Individual SNPs histograms by genotype and dyslexia status. Dyslexic parents are plotted to the left, and typically reading parents, to the right.*

## My First PCR Gel



From personal archive: Genotyping 10 mice samples for training purposes. First column shows the reference values, the following 10 columns are the individual samples (first and seventh did not work well); there were all three genotypes present. Last column was an NTC.

## Appendix III

---

### III.I Noisy or Artifactual Data Inspection and Quality Control

For 13 infants, a 6Hz mechanical noise of an unidentified origin was present (the peak frequency and its harmonics suggests that the noise was originated by a fan or a ventilator). There is also 8Hz harmonised noise of a similar nature identified in another two infants. For eleven of those neonates, the noise is only present in between 1-3 individual channels, usually on the same side of the head. For the remaining four neonates, the noise affects all channels.

An example for one of the infants with a 6Hz noise set of channels is given in *Figure III-1* and further investigated in the frequency domain *Figure III-2* below. In the continuous timeseries example data view in *Figure III-1*, it could be seen that the noise affected strongly channels F7 and F8 (marked with red arrows, top panel). However, there were potential temporally constrained spillage effects to other channels as well, “tuned to” the noise and still present after the removal of the two most affected channels (marked by a yellow rectangle in *Figure III-1*, bottom panel). As 6Hz was above the cut-off frequency range of interest for the analyses in the main text, we checked if the noise was also present in the lower frequencies under 5Hz. If EEG appeared normal under 5Hz, the affected channels or epochs were retained for analysis if they were only mildly and temporarily affected, as in the yellow rectangle in *Figure III-1*, or removed if they were affected heavily throughout, as indicated by the red arrows for channels F7 and F8 in the same figure.

For one infant, the noise affected the recording even under 5Hz in most epochs in all the channels, so their dataset was excluded from analysis.

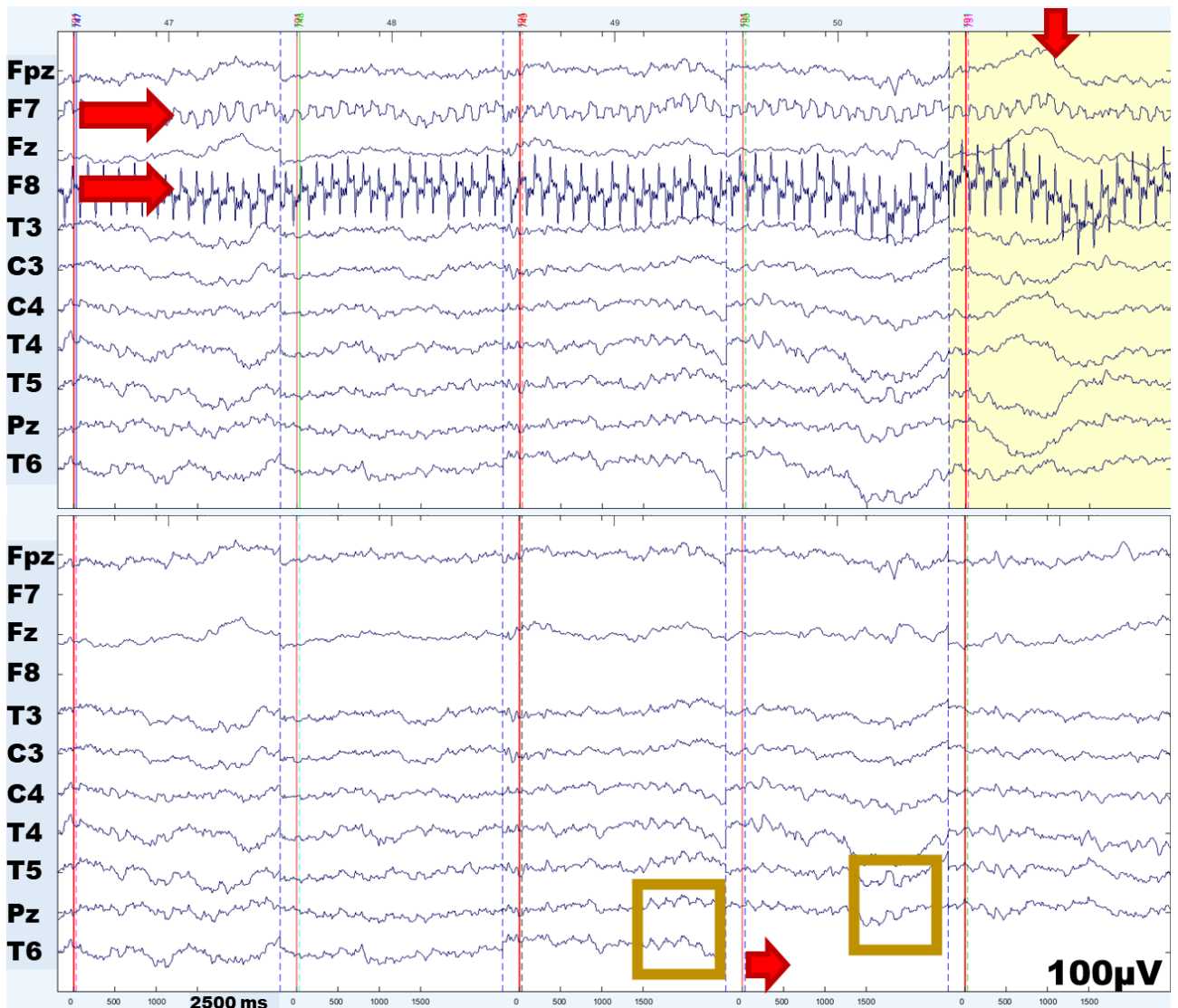


Figure III-1. An example of noisy EEG channels in 5 onset epochs for one infant (top panel); same view of the EEG after rejecting individual channel (bottom panel). Left red arrow keys point to the noisy channels to be rejected, either in just that epoch (T6), or throughout the entire recording (F7 & F8, suspected low-frequency mechanical noise). Bottom-pointing red arrow indicates an onset epoch to be rejected. Yellow rectangles highlight segments with 6Hz activity that was suspected as still artifactual after rejecting the noisy channel (F8) and further investigated.

For the remaining 12 infants, an additional quality-control step was taken to ensure that the EEG recordings under 5Hz were composed of neural activity as opposed to low-frequency artifactual noise. An independent components analysis (ICA) (Jung et al., 2000 in Gwin et al., 2010) on the 0.2-40Hz band-pass filtered data was used to separate 11 orthogonal components, which comprise both neural signal, and noise (Figure III-2).

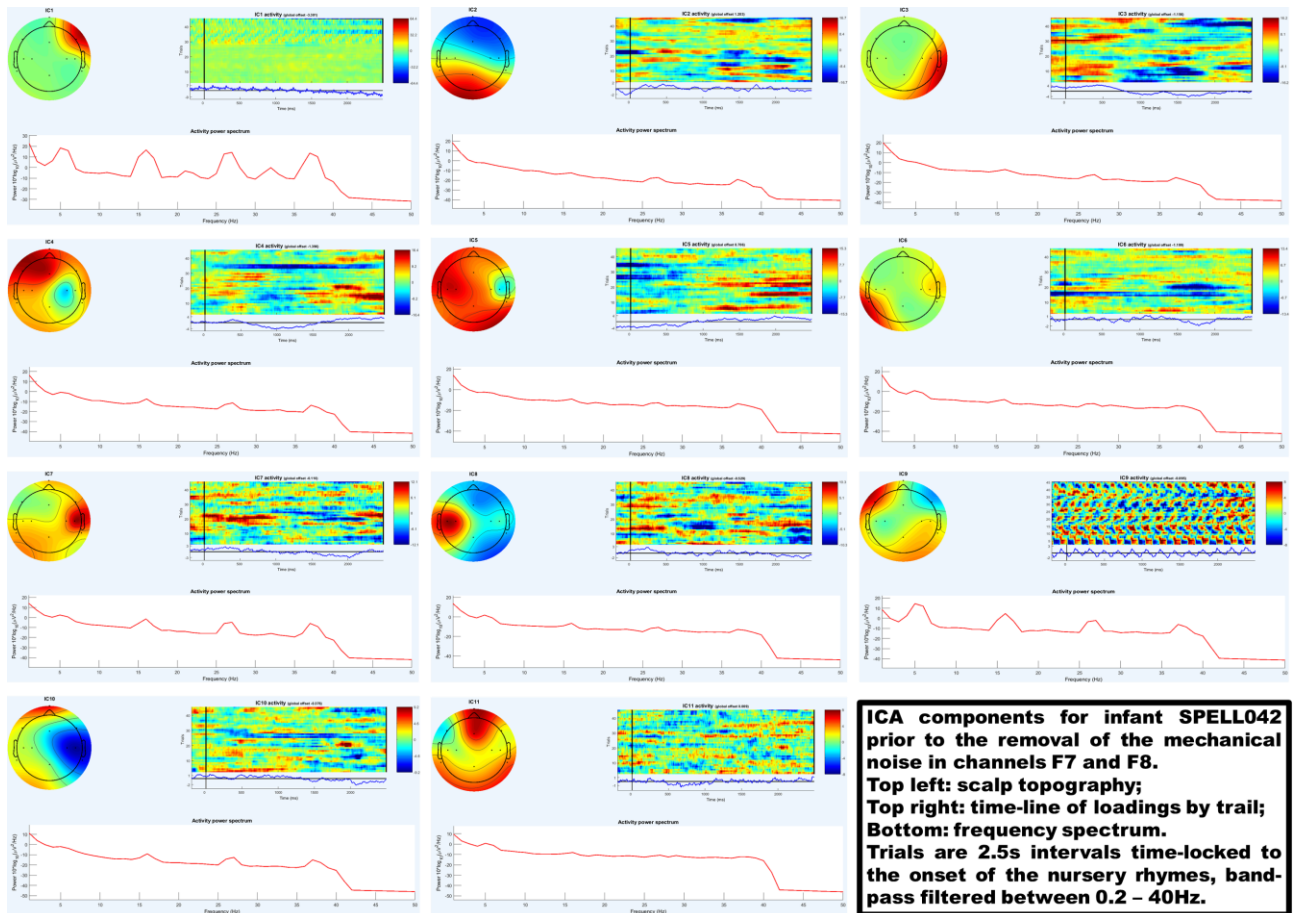


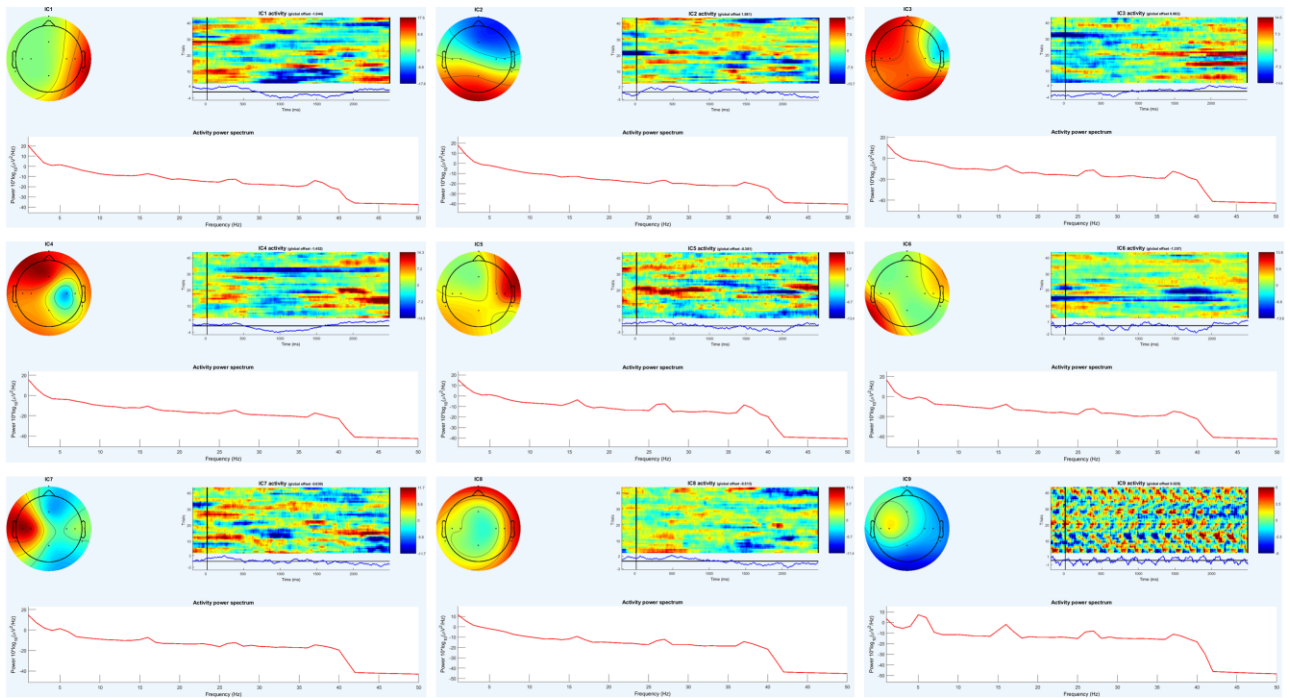
Figure III-2. The 11 orthogonal ICA components for the example infant's data in Figure III-1, computed inclusive of channels F7 & F8. For each component, the headmaps on the top left show the spatial scalp topographies of the component's loadings; the plot on the top right shows the component's timeline by epoch, time-locked to the onset of the nursery rhyme between  $-2s:2.5s$ . The plot at the bottom is the frequency spectrum of the component. The 6Hz noise and its harmonics can be seen affecting all components with different gravity.

ICA is one of the most frequently used techniques for removing artifactual components in adult EEG data but its use with infants is limited and rarely described (Georgieva et al., 2020; Noreika et al., 2020), and it is hardly possible to find published accounts of what neonatal neural components look like. Even in adult EEG pre-processing, using ICA as a cleaning tool, especially without a devoted artifact-detection channel, such as electro-oculogram for eye-blinks for example, is tricky and requires experience in noise pattern recognition. Researchers normally decide a-priori whether they would take a more conservative rejection approach when rejecting components and remove ICs that were certain to represent artifactual activity only, or a more broad-brush rejection strategy in which they only retain a certain predefined neural effect of interest. Neither strategy is

employed here as investigating neonatal ICs is beyond the scope of this doctoral project. Thus, here we did not use ICA here as an artifact rejection tool but merely as a data visualisation tool to establish the extent of effect of the 6Hz or the 8Hz noise on the channels and components comprising the datasets.

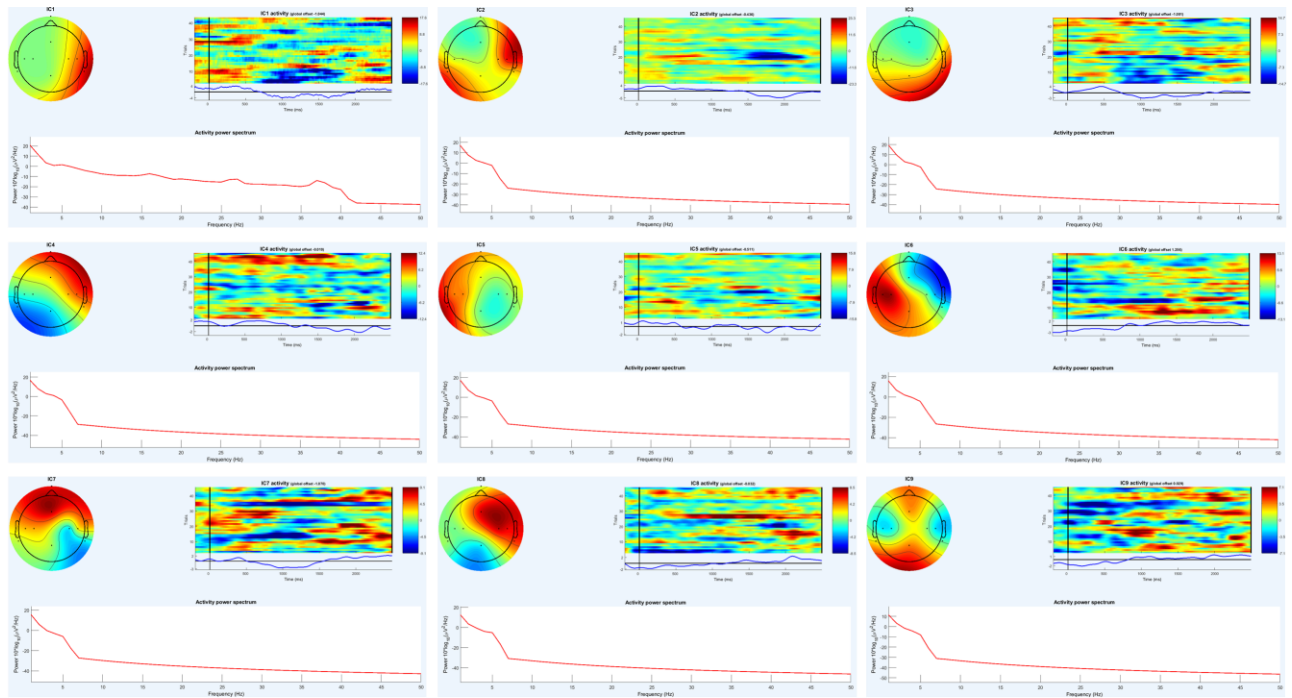
An example of this approach for the infant's dataset presented in *Figure III-1* is demonstrated in *Figure III-2, -3, -4* and *-5*. The original independent components prior to rejecting the noisy channels F7 and F8 were shown in *Figure III-2*. The loadings on ICs 1 and 9 especially were mostly contributed by the 6Hz noise and its harmonics, although it was evident that the rest of the ICs were potentially also affected, especially in the harmonic frequencies.

*Figure III-3* presents the ICs for the same dataset after removing channels F7 and F8 but without rejecting any components (there were only 9 components remaining as ICA always calculates at most as many components as channels were present in the recording). We could see that the most prominent 6Hz noise component IC1 was no longer present, as opposed to IC9 which notably had the lowest loading compared to the rest of the ICs. It can be speculated that this low power artifactual activity was still present because of the spillage effects depicted in the yellow rectangles in *Figure III-1* above. To check if this was indeed induced by the 6Hz noise (and its harmonics), we filtered the dataset under 5.025Hz and checked the ICs of the filtered signal in comparison (*Figure III-4*). It was reassuring to see that the components remaining under 5Hz resembled those extracted from the full .2-40Hz spectrum. As known from previous literature, neonatal EEG tends to be more heavily dominated by slower frequencies (Orekhova et al., 2006; Stroganova et al., 1999), especially when the data were recorded during quiet restfulness (Koolen et al., 2017; Noreika et al., 2020). Thus, it was unsurprising to see some of the major components such as ICs 1 to 3 were still present at this low bandpass cut-off.



**ICA components for infant SPELL042 after removing channels F7 and F8, affected by suspected mechanical noise. No ICAs have been removed. Top left: scalp topography; Top right: time-line of loadings by trial; Bottom: frequency spectrum. Trials are 2.5s intervals time-locked to the onset of the nursery rhymes, band-pass filtered between 0.2–40Hz.**

Figure III-3. The 9 remaining orthogonal ICA components for the example infant's data in Figure III-1, computed excluding channels F7 & F8. For each component, the headmaps on the top left show the spatial scalp topographies of the component's loadings; the plot on the top right shows the component's timeline by epoch, time-locked to the onset of the nursery rhyme between  $-2s:2.5s$ . The plot at the bottom is the frequency spectrum of the component. The 6Hz noise and its harmonics can still be seen in most components but compared to Figure III-2, they affect the lower components more, with the strongest effect seen in component 9.



**ICA components for infant SPELL042 after removing channels F7 and F8, affected by suspected mechanical noise. ICAs recalculated for under 6Hz. Top left: scalp topography; Top right: time-line of loadings by trail; Bottom: frequency spectrum. Trials are 2.5s intervals time-locked to the onset of the nursery rhymes, band-pass filtered between 0.2-5Hz.**

Figure III-4. The 9 remaining orthogonal ICA components for the example infant's data in Figure III-1, computed excluding channels F7 & F8, band-pass filtered at .2-5.25Hz. For each component, the headmaps on the top left show the spatial scalp topographies of the component's loadings; the plot on the top right shows the component's timeline by epoch, time-locked to the onset of the nursery rhyme between -.2s:2.5s. The plot at the bottom is the frequency spectrum of the component. The 6Hz noise and its harmonics can no longer be seen in the powerspectra.

Finally, to confirm that the 6Hz noise was orthogonal to the neural data (i.e. has a potential mechanical source that is fully separable from any neural sources), we took the opposite approach of removing the noise-bearing components IC1 and IC9 as seen in Figure III-2 (again for visualisation purposes only) and inspecting the reconstructed time-series data, in Figure III-5. The same five onset epochs nursery locked to the rhymes were plotted in the top panel of Figure III-5, now with the noise-bearing ICA's removed. Channels F7 and F8 were present in the dataset here and appear clean of the 6Hz noise. The spillage effects marked in the yellow rectangles in Figure III-1 seem to have also been mostly removed with rejecting the two noise-bearing components in this example infant.

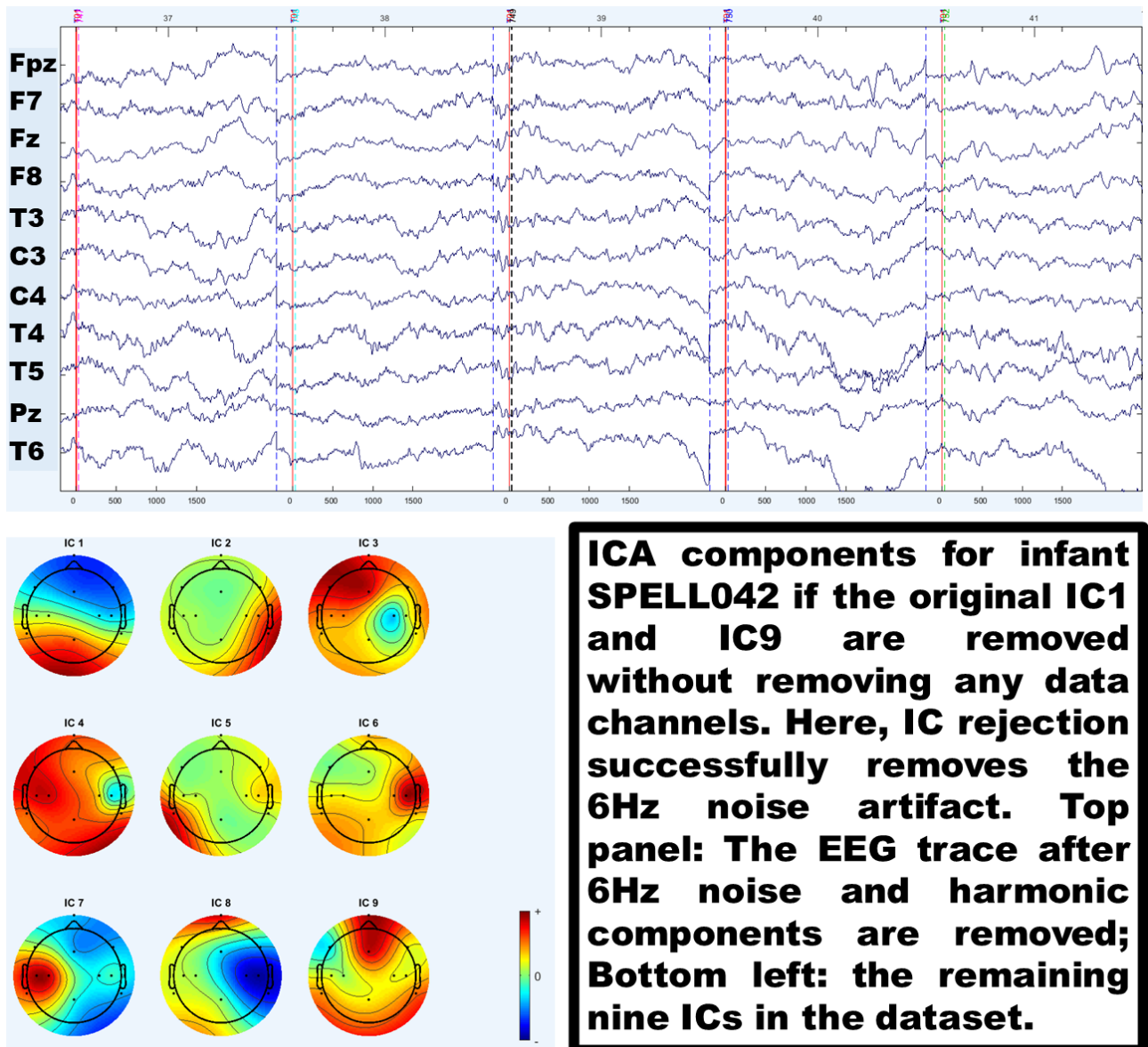


Figure III-5. The EEG timeseries (top) and 9 remaining orthogonal ICA components (bottom left) for the example infant's data in Figure III-1, plotted after rejecting the major noise-bearing components IC1 and IC9, as plotted in Figure III-2. For each component, the headmaps on the bottom left show the spatial scalp topographies of the component's loadings. The EEG timeseries show the same 5 onset epochs as Figure III-1.

The visual inspection quality-control procedure described here was performed for all 12 infants affected by the mechanical noise at 6Hz or 8Hz. To stress again, the datasets for those infants moving forward in the analyses had the affected channels removed, and no ICA rejection has been performed at any pre-processing step for the final datasets – this procedure was undertaken for purely visual inspection and quality control purposes only. An individual infant's dataset affected by the described mechanical noise was only retained

for further analysis if it contained identifiable neural components, and if the mechanical noise was only present above 6Hz. Only frequencies under 5Hz were analysed as the frequencies of interest for both the PLV and the GPDC analyses were at the average syllabic rate of the nursery rhymes between 2-4Hz.

---

### III.II Data Cleaning and Rejection by Individual Recording

*Table III-1. Detailed description of rejected and retained EEG data by infant. The first number in the epochs column identifies the number of epochs (trials) retained, while the numbers ensuing enlist the rejected trials. The first number(s) in the channels column indicate channels rejected in all retained epochs, while the numbers following that corresponded to channels rejected in individual epochs only. Infants grayed out were rejected due to not fitting eligibility criteria, or due to insufficient data recorded or remaining after artifact rejection.*

**Infant ID Total No of Epochs Retained / List of Rejected Epochs Channels Rejected in the Full Recording; / In Individual Epoch(s) Only**

SPELL001	52/ 17, 39, 47, 53, 55, 56	10 in all; /
SPELL002	42/ 1, 4, 17, 22, 24,	3 - missing; /7, 8, 10
SPELL003	52 /2;14; 20; 26; 36; 45	3 - missing; /1, 2, & 11
SPELL004	50 /1,2,5,6,18,29,32,40	none in all; /10 in a few; 1 in 2 epochs
SPELL005	No trigger information recorded in data	
SPELL006	No trigger information recorded in data	
SPELL007	27/ 2,3,6(missing),15,16,17,18,19,20,21,22,23,24,25,26,27,28,29,32,35,37,38,39,42,43,47,48,52,53,54,56	none in all; /11 in 1 epoch
SPELL008	51/ 5,6,11,26,29,37,49	none in all; /3 in 2 epochs
SPELL009	48/ 20,21,35,37,39,40,44,45,47,58	none
SPELL010	32/ 5,9,10,14,15,17,20,21,22,24,26,27,28,31,33,40,41,44,45,46,48,50,51,53,54,57	none in all; /1,2,3,11 in many epochs
SPELL011	46 /6,44,46,49,50,51,52,53,54,55,56,57	none in all; /1,9,10&11 in a few
SPELL012	36 /1,2,3,8,9,11,15,16,17,25,26,27,28,29,30,31,35,36,37,39,40,52,	none in all; /1,2,3 in many
SPELL013	52 /4,9,17,23,37,46	none in all; /1,3,4,9,11 in very few
SPELL014	49 /4,14,31,32,43,45,46,53,	none in all; /
SPELL015	41 /3,4,5,6,7,13,16,17,19,20,23,39,40,43,44,55,58	none
SPELL016	23 /1,2,3,4,5,7,8,11,13,14,16,17,18,19,20,21,22,26,28,30,31,33,34,36,37,40,41,42,43,44,46,48,49,50,51	none in all; /1,2,5&9 in many; 4,8,10&11 in a few
SPELL017	31 /2,3,4,5,6,9,12,13,14,16,17,18,21,22,23,24,26,27,28,29,30,31,32,36,37,38,40,47	none
SPELL018	38 /1,2,3,4,6,7,12,17,19,21,26,27,30,32,49,50,52,53,57,58	none
SPELL019	DATA NOT USEABLE - GRN must have been off but even filtered under 5Hz it is @500uV and synched;	chans 9 & 11 maybe there for 3 epochs and only under 5Hz
SPELL020	41 /4,6,7,8,18,24,29,34,39,40,45,47,48,52,53,57,58	3&10 in all; /1,2,4,5&6 in few, 11 in many
SPELL021	39 /1,4,6,7,8,9,11,12,13,14,15,16,18,23,26,34,36,52,54,	none in all; /2 in many; 1,3,4,7&9 in a couple
SPELL022	52 /5,6,23,44,49,	none in all; /1,2,9&11 in many; 3,4,&7 in a few
SPELL023	35 /	1 in all; /2, 3,4 & 11 in some
SPELL024	54 /27,33,36,37	none in all; /1,6,&10 in many; 2,3,9 in a few
SPELL025	49 /9,27,28,29,43,44,45,48,49	none in all; /1 in a few; 5,6,9 & 11 in a couple
SPELL026	43 /2,22,25,36,40,41,42,43,46,47,50,53,56,57,58	chan 6 in all; /1,4,5,11 in many; 2,3,7&10 in some
SPELL027	33 /3,9,11,12,13,15,20,23,24,26,27,28,30,34,35,37,38,39,40,45,46,51,52,53,56	chan 6 out; /1,8,9,11 in a few; 2,3,5,10 in a couple
SPELL028	47 /34,36,37,38,39,41,42,43,44,45,52,	none in all; /1,3,11 in many; 2,4,8,10 in one
SPELL029	53 /6,12,54,55,56	chan 6 out; /1 in a few; 2,3,5 in one
SPELL030	45 /17,18,21,27,28,37,41,44,45,48,50,52,56	none in all; /5,9,10,11 in many; 1,4,6 in few
SPELL031	46 /1,2,3,5,23,24,25,27,28,33,48,49	none in all; /1,3,6,7&8 in a couple
SPELL032	52 /46,51,52,53,55,58	none in all; /11 in 1 epoch
SPELL033	51 /7,8,10,11,33,34,58	9 in all; /1&3 in a few; 5,9,10 in a couple
SPELL034	45 /	none in all; /1,2,3,4, & 7 in 2 epochs
SPELL035	47 /1,4,8,32,36,41,42,43,47,51,53,	none in all; /1&6 in a few; 2,4,5,7,8,9 & 11 in one
SPELL036	43 /17,18,19,20,32,34,38,42,49	9 in all; /6 in almost all; 1-5,7,8&11 in one or two
SPELL037	39 /1,5,6,7,12,14,16,17,18,26,39,40,41,46,51,52,54,56,57	none in all; /10&11 in many; 1,2,5,8,9 in few
SPELL038	49 /2,3,9,26,27,29,39,52,53	none in all; /11 in many; 2,8,9,&10 in one or two
SPELL039	48 /1,3,4,5,6,17,37,40,53,55	7 and 11 in all; /1&10 in many; 3&9 in a few; 2,4,5&8 in a couple
SPELL040	49 /1,6,19,22,45,46,50,53,58	none in all; 1&3 in many; 2,4,5,6&9 in a few
SPELL041	34 /1,12,13,14,16,20,21,24,26,27,28,31,32,35,36,38,40,44,45,47,48,53,54,58	2 in all; /4,7,8&11 in a few; 1,3,5,6&9 in one or two
SPELL042	46 /1,2,3,4,8,22,30,31,32,45,46,58	none in all (though see notes); /4 in many; 1,2,3,5,6,7 in one; 9 & 11 in a few
SPELL043	43 /3,8,12,14,15,17,19,20,28,29,35,38,39,45,49,	none in all; 7,8&11 in a few; 1,3,4,6,9,10 in one or two
SPELL044	46 /3,5,7,8,12,18,19,32,33,42,48,52,	none in all (though see notes); /6 in many; 1,2,3,4,5,7,8,9&11 in b/n 1-3 nrs
SPELL045	47 /	none in all; /10&11 in a few; 2,3,8,&9 in 2 epochs
SPELL046	39 /1,2,6,9,10,13,14,15,16,17,18,25,26,27,28,32,34,43,49,	2 in all; /4,7,9&11 in many; 1,3,5,6,7 in b/n 1-3 nrs
SPELL047	48 /1,2,3,7,17,31,32,39,44,50,	2 in all; /9&11 in many; 4,5,6,7&8 in one
SPELL048	57 /56	2&3 in all; /1&11 in many; 4,8,9,10 in one or two
SPELL049	30 /2,5,6,7,8,13,18,19,20,21,22,26,32,34,35,39,40,43,44,46,48,49,50,51,52,55,56,58	1,4&5 in all; /2,3,7,8&11 in many; 1,6 & 9 in fewer
SPELL050	15/8,12,13,14,15,16,17,18,19,20,21,22,23,24,26,27,28,30,31,32,33,34,35,36,37,38,39,40,41,43,44,45,46,4	none in all but see notes; /5 in many; 1,2,3,4&11 in one
SPELL051	51 /2,4,5,6,7,16,46	5 in all; 7 in most, 4,6,8,11 in a couple
SPELL052	Baby did not produce any useable data!	
SPELL053	23 /1,2,3,5,7,8,10,11,12,13,14,15,16,17,18,23,27,28,29,38,40,42,45,46,47,49,50,51	none in all; /1,2,9,10 & 11 in many; 3:8 in 1:3 channels
SPELL054	Baby did not produce any useable data!	
SPELL055	Baby did not produce any useable data! - even below 5Hz and with re-referencing. GND most likely was not set up properly	
SPELL056	29 /2,3,4,7,8,9,16,17,18,19,24,25,26,29,33,34,35,36,37,39,43,50,51,52,53,55	none in all; /3,5,6,9&11 in many; 4,7,8,10 in a few; 2 in two
SPELL057	39 /9,13,14,15,16,20,21,22,23,24,25,29,35,36,41,44,50, 51,58	none in all; /11 in many; 1,3,4,5,6,9&10 in a few
SPELL058	8 /2,5,6,8,12,13,14,15,17,18,19,20	none in all; /6,9&10 in one or two
SPELL059	51 /1,2,3,4,6,8,9,10,11,12,13,14,15,16,17,18,19,20,21,22,24,26,27,28,29,30,31,32,33,34,35,36,37,38,39,40,4	chan 1 in all; 11 in 1 & 4
SPELL060	1,42,43,44,45,46,47,48,49,50,51,52,53,54,55,56,57	none in all; 10 & 11 in one or two
SPELL061	51 /1,2,6,7,31,46,56	chan7 in all; 4&6 in one/two
SPELL062	8 /1,2,7,8,9,10,11,12,13,15,19,20,21,22,23,24,25,26	none in all; 7 in most; 2&3 in many; 1,6,8,9,10,11 in a few
SPELL063	35 /1,2,6,9,10,11,12,13,14,15,16,17,19,20,24,25,27,28,40,41,44,47,54	none in all; 1,2,5,7:11 in only b/n 1-3 epochs
SPELL064	47 /5,6,7,24,27,28,31,39,42,49,51	none in all; 1,2,3,6,&7 in many; 4,5,8,9,11 in a few
SPELL065	39 /3,4,5,6,10,16,17,18,19,21,22,23,30,33,47,53,56,57,58	none in all; 6,7,8,11 in many; 2,5,9,10 in a couple
SPELL066	15 /2,5,6,7,11,13,14,16,19,22,23,24,26,27,30,31,32,33,34,35	
SPELL066	Baby did not produce any useable data!	
SPELL067	52 /11,20,33,51,52,58	none in all (though see notes re chan 7!); 7 in many; 1,2,5,8,9,10&11 in a couple
SPELL068	41 /4,8,10,13,19,21,22,26,27,33,40,41,42,43,51,52,53,	none in all; 7 in many; all others in a couple only
SPELL069	48 /1,12,13,20,21,32,41,45,54,57	none in all; 9 in many; 1,2,3,4,5,6,7,8&11 in a couple only
SPELL070	28 /5,7,14,15,16,18,20,23,28,29,33,34,35,36,37,38,40,41,43,44,45,47,48,49,50,52,53,54,55,58	none in all;
SPELL071	32 /5,6,7,11,12,13,16,17,18,19,21,27,28,29,30,31,35,36,40,41,46,47,48,49,53	
SPELL072	50 /1,2,17,23,24,25,41,45	none in all; 1,2,3,4,6,7,8,10,11 in only a couple
SPELL073	36 /4,11,12,15,18,20,21,28,29,31,32,33,36,45,46,47,48,50,51,52,53,55,	
SPELL074	45 /1,3,4,5,6,8,14,15,17,19,24,35,43	none in all; /3 in many; 1,2,4,5,6,7,8,9,10&11 in a couple
SPELL075	57 /46	none
SPELL076	56 /4,58	none in all; 1,5,7,8,9,10,11 in a couple
SPELL077	43 /4,5,6,9,10,11,23,25,29,30,35,37,38,42,48	none in all; 3,4,6,9,10 in a couple only
SPELL078	48 /11,16,19,28,30,35,47,54,55,58	none in all; 4&9 in many; 1,2,5,6,7,8,10&11 in a couple
SPELL079	48 /8,11,13,27,29,39,44,48,55,57	none in all; 1,2,3,4,5,8,9,11 in a couple only
SPELL080	52 /17,34,37,39,41,43	none in all; 2,3,4,5,6,7,8&11 in a couple only
SPELL081	49 /3,4,26,32,36,40,47,56,57	none in all; 9 in many; 4,5,&11 in one or two
SPELL082	37 /2,3,5,6,7,9,10,11,18,20,22,23,29,30,38,39,40,43,44,52,58	none in all; 1,3,4&11 in a couple
SPELL083	50 /5,7,24,25,48,55,56,58	none in all; 6&7 in a few; 2,4,5,8,9,10&11 in one or two
SPELL084	51 /2,3,4,5,13,18,54	none in all; 7 in a few; 1,8,11 in one or two
SPELL085	34 /	
SPELL086	37 /2,3,5,7,8,10,12,15,17,23,25,26,27,32,33,34,35,37,54,55,57	none in all; 1,2,3,4,7,9,10&11 in some
SPELL087	34 /10,11,15,17,18,19,20,21,25,27,28,29,30,35,36,37,38,39,40,44,45,48,49,52	none in all; 1,2,3&4 in some
SPELL088	34 /5,6,7,11,15,16,17,,19,20,22,31,32,40,43,44,45,47,50,53,54,55,56,57,58	none in all; 1,3,4,5,6&9 in few; 7,8&11 in many
SPELL089	46 /	6 in most; /1&9 in a couple
SPELL090	33 /1,2,7,8,9,18,19,22,24,27,28,29,30,32,36,37,39,41,49,52,54,55,56,57,58	none in all; /1,2,3 & 5 in many
SPELL091	3 /1,2,6	5 in all; all rest ok
SPELL092	17/4,5,9,10,11,12,14,15,16,17,19,20,21,22,23,24,25,26,28,29,31,34,35,37,39,40,41,42,43,44,46,49,50,52,5	1,4,5,6,7,8&10 in all, 9&11 in most; baby had only two viable channels in the whole recording - 2&3
SPELL093	35 /11,15,17,25,26,27,28,29,31,33,34,35,36,39,40,41,42,43,44,47,56,57,58	6,7 in all; /2,3,4,10&11 in many
SPELL094	47 /25,26,33,42,44,45,54,55,56,57	none in all; /5,7,9,11 in a few; 1,2,3,8,10 in a couple
SPELL095	48 /9,11,13,15,17,31,32,33,42,43	none
SPELL096	27/	none in all; /3,6,9,11
SPELL097	49 /19,20,42,43,44,45,49,54,58	none
SPELL098	30 /2,4,5,7,11,13,14,15,17,18,19,20,21,22,23,28,29,30,31,32,36,38,39,40,43,46,48,56	none in all; /1-9 & 11 in many
SPELL099	52/	1 in all; /8 in some, 3 in 2 epochs
SPELL100	37 /1,2,3,4,5,6,7,8,9,10,11,12,13,15,28,37,44,45,46,47,58	none in all; /7 & 3 in many, 2&4 in one

### III.III Nursery Rhymes Used in Analyses

23 unique NRs by 6 different female speakers were used for all analyses. *Table III-1* details the nursery rhymes by speaker.

*Table III-2. Detailed description of the nursery rhymes included in the analyses, derived from the corpus metadata: [https://figshare.com/articles/SAMPH\\_CDS/1318572](https://figshare.com/articles/SAMPH_CDS/1318572) (Leong & Goswami, 2015).*

List of Nursery Rhymes In the Analysis						Speaker 1 CDS		Speaker 2 CDS		Speaker 3 CDS		Speaker 4 CDS		Speaker 5 CDS		Speaker 6 CDS		
File No	Nursery Rhyme	Music Time Signat	Rhyth mic Meter	No lines	Repeti tions	Total No Syll	Length (s)	Rate (syll/sec)	Length (s)	Rate (syll/sec)								
1	Baa Baa Black Sheep	2/4	Duple	5	2	76									27.2	2.8		
2	Once I Caught a Fish Alive	4/4	Duple	6	2	106			39.2	2.7			43.9	2.4				
4	Old MacDonald Had a Farm	4/4	Duple	8	2	118									32.5	3.6		
5	Twinkle Twinkle Little Star	4/4	Duple	9	2	84	31.8	2.6										
6	London Bridge is Falling Down	4/4	Duple	10	1	72			24.5	2.9								
7	Mary Had a Little Lamb	4/4	Duple	11	1	111	35.5	3.1	29.9	3.7								
8	Polly Put the Kettle On	2/4	Duple	12	2	102			26.1	3.9			38	2.7			28.1	3.6
11	Mary Mary Quite Contrary	4/4	Duple	15	3	90			24.3	3.7	28.2	3.2	34.3	2.6				
12	Simple Simon Met a Pieman	4/4	Duple	16	2	116	34.3	3.4										
15	Lucy Lockett	4/4	Duple	19	3	84	24.1	3.5										
16	Cobbler Cobbler Mend My Shoe	4/4	Duple	20	3	84	32.3	2.6					36.1	2.3	28.9	2.9		
18	I'm a Little Teapot	4/4	Duple	22	3	96	39.5	2.4										
19	Sing a Song of Sixpence	2/4	Duple	23	1	97	26.6	3.6			24.8	3.9						
20	Wee Willie Winkie	2/4	Duple	24	2	84	24.8	3.4	25.1	3.3	22.9	3.7					23.9	3.5
22	The Wheels on the Bus	4/4	Duple	26	1	54	19.8	2.7	18.8	2.9	20.2	2.7	24.3	2.2			19.5	2.8
23	Three Little Monkeys	N.A.	Duple	27	1	111	34	3.3	33.2	3.3			39.5	2.8	43.3	2.6		
24	Grand Old Duke of York	4/4	Duple	28	1	62	16.7	3.7	17.5	3.5			18.9	3.3				
25	Incy Wincy Spider	6/4	Duple	29	2	92	30.6	3	31.8	2.9							38	2.4
26	Jack and Jill	6/4	Duple	30	3	84			25.2	3.3	26.9	3.1						
27	Humpty Dumpty	6/4	Duple	31	3	108	30.9	3.5	27.1	4	29.1	3.7	36	3				
28	Ring-a-Ring-a-Roses	6/4	Duple	32	3	69	22.6	3.1	23.6	2.9	22.1	3.1	24.8	2.8	19.7	3.5		
29	Row Row Row Your Boat	6/4	Duple	33	1	81	23.1	3.5	24.1	3.4					21.5	3.8	30.5	2.7
30	Hickory Dickory Dock	6/4	Duple	34	3	84	23.2	3.6					32.6	2.6				

## Appendix IV

### IV. I Negative PLV onset peak latencies.

Collectively across all infants, channels, and nursery rhymes onset epochs, between 20-25% of all PLV peaks measured in the onset time-window between  $-2:2.5$ s around the stimulus presentation, had a negative or a zero latency. Thus, only 75% of all trials above any of the tested surrogate thresholds have a positive latency. In practice, this means that the highest phase-locking value between the EEG and the speech envelope of the nursery rhyme in 25% of the cases occurred prior to stimulus onset. Essentially, the distribution of phase differences between the speech and EEG time series within those trials were clustered more when time points prior to the stimulus onset were included, compared to when they were not. As we noted in *Chapter 3 Methods*, some of the neonatal recordings have delayed timing issues with an estimated average of about 49ms. This means that we have a reason to suspect that at least some of the negative PLV peak latencies occurring within 50ms prior to the indicated nursery rhyme onset could be misplaced in time and could in reality have occurred within the first 50ms during the stimulus presentation. However, this explanation does not seem to fit fully the data. The negative PLV peak latencies in the range of  $-60:0$ ms (11% of all detected PLV peaks at the 97.5% individual surrogate threshold and nearly half of all negative peaks detected at the same threshold) are present for 64 infants, that is nearly all infants contributing to the PLV paper dataset (N=86), for most of whom we have either no reason to suspect timing delay issues or have confirm that there were none. Additionally, both infants with and without suspected timing issues, have the same range of negative PLV latencies for this time-window, between 1 to 5 negative peak latencies per individual infant. Finally, the other half of the negative PLV peaks had an even earlier latency of between  $-200:-60$ ms, and these could not be readily contributed to late trigger issues. These earlier peaks represent 15% of the total PLV peak count and are again generated by nearly all infants in the dataset (65 individuals, ranging between 1 to 7 peaks per individual infant).

Due to the trigger delay issues in some infants, all PLV peaks occurring within  $-/+50$ ms around stimulus onset were not included in the main PLV analyses. To test whether the negative PLV peak latencies were due to another variable, such as the time lapse since the previous nursery rhymes was presented and whether the syllabic rhythm of the previous nursery rhyme accounted for the distribution of the negative times (i.e. due to potential

entrainment effects if the inter-trial interval (ITI) lasted <1s), regression analyses were ran on the negative PLV peak latencies, described below. No significant effects were found, however.

***Regression effect of the inter-trial interval to the previous nursery rhyme on the negative PLV peak latencies***

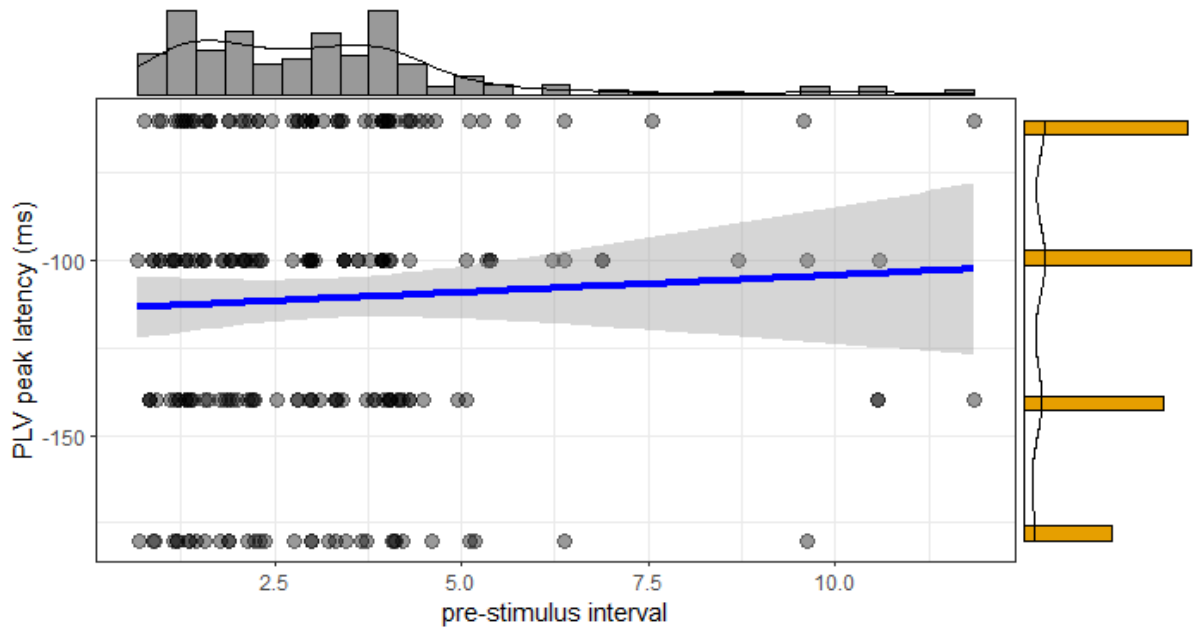
We could not find any relationship between the interval since the previous nursery rhyme and the latency of the PLV peak, whether I look at it in a simple regression model, or in a Best Subset regression with the other descriptive variables: INFANTID, the syllabic rate of the current or the previous nursery rhyme, the number of contributed nursery rhymes by the infant, the channel or the infant's parental risk status. There was still no effect if we only look at the negative latencies. The Figures below show the simple regression coefficients between the inter-trial interval and the peak latency for all latencies, and for the negative latencies only.

There were potentially other influences at play that we did not account for here. The option remained that some processes of anticipation or entrainment were at play. It was also possible that there were still other delays in the EEG triggering system which we were not aware of – this possibility would be very difficult to refute conclusively at this stage. There was also the option of intrinsic noise in the PLV measurements, or in fact, in the underlying neural activity. Unfortunately, again, there are not many PLV peaks of negative latency reported priorly, so it is difficult to generate predictions of possible causes based on previous literature.

**A)**

The Effect of the Pre-stimulus Interval on the Latency of the PLV pe

$t_{\text{Student}}(213) = 0.87, p = 0.387, \hat{r}_{\text{Winsorized}} = 0.06, \text{CI}_{95\%} [-0.08, 0.19], n_{\text{pairs}} = 215$



**B)**

The Effect of the Pre-stimulus Interval on the Latency of the PLV pe

$t_{\text{Student}}(1007) = 1.04, p = 0.300, \hat{r}_{\text{Winsorized}} = 0.03, \text{CI}_{95\%} [-0.03, 0.09], n_{\text{pairs}} = 1,009$

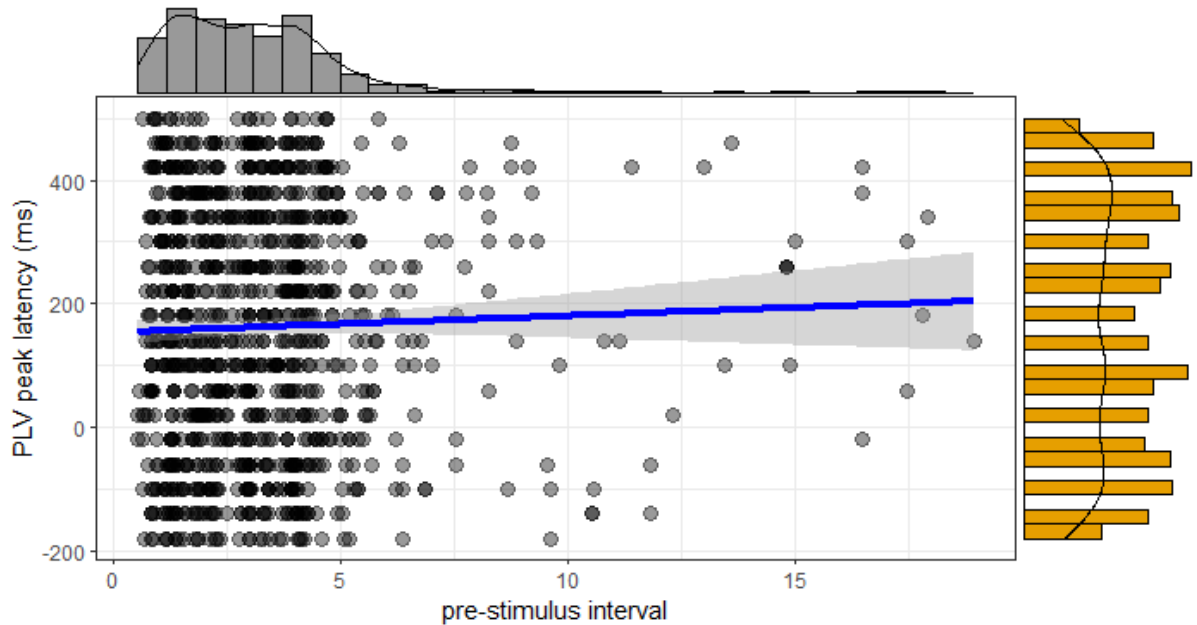


Figure IV-1. A scatterplot of negative PLV onset latencies against the ITI from the previous nursery rhyme (A); a scatterplot of the positive and negative PLV onset latencies against the ITI (B). The bars against the axes are histograms of the PLV onsets (y axis) and the ITI (x axis). The blue line is the fitted regression line, with the 95% confidence intervals shaded in gray.

## IV.II Exploratory Regression Analysis based on the 98% Surrogate Threshold.

As the retrospective power analysis of the effects of familial risk on the latency of the PLV onset peaks identified that thresholding over 98% of the surrogate distribution had the highest power of effect (N=84-1=83, 43 at low risk), the exploratory regression analyses were also run for the 98% threshold.

For the strength of the PLV peaks, the backward stepwise regression identified two DCDC2 SNPs to significantly predict the peak PLV values: rs807701 at  $F_{(2,78)}=4.01$ ,  $p<.023$ ,  $\eta^2 = .09$ ; and rs793842 at  $F_{(2,78)} = 3.25$ ,  $p<.044$ ,  $\eta^2 = .08$ . The model with three variables was significant at  $F_{(4,78)} = 2.51$ ,  $p<.049$ ,  $R^2_{adj} = .069$ . Five factors were selected as the best subset, with the same two DCDC2 SNPs significantly predicting the distribution of PLV onset peaks in this model: rs807701 at  $F_{(2,78)}=4.85$ ,  $p<.011$ ,  $\eta^2 = .12$ ; and rs793842 at  $F_{(2,78)} = 3.62$ ,  $p<.032$ ,  $\eta^2 = .09$ . The full model with five variables was not significant at  $F_{(10,72)} = 1.91$ ,  $p=.057$ ,  $R^2_{adj} = .100$  (Table IV-1 below).

For the latency of the PLV onset peaks above the 98% surrogate distribution threshold, the backward stepwise regression retained two factors, with one significantly predicting the latency values: Parental Risk at  $F_{(2,78)}=7.28$ ,  $p<.002$ ,  $\eta^2 = .16$ ; and one non-significant with a small effect size at rs9853895 (ROBO1)  $F_{(2,78)} = 3.02$ ,  $p=.055$ ,  $\eta^2 = .07$ . The model with three variables was significant at  $F_{(4,78)} = 4.80$ ,  $p<.002$ ,  $R^2_{adj} = .157$ . The best subset model comprised five factors in total, with two of them significantly predicting the latency values: Parental Risk at  $F_{(2,72)}=7.60$ ,  $p<.001$ ,  $\eta^2 = .17$ ; rs9853895 (ROBO1) at  $F_{(2,72)} = 3.81$ ,  $p<.027$ ,  $\eta^2 = .10$ ; and the second ROBO1 SNP rs333491 was not significant at  $F_{(2,78)}= 2.70$ ,  $p=.074$ . This model with five variables was significant at  $F_{(10,72)}= 3.16$ ,  $p<.003$ ,  $R^2_{adj} = .209$ .

Table IV-1. Results from the regression models for the two dependent variables: the latency and strength of the normalized PLV onset peaks at above 98% of the surrogate threshold distribution.

<b>PLV Peak Latency</b>	<b>Stepwise backward removal [.05-.10]</b>	<b>Best Subset based on Adj R<sup>2</sup></b>
<b>N vars in the model</b>	1	5
<b>Variables at p&lt;.05</b>	Parental Risk: $F_{(2,78)}=7.28, p<.002$ ; rs9853895: $F_{(2,78)}=3.02, p=.055$ .	Parental Risk: $F_{(2,72)}=7.60, p<.001$ ; rs9853895: $F_{(2,72)}=3.81, p<.027$ ; rs333491: $F_{(2,72)}=2.70, p=.074$ .
<b>Variance explained (Adj R<sup>2</sup>)</b>	15.65%	20.86%

<b>PLV Peak Strength</b>	<b>Stepwise backward removal [.05-.10]</b>	<b>Best Subset based on Adj R<sup>2</sup></b>
<b>N vars in the model</b>	2	5
<b>Variables at p&lt;.05</b>	rs807701: $F_{(2,78)}=4.01, p<.023$ ; rs793842: $F_{(2,78)}=3.25, p<.044$ .	rs807701: $F_{(2,72)}=4.85, p<.011$ ; rs793842: $F_{(2,72)}=3.62, p<.032$ .
<b>Variance explained (Adj R<sup>2</sup>)</b>	6.88%	10.03%

### IV.III The Family of LME models describing the top 1% variance explained against the lowest information criteria (continued from the main text)

Tables IV-2 And IV-3 below, show the fixed effects parameters in the most parsimonious models according to the B/AIC (B1) and (A1), as identified in the main text:

Table IV-2. Fixed effects coefficients in the most parsimonious model according to the BIC (model B1 in the main text).

<b>LME Model (B1): Fixed effects coefficients (95% CIs)</b>							
<b>Name</b>	<b>Estimate</b>	<b>SE</b>	<b>tStat</b>	<b>DF</b>	<b>pValue</b>	<b>Lower</b>	<b>Upper</b>
'(Intercept)'	263.10	9.74	27.01	704	0.000	243.97	282.22
'ParentOfOrg_M'	49.28	18.54	2.66	704	0.008	12.87	85.68
'ParentOfOrg_F'	9.40	15.20	0.62	704	0.537	-20.44	39.24

Table IV-3. Fixed effects coefficients in the most parsimonious model according to the AIC (model A1 in the main text).

<b>LME Model (A1): Fixed effects coefficients (95% CIs)</b>							
<b>Effect</b>	<b>Estimate</b>	<b>SE</b>	<b>tStat</b>	<b>DF</b>	<b>pValue</b>	<b>Lower</b>	<b>Upper</b>
'(Intercept)'	226.60	26.51	8.55	701	0.000	174.56	278.65
'rs333491'	-14.34	8.66	-1.66	701	0.098	-31.34	2.65
'rs9853895'	26.90	9.83	2.74	701	0.006	7.59	46.20
'Gender_M'	20.67	13.21	1.56	701	0.118	-5.27	46.61
<b>ParentalRisk_M'</b>	<b>51.56</b>	<b>17.43</b>	<b>2.96</b>	<b>701</b>	<b>0.003</b>	<b>17.35</b>	<b>85.77</b>
ParentalRisk_F'	22.58	14.99	1.51	701	0.132	-6.85	52.00

Furthermore, the tables of fixed effects coefficients of the two most parsimonious models identified amongst the top 1% of models with the highest variance explained as measured by  $R^2$  (B2 and A2 in the main text), are shown below.

Table IV-4. Fixed effects coefficients in the most parsimonious model according to the BIC at the top 1% of  $R^2$  values (model B2 in the main text).

<b>LME Model (B2): Fixed effects coefficients (95% CIs)</b>							
<b>Name</b>	<b>Estimate</b>	<b>SE</b>	<b>tStat</b>	<b>DF</b>	<b>pValue</b>	<b>Lower</b>	<b>Upper</b>
'(Intercept)'	<b>352.35</b>	<b>105.78</b>	<b>3.33</b>	<b>665</b>	<b>0.001</b>	<b>144.65</b>	<b>560.06</b>
'CH_'C4''	-236.95	141.20	-1.68	665	0.094	-514.20	40.30
'CH_'Pz''	-36.74	135.06	-0.27	665	0.786	-301.93	228.45
'CH_'T3''	-77.67	137.17	-0.57	665	0.571	-347.01	191.67
'CH_'T4''	<b>-368.54</b>	<b>138.16</b>	<b>-2.67</b>	<b>665</b>	<b>0.008</b>	<b>-639.82</b>	<b>-97.25</b>
'CH_'T5''	51.07	132.92	0.38	665	0.701	-209.93	312.08
'CH_'T6''	-90.04	145.52	-0.62	665	0.536	-375.76	195.69
'rs9853895'	-21.02	24.89	-0.84	665	0.399	-69.90	27.86
ParentalRisk_M'	56.75	50.62	1.12	665	0.263	-42.65	156.14
ParentalRisk_F'	-11.50	28.79	-0.40	665	0.690	-68.04	45.03
'BirthWeight'	-0.03	0.03	-1.21	665	0.226	-0.08	0.02
'nrs'	8.54	4.96	1.72	665	0.086	-1.20	18.28
'CH_'C4':rs9853895'	45.72	31.72	1.44	665	0.150	-16.56	108.00
'CH_'Pz':rs9853895'	<b>60.07</b>	<b>30.28</b>	<b>1.98</b>	<b>665</b>	<b>0.048</b>	<b>0.62</b>	<b>119.52</b>
'CH_'T3':rs9853895'	33.70	28.80	1.17	665	0.242	-22.86	90.25
'CH_'T4':rs9853895'	<b>83.39</b>	<b>30.92</b>	<b>2.70</b>	<b>665</b>	<b>0.007</b>	<b>22.69</b>	<b>144.10</b>
'CH_'T5':rs9853895'	<b>60.42</b>	<b>29.58</b>	<b>2.04</b>	<b>665</b>	<b>0.041</b>	<b>2.34</b>	<b>118.50</b>
'CH_'T6':rs9853895'	20.87	32.21	0.65	665	0.517	-42.37	84.11
CH_'C4':ParentalRisk_M'	-60.86	60.38	-1.01	665	0.314	-179.41	57.70
CH_'Pz':ParentalRisk_M'	5.51	62.05	0.09	665	0.929	-116.33	127.34
CH_'T3':ParentalRisk_M'	-5.06	57.02	-0.09	665	0.929	-117.02	106.90
CH_'T4':ParentalRisk_M'	6.10	60.99	0.10	665	0.920	-113.66	125.86
CH_'T5':ParentalRisk_M'	-9.94	57.34	-0.17	665	0.862	-122.53	102.65
CH_'T6':ParentalRisk_M'	-8.63	59.71	-0.14	665	0.885	-125.87	108.62
CH_'C4':ParentalRisk_F'	37.77	41.16	0.92	665	0.359	-43.05	118.59
CH_'Pz':ParentalRisk_F'	30.55	39.74	0.77	665	0.442	-47.48	108.58
CH_'T3':ParentalRisk_F'	-12.03	35.75	-0.34	665	0.737	-82.23	58.16
CH_'T4':ParentalRisk_F'	31.40	36.43	0.86	665	0.389	-40.13	102.93
CH_'T5':ParentalRisk_F'	48.10	38.40	1.25	665	0.211	-27.30	123.50
CH_'T6':ParentalRisk_F'	32.07	39.42	0.81	665	0.416	-45.33	109.47
'CH_'C4':BirthWeight'	0.06	0.04	1.69	665	0.091	-0.01	0.13
'CH_'Pz':BirthWeight'	0.01	0.04	0.23	665	0.822	-0.06	0.08
'CH_'T3':BirthWeight'	0.03	0.03	0.91	665	0.361	-0.04	0.10
'CH_'T4':BirthWeight'	<b>0.09</b>	<b>0.04</b>	<b>2.38</b>	<b>665</b>	<b>0.018</b>	<b>0.02</b>	<b>0.16</b>
'CH_'T5':BirthWeight'	-0.03	0.03	-0.94	665	0.349	-0.10	0.03
'CH_'T6':BirthWeight'	0.04	0.04	1.22	665	0.225	-0.03	0.12
'CH_'C4':nrs'	-8.57	6.54	-1.31	665	0.190	-21.42	4.27
'CH_'Pz':nrs'	<b>-15.29</b>	<b>6.57</b>	<b>-2.33</b>	<b>665</b>	<b>0.020</b>	<b>-28.19</b>	<b>-2.39</b>
'CH_'T3':nrs'	-11.05	5.94	-1.86	665	0.063	-22.72	0.62
'CH_'T4':nrs'	-9.58	6.58	-1.45	665	0.146	-22.51	3.35
'CH_'T5':nrs'	-6.80	5.99	-1.14	665	0.256	-18.56	4.96
'CH_'T6':nrs'	<b>-13.70</b>	<b>6.40</b>	<b>-2.14</b>	<b>665</b>	<b>0.033</b>	<b>-26.26</b>	<b>-1.14</b>

Table IV-5. Fixed effects coefficients in the most parsimonious model according to the AIC at the top 1% of  $R^2$  values (model B2 in the main text).

<b>LME Model (A2): Fixed effects coefficients (95% CIs)</b>							
<b>Name</b>	<b>Estimate</b>	<b>SE</b>	<b>tStat</b>	<b>DF</b>	<b>pValue</b>	<b>Lower</b>	<b>Upper</b>
'(Intercept)'	<b>533.59</b>	<b>117.47</b>	<b>4.54</b>	<b>656</b>	<b>0.000</b>	<b>302.92</b>	<b>764.25</b>
'CH_'C4''	<b>-292.27</b>	<b>140.11</b>	<b>-2.09</b>	<b>656</b>	<b>0.037</b>	<b>-567.39</b>	<b>-17.15</b>
'CH_'Pz''	-50.56	134.20	-0.38	656	0.706	-314.07	212.94
'CH_'T3''	-100.13	136.56	-0.73	656	0.464	-368.28	168.02
'CH_'T4''	<b>-399.94</b>	<b>138.00</b>	<b>-2.90</b>	<b>656</b>	<b>0.004</b>	<b>-670.91</b>	<b>-128.96</b>
'CH_'T5''	45.10	132.75	0.34	656	0.734	-215.56	305.77
'CH_'T6''	-98.90	145.11	-0.68	656	0.496	-383.83	186.03
'rs333491'	<b>-75.77</b>	<b>27.23</b>	<b>-2.78</b>	<b>656</b>	<b>0.006</b>	<b>-129.23</b>	<b>-22.31</b>
'rs9853895'	-28.07	24.19	-1.16	656	0.246	-75.57	19.43
<b>Sex_M'</b>	<b>44.68</b>	<b>13.76</b>	<b>3.25</b>	<b>656</b>	<b>0.001</b>	<b>17.66</b>	<b>71.69</b>
ParentalRisk_M'	-293.28	161.71	-1.81	656	0.070	-610.82	24.26
ParentalRisk_F'	-1.53	117.29	-0.01	656	0.990	-231.83	228.77
<b>'BirthWeight'</b>	<b>-0.05</b>	<b>0.03</b>	<b>-2.03</b>	<b>656</b>	<b>0.043</b>	<b>-0.11</b>	<b>0.00</b>
'nrs'	-5.32	7.97	-0.67	656	0.505	-20.97	10.33
'CH_'C4':rs9853895'	52.61	31.44	1.67	656	0.095	-9.13	114.35
'CH_'Pz':rs9853895'	<b>59.25</b>	<b>29.97</b>	<b>1.98</b>	<b>656</b>	<b>0.048</b>	<b>0.40</b>	<b>118.09</b>
'CH_'T3':rs9853895'	33.29	28.60	1.16	656	0.245	-22.87	89.44
'CH_'T4':rs9853895'	<b>88.39</b>	<b>30.68</b>	<b>2.88</b>	<b>656</b>	<b>0.004</b>	<b>28.16</b>	<b>148.62</b>
<b>CH_'T5':rs9853895'</b>	<b>61.28</b>	<b>29.28</b>	<b>2.09</b>	<b>656</b>	<b>0.037</b>	<b>3.78</b>	<b>118.77</b>
'CH_'T6':rs9853895'	24.12	31.92	0.76	656	0.450	-38.56	86.79
CH_'C4':ParentalRisk_M'	-53.48	60.07	-0.89	656	0.374	-171.43	64.46
CH_'Pz':ParentalRisk_M'	15.66	61.68	0.25	656	0.800	-105.46	136.77
CH_'T3':ParentalRisk_M'	-1.97	56.80	-0.03	656	0.972	-113.50	109.56
CH_'T4':ParentalRisk_M'	25.45	60.68	0.42	656	0.675	-93.70	144.60
CH_'T5':ParentalRisk_M'	6.23	57.01	0.11	656	0.913	-105.71	118.17
CH_'T6':ParentalRisk_M'	2.33	59.42	0.04	656	0.969	-114.33	119.00
CH_'C4':ParentalRisk_F'	38.36	40.86	0.94	656	0.348	-41.87	118.58
CH_'Pz':ParentalRisk_F'	25.31	39.71	0.64	656	0.524	-52.66	103.28
CH_'T3':ParentalRisk_F'	-5.72	35.60	-0.16	656	0.873	-75.63	64.19
CH_'T4':ParentalRisk_F'	35.76	36.15	0.99	656	0.323	-35.22	106.74
CH_'T5':ParentalRisk_F'	58.58	38.18	1.53	656	0.125	-16.38	133.54
CH_'T6':ParentalRisk_F'	30.02	39.05	0.77	656	0.442	-46.66	106.70
<b>rs333491:ParentalRisk_M'</b>	<b>53.90</b>	<b>25.26</b>	<b>2.13</b>	<b>656</b>	<b>0.033</b>	<b>4.31</b>	<b>103.49</b>
rs333491:ParentalRisk_F'	-28.48	19.81	-1.44	656	0.151	-67.37	10.42
'CH_'C4':BirthWeight'	<b>0.07</b>	<b>0.04</b>	<b>2.00</b>	<b>656</b>	<b>0.046</b>	<b>0.00</b>	<b>0.14</b>
'CH_'Pz':BirthWeight'	0.01	0.04	0.34	656	0.733	-0.06	0.08
'CH_'T3':BirthWeight'	0.03	0.03	0.98	656	0.329	-0.03	0.10
'CH_'T4':BirthWeight'	<b>0.09</b>	<b>0.04</b>	<b>2.43</b>	<b>656</b>	<b>0.015</b>	<b>0.02</b>	<b>0.16</b>
'CH_'T5':BirthWeight'	-0.04	0.03	-1.08	656	0.281	-0.10	0.03
'CH_'T6':BirthWeight'	0.04	0.04	1.19	656	0.234	-0.03	0.11
<b>ParentalRisk_M:BirthWeight'</b>	<b>0.10</b>	<b>0.05</b>	<b>2.13</b>	<b>656</b>	<b>0.034</b>	<b>0.01</b>	<b>0.19</b>
ParentalRisk_F:BirthWeight'	0.03	0.03	1.03	656	0.305	-0.03	0.09
'CH_'C4':nrs'	-8.02	6.50	-1.24	656	0.217	-20.78	4.73
'CH_'Pz':nrs'	<b>-15.59</b>	<b>6.50</b>	<b>-2.40</b>	<b>656</b>	<b>0.017</b>	<b>-28.36</b>	<b>-2.82</b>
'CH_'T3':nrs'	-9.88	5.93	-1.67	656	0.096	-21.53	1.76
'CH_'T4':nrs'	-8.81	6.56	-1.34	656	0.180	-21.70	4.07
'CH_'T5':nrs'	-5.41	5.96	-0.91	656	0.364	-17.11	6.29
'CH_'T6':nrs'	<b>-13.48</b>	<b>6.36</b>	<b>-2.12</b>	<b>656</b>	<b>0.034</b>	<b>-25.96</b>	<b>-0.99</b>
'rs333491:nrs'	<b>8.77</b>	<b>3.28</b>	<b>2.67</b>	<b>656</b>	<b>0.008</b>	<b>2.32</b>	<b>15.21</b>
<b>ParentalRisk_M:nrs'</b>	<b>-11.61</b>	<b>5.65</b>	<b>-2.05</b>	<b>656</b>	<b>0.041</b>	<b>-22.71</b>	<b>-0.50</b>
ParentalRisk_F:nrs'	-8.05	5.22	-1.54	656	0.123	-18.30	2.19

Finally, Table IV-6 presents the FE parameters for the model with the highest variance explained of 39.24% as measured by the adjusted R<sup>2</sup>=.39239 (ordinary R<sup>2</sup>=.43886), AIC=8909.5, BIC=9178.6, LogLikelihood= -4395.7 (marked in red in Figure 4-4). The model was given by the formula:

$$\begin{aligned} & \text{'LAT} \sim 1 + \text{N}^{\circ}\text{NurseryRhymes} * \text{rs333491} + \text{N}^{\circ}\text{NurseryRhymes} * \text{Channel} + \\ & \text{Gender} * \text{BirthWeight} + \text{Gender} * \text{Channel} + \text{BirthWeight} * \text{rs9853895} + \text{BirthWeight} * \text{Channel} \\ & + \text{BirthWeight} * \text{ParentalRisk} + \text{rs9853895} * \text{Channel} + \text{Channel} * \text{ParentalRisk} + (1|\text{ITI}) + \\ & (1|\text{INFANTID}) + (1|\text{SR\_prev}) \end{aligned}$$

Table IV-6. Fixed effects coefficients in the model with the highest R<sup>2</sup> parameter overall.

<b>LME Model (Highest R<sup>2</sup>): Fixed effects coefficients (95% CIs)</b>							
<b>Name</b>	<b>Estimate</b>	<b>SE</b>	<b>tStat</b>	<b>DF</b>	<b>pValue</b>	<b>Lower</b>	<b>Upper</b>
'(Intercept)'	<b>593.98</b>	<b>187.02</b>	<b>3.18</b>	<b>652</b>	<b>0.002</b>	<b>226.76</b>	<b>961.21</b>
'CH_'C4''	<b>-280.04</b>	<b>140.64</b>	<b>-1.99</b>	<b>652</b>	<b>0.047</b>	<b>-556.21</b>	<b>-3.87</b>
'CH_'Pz''	-20.36	135.41	-0.15	652	0.881	-286.26	245.54
'CH_'T3''	-84.58	137.21	-0.62	652	0.538	-354.01	184.86
'CH_'T4''	<b>-390.21</b>	<b>137.83</b>	<b>-2.83</b>	<b>652</b>	<b>0.005</b>	<b>-660.86</b>	<b>-119.56</b>
'CH_'T5''	35.14	133.85	0.26	652	0.793	-227.68	297.96
'CH_'T6''	-54.99	147.64	-0.37	652	0.710	-344.88	234.92
'rs333491'	<b>-64.80</b>	<b>25.19</b>	<b>-2.57</b>	<b>652</b>	<b>0.010</b>	<b>-114.28</b>	<b>-15.33</b>
'rs9853895'	-81.11	73.17	-1.11	652	0.268	-224.79	62.56
Sex_M'	70.60	102.03	0.69	652	0.489	-129.74	270.95
ParentalRisk_M'	-148.80	153.98	-0.97	652	0.334	-451.16	153.57
ParentalRisk_F'	-115.98	127.83	-0.91	652	0.365	-366.98	135.02
'BirthWeight'	-0.07	0.05	-1.39	652	0.165	-0.17	0.03
'nrs'	-5.32	8.03	-0.66	652	0.508	-21.08	10.44
'CH_'C4':rs9853895'	52.31	31.54	1.66	652	0.098	-9.62	114.24
'CH_'Pz':rs9853895'	56.70	30.00	1.89	652	0.059	-2.21	115.62
'CH_'T3':rs9853895'	31.30	28.55	1.10	652	0.273	-24.76	87.36
'CH_'T4':rs9853895'	<b>85.89</b>	<b>30.68</b>	<b>2.80</b>	<b>652</b>	<b>0.005</b>	<b>25.65</b>	<b>146.13</b>
'CH_'T5':rs9853895'	<b>61.90</b>	<b>29.39</b>	<b>2.11</b>	<b>652</b>	<b>0.036</b>	<b>4.19</b>	<b>119.61</b>
'CH_'T6':rs9853895'	21.96	31.94	0.69	652	0.492	-40.75	84.67
CH_'C4':Sex_M'	-9.19	35.72	-0.26	652	0.797	-79.34	60.95
CH_'Pz':Sex_M'	-16.87	35.87	-0.47	652	0.638	-87.30	53.57
CH_'T3':Sex_M'	22.27	33.37	0.67	652	0.505	-43.26	87.79
CH_'T4':Sex_M'	5.41	36.45	0.15	652	0.882	-66.16	76.98
CH_'T5':Sex_M'	21.44	35.56	0.60	652	0.547	-48.40	91.27
CH_'T6':Sex_M'	31.07	37.63	0.83	652	0.409	-42.82	104.95
CH_'C4':ParentalRisk_M'	-53.17	60.04	-0.89	652	0.376	-171.07	64.73
CH_'Pz':ParentalRisk_M'	17.32	61.66	0.28	652	0.779	-103.76	138.40
CH_'T3':ParentalRisk_M'	3.06	57.04	0.05	652	0.957	-108.93	115.06
CH_'T4':ParentalRisk_M'	24.50	60.61	0.40	652	0.686	-94.51	143.51
CH_'T5':ParentalRisk_M'	6.62	57.08	0.12	652	0.908	-105.46	118.70
CH_'T6':ParentalRisk_M'	3.21	59.35	0.05	652	0.957	-113.33	119.75
CH_'C4':ParentalRisk_F'	41.29	41.38	1.00	652	0.319	-39.96	122.54
CH_'Pz':ParentalRisk_F'	24.55	40.89	0.60	652	0.548	-55.75	104.85
CH_'T3':ParentalRisk_F'	-0.15	37.04	0.00	652	0.997	-72.89	72.59
CH_'T4':ParentalRisk_F'	39.55	37.27	1.06	652	0.289	-33.63	112.73
CH_'T5':ParentalRisk_F'	67.86	40.70	1.67	652	0.096	-12.07	147.78
CH_'T6':ParentalRisk_F'	45.01	40.26	1.12	652	0.264	-34.05	124.07
'CH_'C4':BirthWeight'	0.07	0.04	1.93	652	0.055	0.00	0.14
'CH_'Pz':BirthWeight'	0.01	0.04	0.17	652	0.861	-0.06	0.08
'CH_'T3':BirthWeight'	0.03	0.03	0.78	652	0.438	-0.04	0.10
'CH_'T4':BirthWeight'	<b>0.09</b>	<b>0.04</b>	<b>2.40</b>	<b>652</b>	<b>0.017</b>	<b>0.02</b>	<b>0.16</b>
'CH_'T5':BirthWeight'	-0.04	0.03	-1.07	652	0.284	-0.10	0.03
'CH_'T6':BirthWeight'	0.03	0.04	0.71	652	0.479	-0.05	0.10
'rs9853895:BirthWeight'	0.02	0.02	0.91	652	0.366	-0.02	0.06
Sex_M:BirthWeight'	-0.01	0.03	-0.50	652	0.619	-0.07	0.04
ParentalRisk_M:BirthWeig	0.06	0.05	1.27	652	0.204	-0.03	0.15
ParentalRisk_F:BirthWeigl	0.03	0.04	0.87	652	0.384	-0.04	0.10
'CH_'C4':nrs'	-8.32	6.50	-1.28	652	0.201	-21.09	4.45
'CH_'Pz':nrs'	<b>-14.67</b>	<b>6.56</b>	<b>-2.24</b>	<b>652</b>	<b>0.026</b>	<b>-27.54</b>	<b>-1.79</b>
'CH_'T3':nrs'	-9.97	5.90	-1.69	652	0.092	-21.56	1.63
'CH_'T4':nrs'	-9.36	6.79	-1.38	652	0.169	-22.69	3.97
'CH_'T5':nrs'	-5.70	5.95	-0.96	652	0.339	-17.38	5.99
'CH_'T6':nrs'	<b>-14.22</b>	<b>6.45</b>	<b>-2.21</b>	<b>652</b>	<b>0.028</b>	<b>-26.88</b>	<b>-1.56</b>
'rs333491:nrs'	<b>6.71</b>	<b>3.29</b>	<b>2.04</b>	<b>652</b>	<b>0.042</b>	<b>0.25</b>	<b>13.17</b>
'rs333491:nrs'	<b>6.71</b>	<b>3.29</b>	<b>2.04</b>	<b>652</b>	<b>0.042</b>	<b>0.25</b>	<b>13.17</b>

The formula describing the models in the smaller initial peak region of the adjusted R<sup>2</sup> distributions in *Figure 4-4* (in *Chapter 4*), at the highest R<sup>2</sup> value atop the steepest AIC and BIC growth (marked as a red dot at the zoomed-in panel underneath) were, for BIC:

Model ID 134

'LAT ~ 1 + N°NurseryRhymes\*rs333491 + N°NurseryRhymes\*Channel + Gender\*BirthWeight + BirthWeight\*Channel + BirthWeight\*ParentOfOrg + rs9853895\*Channel + Channel\*ParentOfOrg + (1|ITI) + (1|INFANTID) + (1|SR\_prev)'

Model ID 262

'LAT ~ 1 + N°NurseryRhymes\*rs333491 + N°NurseryRhymes\*Channel + Gender\*BirthWeight + BirthWeight\*rs9853895 + BirthWeight\*Channel + BirthWeight\*ParentOfOrg + rs9853895\*Channel + Channel\*ParentOfOrg + (1|ITI) + (1|INFANTID) + (1|SR\_prev)'

Model ID 1880

'LAT~ 1 + N°NurseryRhymes\*rs333491 + N°NurseryRhymes\*Channel + Gender\*Channel + BirthWeight\*Channel + BirthWeight\*ParentOfOrg + rs9853895\*Channel + Channel\*ParentOfOrg + (1|ITI) + (1|INFANTID) + (1|SR\_prev)'

And for AIC:

Model ID 191

'LAT ~ 1 + N°NurseryRhymes\*rs333491 + N°NurseryRhymes\*Channel + Gender\*BirthWeight + BirthWeight\*Channel + BirthWeight\*ParentOfOrg + rs9853895\*Channel + Channel\*ParentOfOrg + (1|ITI) + (1|INFANTID) + (1|SR\_prev)'

Model ID 403

'LAT ~ 1 + N°NurseryRhymes\*rs333491 + N°NurseryRhymes\*Channel + Gender\*BirthWeight + BirthWeight\*rs9853895 + BirthWeight\*Channel + BirthWeight\*ParentOfOrg + rs9853895\*Channel + Channel\*ParentOfOrg + (1|ITI) + (1|INFANTID) + (1|SR\_prev)'

## Model ID 2146

'LAT~ 1 + N°NurseryRhymes\*rs333491 + N°NurseryRhymes\*Channel + Gender\*BirthWeight + Gender\*Channel + Gender\*ParentOfOrg + BirthWeight\*rs985385 + BirthWeight\*Channel + rs9853895\*Channel + Channel\*ParentOfOrg + (1|ITI) + (1|INFANTID) + (1|SR\_prev)'

#### IV.IV Effects of Other Variables in the LME models

The most parsimonious model identified by the AIC selected the alongside the parental dyslexia variable, also the two ROBO1 SNPs, rs9853895 and rs333491 (the A1 model, fixed effects parameters are shown in *Table IV-3*). The effects by trial of most reliable ROBO1 SNP predictor was shown in *Figures 4-7* in the main text. Below, the effects of the two ROBO1 genes by infant are plotted against the infants' mean PLV peak latency in *Figures IV-2* and *IV-3*, respectively. Both ROBO1 SNPs had a significant predictive effect on the latency of the PLV peak in a post-hoc anal

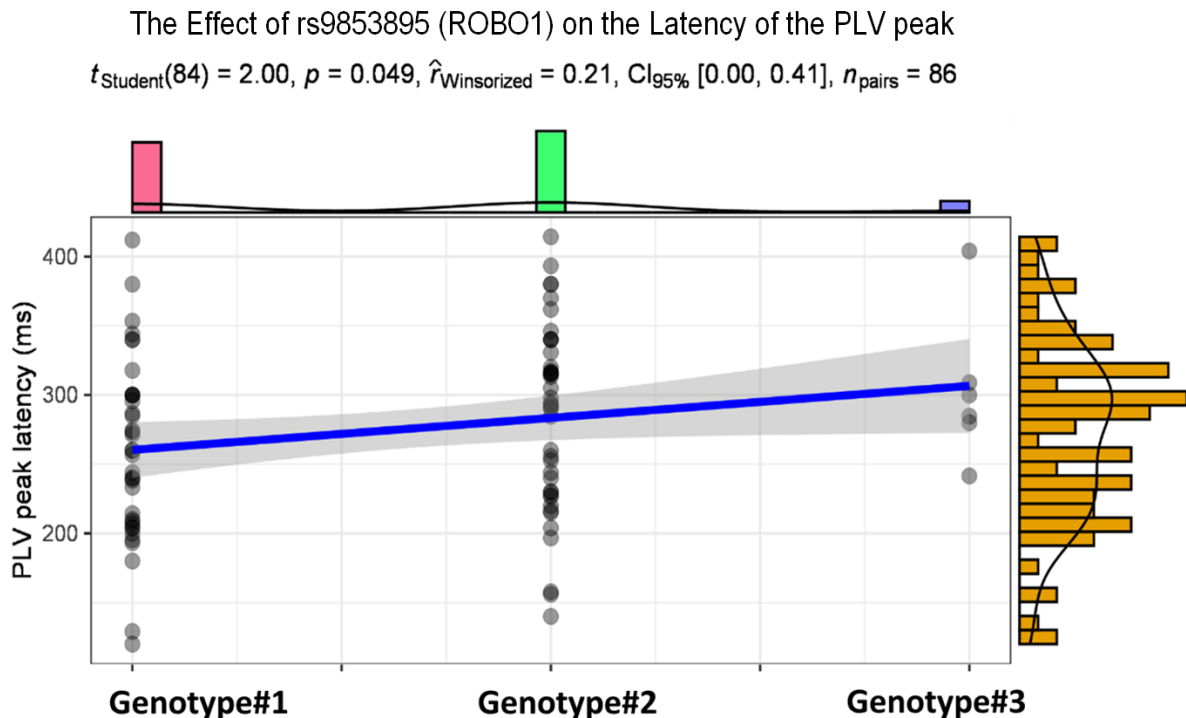
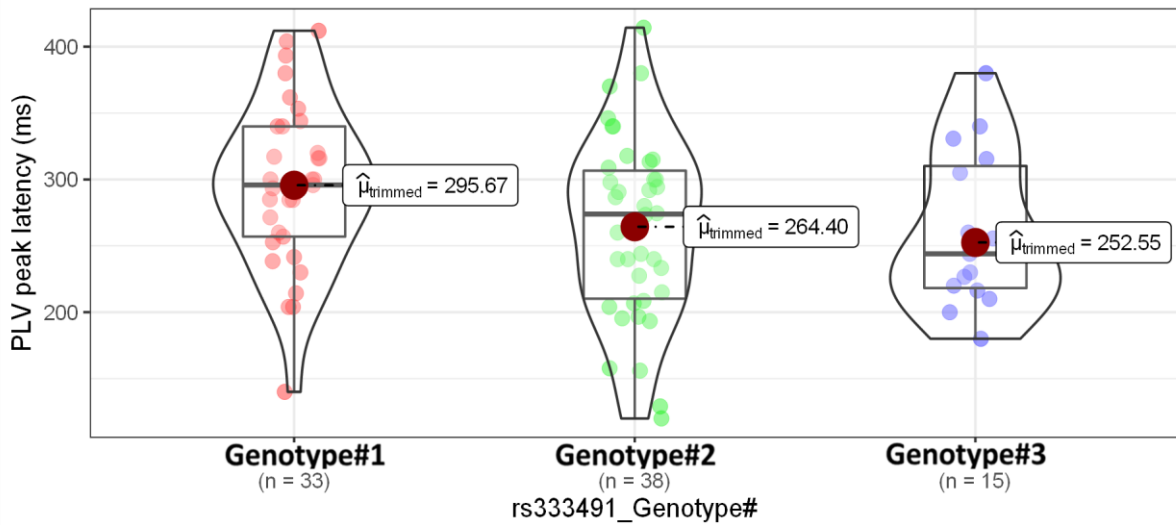


Figure IV-2. A scatterplot of the PLV onset latencies (y-axis) against the infants' rs9853895 (ROBO1) genotype (x-axis), at the individual infant's level.

Conversly, the fixed effects of the **ROBO1 SNP rs333491** went in the opposite direction and infants carrying Genotype#1 tended to have slower PLV peaks compared those with genotype#2 and genotype#3 when the distribution of the individual peaks latencies were plotted (*Figure 4-8B*, n.s.), as well as when the average latency for each infant is plotted against their genotype (*Figure 4-8A*). Again, the robust one-way ANOVA with three levels of the rs333491 variable, one for each genotype, was not significant at  $p = .079$ .

**A) The Effect of rs333491 (ROBO1) on the Latency of the PLV peak**

$F_{\text{trimmed-means}}(2,21.96) = 2.86, p = 0.079, \hat{\xi} = 0.37, CI_{95\%} [0.13, 0.64], n_{\text{obs}} = 86$



Pairwise test: Yuen's trimmed means test; Comparisons shown: **only significant**

**B) The Effect of rs333491 (ROBO1) on the Latency of the PLV peak**

$\log_e(S) = 18.05, p = 0.007, \hat{\rho}_{\text{Spearman}} = -0.10, CI_{95\%} [-0.17, -0.03], n_{\text{pairs}} = 723$

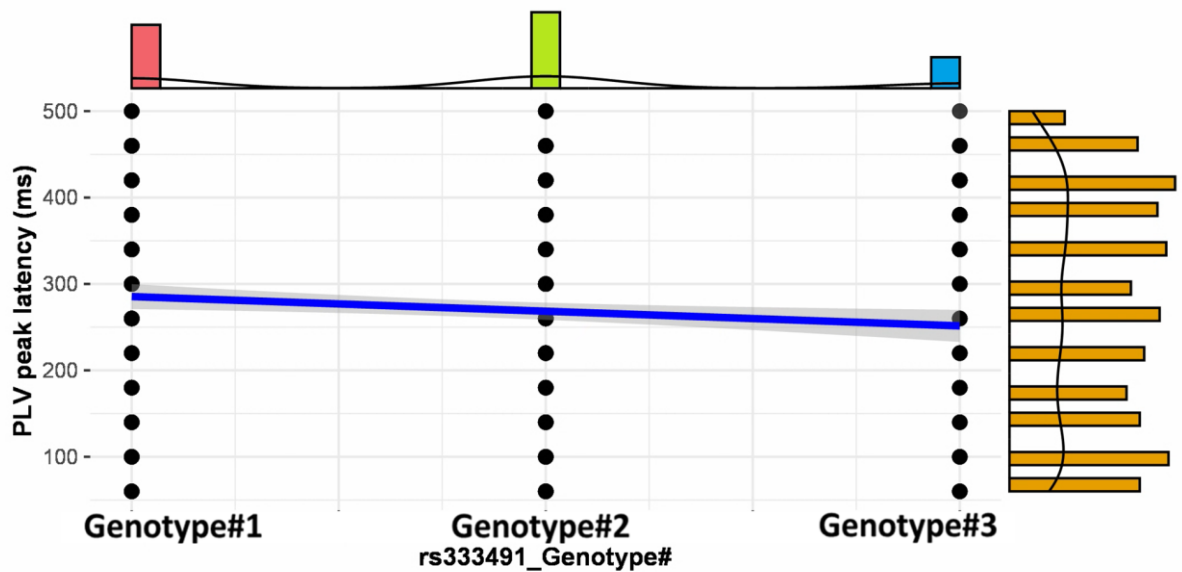


Figure IV-3. A violin plot for infant's mean latency (A) and a regression line for individual trials (B), demonstrating the effects of rs333491 genotype on the latency of the PLV onset peaks. A: at every dot represents a mean latency for the infant PLV onset peaks (Scatterplot of the effect by infants is in Appendix IV.IV, Figure IV-3); B: every dot represent latency on an individual trial. M=maternal; F=paternal; O=low risk group. Statistics reported are for the robust Yuen's trimmed mean test using 80% of the total distribution of values to deal with potential outliers (referred to in the text as robust ANOVA).

No effects of the infant's sex or weight at birth were observed at the individual infant level, as depicted in Figures IV-4 and IV-5 below. There is also no effect of the number of nursery rhymes contributed by each infant (Figure IV-6).

The Effect of Infant's Sex on the Latency of the PLV peak

$$t_{\text{Yuen}}(43.09) = 1.17, p = 0.249, \hat{\xi} = 0.19, \text{CI}_{95\%} [0.00, 0.44], n_{\text{obs}} = 86$$

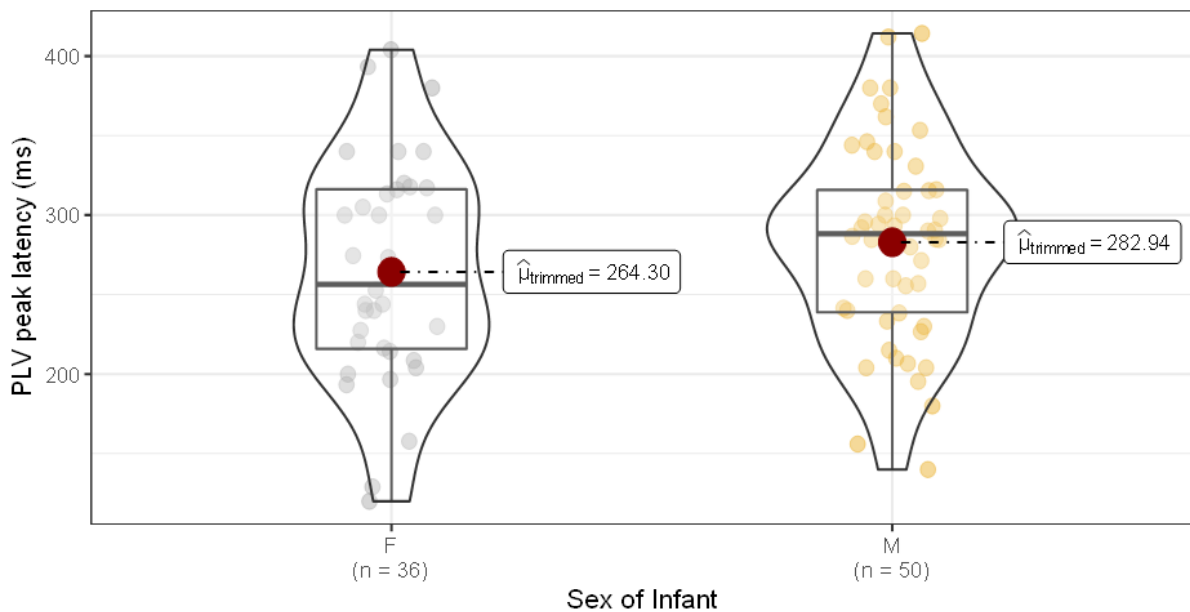


Figure IV-4. A violin plot of the effect of infants' sex (x-axis) on the latency of the PLV onset peaks (y-axis), at the individual infant's level. The red dots present the trimmed mean by group. Robust (trimmed means) t-test statistics are reported in the header.

### The Effect of Infant's Birthweight on their Latency of the PLV peak

$t_{\text{Student}}(84) = -1.07, p = 0.287, \hat{r}_{\text{Winsorized}} = -0.12, \text{CI}_{95\%} [-0.32, 0.10], n_{\text{pairs}} = 86$

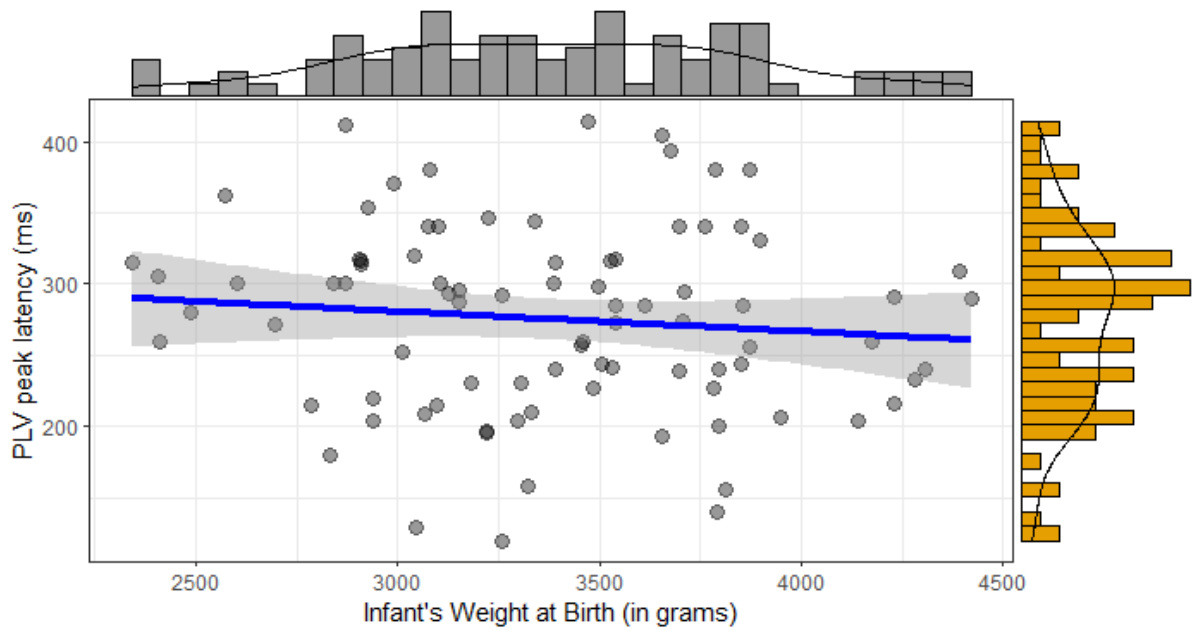


Figure IV-5. A scatterplot of the PLV onset latencies (y-axis) against the infants' average birthweight (x-axis), at the individual infant's level.

### The Number of Nursery Rhymes per Infant

$t_{\text{Student}}(84) = 0.04, p = 0.969, \hat{r}_{\text{Winsorized}} = 0.00, \text{CI}_{95\%} [-0.21, 0.22], n_{\text{pairs}} = 86$

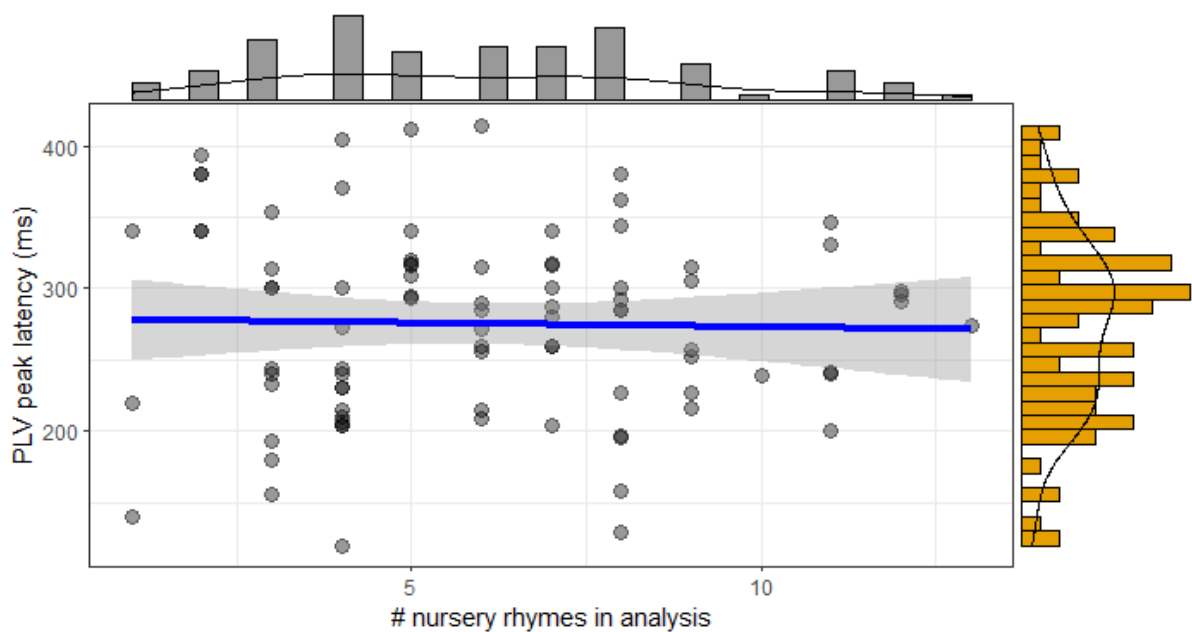


Figure IV-6. A scatterplot of the PLV onset latencies (y-axis) against the number of nursery rhymes contributed to the analysis by each infant (x-axis), at the individual infant's level.

# Appendix V

---

## V.1 Noisy Channels Correction Attempts

To estimate the positive covariance matrix when calculating the GPDC, all channels had to be present in the network, and none could be derived fully from the neighbouring channels. The GPDC input covariance matrix needed to calculate the instantaneous coherence between the input and output vectors had 3 criteria: it had to be square, symmetrical, and positively defined. A singular matrix could not be positively defined, that is, we could not generate a covariance matrix if one of its vectors could be expressed as a linear combination or otherwise determined from (a subset of) the others. This meant that if there were noisy channels amongst those selected for the GPDC calculations, they could not be simply rejected. They had to be reintroduced to the dataset, either via an interpolation, or by replacing them with dummy variable with distribution characteristics close to those of the remaining channels.

Thus, with a sparse network of only 11 EEG channels in the neonatal EEG, the interpolation of missing channels could not successfully circumvent the singularity problem in the input matrix, as the input time-series vectors were not independent enough from each other. Alternatively, we attempted recreating the rejected channels as dummy vectors. Unfortunately, the dummy vectors could not be input as a zero, or a random number as those would distort the structure of the covariance matrix and the calculated model outputs. Instead, we tested inputting a series of random numbers tied to the distribution of the remaining channel-values at each timepoint. In doing so, for each timepoint, we generated a random value from within 95% of the standard normal distribution and weighted the standard deviation of the real channels by it and added it to their mean value. Thus, we retained the structure of the distribution of the input timeseries matrix without introducing outlier distortions, while at the same time retaining enough randomness in the dummy timeseries to estimate the input covariate matrix for the instantaneous model. Finally, in the output structure, we removed again the dummy channels, thus retaining the resulting directed coherence values only for the true EEG channels.

The described dummy variable simulation procedure allowed for the calculation of the instantaneous effects of the partial directed coherence matrix. However, it was not a validated procedure, and it had not been tested for robustness against a known-outcome data series. Given that 21% infants had at least one channel removed in all nursery rhyme epochs, with an even larger proportion of 80% of infants having one or more channels removed in some epochs only (see *Appendix III.II* above), we deemed unjustified using a non-validated method to simulate and substitute such a large proportion of the EEG datasets. Instead, we opted for the more stringent approach of focusing the GPDC analyses on a selected number of channels, justified by their positioning on the head. Thus, channels T3, T4, C3 and C4 were the only ones included in the GPDC analyses. These four channels seemed spared from noise in most infants. Additionally, as the temporal-central areas are important for auditory language information processing, these channels expected to show an effect in response to the nursery rhymes stimuli presented to the infants.

---

## V.II Normalised GPDC Scores by Connection and Familial Risk Group

We observed the same pattern as described in *Chapter 5* of left-hemisphere connections above and right-hemisphere connections under the 95% surrogate threshold when considering only the infants at low familial risk of dyslexia (*Table V-1*). Only three connections remained significantly above the surrogate threshold after FDR (BH) correction in the low-risk group:

T3->C3:  $M=.286$  ( $SE=.025$ ),  $t_{(38)} = 11.6311$ ,  $p < .0000$ ;

C4->T4:  $M=.180$  ( $SE=.023$ ),  $t_{(38)} = 7.6955$ ,  $p < .0000$ ;

T3->T4:  $M=.039$  ( $SE=.016$ ),  $t_{(38)} = 2.377$ ,  $p < .0339$ .

Table V-1. Average normalised GPDC values for each channel-to-channel connection pairs in the low-risk group, tested against no difference to baseline ( $M=0$ ; BH-FDR corrected). The three pairwise connections significantly above the 95% threshold are highlighted in bold.

Low Family Risk: Test of means against 95%tile Surrogate Threshold								
T <sup>2</sup> (casewise MD)=637.957 F(12,27)=37.77 p=.00000								
Variable	Mean	Std.Dv.	N	Std.Err.	t-value	df	p	BH-FDR q
'C3'-'C4'	0.017	0.089	39	0.014	1.221	38	0.229	0.250
'C3'-'T3'	-0.026	0.035	39	0.006	-4.696	38	0.000	0.000
'C3'-'T4'	0.009	0.053	39	0.008	1.027	38	0.311	0.311
'C4'-'C3'	-0.035	0.021	39	0.003	-10.620	38	0.000	0.000
'C4'-'T3'	-0.018	0.049	39	0.008	-2.238	38	0.031	0.042
'C4'-'T4'	<b>0.180</b>	<b>0.146</b>	<b>39</b>	<b>0.023</b>	<b>7.695</b>	<b>38</b>	<b>0.000</b>	<b>0.000</b>
'T3'-'C3'	<b>0.286</b>	<b>0.153</b>	<b>39</b>	<b>0.025</b>	<b>11.631</b>	<b>38</b>	<b>0.000</b>	<b>0.000</b>
'T3'-'C4'	<b>0.029</b>	<b>0.085</b>	<b>39</b>	<b>0.014</b>	<b>2.095</b>	<b>38</b>	<b>0.043</b>	<b>0.051</b>
'T3'-'T4'	<b>0.038</b>	<b>0.101</b>	<b>39</b>	<b>0.016</b>	<b>2.377</b>	<b>38</b>	<b>0.023</b>	<b>0.034</b>
'T4'-'C3'	-0.025	0.021	39	0.003	-7.586	38	0.000	0.000
'T4'-'C4'	-0.020	0.026	39	0.004	-4.851	38	0.000	0.000
'T4'-'T3'	-0.018	0.025	39	0.004	-4.572	38	0.000	0.000

In the group of infants at high familial risk, the same four connections remained significantly above threshold after FDR correction, as in the full dataset in *Chapter 5* (Table V-2, T3->T4 was just above).

T3->C3:  $M=.262$  ( $SE=.030$ ),  $t_{(37)} = 8.7983$ ,  $p < .0000$ ;

C4->T4:  $M=.175$  ( $SE=.026$ ),  $t_{(37)} = 6.6616$ ,  $p < .0000$ ;

T3->T4:  $M=.025$  ( $SE=.012$ ),  $t_{(37)} = 2.12$ ,  $p < .0489$ ;

T3->C4:  $M=.031$  ( $SE=.009$ ),  $t_{(37)} = 3.2699$ ,  $p < .0035$ .

Table V-2. Average normalised GPDC values for each channel-to-channel connection pairs in the high-risk group, tested against no difference to baseline ( $M=0$ ; BH-FDR corrected). The four pairwise connections significantly above the 95% threshold are highlighted in bold.

<b>High Family Risk: Test of means against 95%tile Surrogate Threshold</b>								
<b>T<sup>2</sup>(casewise MD)=1076.19 F(12,25)=62.28 p=.00000</b>								
<b>Variable</b>	<b>Mean</b>	<b>Std.Dv.</b>	<b>N</b>	<b>Std.Err.</b>	<b>t-value</b>	<b>df</b>	<b>p</b>	<b>BH-FDR q</b>
'C3'-'C4'	0.016	0.061	37	0.010	1.588	36	0.121	0.132
'C3'-'T3'	-0.038	0.020	37	0.003	-11.647	36	0.000	0.000
'C3'-'T4'	-0.010	0.039	37	0.006	-1.515	36	0.139	0.139
'C4'-'C3'	-0.038	0.019	37	0.003	-12.390	36	0.000	0.000
'C4'-'T3'	-0.024	0.040	37	0.007	-3.669	36	0.001	0.001
<b>'C4'-'T4'</b>	<b>0.170</b>	<b>0.161</b>	<b>37</b>	<b>0.026</b>	<b>6.422</b>	<b>36</b>	<b>0.000</b>	<b>0.000</b>
<b>'T3'-'C3'</b>	<b>0.263</b>	<b>0.186</b>	<b>37</b>	<b>0.031</b>	<b>8.582</b>	<b>36</b>	<b>0.000</b>	<b>0.000</b>
<b>'T3'-'C4'</b>	<b>0.030</b>	<b>0.059</b>	<b>37</b>	<b>0.010</b>	<b>3.092</b>	<b>36</b>	<b>0.004</b>	<b>0.006</b>
<b>'T3'-'T4'</b>	<b>0.026</b>	<b>0.072</b>	<b>37</b>	<b>0.012</b>	<b>2.177</b>	<b>36</b>	<b>0.036</b>	<b>0.043</b>
'T4'-'C3'	-0.030	0.017	37	0.003	-10.670	36	0.000	0.000
'T4'-'C4'	-0.026	0.018	37	0.003	-8.779	36	0.000	0.000
'T4'-'T3'	-0.017	0.035	37	0.006	-2.871	36	0.007	0.009

### ***In-built Sanity Checks:***

Finally, GPDC had an inbuilt positive control within the current experimental design as a directed measure of connectivity. We could not allow for the possibility of any causal influences going from the brain signal towards the speech-sound recording. Therefore, there could have been no flow of information going from the brain to the nursery rhymes, the directed coherence from the EEG channels to the speech signal should be consistently under the threshold for all four connections: T3->NRs; C3->NRs; C4->NRs; T4->NRs. When tested against the 95tile threshold, all four connections were significantly and consistently below it in double-sided t-tests of mean against a constant reference value of the threshold:

T3->NRs  $t_{(78)} = -97.2169$ ,  $p < .0000$ ,  $M = -.0364$  ( $SE=.000375$ ), range =  $-.0434 : -.0271$ ;

T4->NRs  $t_{(78)} = -56.7848$ ,  $p < .0000$ ,  $M = -.0359$  ( $SE=.000633$ ), range =  $-.0441 : .0002$ ;

C3->NRs  $t_{(78)} = -80.6593$ ,  $p < .0000$ ,  $M = -.0394$  ( $SE=.000489$ ), range =  $-.0461 : -.0162$ ;

C4->NRs  $t_{(78)} = -90.8846$ ,  $p < .0000$ ,  $M = -.0425$  ( $SE=.000468$ ), range =  $-.0494 : -.0307$ .

For each infant, each individual directed coherence value sent from an EEG channel to the nursery rhymes was checked against the 95% surrogate threshold. Looking at the individual values per infant voxel-by-voxel, without averaging, there was only one positive

value (i.e. above threshold) for all infants and all voxels at 240ms post stimulus onset (Baby 16, T4->NRs, GPDC= .0001862).

### V.III FDR Corrections on the Three GLMs by Gene

For the 44 possible effects tested in the three GLMs testing in *Chapter 5*, one for each gene, a FDR-BH correction was calculated for all p-values. *Table V-3* below shows the cumulative number of significant calls at each alpha level, and the corresponding number of p, Storey-q and BH-q values below it.

*Table V-3. Cumulative number of significant calls by different alpha cut-off levels (p-value), and the estimated Storey (q-values) and BH (local FDR) values.  $\pi_0^{\wedge}$  here is the estimate of the proportion of effects fulfilling the null hypothesis (i.e. non-significant effects).*

qvalue(p = p)						
$\pi_0^{\wedge}$ : 0.4497926						
Cumulative number of significant calls:						
	<0.001	<0.01	<0.025	<0.05	<0.1	<1
p-value	6	6	7	9	11	44
q-value	6	6	6	7	9	44
local FDR	6	6	6	6	6	44

False Discovery Rate was estimated over all effects in all three genes, applying both the Benjamini-Hochberg (BH) and the Storey methods, and associated error-rate q-values are reported alongside the raw p-values. Storey's FDR estimate was more powerful than BH q estimate when comparing less than 100 effects. The q-value indicated how many false positives should have been expected after choosing a significance limit (i.e. at the given p-value). For example, here, at  $p < .015$  we had  $q = .04$ , that meant that only 4% of all p-values  $\leq .015$  were likely to have been false positives. Thus, as we had 7 effects at  $p \leq .015$ , then 0.28 (fewer than 1) of those effects were likely to have been a false positive. On the other hand, at  $p = .035$ , we had  $q = .08$  or 8% of the 9 effects, that is closer to one (0.72) of the tests at  $p < .035$  could have been a false positive. Ideally, we would have liked less than 5% of false positive tests (i.e  $q < .05$ ) at any p-value cut-off. *Figure V-1* shows the distribution of p-values for the effects tested here at  $\pi_0^{\wedge} = .45$ , and the corresponding FRD estimated by the Storey q-values and the local FRD, while *Figure V-2* shows the evolution of the  $\pi_0^{\wedge}$  estimates, and

of the q-values as a function of the number of significant effects, and the number of estimated false positives among those.

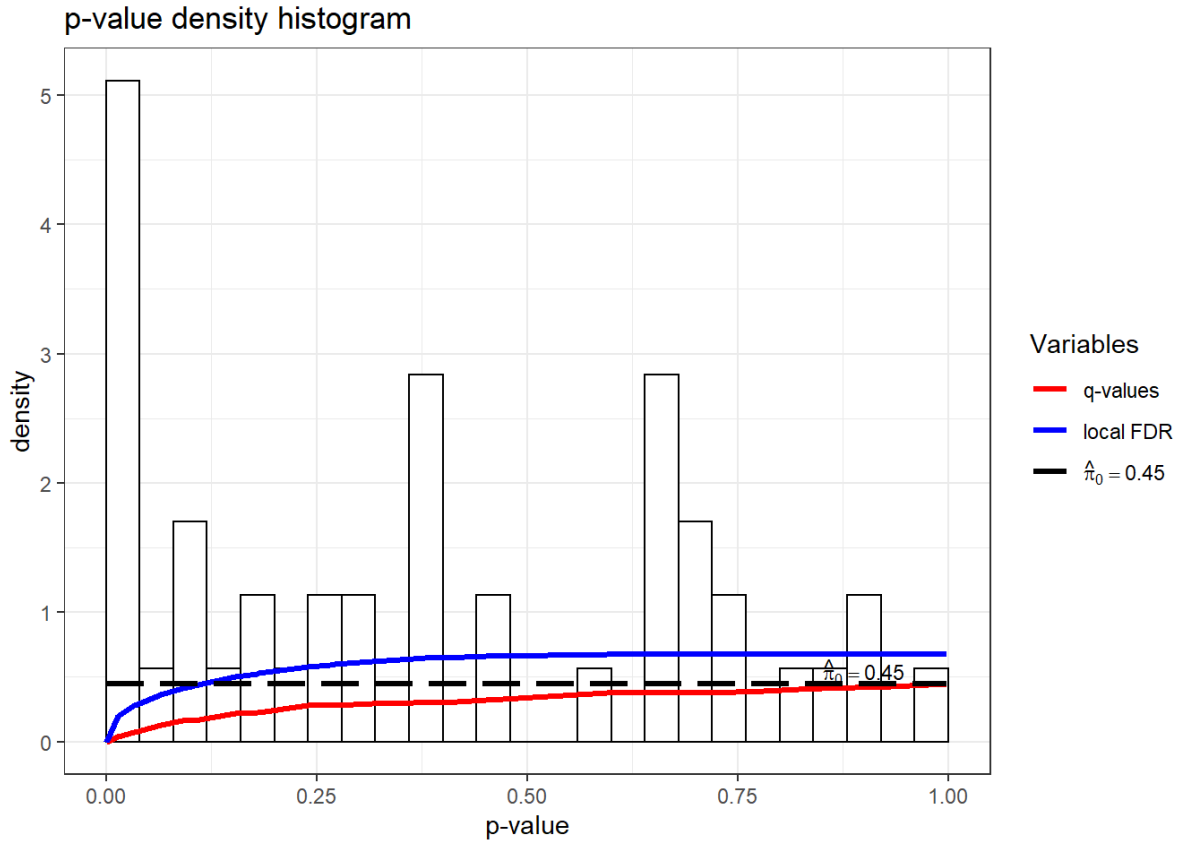


Figure V-1. A histogram of the distribution of the p-values of all effects tested (44), at the  $\hat{\pi}_0 = 0.45$  (the black dotted line). The red line shows the evolution of the Storey-q FDR estimate, and the blue line indicates the evolution of the calculated local FDR estimate.

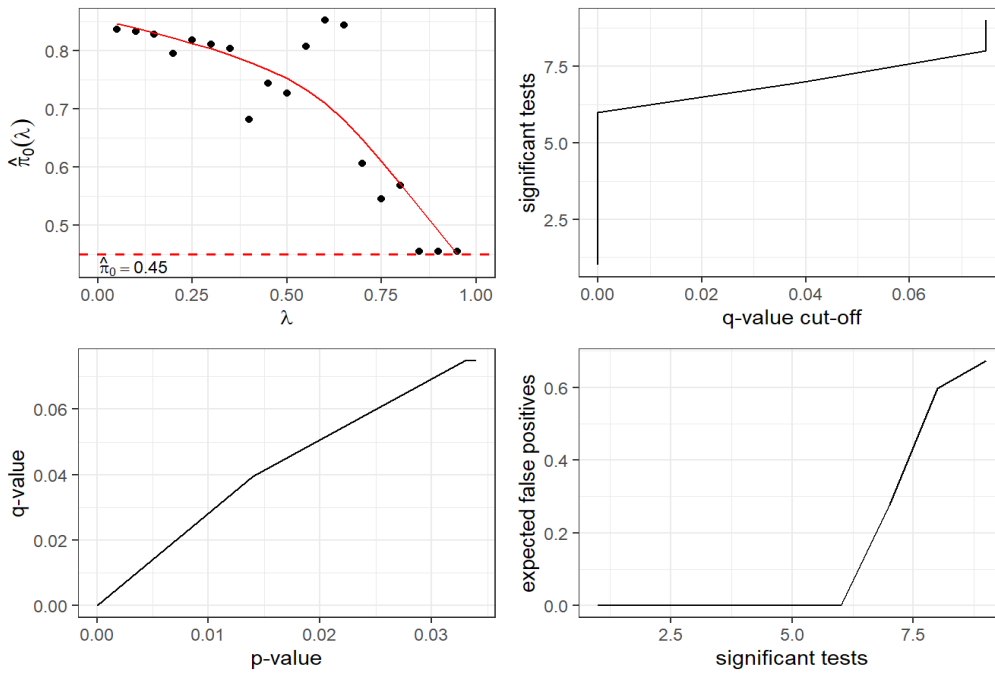


Figure V-2. Top left: the  $\hat{\pi}_0$  estimate of the proportion of true null hypotheses against the tuning parameter  $\lambda$  (the estimated proportion of true alternative hypotheses is  $1-\hat{\pi}_0$ ). Top right: the number of significant tests at each q-value; Bottom left: the q-values as a function of the p-values for the model estimates; Bottom right: the number of false positive effects as a function of the total number of significant effects in the models tested.

Table V-4 below enlists all effects in the 3 GLMs by gene. The graphs in Figure V-2 demonstrate that out of the 44 p-values to the effects in Table V-4, we could confidently trust that seven positive results (three intercepts and three main effects of *Connection* and one *Connection*  $\times$  *ROBO1* SNP interaction) for the alternative hypotheses have no type I error at  $p < .015$  or  $q < .04$ .

Table V-4. All 44 effects in the three GLMs corresponding to the three genes. Raw p-values, and their associated FDR BH, local FDR and Storey q estimates. The values highlighted in red had an uncorrected p-value under 5% alpha, those highlighted in blue – under 10% of type I error.:

		pvals	BH-q	FDR	Storey-q
1	Intercept	0.000	0.000	0.000	0.000
2	FamRisk	0.180	0.498	0.526	0.224
3	"rs793842"	0.650	0.837	0.674	0.377
4	"rs807701"	0.595	0.837	0.674	0.377
5	rs7751169	0.105	0.355	0.435	0.160
6	FamRisk**rs793842"	0.451	0.713	0.664	0.321
7	FamRisk**rs807701"	0.890	0.931	0.674	0.419
8	FamRisk*rs7751169	0.316	0.662	0.620	0.298
9	CONNECT	0.000	0.000	0.000	0.000
10	CONNECT*FamRisk	0.266	0.630	0.593	0.283
11	CONNECT**rs793842"	0.704	0.837	0.674	0.377
12	CONNECT**rs807701"	0.272	0.630	0.596	0.283
13	CONNECT*rs7751169	0.033	0.166	0.279	0.075
14	CONNECT*FamRisk**rs793842"	0.668	0.837	0.674	0.377
15	CONNECT*FamRisk**rs807701"	0.998	0.998	0.674	0.449
16	CONNECT*FamRisk*rs7751169	0.697	0.837	0.674	0.377
17	Intercept	0.000	0.000	0.000	0.000
18	FamRisk	0.454	0.713	0.665	0.321
19	rs3743204	0.643	0.837	0.674	0.377
20	FamRisk*rs3743204	0.666	0.837	0.674	0.377
21	CONNECT	0.000	0.000	0.000	0.000
22	CONNECT*FamRisk	0.316	0.662	0.620	0.298
23	CONNECT*rs3743204	0.823	0.905	0.674	0.407
24	CONNECT*FamRisk*rs3743204	0.675	0.837	0.674	0.377
25	Intercept	0.000	0.000	0.000	0.000
26	FamRisk	0.391	0.675	0.649	0.304
27	"rs333491"	0.065	0.286	0.363	0.129
28	rs9853895	0.091	0.355	0.413	0.160
29	rs6803202	0.760	0.857	0.674	0.386
30	rs7644521	0.399	0.675	0.652	0.304
31	FamRisk**rs333491"	0.154	0.484	0.499	0.218
32	FamRisk*rs9853895	0.181	0.498	0.527	0.224
33	FamRisk*rs6803202	0.850	0.912	0.674	0.410
34	FamRisk*rs7644521	0.748	0.857	0.674	0.386
35	CONNECT	0.000	0.000	0.000	0.000
36	CONNECT*FamRisk	0.691	0.837	0.674	0.377
37	CONNECT**rs333491"	0.101	0.355	0.429	0.160
38	CONNECT*rs9853895	0.014	0.088	0.199	0.040
39	CONNECT*rs6803202	0.240	0.621	0.576	0.279
40	CONNECT*rs7644521	0.365	0.675	0.640	0.304
41	CONNECT*FamRisk**rs333491"	0.034	0.166	0.282	0.075
42	CONNECT*FamRisk*rs9853895	0.379	0.675	0.645	0.304
43	CONNECT*FamRisk*rs6803202	0.390	0.675	0.649	0.304
44	CONNECT*FamRisk*rs7644521	0.910	0.931	0.674	0.419

## V.IV Controlling for number of nursery rhymes by infant

Multivariate t-tests on the coherence values above the surrogate threshold showed that neither connection significantly differed between high and low risk infants, and there was no significant group difference overall. The relevant t-tests are shown in *Table V-5*.

*Table V-5. Four t-tests (one for each pairwise connection) on the differences in normalised GPDC between the high (1) and low (0) familial risk groups. No differences were found. Multivariate t of the group differences is reported in the header.*

T-tests; Grouping: FamRisk (inp_current_ss_cc_240_95)									
Group 1: 1; Group 2: 0									
Hotelling T <sup>2</sup> =1.20265 F(4,71)=.28847 p=.88454									
Variable	Mean	Mean	t-value	df	p	Valid N	Valid N	Std.Dev.	Std.Dev.
	FamRisk=1	FamRisk=0				FamRisk=1	FamRisk=0	FamRisk=1	FamRisk=0
'T3'-'C3'	0.2627	0.2856	-0.5870	74	0.5590	37	39	0.1862	0.1533
'C4'-'T4'	0.1700	0.1801	-0.2879	74	0.7743	37	39	0.1610	0.1462
'T3'-'C4'	0.0299	0.0287	0.0722	74	0.9426	37	39	0.0588	0.0854
'T3'-'T4'	0.0257	0.0385	-0.6292	74	0.5311	37	39	0.0719	0.1011

However, there was a wide spread in the number of nursery rhymes contributed by each infant, ranging from 3 to 38. Still, the high and low familial risk groups did not differ in the mean number of nursery rhymes contributed by each infant,  $t_{(74)}=.16$ ,  $p=.88$ , n.s (*Table V-6*), nor in the distribution of the number of nursery rhymes contributed in each group (*Figure V-3*).

*Table V-6. T-test results on the high (1) and low (0) familial risk group differences between the number of nursery rhymes contributed to the analyses by each infant.*

T-tests; Grouping: FamRisk (inp_current_ss_cc_240_95)									
Group 1: 1									
Group 2: 0									
Variable	Mean	Mean	t-value	df	p	Valid N	Valid N	Std.Dev.	Std.Dev.
	FamRisk=1	FamRisk=0				FamRisk=1	FamRisk=0	FamRisk=1	FamRisk=0
nr_count	24.5405	24.2051	0.1573	74	0.8754	37	39	9.1122	9.4540

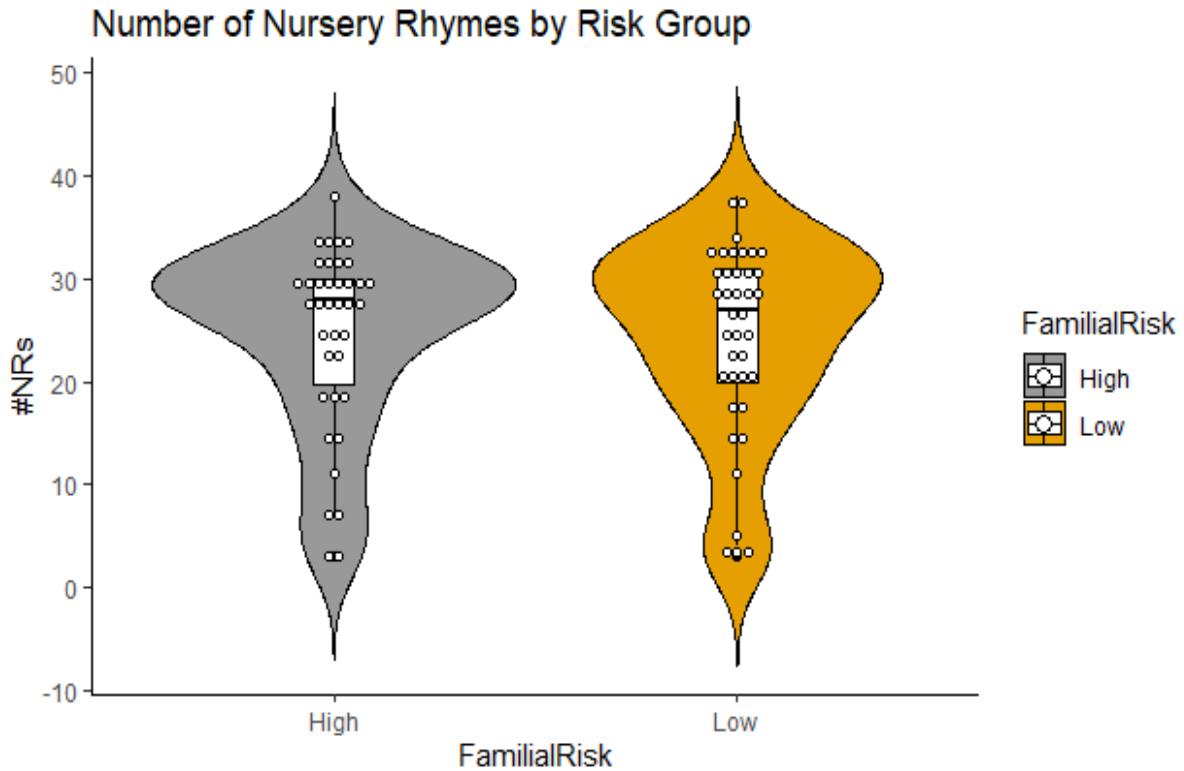


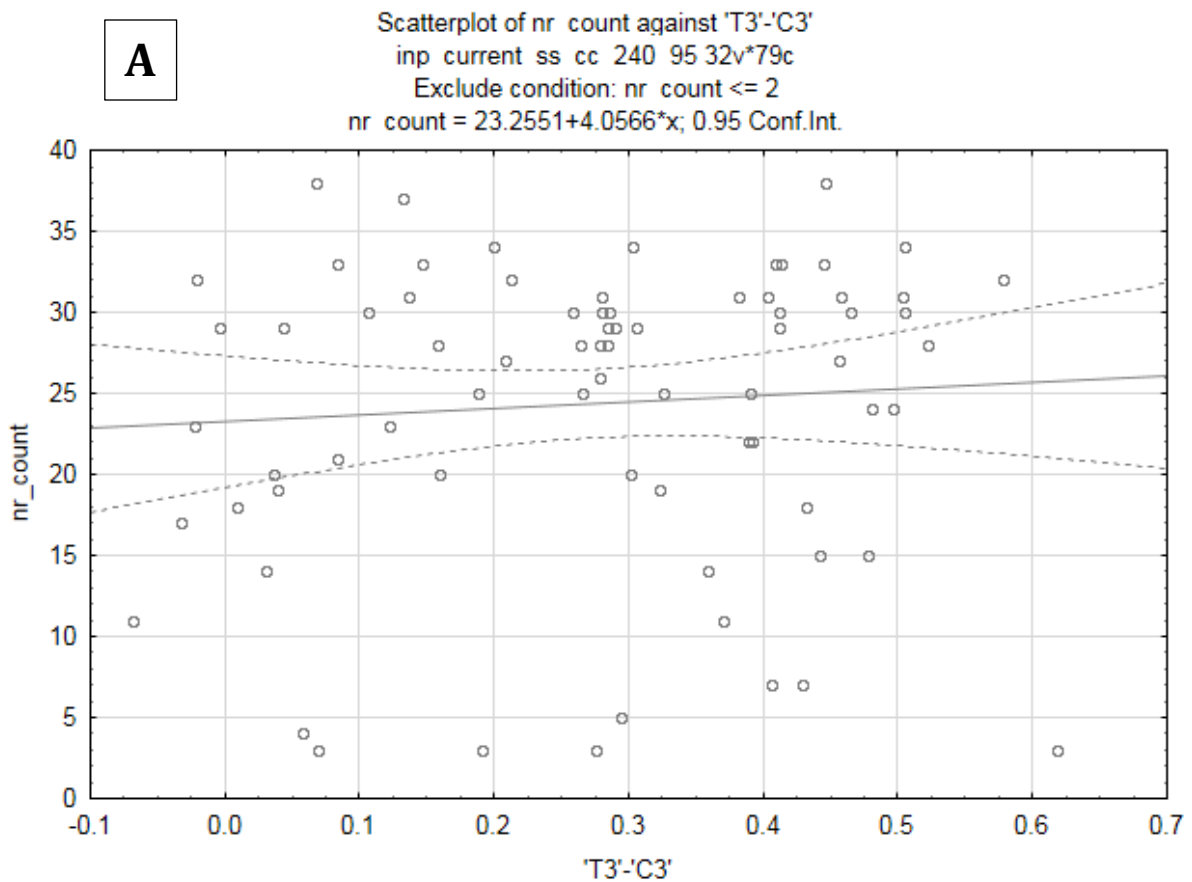
Figure V-3. The Distribution of the number of nursery rhymes contributed by each infant to the analyses, split by familial risk group.

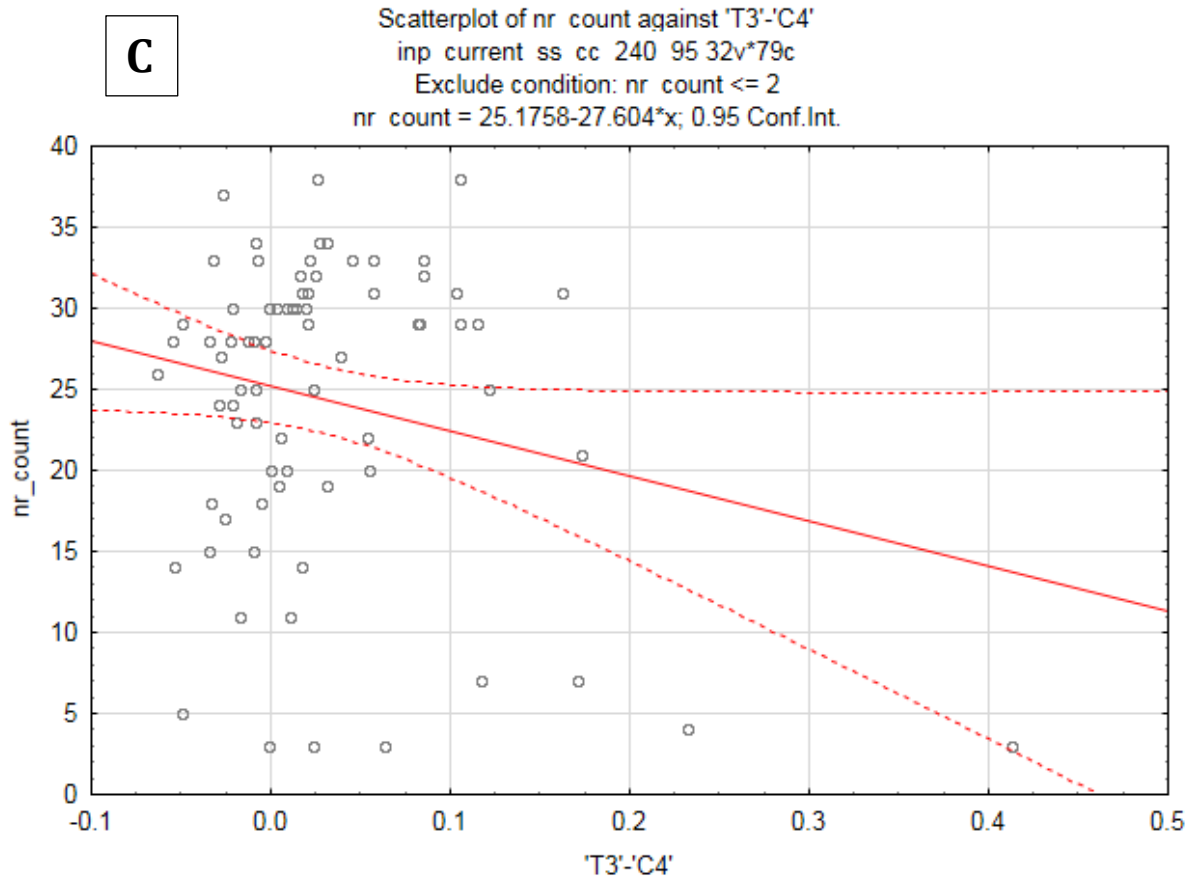
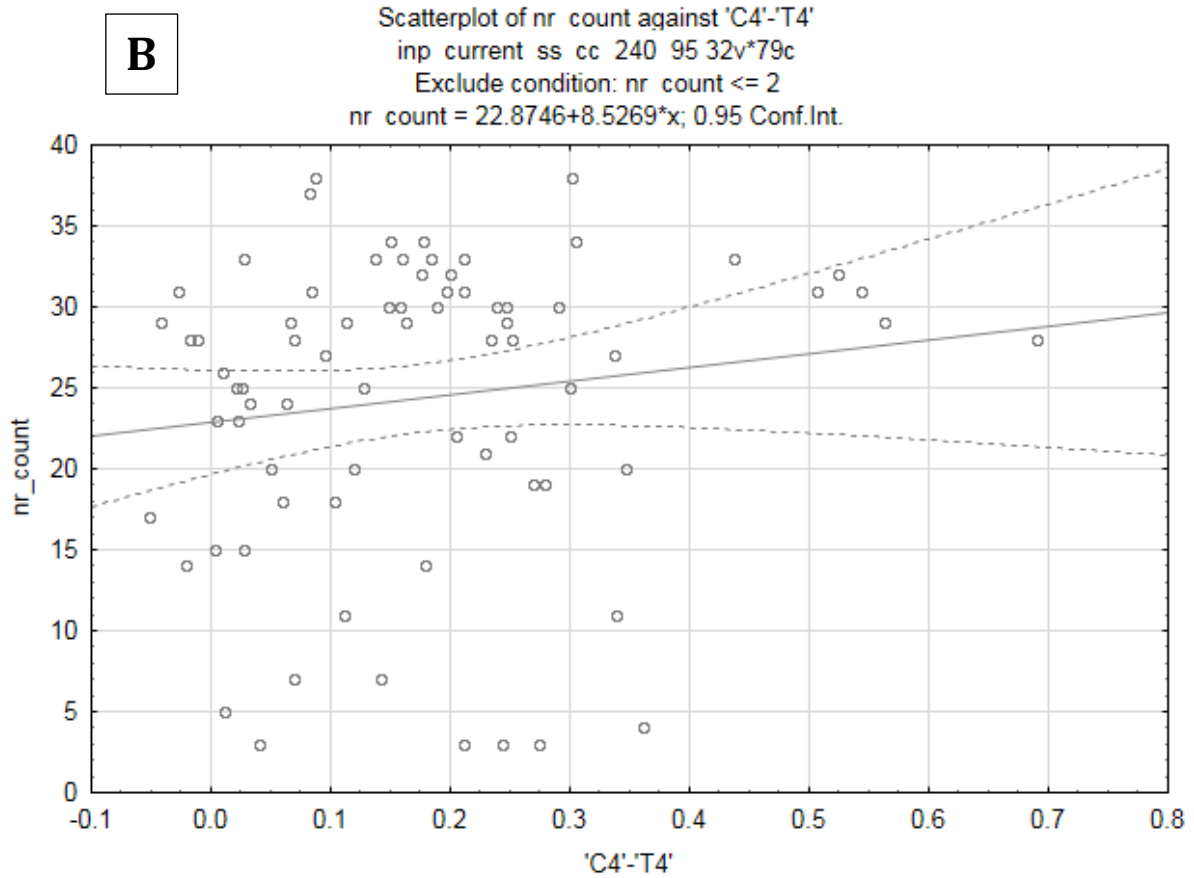
Additionally, a general linear model was run on the normalised GPDC values for each pairwise connection to estimate the predictive power of number of nursery rhymes contributed to the analyses by each infant. The number of nursery rhymes did not predict the GPDC scores for the short-range ipsilateral hemisphere connections T3->C3 ( $F_{(26,49)} = .98, p=.50, n.s.$ ) and T4->C4 ( $F_{(26,49)} = .71, p=.82, n.s.$ ). However, it did significantly explain the coherence in the weaker contralateral connections T3->C4 ( $F_{(26,49)} = 2.06, p<.015, adj R^2=.27$ ) and T3->T4 ( $F_{(26,49)} = 3.78, p<.001, adj R^2=.49$ ), as shown in Table V-7 below.

Table V-7. A general linear regression model on the normalised GPDC values for each pairwise connection predicted by the number of nursery rhymes contributed to the analyses by each infant.

Test of SS Whole Model vs. SS Residual (inp_current_ss_cc_240_95)											
Dependent	Multiple R	Multiple R <sup>2</sup>	Adjusted R <sup>2</sup>	SS Model	df Model	MS Model	SS Residual	df Residual	MS Residual	F	p
'T3'-'C3'	0.5857	0.3430	-0.0056	0.7380	26	0.0284	1.4136	49	0.0288	0.9839	0.5047
'C4'-'T4'	0.5243	0.2749	-0.1098	0.4804	26	0.0185	1.2668	49	0.0259	0.7146	0.8210
'T3'-'C4'	0.7226	0.5221	0.2685	0.2097	26	0.0081	0.1920	49	0.0039	2.0589	0.0145
'T3'-'T4'	0.8168	0.6671	0.4905	0.3853	26	0.0148	0.1923	49	0.0039	3.7768	0.0000

The distributions of the normalised GPDC values for each pairwise connection against the number of contributing nursery rhymes, are shown in *Figure V-7*. In the two ipsilateral connections (*Figure V-4A & B*), there was no relationship between the number of nursery rhymes and the normalised GPDC values, as indicated by the flat gray line across the plots. On the other hand, in the two contralateral connections, plotted in *Figure V-4C & D*, there was a negative relationship between the number of nursery rhymes and the GPDC values, as indicated by the downward red lines. The GPDCs values were lower with the higher number of nursery rhymes in both those connections. This meant that any positive results in the main analyses for the two weaker contralateral connections should have been interpreted with caution as they could be driven by the mere number of trials contributed to the relevant analyses, and not by the metric of interest. It should be noted still that the relationship between the number of trial and the GPDC values in the two contralateral connections could have been due to a few outliers, as can be seen from the distributions in *Figure V-4C & D*. As the two contralateral connections did not show any significant effects in the main analyses and the relationships described here were of no theoretical interest, they were not investigated any further.





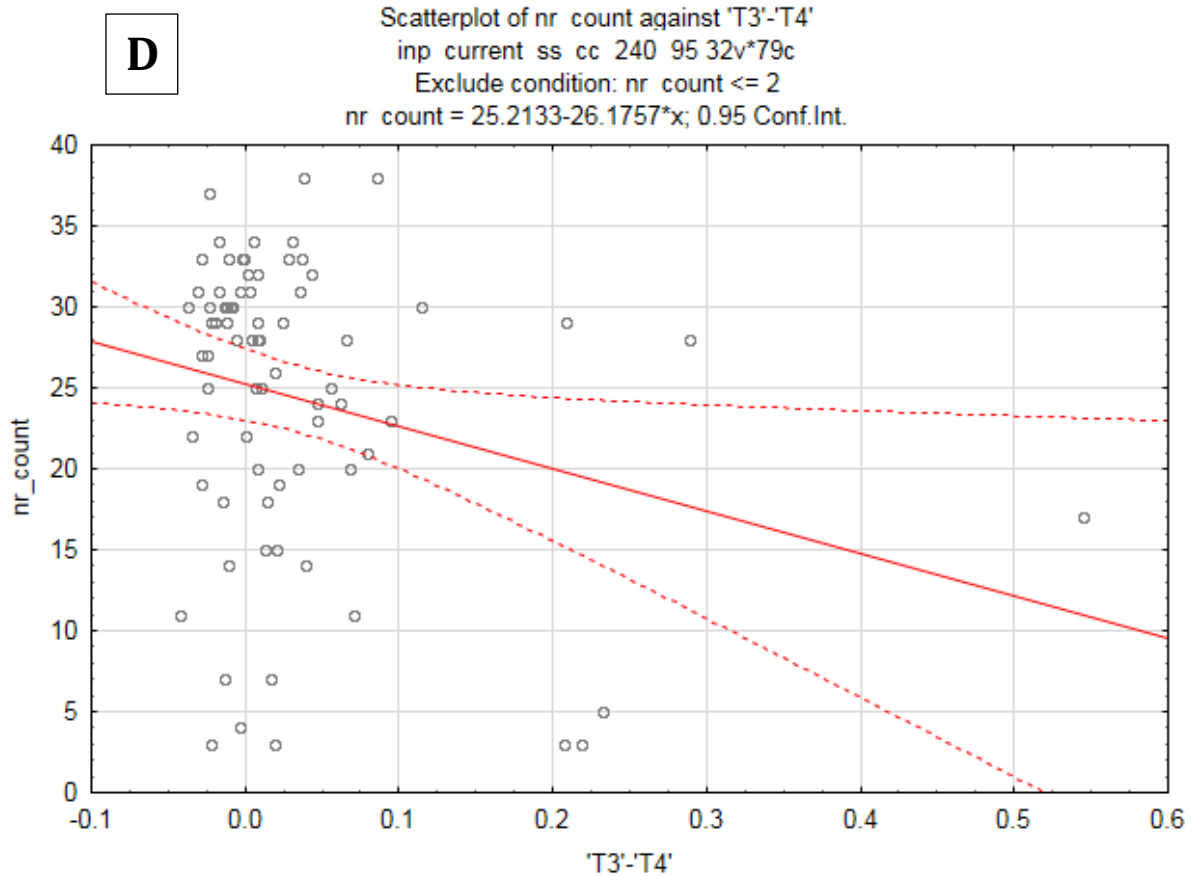


Figure V-4. Scatterplots on the distribution of the normalised GPDC values ( $x$  axis) against the number of contributing nursery rhymes for each infant ( $y$ -axis) in each pairwise connection: A) T3->C3; B) C4->T4; C) T3->C4; D) T3->T4. Solid middle line is the regression line for each pairwise connection plot, the dotted lines are around it are the 95% confidence intervals. The gray lines (in A & B) represent a non-significant regression fit; the red lines (in C & D) show a significant negative relationship.

# Appendix VI

## VI.I PEEPS Protocol & Stimuli Adaptation for Online Administration

### Before the meeting

1. Send parent details for joining the meeting together with information on the nature of the task and the role they will be expected to play
2. Explain to the parents that we would like to go over all 40 words and ask if it is OK to book more than one session if the baby is not happy enough/not paying attention to go over all pictures in one go.
3. Ensure that you have all the materials needed for conducting the experiment within reach
  - a. Slideshow of images in presenter mode
  - b. Toy car
  - c. Flashlight
  - d. Doll
  - e. Cup
  - f. Bag with easily identifiable metal zipper
4. You should make sure that you conduct the experiment in a quiet room with a neutral background and all interruptions are minimised.
5. Check that the volume on your computer is turned up and the webcam is working.

### Before starting the task

1. Say hello to the parent and child once they have joined the meeting and introduce yourself. Use the child's name and wave at them making sure that they can see you and are paying attention to the screen.
2. The child should be free to move around during the experiment, but please ask the parent to make sure that they move the camera to track the child if they move out of view. Also remind them to hide any dummies/ pacifiers for the duration of the experiment.
3. You should sit up straight in your chair facing the camera ensuring that your face and shoulders are visible in the video on screen. The video camera should be centred on your face. Check with the parent that they can see and hear you.
4. Start sharing your presentation and check with the parent that they can see both the presentation that is shared on screen and your video.
5. Check with the parent that they understand the nature of the task and they consent to being recorded.
  - a. The parent will be asked to participate during the 'warm-up' exercise, but they should try not to prompt the child during the task itself.
  - b. During the task, they will have to click between the presentation that is shared on screen and your video (which should be visible in a small box at the bottom right hand corner of the screen). When a
  - c. Please ask the parent to bring the child's attention back to the screen if they become distracted. They can point to your video on screen and direct the child's

- attention to the images shown e.g. “Look at this nice picture”/ “Look at the lady - what is she doing?”
- d. If the child becomes upset at any point during the task ask them to let you know if they feel that a break is necessary.
  - e. Ask the parent if they would be willing to help with delivering the task, if the child offers no response at all.
6. Once the above have been agreed with the parent and they have agreed to having the meeting recorded, proceed with the warm-up exercise, as described below.

### Warm-up exercise

Ask the parent to make sure that your video is maximised on screen so they can see you. Adopt and enthusiastic tone throughout and try to make eye contact with the child.

#### Introduction

- “(Child’s name), do you want to play a game?”
- “Mummy/ Daddy, do you want to play a game?”
- “Yay” (clap) “Let’s all play a game together!”

#### Part 1 – Head, shoulders, knees and toes

- “Let’s start by singing a song.”
- Sing the start of “Head, shoulders, knees and toes” pointing to the relevant parts of your body

*Head, shoulders, knees and toes, knees and toes*

*Head, shoulders, knees and toes, knees and toes*

- “This is my favourite song. Mummy/Daddy can you sing along with me?”

*Head, shoulders, knees and toes, knees and toes*

*Head, shoulders, knees and toes, knees and toes*

*And eyes and ears and mouth and mouth and nose*

*Head, shoulders, knees and toes, knees and toes*

- “That was fun! Shall we sing it again?” (Hopefully the child will say “Again”)
- Repeat the song one more time
- “That was fun! Shall we play another game?”

#### Part 2 – Words and images

- Explain to parent(s) that we will use the book to practice the “naming game”; ask them to join in naming the animals they see and demonstrate to baby how to name pictures on the screen.
- “I brought a book for us to read together. Mummy/Daddy, can you help me read this book?”
- “Click on the picture to see the book”
- When the story is done, thank the parent.
- “Are we ready for our next game now?”

- Ask the parent to click on your video again and confirm that they are ready to start the experiment

### Performing the task

1. Begin the recording and press 'Record'. Check that the meeting is being recorded before you proceed
2. Introduce the task to the child. Use the child's name to draw their attention to the screen. "Do you want to see some pictures? I'm going to show you some pictures and some nice toys. I want you to tell me what they are. Mummy/Daddy, can you click on the pictures?"
3. Use a cheery, enthusiastic tone when speaking to the child. Make sure that you look at the child and say their name as you move between slides to keep them engaged.
4. With each image, action, body part or sound use the levels of elicitation detailed in the table below.
5. You can use 2 prompts for each level of elicitation so a maximum of 6 attempts per word, each time allowing approximately 5 seconds for the child to utter the word. For example for the image of a Baby, you would use the following prompts:
  - i. "What is this?"
  - ii. "What do you see?"
  - iii. "Is this a Baby or a Mummy?"
  - iv. "Is this a *Baby* or is it a Mummy?" (stress the word Baby)
  - v. "This is a Baby. Say Baby"
  - vi. "Say Baby"
7. When asking the questions, make sure you use the child's word occasionally to focus their attention and use encouraging words, as appropriate: "Good try!" / "That's very good!" / "Well done!".
8. If the child utters the correct word spontaneously upon seeing the image, mark this on the scoring sheet and move on to the next word.
9. If they offer a word that sounds like the target word but is not correct try to seek clarification. For instance, if the child says 'Nana' when seeing the picture of a banana, ask them to repeat it using the prompts as outlined in the table (level 1 then level 2 then level 3). Try to get as clear an utterance as possible,
10. Record the child's best attempt in the scoring sheet. You should write down the word as they said it. Tick Word Shape Match (WSM) if their utterance is a good match for the target word (taking into account number of syllables, CV structure and stress pattern). Tick All Consonants Match (ACM) if they correctly produce all the key consonants in the word.
11. If no utterance is offered after all 6 prompts have been exhausted, move on to the next word and tick 'No utterance'
12. If the child's utterance bears no resemblance to the word you were seeking to elicit e.g. 'Nana' for Ball, record their actual utterance in the scoring sheet and leave the Word Shape Match and All Consonants Match boxes unticked.
13. The task will be delivered in blocks of 5 stimuli with a short animation video between each two blocks. Please ask the parent to click on the presentation when the block is complete (if it is not already up). You can play the video by simply clicking on the slide.

14. The child might become distracted or upset during the task or the parent may feel that they need a break. If this happens pause the recording and restart the task and the recording when they are ready to do so. Make a note of this on your scoring sheet.
15. It is also possible that the child refuses to engage with the task altogether. If they offer no utterance, try the first 10 stimuli (with the break in between the two blocks of 5 stimuli) and then discuss with the parent. You can offer to send them the task protocol and ask them to perform the task while you observe. Alternatively, they may feel it would be more appropriate to reschedule the experiment for another.
16. If the child does produce utterances, but none of the utterances produced are correct. (for instance, if the child says 'Nana' for every stimulus), try the first 15 stimuli and then discuss with the parent. If the parent feels that their child should know these words because they have said them previously, you can suggest rescheduling the experiment for another time in order to get a more accurate representation of the child's expressive vocabulary.

## BASIC WORD LIST

	Word	Category	Level 1	Level 2	Level 3
			2 prompts	2 prompts - repeat question if necessary	2 prompts - repeat instruction if necessary
<b>Group 1</b>					
1	BABY	Image 	“What is this?”  “What do you see?”	“Is this a Baby or a Mummy?”	“This is a Baby. Say Baby.”
22	HAT	Image 	“What is this?”  “What do you see?”	“Is it a Hat or a Coat?”	“This is a Hat. Say Hat.”
38	TRUCK	Image 	“What is this?”  “What do you see?”	“Is it a Truck or is it a Boat?”	“This is a Truck. Say Truck”
Reward video					

## Group 2

25	LIGHT	Action <i>See instructions below</i>	“What is this?”  “What do you see?”	“Is this a Light or a Book?”	“This is a Light. Say Light.”
<ul style="list-style-type: none"> <li>● <i>Pick up the flashlight with your right hand and hold it horizontal to the camera in front of your face with the light facing to the left.</i></li> <li>● <i>Turn it on and angle it 15 degrees to the right so that the child can see the light but you avoid the light being directly reflected in the camera.</i></li> </ul>					
12	DOLL	Object <i>See instructions below</i>	“What is this?”  “What am I holding?”	“Is this a Doll or a Car?”	“This is a Doll. Say Doll.”
<ul style="list-style-type: none"> <li>● <i>Pick up the doll and hold it in front of the camera with both hands so that the child can see it.</i></li> <li>● <i>Wave the doll slightly to attract attention and ask the question.</i></li> </ul>					
39	TUMMY	Body part <i>See instructions below</i>	“What is this?”  “What am I pointing to?”	“Is this a Tummy or a Face?”	“This is the Tummy. Say Tummy.”
<ul style="list-style-type: none"> <li>● <i>Pick up the doll toy with your right hand and hold it in front of the camera.</i></li> <li>● <i>Introduce the doll to the child: “This is my Doll. Do you remember it?”</i></li> <li>● <i>Lift up the doll so that the child can clearly see the doll’s tummy in the centre of the camera</i></li> <li>● <i>Holding the doll with your right hand, point to the doll’s tummy with your left hand then rub the doll’s tummy in a circular motion.</i></li> <li>● <i>Repeat the action for each level of elicitation</i></li> </ul>					
Reward video					

Group 3

30	PEEK-A-BOO	Action <i>See instructions below</i>	"What am I playing?"  "What do I say when I play this game?"	"Am I playing Peek-a-boo or am I playing Hide and Seek?"	"Peek-a-boo. Say Peek-a-boo."
----	------------	---	--	--	-------------------------------

- *Cover your face with both hands.*
- *Count to 3 and then reveal your face and smile at the child.*
- *You should open your hands as if opening two doors, with your thumbs remaining in contact with the side of your face.*
- *Repeat the action before asking the child the question.*
- *You should check that they are watching you on the camera.*

19	GO	Action <i>See instructions below</i>	"What did the car do?"  "What will the car do now?"	"Will the car Go or Fly?"	"Go. Say Go."
----	----	---	---	---------------------------	---------------

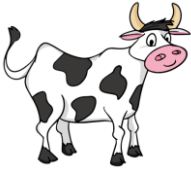
- *Pick up the toy car with your right hand and hold it in front of the camera.*
- *Introduce the toy to the child: "This is my Car. It's very fast. Do you like it?"*
- *Lift your left arm and position it so that it is horizontal to the camera with your fingers flat and close together (palm down). Your forearm should be 20 cm in front of your face at the level of your chin. You are creating a 'bridge' for the toy car with your forearm.*
- *Place the car on the fingers of your left hand and with your right hand gently push the car along your left forearm.*
- *Bring the car back to its initial position (at the tip of the fingers of the left hand) and ask your first question.*
- *Repeat this action for each level of elicitation.*

34	ROCK	Action <i>See instructions below</i>	"What am I doing?"	"Did I Rock the baby or did I Kiss the baby?"	"Rock. Say Rock."
----	------	---	--------------------	---	-------------------

- *Pick up the doll with both hands and hold it up in front of the camera.*
- *Introduce the doll to the child 'This is my doll. Do you remember it?'*
- *Cradle the doll with the doll's head resting on your right elbow and your left hand supporting the doll's feet. Interlock your fingers to form a cradle.*
- *Gently rock the doll back and forth for 5 seconds and then ask your question.*
- *Repeat the rocking motion before each question you ask.*

Reward video

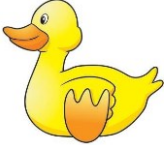
## Group 4

3	BALLOON	Image 	"What is this?"  "What do you see?"	"Is this a Balloon or a Flower?"	"This is a Balloon. Say Balloon."
9	COW	Image 	"What is this?"  "What do you see?"	"Is this a Cow or a Bear?"	"This is a Cow. Say Cow."
11	DOG	Image 	"What is this?"  "What do you see?"	"Is this a Dog or a Bee?"	"This is a Dog. Say Dog."
Reward video					

## Group 5

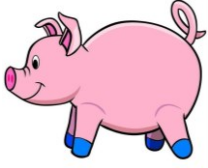
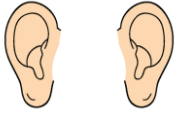
15	EYE	Body part 	“What is this?”  “What do you see?”	“Is this an Eye or is it an Arm?”	“This is an Eye. Say Eye”
<p><i>Instructions for eliciting body part word if image is not recognized by child:</i></p> <ul style="list-style-type: none"> <li>● Ask the parent to select your video. If you normally wear glasses take them off for this part of the task.</li> <li>● Point to your right eye with the index finger of your right hand, gently touching the inferior eyelid.</li> <li>● Your hand should be at a 45-degree angle relative to the side of your face.</li> <li>● Ask ‘What is this?’ / ‘What am I pointing to?’</li> <li>● Repeat level 2 and 3 prompts as above if necessary.</li> </ul>					
29	NOSE	Body part 	“What is this?”  “What do you see?”	“Is this my Nose or my Thumb?”	“This is my Nose. Say Nose”
<p><i>Instructions for eliciting body part word if image is not recognized by child:</i></p> <ul style="list-style-type: none"> <li>● Ask the parent to select your video.</li> <li>● Point to your nose with the index finger of your right hand, gently touching the side of your right nostril.</li> <li>● Your hand should be at a 45-degree angle relative to the side of your face.</li> <li>● Ask ‘What is this?’ / ‘What am I pointing to?’</li> <li>● Repeat level 2 and 3 prompts as above if necessary.</li> </ul>					
10	CUP	Image 	“What is this?”  “What do you see?”	“Is this a Cup or a Bowl?”	“This is a Cup. Say Cup.”
Reward video					

## Group 6

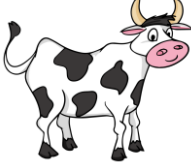
13	DUCK	Image 	“What is this?”  “What do you see?”	“Is this a Duck or is it a Frog?”	“This is a Duck. Say Duck.”
32	PUPPY/ DOGGY	Image 	“What is this?”  “What do you see?”	“Is this a Puppy or is it a Bunny?”	“This is a Puppy. Say Puppy”
16	FINGER	Body part 	“What is this?”  “What do you see?”	“Is this a Finger or an Elbow?”	“This is a Finger. Say Finger”
<p><i>Instructions for eliciting body part word if image is not recognized by child:</i></p> <ul style="list-style-type: none"> <li>● Ask the parent to select your video.</li> <li>● Lift your left hand in front of your face (20 cm away from your face, palm facing the camera).</li> <li>● The index finger of your left hand should be pointing up with the other fingers curled inwards towards the palm.</li> <li>● Point to your left index finger with the index finger of your right hand, touching the side of the left index finger with the right index finger (half-way along the finger).</li> <li>● Ask ‘What is this?’ / ‘What am I pointing to?’</li> <li>● Repeat level 2 and 3 prompts as above if necessary.</li> </ul>					
Reward video					

## Group 7

5	BED	Image 	“What is this?”  “What do you see?”	“Is this a Bed or a Chair?”	“This is a Bed. Say Bed.”
18	FOOT	Body part 	“What is this?”  “What do you see?”	“Is this a Foot or a Head?”	“This is a Foot. Say Foot.”
<p><i>Instructions for eliciting body part word if image is not recognized by child:</i></p> <ul style="list-style-type: none"> <li>● Ask the parent to select your video</li> <li>● Pick up the doll toy with your left hand and hold it in front of the camera.</li> <li>● Introduce the doll to the child: “This is my Doll. Do you remember it?”</li> <li>● Lift up the doll so that the child can clearly see the doll’s legs and feet in the centre of the camera</li> <li>● Holding the doll with your left hand, grab the doll’s right ankle between your right thumb (positioned posteriorly) and your right index finger (positioned anteriorly) and push the doll’s foot or lower leg forward by 30 degrees.</li> <li>● Wiggle the doll’s foot and then, keeping your thumb where it is, move your index finger to the side of the foot touching it gently.</li> <li>● You can try different positions with your fingers to move the doll’s right foot (as necessary).</li> <li>● Ask ‘What is this?’ / ‘What am I pointing to?’</li> <li>● Repeat level 2 and 3 prompts as above if necessary.</li> </ul>					
27	MOUSE	Image 	“What is this?”  “What do you see?”	“Is this a Mouse or a Snake?”	“This is a Mouse. Say Mouse.”
Reward video					
Group 8					
31	PIG	Image	“What is this?”  “What do you	“Is this a Pig or is Goat?”	“This is a Pig. Say Pig”

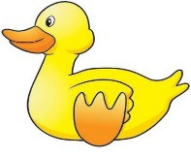
			see?"		
14	EAR	Body part 	"What is this?"  "What do you see?"	"Is this an Ear or is a Neck?"	"This is an Ear. Say Ear"
<p><i>Instructions for eliciting body part word if image is not recognized by child:</i></p> <ul style="list-style-type: none"> <li>● Ask the parent to select your video</li> <li>● Point to your right ear with the index finger of your right hand making sure you touch the helix as you do so.</li> <li>● Your head should be slightly turned to the left (by 15 degrees) so that the child can clearly see your ear on the camera.</li> <li>● Your gaze should remain directed at the child</li> <li>● If you have long hair you should make sure it is tucked behind the ear. Avoid wearing distracting earrings.</li> <li>● Ask 'What is this?' / 'What am I pointing to?'</li> <li>● Repeat level 2 and 3 prompts as above if necessary.</li> </ul>					
28	MOUTH	Body part 	"What is this?"  "What do you see?"	"Is this a Mouth or a Leg?"	"This is a Mouth. Say Mouth"
<p><i>Instructions for eliciting body part word if image is not recognized by child:</i></p> <ul style="list-style-type: none"> <li>● Ask the parent to select your video</li> <li>● Point to your mouth with the index finger of your right hand, gently touching your lower lip</li> <li>● Your hand should be at a 45-degree angle relative to the side of your face.</li> <li>● Ask 'What is this?' / 'What am I pointing to?'</li> <li>● Repeat level 2 and 3 prompts as above if necessary.</li> </ul>					
Reward video					

Group 9

17	FISH	Image 	"What is this?"  "What do you see?"	"Is it a Fish or a Swan?"	"This is a Fish. Say Fish."
24	KITTY/ CAT	Image 	"What is this?"  "What do you see?"	"Is it a Kitty or a Birdie?"	"This is a Kitty. Say Kitty."
26	MOO	Sound elicited by image 	"What does the cow say?"  "What noise does the cow make?"	"Does the cow say Moo or Baa?"	"The cow says Moo. Say Moo."

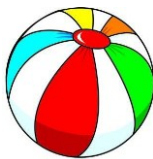
Reward video

Group 10

6	BIB	Image 	"What is this?"  "What do you see?"	"Is this a Bib or a Toy?"	"This is a Bib. Say Bib."
33	QUACK	Sound elicited by image 	"What does the duck say?"  "What noise does the duck make?"	"Does the duck say Quack or Miaow?"	"The duck says Quack. Say Quack."
40	WOOF	Sound elicited by image 	"What does the doggy say?"  "What noise does the doggy make?"	"Does the doggy say Woof or Neigh?"	"The doggy says Woof. Say Woof."

Reward video

Group 11

20	HAIR	Body part 	"What is this?"  "What do you see?"	"Is this Hair or Teeth?"	"This is Hair. Say Hair."
<p><i>Instructions for eliciting body part word if image is not recognized by child:</i></p> <ul style="list-style-type: none"> <li>● Ask the parent to select your video.</li> <li>● With your right hand pick up a strand of hair making sure the child can see it.</li> <li>● If you have long hair, lift your hair so that it is at a 60-degree angle from your head (measured inferiorly).</li> <li>● If your hair is in a ponytail, turn your head 15 degrees to the left and lift your ponytail, while still directing your gaze towards the camera.</li> <li>● If your hair is short, pick up a strand of hair from the top (right side of your head) and tilt your head forward slightly.</li> <li>● Ask 'What is this?' / 'What am I pointing to?'</li> <li>● Repeat level 2 and 3 prompts as above if necessary.</li> </ul>					
37	TOE	Body part 	"What is this?"  "What am I pointing to?"	"Is this a Toe or a Chin?"	"This is a Toe. Say Toe."
<p><i>Instructions for eliciting body part word if image is not recognized by child:</i></p> <ul style="list-style-type: none"> <li>● Ask the parent to select your video.</li> <li>● Pick up the doll with your right hand and hold it in front of the camera.</li> <li>● Introduce the doll to the child: "This is my Doll. Do you remember it?"</li> <li>● Lift up the doll so that the child can clearly see the doll's legs and feet in the centre of the camera</li> <li>● Holding the doll with your right hand, hold the doll's right foot with your left hand (between the thumb and index finger) and push the foot forward by 30 degrees.</li> <li>● Keeping your thumb where it is, move your left index finger to the side of the foot pointing at the big toe.</li> <li>● Ask 'What is this?' / 'What am I pointing to?'</li> <li>● Repeat level 2 and 3 prompts as above if necessary.</li> </ul>					
2	BALL	Image 	"What is this?"  "What do you see?"	"Is this a Ball or a Can?"	"This is a Ball. Say Ball."

Reward video

Group 12

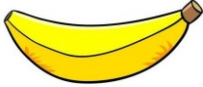
7	CHEESE	Image 	“What is this?”  “What do you see?”	“Is this Cheese or Soup?”	“This is Cheese, Say Cheese.”
35	SHOE	Image 	“What is this?”  “What do you see?”	“Is this a Shoe or a Dress?”	“This is a Shoe. Say Shoe.”
21	HAND	Body part 	“What is this?”  “What do you see?”	“Is this a Hand or a Knee?”	“This is a Hand. Say Hand.”

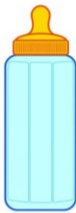
*Instructions for eliciting body part word if image is not recognized by child:*

- Ask the parent to select your video.
- Raise your left hand in front of your face (20 cm away), with the palm facing the camera and your fingers spread out.
- First wave your left hand in front of the camera.
- Next with the index finger of your right hand, point towards your left hand. You should not touch the left hand and the index finger of your right hand should be positioned horizontally, at the level of the tip of your left thumb.
- Ask ‘What is this?’ / ‘What am I pointing to?’
- Repeat level 2 and 3 prompts as above if necessary.

Reward video

Group 13

4	BANANA	Image 	"What is this?"  "What do you see?"	"Is this a Banana or a Coconut?"	"This is a Banana. Say Banana."
8	COOKIE/ BISCUIT	Image 	"What is this?"  "What do you see?"	"Is this a Cookie or an Apple?"	"This is a Cookie. Say Cookie."
23	JUICE	Image 	"What is this?"  "What do you see?"	"Is it Juice or Tea?"	"This is Juice. Say Juice."
36	SOCK	Image 	"What is this?"  "What do you see?"	"Is this a Sock or a Cap?"	"This is a Sock. Say Sock."
Reward video					

EXPANDED WORD LIST					
	Word	Category	Level 1	Level 2	Level 3
			2 prompts	2 prompts - repeat question if necessary	2 prompts - repeat instruction if necessary
41	BELLY BUTTON	Body part <i>See instructions below</i>	“What is this?”  “What am I pointing to?”	“Is this a Belly Button or a Fingernail?”	“This is the Belly button. Say Belly button.”
	<ul style="list-style-type: none"> <li>• Pick up the doll toy with your right hand and hold it in front of the camera.</li> <li>• Introduce the doll to the child: “This is my Doll. Do you remember it?”</li> <li>• Lift up the doll so that the child can clearly see the doll’s tummy in the centre of the camera</li> <li>• Holding the doll with your right hand, point to the doll’s belly button.</li> <li>• If the child looks confused, try pressing on the doll’s belly button.</li> </ul>				
42	BLANKET	Image 	“What is this?”  “What do you see?”	“Is this a Blanket or a Window?”	“This is a Blanket. Say Blanket.”
43	BLOCK	Image 	“What is this?”  “What do you see?”	“Is this a Block or a House?”	“This is a Block. Say Block.”
44	BOTTLE	Image 	“What is this?”  “What do you see?”	“Is this a Bottle or a Plate?”	“This is a Bottle. Say Bottle.”

45	BUG	Image 	“What is this?”  “What do you see?”	“Is this a Bug or a Shark?”	“This is a Bug. Say Bug.”
46	CHICKEN	Image 	“What is this?”  “What do you see?”	“Is this a Chicken or a Horse?”	“This is a Chicken. Say Chicken.”
47	COMB	Image 	“What is this?”  “What do you see?”	“Is this a Comb or a Pen ?”	“This is a Comb. Say Comb.”
48	DIAPER/ NAPPIES	Image 	“What is this?”  “What do you see?”	“Is this a Nappy/ Diaper or a Jumper?”	“This is a Nappy/ Diaper. Say Nappy/ Diaper.”
49	ELEPHANT	Image 	“What is this?”  “What do you see?”	“Is this an Elephant or a Giraffe?”	“This is an Elephant. Say Elephant.”
50	DRINK	Action	“What am I doing?”  “What do I do with the cup?”	“Do I Drink from the cup or Eat from the cup?”	“Drink. Say Drink.”
<ul style="list-style-type: none"> <li>• Pick up the cup with your right hand and lift it to your lips as if you were taking a drink.</li> <li>• As you do this make sure that the child is watching you and repeat the action if necessary before asking the question.</li> </ul>					

51	LION	Image 	“What is this?”  “What do you see?”	“Is this a Lion or a Turtle?”	“This is a Lion. Say Lion.”
52	MONKEY	Image 	“What is this?”  “What do you see?”	“Is this a Monkey or a Tiger?”	“This is a Monkey. Say Monkey.”
53	SHEEP	Image 	“What is this?”  “What do you see?”	“Is this a Sheep or an Ant?”	“This is a Sheep. Say Sheep.”
54	SOAP	Image 	“What is this?”  “What do you see?”	“Is this Soap or a Brush?”	“This is Soap. Say Soap.”
55	SPOON	Image 	“What is this?”  “What do you see?”	“Is this a Spoon or a Pot?”	“This is a Spoon. Say Spoon.”
56	STOP	Action <i>See instructions below</i>	“What did the car do?”  “What will the car do now?”	“Did the car stop or fall?”  “Did you see the car <i>stop</i> or did you see it fall?”	“Stop. Say Stop.”

			<ul style="list-style-type: none"> <li>● Pick up the toy car with your right hand and hold it in front of the camera so that the child can clearly see what it is .</li> <li>● Introduce the toy to the child: "This is my car. Do you remember it?"</li> <li>● Hold the car up with your right hand and gently move it from the right side to the left side, lifting up your left hand as if to stop the car. Just before the car reaches your left hand stop the car mid air and ask the question.</li> <li>● Repeat the action as you ask the second question.</li> </ul>		
57	TONGUE	Body part <i>See instructions below</i>	<p>"What is this?"</p> <p>"What did I point to?"</p>	"Is this my Tongue or my Heart?"	"This is my Tongue. Say Tongue."
	<ul style="list-style-type: none"> <li>● Say the child's name to ensure that they are looking at you.</li> <li>● Smile then stick out your tongue</li> <li>● Point to your tongue with the index finger of your right hand, without touching your tongue.</li> <li>● Ask the question, then repeat the action, to make sure the child notices you sticking out your tongue.</li> </ul>				
58	TRAIN	Image 	<p>"What is this?"</p> <p>"What do you see?"</p>	"Is this a Train or a Bus?"	"This is a Train. Say Train."
59	WATCH	Image 	<p>"What is this?"</p> <p>"What do you see?"</p>	"Is this a Watch or a Key?"	"This is a Watch. Say Watch."
60	ZIPPER	Action/ Object <i>See instructions below</i>	<p>"What is this?"</p> <p>"What am I doing?"</p>	"Is this a Zipper or a Button?"	"This is a Zipper. Say Zipper".
	<ul style="list-style-type: none"> <li>● Pick up the bag with the zipper and hold it in front of the camera, slightly tilted towards the child so that they can clearly see the zipper.</li> <li>● Open and close the zipper slowly</li> <li>● Repeat the action each time you ask a question.</li> </ul>				

## Appendix VII

### VII.I Relevant Research Output During PhD Program

#### Presentations

##### Academic

1. Georgieva S., Austin T., Belteki G., Kourtzi Z., & Leong, V. (April, 2019). Genetic Influences on Early Brain Development: Learning from changes in neuronal oscillations. (April 2018). *Conference Talk, Newnham College Annual Graduate Conference, Cambridge, UK. (1<sup>st</sup> Place Award (GBP25) for Best Presentation)*
2. Georgieva S., Austin T., Belteki G., Kourtzi Z., & Leong, V. (March, 2019). A Neurogenetic Study of Dyslexia Risk in Neonates. *Early Career Investigator Blitz Talk and Poster Presentation. 31<sup>st</sup> Cambridge Neuroscience Seminar.*
3. Georgieva S., Austin T., Belteki G., Kourtzi Z., & Leong, V. (August, 2019). A Neurogenetic Study of Dyslexia Risk in Neonates. *Slam Talk and Poster Presentation. 11<sup>st</sup> Annual Meeting of the Society for the Neurobiology of Language, Helsinki, Finland. (GARS Research and Travel Award, GBP960).*

##### Public Engagement

4. Georgieva, Lester, Noreika, Yilmaz, Wass & Leong (Feb, 2018). Topographical and Spectral Signatures of Infant Movement Artifacts in EEG. *Public Talk, 5<sup>th</sup> Cantabulgarian Conference, Bulgarian Embassy in London, UK.*
5. Georgieva S., Austin T., Belteki G., Kourtzi Z., & Leong, V. (April, 2019). A Neurogenetic Study of Dyslexia Risk in Neonates. *Public Engagement talk, CamBrain/PNN Neurotalks at the pub, Cambridge, UK.*
6. Georgieva S., Austin T., Belteki G., Kourtzi Z., & Leong, V. (April, 2019). A Neurogenetic Study of Dyslexia Risk in Neonates. *Pudding Seminar Public Talk at Newnham College, University of Cambridge.*

##### Grants

7. Georgieva S., Leong V., Kourtzi Z. (June 2020). Understanding Gene-Environment Interactions in the Etiology of Dyslexia During Infancy. *G C Grindley Fund Award (GBP2500) – given in 2020 for exceptional circumstances surrounding the COVID 19 crisis.*

#### Journal Papers

1. Georgieva S., Lester S., Noreika V., Yilmaz M. N., Wass S., & Leong V (2020). Toward the Understanding of Topographical and Spectral Signatures of Infant Movement Artifacts in Naturalistic EEG. *Frontiers in Neuroscience, 14* 352. <https://doi.org/10.3389/fnins.2020.00352>.
2. Noreika, V., Georgieva, S., Wass, S., & Leong, V. (2020). 14 challenges and their solutions for conducting social neuroscience and longitudinal EEG research with infants. *Infant Behavior and Development, 58*(June 2019), 101393. <https://doi.org/10.1016/j.infbeh.2019.101393>

## VII.II Methods Paper One

OPEN ACCESS

Lancaster University, United Kingdom

\*Correspondence: Stanimira Georgieva

Edited by:  
Guillaume Dumas,  
Institut Pasteur, France

Reviewed by:  
Hoshinori Kanazawa,  
The University of Tokyo, Japan  
Kirsty Jayne Dunn,

Jonathan Levy,  
Aalto University, Finland

Specialty section:  
This article was submitted to  
Brain Imaging Methods, a section of the journal  
Frontiers in Neuroscience



METHODS  
published:28April2020 0  
doi:10.3389/fnins.2020.00352



Received: 05 February 2019

Accepted: 23 March 2020

Published: 28 April 2020

Citation:

Georgieva S, Lester S, Noreika V,  
Yilmaz MN, Wass S and Leong V  
(2020) Toward the Understanding of Topographical and Spectral  
Signatures of Infant Movement  
Artifacts in Naturalistic EEG.  
*Front. Neurosci.* 14:352. doi: 10.3389/fnins.2020.00352

# Toward the Understanding of Topographical and Spectral Signatures of Infant Movement Artifacts in Naturalistic EEG

Stanimira Georgieva<sup>1\*</sup>, Suzannah Lester<sup>1</sup>, Valdas Noreika<sup>1</sup>, Meryem Nazli Yilmaz<sup>1</sup>,  
Sam Wass<sup>2</sup> and Victoria Leong<sup>1,3</sup>

<sup>1</sup> Department of Psychology, University of Cambridge, Cambridge, United Kingdom, <sup>2</sup> Department of Psychology, University of East London, London, United Kingdom, <sup>3</sup> Division of Psychology, Nanyang Technological University, Singapore, Singapore

Electroencephalography (EEG) is perhaps the most widely used brain-imaging technique for pediatric populations. However, EEG signals are prone to distortion by motion. Compared to adults, infants' motion is both more frequent and less stereotypical yet motion effects on the infant EEG signal are largely undocumented. Here, we present a systematic assessment of naturalistic motion effects on the infant EEG signal. EEG recordings were performed with 14 infants (12 analyzed) who passively watched movies whilst spontaneously producing periods of bodily movement and rest. Each infant produced an average of 38.3 s (SD = 14.7 s) of rest and 18.8 s (SD = 17.9 s) of single motion

segments for the final analysis. Five types of infant motions were analyzed: Jaw movements, and Limb movements of the Hand, Arm, Foot, and Leg. Significant movement-related distortions of the EEG signal were detected using cluster-based permutation analysis. This analysis revealed that, relative to resting state, infants' Jaw and Arm movements produced significant *increases* in beta (~15 Hz) power, particularly over peripheral sites. Jaw movements produced more anteriorly located effects than Arm movements, which were most pronounced over posterior parietal and occipital sites. The cluster analysis also revealed trends toward *decreased* power in the theta and alpha bands observed over central topographies for all motion types. However, given the very limited quantity of infant data in this study, caution is recommended in interpreting these findings before subsequent replications are conducted. Nonetheless, this work is an important first step to inform future development of methods for addressing EEG motion-related artifacts. This work also supports wider use of naturalistic paradigms in social and developmental neuroscience.

Keywords: electroencephalography, signal distortion, motion artifacts, infants, naturalistic paradigm

## INTRODUCTION

### Motion in EEG Measurements

Electroencephalography (EEG) is a widely used brain imaging technique for both adult and pediatric populations, owing to its low risk to the individual (Teplan, 2002) and ease of application (De Haan, 2013). In particular, rising interest in the neural processes that play a critical part in early emotional, social, and cognitive development has led to an increased use of EEG with infants and young children (Saby and Marshall, 2012). For decades, research in infants and young children has employed EEG as a methodology to understand the neural processes involved in numerous aspects of early cognitive development (Maguire et al., 2014). Like the adult EEG signal, infant EEG can be decomposed into different frequency bands such as delta (1–3 Hz), theta (3–6 Hz), alpha (6–9 Hz), beta (9–20 Hz), and gamma (>20 Hz), although infant oscillations are generally slower than that of their functional equivalents in adults (Orekhova et al., 1999). Neural activity in different bands has been shown to be of functional significance for the study of a wide range of developmental phenomena including attention (e.g., theta and alpha bands: Xie et al., 2018), face and emotion processing (e.g., alpha band: Batty et al., 2011; Dawson et al., 2012), early language acquisition (Kuhl, 2010), object recognition (Reynolds, 2015), memory (Richards et al., 2010), auditory processing (Telkemeyer et al., 2011), action perception and production, imitation (e.g., alpha band, van Elk et al., 2008; Marshall et al., 2011), and interpersonal synchronization (e.g., alpha and theta bands: Leong et al., 2017; Wass et al., 2018). In particular, early language acquisition research uses brain-to-speech coupling (a measure of how accurately neural oscillatory activity tracks dynamic rhythmic patterns in the speech signal) to study infant-directed speech perception across a number of frequency bands: delta – corresponding to prosodic stress patterns in the speech signal (Leong et al., 2017); theta – representative of the syllabic rate in the English language (Leong et al., 2017; Kalashnikova et al., 2018); and alpha – corresponding to phonemic/onset-rime patterns in speech (Leong et al., 2017). Further, frontal high gamma activity in infants has been associated with the ability to discriminate native from non-native phonetic sounds (55–75 Hz: Peña et al., 2010), and also with inhibitory control and attention shifting skills (31–50 Hz: Benasich et al., 2008). Finally, alpha band power and coherence have been shown to change developmentally in relation to working memory and encoding tasks (Bell and Wolfe, 2007; Köster et al., 2017), while frontal and parietal theta is particularly associated with perceptual binding in learning (Köster et al., 2017).

However, EEG recordings are highly prone to interference by both biological factors (such as electromyogenic activity, the electrical activity produced by voluntary or automatic muscle contractions) and non-biological factors (such as electrical line noise) (Nathan and Contreras-Vidal, 2015). In particular, artifacts induced by motion (such as head motion, jaw motion, or blinking) are a major and common source of EEG distortion. These distortions can result in misinterpretation of underlying neural processes or sources; or to the inaccurate detection and diagnosis of brain disorders (Guerrero-Mosquera et al., 2012). For example, in a concurrent EEG and eye-tracking paradigm, Yuval-Greenberg et al. (2008) showed that the most likely source of the induced gamma-band EEG response – an EEG waveform associated with visual object representation, recognition and attention – were small eye movements made at the onset of each stimulus, rather than a neural response to the stimuli *per se*. Köster (2017) highlighted that a similar, if not worse, problem may exist for infant EEG analyses utilizing activity in the 25–35 Hz gamma range. It has not yet been clarified whether microsaccades (tiny involuntary fixation-related eye-movements) can be measured in infants, whether they generate similar EEG artifacts, and whether the correction methods used for adult EEG signals are applicable to infant data (Kampis et al., 2016).

For adult populations, motion artifacts can be avoided or minimized by direct instruction, such as asking participants to only swallow and blink between trials or during other defined periods and asking them to avoid significant head and facial muscle contractions during critical periods of recordings (Reis et al., 2014). However, this strategy is less effective for clinical and pediatric populations whose ability to understand and comply with verbal instruction is greatly reduced. Young infants present a particular challenge in this regard, as they have a high natural tendency for movement, which cannot be constrained by instruction. Indeed, it is widely acknowledged that EEG recordings produced by infants and young children are heavily contaminated by various motion artifacts, including gross motor movements and eye blinks (Bell and Cuevas, 2012).

One common strategy used in infancy paradigms is to reduce motion indirectly through attentional capture – that is, the experimenter monitors the infants' attentional state through a video feed and only delivers experimental stimuli during attentive periods when the infant is relatively still. However, as exemplified in **Supplementary Table S1 (Supplementary Material)**, our own studies suggest that even when contingently delivered screenbased stimuli are used (including cartoons, real language, and artificial language stimuli), infant movement (i.e., facial, limb or postural movement) is still present throughout 60–70% of the total stimulus presentation time. In more naturalistic paradigms, in which infants are not watching a computer monitor but engaged in social interaction, we might expect that artifacts will be even more prevalent.

### Naturalistic Social Paradigms

The necessity for ecological validity in experimental developmental psychology has been emphasized for decades (Tunnell, 1977; Fabes et al., 2000). It is accepted that the combination of experimental and naturalistic research methods offers a more complete insight into child development (Dahl, 2016). The use of naturalistic methods is more common in social science research than in the neurosciences. However, across a number of neuroscience sub-fields, such as developmental and social neuroscience, the balance is beginning to shift in favor of EEG paradigms with greater ecological validity (for example, see Babiloni et al., 2007; Lindenberger et al., 2009; Dumas et al., 2010, 2011, 2014). Still, a tension exists between the ecological benefits conferred by naturalistic social interaction, and the generation of EEG artifacts from participants' social behavior (e.g., facial and gesticulatory movements). Observational

assessments of behavior in the “real world,” such as in the home or school environment, have higher ecological validity than assessments that occur within structured experiments in laboratory settings, where participants typically perform screen-based tasks that require little or no social interaction. The lack of social interaction is a particular issue for infancy studies. Humans are a social species (Schilbach et al., 2013) and most attention and learning during the crucial early years of life takes place in social settings. For example, social factors influence attention allocation: when a parent pays attention to a particular object during social interaction with their infant, infants’ own attention to the object is increased (Yu and Smith, 2016; Wass et al., 2018). Therefore, when social interaction is excluded from infant experimental paradigms, this can affect the validity and generalizability of early cognition studies.

However, real-world measurements also carry the disadvantage of less (or no) control over key environmental variables that can affect behavior, leading to increased intersubject variability. As a compromise, naturalistic laboratory settings allow for some controlled task-based variation between participants and facilitate the emergence of more natural behavior whilst at the same time minimizing environmental variation (Noris et al., 2012; TamisLeMonda et al., 2017). For example, with infants, such compromises may allow for parental social interaction within a semi-scripted paradigm.

#### Common EEG Motion Artifacts

Neural activity at the scalp level is low in amplitude compared to other sources of electrical activity, such as electrical potentials generated by muscle activity and environmental electrical noise (i.e., a low signal-to-noise ratio). Amplification that is applied to the neural signal also amplifies non-neural contaminants, and therefore does not improve neural signal detection. Myogenic EEG artifacts that arise from involuntary movements supporting the physiological functioning of the body, such as heartbeat and respiratory torso movements, can be monitored using a devoted channel, such as an electrocardiogram (ECG), which can significantly improve automated detection and removal strategies (Klados et al., 2011). By contrast, voluntary movement, such as motion generated by the jaw, head, body and limb, are both less easy to monitor through a devoted channel, and less frequently addressed in the literature. For example, in an extensive review of methods for EEG artifact detection and rejection, Islam et al. (2016) found that across 46 publications that were reviewed, over 70% focused solely on automatic movements, with the rest only partially addressing forms of voluntary action. Perhaps best understood are the effects of eye and jaw motions. However, this literature pertains almost exclusively to adults, and very little is known about the nature of motion artifacts in *infant* EEG signals.

A single eye movement can produce a number of artifacts that arise from different mechanisms (e.g., eye rotations and blinks) and differ in their amplitude and spectral properties (Plöchl et al., 2012). Eye movements can introduce systematic biases in both adult (Yuval-Greenberg et al., 2008; Keren et al., 2010) and infant (Köster, 2017) EEG analyses. Jaw movements are another major source of EEG artifacts. In experimental paradigms, jaw motion commonly occurs as a corollary of speech production (Ganushchak et al., 2011). Jaw motion causes significant distortion to EEG signals due to facial myogenic potentials originating from contractions of the frontalis and temporalis muscles when tensing or clenching the jaws (Sweeney et al., 2012). Speech-related articulatory motions are known to reduce the signal-to-noise ratio of neural signals that relate to cognition (Brooker and Donald, 1980). For instance, the myogenic potential generated by the temporalis muscle, used for closing the lower jaw, spreads widely over the scalp frontal/temporal/parietal locations, generating large broadband artifacts in the EEG signals measured over these regions (Brooker and Donald, 1980).

Myogenic artifacts are more problematic for infant than adult measurements since involuntary physiological activity such as heartbeat and blinks are less stereotypical than adults' and therefore more difficult to identify in the EEG recording (Fujioka et al., 2011). A further complication arises from infants' tendency to move abruptly and frequently, which creates temporary displacement of channels on the scalp and high-amplitude artifacts (Fujioka et al., 2011; Bell and Cuevas, 2012; Hoehl and Wahl, 2012). Hence, artifacts arising in infant EEG are more challenging to identify and remove using the de-noising procedures normally applicable to adult EEG.

### Current Strategies for Addressing Motion Artifacts

There are two major approaches to addressing the problem of movement-related artifacts in EEG data. Researchers typically (1) exclude artifact-contaminated segments by employing strict rejection procedures/thresholds; or (2) attempt to remove artifacts from data using correction procedures such as independent component analysis (ICA) (Gwin et al., 2010). The first approach (artifact exclusion) is conservative and may entail considerable data loss, especially with infant participants (Fujioka et al., 2011; also see **Supplementary Table S1**), potentially leading to skewed data and subsequent misinterpretation. Therefore, there is increasing interest in correction procedures that permit the accurate identification and removal of artifacts from EEG data without a significant compromise to the integrity of underlying neural activity.

Several methods have been proposed for the detection and removal of physiologically generated artifacts from the EEG signal. These include the use of linear regression (Klados et al., 2011), Independent Component Analysis (ICA), and blind source separation (BSS) based on Canonical Correlation Analysis (CCA, Vos et al., 2010), to separate the neural signal from interfering electrical signals in the EEG trace. However, none of these methods is able to completely remove motion artifacts from the EEG signal and may even remove some genuine neural activity of interest. As noted by Islam et al. (2016), current artifact detection-removal methods are sub-optimal because these methods typically only address a single artifact class and necessitate dedicated reference channels, and moreover, frequently result in overcorrection. For example, a common approach to addressing some classes of stereotypical artifacts (such as eye blinks) is to include an observed reference channel that independently measures the artifact signal (i.e., EOG for eye muscles, ECG for heartbeat). Next, linear regression or ICA may be employed to estimate the similarities between the

EEG signal and the reference signal, permitting removal of the artifact estimate from the EEG signal (Klados et al., 2011). ICA does not require the presence of a reference signal (although it can improve performance, see Plöchl et al., 2012), and is therefore a widely used approach for artifact removal (Chaumon et al., 2015). While all these approaches can be successful for highly stereotypical artifacts (such as heartbeats and eye-blinks in adults), they fail for less stereotypical artifacts that particularly affect infant EEG as these methods are designed to extract repetitive patterns in the signal over many occurrences of the same type of noise (where each noise occurrence presents with a similar shape and form). Further, the placement of additional reference channels (e.g., under the eyes) may not be well tolerated by pediatric participants.

Two correction approaches that have been successfully applied in infant EEG studies are *Independent Channel Rejection* (He et al., 2007) and *Artifact Blocking* (Fujioka et al., 2011). Both methods only eliminate data in trials and/or channels where there is an artifact (defined by amplitude displacement above a certain absolute threshold), without removing the whole trial or channel. Thus, these methods ameliorate the problem of data loss due to artifact rejection and

have been used in a number of research studies as a pre-processing data cleaning strategy (i.e., Corrigan and Trainor, 2014; Folland et al., 2014; Slugocki and Trainor, 2014; Trainor et al., 2014; Agyei et al., 2016). However, these strategies still rely on the successful classification of portions of the EEG signal as artifactual, which is itself a non-trivial task. Classification often relies either on some form of automated pattern-recognition (i.e., machinelearning classifiers) or a combination of automated and manual identification (i.e., ICA where components are rejected by eye). EEG pattern-recognition is challenging due to the large amount of natural variation in the signal, which is exacerbated further by the presence of sporadic artifactual activity, hindering accurate classification.

Newer machine learning approaches have begun to be employed for automatic classification of artifactual and nonartifactual segments of EEG signals. These methods are particularly applicable to motion-related distortions which are less stereotypical. For example, O'Regan et al. (2010) trained a classifier to segregate different types of artifactual neural EEG signals. In their study, 19 adult participants were instructed to perform 32 types of head actions that had previously been related to distortions in ambulatory EEG, including head shaking, rolling, nodding, jaw clenching, lowering and raising of eyebrows. A classifier using linear discriminant analysis was trained from a random selection of 20% of the data and resulted in up to 76.49% accuracy in distinguishing head-motion contaminated EEG. Similarly, Lawhern et al. (2012) investigated methods for automatic detection and classification of EEG artifacts generated by different types of jaw and eye movements. An autoregressive model using a Maximum Likelihood Estimator was used to estimate features for a support vector machine classifier. The procedure was successful in differentiating between broad classes of artifacts (i.e., jaw and eye); but it tended to group together more specific artifacts from a common source. However, the error rate of falsely classifying epochs with no artifacts was low (the reported average accuracy for 5 out of 7 participants was over 96%, and over 81% for the remaining 2). Therefore, newer machine learning approaches may, in future, have strong utility for the detection of more complex classes of motion artifacts. It is anticipated that the data from the current study could be used, in future, to inform the development of such new tools for artifact identification in infant EEG signals.

#### Pilot Study to Assess Common Infant Movement Types and Their Prevalence in a Naturalistic Task

A pilot study was conducted to identify the most prevalent infant motions in a naturalistic play setting where infant participants interacted with toys in a social or non-social context. We were interested in identifying motion patterns elicited during social interaction, as naturalistic developmental paradigms often include, or at least permit social interaction. Hence, we identified the most common infant motions produced during naturalistic object-oriented play and also investigated how these differed between social and non-social experimental conditions. The full inventory of infant movements analyzed included Talking, Chewing, Whining, Side-to-Side neck movements, Up and Down neck movements, Small Hand, Small Foot, Large Arm and Large Leg movements. The pilot study is fully described in **Supplementary Material** section "Pilot Study 1." Our results revealed that across both play conditions, infant motion was present over 95% of the time, which represents near-continuous contamination of the EEG signal. We further noted that the most commonly occurring types of infant motion were small hand and large arm movements, which is unsurprising given that the paradigm involved object-oriented play. When further considering the types of motions that occurred as a function of play condition (social or non-social), we found that an increase in motion frequency was observed during non-social relative to social play for chewing and nodding movements, and no difference was observed for

limb (arm and leg) movements and talking/whining. This pattern suggests that when actively engaged in play with their parents, infants were less distracted and therefore showed a lower tendency to move. **Supplementary Material** section “Results” presents a detailed account of the full set of results from the pilot study.

### Study Aims

The high prevalence of movement observed during the pilot study motivated a more detailed study seeking to identify the spectral and topographical effects of movement on the infant EEG signal. As the removal of artifacts from EEG data is restricted by current methodological limitations, and clinical and infant populations are unable to comply with directions to reduce movement to lessen distortion of the signal, there is a clear need for research to report how these artifacts distort EEG data. Accordingly, the major aim of this work is to investigate the individual topological and spectral features of commonly occurring motion-related EEG artifacts in infants, as compared to resting state EEG measurements.

## METHODS

### Participants

Fourteen infants participated in the study. There were 6 boys and 8 girls in the group, with an average age of 338.85 days ( $SD = 59.59$ ). Two infants produced insufficient resting state data due to fussiness, and so were excluded from the analysis. The remaining 12 infants comprised 5 boys and 7 girls, with an average age of 325.5 days ( $SD = 51.77$ ). All mothers reported no neurological problems and normal hearing and vision for their infants. Participants also took part in other separate experiments on the same day as the current study, but these data are unrelated to the current study and will not be reported. This study was approved by the Cambridge Psychology Research Ethics Committee, and parents provided written informed consent on behalf of their children.

### Materials

For the duration of this experiment, the infants saw a series of brief age-appropriate videos. The videos included familiar nursery rhymes (such as “Twinkle Twinkle Little Star”) that were sung by a female adult, interspersed with different (static) cartoon pictures. All infants saw the same set of videos, presented in a counterbalanced order. The videos lasted up to 22.77 min in total.

### Protocol

Here, infants’ spontaneous motions during passive video viewing were analyzed. As shown in **Figure 1**, infants passively watched videos while seated in a high chair, with their mothers seated adjacent to them. A passive (video viewing) task was used in order to allow us to better assess the individual contribution of each motion type. As noted in section “Pilot Study to Assess Common Infant Movement Types and Their Prevalence in a Naturalistic Task” and detailed in **Supplementary Material** section 2.2, during object-oriented play, motions typically cooccurred because infants were actively exploring the toy objects (e.g., infants picked up the toy with their hands whilst bending their necks downward to inspect it). In the recorded EEG signal, the effects of these co-occurring motions would mix and overlap spectrally and topographically, making it very difficult to isolate the individual effects. In a passive paradigm, infants were more likely to make only one type of motion at a time, providing unambiguous exemplars for

analysis<sup>21</sup>. The passive design also had the added advantage of optimizing the comparability of motion-related EEG with infant “resting state” EEG. Infant resting state EEG is typically recorded whilst infants quietly watch a screen with some non-arousing video presentation (Bell and Cuevas, 2012). This protocol minimizes frequent eye and motor movements, although some isolated movement by infants always occurs. Here, we capitalized on these isolated infant motions in order to collect both motion-related EEG and resting state EEG *within the same recording*.

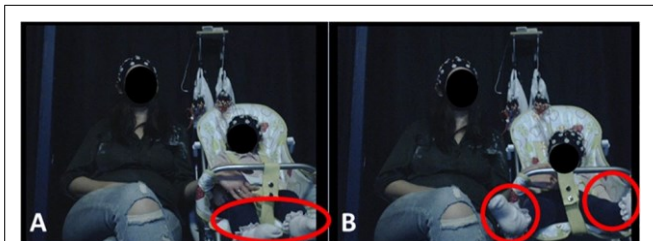


FIGURE 1 | Experimental Setup. Infants were seated on a highchair next to their mothers. A camera, placed in a central location in front of participants, recorded infants' behavior and motions. (A) (left) illustrates resting state behavior, when the infant showed no visible motion. (B) (right) illustrates leg movement by the infant. Written informed consent was obtained from the parents for the publication of these images.

## EEG Acquisition

A 32-channel BIOPAC Mobita mobile amplifier was used with an Easycap electrode system. Electrodes were placed according to the 10–20 international system for electrode placement (see **Figure 3D**). Data were acquired using Acqknowledge 5.0 software, at a 500 Hz sampling rate. The ground electrode was affixed to the back of the neck as this location is the least invasive for infants.

The 12 infants included in the final analysis produced an average of 325.5 s (SD = 51.8 s, range 274–448 s) of raw continuous EEG recording, which included periods of rest and of spontaneous motion. The raw EEG recording was then segmented to chunks containing only either rest, or a single motion, as operationally defined in later sections.

## Video Recordings

A Logitech High-Definition Professional Web-camera recorded infants' behavior (at 30 frames per second) throughout the session. Afterward, each video was manually screened frame-by-frame and coded to ascertain the start and end times of each motion type of interest, and of the resting state periods.

## Video Coding

The motion and rest timings were manually extracted from each video by video coding. Three trained video-coders noted the onset and offset time of each motion or rest period by looking through the recorded video frame by frame.

## Resting State

<sup>21</sup> Note that we also ran a second pilot study (described in **Supplementary Material** section “Supplementary Pilot Study 2 on Actively-Elicited Motion”), where an infant-adult dyad actively modeled the motions observed in the first pilot study using the same toys to elicit the same motions for the infant. In this second pilot study, the infant produced collectively more than 3 h of EEG recording over the course of three separate testing sessions; the adult produced around 20 h of EEG over 7 testing sessions. Similar to the first behavioral-only pilot study, the cooccurrence of motion was very high in this active protocol and we were unable to identify sufficient isolated repetitions for each infant motion. This necessitated the choice of a passive paradigm for the main study.

Resting state periods were strictly defined as periods during which the infant exhibited fixated gaze with no visible facial or bodily motion and maintained this state for at least half a second. Periods with any visible motion were excluded. On average, infants produced 49.2 s of resting data (SD = 24.4) prior to pre-processing, and 38.3 s (SD = 14.7) of clean resting data after pre-processing.

### Motion Artifacts

Five types of *infant* motions were selected for the analysis. These included: Jaw movements (e.g., talking/babbling and chewing), and Limb Movements (LMs) of the Hand, Arm, Foot and Leg. Only motions lasting for longer than 250 ms were included for the analysis. An additional inclusion criterion was that only one motion should be present at any time – periods containing overlapping motions were excluded from the analysis. Identical to the resting state data, during motion, infants' gaze was fixed and no eye-movements other than blinks were present. Infants produced an average of 22.2 s of data per motion type

(SD = 19.6 s) prior to data-cleaning, and an average of 18.8 s (SD = 17.9 s) of pre-processed data were included in the final analysis. A detailed operational definition of each one of these motions is given in **Supplementary Material** sections “Facial Motion Descriptives,” “Body Movement Descriptives,” and “Head Movement Descriptives.” We focused on these motions because they were the most prevalent types of motions made by infants in the pilot study. Statistical stratification was performed to assess the effect of data duration differences on the main reported results (described in **Supplementary Material** section “Statistical Stratification to Assess for Effects of Data Duration Differences Across Conditions”).

### Video-EEG Synchronization

Video recordings were synchronized to the EEG signal by sending triggers via a radio frequency transmitter which marked the EEG trace and produced a light signal that was visible on the video recording. Synchronization was performed manually by recording the exact frame at which the onset of the synchronization light signal occurred. Thus, the synchronization accuracy was limited to the temporal resolution of the video frame rate, which was 30 frames per second (33 ms).

### EEG Acquisition and Analysis

#### EEG Pre-processing

Noisy channels with raw amplitude fluctuations above 100  $\mu$ V above the rest of the channels for over 25% of the recording session were rejected. **Table 1** shows the number and location of rejected channels for each infant. Next, the data were rereferenced to the average of the remaining channels. EEG segments containing each type of motion were concatenated, creating separate continuous datasets for each motion type, and for the resting state. These concatenated data were then visually inspected for eye-blinks and high amplitude fluctuations, which were removed unless directly arising from the modeled action.

TABLE 1 | EEG channels rejected for each infant and movement type.

Infant ID	Rejected channels					
	RS	Jaw	Hand	Arm	Foot	Leg
1	-	-	-	-	-	-
2	-	-	-	-	-	-

3	CP5	-	-	CP5	-	CP5
4	-	-	-	-	-	-
5	-	-	-	-	-	-
6	T7, TP9	T7, TP9	-	TP9, P7	-	TP9
7	TP9	-	TP9	TP9	-	TP9
8	-	-	-	-	-	-
9	-	-	-	-	-	-
10	C3, CP2	-	C3, CP2	-	-	-
11	-	-	-	Cz, TP9	TP9	Cz
12	T7	-	-	-	-	T7

RS, resting state.

### EEG Power Analysis

To describe the topographical distribution of power by frequency for each condition (rest or single motion type), raw power scores were transformed into z-scores to permit averaging across individual infants in a standardized manner. First, each continuous dataset per condition and infant was divided into non-overlapping 1-second-long epochs. A Fast Fourier Transform (FFT) was performed for each epoch, yielding 3dimensional estimates of spectral power (channel  $\times$  frequency bin  $\times$  epoch) for each infant and condition. Next, for each frequency bin, the sample mean of all epochs and channels was subtracted from the sample mean for each channel (averaged over epochs). This differenced data were then divided by the sample standard deviation of all epochs and all channels per frequency bin to derive the normalized power spectra z-scores, as described in eq. (1) below:

$$z_{pow(c,f)}^{(infant, cond)} = \frac{mean_e(pow_{(c,infant,f), cond}) - mean_e(mean_c(pow_{(infant, cond)}))}{stdev_e(mean_c(pow_{(infant, cond)}))}$$

where  $c$  = channel;  $f$  = frequency bin;  $e$  = epoch (1)

For each condition, the standardized power spectra for each channel were then averaged across all infants, according to eq. (2).

$$mean\_z\_pow_{(c,f)}^{(cond)} = \frac{P_{infant} z_{pow_{(c,cond,f)}}}{n_{infant}} \quad (2)$$

For clarity of reporting, spectral power in the following scalp topographical plots is reported as averaged over pre-defined frequency bands. As infant oscillations are generally slower than their functional equivalents in adults (Orekhova et al., 1999), the standard EEG frequency bands were downward-adjusted accordingly: delta (1–3 Hz), theta (3–6 Hz), alpha (6–9 Hz), low beta (9–13 Hz), and high beta (13–20 Hz) (Leong et al., 2017).

### Cluster-Based Permutation Test of Motion-Related Power Changes

Statistical comparison of spectral power differences between motion and resting state data was conducted using the Matlab-based toolbox, Fieldtrip (Oostenveld et al., 2011). First, frequency decomposition of the pre-processed data was performed using a multi-taper FFT based on discrete prolate spheroidal sequences (DPSS) and 2 Hz smoothing frequency, for the frequency range of interest 0.1–20 Hz (*ft\_freqanalysis*). The derived power spectra ( $\mu\text{V}^2/\text{Hz}$ ) during the resting state and each motion type were thus calculated separately for each infant, and then a grand-average was calculated across infants using *ft\_freqgrandaverage*. Next, statistically significant differences in power between each motion type and the resting state were assessed at the group level by conducting a within-subject non-parametric cluster-permutation test. We corrected for multiple comparisons using Monte-Carlo estimates of the two-tailed significance probabilities ( $\alpha = 0.05$ ) from the permutation distribution based on 10,000 permutation cycles, using Fieldtrip's function *ft\_freqstatistics*. This procedure identified clusters of neighboring sensors where the EEG power differed significantly between a specific type of motion and the resting state data (in either direction), and is particularly suitable for use with non-parametric datasets (Maris and Oostenveld, 2007). Clusters were defined with a minimum of three sensors per cluster (with one unit distance between neighboring sensors, and yielding an average of 6–7 neighbors per sensor).

## RESULTS

### Motion Types and (Isolated) Prevalence

The total duration of each type of motion (occurring in isolation) for each infant is shown in **Table 2**. All 12 infants whose data were analyzed produced motion in at least two out of five motion categories. As not all the infants spontaneously produced all types of motion, the number of participants analyzed for each motion type varied between 4 and 10 (see **Table 2**).

Note that there was a difference in the prevalence of the same motions reported in the behavioral pilot study and here. This is because the behavioral pilot (see **Supplementary Figure S3** in **Supplementary Material** section “Results”) considered all occurrences of motion present during the task

TABLE 2 | Total duration (in seconds) of clean pre-processed isolated motion and resting state EEG contributed for the final analysis by each infant.

InfantID	Totaldurationcontributed(s)					
	RS	Jaw	Hand	Arm	Foot	Leg
1	15	8	7	5	4	19
2	46	–	14	11	8	27
3	53	8	–	10	–	57
4	33	14	–	6	–	–
5	10	18	12	10	4	18
6	36	10	27	11	–	21
7	34	–	25	28	–	14
8	36	4	–	–	–	4
9	44	–	41	9	–	5
10	59	–	27	–	–	–
11	54	–	36	27	93	51
12	40	–	–	5	–	6

Average(SD) 38.3(14.7) 10.3(5) 23.6(11.9) 12.2(8.4) 27.3(43.9) 22.2(18.4)

(including co-occurring motion), whereas here we only report isolated motion.

## Scalp Topographies by Frequency Band

### Resting State

As shown in **Figure 2A**, infants' resting state scalp topology was characterized by high power over posterior regions in delta and theta bands, and high alpha power over centroparietal regions. Additionally, beta power was higher over bilateral orbitofrontal regions, while it was relatively lower over bilateral temporal regions, which could reflect the presence of oculomotor activity (such as microsaccades). Individual plots for each infant's resting state scalp topologies are presented in **Supplementary Figure S4A (Supplementary Material section "Individual Infants' Scalp Topographies During Resting State and Motion")**.

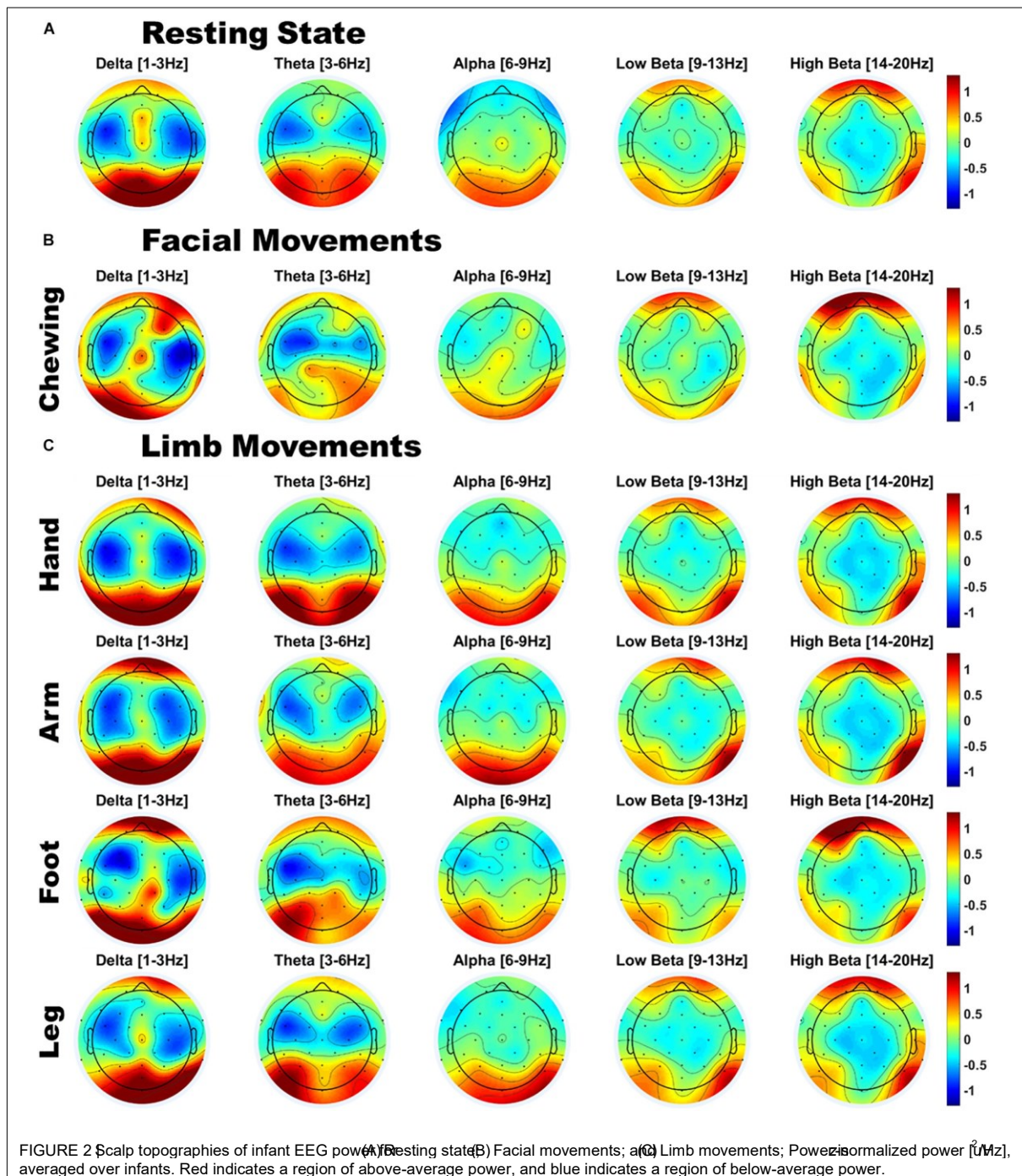
### Movement

Compared to resting state EEG, the scalp topology of infants' movement EEG also showed a broadly similar pattern of high delta/theta power over posterior regions and high beta power over orbitofrontal regions (see **Figures 2B,C**). However, visual inspection also indicated variations in scalp topography by movement class. To assess whether there were significant patterns of spectral and topographical difference in the power spectra of motion relative to the resting state data, a cluster permutation analysis was applied (see section "EEG Acquisition and Analysis"). Individual plots for each infant's motion-related scalp topologies are presented separately for each motion type in **Supplementary Figures S4B–F (Supplementary Material section "Individual Infants' Scalp Topographies During Resting State and Motion")**. Here, the group average topologies are presented.

### Motion-Related Differences in Spectral Power and Topography

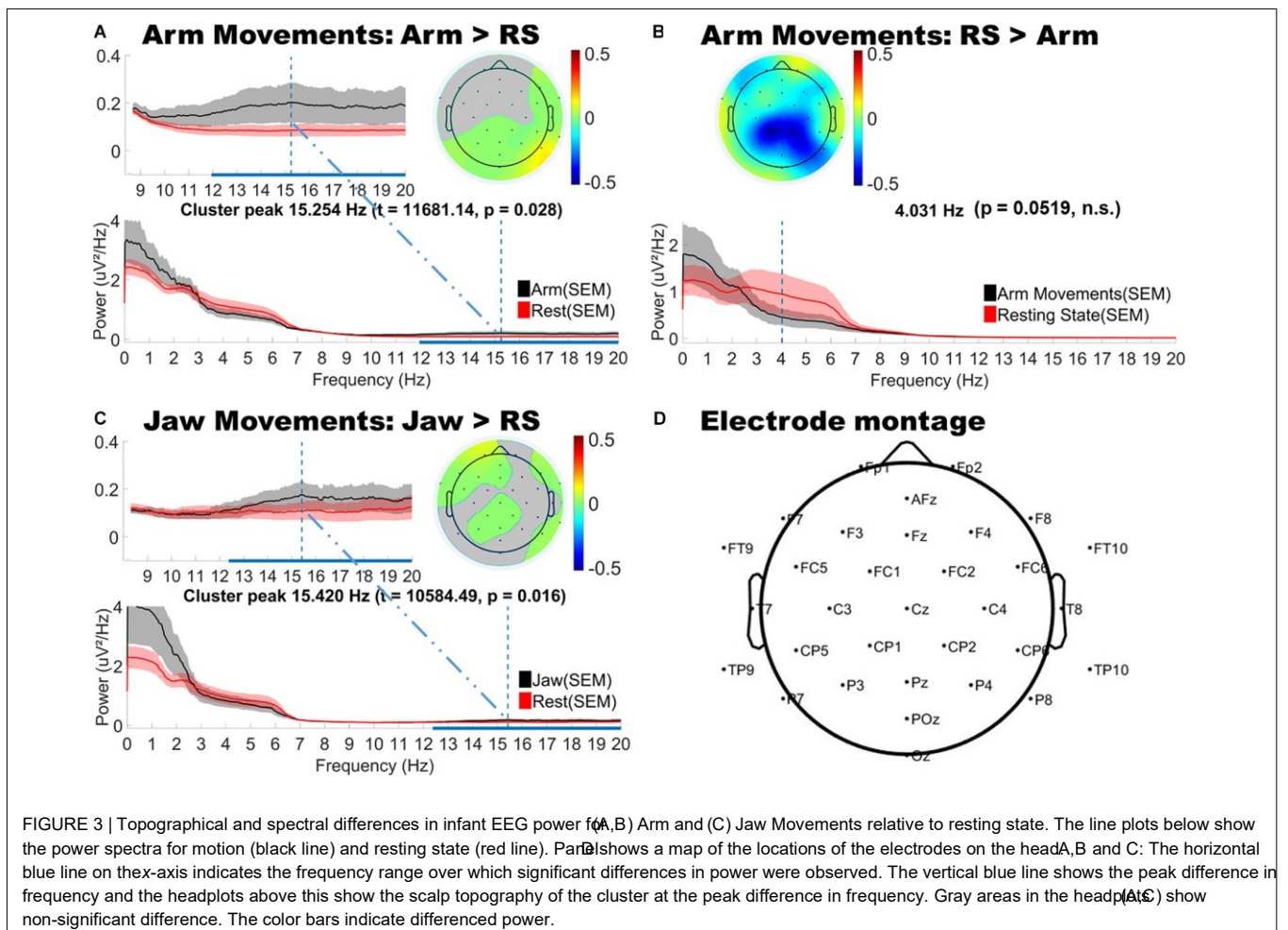
As shown in **Figure 3**, jaw movements and upper limb movements (arm) did indeed produce significantly *increased* low and high beta (12–20 Hz) power, peaking at around 15 Hz for both motion types and most strongly observed at peripheral sites. Jaw movements generally produced anteriorly located increases in beta power, particularly over frontal and fronto-temporal regions bilaterally. Smaller central increases in beta power were also observed. By contrast, arm movements mainly generated posterior increases in beta power, strongest over posterior parietal and occipital sites. Lower limb movements (foot and leg) and hand movements produced no significant changes as compared to the infants' resting state topography.

The cluster analysis also revealed trends toward *decreased* power in the theta and alpha bands, however, these did not reach statistical significance ( $p = 0.0519$ ). These trends in theta and alpha decreases were consistently observed over central topographies for all motion types (see **Figure 3B** for example).



## DISCUSSION

Electroencephalography recordings are highly prone to the misinterpretation of underlying neural processes, or even the inaccurate detection and diagnosis of brain disorders (Guerrero-Mosquera et al., 2012). Young infants present a distortion by motion-related artifacts, which can result in particular challenge as they have a high natural tendency for movement, which cannot be constrained by instruction. This work represents the first systematic assessment of the effects of naturalistic (social) infant motion on the recorded EEG signal. It is intended that this work will build toward a more comprehensive database or “Artifact Library” which could later serve as a common resource for EEG researchers in social and developmental neuroscience.



In a behavioral pilot study, we assessed the prevalence of motion in adult-infant dyads during social and non-social naturalistic play paradigms. We observed that motion occurred >95% of the time, for both infants and adults, and in both types of social play settings. For such datasets, it would not be feasible to adopt a simple approach of rejecting (excluding) all motion-contaminated data, as this would entail losing an unacceptably high proportion of data. However, before artifact removal methods (such as ICA or CCA) can be effectively applied to the EEG signal, it is first necessary to understand the exact distortion that these motions would produce. Accordingly, the current study attempted to document the topographical and spectral properties of each of the most prevalent (frequently occurring) types of motion that were observed in the behavioral pilot. Here, infants' motions, produced one at a time during a passive

video-viewing paradigm, were analyzed. The spectral properties of these motion-contaminated signals were then contrasted against a resting state baseline.

In general, the infants' motions generated only a few significant deviations from the resting state power spectrum. Upper limb movements (arm) and jaw movements (e.g., chewing) produced stronger and more widespread artifacts than hand movements and lower limb movements (foot and leg). Further, infants' arm and jaw movement artifacts were both characterized by *increased* beta power which was most evident at peripheral sites. Jaw movements generated mainly anteriorly located increases in beta power over frontal and fronto-central sites whereas arm movements produced strong posterior increases in beta power over parietal and occipital regions. By contrast, lower limb and hand movements produced no discernible changes in infants' spectral power.

One potential explanation for the apparent limited effects of motion contamination in infants' EEG data could be that insufficient data were collected from infants to reveal true differences. Data from only 12 infants were included in the final analysis, with an average of 38.3 s (14.7) of rest and of 18.8 s (SD = 17.9 s) of single motion segments per infant. However, this explanation is unlikely as the main results were visually similar to the effects of motion described in our supplementary study where the number of trials produced by the infant was comparable to the data quantity produced in a controlled laboratory experiment with an adult (e.g., the mother of the infant produced a 450 s of resting state data compared to 328 s produced by the infant; and the infant also had a higher number of recorded instances for all motion types than his mother). An alternative explanation could be a bias in data quantity in favor of the resting state condition. However, an additional clusterbased permutation analysis on a stratified subsample of the data (reported in **Supplementary Material** section "Statistical Stratification to Assess for Effects of Data Duration Differences Across Conditions") following the original protocol showed that Arm-related effects were virtually identical. Although the Jaw-related effects did not reach significance in the stratified subsample (due to loss of power), similar spectral trends in the data were observed. These supplementary analyses confirm that data duration differences did not introduce systematic biases into the results. Furthermore, it should be noted that infants' resting state data differed qualitatively from resting state data that is typically collected from adults. Since we could not instruct infants to produce a state of rest, their resting state data was collected incidentally (e.g., whilst watching a video) and periods of nonmotion were identified through video coding. This protocol of recording continuous EEG and selecting relevant segments offline is frequently used in infant research (e.g., Orekhova et al., 2014). Still, it is possible that this procedure inadvertently included some tonic muscle activity that was not visible on video, leading to an underestimation of the true extent of the effects of motion on the infant's EEG signal.

Although not statistically significant, we observed trends toward decreased theta and alpha power at central sites associated with all motion types. Alpha or "mu rhythm" suppression has been well-documented in infants and young children in relation to both action production and action observation (Liao et al., 2015). For example, Marshall et al. (2011) reported suppression effects in the 6–9 Hz range, broadly distributed over the scalp, when 14-month old infants were engaged in action observation in a social context. This raises the question of whether the movement-related suppression effects observed here are truly "artifactual", since they could also reflect the cognitive or social processes that underpin infants' action generation, and therefore are more in the realm of confounding neural processes as opposed to truly artifactual signals that originate from peripheral muscle or electrode movement. According to this view, only unintentional or involuntary movement produces truly artifactual effects. However, to definitively separate these effects would require concurrent measures of intentionality and

cognitive processing, along with active and passive manipulations of participant motion, which are beyond the scope of the current study.

#### Implications for EEG Research Using Naturalistic Paradigms

The growth of naturalistic EEG paradigms reflects the view that movement is a natural neural state (Makeig et al., 2009) and that cognitive processes themselves are embodied

(Gramann et al., 2011). The brain maintains representations of its internal (proprioception) and external (motor behavior and audio-visual scene) environment – and these representations are constantly, dynamically updated through action. To study cognition in this holistic and action-oriented way, new technologies and imaging methods are required, such as mobile sensors that can synchronously image the brain (i.e., wireless EEG) and the body (i.e., motion capture) and perform online registration of the two modalities. One such system is the sensor technology for mobile brain/body imaging (MoBI) which has shown promising results for studying changes in the EEG power spectrum in relation to participants' gait during locomotion (Gramann et al., 2011). The MoBI system has also been used to localize independent components in relation to motions such as head-turning, pointing, and walking in a 3D virtual reality orientation task (Makeig et al., 2009). However, when such sophisticated methods for tracking and removing EEG artifacts are not available, precautions should be taken when analyzing data from naturalistic paradigms, as discussed next.

Our results indicated that for infants, one likely effect of motion was reduced EEG power over central sites in the theta and alpha bands. Accordingly, if EEG researchers are investigating phenomena where infant alpha band effects are predicted (e.g., mu de-synchronization or emotion-related frontal alpha asymmetry), care must be taken to avoid including confounding jaw or limb motions, which can independently create changes in alpha band power across frontal and central sites. Additionally, EEG researchers studying speech perception or brain-to-speech synchronization in the beta bands might be cautious when interpreting results if jaw or arm motion is present during stimulus presentation. For example, jaw motions may provide a confounding factor when infants suck on a teething toy whilst watching screen-based experimental stimuli. It is important that experimenters check, and report (e.g., by video coding) the relative occurrence of these movement artifacts in infant participants across experimental conditions and groups, to verify that any reported results cannot be explained by differences in patterns of movement. Further, we also found that infants' peripheral EEG channels were particularly vulnerable to motion-related power increases, and therefore recommend particular caution (or exclusion) when analyzing these channels.

#### Implications for EEG Research Using ERP Paradigms

Motion artifacts present a different set of challenges for research employing the use of evoked-response potentials (ERPs, sometimes also referred to as event-related potentials). ERPs measure changes in the electrical potential of the EEG trace in response to a discrete event in time, in some or all electrodes. ERPs are thus time-locked responses averaged over a number of repetitions (trials) of the same event. The measurement of ERPs is perhaps the most widely used EEG method in the infant literature. ERPs have been used to study face perception (e.g., de Haan and Nelson, 1999; Halit et al., 2004); visual recognition memory (deRegnier et al., 1997); the maturation of auditory perception (e.g., Kushnerenko et al., 2002); auditory recognition memory (e.g., deRegnier et al., 2000, 2002); word recognition and language processing of phrases based on intonation (Mannel and Friederici, 2009; Mannel et al., 2013). The negative central component (NC), which is the developmentally earliest described endogenous ERP component, is present in newborn infants (Nelson, 1996) and has been associated with aspects

of attention (e.g., Richards, 2003), memory (e.g., Nelson et al., 1998; Pascalis et al., 1998; Lukowski et al., 2005), and face recognition (e.g., de Haan and Nelson, 1997). By far the most widely used and reported ERP component in the developmental literature is the mismatch negativity (MMN), a negative deflection which arises as a pre-attentive response (Kraus and Naatanen, 1995) to an oddball stimulus embedded within a sequence of standard stimuli (the typical probability of the oddball stimulus is about 10–20%).

The MMN is implicated in the discrimination of phonemes (e.g., Winkler et al., 1999) and native vs. non-native stress patterns (e.g., Weber et al., 2004, 2005), and also in the ability to perceive complex statistical regularities such as embedding (nesting rules between stimuli) (e.g., Winkler et al., 2018).

Unless motion is time-locked to the neural phenomenon of interest (e.g., saccades to visual stimulus onset), the effect of motion will vary from one trial to the next, introducing a random (rather than systematic) bias. However, sufficient repetitions will decrease the effects of non-time-locked motion on the ERP signal. Nonetheless, a high prevalence of motion in an ERP paradigm may still reduce the signal-to-noise ratio (SNR) of the effect of interest, when compared to motion-free data of a similar quantity. A reduced SNR has two main effects on the ERP: (1) it reduces the amplitude of the ERP and (2) reduces the precision with which the latency of EEG components can be estimated. These effects also depend on the exact topography of the ERP component of interest. Future studies are needed to investigate these effects in more detail.

The current study may be of particular relevance to ERP research in situations where the amplitude or latency of the neural response is related to neuro-oscillatory processes in one or more frequency bands. Such event-related oscillations (EROs; Csibra and Johnson, 2007), also referred to as event-related synchronisation (ERS), are frequency-band specific bursts in EEG activity that are loosely time-locked to a specific event (for example, the gamma bursts described in the Introduction section “Motion in EEG Measurements”). EROs represent a sustained response to stimulation and have been used to study rapid auditory processing and acoustic change detection (e.g., theta: Musacchia et al., 2015; theta and gamma: Musacchia et al., 2017; Cantiani et al., 2019); infant-directed speech processing (delta and theta: Zhang et al., 2011); discrimination of native and non-native syllable contrasts (delta, theta and gamma: Ortiz-Mantilla et al., 2013); and perceptual binding and object permanence (broadband gamma: Csibra et al., 2000) in young infants. Accordingly, motion which affects spectral power in the frequency band(s) of interest would confound the detection and accurate measurement of the ERO/ERS event. Still, it is worth noting that an ERO/ERS (as well as any other ERP) study design would be less affected by random non-timelocked motion-related artifacts than designs using continuous data analysis, for example when studying naturalistic social interactions, sustained attention, connectivity, or resting-state default-mode networks, to name a few.

Another interdependency between neural oscillatory processing and ERPs is through variations in attentional state. Different attentional processes (alerting, orienting, executive control, sustained attention) are strongly correlated to the neural activity in the theta and alpha bands (in infants and adults: Fan et al., 2007; Xie et al., 2017), but also to beta and gamma band activity (in adults: Fan et al., 2007). The amplitude and latency of attention-related ERP components is modulated by attentional state (e.g., Fu et al., 2005; for review, see Luck et al., 2000), and also by underlying endogenous oscillatory fluctuations in theta and alpha bands (e.g., Buzsaki, 2006; Vanderperren et al., 2008; Harris et al., 2018). Therefore, one may envisage a scenario in which frontal/central alpha desynchronization, which is related to sustained attention in infants between 10 and 12 months (Xie et al., 2017), is potentially affected by infant

hand motions that decrease central theta/alpha power and become more frequent during periods of infant inattention. This in turn may produce systematic artifactual differences in the measured ERPs to stimuli presented within a sustained attention paradigm.

It is important to note that based on the current study alone, it is not possible to estimate how the effect sizes of measurements (ERP or time/frequency-based) in a given paradigm compare to the effect sizes of these artifacts. Therefore, EEG researchers may need to assess whether the betweencondition effects in their experiment are significantly affected by motion artifacts, especially in cases where there is a difference in movement between conditions, or where the phenomenon under investigation may be biased by motion.

#### Implications for ICA Artifact Removal

Independent component analysis is one of the most frequently used techniques for removing motion artifacts from adult EEG data. However, its use in infant EEG is still limited as the spectrotemporal signatures of motion in infant EEG are not as well described as adults'. To assess whether the findings of the current study may be used to guide and improve ICA correction of infant EEG data, we conducted a case study using infant Arm movement data. Arm movements were selected since this class of motion generated the most widespread artifactual effects. The full details of this supplementary analysis are provided in **Supplementary Material** section "ICA Analysis." Briefly, independent components (ICs) were rejected in two stages: (1) ICs clearly pertaining to eye movements (blinks and saccades) were removed from both Resting State (RS) and Arm movement data, and (2) ICs specifically related to Arm movement whose identification was guided by the spectral difference maps produced in the main "Results" section – were only removed from Arm movement segments. Next, we computed the spectral topographic difference maps of the "cleaned" Arm movement data with respect to the RS data, using the same statistical procedure as in the main "Results" section. We found that guided-ICA was indeed successful in removing infants' Arm movement-related artifacts. Although both positive and negative differences clusters were still present, none of them reached significance. Still, it has to be cautioned that even when guided, the ICA procedure was most likely unable to fully separate Arm movements from other similar but non-related neural activity (we noted that Arm movement-related activity was observed to be spread across 3–6 different ICs in individual infants). Thus, some Arm-movement related activity may have remained in ICs that were not removed. In summary, the results presented in this study (specifically **Figure 3**) may indeed be used to guide the targeted removal of jaw and arm movement-related ICs from the infant EEG signal. This may have some benefit in reducing the impact of excessive motion, but is unlikely to completely eliminate artifactual motion effects.

#### Limitations and Future Directions

The major limitation to the current work is that the study was conducted with a small sample size ( $N = 12$ ). This limits the wider generalizability of these findings, as individuals may differ substantially in their motion patterns, and also in the effects of motion on their EEG signals. Further, given the higher variability of infant (as compared to adult) data and lower signal-to-noise ratio, it is possible that significant effects could have been missed, thereby underestimating the effect of motion on the EEG signal. Therefore, given the very limited quantity of the infant data reported here, caution is recommended in interpreting these findings before subsequent replications are conducted.

The second major limitation of this work is the use of a passive (video-watching) as opposed to an active (i.e., play) paradigm to facilitate better isolation of the effects of individual motions (i.e., reduce the co-occurrence of different motion types). As we were concerned that the

movements produced by infants in a passive paradigm may differ from movements during an active task, we conducted a supplementary study in which we repeatedly elicited each type of motion from one mother-infant pair, whilst their EEG was recorded. This analysis (fully detailed in **Supplementary Material** section “Supplementary Pilot Study 2 on Actively-Elicited Motion”) revealed that, similar to what we observed in the current study, the infant’s motions generated only a few significant deviations from his resting state power spectrum, and the effects of upper limb movement were larger than the effects produced by chewing or lower limb movement. Unlike in the current study, *decreases* in alpha power (mainly over fronto-central, central and centro-parietal regions) produced by the upper limb movements did reach significance in the **supplementary study**. Significant *increases* in spectral power in peripheral scalp regions were also present when the infant was “modeling” upper limb and chewing movements, similar to the results observed in the current study when those motions occurred spontaneously. In future, a study actively modeling all motions with a larger number of infants is needed to ensure the replicability and generalizability of the current findings. Also, building on this work, future studies are required to explore the impact of multiple co-occurring motion types on the infant EEG signal. However, the current study, though highly limited, is an important first step in this direction.

Finally, it should also be noted that, as infants’ EEG signals were acquired whilst they were watching a movie, the neural activations recorded would also reflect sensory and cognitive processing of the video stimuli, in addition to the motion-related activity of interest. However, given that the resting state recordings were also obtained during the *same* movie stimuli, the subtraction procedure employed here should result in the removal of most common perceptual effects. Nonetheless, it is possible that infants moved more during some parts of the movie than others (e.g., sections that were more interesting or arousing), leading to potential biases in the data. Future studies may consider the use of video stimuli that present uniform stimulation throughout the task.

Despite these limitations, the current work is a necessary first step toward a better understanding of the effects of motion on infant EEG data. Further studies with a larger number of participants, and a wider range of modeled motions (collected across different social interactive scenarios) will be necessary to ascertain the extent to which these effects are generalizable, and to inform the future development of methods for EEG artifact removal.

#### DATA AVAILABILITY STATEMENT

The anonymised and non personally-identifiable EEG datasets generated for this study are available on request to the corresponding author.

#### ETHICS STATEMENT

This study was approved by the Cambridge Psychology Research Ethics Committee, and parents provided written informed consent on behalf of their children.

#### AUTHOR CONTRIBUTIONS

SG and VL designed the study. SG, SL, and MY contributed to data collection and coding. SG, SL, VN, SW, and VL completed the data analysis and contributed in the writing and revisions of the manuscript.

## FUNDING

This research was funded by a UK Economic and Social Research Council (ESRC) Transforming Social Sciences Grant ES/N006461/1 to VL and SW, a Nanyang Technological University start-up Grant M4081585.SS0 to VL, a Ministry of Education (Singapore) Tier 1 Grant M4012105.SS0 to VL, an ESRC Future Research Leaders Fellowship ES/N017560/1 to SW, and a Rosetrees Medical Trust Ph.D. Studentship A1414 to SG. A version of this manuscript has been released as a Pre-Print on bioRxiv 206029; doi: <https://doi.org/10.1101/206029> (Georgieva et al., 2018).

## SUPPLEMENTARY MATERIAL

The Supplementary Material for this article can be found online at: <https://www.frontiersin.org/articles/10.3389/fnins.2020.00352/full#supplementary-material>

## REFERENCES

- Ageyi, S. B., Van Der, W., Audrey, L. H., and Van Der, M. (2016). Neuropsychologia Longitudinal study of preterm and full-term infants : high-density EEG analyses of cortical activity in response to visual motion. *Neuropsychologia* 84, 89–104. doi: 10.1016/j.neuropsychologia.2016.02.001
- Babiloni, F., Astolfi, L., Cincotti, F., Mattia, D., Tocci, A., Tarantino, A., et al. (2007). "Cortical activity and connectivity of human brain during the prisoner's dilemma: an EEG hyperscanning study," in *Engineering in Medicine and Biology Society, 2007. EMBS 2007. 29th Annual International Conference of the IEEE*, Piscataway, NJ: IEEE, 4953–4956.
- Batty, M., Meaux, E., Wittmeyer, K., Rogé, B., and Taylor, M. J. (2011). Early processing of emotional faces in children with autism: an event-related potential study. *J. Exp. Child Psychol.* 109, 430–444. doi: 10.1016/j.jecp.2011.02.001
- Bell, M. A., and Wolfe, C. D. (2007). Changes in brain functioning from infancy to early childhood: evidence from EEG power and coherence during working memory tasks. *Dev. Neuropsychol.* 31, 21–38. doi: 10.1207/s15326942dn3101\_2
- Bell, M. A., and Cuevas, K. (2012). Using EEG to study cognitive development : issues and practices. *J. Cogn. Dev.* 13, 281–294. doi: 10.1080/15248372.2012.691143
- Benasich, A. A., Gou, Z., Choudhury, N., and Harris, K. D. (2008). Early cognitive and language skills are linked to resting frontal gamma power across the first 3 years. *Behav. Brain Res.* 195, 215–222. doi: 10.1016/j.bbr.2008.08.049
- Brooker, B. H., and Donald, M. W. (1980). Contribution of the speech musculature to apparent human EEG asymmetries prior to vocalization. *Brain Lang.* 9, 226–245. doi: 10.1016/0093-934X(80)90143-1
- Buzsaki, G. (2006). *Rhythms of the Brain*. New York, NY: Oxford University Press.
- Cantiani, C., Ortiz-Mantilla, S., Riva, V., Piazza, C., Bettoni, R., Musacchi, G., et al. (2019). Reduced left-lateralized pattern of event-related EEG oscillations in infants at familial risk for language and learning impairment. *Neuroimage Clin.* 22:101778. doi: 10.1016/j.nicl.2019.101778
- Chaumon, M., Bishop, D. V., and Busch, N. A. (2015). A practical guide to the selection of independent components of the electroencephalogram for artifact correction. *J. Neurosci. Methods* 250, 47–63. doi: 10.1016/j.jneumeth.2015.02.025
- Corrigall, K. A., and Trainor, L. J. (2014). Enculturation to musical pitch structure in young children : evidence from behavioral and electrophysiological methods. *Dev. Sci.* 17, 142–158. doi: 10.1111/desc.12100
- Csibra, G., Davis, G., Spratling, M. W., and Johnson, M. H. (2000). Gamma oscillations and object processing in the infant brain. *Science* 290, 1582–1585. doi: 10.1126/science.290.5496.1582
- Csibra, G., and Johnson, M.H. (2007). "Investigating event-related oscillations in infancy," in *Infant EEG and Event-Related Potentials*, ed M. de Haan, (Hove: Psychology Press), 289–304.
- Dahl, A. (2016). Ecological commitments: why developmental science needs naturalistic methods. *Child Dev. Perspect.* 11, 79–84. doi: 10.1111/cdep.12217
- Dawson, G., Jones, E. J., Merkle, K., Venema, K., Lowy, R., Faja, S., et al. (2012). Early behavioral intervention is associated with normalized brain activity in young children with autism. *J. Am. Acad. Child Adolesc. Psychiatry* 51, 1150–1159. doi: 10.1016/j.jaac.2012.08.018
- De Haan, M. (Ed.). (2013). *Infant EEG and Event-Related Potentials*. Hove: Psychology Press.
- de Haan, M., and Nelson, C. A. (1997). Recognition of the mother's face by 6-month-old infants: a neurobehavioral study. *Child Dev.* 68, 187–210. doi: 10.1111/j.1467-8624.1997.tb01935.x de Haan, M., and Nelson, C. A. (1999). Brain activity differentiates face and object processing by 6-month-old infants. *Dev. Psychol.* 34, 1114–1121.
- deRegnier, R. A., Georgieff, M. K., and Nelson, C. A. (1997). Visual event-related brain potentials in 4-month-old infants at risk of neurodevelopmental impairments. *Dev. Psychol.* 30, 11–28. doi: 10.1002/(SICI)1098-2302(199701)30:1<11::AID-DEV2>3.0.CO;2-Y
- deRegnier, RA., Nelson, CA., Thomas, KM., Wewerka, S., and Georgieff, MK. (2000). Neurophysiologic evaluation of auditory recognition memory in healthy newborn infants and infants of diabetic mothers. *J. Pediatr.* 137, 777–784. doi: 10.1067/mpd.2000.109149

- deRegnier, R., Wewerka, S., Georgieff, M. K., and Mattia, F., Nelson, C. A. (2002). Influences of postconceptional age and postnatal experience on the development of auditory recognition memory in the newborn infant. *Dev. Psychobiol.* 41, 216–225. doi: 10.1002/dev.10070
- Dumas, G., Lachat, F., Martinerie, J., Nadel, J., and George, N. (2011). From social behaviour to brain synchronization: review and perspectives in hyperscanning. *Irmb* 32, 48–53. doi: 10.1016/j.irbm.2011.01.002
- Dumas, G., Nadel, J., Soussignan, R., Martinerie, J., and Garnero, L. (2010). Interbrain synchronization during social interaction. *PLoS One* 5:8. doi: 10.1371/journal.pone.0012166
- Dumas, G., Laroche, J., and Lehmann, A. (2014). Your body, my body, our coupling moves our bodies. *Front. Hum. Neurosci.* 8:1004
- Fabes, R. A., Martin, C. L., Hanish, L. D., and Updegraff, K. A. (2000). Criteria for evaluating the significance of developmental research in the twenty-first century: force and counterforce. *Child Dev.* 71, 212–221. doi: 10.1111/1467-8624.00136
- Fan, J., Byrne, J., Worden, M. S., Guise, K. G., McCandliss, B. D., Fossella, J., et al. (2007). The relation of brain oscillations to attentional networks. *J. Neurosci.* 27, 6197–6206. doi: 10.1523/jneurosci.1833-07.2007
- Folland, N. A., Butler, B. E., Payne, J. E., and Trainor, L. J. (2014). Cortical representations sensitive to the number of perceived auditory objects emerge between 2 and 4 months of age?. *Electroencephalogr. Clin. Neurophysiol. Suppl.* 106, 1060–1067. doi: 10.1162/jocn\_a\_00764
- Fu, S., Caggiano, D. M., Greenwood, P. M., and Parasuraman, R. (2005). Event-related potentials reveal dissociable mechanisms for orienting and focusing visuospatial attention. *Brain Res. Cogn. Brain Res.* 23, 341–353. doi: 10.1016/j.cogbrainres.2004.11.014
- Fujioka, T., Mourad, N., He, C., and Trainor, L. J. (2011). Comparison of artifact correction methods for infant EEG applied to extraction of event-related potential signals. *Clin. Neurophysiol.* 122, 43–51. doi: 10.1016/j.clinph.2010.04.036
- Ganushchak, L., Christoffels, I., and Schiller, N. O. (2011). The use of electroencephalography in language production research: a review. *Front. Psychol.* 2:208. doi: 10.3389/fpsyg.2011.00208
- Georgieva, S., Lester, S., Yilmaz, M., Wass, S., and Leong, V. (2018). Topographical and spectral signatures of infant and adult movement artifacts in naturalistic EEG. *BioRxiv* [Preprint]. doi: 10.1101/206029
- Gramann, K., Gwin, J. T., Ferris, D. P., Oie, K., Jung, T. P., Lin, C. T., et al. (2011). Cognition in action: Imaging brain/body dynamics in mobile humans. *Rev. Neurosci.* 22, 593–608. doi: 10.1515/RNS.2011.047
- Guerrero-Mosquera, C., Navia-Vazquez, A., and Trigueros, A. M. (2012). *EEG Signal Processing for Epilepsy*. London: INTECH Open Access Publisher
- Gwin, J. T., Gramann, K., Makeig, S., and Ferris, D. P. (2010). Removal of movement artifact from high-density EEG recorded during walking and running. *J. Neurophysiol.* 103, 3526–3534. doi: 10.1152/jn.00105.2010
- Halit, H., Csibra, G., Volein, Á., and Johnson, M. H. (2004). Face-sensitive cortical processing in early infancy. *J. Child Psychol. Psychiatry* 45, 1228–1233
- Harris, A. M., Dux, P. E., and Mattingley, J. B. (2018). Detecting unattended stimuli depends on the phase of prestimulus neural oscillations. *J. Neurosci.* 38, 3092–3101. doi: 10.1523/JNEUROSCI.3006-17.2018
- He, C., Hotson, L., and Trainor, L. J. (2007). Mismatch responses to pitch changes in early infancy. *J. Cogn. Neurosci.* 19, 878–892. doi: 10.1162/jocn.2007.19.5.878
- Hoehl, S., and Wahl, S. (2012). Recording infant ERP data for cognitive. *Dev. Neuropsychol.* 37, 87–209. doi: 10.1080/87565641.2011.627958
- Islam, M. K., Rastegarnia, A., and Yang, Z. (2016). Methods for artifact detection and removal from scalp EEG: a review. *Neurophysiol. Clin. Clin. Neurophysiol.* 46, 287–305. doi: 10.1016/j.neucli.2016.07.002
- Kalashnikova, M., Peter, V., Di Liberto, G. M., Lalor, E. C., and Burnham, D. (2018). Infant-directed speech facilitates seven-month-old infants' cortical tracking of speech. *Sci. Rep.* 8:13745.
- Kampis, D., Parise, E., Csibra, G., and Kovács, Á. M. (2016). On potential ocular artefacts in infant electroencephalogram: a reply to comments by Köster. *Proc. R. Soc. B: Biol. Sci.* 283:20161285. doi: 10.1098/rspb.2016.1285
- Keren, A. S., Yuval-Greenberg, S., and Deouell, L. Y. (2010). Saccadic spike potentials in gamma-band EEG: characterization, detection and suppression. *NeuroImage* 49, 2248–2263. doi: 10.1016/j.neuroimage.2009.10.057
- Klados, M. A., Papadelis, C., Braun, C., and Bamidis, P. D. (2011). REG-ICA: a hybrid methodology combining blind source separation and regression techniques for the rejection of ocular artifacts. *Biomed. Signal Process. Control* 6, 291–300. doi: 10.1016/j.bspc.2011.02.001
- Köster, M. (2017). What about microsaccades in the electroencephalogram of infants? *Proc. Biol. Sci.* 283: 20160739. doi: 10.1098/rspb.2016.0739
- Köster, M., Haese, A., and Czernochowski, D. (2017). Neuronal oscillations reveal the processes underlying intentional compared to incidental learning in children and young adults. *PLoS One* 12:e0182540. doi: 10.1371/journal.pone.0182540
- Kraus, N., and Naatane, R. eds (1995). Mismatch negativity as an index of central auditory function. *Ea.r Hear. Special Issue* 16, 38–51.
- Kuhl, P. K. (2010). Brain mechanisms in early language acquisition. *Neuron* 67, 713–727. doi: 10.1016/j.neuron.2010.08.038
- Kushnerenko, E., Ceponiene, R., Balan, P., Fellman, V., Huotilaine, M., and Naatane, R. (2002). Maturation of the auditory event-related potentials during the first year of life. *Neuroreport* 13, 47–51. doi: 10.1097/00001756-200201210-00014

- Lawhern, V., Hairston, W. D., McDowell, K., Westerfield, M., and Robbins, K. (2012). Detection and classification of subject-generated artifacts in EEG signals using autoregressive models. *J. Neurosci. Methods* 208, 181–189. doi: 10.1016/j.jneumeth.2012.05.017
- Leong, V., Byrne, E., Clackson, K., Georgieva, S., Lam, S., and Wass, S. (2017). Speaker gaze increases information coupling between infant and adult brains. *Proc. Natl. Acad. Sci. U.S.A.* 114:201702493. doi: 10.1073/pnas.1702493114
- Liao, Y., Acar, Z. A., Makeig, S., and Deak, G. (2015). EEG imaging of toddlers during dyadic turn-taking: mu-rhythm modulation while producing or observing social actions. *NeuroImage* 112, 52–60. doi: 10.1016/j.neuroimage.2015.02.055
- Lindenberger, U., Li, S. C., Gruber, W., and Müller, V. (2009). Brains swinging in concert: cortical phase synchronization while playing guitar. *BMC Neurosci.* 10:22. doi: 10.1186/1471-2202-10-22
- Luck, S. J., Woodman, G. F., and Vogel, E. K. (2000). Event-related potential studies of attention. *Trends Cogn. Sci.* 4, 432–440.
- Lukowski, A. F., Wiebe, S. A., Haight, J. C., DeBoer, T., Nelson, C. A., and Bauer, P. J. (2005). Forming a stable memory representation in the first year of life: why imitation is more than child's play. *Dev. Sci.* 8, 279–298. doi: 10.1111/j.1467-7687.2005.00415.x
- Maguire, M. J., Magnon, G., and Fitzhugh, A. E. (2014). Improving data retention in EEG research with children using child-centered eye tracking. *J. Neurosci. Methods* 238, 78–81. doi: 10.1016/j.jneumeth.2014.09.014
- Makeig, S., Gramann, K., Jung, T. P., Sejnowski, T. J., and Poizner, H. (2009). Linking brain, mind and behavior. *Int. J. Psychophysiol.* 73, 95–100. doi: 10.1016/j.ijpsycho.2008.11.008
- Mannel, C., and Friederici, A. D. (2009). Pauses and intonational phrasing: ERP studies in 5-month-old German infants and adults. *J. Cogn. Neurosci.* 21, 1988–2006. doi: 10.1162/jocn.2009.21221
- Mannel, C., Schipke, C. S., and Friederici, A. D. (2013). The role of pause as a prosodic boundary marker: language ERP studies in German 3- and 6-year-olds. *Dev. Cogn. Neurosci.* 5, 86–94. doi: 10.1016/j.dcn.2013.01.003
- Maris, E., and Oostenveld, R. (2007). Nonparametric statistical testing of EEG- and MEG-data. *J. Neurosci. Methods* 164, 177–190. doi: 10.1016/j.jneumeth.2007.03.024
- Marshall, P. J., Young, T., and Meltzoff, A. N. (2011). Neural correlates of action observation and execution in 14-month-old infants: an event-related EEG desynchronization study. *Dev. Sci.* 14, 474–480. doi: 10.1111/j.1467-7687.2010.00991.x
- Musacchia, G., Ortiz-Mantilla, S., Choudhury, N., Realpe-Bonilla, T., Roesler, C., Benasich, A. A., et al. (2017). Active auditory experience in infancy promotes brain plasticity in theta and gamma oscillations. *Dev. Cogn. Neurosci.* 26, 9–19. doi: 10.1016/j.dcn.2017.04.004
- Musacchia, G., Ortiz-Mantilla, S., Realpe-Bonilla, T., Roesler, C. P., and Benasich, A. A. (2015). Infant auditory processing and event-related brain oscillations. *J. Vis. Exp.* 101:e52420. doi: 10.3791/52420
- Nathan, K., and Contreras-Vidal, J. L. (2015). Negligible motion artifacts in scalp electroencephalography (EEG) during treadmill walking. *Front. Hum. Neurosci.* 9:708. doi: 10.3389/fnhum.2015.00708
- Nelson, C. A. (1996). "Electrophysiological correlates of memory development in the first year of life," in *Biological and Neuropsychological Mechanisms: Life Span Developmental Psychology*, eds H Reese, & M Fransen, (Hillsdale, NJ: Lawrence Erlbaum Associates Inc), 95–131.
- Nelson, C., Thomas, K., de Haan, M., and Wewerka, S. (1998). Delayed recognition memory in infants and adults as revealed by event-related potentials. *Int. J. Psychophysiol.* 29, 145–165. doi: 10.1016/s0167-8760(98)00014-2
- Noris, B., Nadel, J., Barker, M., Hadjikhani, N., and Billard, A. (2012). Investigating gaze of children with ASD in naturalistic settings. *PLoS One* 7:e44144. doi: 10.1371/journal.pone.0044144
- Oostenveld, R., Fries, P., Maris, E., and Schoffelen, J. -M. (2011). FieldTrip: open source software for advanced analysis of MEG, EEG, and invasive electrophysiological data. *Comput. Intell. Neurosci.* 2011:156869. doi: 10.1155/2011/156869
- O'Regan, S., Faul, S., and Marnane, W. (2010). "Automatic detection of EEG artefacts arising from head movements. In engineering in medicine and biology society (EMBC)," in *2010 Annual International Conference of the IEEE, Piscataway, NJ*: IEEE, 6353–6356.
- Orekhova, E. V., Stroganova, T. A., and Posikera, I. N. (1999). Theta synchronization during sustained anticipatory attention in infants over the second half of the first year of life. *Int. J. Psychophysiol.* 32, 151–172. doi: 10.1016/s0167-8760(99)00011-2
- Orekhova, E. V., Elsabbagh, M., Jones, E. J., Dawson, G., Charman, T., Johnson, M. H. et al. (2014). EEG hyper-connectivity in high-risk infants is associated with later autism. *J. Neurodev. Disord.* 6:40. doi: 10.1186/1866-1955-6-40
- Ortiz-Mantilla, S., Hamalainen, J. A., Musacchia, G., and Benasich, A. A. (2013). Enhancement of gamma oscillations indicates preferential processing of native over foreign phonemic contrasts in infants. *J. Neurosci.* 33, 18746–18754. doi: 10.1523/JNEUROSCI.3260-13.2013
- Pascalis, O., de Haan, M., Nelson, C. A., and de Schonen, S. (1998). Longterm recognition assessed by visual paired comparison in 3- and 6-month-old infants. *J. Exp. Psychol. Learn. Mem. Cogn.* 24, 249–260. doi: 10.1037/0278-7393.24.1.249
- Peña, M., Pittaluga, E., and Mehler, J. (2010). Language acquisition in premature and full-term infants. *Proc. Natl. Acad. Sci. U.S.A.* 107, 3823–3828. doi: 10.1073/pnas.0914326107
- Plöchl, M., Ossandón, J. P., and König, P. (2012). Combining EEG and eye tracking: identification, characterization, and correction of eye movement artifacts in electroencephalographic data. *Front. Hum. Neurosci.* 6:278. doi: 10.3389/fnhum.2012.00278
- Reis, P. M., Hebenstreit, F., Gabsteiger, F., von Tscherner, V., and Lochmann, M. (2014). Methodological aspects of EEG and body dynamics measurements during motion. *Front. Hum. Neurosci.* 8:156. doi: 10.3389/fnhum.2014.00156
- Reynolds, G. D. (2015). Infant visual attention and object recognition. *Behav. Brain Res.* 285, 34–43. doi: 10.1016/j.bbr.2015.01.015

- Richards, J. E. (2003). Attention affects the recognition of briefly presented visual stimuli in infants: an ERP study. *Dev. Sci.* 6, 312–328. doi: 10.1111/1467-7687.00287
- Richards, J. E., Reynolds, G. D., and Courage, M. L. (2010). The Neural Bases of Infant Attention. *Curr. Dir. Psycho. Sci.* 19, 41–46. doi: 10.1177/0963721409360003
- Saby, J. N., and Marshall, P. J. (2012). The utility of EEG band power analysis in the study of infancy and early childhood. *Dev. Neuropsychol.* 37, 253–723. doi: 10.1080/87565641.2011.614663
- Schilbach, L., Timmermans, B., Reddy, V., Costall, A., Bente, G., Schlicht, T., et al. (2013). Toward a second-person neuroscience 1. *Behav. Brain Sci.* 36, 393–414. doi: 10.3389/fpsy.2013.00123
- Slugocki, C., and Trainor, L. J. (2014). Cortical indices of sound localization mature monotonically in early infancy. *Eur. J. Neurosci.* 40, 3608–3619. doi: 10.1111/ejn.12741
- Sweeney, K. T., Ward, T. E., and McLoone, S. F. (2012). Artifact removal in physiological signals—Practices and possibilities. *IEEE Trans. Inf. Technol. Biomed.* 16, 488–500. doi: 10.1109/TITB.2012.2188536
- Tamis-LeMonda, C. S., Kuchirko, Y., Luo, R., Escobar, K., and Bornstein, M. H. (2017). Power in methods: language to infants in structured and naturalistic contexts. *Dev. Sci.* 20:10.1111/desc.12456. doi: 10.1111/desc.12456
- Telkemeyer, S., Rossi, S., Nierhaus, T., Steinbrink, J., Obrig, H., Wartenburger, I., et al. (2011). Acoustic processing of temporally modulated sounds in infants: evidence from a combined near-infrared spectroscopy and EEG study. *Front. Psychol.* 2:62. doi: 10.3389/fpsyg.2011.00062
- Teplan, M. (2002). Fundamentals of EEG measurement. *Meas. Sci. Revi.* 2, 1–11.
- Trainor, L. J., Lee, K., and Bosnyak, D. J. (2014). Cortical plasticity in 4-month-old infants : specific effects of experience with cortical plasticity in 4-month-old infants : specific effects of experience with musical timbres. *Brain Topogr* 24, 192–203. doi: 10.1007/s10548-011-0177-y
- Tunnell, G. B. (1977). Three dimensions of naturalness: an expanded definition of field research. *Psychol. Bull.* 84, 426–443. doi: 10.1037/0033-2909.84.3.426
- van Elk, M., van Schie, H.T., Hunnius, S., Vesper, C., and Bekkering, H. (2008). You'll never crawl alone: neurophysiological evidence for experiencedependent motor resonance in infancy. *NeuroImage* 43, 808–814. doi: 10.1016/j.neuroimage.2008.07.057
- Vanderperren, K., Hunyadi, B., DeVos, M., Mennes, M., Wouters, H., Vanrumste, B., et al. (2008). Reduction of alpha distortion in event related potentials. *IFMBE Proc.* 22:1298–1301. doi: 10.1007/978-3-540-89208-3\_309
- Vos, D. M., Riès, S., Vanderperren, K., Vanrumste, B., Alario, F. X., Huffel, V. S., and Burle, B. (2010). Removal of muscle artifacts from EEG recordings of spoken language production. *Neuroinform.* 8, 135–150. doi: 10.1007/s12021-0109071-0
- Wass, S. V., Noreika, V., Georgieva, S., Clackson, K., Brightman, L., Nutbrown, R., et al. (2018). Parental neural responsivity to infants' visual attention: how mature brains influence immature brains during social interaction. *PLoS Biol.* 16:e2006328. doi: 10.1371/journal.pbio.2006328
- Weber, C., Hahne, A., Friedrich, M., and Friederici, A. D. (2004). Discrimination of word stress in early infant perception: electrophysiological evidence. *Cogn. Brain Res.* 18, 149–161. doi: 10.1016/j.cogbrainres.2003.10.001
- Winkler, I., Lehtokoski, A., Alku, P., Vainio, M., Czigler, I., Csepe, V., et al. (1999). Pre-attentive detection of vowel contrasts utilizes both phonetic and auditory memory representations. *Cogn. Brain Res.* 7, 357–369. doi: 10.1016/s0926-6410(98)00039-1
- Winkler, M., Mueller, J. L., Friederici, A. D., and Männel, C. (2018). Infant cognition includes the potentially human-unique ability to encode embedding. *Sci. Adv.* 4:eaar8334 doi: 10.1126/sciadv.aar8334
- Weber, C., Hahne, A., Friedrich, M., and Friederici, A. D. (2005). Reduced stress pattern discrimination in 5-month-olds as a marker of risk for later language impairment: neurophysiological evidence. *Cogn. Brain Res.* 25, 180–187. doi: 10.1016/j.cogbrainres.2005.05.007
- Xie, W., Mallin, B. M., and Richards, J. E. (2017). Development of infant sustained attention and its relation to EEG oscillations: an EEG and cortical source analysis study. *Dev. Sci.* 21:e12562. doi: 10.1111/desc.12562
- Xie, W., Mallin, B. M., and Richards, J. E. (2018). Development of brain functional connectivity and its relation to infant sustained attention in the first year of life. *Dev. Sci.* 22:e12703. doi: 10.1111/desc.12703
- Yu, C., and Smith, L. B. (2016). The social origins of sustained attention in one-year-old human infants. *Curr. Biol.* 26, 1235–1240. doi: 10.1016/j.cub.2016.03.026
- Yuval-Greenberg, S., Tomer, O., Keren, A. S., Nelken, I., and Deouell, L. Y. (2008). Transient induced gamma-band response in EEG as a manifestation of miniature saccades. *Neuron* 58, 429–441. doi: 10.1016/j.neuron.2008.03.027
- Zhang, Y., Koerner, T., Miller, S., Grice-Patil, Z., Svec, A., Akbari, D., et al. (2011). Carney, E. Neural coding of formant-exaggerated speech in the infant brain. *Dev. Sci.* 14, 566–581 doi: 10.1111/j.1467-7687.2010.01004.x

**Conflict of Interest:** The authors declare that the research was conducted in the absence of any commercial or financial relationships that could be construed as a potential conflict of interest.

Copyright © 2020 Georgieva, Lester, Noreika, Yilmaz, Wass and Leong. This is an open-access article distributed under the terms of the Creative Commons Attribution License (CC BY). The use, distribution or reproduction in other forums is permitted, provided the original author(s) and the copyright owner(s) are credited and that the original publication in this journal is cited, in accordance with accepted academic practice. No use, distribution or reproduction is permitted which does not comply with these terms.

## VII.III Methods Paper Two (Author's Own Copy)

### **14 challenges and their solutions for conducting social neuroscience and longitudinal EEG research with infants**

Valdas Noreika<sup>1,\*</sup>, Stanimira Georgieva<sup>1</sup>, Sam Wass<sup>3</sup>, Victoria Leong<sup>1,2</sup>

<sup>1</sup> Department of Psychology, University of Cambridge, Cambridge, UK

<sup>2</sup> Division of Psychology, Nanyang Technological University, Singapore

<sup>3</sup> School of Psychology, University of East London, London, UK

\* Corresponding author.

## Highlights

- EEG solutions developed for adult research do not always hold when testing infants
- Unique solutions are required for the emerging infant-adult dual EEG studies
- Challenges related to the study design are data attrition and varying arousal
- Data acquisition require optimal electrode placement and equipment synchronisation
- Changing head anatomy, myogenic artifacts and EEG rhythms challenge data analysis

## Abstract

The use of electroencephalography (EEG) to study infant brain development is a growing trend. In addition to classical longitudinal designs that study the development of neural, cognitive and behavioural functions, new areas of EEG application are emerging, such as novel social neuroscience paradigms using dual infant-adult EEG recordings. However, most of the experimental designs, analysis methods, as well as EEG hardware were originally developed for single-person adult research. When applied to study infant development, adult-based solutions often pose unique problems that may go unrecognised. Here, we identify 14 challenges that infant EEG researchers may encounter when designing new experiments, collecting data, and conducting data analysis. Challenges related to the experimental design are: (1) small sample size and data attrition, and (2) varying arousal in younger infants. Challenges related to data acquisition are: (3) determining the optimal location for reference and ground electrodes, (4) control of impedance when testing with the high-density sponge electrode nets, (5) poor fit of standard EEG caps to the varying infant head shapes, and (6) ensuring a high degree of temporal synchronisation between amplifiers and recording devices

during dual-EEG acquisition. Challenges related to the analysis of longitudinal and social neuroscience datasets are: (7) developmental changes in head anatomy, (8) prevalence and diversity of infant myogenic artefacts, (9) a lack of stereotypical topography of eye movements needed for the ICA-based data cleaning, (10) and relatively high inter-individual variability of EEG responses in younger cohorts. Additional challenges for the analysis of dual EEG data are: (11) developmental shifts in canonical EEG rhythms and difficulties in differentiating true inter-personal synchrony from spurious synchrony due to (12) common intrinsic properties of the signal and (13) shared external perturbation. Finally, (14) there is a lack of test-retest reliability studies of infant EEG. We describe each of these challenges and suggest possible solutions. While we focus specifically on the social neuroscience and longitudinal research, many of the issues we raise are relevant for all fields of infant EEG research.

**Keywords:** infant; electroencephalography (EEG); longitudinal design; methodology; social neuroscience.

## **Introduction**

The use of electroencephalography (EEG) to study infant brain development has undergone a slow but steady increase in recent decades. A PubMed search using the words “newborn / neonate / neonatal / baby / infant” and “EEG / electroencephalography / ERP / event-related potential” in the Title or Abstract returned 36 studies published in 1998, 90 studies published in 2008, and 197 studies published in 2018. The rich history of infant EEG research dates back to the 1930s, when J. Roy Smith (1938a-c, 1939) carried out seminal studies on the development of awake and sleep EEG rhythms, including alpha waves, during normal infancy

and childhood. Research of infant EEG consolidated in the 1960s and 1970s when basic research into normal infant EEG development (e.g. Hagne, 1968, 1972) extended to examine EEG of premature infants (e.g. Parmelee Jr et al., 1968; Weitzman & Graziani, 1968). While in the subsequent decades infant EEG studies were mostly clinical, e.g. aiming to assess sources of epileptic seizures (Clancy & Legido, 1991) or the effects of exposure to addictive substances (Legido et al., 1992), more recent studies have started to address psychological and cognitive neuroscience topics, such as language development (Kühn-Popp et al., 2016) and gaze monitoring (Hoehl et al., 2014).

EEG research in developmental social neuroscience has used a range of paradigms (see Figure 1). Historically the majority have been ERP studies that typically examine infants' neural responses to static pictures of faces. Well-studied contrasts include differential neural responses to face vs non-face stimuli (e.g. Halit et al., 2004); to faces either gazing directly to the camera, or with gaze averted (e.g. Farroni et al., 2002); and to faces with different emotional expressions (e.g. Nelson & De Haan, 1996).

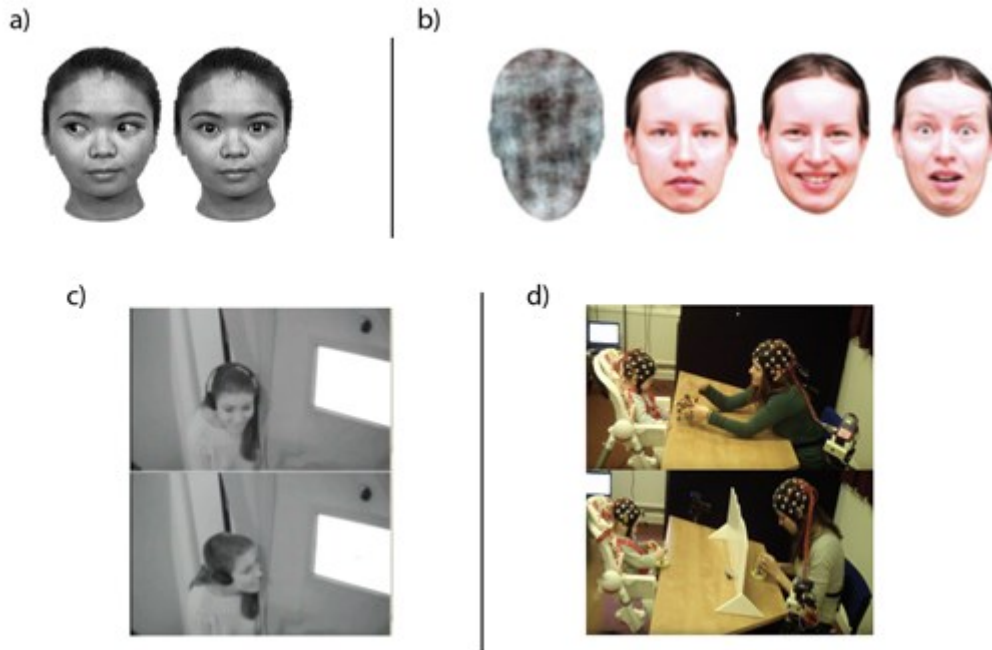


**Figure 1** | Illustrating the range of EEG paradigms used in infant social neuroscience research. a) static images showing direct and averted gaze (reproduced from Farroni et al. (2002), Copyright © 2002, The National Academy of Sciences); b) static images showing different emotional expressions (reproduced with permission from Leppänen et al. (2011)); c) interactions featuring a live experimenter and screen-based stimuli (reproduced with permission from Hoehl et al. (2014)); d) live, tabletop interactions with dual EEG recording, reproduced from Wass et al. (2018).

While the strength of these paradigms is their high reproducibility, a limitation is that the paradigms lack ecological validity. Recognising this, other studies have examined differential ERP responses to direct and averted gaze – but including live actors, with onsets and offsets controlled by showing real faces through a computer-controlled electronic shutter (Pönkänen et al., 2011). Other studies have presented dynamic videos of actors talking to the camera (Jones et al., 2015), or real live interactions (Reid et al., 2011), and analysed them using Fourier-transform-based analyses to examine topographic changes in activity across frequencies between social and non-social conditions. Other studies have used conditions in which a live

adult experimenter gazes first at the infant's face and then to a computer-displayed novel object, while the infant's neural response to the object is measured (Striano et al., 2006; Hoehl et al., 2014).

Although more ecologically valid, one further limitation of these studies is that, by only recording from a single participant at once, they are unable to capture the interpersonal dynamics of how information is shared between two interacting partners during social interaction (Schilbach et al., 2013). To address this, researchers have recently started to build on methodological innovations in adult research (Lachat & George, 2012; Liu et al., 2018) that allows the recording of dual EEG from infants and their adult social partners concurrently *during* an interaction. Types of interaction studied include semi-structured interactions with an unfamiliar adult (Leong et al., 2017), and tabletop play or other cooperative activities with a parent (Wass et al., 2018). Analyses typically concentrate on measuring either Granger-causal relationships between the infant's and adult's brain activity and attention (Granger, 1969), or concurrent synchrony (Lachaux et al., 1999).

One problem common for infancy researchers is that most of the hardware and analysis methods, as well as EEG hardware, were originally developed for adult research. When applied to the study of infant development, adult-based solutions often pose unique problems that may go unrecognised. In addition, some of the more newly developed techniques, such as dual EEG recording, pose specific methodological challenges that have been little discussed hitherto. Here, we identify 14 challenges that infant EEG researchers may encounter when designing new experiments, collecting data and conducting data analysis. Several of the methodological problems and possible solutions that we describe in the following are specific to the dual EEG analyses, whereas others are relevant for all areas of infant EEG research, including

longitudinal and cross-sectional designs. Given that our aim is to illustrate the identified problems and suggest possible solutions rather than provide an extensive review of infant EEG research, the citation of the infant EEG literature will be selective. The key terms used in the following sections are introduced in Table 1, including suggested references for more information.

**Table 1.** Key terms related to the acquisition and analysis of EEG data

<b>Concept</b>	<b>Description</b>
Dual EEG	Concurrent acquisition of electroencephalography signals from two different individuals, typically for the purpose of obtaining measures of interpersonal synchronisation. This method is also known as hyperscanning. Babiloni & Astolfi, 2014.
Electrode placement	The positioning of EEG electrodes on the scalp, based on pre-determined anatomical landmarks, e.g. distance from inion. Electrode placement can be carried out manually by calculating the location of each electrode, or – more frequently – by placing an age-appropriate EEG cap/net with fixed electrode positions. Fisch & Spehlmann, 1999.
Event-related potentials	Stereotypical patterns of EEG voltage fluctuation that are time-locked to specific sensory stimuli or motor responses. Due to the high amplitude of stimulus-unrelated background EEG activity, the repetition of tens or hundreds of trials per condition is usually required for a reliable estimation of event-related potentials. Luck, 2014.
Granger causality	A directional measure of how one time-series (x) forward-predicts another time series (y), after taking into account the self-predictive past values of y. Granger, 1969.

Ground electrode	An electrode used for common-mode rejection: it takes signals read by all electrodes, such as power line noise (50/60 Hz), and cancels them out of the EEG recordings. In adult studies, this is often placed on the forehead or cheek. Nunez & Srinivasan, 2006.
Impedance	The degree of opposition to alternating current (AC) flow, arising from the combined effects of resistance and reactance. Generally, the higher the impedance of an EEG electrode on the scalp, the smaller the amplitude of the signal recorded by that electrode. The electrode contact impedance is usually kept below 10 k $\Omega$ , although much higher impedance values (<100 k $\Omega$ ) are acceptable when using the high-density Philips-EGI Geodesic Sensor nets. Nunez & Srinivasan, 2006.
Phase coupling	A measure of the association between the on-going oscillatory phase of two EEG time series (e.g. recorded by different electrodes or different individuals). Phase coupling may be assessed by a wide range of metrics, such as the phase-locking value (PLV), phase lag index, mutual information, etc. Cohen, 2014.
Reference electrode	The EEG signal recorded at each electrode is a difference between the signal measured by the electrode itself and another “reference electrode”. In a unipolar montage, the reference electrode is typically placed on the vertex, nose or mastoid. In a bipolar montage, there is a separate reference electrode for each data channel. Nunez & Srinivasan, 2006.
Resting-state	A neuroimaging paradigm in which participants are instructed to relax and stay still without engaging in an active task. In infants, resting-state recordings simulate periods of quiet wakefulness with minimal motor activity. Anderson & Perone, 2018.

Rhythms	The EEG signal is partially composed of neuronal oscillations which can be functionally separated into different frequency ranges, often referred to as EEG rhythms or frequency bands. One classic example is the alpha rhythm (8-12 Hz in adults and 6-9 Hz in infants), which peaks in amplitude over occipital channels during eyes-closed relaxed wakefulness. Buzsaki, 2006.
Source localisation	Identification of the source(s) within the brain from which an EEG signal (or an element of the signal) originates. It involves the prediction of EEG potentials from a model of neural sources (termed as the forward problem) and the estimation of the neural sources from EEG potentials (termed as the inverse problem). Michel & Brunet, 2019.
Spectral power	The squared amplitude of the neural signal typically integrated over a range of signal frequencies. Commonly computed using a Fast Fourier Transform (FFT). Spectral power is usually measured in continuous EEG datasets. Cohen, 2014.

## 1. Experimental design

### *1.1 Sample size and data attrition for infant neuroimaging studies*

#### **Problem:**

Compared to adult studies, infant neuroimaging studies typically suffer from a higher rate of data attrition due to infant non-compliance and signal contamination by motion-related

artefacts (Bell & Cuevas, 2012). Whereas adults may be instructed to avoid movement, this strategy is ineffective for paediatric populations. A proportion of infants who attend sessions will either be too fussy or irritable for the EEG cap to be applied in the first place - or will become too upset when the cap is applied, meaning that it immediately has to be removed before data can be collected (see De Haan, 2013, pp 17-18). Furthermore, for some infants, their amount of movement artefact-free data may not meet minimum requirements for data analysis. For example, in resting state paradigms, it is recommended that at least 40-60s of usable data per participant is required for consistent and reliable results (Salinsky et al, 1991; Lund et al, 1995). Therefore, infants who do not contribute to this minimum amount of movement-free data will have to be excluded entirely from analyses. This results in a lower fraction of usable data per participant, and potentially fewer usable datasets (e.g. if minimum requirements for data analysis in terms of artefact-free data duration or usable trials are not met). The problem of data attrition is compounded for naturalistic paradigms (such as free play), and also for dyadic protocols in which the computation of synchronicity measures requires both partners to concurrently contribute artefact-free data segments. As shown in Table 2, even when infants are watching engaging screen-based stimuli (such as cartoons or nursery rhymes), infant motion (including facial, limb and postural movement) is still present between 60-70% of the time. In a naturalistic free-play paradigm, motion is present almost continuously. This high rate of motion contamination strongly motivates the development of robust algorithms for data cleaning, and a better understanding of the specific effects of different classes of motion on the neural signal (see section 3.2 for further discussion on these points).

**Table 2.** Prevalence of infant motion during four different experimental paradigms expressed as a percentage of the total experiment time.

<b>Stimulus</b>	<b>Cartoon clips</b> <i>N = 11</i>	<b>Speech (nursery rhymes)</b> <i>N = 24</i>	<b>Speech (artificial language)</b> <i>N = 14</i>	<b>Tabletop free play</b> <i>N = 5</i>
Average prevalence of infant movement (% of total stimulus presentation time)	59.2%	70.1%	71.0%	>95%

**Note.** The first three experiments were screen-based (i.e. infants watched either cartoon clips, natural speech or artificial speech respectively), whilst the last experiment involved free play across a tabletop with mothers. Infants were video-recorded during each paradigm and the recordings were manually coded for segments free of muscle movements of any kind. Here we report the average (across all infant participants) amount of time while performing the task and moving simultaneously. Authors' unpublished data.

### **Solution:**

The usable fraction of infant neural data will depend on a range of factors, including the nature of the experimental paradigm (e.g. screen-based or interaction-based), the age of infant participants (older infants are capable of a wider range of motion), the sensitivity of the recording device to motion (and effectiveness of motion artefact removal techniques), and the spectral and topographical properties of the neural effect of interest. In the case of an EEG dyadic interactive paradigm involving infants (e.g. Leong et al, 2017; Wass et al, 2018; Leong et al, 2019), we have previously noted a data attrition rate of ~50%. This suggests that studies may need to recruit and test twice the number of participants (dyads) than would be required based on standard power calculations. In the future, the advent of next-generation brain imaging systems such as Optically Pumped Magnetometer (OPM) MEG systems (Boto et al, 2018) which afford higher signal-to-noise ratios and greater robustness to motion artefact

contamination, and better motion artefact cleaning methods (see Section 3.2) could permit high-fidelity and lower attrition neural data collection even in real-world naturalistic paradigms.

### *1.2 Varying arousal in younger infants*

#### **Problem:**

Both longitudinal and dual EEG data can be affected by variations in infant arousal state. Infant behaviour can range from a highly agitated state (hyperarousal) to peaceful rest or even sleep in just a few minutes. Due to the relatively high ratio between sleeping and waking hours in neonates and infants as well as numerous EEG artefacts linked to neonate-typical motor activities during waking, such as sucking, crying, defecating and moving limbs (see Section 3.2), most of the EEG measurements of newborns are carried out during “quiet” non-rapid eye movement (NREM) sleep. However, while recordings during sleep improve the EEG signal-to-noise ratio, the obtained results may not be straightforward to interpret. In adults, even a mild decrease in arousal shifts the brain into a different mode of processing compared to the waking brain, affecting EEG event-related potentials (ERP), spectral power, and connectivity measures (Ogilvie, 2001). Consequently, EEG results obtained during drowsiness or sleep cannot be directly interpreted in terms of brain functioning during waking hours. Early studies in infants suggested that neurobehavioural states of arousal (waking, NREM sleep and REM sleep) do not affect ERP characteristics in newborn infants (Hirasawa et al., 2002; Martynova et al., 2003), justifying infant testing during drowsiness and quiet sleep. However, subsequent research soon demonstrated such effects, including a significant increase of auditory ERP amplitude during quiet sleep compared to awake periods in 8 week old healthy infants

(Friedrich et al., 2004; see Figure 2), and a change in the topography of mismatch responses as a function of alertness (Otte et al., 2013).

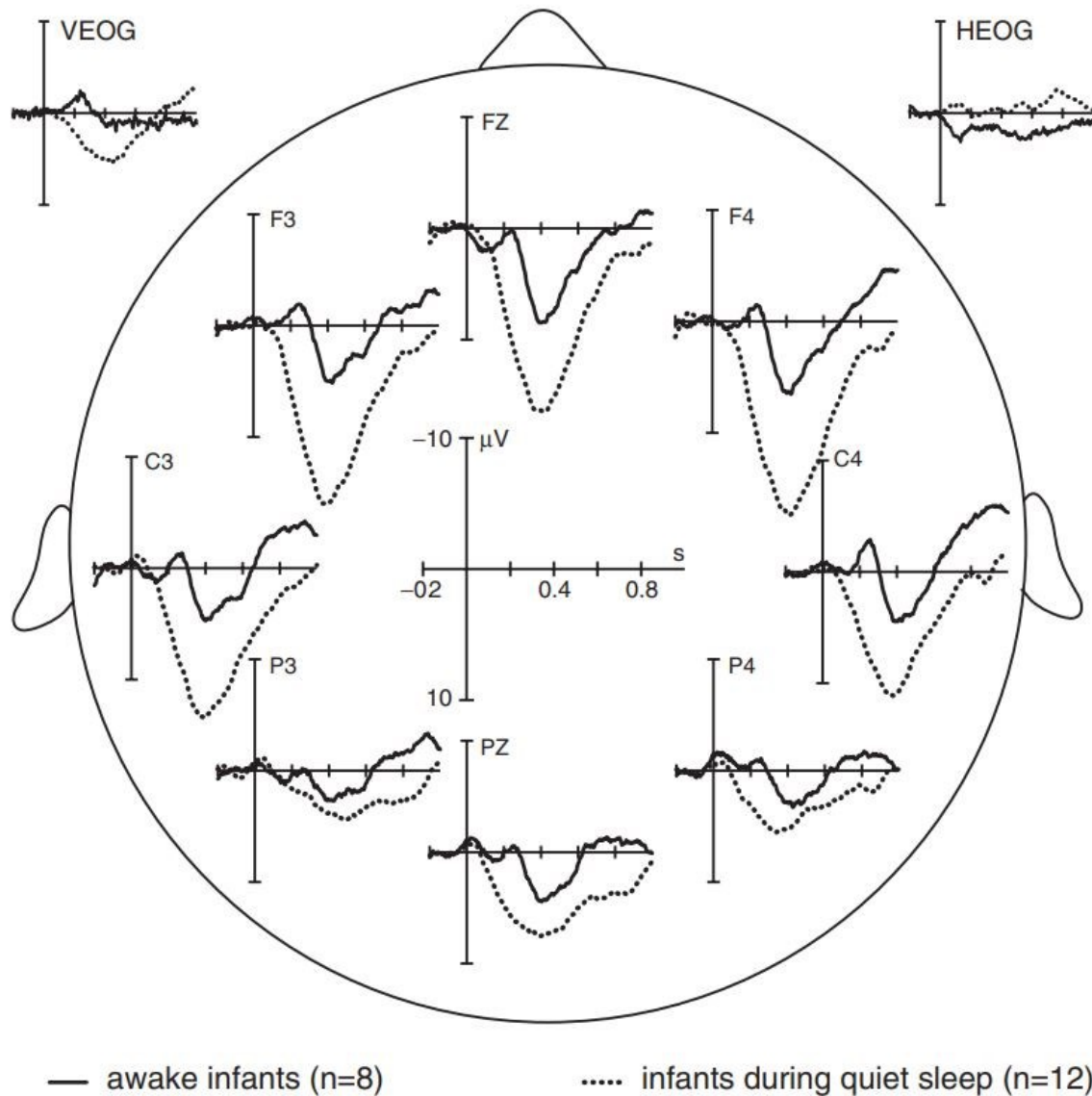


**Figure 2** | Auditory difference waves (deviant minus standard) in 8 weeks-old infants show an increase of amplitude in quiet sleep compared to the awake state. Reproduced with permission from Friedrich et al. (2004).

Thus, infant EEG findings obtained during low levels of arousal should be interpreted cautiously when compared to datasets collected during periods of high arousal. The sleep

confound is particularly problematic for longitudinal or cross-sectional EEG studies that compare younger sleeping infants with older awake infants. In such cases, an identified EEG change as a function of age may simply reflect EEG differences between different levels of arousal. EEG recordings carried out during sleep for all age groups would not necessarily solve the problem, as the characteristics of sleep EEG change substantially during the first year of life, e.g. multifocal sharp waves are frequently observed during sleep in the neonates but not in older infants (Hagne, 1972). Similarly, dual EEG measurements can be confounded if one partner of a dyad is more agitated or drowsy than the other partner. Given that changing levels of arousal can shift background EEG activity towards faster or slower frequencies, this would likely reduce cross-brain synchronisation indices.

**Solution:**

A stable level of infant's arousal can be maintained by running a series of short 1-3 min experimental blocks with breaks lasting as long as needed in order to guide infants' arousal to the desired level. It is also critical that experimental scripts for stimuli presentation and data acquisition can be delivered in a contingent manner in response to changes in infants' behaviour and arousal state. Finally, data containing episodes of hyper- or hypo-arousal should be analyzed cautiously, either removing them or sorting into arousal bins and analyzing them separately.

When data acquisition during awake-only periods is not feasible in longitudinal or cross-sectional studies, such as when testing newborns, arousal level can be assessed in 20-30 sec epochs by manually scoring video recordings of infant's behaviour and/or scoring the level of arousal (awake, NREM sleep, REM sleep) from EOG and EEG recordings. Grigg-Damberger et al. (2007) summarise guidelines for the visual scoring of arousal and sleep in infants and

children. There is also an increasing use of automated actigraphy-based assessment of sleep/wake patterns in paediatric research (Meltzer et al., 2012). The obtained arousal indices could be entered as covariates in statistical models testing experimental hypotheses.

## **2. Data acquisition**

### *2.1 Determining the optimal location for reference and ground electrodes*

#### **Problem:**

There are two major considerations to take into account when choosing a reference and the common ground (if applicable) electrode locations for infant EEG acquisition. The first consideration (more relevant to the common ground electrode if a given system uses such) is stability - choosing a location that is least vulnerable to motion-related displacement. The second consideration (more relevant to the reference electrode) is the topography of the effect that is being studied and comparability (in terms of the location and polarity of the predicted effect) to previous literature. Both of these considerations are also relevant to adult EEG, but adult participants are amenable to instruction (e.g. to stay still) and can more easily tolerate electrodes attached to different locations (e.g. nose, mastoid, and ear lobe). The issue is additionally complicated by developmental changes within the infant population.

#### **Solution:**

Regarding the common ground, the exact location on the participant is of relatively low consequence (Light et al., 2010), as long as the electrode is well attached and is not easily displaced by movement, e.g. when placed on the head or over a vertebra on the back of the neck. If an EEG cap is used, a recording channel is sometimes sacrificed for the common

ground, which may not be ideal in a low-density system. In these cases, the back-of-the-neck vertebra is an acceptable alternative, as long as care is taken to attach it stably, avoiding its loosening during the recording session. For this, it should not be placed too high as that would make it vulnerable to head movements, or too low, where it might pick up physiological movements such as breathing and heart-beat. The length of the wire should also be carefully considered, as it should give enough leeway for the infant to be able to lean forward without compromising the attachment of the actual electrode. Importantly, unlike with adults, the nose is a poor location of choice for infants (even neonates) given its high visibility and the potential for distraction.

The optimal location of the reference electrode has generated heated debate in the literature. Most amplifiers do not distinguish between recording and reference electrodes (Nunez & Srinivasan, 2006) - rather, they amplify the difference between pairs of scalp locations, and the resulting amplified potential is proportional to that difference. Since this manipulation is linear, in most systems the online reference can be recovered and the recording can be re-referenced offline. Additionally, as EEG is recorded as a difference of potentials, in an ideal world, the reference electrode would be symmetrically spaced from all other channels, and it should not record brain activity, so as to not have any brain activity subtracted out in the referencing process. Thus, for adults, the nose, earlobes, and mastoids (although they are on the head, the bone behind the temporal bone is thicker and provides a larger distance from the brain compared to the rest of the scalp sensors) are preferred sites (Op de Beeck & Nakatani, 2019). However, these locations are not easily tolerated by infants, and different locations are more tolerable for different ages, which immediately poses a problem in dual EEG designs, as placing reference at different locations for each partner of the dyad would affect EEG data differently. The mastoid location is well tolerated during recording, but placing reference

electrodes at this location often causes distress to infants during removal because adhesive stickers that are used to attach the electrodes securely can easily pick up longer hairs. Therefore, careful consideration should be given to the safe and speedy removal of electrodes from mastoid locations for infants.

Perhaps the most frequently applied solution is to use Cz as a reference channel (Heohl & Wahl, 2012). Its location is symmetrical to all other channels, it is a fairly protected location from motion artefacts, and it allows for shorter setting up and removal time, especially if a cap is used. This solution has three potential pitfalls, however. First, it sacrifices a recording channel, which is not desirable in low-density systems. Second, if the infant has thick hair growth, getting a good connection and low impedance might be difficult. Finally, the central location is maximal for certain forms of brain activity, and this activity would be subtracted in the referencing process. Evidently, there is no perfect solution when it comes to the location of the reference channel in infant EEG. The decision should be informed by considerations such as the setup (high or low density); the age of the participants; the experimental question and design (is it a dual EEG study); and finally and most importantly, the published literature - changing the reference location can change the direction of the dipole that is being measured, and the topography of effects.

## *2.2 Control of impedance when testing with the high-density sponge electrode nets*

### **Problem:**

Of the different equipment setups available to researchers who wish to record infant EEG, one important distinction is between saline- and gel-based systems. For gel-based systems (such as those from Biosemi, Neuroelectronics, and Biopac), each electrode must have electrolyte gel

manually inserted after application of the net or cap before recording can start. For saline-based systems (such as the EGI/Phillips system) each electrode contains a small sponge, and the entire net is soaked in electrolyte before it is applied to the infant's head. The advantage of these systems is that, because each electrode does not need a manual injection of electrode gel, high-density recordings (e.g. with 128 electrodes and more) can be taken from infants, who otherwise would not tolerate a long process of applying a high-density net prior to recording.

One disadvantage of a saline-based system is that the connectivity between electrodes and scalp relies on the presence of the saline solution. As the recording progresses, and the saline solution evaporates, impedances can increase over time, systematically decreasing data quality towards the end of the recording session.

**Solution:**

First, recording sessions using saline-based nets should be kept brief (e.g. no more than ~20 minutes per continuous session). If longer recordings are necessary, testing can be interrupted and the saline solution reapplied, electrode by electrode, using a pipette, and without removing the net. Second, if comparisons are planned between conditions, ensure that the order in which conditions are presented is counterbalanced between participants, to avoid the possibility that systematically higher impedances later in a testing session may influence results. Finally, if planned analyses will focus on a subset of electrodes, ensure that these electrodes are manually checked, by viewing the impedances both before and during testing.

*2.3 Poor fit of standard EEG caps to the varying shapes of infants' heads*

**Problem:**

Poor fit of standard EEG caps is a common problem for measurements with young infants. This arises in part from the fact that the fontanelles (“soft gaps” between the cranial bones made of connective rather than bone tissue) are still malleable during early infancy and therefore the shape of the infant’s skull (therefore, head), can change dramatically, especially in the first week of life (Baum & Searls, 1971). Furthermore, changes in infants’ head shape can be non-linear in the first weeks of life of pre-term infants (Souza et al., 1976; see Figure 3). This can be problematic in longitudinal study designs when an infant is tested at birth and then again later in life, as the exact location where the electrodes lie using a standard cap can vary slightly between the ages. This may or may not pose a problem depending on how sensitive the research question is to the topography of the effect. The fontanelles normally close up slowly starting at about 3 months, with the process continuing to 18 months and beyond (Duc & Largo, 1986; Hansman, 1966), but these gradual changes are small and are only likely to be problematic with very low density setups, i.e. fewer than 8 recording channels.

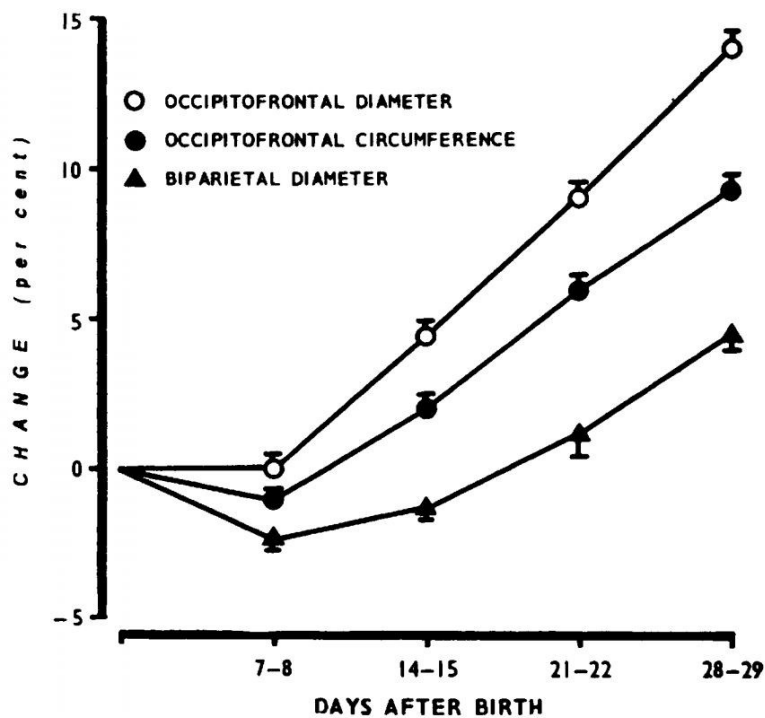


**Figure 3** | Percentage changes (y axis) of the head shape during the first month in preterm infants born by vaginal delivery at 26-35 weeks' gestational age. Reproduced with permission from Souza et al. (1976).

**Solution:**

In a clinical setting, where precision in topography and electrode placement are essential, the most frequent use of EEG involves only one or two recording channels (plus a reference/common ground). These electrodes are individually glued using a conductive paste to a specific location on the scalp irrespective of the shape of the infant's head (e.g. for monitoring seizures).

In neonatal and early infancy research, a low-density (typically between 3-32 channels) setup is more practical and likely to be used than a high-density setup (32-128 channels) (DeBoer, Scott & Nelson, 2007). With the lower number of channels to be attached, they can be applied individually, though time and care should be taken to correctly identify each channel's location, which depending on the setting and the state/mood of the infant, can be more or less practical. The manual application of channels may be more prone to human error than the application of a cap. However, given the high variability in head-shapes of infants < 3 months old, if the experimenters are well trained and experienced, and the exact rather than approximate location of channels is essential, individual application of channels may be prescribed. In high density systems, however, this would simply not be practical. In infants older than 6 months, where generally higher-density (32+ channels) systems are preferred, and where there is little indication of greater head-shape variability than in adults, using a stretchy cap is appropriate standard practice.

#### *2.4 Ensuring a high degree of temporal synchronisation between amplifiers and recording devices – dual EEG acquisition*

**Problem:**

Data analyses for dual EEG data require that the different recording devices used have a very high degree of temporal synchronisation. When measuring brain activity at 10Hz, for example, for which one complete oscillation lasts 100ms, a variable recording error of even tens of milliseconds can be detrimental in estimating the phase of a signal. Similar considerations apply to time synchronisation between video recordings and EEG data. Our experience suggests that certain EEG recording systems, and many cameras, can periodically skip short segments of data during recording, particularly in cases when the data sampling rate is high and the memory/hard disk write speed of the system is limited.

**Solution:**

First, ensure that, wherever possible, one amp rather than two separate amps is used for the EEG data acquisition. This eliminates problems of ensuring accurate synchronisation between the two (or more) EEG data-streams. If this solution is not possible, such as when synchronising the EEG data with external video cameras, then a regular TTL pulse may be sent (from a separate computer) which inserts a periodic event into the EEG recording(s), and simultaneously sends a signal (e.g. by lighting an LED) which is visible to the video cameras. Synchronisation of the EEG to the video can be ensured by hand-coding the frames in which the LED light is first visible. Rather than synchronising once, this same process should be repeated throughout the recording, in case of short periods of missing data (e.g. dropped frames) mid-way through recording.

### 3. Analysis of longitudinal and social neuroscience datasets – single participant data

#### *3.1 Developmental changes in head anatomy affect EEG source localisation*

##### **Problem:**

Major advancements are being made in computational methods for modelling neurodevelopment changes of sources of EEG signals during infancy (e.g. Reynolds & Richards, 2009; Xie & Richards, 2017). However, this is challenging because significant changes in head anatomy occur during the first years of life, which affect skull conductivity and the propagation of electrical signals that are measured at the scalp (Odabae et al., 2014). For several months following birth, the neonatal cranial bones are not fully fused. Rather, the skull bones are separated by fontanels (soft membranous sutures) that accommodate the stretching and deformation which occurs during birth and subsequent growth of the brain (Weickenmeier et al., 2017). Fontanels are initially relatively small during delivery but can expand up to 3-4 cm in width in the first few months of life (Popich & Smith, 1972; Pedroso et al., 2008). In healthy children, the anterior fontanel (the most prominent diamond-shaped membrane-filled space located between the two frontal and two parietal skull bones) is generally the last to close (due to ossification of the bones of the skull). The anterior fontanel persists until around 18 months after birth and sometimes for several years (Hansman, 1966). Fontanels influence the volume currents that accompany primary currents generated by active neuronal populations. Modelling data suggest that the influence of fontanels is akin to that of holes (Benar & Gotman, 2002) and zones of higher conductivity (Ollikainen et al, 1999) in the adult skull. Specifically, Roche-Labarbe et al (2008) reported that in their source localisation analyses, when the infant fontanel was modelled as a thinner resistive skull zone, this caused a modest dipole shift towards the fontanel region.

As the thickness of the skull increases from 1 to 2 mm at birth to several millimetres during early adulthood, its conductivity concomitantly decreases (Gibson et al, 2000; Hansman, 1966). In adults, there is high individual variability in skull conductivity (Goncalves et al, 2003), which suggests that infant skull conductivity may vary considerably across participants as well. Infant source localisation modelling studies have shown that changes in skull layer conductivity tend to affect the magnitude and position of dipoles to a larger extent than their orientation (Roche-Labarbe et al, 2008; Lew et al, 2013).

**Solution:**

Currently, most available source localisation techniques for infants do not compensate for factors such as skull thickness, density, and fontanel closure. Although high-density EEG arrays may offer promising potential for estimating sources of neural activity in infants, it is recommended that attempts at source localisation are combined with, and constrained by, strong theoretical and anatomical predictions. In particular, attempts to develop developmentally-appropriate head models (e.g. Lew et al, 2013) may improve the feasibility of source localisation for infants in the future. Azizollahi et al. (2018) have recently developed promising head models for the forward solution in EEG source localisation that take into account variable conductivity of fontanels; follow up research is needed to test the proposed solutions at different stages of fontanel closure.

### *3.2 Prevalence and diversity of infant myogenic artefacts*

**Problem:**

For paediatric populations, motion is almost unavoidable during experimental recordings. In EEG, myogenic artefacts are more problematic for the infant than adult measurements since involuntary physiological activity such as heartbeat and blinks are less stereotypical and therefore more difficult to identify and remove using the de-noising procedures normally applicable to adult EEG (Fujioka, Mourad, He, & Trainor, 2011). A further complication arises from infants' tendency to move abruptly and frequently, which creates temporary displacement of channels on the scalp (Bell, & Cuevas, 2012; Fujioka et al., 2011; Hoehl & Wahl, 2012).

As demonstrated in Table 2 (Section 1.1), the prevalence of movement during the time on task can be up to >95% in naturalistic interactive paradigms. Muscular activities can be grouped in the head-neck-face category and the bodily-limb movement category. We generally find that the former is more problematic in terms of prevalence, and in terms of broadband artefactual effects on the EEG signal.

Two representatives of the first category worth mentioning are eye and jaw movements. They occur from birth (i.e. blinking, sucking reflex, yawning, rooting, crying) and continue to occur frequently in experimental conditions by 18 months and beyond. The proximity of muscular generators of these motions to the EEG electrodes and their repetitive nature makes them particularly problematic for the EEG researcher. While the effects of eye-blinks on EEG are somewhat better studied in the literature and can be detected using a dedicated channel, or eye-tracker (Plöchl, Ossandón, J., & König, 2012), jaw motions are more challenging to both detect and correct, and are known to reduce the signal-to-noise ratio of neural signals that relate to cognition (Brooker & Donald, 1980).

In the body-limb movement category, we find that upper limb movements (arms and hands) create the most artefactual spectral signature in infant EEG during naturalistic play in the age group around 12 months (see Figure 4). A problematic feature of these sets of motion artefacts is that they do not necessarily produce obviously artefactual activity in raw EEG - i.e. the amplitude and temporal features of the electrode traces may not change much compared to when the infant (although this is also true for adults) is apparently still. Therefore, contamination from these forms of muscular activity may remain undetectable by automated pre-processing procedures, and indeed during manual artefact rejection (see Figure 5).

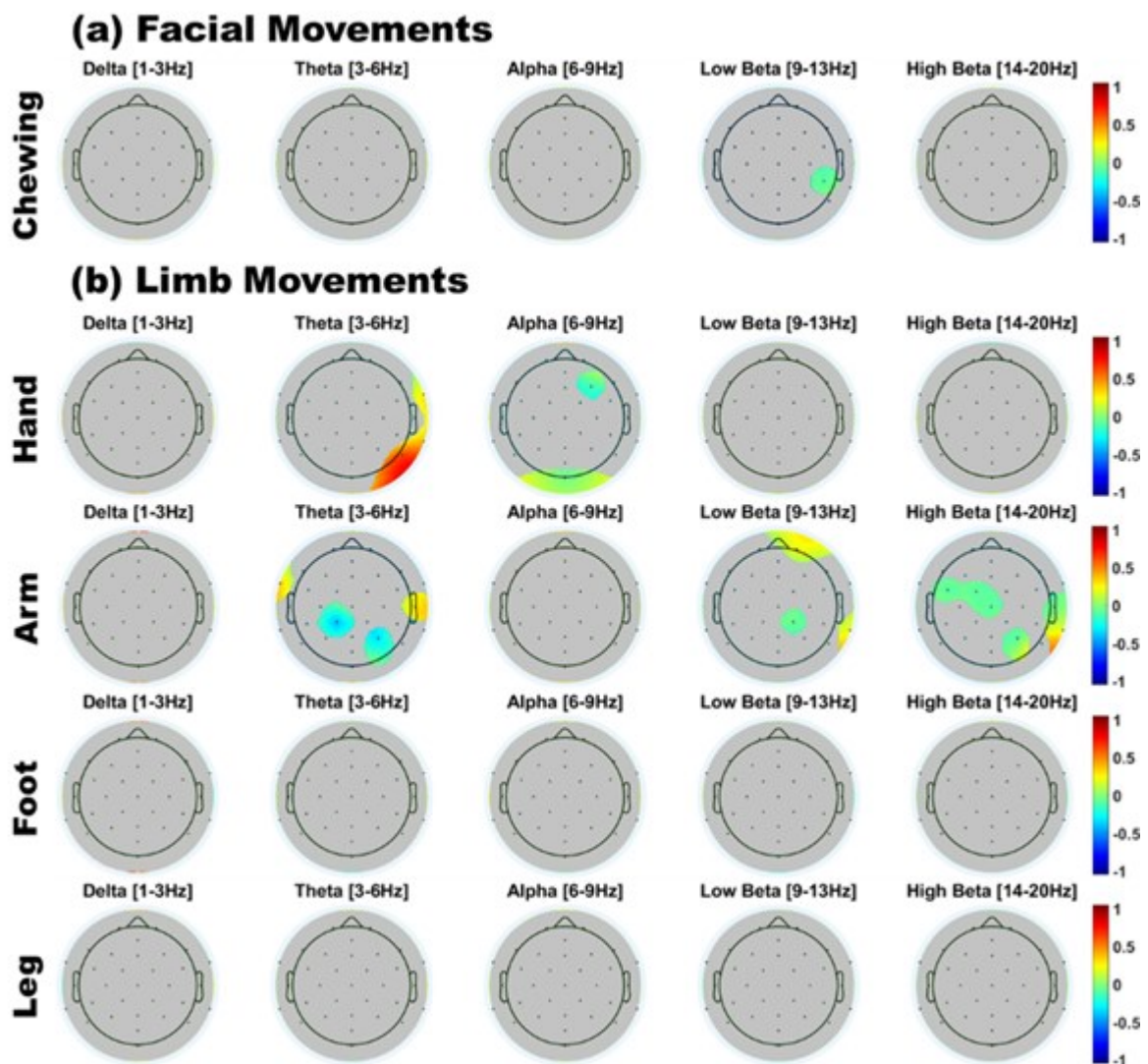


**Figure 4** | Scalp topography of significant differences (Cohen's D-values) between a) facial movements or b) limb movements, and resting state. In each subplot, only scalp regions where significant power differences were observed (Benjamin-Hochberg FDR corrected at  $p < .05$ ) are shown in colour. Grey = nonsignificant result; red = higher power during movement; blue = higher power during resting state. Fourteen infants participated in the study. There were 6 boys and 8 girls in the group, with an average age of 338.85 days (SD = 59.59). Two infants produced insufficient resting state data due to fussiness, and so were excluded from the analysis. The remaining 12 infants comprised 5 boys and 7 girls, with an average age of 325.5 days (SD = 51.77). Facial movements are represented by 6 infants, hand and arm movements – by 8 infants, and foot and leg movements – by 10 infants. The study was approved by the Cambridge Psychology Research Ethics Committee, and parents provided written informed consent on behalf of their children. Authors' data (Georgieva et al., 2018).

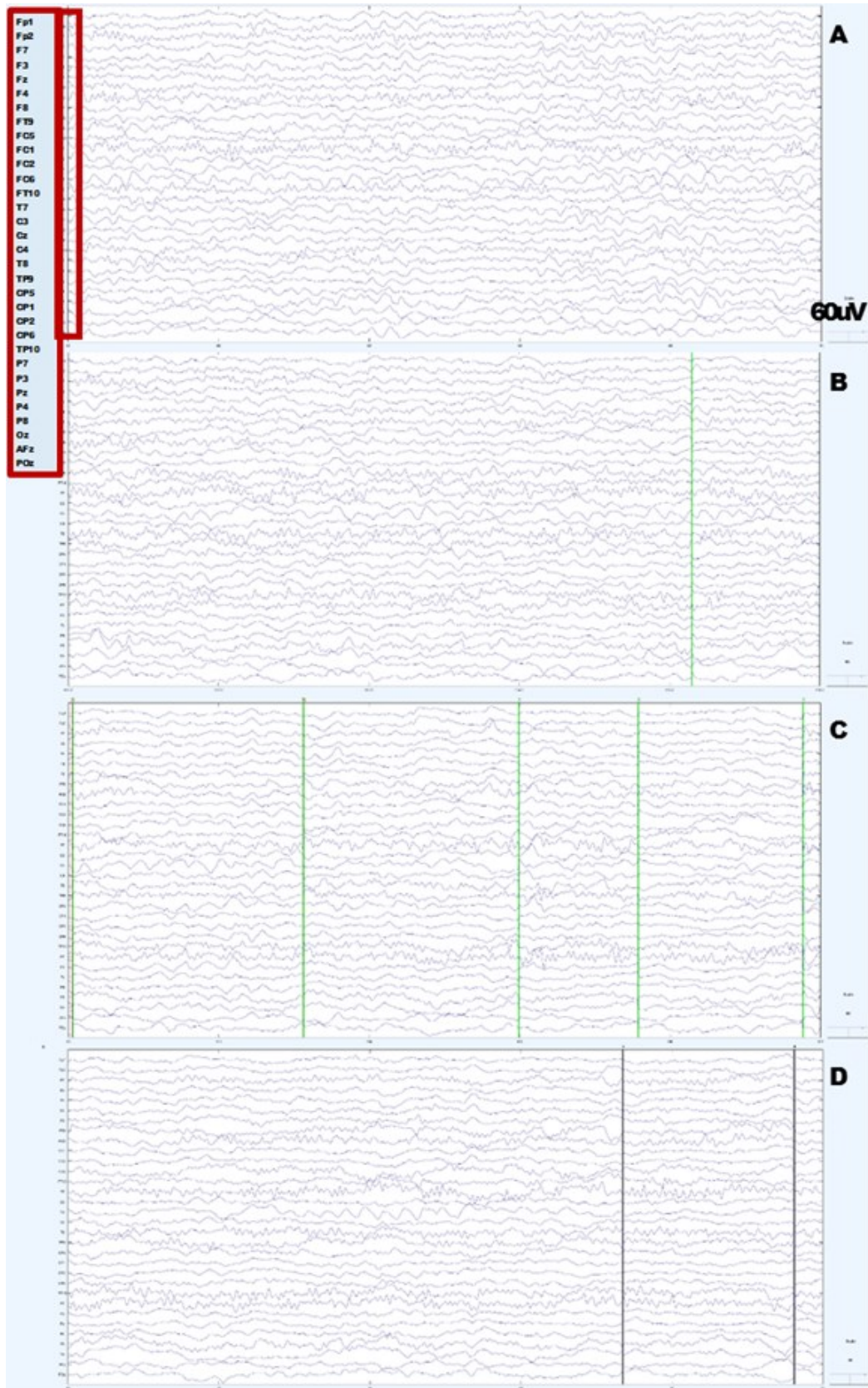


**Figure 5** | Infant raw EEG (filtered and average re-referenced) segment from continuous recording. All figures show 5 seconds of continuous recording during a) infant resting state, b) infant hand movements, c) infant arm movements, and d) infant talking/babbling. Note that

timepoints where movements were made (marked as vertical lines) do not produce easily identifiable changes in the EEG signal. Authors' unpublished data.

In cases where the electrical trace displacement is not as stereotypical as with blinking, one could try to isolate signal distortion by comparing its frequency spectra with that of resting state activity. However, when interpreting muscle generated artefactual activity in EEG, using infant “resting state” activity as a gold standard is questionable in its own right. It is difficult to ascertain with confidence that an infant’s EEG recording is movement free; even when there is no apparent motion. For example, there might be gentle continuous sucking that occurs at ~2-4Hz, which would increase delta or theta power in temporal electrode regions. Such activity would be virtually undetectable without additional EMG electrodes over the jaw area - and these are nearly never used in infant EEG research.

**Solution:**

As there is no efficacious method for eliminating infant motion during EEG experiments, it is essential to understand (1) the characteristic effects on typical infant motions on the EEG signal, (2) the motions most likely to be exhibited at the age of interest, (3) the motions most likely to be present in the paradigm, and (4) the effect of motion on different EEG metrics (e.g. connectivity or spectral measures).

To address the problem of movement-related artefacts in adult EEG data, researchers traditionally exclude artefact-contaminated segments by employing strict rejection thresholds. However, when applied to infants, the artefact exclusion approach may entail considerable data loss (Fujioka et al., 2011), and there is an increasing interest in correction procedures that permit the accurate identification and removal of artefacts from infant EEG without

significantly compromising the integrity of underlying neural activity (Gwin et al., 2010; He, Hotson, & Trainor, 2007; Fujioka et al., 2011). Yet, while various methods can ameliorate the problem of data loss due to artefact rejection, and they have been used in a number of research studies as a cleaning strategy for data pre-processing (Agyei, Weel, & Meer, 2016; Corrigan & Trainor, 2014; Folland, Butler, Payne, & Trainor, 2014; Slugocki & Trainor, 2014; Trainor, Lee, & Bosnyak, 2014), these strategies still rely on the successful classification of portions of the EEG signal as artefactual, which is itself a non-trivial task.

In order to assess whether the artefactual activity is likely to inflate or reduce the effect that researchers are testing, systematic control analyses should be carried out on how specific movement artefacts distort infant EEG data. We have successfully employed this strategy with jaw movements artefacts in a study where an adult sang nursery rhymes for the infants and her EEG was recorded during speech production (Leong et al., 2017). We quantified the spectral and topographical signatures of the production of nursery rhymes and compared those to a silent resting state in order to quantify the effect of speech production artefacts on our measures of interest (connectivity patterns). Furthermore, in more recent work, we attempted to catalogue a detailed descriptive library of the most prominent motions produced by infants, and their respective artefactual influence on the EEG recordings (Georgieva et al., 2018). Accordingly, we investigated their topological and spectral features as compared to resting state EEG in the major frequency bands of interest (0.05 - 20 Hz). While this library is by no means exhaustive, we hope that it can be further developed as a tool to identify which dimensions of EEG signal are the most vulnerable to biases introduced by artefactual muscle activity.

### *3.3 A lack of stereotypical topography of infants' eye movements needed for the ICA-based data cleaning*

**Problem:**

Given that infants cannot be instructed to avoid blinking during critical periods of stimuli presentation, infant task-related EEG data can become contaminated with a much higher proportion of eye-movement related noise than adult EEG. This poses data comparability issues for dual EEG studies that require a comparable signal-to-noise ratio for the accurate estimation of cross-brain synchronisation. Stereotypical EEG artefacts, such as those caused by blinks and saccades, can be efficiently identified and removed from the signal using Independent Component Analysis (ICA), which separates a multivariate signal into additive subcomponents that are linearly mixed in several EEG channels (Makeig et al., 1996; Vigario, 1997). In adult EEG research, ICA-based decomposition of signal is perhaps the most commonly used method of data cleaning, and there is also an increasing use of ICA in infant research. However, while ICA is very efficient in identifying eye-movement related artefacts in the adult populations, it often fails to identify components driven by blinks and saccades in infants (see Figure 6). In some other cases of ICA of infant EEG, eye movement noise spreads across a large number of components (Fujioka et al., 2011), as it is not as temporally and spatially confined as in adults (Bell & Wolfe, 2008). Also, given that infant background EEG activity is relatively slow in frequency but high in amplitude (Bell & Wolfe, 2008), its spectral and spatial patterns can overlap with those caused by eye movements, further obstructing ICA-based decomposition of the signal.

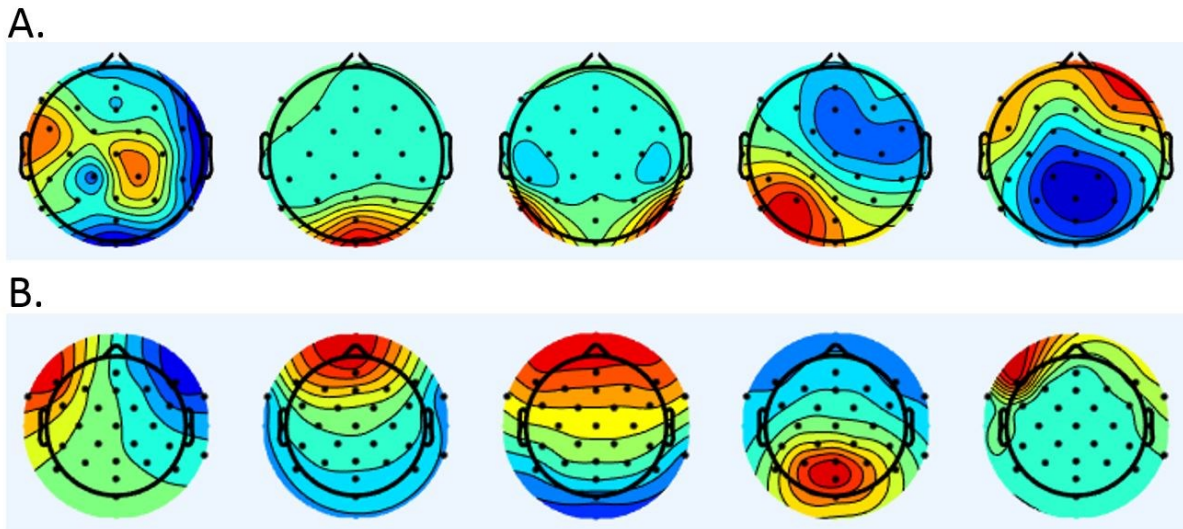


**Figure 6** | Topographic representation of the first five independent components, ordered from the largest to smallest by the magnitude of EEG signal explained, calculated from a) infant (9.5 months) and b) mother (32 y.o.) datasets of the same dyad. The first two components in the mother's dataset represent eye movements (saccades and blinks), whereas eye movement-related components are missing from the ICA decomposition of the infant's dataset. Authors' unpublished data.

### **Solution:**

While most of the EEG studies using ICA for data cleaning rely on the Runica (Makeig et al., 1996) or FastICA (Hyvärinen & Oja, 1997) algorithms, there is a large body of signal processing literature investigating other ICA solutions, and some of them could be more efficient for the processing of infant data. For instance, Miljkovic et al. (2010) compared the efficiency of RobustICA, SOBI, JADE, and BSS-CCA algorithms to extract ECG artefacts from neonatal EEG signal, and found their sensitivity to vary from 0.73 to 0.85 with SOBI and BSS-CCA methods being more efficient than RobustICA and BSS-CCA. A similar systematic research is needed to compare the efficiency of different ICA methods for cleaning both infant and adult EEG datasets. Finally, when ICA-based algorithms fail, other artefact cleaning methods should be applied, such as Artefact Blocking algorithm, which can efficiently process

both infant and adult datasets (Fujioka et al., 2011; Mourad et al., 2007). It multiplies the observed data matrix by a blocking matrix that eliminates high amplitude artefacts, such as blinks, saccades or head movements, while linearly transforming the other EEG sources with minimal distortion.

### *3.4 Relatively high inter-individual variability of EEG responses in younger cohorts*

#### **Problem:**

In EEG studies with infants, two inherent problems are that shorter periods of data recording must be used, and that data quality during these recordings is more variable, due to the increased prevalence of artefacts. In addition, one further problem is that intra-individual variability in neural responses is inherently higher in infants (De Haan, 2013). This higher variability arises from a number of sources, including variable arousal states (see section 1.2), movement artefacts and non-compliance (see section 3.2), and rapid developmental maturation of brain structures (see sections 2.3 & 3.1). This high variability means that a larger number of samples must be taken to obtain an accurate average value. And, finally, due to differential rates of development and brain maturation, inter-individual variability in responses is also higher in younger cohorts. Taken together, these problems pose serious signal-to-noise challenges in infant EEG studies.

#### **Solution:**

Practical steps that can be taken to address these problems are: i) aiming for a smaller number of conditions, allowing more (and therefore more accurate) data to be collected for each condition; ii) splitting data collection, where possible, across a number of different shorter sessions, or interspersing an experimental condition with engaging TV clips, in order to

maximise data retention. Analytical steps that can be taken include inserted the amount of data collected in as a covariate into statistical analyses.

#### **4. Analysis of dual EEG data**

##### *4.1 Developmental shifts in canonical EEG rhythms*

###### **Problem:**

During the early years, rapid developmental changes in brain activity occur (Haartsen et al., 2016), and canonical EEG rhythms change over development (Anderson & Perone, 2018; Hagne, 1968). For example, Stroganova and colleagues (1999) found that alpha activity is slower during infancy than during early childhood and later in life (see Figure 7A), although it functionally and topographically corresponds to posterior alpha in adults, and that theta activity is also lower (Orekhova et al., 2006). Marshall and colleagues (2002) found, similarly, changes in relative 6-9 Hz power from 5 months to 4 years of age, with peak frequency increasing from 4 Hz (over parietal and occipital sites) and 7 Hz (over central and frontal sites) at 5 months to about 8 Hz by 2 years and 9 Hz by 4 years (widespread over the scalp) (see Figure 7B). They also observed stable individual differences in relative alpha power from 10 months to 4 years (but not 5 months to 10 months).

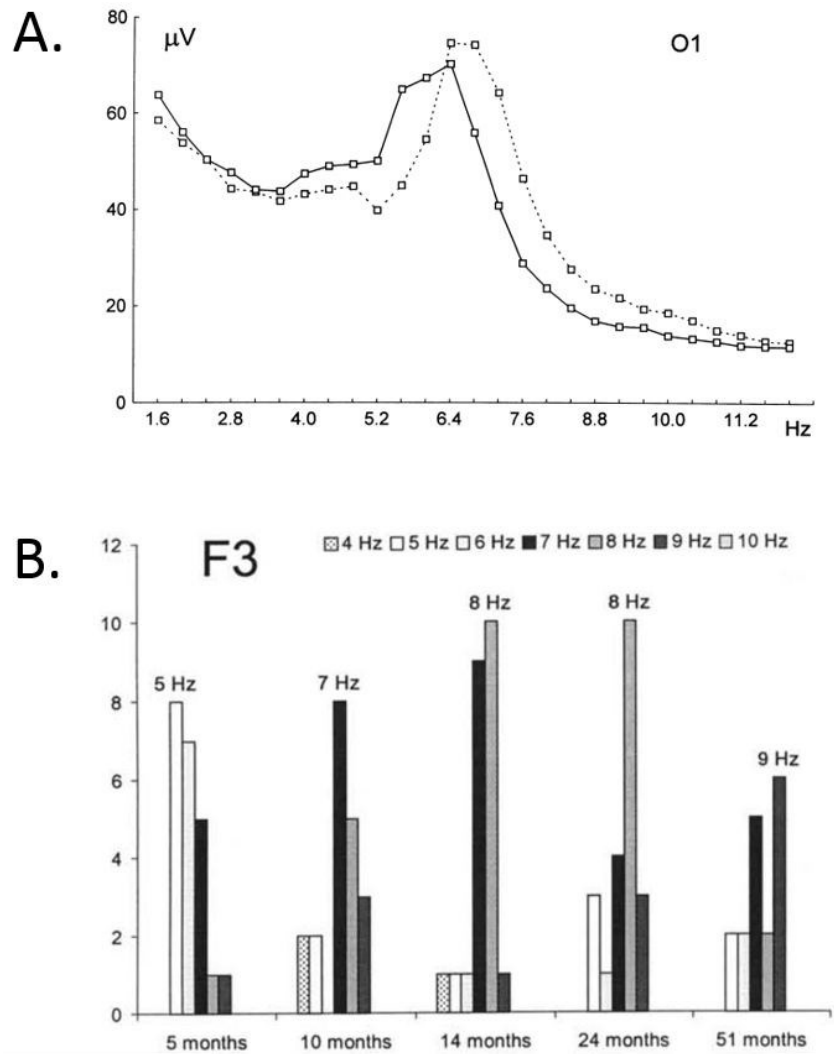


**Figure 7 | (A)** A developmental shift in the alpha frequency range observed from the age of 8 months (solid line) to the age of 11 (dashed line). Reproduced with permission from Stroganova et al. (1999). **(B)** The number of participants from five age groups depicted as vertical bars, whose peak frequency fell at a specific 1 Hz bin within the 4–9 Hz range, recorded from the left frontal electrode F3. A peak frequency shift can be observed from 5 Hz at the age of 5 months to 9 Hz at the age of 51 months. Reproduced with permission from Marshall et al. (2002).

Such developmental shifts in EEG rhythms present problems for dual infant-adult EEG analyses, as most of the analytical algorithms used to study inter-brain connectivity, such as phase locking value (PLV; Lachaux et al., 1999) or weighted phase lag index (wPLI; Vinck et al., 2011), estimate phase coupling of identical frequencies extracted from two time series.

Given that peak frequencies of oscillatory rhythms are slower in infants compared to adults, such analyses are likely to assess phase coupling of different frequency bands between dyad partners. For instance, a 6 Hz coupling between an 8 month old infant and her mother would estimate synchronisation between alpha oscillations in infant and theta oscillations in mother. Given that different frequency ranges may have different functional roles, such coupling may be suboptimal for the identification of functionally significant inter-brain synchronisation.

**Solution:**

As an alternative to the single-frequency coupling, inter-brain connectivity can be assessed using cross-frequency coupling techniques (Canolty & Knight, 2010; Cohen, 2014). In the phase-amplitude coupling analysis, an oscillation phase in one time series is correlated with an oscillation amplitude in another time series. Importantly, the frequency of oscillations does not need to match between the two time series, enabling coupling between different frequency bins, e.g. 6 Hz alpha phase in infant and 10 Hz alpha amplitude in mother. Likewise, the power of different frequency bins can be correlated between two time series (infant and mother) in the amplitude-amplitude coupling. Alternatively to the cross-frequency coupling methods that rely on the analysis of narrow frequency bins, inter-brain connectivity could be assessed using connectivity indices that are not limited to a single narrow frequency bin. For instance, weighted symbolic mutual information (wSMI; King et al., 2013) estimates the probability of co-occurrence of symbolic signal patterns in two times series at a rather low frequency specificity. While symbols formed by three elements separated by 32 ms have peak sensitivity at 8 Hz, they represent ~2-11 Hz range of frequencies, which would arguably cover alpha peaks for both infants and adults (King et al., 2013).

#### *4.2 Differentiating inter-personal synchrony from spurious synchrony due to common intrinsic properties of the signal*

##### **Problem:**

Dual neuroimaging studies usually examine synchrony in one of two modes. The first is concurrent synchrony ('when X is high, Y is high'), which can be assessed either by measuring covariance in the amplitude or power of the signal or by measuring the phase of the signal (e.g. phase-locking value; Lachaux et al., 1999). The second is sequential synchrony ('changes in X forward-predict changes in Y') (often known as Granger-causality; Granger, 1969) which can again be assessed based on the amplitude, power, or phase of the signal (e.g. Partial Directed Coherence; Baccalá & Sameshima, 2001).

One challenge to researchers measuring synchrony is that neural activity itself has certain common properties. For example, two adults, each with a dominant alpha rhythm of 10Hz, might be expected to show fairly consistent phase relationships between their alpha rhythms even if there was no communication between them. Similar considerations apply when considering variability in amplitude and power of the signal, where common oscillatory activity may be attributable to other sources (such as heart beat; Schmueli et al., 2007).

##### **Solution:**

Because of this inherent problem, most hyperscanning studies do not simply measure phase coupling between individuals, but rather compare the degree of coupling between different experimental conditions. Ideally, the two conditions should be held as constant as possible except for the particular parameter (e.g. the presence or absence of social interaction) which is of interest.

Second, from an analytical perspective, researchers (Burgess, 2013) have argued that, perhaps particularly for EEG, where analyses tend to focus on the oscillatory components, the simple presence of consistent phase differences between two EEG signals is perhaps too inclusive a definition of synchrony, and that Granger-causal measures such as Partial Directed Coherence may give fewer false-positive results (Burgess, 2013).

One recommended analytical solution is to perform a bootstrapping analysis in which corresponding epochs from the dyad are temporally translocated ('shuffled') with respect to each other, and synchrony is re-computed multiple times, in order to estimate the likelihood that the synchrony observed in the paired datasets would have been observed by chance. In doing this, care should be taken to ensure that sufficiently large epochs are used to ensure that lower frequency information is not distorted (which can be challenging in infant datasets, as any longer segments of usable data can be rare).

#### *4.3 Differentiating inter-personal synchrony from spurious synchrony due to shared external perturbation*

##### **Problem:**

The second problem facing researchers measuring inter-personal synchrony is that neural activity is also influenced by common external perturbation due to the environment, e.g. sounds or visual stimuli in the lab. For example, neural activity synchronises to temporal structures in speech (Giraud & Poeppel, 2012), and hence any words uttered during EEG recording could boost spurious synchrony by triggering similar neural responses in both partners of the dyad. Differentiating neural inter-personal synchrony from synchrony attributable to shared external

perturbation can be non-trivial (Fairhurst & Dumas, 2019). This is particularly true for naturalistic paradigms where factors such as the acoustic input cannot be completely controlled for across participants.

Similar considerations apply to analyses examining event-related change. Burgess showed that measures such as Phase-Locking value are sensitive to changes in the variance of the marginal distributions from the expected phase. Therefore, phase resetting time-locked to a stimulus can create the appearance of increases in phase synchrony, even when this is not the case (Burgess, 2013).

**Solution:**

A bootstrapping analysis in which chunks are translocated - either within a dyad over time or between dyads – does not control for this confound in cases where the environmental input is inconsistent across time, or across dyads. In cases where external stimulation cannot be adequately controlled for, the solution to this problem is non-trivial (Fairhurst & Dumas, 2019). As with section 4.2 above, an optimal experimental design will not just measure synchrony per se, but examine how synchrony changes relative to different experimental conditions – e.g. in the presence or absence of social interaction. Ideally, the level of external stimulation should be constant between these conditions. In addition, separate analyses can be conducted to identify the influence of external perturbation in each partner individually (e.g. speech-brain synchrony, in the case of an experiment where one or both of the partners is talking). And then, separately, an analysis can be conducted to show that speech-brain synchrony *does not* differ between conditions for either individual 1 or individual 2, but that brain-to-brain synchrony *does*.

## 5. Test-retest reliability of EEG measurement in infants

### **Problem:**

The stability and reliability of a testing instrument over time is one of the critical requirements for reproducible experimental research. In response to the replication crisis in cognitive sciences, cognitive neuroscientists have begun to show a growing interest in the test-retest reliability of their paradigms and brain measures, and several recent studies have assessed the test-retest reliability of EEG measurements in infants.

Munsters et al. (2019) reported the test-retest reliability of ERPs evoked by neutral, fearful and happy faces presented in low or high-frequency conditions to 9–10 month-old infants (N=31), who were tested twice within two weeks. Substantial reliability was observed for the amplitude of the earliest N290 component (Intraclass correlation (ICC)=0.76), and moderate reliability was observed for the amplitude of components P400 (ICC=0.58) and Nc (ICC=0.57) (see Figure 8A). These findings suggest that the reliability of the early sensory potentials might be generally higher than the reliability of later potentials that reflect more complex and variable cognitive processes.

van der Velde et al. (2019) estimated the test-retest reliability of EEG connectivity and network characteristics in 10 month-old infants (N=60), who were tested twice one week apart while watching videos on a computer screen. The reliability of the global phase lag index (PLI) was excellent for theta and alpha frequency bands (3-12 Hz; intraclass correlation coefficient (ICC)=[0.84-0.91]), and mediocre to good for delta, beta and gamma bands (ICC=[0.60-0.72]). Similarly, the test-retest reliability for the graph measures (Average clustering coefficient and Characteristic path length) calculated from the PLI matrices was

excellent for theta and alpha frequency bands (ICC=[0.84-0.91]), and mediocre to good for delta, beta and gamma bands (ICC=[0.53-0.73]). However, considerably lower reliability was observed for the Small-worldness Index for all frequency bands (ICC=[0.13-0.67]). Thus, EEG connectivity and network characteristics can be reliably assessed in 10 month-old infants (see Figure 8B), although reliability is strongly dependent on the frequency band and specific graph index.

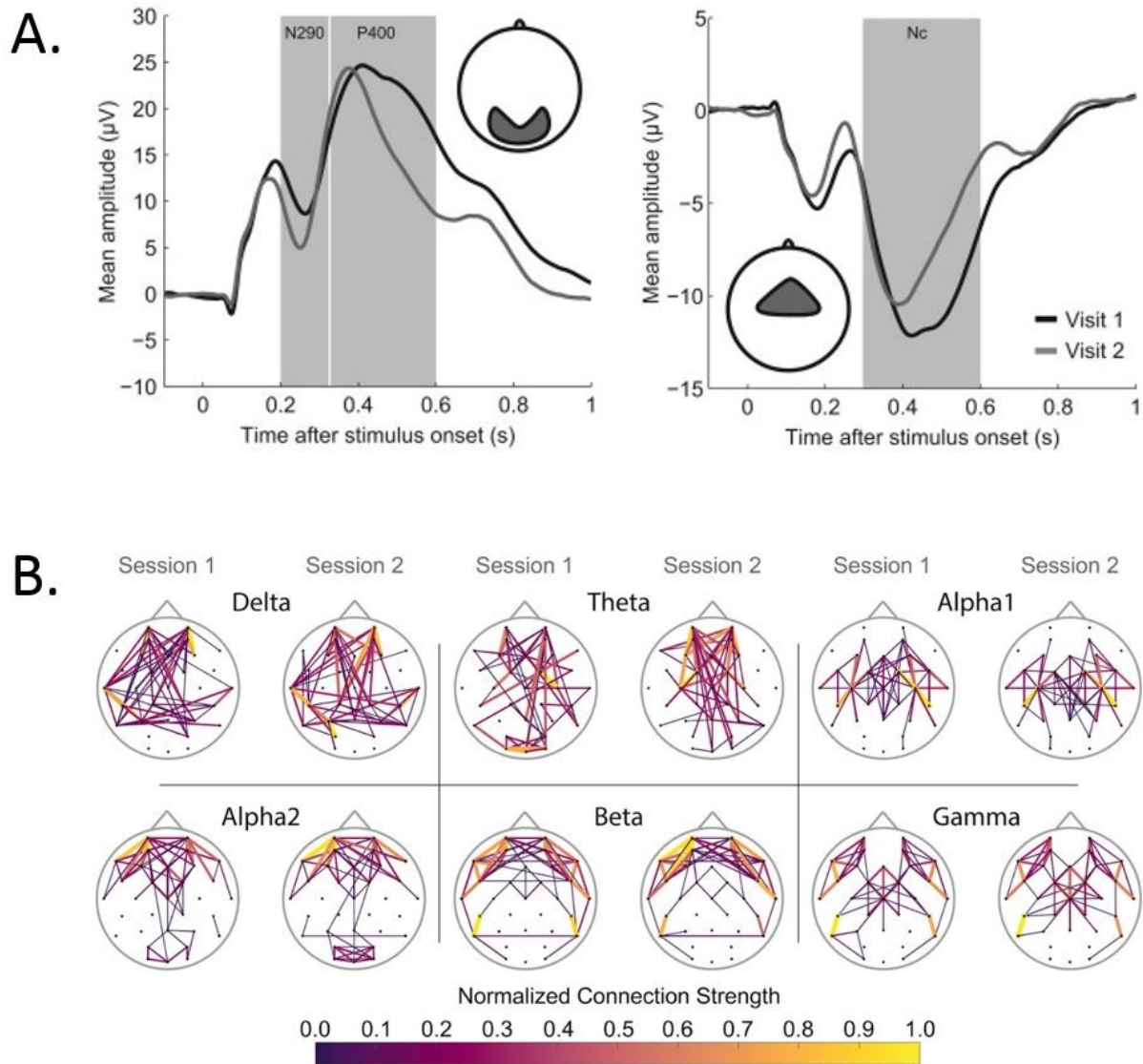


**Figure 8** | (A) Areal average of ERP to face stimuli in 9-10 month-old infants show a larger amplitude decrease for the later components during the second session. Reproduced with permission from Munsters et al. (2019). (B) Averaged PLI connectivity maps with the 12% strongest connections in 10 month-old infants indicate great similarity between two sessions. Reproduced from van der Velde et al. (2019), following the Creative Commons Attribution License (CC BY).

Overall, these studies demonstrate substantial reliability of specific EEG measures in both active and passive tasks. However, given that ICC is not equally high across all ERP components, frequency bands, and graph indices, the reliability of any new or untested EEG measure cannot be inferred from the reliability of related measures. Furthermore, while

reliability was relatively high for the averaged ERP data (Munsters et al., 2019), specific experimental manipulations showed low reliability. In particular, even though there were significant ERP effects of face emotion and an emotion x spatial frequency interaction, these experimental manipulations yielded very low reliability ( $ICC=[-0.33-0.15]$ ), suggesting that reliability of psychological manipulations may be much lower than the reliability of purely neurophysiological measurements.

**Solution:**

Ideally, the introduction of a new experimental manipulation and/or a new EEG analysis method should be accompanied by the estimation of its test-retest reliability. This is particularly important for the assessment of complex statistical interactions and new areas of research, such as dual EEG interactions between infants and adults.

**Concluding note**

Most of the EEG acquisition and analysis techniques have been developed to study adults, and hence their adaptation for infant research should always be carefully scrutinised. While longitudinal and social neuroscience studies using infant EEG become increasingly sophisticated (e.g. using dual EEG paradigms), new unique methodological challenges will continue to be identified. This requires infant EEG labs to invest time and resources into building technical and signal processing expertise that is not always available in the research centres dedicated to studying developmental psychology. With human cognitive neuroscience becoming increasingly specialised and technically and computationally challenging, a close collaboration between infant EEG and methods-oriented labs is desirable if not necessary.

## Acknowledgements

This research was funded by an ESRC Transforming Social Sciences collaboration grant (ES/N006461/1) to VL and SW, and by ESRC FRL Fellowship (ES/N017560/1) to SW. We thank Emma Bruce-Gardyne for proofreading the manuscript.

## References

Agyei, S. B., van der Weel, F. R. R., & van der Meer, A. L. H. (2016). Longitudinal study of preterm and full-term infants: High-density EEG analyses of cortical activity in response to visual motion. *Neuropsychologia*, *84*, 89–104.

Anderson, A. J., & Perone, S. (2018). Developmental change in the resting state electroencephalogram: insights into cognition and the brain. *Brain and Cognition*, *126*, 40-52.

Azizollahi, H., Darbas, M., Diallo, M. M., El Badia, A., & Lohrengel, S. (2018). EEG in neonates: Forward modeling and sensitivity analysis with respect to variations of the conductivity. *Mathematical Biosciences & Engineering*, *15*, 905-932.

Babiloni, F., & Astolfi, L. (2014). Social neuroscience and hyperscanning techniques: past, present and future. *Neuroscience & Biobehavioral Reviews*, *44*, 76-93.

Baccalá, L. A., & Sameshima, K. (2001). Partial directed coherence: a new concept in neural structure determination. *Biological Cybernetics*, *84*, 463-474.

Baum, J. D., & Searls, D. (1971). Head shape and size of newborn infants. *Developmental Medicine & Child Neurology*, *13*, 572-575.

Bell, M. A., & Cuevas, K. (2012). Using EEG to study cognitive development: issues and practices. *Journal of Cognition and Development*, *13*: 3. Doi: 10.1080/15248372.2012.691143

Bell, M.A., & Wolfe, C.D. (2008). The use of the electroencephalogram in research on cognitive development. L.A. Schmidt, S.J. Segalowitz (Eds.), *Developmental Psychophysiology: Theory, Systems, and Methods*, pp. 150-170. Cambridge University Press, New York.

Béнар C.-G., & Gotman, J. (2002). Modeling of post-surgical brain and skull defects in the EEG inverse problem with the boundary element method. *Clinical Neurophysiology*, *113*, 48–56.

Brooker, B. H., & Donald, M. W. (1980). Contribution of the speech musculature to apparent human EEG asymmetries prior to vocalization. *Brain and Language*, *9*, 226–245.

Boto, E., Holmes, N., Leggett, J., Roberts, G., Shah, V., Meyer, S. S., ... Brookes, M. J. (2018). Moving magnetoencephalography towards real-world applications with a wearable system. *Nature*, *555*, 657–661.

Burgess, A. P. (2013). On the interpretation of synchronisation in EEG hyperscanning studies: a cautionary note. *Frontiers in Human Neuroscience*, 7, 881. Doi: 10.3389/fnhum.2013.00881

Buzsaki, G. (2006). *Rhythms of the Brain*. Oxford University Press.

Canolty, R. T., & Knight, R. T. (2010). The functional role of cross-frequency coupling. *Trends in Cognitive Sciences*, 14, 506-515.

Clancy, R. R., & Legido, A. (1991). Postnatal epilepsy after EEG-confirmed neonatal seizures. *Epilepsia*, 32, 69-76.

Cohen, M. X. (2014). *Analyzing Neural Time Series Data: Theory and Practice*. MIT press.

Corrigall, K. A., & Trainor, L. J. (2014). Enculturation to musical pitch structure in young children : evidence from behavioral and electrophysiological methods. *Developmental Science*, 17, 142–158.

DeBoer, T., Scott, L. S., & Nelson, C. A. (2007). Methods for acquiring and analyzing infant event-related potentials. In M de Haan (Ed.) *Infant EEG and Event-Related Potentials*, pp. 5–37. New York, NY: Psychology Press.

De Haan, M. (2013). *Infant EEG and Event-Related Potentials*. New York, NY: Psychology Press.

Duc, G., & Largo, R. H. (1986). Anterior fontanel: size and closure in term and preterm infants. *Pediatrics*, *78*, 904-908.

Fairhurst, M., & Dumas, G. (2019). Reciprocity and alignment: quantifying coupling in dynamic interactions. PsyArXiv, Preprint Doi: 10.31234/osf.io/nmg4x

Farroni, T., Csibra, G., Simion, F., & Johnson, M. H. (2002). Eye contact detection in humans from birth. *Proceedings of the National Academy of Sciences*, *99*, 9602-9605.

Fisch, B. J., & Spehlmann, R. (1999). *Fisch and Spehlmann's EEG Primer: Basic Principles of Digital and Analog EEG*. Elsevier Health Sciences.

Folland, N. A., Butler, B. E., Payne, J. E., & Trainor, L. J. (2014). Cortical representations sensitive to the number of perceived auditory objects emerge between 2 and 4 months of age: electrophysiological evidence. *Journal of Cognitive Neuroscience*, *27*, 1060-1067.

Friedrich, M., Weber, C., & Friederici, A. D. (2004). Electrophysiological evidence for delayed mismatch response in infants at-risk for specific language impairment. *Psychophysiology*, *41*, 772-782.

Fujioka, T., Mourad, N., He, C., & Trainor, L. J. (2011). Comparison of artefact correction methods for infant EEG applied to extraction of event-related potential signals. *Clinical Neurophysiology*, *122*, 43-51.

Georgieva, S., Lester, S., Yilmaz, M., Wass, S., & Leong, V. (2018). Topographical and spectral signatures of infant and adult movement artefacts in naturalistic EEG. *bioRxiv*, 206029. Doi: 10.1101/206029

Gibson, A., Bayford, R. H., & Holder, D. S. (2000). Two-dimensional finite element modelling of the neonatal head. *Physiological Measurement*, 21, 45-52.

Giraud, A. L., & Poeppel, D. (2012). Cortical oscillations and speech processing: emerging computational principles and operations. *Nature Neuroscience*, 15, 511-517.

Gonçalves, S. I., de Munck, J. C., Verbunt, J. P., Bijma, F., Heethaar, R. M., & da Silva, F. L. (2003). In vivo measurement of the brain and skull resistivities using an EIT-based method and realistic models for the head. *IEEE Transactions on Biomedical Engineering*, 50, 754-767.

Granger, C. W. (1969). Investigating causal relations by econometric models and cross-spectral methods. *Econometrica: Journal of the Econometric Society*, 37, 424-438.

Grigg-Damberger, M., Gozal, D., Marcus, C. L., Quan, S. F., Rosen, C. L., Chervin, R. D., ... & Iber, C. (2007). The visual scoring of sleep and arousal in infants and children. *Journal of Clinical Sleep Medicine*, 3, 201-240.

Gwin, J. T., Gramann, K., Makeig, S., & Ferris, D. P. (2010). Removal of movement artefact from high-density EEG recorded during walking and running. *Journal of Neurophysiology*, 103, 3526-3534.

Haartsen, R., Jones, E. J., & Johnson, M. H. (2016). Human brain development over the early years. *Current Opinion in Behavioral Sciences*, *10*, 149-154.

Hagne, I. (1968). Development of the waking EEG in normal infants during the first year of life. In P. Kellaway and I. Petersen (Eds.) *Clinical Electroencephalography of Children*, pp. 97-118. Almqvist & Wiksell, Stockholm.

Hagne, I. (1972). Development of the sleep EEG in normal infants during the first year of life. *Acta Paediatrica*, *61*, 25-53.

Halit, H., Csibra, G., Volein, A., & Johnson, M. H. (2004). Face-sensitive cortical processing in early infancy. *Journal of Child Psychology and Psychiatry*, *45*, 1228-1234.

Hansman, C. F. (1966). Growth of interorbital distance and skull thickness as observed in roentgenographic measurements. *Radiology*, *86*, 87-96.

He, C., Hotson, L., & Trainor, L. J. (2007). Mismatch responses to pitch changes in early infancy. *Journal of Cognitive Neuroscience*, *19*, 878-892.

Hirasawa, K., Kurihara, M., & Konishi, Y. (2002). The relationship between mismatch negativity and arousal level. Can mismatch negativity be an index for evaluating the arousal level in infants? *Sleep Medicine*, *3*, S45-S48.

Hoehl, S., Michel, C., Reid, V. M., Parise, E., & Striano, T. (2014). Eye contact during live social interaction modulates infants' oscillatory brain activity. *Social Neuroscience, 9*, 300-308.

Hoehl, S., & Wahl, S. (2012). Recording infant ERP data for cognitive research. *Developmental Neuropsychology, 37*, 187-209.

Hyvärinen, A., & Oja, E. (1997). A fast fixed-point algorithm for independent component analysis. *Neural computation, 9*, 1483-1492.

Jones, E. J., Venema, K., Lowy, R., Earl, R. K., & Webb, S. J. (2015). Developmental changes in infant brain activity during naturalistic social experiences. *Developmental Psychobiology, 57*, 842-853.

King, J. R., Sitt, J. D., Faugeras, F., Rohaut, B., El Karoui, I., Cohen, L., ... & Dehaene, S. (2013). Information sharing in the brain indexes consciousness in noncommunicative patients. *Current Biology, 23*, 1914-1919.

Kühn-Popp, N., Kristen, S., Paulus, M., Meinhardt, J., & Sodian, B. (2016). Left hemisphere EEG coherence in infancy predicts infant declarative pointing and preschool epistemic language. *Social Neuroscience, 11*, 49-59.

Lachat, F., & George, N. (2012). Oscillatory brain correlates of live joint attention: a dual-EEG study. *Frontiers in Human Neuroscience, 6*, 156. Doi: 10.3389/fnhum.2012.00156

Lachaux, J. P., Rodriguez, E., Martinerie, J., & Varela, F. J. (1999). Measuring phase synchrony in brain signals. *Human Brain Mapping, 8*, 194-208.

Legido, A., Clancy, R. R., Spitzer, A. R., & Finnegan, L. P. (1992). Electroencephalographic and behavioral-state studies in infants of cocaine-addicted mothers. *American Journal of Diseases of Children, 146*, 748-752.

Leong, V., Byrne, E., Clackson, K., Harte, N., Lam, S., & Wass, S. (2017). Speaker gaze changes information coupling between infant and adult brains. *Proceedings of the National Academy of Sciences, 114*, 13290-13295.

Leong, V., Noreika, V., Clackson, K., Georgieva, S., Brightman, L., Nutbrown, R., ... & Wass, S. (2019). Mother-infant interpersonal neural connectivity predicts infants' social learning. *PsyArXiv*, Preprint Doi: 10.31234/osf.io/gueaq

Leppänen, J. M., Peltola, M. J., Puura, K., Mäntymaa, M., Mononen, N., & Lehtimäki, T. (2011). Serotonin and early cognitive development: variation in the tryptophan hydroxylase 2 gene is associated with visual attention in 7-month-old infants. *Journal of Child Psychology and Psychiatry, 52*, 1144-1152.

Lew, S., Sliva, D. D., Choe, M. S., Grant, P. E., Okada, Y., Wolters, C. H., & Hämäläinen, M. S. (2013). Effects of sutures and fontanels on MEG and EEG source analysis in a realistic infant head model. *NeuroImage, 76*, 282-293.

Light, G. A., Williams, L. E., Minow, F., Sprock, J., Rissling, A., Sharp, R., ... & Braff, D. L. (2010). Electroencephalography (EEG) and event-related potentials (ERPs) with human participants. *Current Protocols in Neuroscience*, 52, 6-25.

Liu, D., Liu, S., Liu, X., Zhang, C., Li, A., Jin, C., ... & Zhang, X. (2018). Interactive brain activity: review and progress on EEG-based hyperscanning in social interactions. *Frontiers in Psychology*, 9, 1862. Doi: 10.3389/fpsyg.2018.01862

Luck, S. J. (2014). *An Introduction to the Event-Related Potential Technique* (2<sup>nd</sup> edition). MIT press.

Lund, T. R., Sponheim, S. R., Iacono, W. G., & Clementz, B. A. (1995). Internal consistency reliability of resting EEG power spectra in schizophrenic and normal subjects. *Psychophysiology*, 32, 66-71.

Makeig, S., Bell, A. J., Jung, T. P., & Sejnowski, T. J. (1996). Independent component analysis of electroencephalographic data. *Advances in Neural Information Processing Systems*, 8, 145-151.

Marshall, P. J., Bar-Haim, Y., & Fox, N. A. (2002). Development of the EEG from 5 months to 4 years of age. *Clinical Neurophysiology*, 113, 1199-1208.

Martynova, O., Kirjavainen, J., & Cheour, M. (2003). Mismatch negativity and late discriminative negativity in sleeping human newborns. *Neuroscience Letters*, 340, 75-78.

Meltzer, L. J., Montgomery-Downs, H. E., Insana, S. P., & Walsh, C. M. (2012). Use of actigraphy for assessment in pediatric sleep research. *Sleep Medicine Reviews, 16*, 463-475.

Michel, C. M., & Brunet, D. (2019). EEG Source Imaging: a practical review of the analysis steps. *Frontiers in Neurology, 10*, 325. Doi: [10.3389/fneur.2019.00325](https://doi.org/10.3389/fneur.2019.00325)

Miljković, N., Matić, V., Van Huffel, S., & Popović, M. B. (2010, September). Independent Component Analysis (ICA) methods for neonatal EEG artefact extraction: Sensitivity to variation of artefact properties. In *10th Symposium on Neural Network Applications in Electrical Engineering* (pp. 19-21). IEEE.

<https://ieeexplore.ieee.org/abstract/document/5644041>

Mourad, N., Reilly, J. P., de Bruin, H., Hasey, G., & MacCrimmon, D. (2007, April). A simple and fast algorithm for automatic suppression of high-amplitude artefacts in EEG data. In *2007 IEEE International Conference on Acoustics, Speech and Signal Processing-ICASSP'07* (pp. 393-396). IEEE. <https://ieeexplore.ieee.org/abstract/document/4217099>

Munsters, N. M., van Ravenswaaij, H., van den Boomen, C., & Kemner, C. (2019). Test-retest reliability of infant event related potentials evoked by faces. *Neuropsychologia, 126*, 20-26.

Nelson, C. A., & De Haan, M. (1996). Neural correlates of infants' visual responsiveness to facial expressions of emotion. *Developmental Psychobiology, 29*, 577-595.

Nunez, P. L., & Srinivasan, R. (2006). *Electric Fields of the Brain: The Neurophysics of EEG*. Oxford University Press.

Odabae, M., Tokariev, A., Layeghy, S., Mesbah, M., Colditz, P. B., Ramon, C., & Vanhatalo, S. (2014). Neonatal EEG at scalp is focal and implies high skull conductivity in realistic neonatal head models. *Neuroimage*, *96*, 73-80.

Ogilvie, R. D. (2001). The process of falling asleep. *Sleep Medicine Reviews*, *5*, 247-270.

Ollikainen, J. O., Vauhkonen, M., Karjalainen, P. A., & Kaipio, J. P. (1999). Effects of local skull inhomogeneities on EEG source estimation. *Medical Engineering & Physics*, *21*, 143-154.

Op de Beeck, H. & Nakatani, C. (2019). *Introduction to Human Neuroimaging*. Cambridge University Press.

Orehova, E. V., Stroganova, T. A., Posikera, I. N., & Elam, M. (2006). EEG theta rhythm in infants and preschool children. *Clinical Neurophysiology*, *117*, 1047-1062.

Otte, R. A., Winkler, I., Braeken, M. A. K. A., Stekelenburg, J. J., Van der Stelt, O., & Van den Bergh, B. R. H. (2013). Detecting violations of temporal regularities in waking and sleeping two-month-old infants. *Biological Psychology*, *92*, 315-322.

Parmelee Jr, A. H., Schulte, F. J., Akiyama, Y., Wenner, W. H., Schultz, M. A., & Stern, E. (1968). Maturation of EEG activity during sleep in premature infants.

*Electroencephalography and Clinical Neurophysiology*, 24, 319-329.

Pedroso, F. S., Rotta, N., Quintal, A., & Giordani, G. (2008). Evolution of anterior fontanel size in normal infants in the first year of life. *Journal of Child Neurology*, 23, 1419-1423.

Plöchl, M., Ossandón, J., & König, P. (2012). Combining EEG and eye tracking:

identification, characterization, and correction of eye movement artefacts in

electroencephalographic data. *Frontiers in Human Neuroscience*, 6: 278. Doi:

10.3389/fnhum.2012.00278

Pönkänen, L. M., Peltola, M. J., & Hietanen, J. K. (2011). The observer observed: Frontal EEG asymmetry and autonomic responses differentiate between another person's direct and averted gaze when the face is seen live. *International Journal of Psychophysiology*, 82, 180-187.

Popich, G. A., & Smith, D. W. (1972). Fontanels: range of normal size. *The Journal of Pediatrics*, 80, 749-752.

Reid, V. M., Striano, T., & Iacoboni, M. (2011). Neural correlates of dyadic interaction during infancy. *Developmental Cognitive Neuroscience*, 1, 124-130.

Reynolds, G. D., & Richards, J. E. (2009). Cortical source localisation of infant cognition. *Developmental Neuropsychology*, 34, 312-329.

Roche-Labarbe, N., Aarabi, A., Kongolo, G., Gondry-Jouet, C., Dümpelmann, M., Grebe, R., & Wallois, F. (2008). High-resolution electroencephalography and source localisation in neonates. *Human Brain Mapping, 29*, 167-176.

Salinsky, M. C., Oken, B. S., & Morehead, L. (1991). Test-retest reliability in EEG frequency analysis. *Electroencephalography and Clinical Neurophysiology, 79*, 382-392.

Schilbach, L., Timmermans, B., Reddy, V., Costall, A., Bente, G., Schlicht, T., & Vogeley, K. (2013). Toward a second-person neuroscience. *Behavioral and Brain Sciences, 36*, 393-414.

Shmueli, K., van Gelderen, P., de Zwart, J. A., Horovitz, S. G., Fukunaga, M., Jansma, J. M., & Duyn, J. H. (2007). Low-frequency fluctuations in the cardiac rate as a source of variance in the resting-state fMRI BOLD signal. *Neuroimage, 38*, 306-320.

Slugocki, C., & Trainor, L. J. (2014). Cortical indices of sound localisation mature monotonically in early infancy. *European Journal of Neuroscience, 40*, 3608-3619.

Smith, J. R. (1938a). The electroencephalogram during normal infancy and childhood: I. Rhythmic activities present in the neonate and their subsequent development. *The Pedagogical Seminary and Journal of Genetic Psychology, 53*, 431-453.

Smith, J. R. (1938b). The electroencephalogram during normal infancy and childhood: II. The nature of the growth of the alpha waves. *The Pedagogical Seminary and Journal of Genetic Psychology*, 53, 455-469.

Smith, J. R. (1938c). The electroencephalogram during normal infancy and childhood: III. Preliminary observations on the pattern sequence during sleep. *The Pedagogical Seminary and Journal of Genetic Psychology*, 53, 471-482.

Smith, J. R. (1939). The “occipital” and “pre-central” alpha rhythms during the first two years. *The Journal of Psychology*, 7, 223-226.

Souza, S. W., Ross, J., & Milner, R. D. (1976). Alterations in head shape of newborn infants after caesarean section or vaginal delivery. *Archives of Disease in Childhood*, 51, 624-627.

Striano, T., Reid, V. M., & Hoehl, S. (2006). Neural mechanisms of joint attention in infancy. *European Journal of Neuroscience*, 23, 2819-2823.

Stroganova, T. A., Orekhova, E. V., & Posikera, I. N. (1999). EEG alpha rhythm in infants. *Clinical Neurophysiology*, 110, 997-1012.

Trainor, L. J., Lee, K., & Bosnyak, D. J. (2011). Cortical plasticity in 4-month-old infants: specific effects of experience with musical timbres. *Brain Topography* 24, 192. Doi: 10.1007/s10548-011-0177-y

van der Velde, B., Haartsen, R., & Kemner, C. (2019). Test-retest reliability of EEG network characteristics in infants. *Brain and Behavior*, e01269. Doi: 10.1002/brb3.1269

Vigário, R. N. (1997). Extraction of ocular artefacts from EEG using independent component analysis. *Electroencephalography and Clinical Neurophysiology*, 103, 395-404.

Vinck, M., Oostenveld, R., Van Wingerden, M., Battaglia, F., & Pennartz, C. M. (2011). An improved index of phase-synchronisation for electrophysiological data in the presence of volume-conduction, noise and sample-size bias. *Neuroimage*, 55, 1548-1565.

Wass, S.V., Noreika, V., Georgieva, S., Clackson, K., Brightman, L., Nutbrown, R., Santamaria, L., & Leong, V. (2018). Parental neural responsivity to infants' visual attention: how mature brains influence immature brains during social interaction. *PloS Biology*, 16: e2006328. Doi: 10.1371/journal.pbio.2006328

Weickenmeier, J., Fischer, C., Carter, D., Kuhl, E., & Goriely, A. (2017). Dimensional, geometrical, and physical constraints in skull growth. *Physical Review Letters*, 118, 248101.

Weitzman, E. D., & Graziani, L. J. (1968). Maturation and topography of the auditory evoked response of the prematurely born infant. *Developmental Psychobiology: The Journal of the International Society for Developmental Psychobiology*, 1, 79-89.

Xie, W., & Richards, J. E. (2017). The relation between infant covert orienting, sustained attention and brain activity. *Brain Topography*, 30, 198-219.